

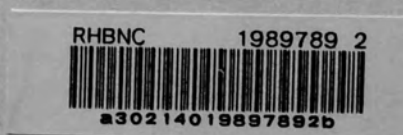
PALAEOENVIRONMENTAL STUDIES
IN MID-TERTIARY CARBONATES
OF SW SICILY

by
ROBIN CRAWFORD, BSc, FGS

Department of Geology
Bedford College
University of London

Submitted for the degree of
Doctor of Philosophy

June 1984



ProQuest Number: 10098965

All rights reserved

INFORMATION TO ALL USERS

The quality of this reproduction is dependent upon the quality of the copy submitted.

In the unlikely event that the author did not send a complete manuscript and there are missing pages, these will be noted. Also, if material had to be removed, a note will indicate the deletion.



ProQuest 10098965

Published by ProQuest LLC(2016). Copyright of the Dissertation is held by the Author.

All rights reserved.

This work is protected against unauthorized copying under Title 17, United States Code.
Microform Edition © ProQuest LLC.

ProQuest LLC
789 East Eisenhower Parkway
P.O. Box 1346
Ann Arbor, MI 48106-1346

ABSTRACT

Upper Oligocene limestones up to c. 50 m thick form disconnected outcrops within a 20 km radius of Sciacca in southwest Sicily. Two facies are present: foraminiferal grainstone-packstones (dominated by large benthonic foraminifera, particularly *Lepidocyclines*), and rhodalithic algal packstone-wackestones (in which eight species of coralline red algae are present). Petrology, fauna and flora indicate deposition in cool oxygenated waters of normal marine salinity at depths of 80-250 m in tropical-subtropical latitudes; the two facies representing differences in local water depth and turbulence. Rare feldspars within the limestones are diagenetic, with a variable sodic alio-
class - calcic alio-orthoclase composition related to localised synchronous glauconitisation.

*"What we see now is like a dim
image in a mirror"*

The limestones rest conformably on Cretaceous/Eocene carbonates, locally burrowed by *Thalassoides paradoxus*. A basal conglomerate contains both locally derived limestone cobbles and allochthonous phosphatized Eocene pebbles. All phosphate occurs as francolite replacing limestone. Features of major, trace and Rare Earth elements clearly differentiate these phosphates from Lower Miocene phosphorites of both southeast Sicily and the Maltese Islands, which have a very similar geochemistry.

1 COR. 13: 12

Lower Miocene limestones form similar outcrops generally to the north of the Upper Oligocene limestones and comprise a glauconitic limestone facies and a sandy limestone facies. Glauconite occurs as ubiquitous pellets, its geochemistry indicating formation by a gradual alteration of calcium carbonate. Petrology indicates deposition of the sediments in an outer shelf environment. Field relations of the two facies indicate that the Western Sicily Bridge (zone) was a positive structural feature from basal Miocene times, acting as a barrier to the arduaceous Numidian Flysch facies derived from the west-southwest.

Purity of the Oligocene - Miocene limestones has been greatly reduced by reprecipitation and by phases of both early submarine and late

ABSTRACT

Upper Oligocene limestones up to c.50 m thick form disconnected outcrops within a 20 km radius of Sciacca in southwest Sicily. Two facies are present: foraminiferal grainstone-packstones (dominated by large benthonic foraminifera, particularly *Lepidocyclines*), and rhodolithic algal packstone-wackestones (in which eight species of coralline red algae are present). Petrology, fauna and flora indicate deposition in cool oxygenated waters of normal marine salinity at depths of 80-250 m in tropical subtropical latitudes; the two facies representing differences in local water depth and turbulence. Rare feldspars within the limestones are diagenetic, with a variable sodic oligoclase - calcic anorthoclase composition related to localised synchronous glauconitisation.

The limestones rest disconformably on Cretaceous/Eocene carbonates, locally burrowed by *Thalassinoides paradoxica*. A basal conglomerate contains both locally derived limestone cobbles and allochthonous phosphatised Eocene pebbles. All phosphate occurs as francolite replacing limestone. Features of major, trace and Rare Earth elements clearly differentiate these phosphates from Lower Miocene phosphorites of both southeast Sicily and the Maltese islands, which have a very similar geochemistry.

Lower Miocene limestones form similar outcrops generally to the north of the Upper Oligocene limestones and comprise a glauconitic limestone facies and a sandy limestone facies. Glauconite occurs as ubiquitous pellets, its geochemistry indicating formation by a gradational alteration of calcium carbonate. Petrology indicates deposition of the sediments in an outer shelf environment. Field relations of the two facies indicate that the Western Sicily Bridge (*ant.*) was a positive structural feature from basal Miocene times, acting as a barrier to the arenaceous Numidian Flysch facies derived from the west-southwest.

Porosity of the Oligocene - Miocene limestones has been greatly reduced by compaction and by phases of both early submarine and late

ACKNOWLEDGEMENTS

subaerial diagenesis. Southward thrusting and associated folding post Lower Miocene times have slightly transported the sequences from their original (Saccense) carbonate platform and (Sicani) basin environments.

During my fieldwork in the central Mediterranean area during 1979, 1980 and 1981, the last, in January 1981, associated with a field trip to the Maltese islands sponsored by the Palaeontological Association, London, with Dr E.P.F. Rose as co-ordinating leader.

I thank my supervisor, Dr E.P.F. Rose, for his guidance during the initial fieldwork in 1979 and in 1980; and for much constructive critical help both during the course of research and in the final preparation of this thesis. Thanks are also due for his constant encouragement to meet other scientists from whom I have benefited greatly and which has provided me with a wealth of friends worldwide.

For the provision of resources, I am grateful to the Department of Geology, Bedford College (head: Prof. A.J. Smith) for special purchase of a Landrover for use in the field, to the Department of Geology, King's College, for the use of their NERC funded inductively coupled plasma spectrometer, and for the supervision and assistance of Dr J.N. Walsh and his technical staff; to the Department of Earth Sciences, University of Cambridge, for the use of their NERC funded microprobe and for the supervision of Dr P. Treloar; to the Universities of Palermo and Catania for the use of their libraries where I was able to obtain such local literature otherwise difficult to locate in the United Kingdom, and for the assistance and friendship of Drs R. Catalano and M. Ronga in each university respectively; and to Salvatore Bono, his family and friends in Palermo whose friendship made my visits so doubly memorable.

Many scientists have given their time to discuss and assist the development of this research. I am indebted to: Dr D.R.G. Rossouw (Goldsmiths' College, coralline red algae); Dr R.G. Bromley (Institute of Historic Geology and Palaeontology, Copenhagen, trace fossils); Dr W.C. Burnett (Florida State University, phosphorite and glauconite sedimentology and geochemistry); Dr G. Elliot (British Museum, Natural History, coralline red algae); Mr R.G. Sample (City of London Polytechnic, Mediterranean Tertiary); Dr S.R.A. Keller (University of Cambridge, trace fossils); Prof. G.W. Maschke

ACKNOWLEDGEMENTS

I gratefully acknowledge tenure of a Natural Environment Research Council research studentship during the years 1978-81; also the Council's funding of fieldwork in the central Mediterranean area during 1979, 1980 and 1981, the last, in January 1981, associated with a field trip to the Maltese islands sponsored by the Palaeontological Association, London, with Dr E.P.F. Rose as co-ordinating leader.

I thank my supervisor, Dr E.P.F. Rose, for his guidance during the initial fieldwork in 1979 and in 1980; and for much constructive critical help both during the course of research and in the final preparation of this thesis. Thanks are also due for his constant encouragement to meet other scientists from whom I have benefited greatly and which has provided me with a wealth of friends worldwide.

For the provision of resources, I am grateful to the Department of Geology, Bedford College (Head: Prof. A.J. Smith) for special purchase of a Landrover for use in the field; to the Department of Geology, King's College, for the use of their NERC funded inductively coupled plasma spectrometer, and for the supervision and assistance of Dr J.N. Walsh and his technical staff; to the Department of Earth Sciences, University of Cambridge, for the use of their NERC funded microprobe and for the supervision of Dr P. Treloar; to the Universities of Palermo and Catania for the use of their libraries where I was able to obtain much local literature otherwise difficult to locate in the United Kingdom, and for the assistance and friendship of Drs R. Catalano and M. Romeo in each university respectively; and to Salvatore Bono, his family and friends in Sciacca whose friendship made my visits to Sicily memorable.

Many scientists have given their time to discuss and assist the development of this research. I am indebted to: Dr D.W.G. Bosence (Goldsmiths' College, coralline red algae); Dr R.G. Bromley (Institute of Historic Geology and Palaeontology, Copenhagen, trace fossils); Dr W.C. Burnett (Florida State University, phosphorite and glauconite sedimentology and geochemistry); Dr G. Elliot (British Museum, Natural History, coralline red algae); Mr H.G. Gamble (City of London Polytechnic, Mediterranean Tertiary); Dr S.R.A. Kelley (University of Cambridge, trace fossils); Prof. G.H. Mascle

(University of Paris VI, Sicilian geology); Dr R.T.J. Moody (Kingston Polytechnic, Mediterranean geology); Prof. A.F. Poignant (University of Paris VI, coralline red algae); Dr R. Riding (University College Cardiff, coralline red algae); Dr S.R. Riggs (East Carolina University, phosphorite and glauconite sedimentology); Dr J.D. Smewing (University College Swansea, feldspar geochemistry); and particularly to Dr C.G. Adams (British Museum, Natural History) for much time spent correlating the succession; to Dr R. Catalano (University of Palermo) for lengthy discussions on Sicilian geology in the field; and to Dr H.M. Pedley (Polytechnic of North London) for frequent discussions on the central Mediterranean Tertiary.

My thanks are also expressed to the staff, research students and students of the Bedford College Geology Department who provided an academic environment from which this research has benefited and from which I have enjoyed discussions in all aspects of geology. In particular though, I would like to thank: Dr S.M. Bennett (now with British Petroleum), for discussions on central Mediterranean Tertiary and carbonate sedimentology and diagenesis; Dr G.R. Challis (central Mediterranean geology); Mr J. Elliott (for many hours of lively discussions on Sicilian geology); Dr G.M. Marriner (for guidance in X-ray diffraction analysis); and Dr A.D. Saunders (for much critical comment on the phosphorite and glauconite geochemistry manuscript).

I would also like to thank the technical staff of the Geology Department at Bedford College, particularly Mr Jack Keith who will be missed by all upon his retirement and whose humour and willing helpfulness lightened my research-troubled day. Thanks too, to Mr R.G.C. Jones (technician, Department of Geology, University College, Swansea) who helpfully prepared most of the diagrams and the plates. I am indebted to Mrs Sheila Bishop (Geology Department secretary, Bedford College) for typing this thesis quickly and so well.

Finally, I wish to thank my family and friends for their encouragement and support. In particular, I thank my wife Wendy for making my stay at Bedford College more enjoyable and for enduring the strains imposed during the preparation of this thesis.

C O N T E N T S

| | page |
|---|------|
| Abstract | i |
| Acknowledgements | iii |
| List of Contents | v |
| List of Figures | xi |
| List of Tables | xiv |
| List of Plates | xvi |
| | |
| CHAPTER 1: INTRODUCTION | 1 |
| 1.1 General | 1 |
| 1.2 Regional Setting | 1 |
| 1.3 Structural Setting | 4 |
| 1.4 Stratigraphic Setting | 8 |
| 1.5 Scope of the Thesis | 11 |
| | |
| CHAPTER 2: UPPER OLIGOCENE LIMESTONES | 14 |
| 2.1 Introduction | 14 |
| 2.1.1 General | 14 |
| 2.1.2 Previous Work | 15 |
| 2.1.3 Stratigraphic Nomenclature | 15 |
| 2.1.4 Correlation | 16 |
| 2.2 Base of the Succession | 17 |
| 2.2.1 The Basal Unconformity | 17 |
| 2.2.2 The Basal Conglomerate | 19 |
| 2.3 Stratigraphic Sections | 22 |
| 2.4 Facies | 33 |
| 2.4.1 Introduction | 33 |
| 2.4.2 Rhodolithic algal packstone-wackestone facies | 34 |
| (a) Macrofacies | 34 |
| (b) Microfacies | 34 |
| (c) Diagenesis | 36 |
| 2.4.3 Foraminiferal grainstone-packstone facies | 36 |
| (a) Macrofacies | 36 |
| (b) Microfacies | 37 |
| (c) Diagenesis | 38 |
| 2.4.4 Facies Distribution | 38 |
| 2.4.5 Conclusion | 39 |

| | page |
|--|--------|
| 2.5 Depositional Environment | 40 |
| 2.5.1 Introduction | 40 |
| 2.5.2 Oxidation | 40 |
| 2.5.3 Salinity | 40 |
| 2.5.4 Temperature | 41 |
| 2.5.5 Light Intensity | 43 |
| 2.5.6 Depth | 43 |
| 2.5.7 Water Turbulence | 44 |
| 2.5.8 Summary | 45 |
| 2.6 Palaeogeography of the Saccense Carbonate Platform | 46 |
| 2.6.1 General | 46 |
| 2.6.2 Upper Oligocene | 47 |
| 2.7 Conclusions | 49 |
| CHAPTER 3: LOWER MIOCENE LIMESTONES | 52 |
| 3.1 Introduction | 52 |
| 3.1.1 General | 52 |
| 3.1.2 Previous Work | 53 |
| 3.1.3 Stratigraphic Nomenclature | 53 |
| 3.1.4 Correlation | 54 |
| 3.2 Stratigraphic Sections | 56 |
| 3.3 Facies | 62 |
| 3.3.1 Introduction | 62 |
| 3.3.2 Glauconitic Limestone Facies | 63 |
| (a) Macrofacies | 63 |
| (b) Microfacies | 64 |
| (c) Diagenesis | 65 |
| 3.3.3 Sandy Limestone Facies | 66 |
| (a) Macrofacies | 66 |
| (b) Microfacies | 66 |
| (c) Diagenesis | 68 |
| 3.3.4 Conclusion | 68 |
| 3.4 Depositional Environment | 69 |
| 3.4.1 Glauconitic Limestone Facies | 69 |
| 3.4.2 Sandy Limestone Facies | 70 |
| 3.4.3 Conclusions | 72 |
| 3.5 Regional Setting | 72 |
| 3.6 Conclusions | 77 |

| | page |
|--|------|
| CHAPTER 4: DESCRIPTIVE PALAEOONTOLOGY | 129 |
| 4.1 Coralline Red Algae | 80 |
| 4.1.1 Introduction | 80 |
| 4.1.2 Systematic Palaeontology | 81 |
| 4.1.3 Rhodolithic Growth Form | 91 |
| 4.1.4 Palaeoecology | 94 |
| 4.1.5 Conclusions | 96 |
| 4.2 Trace Fossils | 97 |
| 4.2.1 Introduction | 97 |
| 4.2.2 Systematic Palaeontology | 97 |
| 4.2.3 Palaeoenvironments | 103 |
| 4.2.4 Conclusions | 104 |
| CHAPTER 5: DIAGENESIS | 106 |
| 5.1 Carbonate Diagenesis: Upper Oligocene Limestones | 106 |
| 5.1.1 Introduction | 106 |
| 5.1.2 Cementation | 106 |
| (a) Introduction | 106 |
| (b) First Period | 107 |
| (c) Second Period | 108 |
| (d) Third Period | 109 |
| (e) Fourth Period | 109 |
| (f) Relative Timing | 109 |
| (g) Discussion | 110 |
| 5.1.3 Compaction | 113 |
| (a) Observations | 113 |
| (b) Discussion | 115 |
| 5.1.4 Neomorphism | 117 |
| (a) Introduction | 117 |
| (b) Syntaxial Overgrowths | 117 |
| (c) Discussion | 118 |
| 5.1.5 Syn-cementation pore fillers | 119 |
| (a) Observations | 119 |
| (b) Discussion | 120 |
| 5.1.6 Dolomitisation | 121 |
| 5.1.7 Conclusion | 122 |
| 5.2 Diagenetic Feldspars: Upper Oligocene Limestones | 123 |
| 5.2.1 Introduction | 123 |
| 5.2.2 Microprobe Results | 124 |
| 5.2.3 Discussion | 124 |
| 5.2.4 Conclusion | 128 |

| | page |
|---|------|
| 5.3 Carbonate Diagenesis: Lower Miocene Limestones | 129 |
| 5.3.1 Introduction | 129 |
| 5.3.2 Cementation | 129 |
| (a) Introduction | 129 |
| (b) First Period | 129 |
| (c) Second Period | 130 |
| (d) Discussion | 131 |
| 5.3.3 Compaction | 133 |
| (a) Observations | 133 |
| (b) Discussion | 134 |
| 5.3.4 Conclusions | 135 |
| CHAPTER 6: GLAUCONITE | 137 |
| 6.1 Introduction | 137 |
| 6.2 Occurrence | 137 |
| 6.3 Petrography | 139 |
| 6.4 Geochemistry | 139 |
| 6.4.1 Analysis | 139 |
| 6.4.2 Results | 155 |
| 6.4.3 Discussion | 156 |
| 6.5 Origin of Glauconite | 159 |
| 6.6 Environment of Glauconite Formation | 160 |
| 6.6.1 Salinity and Acidity | 160 |
| 6.6.2 Oxidation | 160 |
| 6.6.3 Temperature | 161 |
| 6.6.4 Water Turbulence | 161 |
| 6.6.5 Water Depth | 162 |
| 6.6.6 Sedimentation Rate | 162 |
| 6.6.7 Summary | 162 |
| 6.7 Conclusions | 163 |
| CHAPTER 7: PHOSPHORITES OF SICILY AND MALTA | 165 |
| 7.1 Introduction | 165 |
| 7.2 Geographic, Stratigraphic and Facies Occurrence | 167 |
| 7.2.1 Southwest Sicily | 167 |
| 7.2.2 Southeast Sicily | 167 |
| 7.2.3 Maltese Islands | 171 |

| | page |
|--|------|
| 7.3 Petrography | 176 |
| 7.3.1 Observations | 176 |
| 7.3.2 Variation with locality | 177 |
| 7.3.3 Discussion | 179 |
| 7.4 Mineralogy | 180 |
| 7.4.1 Analyses | 180 |
| 7.4.2 Results | 181 |
| 7.4.3 Discussion | 185 |
| 7.5 Major Element Geochemistry | 186 |
| 7.5.1 Introduction | 186 |
| 7.5.2 Variation in Abundance of P_2O_5 and SiO_2 | 193 |
| 7.5.3 Variation of Major Elements relative to P_2O_5 | 193 |
| 7.5.4 Variation of Major Elements relative to CaO | 201 |
| 7.5.5 Variation of Fe_2O_3 and Al_2O_3 with Na_2O and K_2O | 207 |
| 7.5.6 Variation of Major Elements with Geographic Area | 207 |
| 7.5.7 Discussion | 207 |
| 7.6 Trace Element Geochemistry | 212 |
| 7.6.1 Introduction | 212 |
| 7.6.2 Variation in Trace Element Absolute Abundances | 212 |
| 7.6.3 Variation of Trace Elements with P_2O_5 | 213 |
| 7.6.4 Variation of Trace Elements with CaO | 213 |
| 7.6.5 Variation of Trace Elements with Geographic Area | 213 |
| 7.6.6 Discussion | 224 |
| 7.7 Yttrium and Rare Earth Element Geochemistry | 226 |
| 7.7.1 Introduction | 226 |
| 7.7.2 Results | 227 |
| 7.7.3 Discussion | 239 |
| 7.8 Phosphorite Palaeogeography, Formation and Environments | 242 |
| 7.8.1 Palaeogeography | 242 |
| 7.8.2 Phosphate Mineral Formation | 243 |
| 7.8.3 Phosphorite Environments | 245 |
| 7.8.4 Central Mediterranean Phosphorites | 246 |
| 7.9 Conclusion | 248 |
| CHAPTER 8: CONCLUSION | 250 |
| 8.1 Stratigraphy | 250 |
| 8.1.1 Upper Oligocene Limestones | 250 |
| 8.1.2 Lower Miocene Limestones | 251 |
| 8.1.3 Palaeogene-Neogene Boundary | 252 |

| LIST OF FIGURES | | page |
|-----------------|--|------|
| 8.2 | Depositional History | 253 |
| 8.2.1 | Upper Oligocene Limestones | 253 |
| 8.2.2 | Lower Miocene Limestones | 255 |
| 8.3 | Diagenetic History | 257 |
| 8.3.1 | Upper Oligocene Limestones | 257 |
| 8.3.2 | Lower Miocene Limestones | 259 |
| 8.4 | Regional Setting | 259 |
| 8.4.1 | General | 259 |
| 8.4.2 | Palaeogeography | 260 |
| 8.4.3 | Facies Distribution and Palaeoenvironments | 263 |
| | REFERENCES | 267 |
| | APPENDIX I: TECHNIQUES | 294 |
| | A1.1 Petrology | 294 |
| | A1.2 Powder Sample Preparation | 295 |
| | A1.3 X-ray Diffraction Analysis | 296 |
| | A1.4 Inductively Coupled Plasma Spectrometry | 296 |
| | (a) Major and Trace Elements | 296 |
| | (b) Rare Earth Elements | 297 |
| | APPENDIX II: ADDITIONAL TABLES | 299 |
| | Table A2.1 Index to samples used in phosphorite study | 300 |
| | Table A2.2 XRD analyses of twenty phosphorite samples | 303 |
| | Table A2.3 Yttrium and REE abundances used in normalisation procedures | 309 |
| | Table A2.4 Published compositions for four standard rocks | 310 |
| | Table A2.5 Trace element concentrations of ten standard rocks | 311 |
| | Table A2.6 Phosphorite localities mentioned in the text | 312 |
| | Table A2.7 W_2O_5 v. $Ca_3(PO_4)_2$ | 313 |
| | Table A2.8 AP_2O_7 v. $Ca_3(PO_4)_2$ | 314 |
| | Table A2.9 AP_2O_7 v. $Ca_3(PO_4)_2$ | 315 |
| | Table A2.10 AP_2O_7 v. $Ca_3(PO_4)_2$ | 316 |

LIST OF FIGURES

| | page | |
|------|--|-----------------------------|
| 1.1 | Location of the study area in southwest Sicily | 2 |
| 1.2 | Location of Sicily in the Mediterranean sea | 3 |
| 1.3 | The tectonic units of Sicily (from Catalano & D'Argenio, 1978) | 6 |
| 1.4 | The palaeogeography of western Sicily (from Catalano & D'Argenio, 1978) | 10 |
| 1.5 | Outcrop and Locality map: Upper Oligocene and Lower Miocene limestones (adapted from Mascle, 1979) | enclosure back pocket |
| 2.1 | Nadorello east locality map | 24 |
| 2.2 | Nadorello east measured stratigraphic section | 26 |
| 2.3 | Carboj Dam measured stratigraphic section | 27 |
| 2.4 | La Conca measured stratigraphic section | 28 |
| 2.5 | Contrada Giovanni measured stratigraphic section | 29 |
| 2.6 | San Biagio west measured stratigraphic section | 30 |
| 2.7 | San Biagio east measured stratigraphic section | 31 |
| 2.8 | Tombe Sicani measured stratigraphic section | 32 |
| 2.9 | Upper Oligocene facies distribution explained by A & B fault control | 48 |
| 2.10 | Upper Oligocene palaeogeography of the Saccense Carbonate Platform | 50 |
| 3.1 | Serra Lunga measured stratigraphic section | 58 |
| 3.2 | Costa del Conte measured stratigraphic section | 59 |
| 3.3 | Battellaro measured stratigraphic section | 60 |
| 3.4 | Mt Cardellia measured stratigraphic section | 61 |
| 3.5 | Lower Miocene facies distribution. A: East-West section. B: North-South section | 75 76 |
| 5.1 | Feldspar geochemistry. Plot of K: Na: Ca ratio | 126 |
| 7.1 | Southeast Sicily locality map. Phosphorite localities mentioned in the text | 168 |
| 7.2 | Maltese islands locality map. Phosphorite localities mentioned in the text | 172 |
| 7.3 | %P ₂ O ₅ v %SiO ₂ | 196 |
| 7.4 | %P ₂ O ₅ v %Fe ₂ O ₃ | 196 |
| 7.5 | %P ₂ O ₅ v %Al ₂ O ₃ | 197 |
| 7.6 | %P ₂ O ₅ v %MgO | 197 |

| | page |
|---|------|
| 7.7 %P ₂ O ₅ v %Na ₂ O | 198 |
| 7.8 %P ₂ O ₅ v %K ₂ O | 198 |
| 7.9 %P ₂ O ₅ v %TiO ₂ | 199 |
| 7.10 %P ₂ O ₅ v %F | 199 |
| 7.11 Bivariate plot showing P ₂ O ₅ against element (oxide) X | 200 |
| 7.12 %CaO v %P ₂ O ₅ | 203 |
| 7.13 %CaO v %SiO ₂ | 203 |
| 7.14 %CaO v %Fe ₂ O ₃ | 204 |
| 7.15 %CaO v %Al ₂ O ₃ | 204 |
| 7.16 %CaO v %MgO | 205 |
| 7.17 %CaO v %Na ₂ O | 205 |
| 7.18 %CaO v %K ₂ O | 206 |
| 7.19 %CaO v %TiO ₂ | 206 |
| 7.20 %Al ₂ O ₃ v %K ₂ O | 209 |
| 7.21 %Fe ₂ O ₃ v %K ₂ O | 209 |
| 7.22 %Al ₂ O ₃ v %Na ₂ O | 210 |
| 7.23 %Fe ₂ O ₃ v %Na ₂ O | 210 |
| 7.24 %P ₂ O ₅ v ppmSc | 215 |
| 7.25 %P ₂ O ₅ v ppmV | 215 |
| 7.26 %P ₂ O ₅ v ppmNi | 216 |
| 7.27 %P ₂ O ₅ v ppmCu | 216 |
| 7.28 %P ₂ O ₅ v ppmSr | 217 |
| 7.29 %P ₂ O ₅ v ppmZr | 217 |
| 7.30 %P ₂ O ₅ v ppmBa | 218 |
| 7.31 %CaO v ppmSc | 220 |
| 7.32 %CaO v ppmV | 220 |
| 7.33 %CaO v ppmNi | 221 |
| 7.34 %CaO v ppmCu | 221 |
| 7.35 %CaO v ppmSr | 222 |
| 7.36 %CaO v ppmZr | 222 |
| 7.37 %CaO v ppmBa | 223 |
| 7.38 Chondrite normalised concentrations of Y and REE for A & B phosphatic clasts from southwest Sicily | 232 |
| 7.39 Chondrite normalised concentrations of Y and REE for phosphatic clasts from (A) southeast Sicily and (B) Maltese islands | 233 |

| | page |
|---|------|
| 7.40 Chondrite normalised concentrations of Y and REE for (A) mean southwest Sicily phosphorite and (B) mean Maltese islands phosphorite and mean southeast Sicily phosphorite | 234 |
| 7.41 Chondrite normalised concentrations of Y and REE for (A) Florida phosphorite standard 120B and (B) south- west Sicily limestones | 235 |
| 7.42A Concentrations of Y and REE normalised by the mean Maltese islands phosphorite for Sicilian phosphorites and a limestone | 237 |
| 7.42B Concentrations of Y and REE normalised by limestone RTB18 for Sicilian and Maltese islands phosphorites | 237 |
| 7.43 Concentrations of Y and REE normalised by Herrmann's (1970) average sediment for (A) Sicilian and Maltese islands phosphorites and (B) Sicilian limestones | 238 |
| 8.1 The palaeogeography of the central Mediterranean area in Upper Oligocene - Lower Miocene times | 261 |

LIST OF TABLES

| | page |
|------|--|
| 5.1 | Feldspar geochemistry. Microprobe analyses of twelve feldspar grains 125 |
| 6.1 | Battellaro, Lower Miocene glauconite pellets: microprobe geochemistry 141 |
| 6.2 | Costa del Conte, Lower Miocene glauconite pellets: microprobe geochemistry 142 |
| 6.3 | Serra Lunga, Lower Miocene glauconite pellets: microprobe geochemistry 143 |
| 6.4 | Cardellia, Lower Miocene glauconite pellets: microprobe geochemistry 144 |
| 6.5A | Lower Miocene glauconitised pellets (Early Stage): microprobe geochemistry 148 |
| 6.5B | Lower Miocene glauconitised pellets (Late Stage): microprobe geochemistry 149 |
| 6.6 | Lower Miocene glauconitised foraminiferid chamber infills: microprobe geochemistry 150 |
| 6.7 | Western Nadorello, Upper Oligocene glauconitised foraminiferid chamber infills: microprobe geochemistry 151 |
| 6.8 | Western Nadorello, Upper Oligocene mineralised echinoid grain: microprobe geochemistry 153 |
| 6.9 | Costa del Conte, Lower Miocene unmineralised echinoid grain and its cement overgrowth: microprobe geochemistry 154 |
| 7.1 | XRD analysis. Mean values of d-spacings and peak intensity for phosphorite samples from SW Sicily, SE Sicily and the Maltese islands 182 |
| 7.2 | XRD data. Values of d-spacing and peak intensity for a synthetic fluorapatite standard (Berry, 1974) and a French Cretaceous carbonate-fluorapatite (Jarvis, 1980) 183 |
| 7.3 | Southwest Sicily phosphorite: major and trace element geochemistry 187 |
| 7.4 | Southwest Sicily phosphorite: major and trace element geochemistry 188 |
| 7.5 | Southeast Sicily phosphorites: major and trace element geochemistry 189 |
| 7.6 | Maltese phosphorites: major and trace element geochemistry 190 |

LIST OF PLATES

| | page |
|--|------|
| 7.7 Maltese phosphorites: major and trace element geochemistry | 191 |
| 7.8 Southwest Sicily limestones: major and trace element geochemistry | 192 |
| 7.9 Southwest Sicily phosphorite: Yttrium and REE geochemistry | 228 |
| 7.10 Southeast Sicily and Maltese phosphorites: Yttrium and REE geochemistry | 229 |
| 7.11 Standards and limestones: Yttrium and REE geochemistry | 230 |

| | |
|--|--|
| 2.4 Corral area, close view of the Eocene - Upper Oligocene unconformity | |
| 2.7 San Diego west measured stratigraphic section | |
| 2.8 San Diego west, close view of the lower reticulate - upper Oligocene unconformity | |
| 2.9 San Diego west, close view of the upper Oligocene basal conglomerate | |
| 2.10 Corral Dam measured stratigraphic section | |
| 2.11 La Conca measured stratigraphic section | |
| 2.12 Contrada Giovanni measured stratigraphic section | |
| 2.13 San Diego west measured stratigraphic section | |
| 2.14 Torre Sicani measured stratigraphic section | |
| 2.15 Madonella east, topographic (topographic) view of the | |
| UPPER OLIGOCENE LIMESTONES: INTERFACES OF THE ANHOLTRIC AND EOCENE-WACHTING FACIES | |
| 2.18 Madonella east, compacted silty foraminiferal packstone, scale 41 x | |
| 2.19 Madonella east, poorly sorted foraminiferal packstone, cement periods 3 and 4. Scale 41 x | |
| 2.20 Madonella east, foraminiferal packstone: umbrella structure, cement periods 3 and 4. Scale 41 x | |
| 2.21 Madonella east, muddy foraminiferal packstone. Scale 105 x | |
| 2.22 Madonella east, foraminiferal packstone: umbrella structure, cement periods 3 and 4. Scale 41 x | |
| 2.23 Madonella east, foraminiferal packstone: umbrella structure, cement periods 3 and 4. Scale 41 x | |
| 2.24 Madonella east, compacted foraminiferal packstone. Scale 41 x | |

LIST OF PLATES

UPPER OLIGOCENE LIMESTONES: FIELD VIEWS

- 2.1 Structure at western Nadorello
- 2.2 Structure near Caltabellotta
- 2.3 Nadorello east measured stratigraphic section
- 2.4 Nadorello east, distal view of the Upper Cretaceous - Upper Oligocene unconformity
- 2.5 Nadorello east, close view of the Upper Cretaceous - Upper Oligocene unconformity
- 2.6 Carboj area, close view of the Eocene - Upper Oligocene unconformity
- 2.7 San Biagio west measured stratigraphic section
- 2.8 San Biagio west, close view of the Upper Cretaceous - Upper Oligocene unconformity
- 2.9 San Biagio west, close view of the Upper Oligocene basal conglomerate
- 2.10 Carboj Dam measured stratigraphic section
- 2.11 La Conca measured stratigraphic section
- 2.12 Contrada Giovanni measured stratigraphic section
- 2.13 San Biagio east measured stratigraphic section
- 2.14 Tombe Sicani measured stratigraphic section
- 2.15 Nadorello east, *Lepidocyclina* (*Eulepidina*) rich horizon

UPPER OLIGOCENE LIMESTONES: MICROFACIES OF THE RHODOLITHIC ALGAL PACKSTONE-WACKESTONE FACIES

- 2.16 Nadorello east, compacted algal foraminiferal packstone. Scale 41 x
- 2.17 Nadorello east, poorly sorted foraminiferal packstone: cement periods 3 and 4. Scale 41 x
- 2.18 Nadorello east, foraminiferal packstone: umbrella structure, cement periods 3 and 4. Scale 41 x
- 2.19 Nadorello east, muddy foraminiferal packstone. Scale 105 x
- 2.20 Nadorello east, foraminiferal packstone: umbrella structure, cement periods 3 and 4. Scale 41 x
- 2.21 Nadorello east, foraminiferal packstone: umbrella structure, cement periods 3 and 4. Scale 41 x
- 2.22 Nadorello east, foraminiferal grainstone: cement periods 3 and 4. Scale 41 x
- 2.23 Nadorello east, compacted foraminiferal packstone. Scale 41 x

2.24 Nadorello east, foraminiferal packstone: cement periods 3 and 4. Scale 41 x

2.25 Nadorello east, foraminiferal packstone: cement periods 3 and 4. Scale 41 x

UPPER OLIGOCENE LIMESTONES: MICROFACIES OF THE FORAMINIFERAL GRAINSTONE-PACKSTONE FACIES

2.26 La Conca, compacted foraminiferal grainstone: algae occupy "interstitial" positions. Scale 41 x

2.27 Carboj Dam, compacted foraminiferal grainstone: bryozoans and echinoids act as preferential sites for period 2 cement. Scale 41 x

2.28 Contrada Giovanni, poorly sorted compacted foraminiferal packstone: echinoid, period 2, cements. Scale 41 x

2.29 Contrada Giovanni, poorly sorted foraminiferal packstone: echinoid, period 2, cements; fracturing of *Heterostegina/Operculina*. Scale 41 x

2.30 San Biagio east, foraminiferal grainstone with common algal debris. Scale 41 x

2.31 Carboj Dam, sorted foraminiferal grainstone from a cross-bedded unit. Scale 41 x

2.32 La Conca, foraminiferal grainstone: abundant *Nephrolepidina*, pressure welded texture. Scale 41 x

2.33 Carboj Dam, foraminiferal grainstone: abundant *Nephrolepidina*. Scale 41 x

2.34 Carboj Dam, bioclastic grainstone: echinoid period 1 and 2 cements. Scale 41 x

LOWER MIOCENE LIMESTONES: FIELD VIEWS

3.1 Serra Lunga measured stratigraphic section

3.2 Costa del Conte measured stratigraphic section

3.3 Battellaro measured stratigraphic section

3.4 Battellaro, close view of the sandy limestones at the top of the Lower Miocene succession

3.5 Mt Cardellia measured stratigraphic section

LOWER MIOCENE LIMESTONES: MICROFACIES OF THE GLAUCONITIC LIMESTONE FACIES

3.6 Costa del Conte, compacted foraminiferal grainstone: abundant *Miogypsina*, glauconite in foraminifera. Scale 41 x

3.7 Costa del Conte, compacted foraminiferal grainstone: glauconite in foraminifera. Scale 41 x

- 3.8 Costa del Conte, foraminiferal grainstone: glauconite in foraminifera. Scale 41 x
- 3.9 Costa del Conte, compacted bioclastic grainstone: glauconite in foraminifera and echinoid grains. Scale 41 x
- 3.10 Battellaro, peel photomicrograph, foraminiferal grainstone: glauconite in foraminifera. Scale 105 x
- 3.11 Battellaro, peel photomicrograph, foraminiferal grainstone: glauconite in foraminifera. Scale 105 x
- 3.12 Battellaro, peel photomicrograph, foraminiferal grainstone: glauconite in foraminifera. Scale 105 x
- 3.13 Battellaro, bioclastic grainstone: common quartz grains and glauconite pellets. Scale 105 x
- 3.14 Cardellia, peel photomicrograph, bioclastic grainstone: glauconite in foraminifera. Scale 41 x
- 3.15 Cardellia, bioclastic grainstone. Scale 105 x
- 3.16 Cardellia, glauconite rich bioclastic grainstone. Scale 105 x
- 3.17 Cardellia, bioclastic grainstone. Scale 105 x
- 3.18 Cardellia, bioclastic grainstone. Scale 105 x
- 3.19 Cardellia, bioclastic grainstone. Scale 105 x

LOWER MIOCENE LIMESTONES: MICROFACIES OF THE SANDY LIMESTONE FACIES

- 3.20 Costa del Conte, sandy limestone. Scale 41 x
- 3.21 Costa del Conte, sandy limestone. Scale 105 x
- 3.22 Battellaro, sandy limestone. Scale 105 x
- 3.23 Battellaro, calcareous sandstone. Scale 41 x
- 3.24 Battellaro, sandy limestone with a calcareous sandstone horizon. Scale 41 x
- 3.25 Serra Lunga, coarse sandy limestone. Scale 105 x
- 3.26 Serra Lunga, coarse sandy limestone. Scale 105 x
- 3.27 Serra Lunga, coarse sandy limestone. Scale 105 x
- 3.28 Cardellia, bioclastic grainstone. Scale 105 x
- 3.29 Cardellia, bioclastic grainstone. Scale 105 x
- 3.30 Cardellia, bioclastic grainstone. Scale 105 x

PALAEONTOLOGY: CORALLINE RED ALGAE
(All photomicrographs are from Nadorello east samples)

- 4.1 *Archaeolithothamnium saipanense*. Scale 41 x
- 4.2 *A. saipanense*. Scale 41 x
- 4.3 *A. saipanense*. Scale 105 x

- 4.4 *A. saipanense*. Scale 105 x
- 4.5 *A. saipanense*. Scale 410 x
- 4.6 *A. saipanense*. Scale 410 x
- 4.7 *Lithothamnium aggregatum*. Scale 105 x
- 4.8 *L. aggregatum*. Scale 105 x
- 4.9 *L. aggregatum*. Scale 410 x
- 4.10 *L. aggregatum*. Scale 41 x
- 4.11 *Lithothamnium cf. marianae*. Scale 41 x
- 4.12 *L. cf. marianae*. Scale 41 x
- 4.13 *L. cf. marianae*. Scale 105 x
- 4.14 *L. cf. marianae*. Scale 410 x
- 4.15 *Lithophyllum ovatum*. Scale 105 x
- 4.16 *L. ovatum*. Scale 410 x
- 4.17 *Lithophyllum personatum*. Scale 41 x
- 4.18 *L. personatum*. Scale 105 x
- 4.19 *L. personatum*. Scale 410 x
- 4.20 *L. personatum*. Scale 410 x
- 4.21 *L. personatum*. Scale 105 x
- 4.22 *Mesophyllum cf. vaughanii*. Scale 41 x
- 4.23 *M. cf. vaughanii*. Scale 41 x
- 4.24 *M. cf. vaughanii*. Scale 105 x
- 4.25 *M. cf. vaughanii*. Scale 105 x
- 4.26 *M. cf. vaughanii*. Scale 410 x
- 4.27 *Lithoporella cf. melobesioides*. Scale 105 x
- 4.28 *L. cf. melobesioides* and *Melobesia cf. cuboides*.
Scale 410 x
- 4.29 *L. cf. melobesioides* and *M. cf. cuboides*. Scale 105 x
- 4.30 *M. cf. cuboides*. Scale 105 x
- 4.31 *M. cf. cuboides*. Scale 410 x
- 4.32 *M. cf. cuboides*. Scale 105 x
- 4.33 Nadorella east, rhodolith compact branching growth form
- 4.34 Nadorello east, rhodolith compact branching growth form
- 4.35 Nadorello east, rhodolith compact-laminar growth form
- 4.36 Nadorello east, rhodolith laminar growth form
- 4.37 Nadorello east, rhodolith open branching growth form
- 4.38 Nadorello east, rhodolith open branching growth form
- 4.39 Contrada Giovanni, rhodolith compact non-branching
growth form

- 4.40 Contrada Giovanni rhodolith compact non-branching growth form

PALAEONTOLOGY: TRACE FOSSILS

- 4.41 Nadorello east, *Thalassinoides paradoxica*, Upper Cretaceous - Upper Oligocene unconformity, Upper Oligocene phosphatic conglomerate
- 4.42 Donnalucata, SE Sicily, *T. paradoxica* and *Trypanites* sp. in a Lower Miocene phosphatised hardground
- 4.43 Donnalucata, SE Sicily, *T. paradoxica*
- 4.44 Donnalucata, SE Sicily, *Thalassinoides suevicus*
- 4.45 Donnalucata, SE Sicily, *T. suevicus*
- 4.46 Donnalucata, SE Sicily, *T. suevicus*
- 4.47 Ragusa, SE Sicily, *T. suevicus*
- 4.48 Ragusa, SE Sicily, *Trypanites weisei* in phosphorite pebbles
- 4.49 Nadorello east, *Trypanites* sp.

DIAGENESIS: UPPER OLIGOCENE LIMESTONES

- 5.1 Carboj Dam, cement periods 1 and 2, compaction post-dates period 2 cement. Scale 105 x
- 5.2 Carboj Dam, cement periods 1 and 2, compaction post-dates period 2 cement. Scale 105 x
- 5.3 Nadorello east, cement periods 1 to 4. Scale 105 x
- 5.4 Nadorello east, cement periods 1 to 4. Scale 41 x
- 5.5 Carboj Dam, cement period 2, scalenohedral to bladed habit. Scale 410 x
- 5.6 Western Nadorello, stained peel colour photomicrograph showing seven zones of alternating non-ferroan and ferroan calcite. Scale 410 x
- 5.7 Nadorello east, cement periods 2 to 4. Scale 41 x
- 5.8 Nadorello east, cement periods 3 and 4. Scale 105 x
- 5.9 Nadorello east, cement periods 3 and 4. Scale 410 x
- 5.10 San Biagio, cement periods 3 and 4. Scale 41 x
- 5.11 Contrada Giovanni, echinoid period 2 cements predate compaction. Scale 41 x
- 5.12 La Conca echinoid period 2 cement predates compaction. Scale 41 x
- 5.13 Nadorello east, compaction of a foraminiferal packstone. Scale 41 x
- 5.14 Carboj Dam, compaction: areal pressure solution contacts and fracturing of grains. Scale 105 x

- 5.15 Carboj Dam, compaction: grain rotation, areal pressure solution contacts, excessive algal pressure solution. Scale 105 x
- 5.16 Tombe Sicani, compaction: fracturing of foraminifera. Scale 105 x
- 5.17 Carboj Dam, compaction: fracturing and pressure solution of foraminifera. Scale 105 x
- 5.18 San Biagio east, compaction: parallel alignment of foraminifera and ductile deformation. Scale 41 x
- 5.19 Contrada Giovanni, compaction: pressure solution of foraminifera against a rock fragment. Scale 41 x
- 5.20 Nadorello east, neomorphism: microspar, pseudospar and echinoid overgrowths. Scale 41 x
- 5.21 Nadorello east, neomorphism: microspar and echinoid overgrowths. Scale 41 x
- 5.22 Tombe Sicani, neomorphism: overgrowths on echinoid grains and foraminifera. Scale 41 x
- 5.23 Tombe Sicani, neomorphism: echinoid overgrowths. Scale 41 x
- 5.24 Nadorello east, syndiagenetic pore filling sediments. Scale 41 x
- 5.25 Nadorello east, syndiagenetic pore filling sediments. Scale 41 x
- 5.26 Nadorello east, syndiagenetic pore filling sediments. Scale 105 x
- 5.27 San Biagio west, syndiagenetic pore filling sediments. Scale 41 x
- 5.28 San Biagio west, syndiagenetic pore filling sediments. Scale 105 x
- 5.29 San Biagio east, dolomitisation. Scale 105 x
- 5.30 Western Nadorello, early diagenetic feldspars. Scale 105 x
- 5.31 Western Nadorello, early diagenetic feldspars. Scale 105 x

DIAGENESIS: LOWER MIOCENE LIMESTONES

- 5.32 Costa del Conte, echinoid cements predate compaction. Scale 41 x
- 5.33 Costa del Conte, cement periods 1 and 2. Scale 105 x
- 5.34 Battellaro, cement periods 1 and 2. Scale 105 x
- 5.35 Mt Cardellia, cement periods 1 and 2. Scale 105 x
- 5.36 Mt Cardellia, cement periods 1 and 2. Scale 105 x
- 5.37 Battellaro, cement periods 1 and 2. Scale 105 x
- 5.38 Costa del Conte, cement periods 1 and 2. Scale 105 x

- 5.39 Costa del Conte, cement periods 1 and 2. Scale 105 x
- 5.40 Battellaro, subpoikilotopic cements of second period generation. Scale 105 x
- 5.41 Battellaro, poikilotopic and subpoikilotopic cements of second period generation. Scale 105 x
- 5.42 Costa del Conte, stained peel colour photomicrograph showing ferroan and non ferroan calcite cements of periods 1 and 2. Scale 105 x
- 5.43 Battellaro, compaction: pressure solution relationships between grains. Scale 105 x
- 5.44 Battellaro, compaction: pressure solution relationships between grains and distortion of the quartz grain lattice. Scale 105 x
- 5.45 Battellaro, compaction: pressure solution relationships between grains. Scale 105 x
- 5.46 Serra Lunga, compaction: fractured quartz grain with fractures filled by period 2 cement. Scale 105 x
- 5.47 Serra Lunga, compaction: fractured quartz grain with fractures filled by period 2 cement. Scale 105 x

GLAUCONITE

- 6.1 Western Nadorello Upper Oligocene, colour photomicrograph of glauconite infilling foraminiferid chambers. Scale 105 x
- 6.2 Western Nadorello Upper Oligocene, colour photomicrograph of glauconite infilling foraminiferid chambers and echinoid grain pores. Scale 105 x

PHOSPHORITES: FIELD VIEWS

- 7.1 Donnalucata, SE Sicily, phosphatised hardground
- 7.2 Ragusa, SE Sicily, general view of the Lower Miocene succession at Contrada le Serre
- 7.3 Ragusa, SE Sicily, phosphorite conglomerates at Contrada le Serre
- 7.4 Maltese islands, Lower Miocene phosphatised hardground and overlying phosphorite conglomerate at the top of the Lower Globigerina Limestone
- 7.5 Maltese islands, Lower Miocene phosphatised hardground and overlying phosphorite conglomerate at the top of the Lower Globigerina Limestone
- 7.6 Maltese islands, Lower Miocene phosphorite conglomerate at the top of the Lower Globigerina Limestone
- 7.7 Maltese islands, Lower Miocene phosphorite conglomerate at the top of the Middle Globigerina Limestone
- 7.8 Maltese islands, Lower Miocene phosphorite conglomerate at the top of the Middle Globigerina Limestone

- 7.9 Maltese islands, Lower Miocene phosphorite conglomerate at the top of the Middle Globigerina Limestone

PHOSPHORITES: MICROFACIES

- 7.10 Nadorello east, dark and opaque and light coloured francolite. Scale 41 x
- 7.11 Nadorello east, dark and opaque and light coloured francolite. Scale 410 x
- 7.12 Donnalucata, SE Sicily, dark and opaque and light coloured francolite. Scale 41 x
- 7.13 Donnalucata, SE Sicily, dark and opaque pellets of francolite. Scale 105 x
- 7.14 Donnalucata, SE Sicily, colour photomicrograph of light coloured francolite. Scale 105 x
- 7.15 Donnalucata, SE Sicily, light coloured francolite: texture with calcite crystals. Scale 105 x
- 7.16 Donnalucata, SE Sicily, light coloured francolite: texture with calcite crystals. Scale 105 x
- 7.17 Maltese islands, francolite coatings on phosphorite clasts. Scale 41 x
- 7.18 Maltese islands, stages of francolite coating on the hard-ground surface at the top of the Lower Globigerina Limestone. Scale 41 x

CHAPTER 1

INTRODUCTION

1.1 General

Rocks described in this thesis comprise some 50 km² of Upper Oligocene - Lower Miocene limestones outcropping in an area 25 km square in the western Sicani mountains situated to the north of Sciacca in southwest Sicily (Fig. 1.1). The island of Sicily is itself of geological interest because of its central Mediterranean position (Fig. 1.2), between the continental areas of Europe and Africa and between the eastern and western Mediterranean hydrographic basins. The western Sicani mountains form one of two areas of Sicily relatively undeformed by Alpine tectonics, preserving a distinctive suite of mid-Tertiary shallow water carbonates. These carbonates span the Palaeogene-Neogene boundary in age, and immediately pre-date the faunal isolation of the Mediterranean brought about by closure of its eastern and western ends towards the end of the Lower Miocene. The area is therefore of more than local interest.

This study is designed to extend and complement recent palaeo-environmental studies by other Bedford College students (Bennett, 1980; Challis, 1980) on similar mid-Tertiary carbonates of the adjacent Maltese islands, and to contribute to the objectives of the UNESCO/IUGS International Geological Correlation Programme (IGCP) Project 25 (Stratigraphic Correlation of the Tethys-Paratethys Neogene), IGCP Project 156 (Phosphorites), the IUGS/ICS "Working Party on the Paleogene-Neogene Boundary", and the IUGS Regional Committee on the Mediterranean Neogene Stratigraphy's "Working Group on Marine Neogene Macrofaunal Palaeoenvironments and Biostratigraphy".

1.2 Regional Setting

Sicily is an island of some 26000 km² measuring 270 km east-west and 180 km (maximum) north-south. It is situated in the central

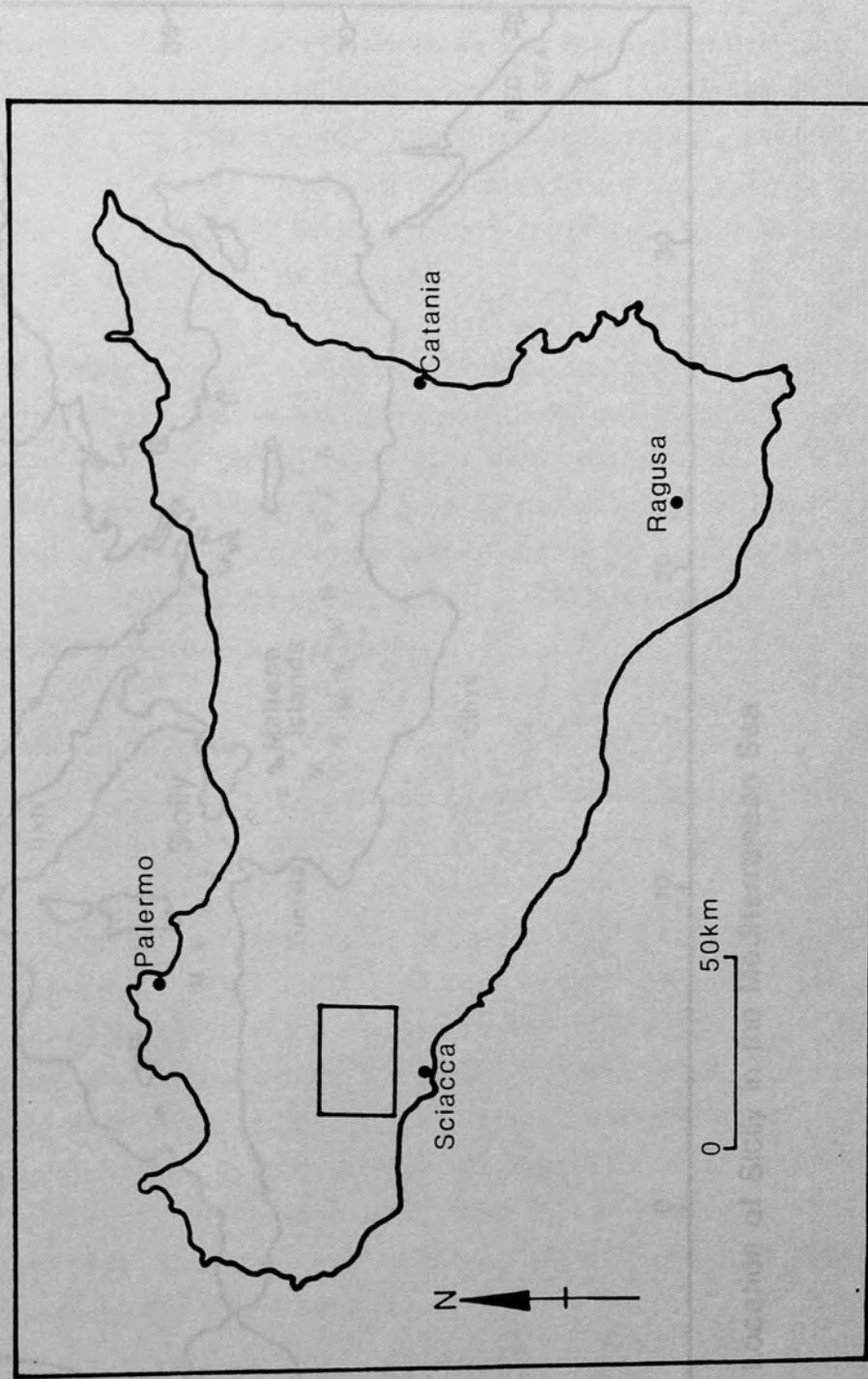


Figure 1.1 Location of the study area in southwest Sicily

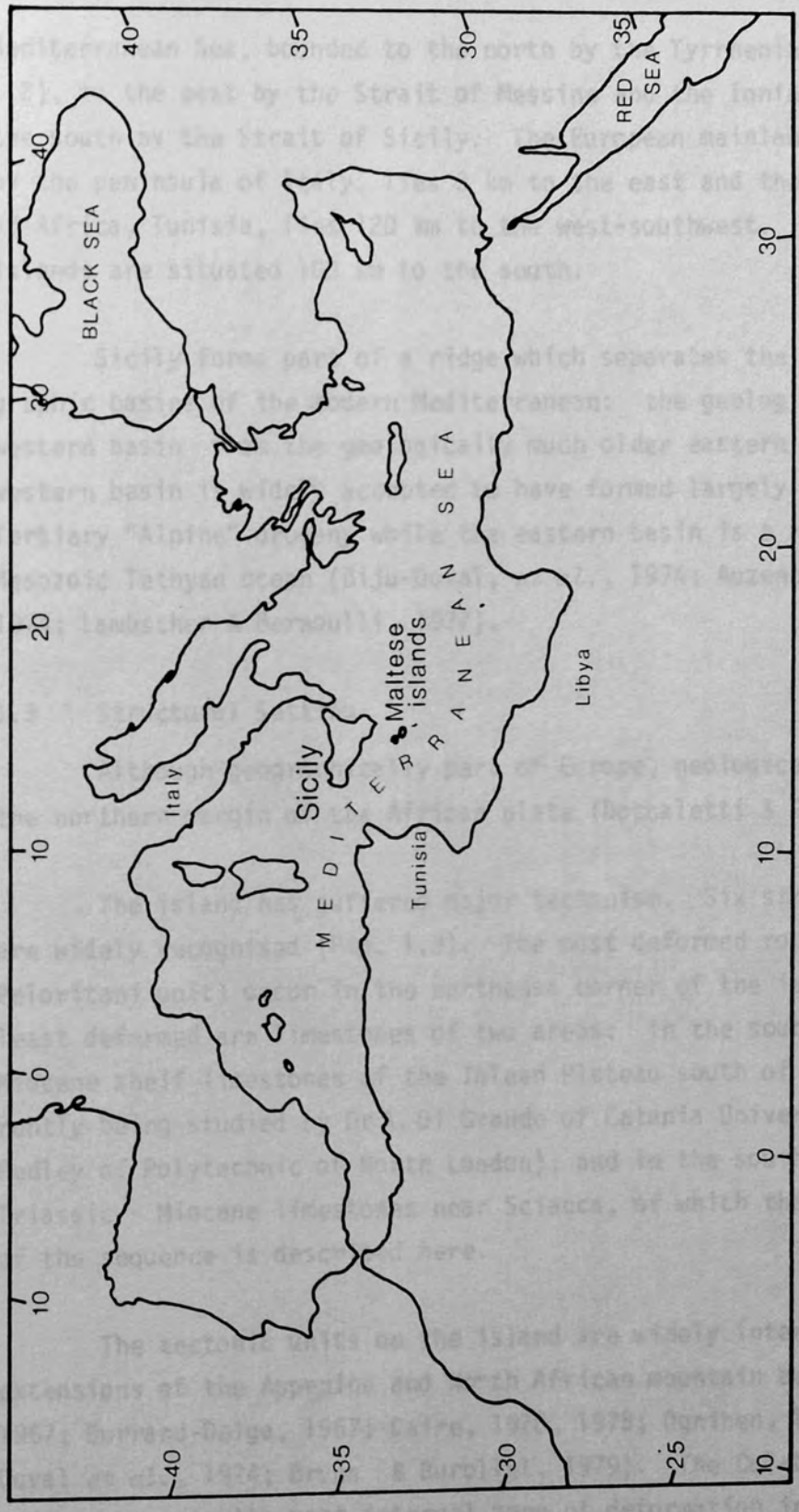


Figure 1.2 Location of Sicily in the Mediterranean Sea

Mediterranean Sea, bounded to the north by the Tyrrhenian Sea (Fig. 1.2), to the east by the Strait of Messina and the Ionian Sea and to the south by the Strait of Sicily. The European mainland, represented by the peninsula of Italy, lies 3 km to the east and the nearest point of Africa, Tunisia, lies 120 km to the west-southwest. The Maltese islands are situated 100 km to the south.

Sicily forms part of a ridge which separates the two main hydrographic basins of the modern Mediterranean: the geologically recent western basin from the geologically much older eastern basin. The western basin is widely accepted to have formed largely during the mid-Tertiary "Alpine" orogeny while the eastern basin is a relict of the Mesozoic Tethyan ocean (Biju-Duval, *et al.*, 1974; Auzende & Olivet, 1974; Lamscher & Bernoulli, 1977).

1.3 Structural Setting

Although geographically part of Europe, geologically Sicily marks the northern margin of the African plate (Boccaletti & Guazzone, 1975).

The island has suffered major tectonism. Six structural units are widely recognised (Fig. 1.3). The most deformed rocks (Calabrian-Peloritani unit) occur in the northeast corner of the island. Those least deformed are limestones of two areas: in the southeast, Eocene - Miocene shelf limestones of the Iblean Plateau south of Catania (currently being studied by Dr A. Di Grande of Catania University and Dr H.M. Pedley of Polytechnic of North London); and in the southwest, the Triassic - Miocene limestones near Sciacca, of which the uppermost part of the sequence is described here.

The tectonic units on the island are widely interpreted as lateral extensions of the Apennine and North African mountain belts (Buroillet, 1967; Durrand-Delga, 1967; Caire, 1970, 1975; Ogniben, 1971, 1973; Biju-Duval *et al.*, 1974; Brunn & Buroillet, 1979). The Calabrian-Peloritani unit represents the most internal zone of deformation in the "Alpine" orogeny, comparable with the Betic of Spain. The undeformed areas of the

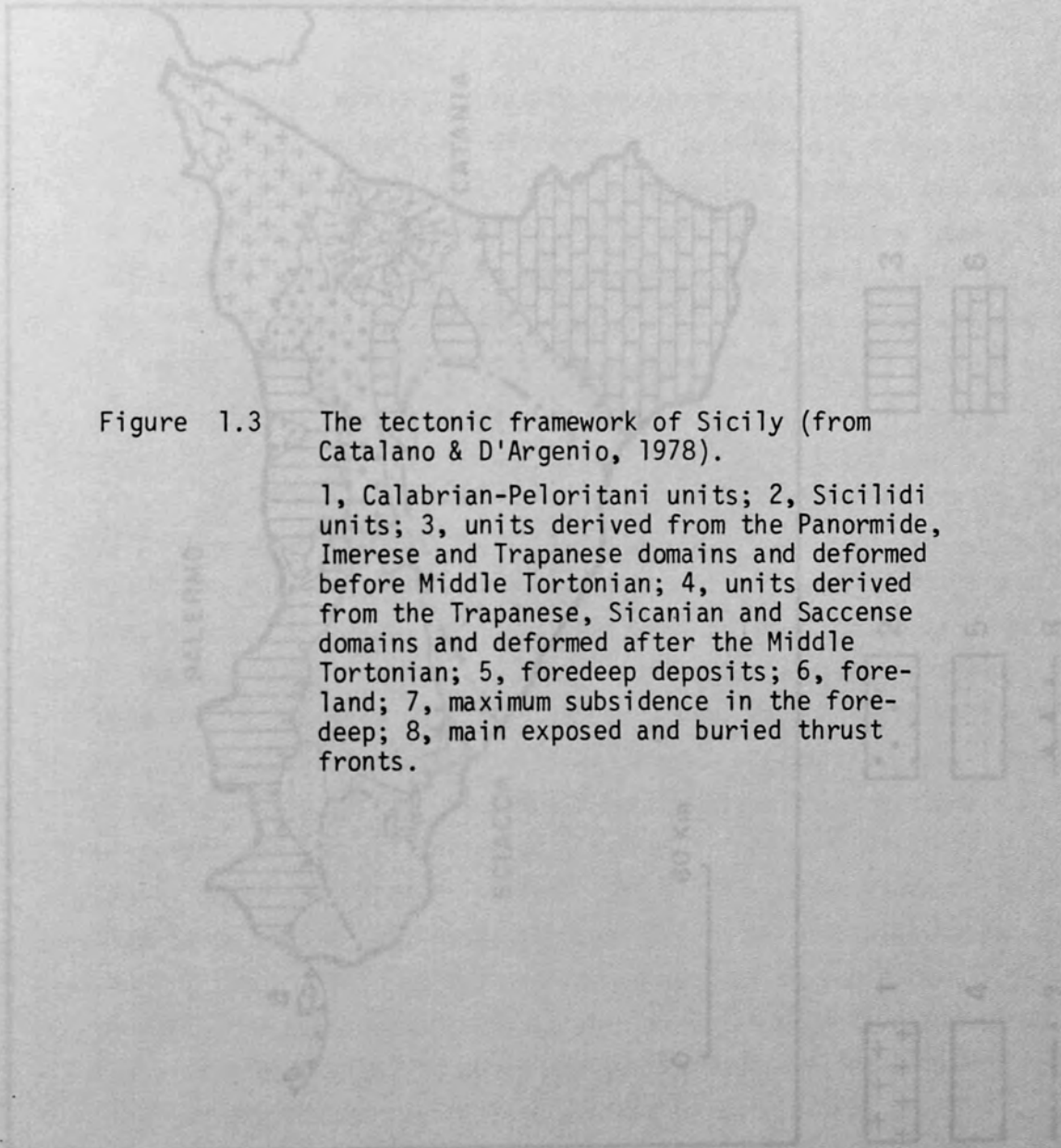


Figure 1.3 The tectonic framework of Sicily (from Catalano & D'Argenio, 1978).

1, Calabrian-Peloritani units; 2, Sicilidi units; 3, units derived from the Panormide, Imerese and Trapanese domains and deformed before Middle Tortonian; 4, units derived from the Trapanese, Sicanian and Saccense domains and deformed after the Middle Tortonian; 5, foredeep deposits; 6, foreland; 7, maximum subsidence in the foredeep; 8, main exposed and buried thrust fronts.

Figure 1.3

Palermo Plateau and of Sciacca are foreland regions, representing the most external zone, comparable with the Pre-Betic of Spain. The widely developed structural units between are comparable with the intermediate Sub-Betic, or to the Tell Atlas of North Africa, the Apennines of Italy, or the Dinarides of Eastern Europe (Burrand-Deijs, 1967;

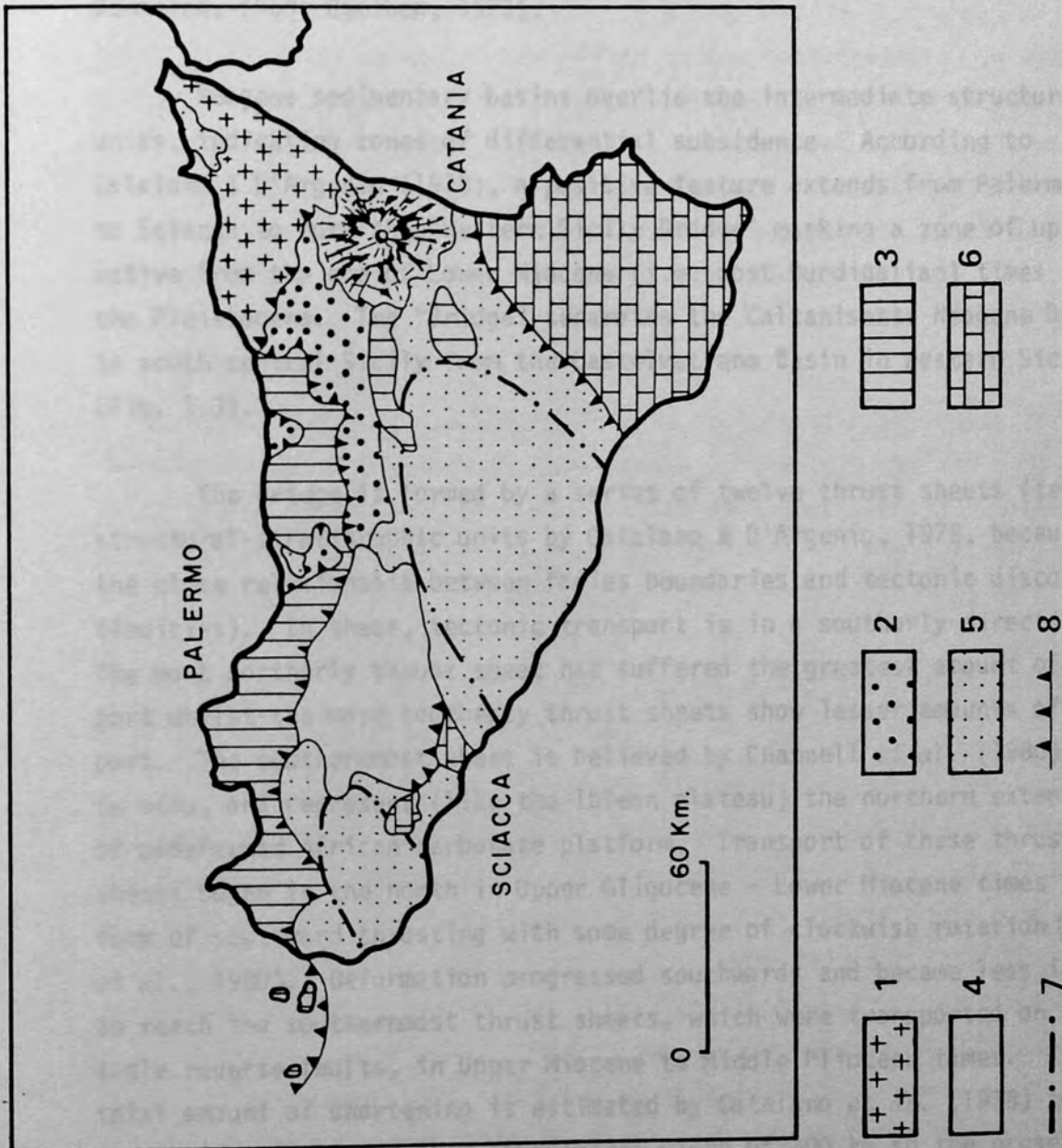


Figure 1.3

Iblean Plateau and of Sciacca are foreland regions, representing the most external zone, comparable with the Pre-Betic of Spain. The widely developed structural units between are comparable with the intermediate Sub-Betic, or to the Tell Atlas of North Africa, the Appenines of Italy, or the Dinarides of Eastern Europe (Durrand-Delga, 1967; Bemmelen, 1969; Ogniben, 1973).

Neogene sedimentary basins overlies the intermediate structural units, indicating zones of differential subsidence. According to Calalano & D'Argenio (1978), a positive feature extends from Palermo to Sciacca to form the "Western Sicily Bridge" marking a zone of uplift active from the end of Lower Miocene (i.e. post Burdigalian) times to the Pleistocene. The "Bridge" separates the Caltanissetta Neogene Basin in south central Sicily from the Castelvetro Basin in western Sicily (Fig. 1.3).

The Bridge is formed by a series of twelve thrust sheets (termed structural-stratigraphic units by Catalano & D'Argenio, 1978, because of the close relationship between facies boundaries and tectonic discontinuities). In these, tectonic transport is in a southerly direction. The most northerly thrust sheet has suffered the greatest amount of transport whilst the more southerly thrust sheets show lesser amounts of transport. The southernmost sheet is believed by Channell *et al.* (1980) to be *in situ*, and represent (like the Iblean plateau) the northern extension of undeformed African carbonate platform. Transport of these thrust sheets began in the north in Upper Oligocene - Lower Miocene times in the form of southward thrusting with some degree of clockwise rotation (Channell *et al.*, 1980). Deformation progressed southwards and became less intense to reach the southernmost thrust sheets, which were transported on high angle reverse faults, in Upper Miocene to Middle Pliocene times. The total amount of shortening is estimated by Catalano *et al.* (1978) to be in the region of 200 km, from an original width of 300 km to the present western Sicily (Palermo-Sciacca) width of 90 km.

This study is concerned with rocks situated on the first, second, third and fifth most southerly thrust sheets, respectively the Mt San

Calogero, Pizzo Telegrafo, Mt Genuardo and Mt Barracu - Mt Colomba structural stratigraphic units of Catalano and D'Argenio (1978). The Mt San Calogero unit is believed to be *in situ* (Channel *et al.* 1980). The amount of tectonic transport of the Pizzo Telegrafo and Mt Genuardo thrust sheets is minimal and was incurred in Upper Miocene and Pliocene times (Catalano & D'Argenio, 1978; Channel *et al.* 1980). It therefore has little effect on the interpretation of Upper Oligocene and Lower Miocene regional environments. The amount of movement on the Mt Barracu - Mt Colomba thrust sheet is probably much greater. The Lower Miocene limestones from this unit were situated some distance northwards in Lower Miocene times, and this must be allowed for in regional palaeoenvironmental interpretations.

1.4 Stratigraphic Setting

Western Sicily represents an area of carbonate platforms and associated basins whose development began in the Triassic and continued until the Lower Miocene, when deformation of the western Sicily continental margin began as a consequence of collision orogeny (Catalano & D'Argenio, 1978, 1981).

Catalano and D'Argenio (1978) distinguish three stages in the overall evolution of western Sicily:

1) Continental rifting (Middle to Upper Triassic). An intracratonic basin (the Lercara Basin) developed in Middle Triassic times, presumably as a response to tensile tectonics. This basin was flanked by carbonate platform facies which were possibly linked along a western prolongation (Scandone *et al.*, 1974). In Upper Triassic (Norian) times an intermediate carbonate platform developed by prolongation from the west, dividing the original basin in two. Three carbonate platforms are therefore associated with two intervening basins, of general east-west trend. These are (from north to south): Panormide Carbonate Platform, Imerese Basin, Trapanese Carbonate Platform, Sicani Basin and Saccense Carbonate Platform (Fig. 1.4). (This palaeogeographic interpretation is well established in the literature and its broad features accepted by a range of different authors: e.g. Broquet *et al.*, 1966; Broquet, 1970;

Figure 1.4 The palaeogeography of western Sicily in Middle Cretaceous to Eocene times (from Catalano & D'Argenio, 1978).

Panormide Carbonate Platform: 1, Internal margin; 2, Foraminiferid, rudistid and Nummulitic shallow water carbonate banks; 3, White to red *Globotruncana* and *Globorotalia* calcilutites (scaglia) with resedimented biocalcarenites; 4, Maastrichtian megabreccias.

Imerese Basin: 5, Radiolarian and globigerinid red marls and calcilutites with resedimented biocalcarenites; 6, Pelagic marls and calcilutites.

Trapani Carbonate Platform: 7, *Globotruncana* and *Globorotalia* white and red calcilutites with intercalations of nummulitid biocalcarenites; 8, Maastrichtian megabreccias in the internal margin.

Sicani Basin: 9, White to red *Globotruncana* and *Globorotalia* calcilutites, red marls and resedimented nummulitid biocalcarenites; 10, Basalts; 11, White and red calcilutites; 12, Maastrichtian megabreccias.

Saccense Carbonate Platform: 13, Grey green and white calcilutites (scaglia).

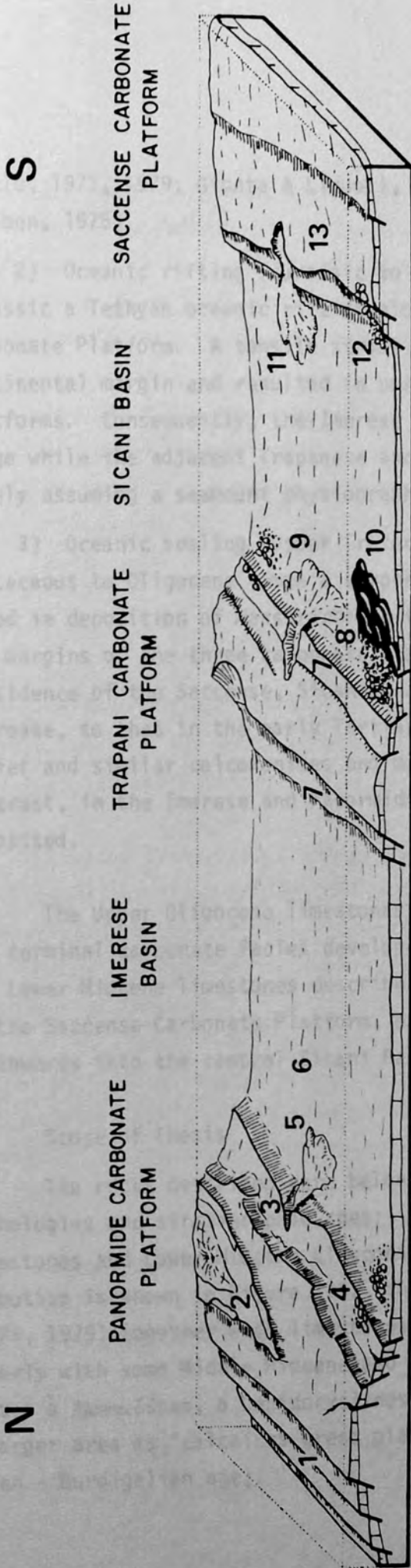
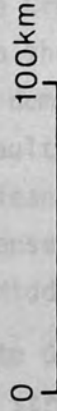


Figure 1.4

Approximate scale:



Masclé, 1973, 1979, Giunta & Liguori, 1973; Scandone *et al.*, 1974; Ogniben, 1975).

2) Oceanic rifting (Jurassic to Middle Cretaceous). During the Jurassic a Tethyan oceanic rift developed to the north of the Panormide Carbonate Platform. A tensile stress field dominated the western Sicily continental margin and resulted in normal faulting of the carbonate platforms. Consequently, the Imerese and Sicani basins tended to enlarge while the adjacent Trapanese and Saccense platforms rapidly sank, widely assuming a seamount physiography by Middle to Upper Jurassic times.

3) Oceanic sealing (Upper Cretaceous to Oligocene). In Upper Cretaceous to Oligocene times a compressive stress regime ensued and resulted in deposition of Maastrichtian fault-generated megabreccias along the margins of the three carbonate platforms (Fig. 1.4). The relative subsidence of the Saccense, Sicani and Trapanese domains tended to decrease, so that in the early Tertiary there was little topographic relief and similar calcarenites and marls were deposited throughout. In contrast, in the Imerese and Panormide domains terrigenous sediments were deposited.

The Upper Oligocene limestones described below comprise part of the terminal carbonate facies developed on the Saccense Carbonate Platform. The Lower Miocene limestones described are situated at the northern margin of the Saccense Carbonate Platform, extending from its northern flank northwards into the central Sicani Basin.

1.5 Scope of Thesis

The rocks described here belong to two quite separate carbonate lithologies and stratigraphic ages: Upper Oligocene algal-foraminiferal limestones and Lower Miocene glauconitic sandy limestones. Their distribution is shown in Figure 1.5. The former unit was mapped by Masclé (1973, 1979) together with limestones of Middle Oligocene age (and mistakenly with some Middle Miocene and Quaternary limestones) as "calcarénites à *Nummulites*, a *Lepidocyclines*"; the latter unit was mapped over a larger area as "calcaires greso glauconieux" of Lower Miocene (Aquitani - Burdigalian age).

The Upper Oligocene limestones are described in Chapter 2. The rocks rest with major unconformity on Cretaceous and Eocene carbonates; have a locally distinctive basal phosphorite conglomerate; and two very distinctive if variably developed facies (algal rhodolithic packstone-wackestone facies and foraminiferal grainstone-packstone facies).

The Lower Miocene limestones are described in detail in Chapter 3. Stratigraphic relationship to the supposedly underlying Upper Oligocene argillaceous rocks is rarely observed, but two facies are readily distinguished: a glauconitic limestone facies and a sandy limestone facies.

Coralline algae are an important component of the Upper Oligocene limestones. Chapter 4 describes eight species from six genera, known elsewhere from the Mediterranean Tertiary but all new to Sicily. Trace fossils (burrows and borings) are also identified for the first time from the Sicilian Tertiary.

Chapter 5 interprets the diagenetic history of the carbonates, shows cementation and compaction to be prominent features, and demonstrates that whereas the Upper Oligocene limestones are characterised by four periods of cementation only two can be recognised in the Lower Miocene limestones.

Geochemical analyses are presented in Chapter 6 to confirm identification of the greenish mineral widespread in the Lower Miocene limestones as glauconite, authigenic in the glauconitic limestone facies, and hence supporting inferences on the original environment of deposition of the rock. Geochemical analyses of phosphorites in Chapter 7 both complement the glauconite analyses, and extend comparison of southwest Sicily into the Iblean Plateau of southeast Sicily and into the well documented Maltese islands.

Chapter 8 concludes with a description of the depositional and diagenetic histories of both the Upper Oligocene and Lower Miocene limestones, describes their palaeogeography, placing them in a central Mediterranean

setting and traces the distribution of similar rhodolithic, foraminiferal and glauconitic facies in the Tethyan realm.

UPPER OLIGOCENE LIMESTONES

Introduction

Location

The localities described in this chapter all lie within the area bounded by the towns of Muro, Sciacca, Ribera, Burgio and Sambuca (Fig. 1.5). The four clusters of outcrop from 0.04 km² to 1.0 km² (see Table 1.1, 1971, map and text.), separated from one another as a result of the effects of late Miocene and Pliocene tectonism (Broquet, 1967; 1971; Catalano & D'Argenio, 1972) and subsequent erosion. The latter is a series which partly encircles the large Mesozoic Sicilian Basin (from west to east) the upland areas of Maggiori, Muro, Sciacca and Ribera (Fig. 1.5). All of these form part of the great and complex thrust sheets of the Western Sicily Intraoceanic Subduction Zone: the Mt. San Calogero thrust sheet (Muro, Sciacca and Ribera), the Mt. San Calogero thrust sheet (Muro, Sciacca and Ribera) and the Pizzo Felagradio thrust sheet (Muro, Sciacca and Ribera).

In the north-east part of the study area the limestones form a series of small outcrops, from 0.04 km² to 0.1 km² to the east of Muro, Sciacca and Ribera. The strata are folded into tight folds, with the axial planes generally steeply inclined to vertical dip (see Fig. 1.5, 1971, map and text.), towards minor thrusting to the south. The outcrops are generally composed of the Upper Oligocene successions, with some lower Oligocene strata, all lying within one kilometre of the road between Muro and Sciacca (Burgio) road. In the west the outcrops are more widely spaced, with gentle easterly and northerly dips. The southern limit of the river Corbo (see Fig. 1.5, 1971, map and text.) including the depression La Cucca are also composed of the Upper Oligocene successions (see Fig. 1.5, 1971, map and text.) and the Mt. San Calogero thrust sheet (Muro, Sciacca and Ribera) and the Pizzo Felagradio thrust sheet (Muro, Sciacca and Ribera). The outcrops have gentle northerly dips. The outcrops are generally composed of the Upper Oligocene successions, with some lower Oligocene strata, all lying within one kilometre of the road between Muro and Sciacca (Burgio) road. In the west the outcrops are more widely spaced, with gentle easterly and northerly dips. The southern limit of the river Corbo (see Fig. 1.5, 1971, map and text.) including the depression La Cucca are also composed of the Upper Oligocene successions (see Fig. 1.5, 1971, map and text.) and the Mt. San Calogero thrust sheet (Muro, Sciacca and Ribera) and the Pizzo Felagradio thrust sheet (Muro, Sciacca and Ribera).

CHAPTER 2

UPPER OLIGOCENE LIMESTONES

2.1 Introduction

2.1.1 General

The limestones described in this chapter all lie within the area bounded by the towns of Menfi, Sciacca, Ribera, Burgio and Sambuca (Fig. 1.5). They form discrete areas of outcrop from 0.04 km² to 5.0 km² in size (Masclé, 1973, 1979, map encl.), separated from one another as the resultant effect of late Miocene and Pliocene tectonism (Broquet *et al.*, 1966; Broquet, 1972; Catalano & D'Argenio, 1978) and subsequent erosion. They form a veneer which partly encircles the large Mesozoic outcrops forming (from west to east) the upland areas of Magaggiari, Arancio, Tardara and Pizzo Telegrafo (Fig. 1.5). All of these form part of the two most southerly thrust sheets of the Western Sicily Bridge thrust pile (Section 1.3): the Mt San Calogero thrust sheet (Magaggiari) and the Pizzo Telegrafo thrust sheet (Arancio, Tardara and Pizzo Telegrafo).

In the south and east of the study area the limestones form a series of outcrops stretching from Nadorello (UB 335800) to the east of Caltabellotta terminating at UB 448606. The strata are folded into tight to open upright folds and commonly show steeply inclined to vertical dips (Plates 2.1, 2.2). (Masclé, 1973, records minor thrusting to the south-west of Caltabellotta causing repetition of the Upper Oligocene succession). These outcrops are easily accessible, all lying within one kilometre of the Sciacca - Caltabellotta - San Carlo (Burgio) road. In the west the limestones form large, more scattered outcrops, with gentle southerly and westerly dips (10-20°), notably: the southern exit of the river Carboj from Contrada Tardara (UB 276647); encircling the depression La Conca and to the west of Contrada Arancio (UB 250666 to UB 260671 and UB 242667 to UB 239689); in small low lying outcrops in Contradas Finocchio and Genovese (UB 234685 to UB 195689). In the north beds have gentle northerly dips (10-30°) and outcrop is plentiful, forming: large crags on the flanks of

the river to the south of the Carboj dam (UB 290662 and UB 296661); a fragmented veneer on contradas Ulma, Pasqualetto, Cesinata and Giovanni (UB 300658 to UB 344667); and a number of craggy outcrops with variable dip within the area of San Biagio (UB 362677 to UB 392673).

2.1.2 Previous Work

Campisi (1968) and Blondeau *et al.* (1972) provide the most recent works concentrating solely on these limestones. Both are primarily concerned with correlation and neither cover the complete extent of outcrop. Other works making reference to these rocks have been of a general nature incorporating much larger areas and stratigraphy, and are usually of structural interest (Caire & Mascle, 1964; Broquet *et al.*, 1966; Mascle, 1967a & b, 1973, 1974, 1979; Catalano & D'Argenio, 1978; Catalano *et al.*, 1978; Channel *et al.*, 1980) or, older works of note type, often on single outcrops and recording preliminary observations on fauna and general rock type (Checchia-Rispoli, 1918; Rigo de Righi, 1954; Ruggieri, 1959, 1961). Mascle, (1973, 1979) produced a geological map (scale 1 : 100 000) of the Scicani Mountains which incorporated the area. Previously, the only maps available of the area were those produced in the late nineteenth century under the direction of Baldacci (1886).

2.1.3 Stratigraphic Nomenclature

The limestones form part of the Ragusa Formation since this was defined by Rigo & Barbieri (1959) to designate Sicilian shelf limestones of Middle Eocene to Middle Miocene age. The type locality of the Formation is at Ragusa in southeast Sicily, but its lateral extent into southwest Sicily was recognised by Rigo & Barbieri and subsequently by Blondeau *et al.* (1972) and Mascle (1973, 1979).

The limestones correlate most closely in lithology with the Irminio Member of the Ragusa Formation as described by Rigo & Barbieri (1959). They also have a similar fauna including *Miogypsina* and *Miogypsinoidea*. However, they have an Upper Oligocene (Chattian) age whereas the Irminio Member is correlated with the Lower Miocene by Rigo & Barbieri (1959).

2.1.4 Correlation

There is disagreement on the age of the limestones. Campisi (1968) dates them as Lower Miocene (Aquitanian) in age whilst Blondeau *et al.* (1972) and Mascle (1973, 1979) date some of the outcrops as uppermost Oligocene ("Oligocene terminal") and others as lowermost Miocene ("Aquitanian inferieur").

Campisi (1968) studied only two stratigraphic sections within the area (one adjacent to Carboj Dam and the other at San Biagio: the Carboj Dam and San Biagio east localities of this work, see Figures 2.3, 2.7). From these he recorded faunas including the benthonic foraminifera *Austrotrillina howchini*, *Eulepidina*, *Nephrolepidina morgani*, *N. sumatrensis* and *Spiroclypeus blankenhorni ornata*. Campisi concluded that this association is Lower Miocene (Aquitanian) in age. In particular he states that *N. morgani* and *N. sumatrensis* are exclusively Miocene forms whilst *A. howchini* and *Eulepidina* are Oligocene forms which become extinct in Lower Miocene times.

According to Blondeau *et al.* (1972) and Mascle (1973, 1979) their limestones of uppermost Oligocene age have a large benthonic foraminiferal assemblage of *Amphistegina cf. lessonii*, *Heterostegina* sp. and *Miogypsinoidea* sp. whilst those of lowermost Miocene, Aquitanian, age contain *Eulepidina* sp., *Nephrolepidina* sp., *Spiroclypeus* sp., *Heterostegina* sp., *Amphistegina cf. lessonii*, *Pararotalia* sp., *Operculina* sp., *Rupertia* sp., *Miogypsina* sp. and *Miogypsina gunteri*.

Dr C.G. Adams (British Museum, Natural History) has examined thirty thin sections from most localities throughout the area and has concluded that these limestones are all Upper Oligocene (Chattian) in age (pers. comm., 1980). Positive evidence for a Chattian age is the presence of *Miogypsinoidea complanatus* which is present, if not abundant, in 30 - 40 thin sections. Where *M. complanatus* is not present, positive identification of Chattian age is not possible. However, the general assemblage of *L. (Eulepidina) dilatata*, *L. (Nephrolepidina)*, *Spiroclypeus*, *Amphistegina*, *Pararotalia*, *Rotalia*, *Cycloclypeus* and *Heterostegina* (determined by Dr Adams) occurs throughout the area (augmented by *Miogypsina*

in the outcrops around Caltabellotta, see Figure 2.8) and therefore, the containing limestones are likely to be of the same Upper Oligocene, Chattian, age.

Campisi's (1968) conclusion that at least some of these limestones are Lower Miocene (Aquitanian) in age may be erroneous since his age indicative fauna includes *N. morgani* and *N. sumatrensis* both of which have been recorded from the Upper Oligocene of Italy (Pieroni, 1965) and the western Pacific (Premoli Silva & Brusa, 1981) respectively.

A significant feature of the Blondeau *et al.* (1972) and Mascle (1973, 1979) identifications is that *Miogypsinoidea* is restricted to the Upper Oligocene in occurrence whilst *Miogypsina* is found in their Lower Miocene, Aquitanian association. *Miogypsina*, however, is known to range from the Chattian into the Lower Miocene (Berggren, 1971), although it does not become abundant until Lower Miocene times. Its absence or restricted occurrence here in a facies within which it might be expected to occur, along with the presence of *Miogypsinoidea complanatus*, suggests that the limestones are Upper Oligocene, Chattian, in age.

2.2 Base of the Succession

2.2.1 The Basal Unconformity

Where seen, the base of the succession is formed by an unconformity. This is clearly exposed at only three localities within the area: Nadorello east; Carboj ravine, San Biagio (see Fig. 1.5). Additional small exposures occur at Mont Gargalupo and east of Caltabellotta. Elsewhere the position of the unconformity can be inferred with some precision, but the plane is obscured by soil and vegetation.

At Nadorello east (Figs 2.1, 2.2, Plates 2.3, 2.4, 2.5) the unconformity is exposed in section at four places. The beds above the unconformity are parallel to, or at a slight angular discordance with, the beds below. The surface of the unconformity is planar, has no marked relief and has been burrowed with *Thalassinoidea paradoxica*. Strata immediately below the unconformity are massively bedded chalks which have

yielded a rich planktonic foraminiferal fauna including *Globotruncana laporenti*, *G. sigali*, *G. coronata*, *G. praeconcaevata* and *G. convexa* (Mascle 1973, 1979) indicative of an Upper Cretaceous date.

At the southern exit of the river Carboj from Contrada Tardara (Plate 2.6) the unconformity is again exposed in an outcrop almost concealed by vegetation midway up the northwest side of the ravine at the northern limit of Tertiary outcrop. The surface of the unconformity is uneven, resulting from an erosion-formed relief of 15-20 cm and subsequent minor normal faulting with downthrow of up to 0.3 m to the northeast. The underlying strata are again massive chinks, but they contain a *Globigerina* and *Globorotalia* fauna indicative of an Eocene age (Campisi, 1968; Mascle, 1973, 1979).

At San Biagio (Fig. 2.6; Plates 2.7, 2.8) the unconformity is exposed in section over a distance of 60-80 m down dip. The surface is rugged (Plate 2.8), forming a local topography of 0.2-0.4 m which is partly the effect of erosion and partly due to tectonic movements which have brecciated the underlying strata: massive chinks of Upper Cretaceous age (Mascle, 1973, 1979) yielding the same fauna as at Nadorello east.

Further small exposures of the unconformity occur to the southeast of Mt Gargalupo (Fig. 1.5) and adjacent to the Caltabellotta - San Carlo road at UB 436602. At both localities the surface is even, with no apparent angular discordance between the limestones above and below the unconformity.

The sediments resting on the unconformity at all the localities have the same faunal assemblage (Section 2.1.4) and therefore the same Upper Oligocene age. The underlying strata vary from Upper Cretaceous to Eocene in age (Campisi, 1968; Mascle, 1973, 1979). The unconformity can therefore be dated as post Eocene, pre Upper Oligocene in age. Evidence from clasts in the basal conglomerate lying immediately above the unconformity confirms that rocks of Upper Cretaceous to Eocene age were being eroded.

The presence of *Thalassinoides paradoxica* burrows (Plate 4.41) at Nadorello east (Section 4.2.2) is an added complication. Although these burrows are in Upper Cretaceous chalk, they are inferred to be Chattian rather than Upper Cretaceous in origin. This Chattian age of burrow formation is suggested for five reasons: the burrows are infilled with Chattian limestone; burrows are absent from the underlying Upper Cretaceous sequence; the burrows show no signs of secondary colonisation by borers, or of mineralisation which might suggest an extended period of exposure on the sea floor; there is no evidence of any burrow infill older than Chattian age to suggest that the burrows were re-excavated and infilled with Chattian material; and the morphology of the burrow system suggests formation during hardground lithification. Presumably, the chalk had remained soft from Upper Cretaceous to Chattian times, but began to lithify when exposed by erosion during the Chattian marine transgression. Exposure of the soft sediment allowed colonisation by burrowing organisms for a short period of time before lithification occurred.

2.2.2 The Basal Conglomerate

A basal conglomerate is clearly exposed at all localities which reveal the basal unconformity: Nadorello east, Carboj ravine and San Biagio (Fig. 1.5). It is, however, better developed at Nadorello east and San Biagio, where it occurs at the base of an algal rhodolithic wackestone-packstone facies, than at Carboj ravine where it occurs below the foraminiferal grainstone-packstone facies. Additional exposures occur at Mt Gargalupo and Rocca Porcaria where the conglomerate is represented by only a few clasts resting on the unconformable surface.

The most extensive outcrop occurs at Nadorello east (Figs 2.1, 2.2, Plates 2.5, 4.41). The conglomerate rests directly upon the plane of unconformity, and is composed of cobbles and pebbles forming a maximum thickness of 0.2 m at the base of a 3.5-6 m thick unit of massive algal foraminiferal limestone. Matrix between the clasts is identical to and continuous with the overlying limestones (described fully in Section 2.4). The conglomerate itself is not a bed with sharp top and

lateral continuity, but rather it forms patches of clasts some 1-10 m in extent lying upon the unconformity.

Five types of clast, within the conglomerate, can be recognised.

1) Bioclasts. Forming some 20% of clasts, these comprise abraded tests of *Lepidocyclina* (*Eulepidina*); abraded algal rhodoliths; and slightly abraded, disassociated valves of the large pectinid bivalve *Chlamys* (valves 60-90 mm in length). Tests of a large (120 mm diameter) echinoid (*Clypeaster*) are also common, generally whole and unabraded.

These clasts show but little evidence of transport. Furthermore, unabraded examples of the same species occur in both the matrix between clasts and within the overlying limestones. The bioclasts are therefore semi-autochthonous, contemporaneous with and from the same environment of origin as the enclosing sediment.

2) Unbored chalks. Angular to sub-angular, non-bored chalk clasts, generally 50-70 mm diameter but reaching 200-300 mm. Some clasts contain Globotruncanid planktonic foraminifera of probable Upper Cretaceous age. Others contain Globigerinid planktonic foraminifera of probable Eocene age. Clasts of Cretaceous age predominate and are abundant at Nadorello east and San Biagio west where the underlying limestones are also of Upper Cretaceous age. Eocene clasts are uncommon.

Shape, age and occasional large size of the clasts are therefore consistent with their local derivation during the Upper Oligocene transgression.

3) Bored chalks. Rounded to sub-rounded oblate shaped bored chalk clasts (80-150 mm diameter) may have borings on both sides, one side, or predominantly one side of the clast. Clast roundness and the presence of borings indicate prolonged transport and relatively prolonged exposure on the sea floor prior to burial. These clasts separately contain both Globotruncanid and Globigerinid planktonic foraminifera; but no relationship between the age of the clasts and the age of

the underlying strata was observed.

Despite obvious evidence for greater transport than the unbored chalks, these clasts are of the same ages and facies, and indicate only erosion of the same (presumably local) Cretaceous and Eocene rocks.

4) Large phosphates. Rounded to sub-rounded, oblate to sub-spherical, phosphatised bored chalk clasts (80-150 mm diameter), have been bored on all surfaces, subsequently abraded (resulting in a shallowing of bores) and phosphatised. They are easily recognised by their brown polished appearance. Their phosphatic nature has been established from thin section petrography and by X-ray diffraction and ICP analysis (Chapter 7). They contained planktonic foraminifera (*Globigerina* and *Globorotalia*) suggest an Eocene age (Adams, pers. comm., 1982). No Upper Cretaceous, Palaeocene or Oligocene phosphatised clasts have been found.

These clasts therefore provide evidence for a significant period of phosphatisation in or adjacent to this southwest Sicily area but of pre Upper Oligocene to Eocene age. Oligocene phosphorites are unknown in Sicily (Catalano, pers. comm., 1980) and indeed the Oligocene marks a phosphorite hiatus worldwide (Cook & McElhinny, 1979; Notholt, 1980b). The nearest Eocene phosphorites occur in central Tunisia (British Sulphur Corp., 1973), and form part of the Cretaceous-Eocene phosphorite province widely represented in North Africa. Despite their large size, these clasts have seemingly been transported into the area from an Eocene phosphorite source outside it. Conditions generating phosphorites in North Africa during the Eocene may have extended closer to Sicily than previously supposed.

5) Small phosphates. Rounded to sub-angular phosphatised chalk clasts (< 5-50 mm diameter) and whole and fragmentary fish teeth. These clasts are not restricted to the basal conglomerate, but can be found dispersed throughout the basal 1.5 m of the overlying limestones.

The basal conglomerate varies laterally with great rapidity, even at a single locality. Thus, in the Nadorello east area (Fig. 2.1) at locality A clasts change from almost exclusively unbored chalks (Plate 2.5) to predominantly bored chalks with some large and small phosphates (Plate 4.41) over a distance of 10 m. At locality B the conglomerate is represented by a single large phosphate clast with a few small phosphates dispersed sparsely throughout the overlying limestones. At C small phosphates predominate with some bored and unbored chalks: the first is found dispersed throughout the basal 1.5 m of the Upper Oligocene, whilst the latter two rest on the unconformable surface.

Elsewhere, at San Biagio west (Fig. 2.6), bored chalks and large phosphates are common whilst unbored chalks are abundant (Plate 2.9) and partly represented by some very large (0.4-0.8 m) bedded boulders. At Mt Gargalupo, Rocca Porcaria and Contrada Pasquelato the conglomerate is represented by only a few large and small phosphate clasts, whilst at Carboj ravine small phosphates predominate.

The basal conglomerate is therefore polygenetic. It is composed of: semi-autochthonous bioclasts, the same species as found in the overlying Upper Oligocene limestones; bored and unbored chalk clasts of the same facies and Cretaceous - Eocene age as those located below the unconformity in the local area; and large and small phosphatised chalk clasts of Eocene age seemingly derived from outside the area of study.

2.3 Stratigraphic Sections

Seven sections through the Upper Oligocene limestones were measured and logged, and are illustrated below by annotated figures and plates. The seven localities were chosen for a variety of reasons including: relatively thick succession; extensive local exposure; favourable weathering characteristics; accessibility; their widespread geographic distribution throughout the area; and, most importantly, for their representative qualities, in that they demonstrate variations and/or consistencies within recognised facies and variations in the basal unconformity and conglomerate.

The precise positions of the localities are shown on the outcrop

map, Figure 1.5. The localities are as follows:

1) Nadorello east. Stratigraphic section, Figure 2.2; locality photograph, Plates 2.3 and 2.4.

The measured section is situated 8 km northeast of Sciacca at UB 351598. It takes the form of a fresh cut surface in a small disused quarry on the northeast extremity of a bedded outcrop.

2) Carboj Dam. Stratigraphic section, Figure 2.3; locality photograph, Plate 2.10.

The measured section is situated 5.5 km southwest of Sambuca, 0.5 km south of Carboj dam on the west side of the river at UB 290662. It is located at a sheltered weathered surface in a cliff outcrop, as indicated in the Plate 2.10.

3) La Conca. Stratigraphic section, Figure 2.4; locality photograph, Plate 2.11.

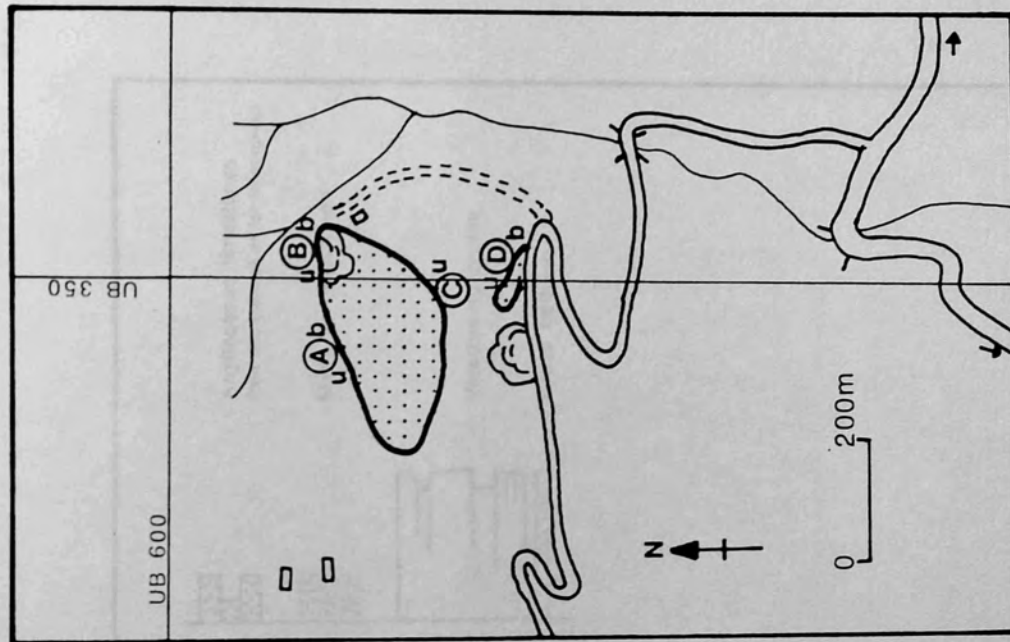
The section is situated 8 km west-southwest of Sambuca and 6 km east northeast of Menfi on the west side of the depression named La Conca at UB 239 673. It was measured on the fresh surface of the east facing side of a now disused quarry.

4) Contrada Giovanni. Stratigraphic section, Figure 2.5; locality photograph, Plate 2.12.

The measured section is situated 2 km south of Sambuca at UB 338668. It takes the form of a sheltered weathered surface on a large outcrop immediately east of some farm buildings on the rough grass covered slopes of Contrada Giovanni.

5) San Biagio west. Stratigraphic section, Figure 2.6; locality photograph, Plate 2.7.

The section is situated 3 km southeast of Sambuca, 1.3 km due west of the San Biagio fortress at UB 363676. It was measured on the east side of a large bedded outcrop immediately north of a cave.



KEY



Upper Oligocene limestones



Quarry



Text locality



Exposed unconformity (U.Cret./U.Olig.)



Burrowed unconformity surface

Figure 2.1 Nadorello east locality map

KEY TO FIGURES 2.2-2.8 and 3.1-3.4

FAUNA



Echinoids



Cidaroid spines



Chlamys



Lepidocyclina (Eulepidina)

FLORA



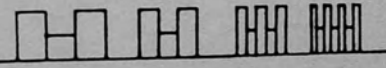
Red algal rhodoliths

LITHOCLASTS



Phosphatised and unphosphatised chalk lithoclasts

LITHOLOGY



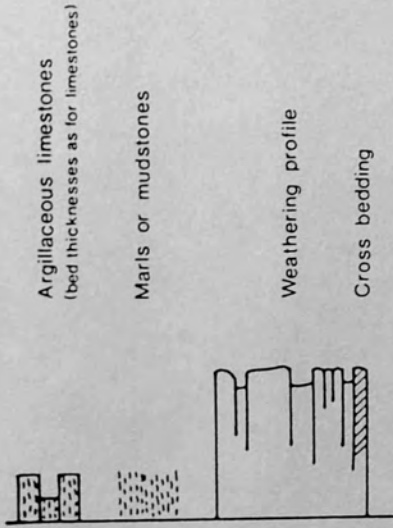
1.0 - 6.0m beds

0.4 - 1.0m beds

0.1 - 0.4m beds

<0.1m beds

Limestones



Argillaceous limestones
(bed thicknesses as for limestones)

Marls or mudstones

Weathering profile

Cross bedding

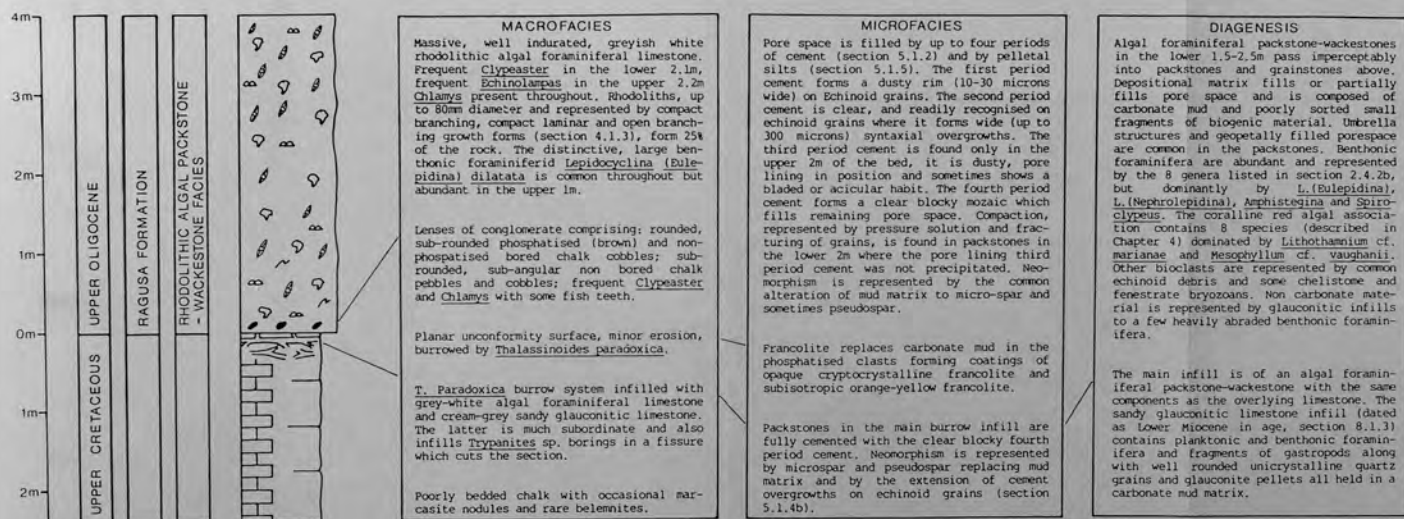


Figure 2.2 Nadorello East measured stratigraphic section.

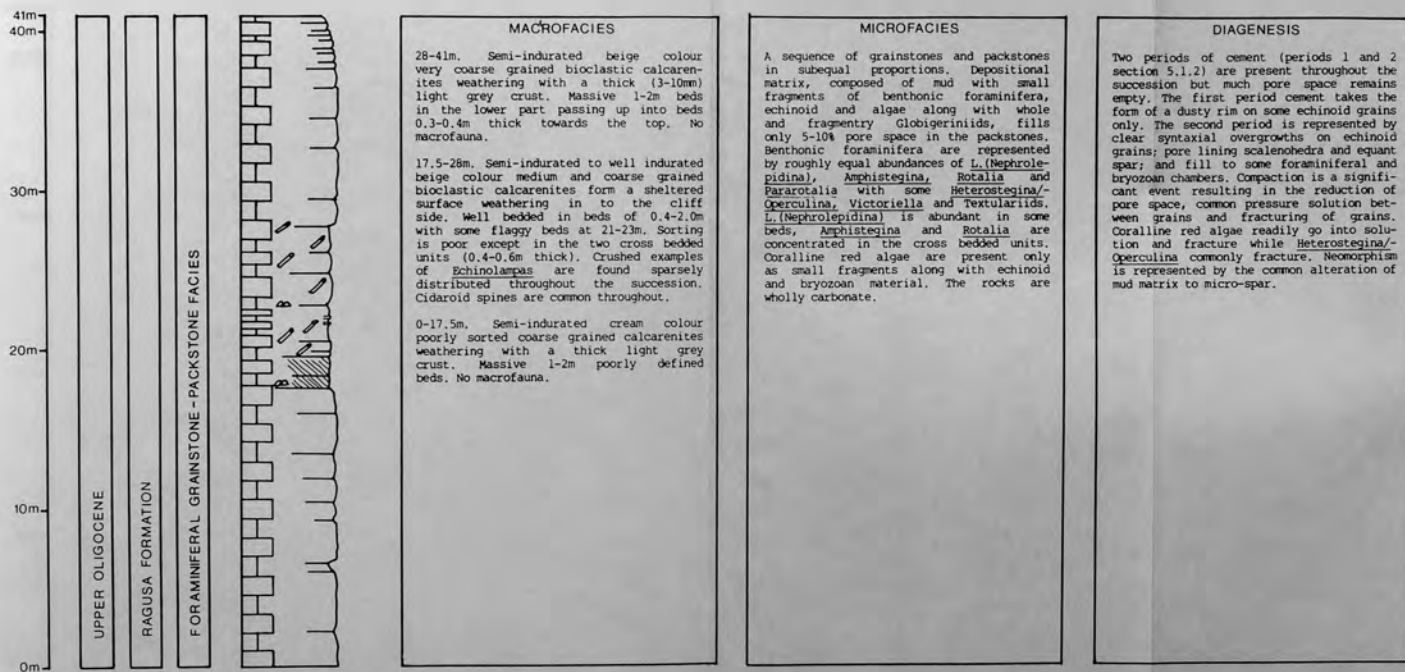


Figure 2.3 Carboj Dam measured stratigraphic section.

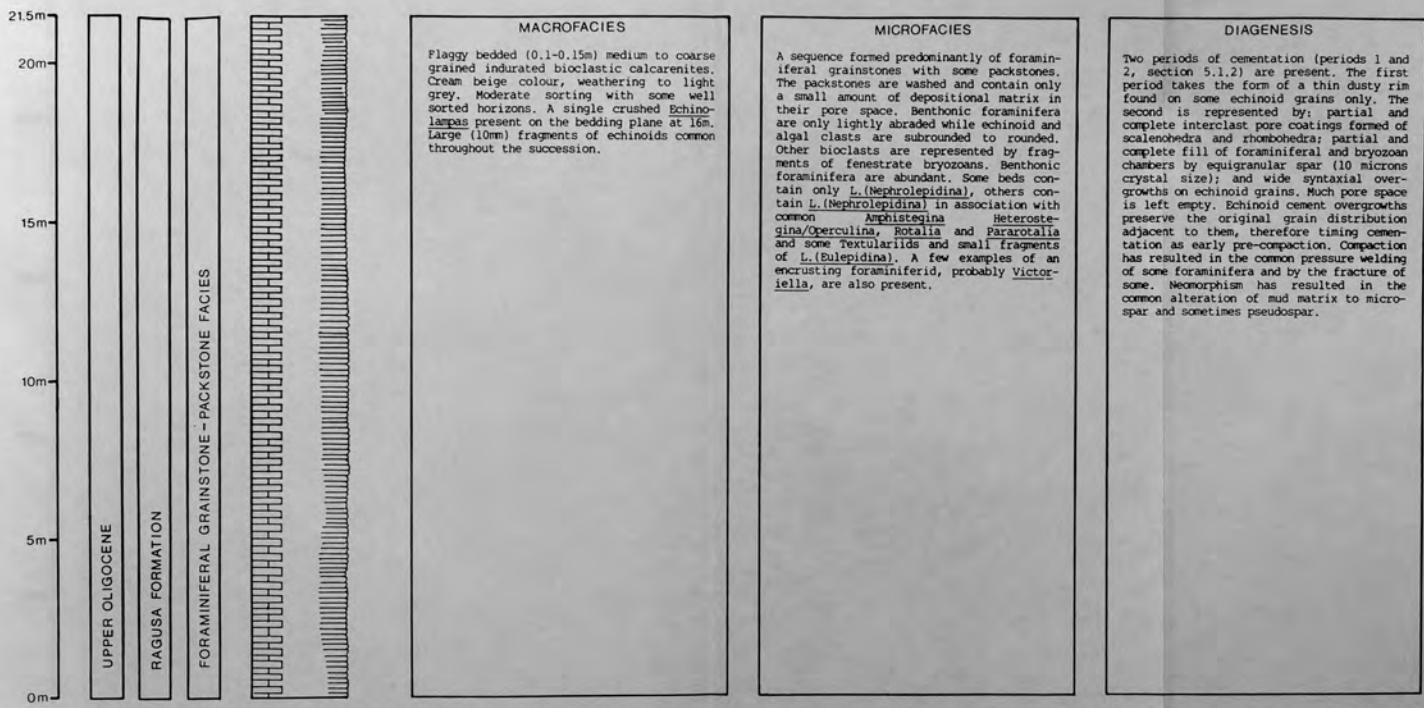


Figure 2.4 La Conca measured stratigraphic section.

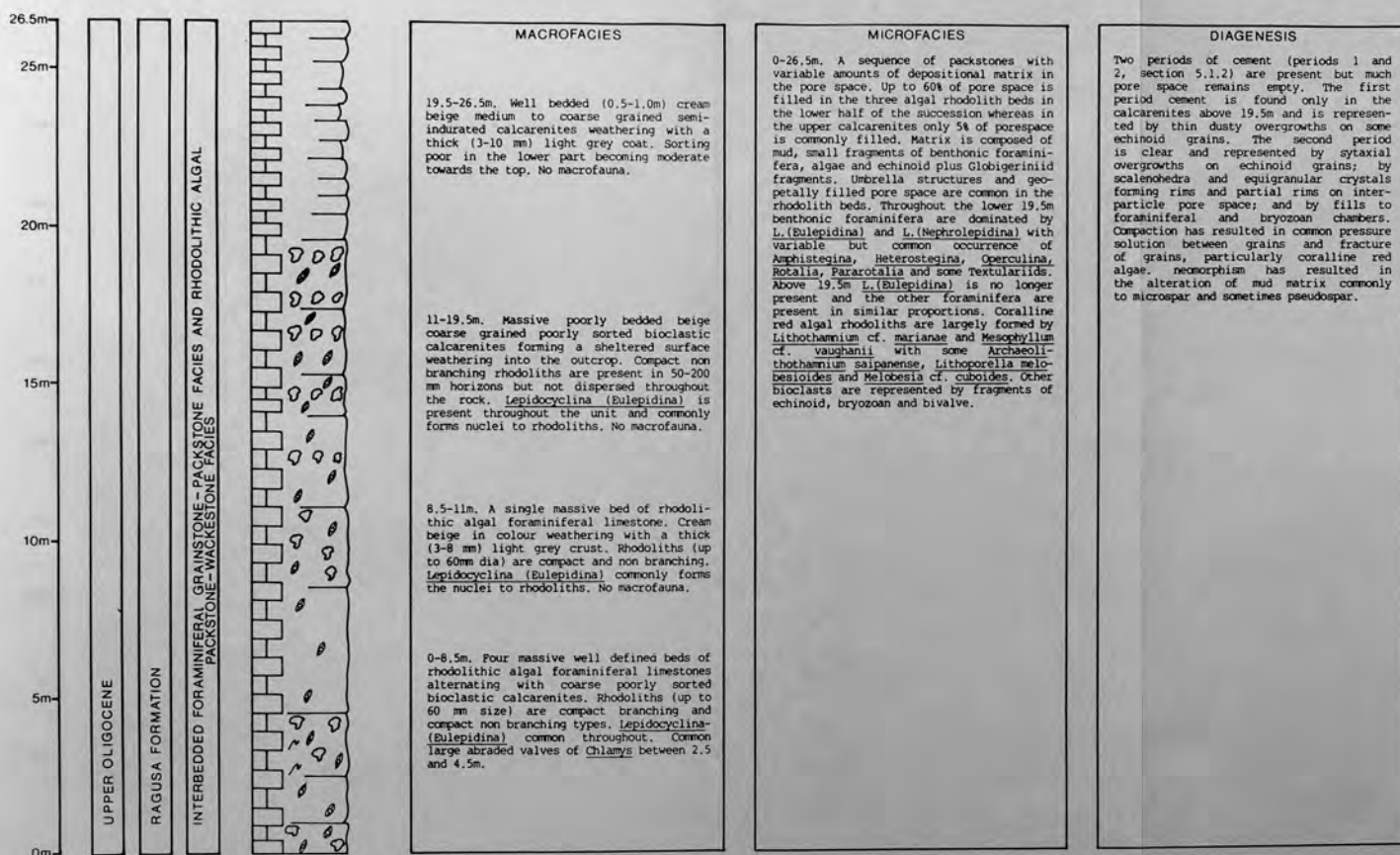


Figure 2.5 Contrada Giovanni measured stratigraphic section.

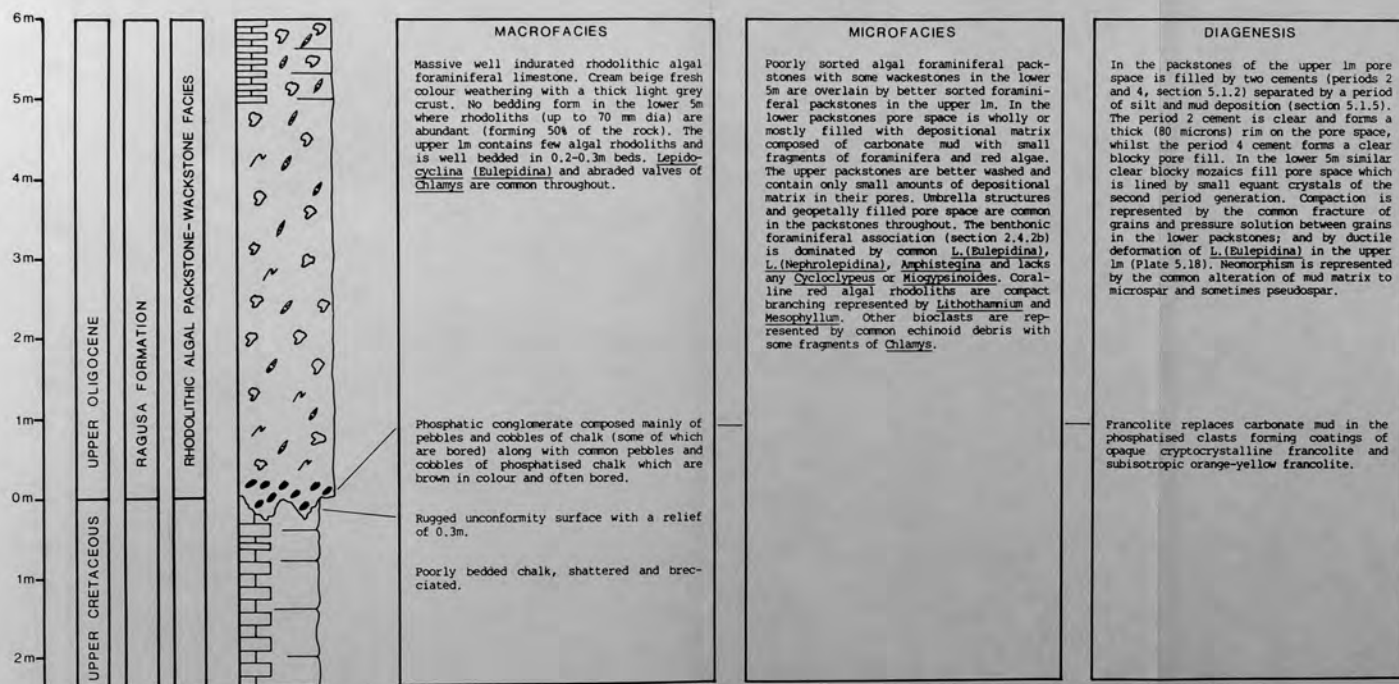


Figure 2.6 San Biagio West measured stratigraphic section.

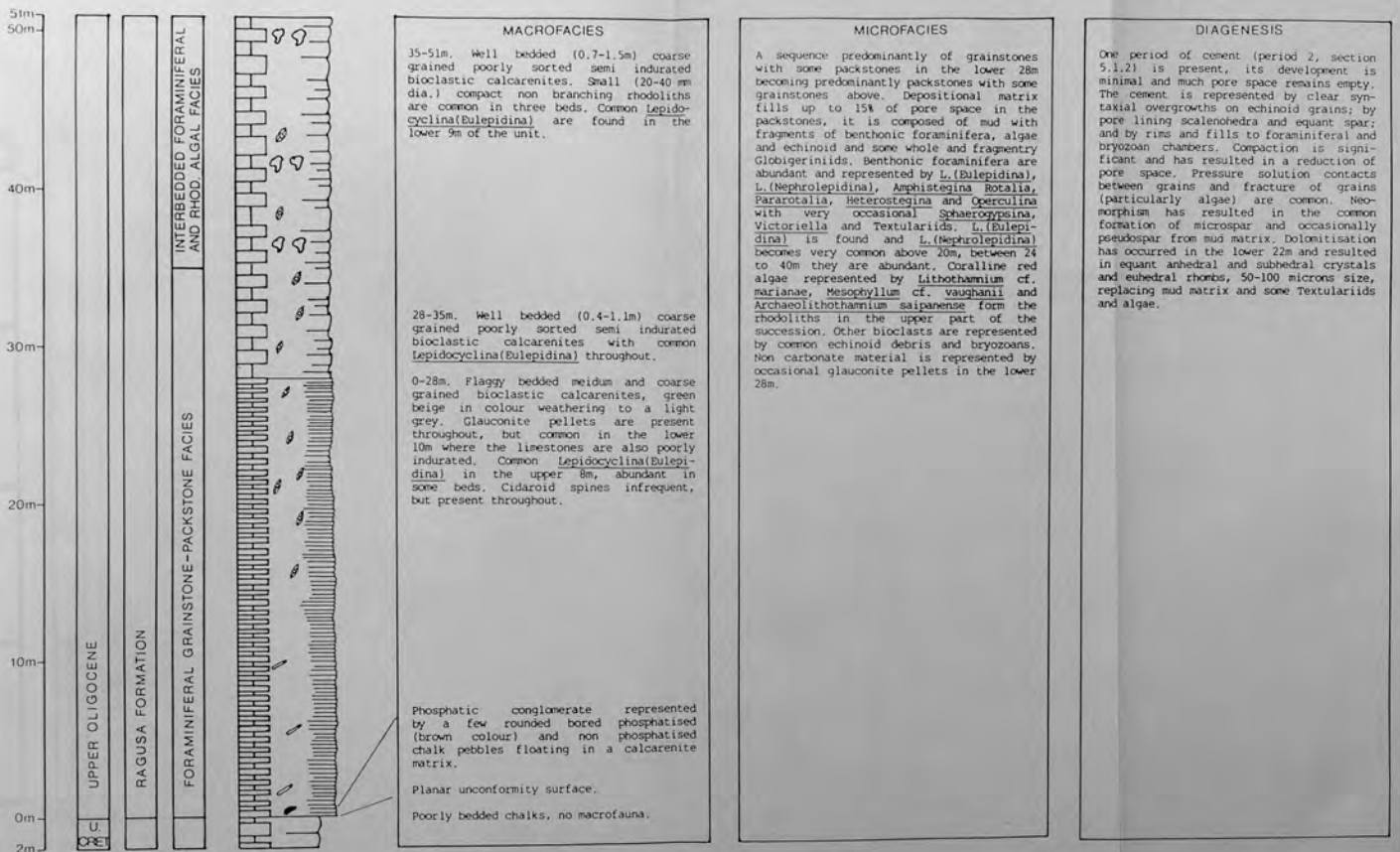


Figure 2.7 San Biagio East measured stratigraphic section.

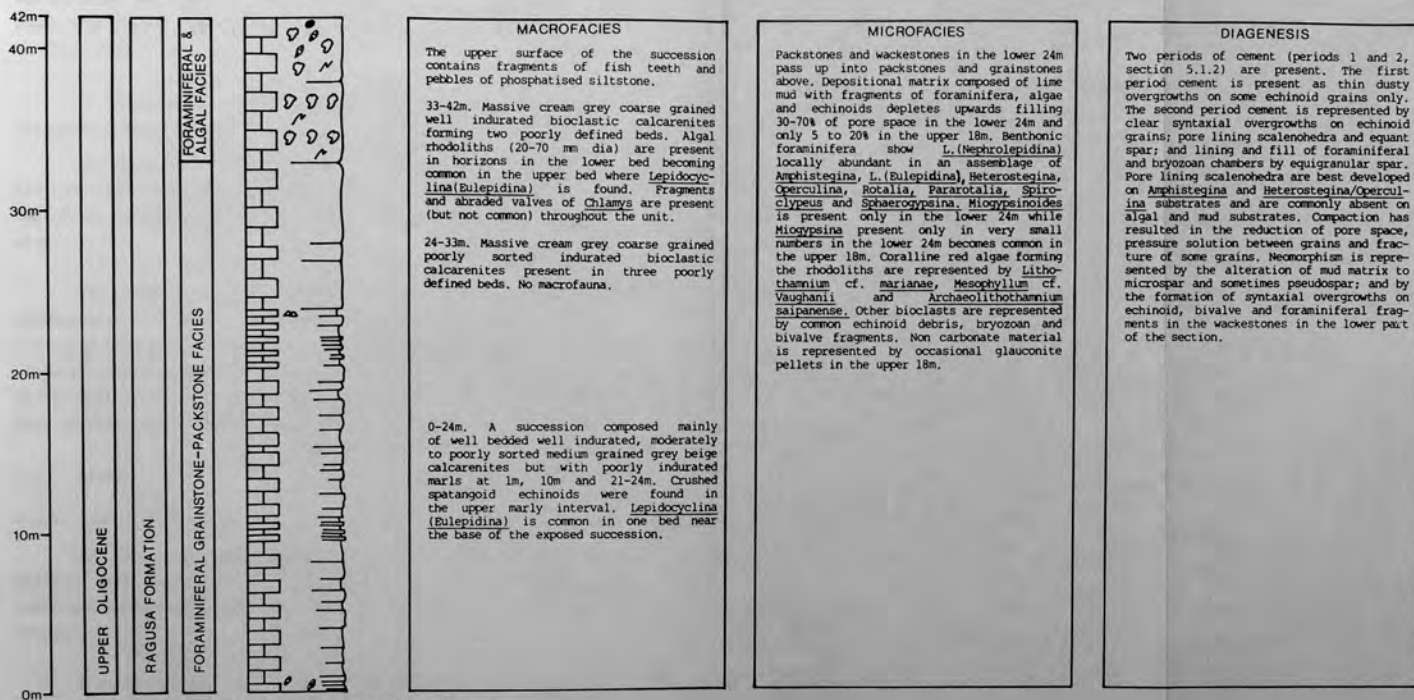


Figure 2.8 Tombe Sicani measured stratigraphic section.

6) San Biago east. Stratigraphic section, Figure 2.7; locality photograph, Plate 2.13.

This section is located 4.5 km east southeast of Sambuca 0.3 km due south of San Biago fortress at UB 376673. It was measured on the steep west facing side of the large outcrop there, dog-legged as shown in Plate 2.13.

7) Tombe Sicani. Stratigraphic section, Figure 2.8; locality photograph, Plate 2.14.

The section is located on the north side of the Sciacca-Caltabellotta road immediately west of Caltabellotta at UB 421601. The top of the succession is marked by the "Tombe Sicani" archaeological site.

The lithologies of these measured, illustrated localities are representative of the two major facies (defined and described in the following section 2.4) found in the Upper Oligocene. They show the range of variation found within the facies and are representative of the outcrop found in their local area. They are placed in the context of facies distribution in the following section.

2.4 Facies

2.4.1 Introduction

Two facies can be recognised in the field, named here, on the basis of their most distinctive constituents, the "rhodolithic algal packstone-wackestone facies" and "foraminiferal grainstone-packstone facies".

Previous workers have not distinguished between these two distinctive facies which differ in: flora, macrofauna, microfauna, basal conglomerate development, underlying rock type and diagenesis. Campisi (1968) terms all the deposits Lepidocycline limestones. Blondeau *et al.* (1972) and Mascle (1973, 1979) failed to recognise the presence of rhodoliths; they describe all the deposits as calcarenites, not distinguishing grainstones, packstones and wackestones.

2.4.2 Rhodolithic Algal Packstone-Wackestone Facies

a) Macrofacies: The thickest and most extensive development of this facies is seen in the Nadorello east area (Figs 2.1, 2.2; Plates 2.3, 2.4, 4.33-4.38) and at San Biagio west (Fig. 2.6; Plate 2.7). At both localities it is represented by a single massive 3.5-6 m bed resting unconformably on Upper Cretaceous chalk with a relatively extensive development of phosphatic conglomerate at the base (see Section 2.2.2). Elsewhere the facies is found as 0.5-2 m interbeds in predominantly "foraminiferal grainstone-packstone facies" successions at Contrada Giovanni (Fig. 2.5), San Biagio east (Fig. 2.7) and Tombe Sicani (Fig. 2.8) and in the areas around these localities. West of Contrada Giovanni in the Carboj and La Conca areas the facies is not seen.

The facies is characterised by common algal rhodoliths in a light grey foraminiferal limestone matrix. The rhodoliths have branching or laminar growth forms at Nadorello east and San Biagio west (Plates 4.33-4.38) whereas at the other localities they have non-branching compact growth forms (Plates 4.39, 4.40) a difference thought to be related to water energy (see Section 5.1.3). This difference is also reflected by the associated macrofauna. At Nadorello east there is a common echinoid fauna of large species of *Clypeaster* and of *Echinolampas* (both determined by Dr E.P.F. Rose, supervisor) with occasional pectinid (*Chlamys*, determined by Mr C.P. Nuttall, British Museum Natural History) bivalves. At San Biagio west *Chlamys* is abundant. Elsewhere, macrofauna is absent except at Contrada Giovanni where *Chlamys* is common. *Lepidocyclina* (*Eulepidina*) is seen in abundance in the upper part of the algal bed at Nadorello east (Plate 2.15).

b) Microfacies: The facies is characterised by algal foraminiferal packstones and wackestones (Plates 2.16-2.19). (These are poorly washed biosparites and packed biomicrites in Folk (1962) terminology). The former are, by far, most common whilst the latter occur only occasionally in patches at some horizons. Settling features such as umbrella structures (Plates 2.20, 2.21) (formed by the large *Lepidocyclina* (*Eulepidina*) *dilatata* and by rhodoliths), and geopetally filled pore space are common. Towards the top of the bed in the measured section at

Nadorello east and at San Biagio west algal rhodoliths become less abundant and the limestones become more washed and in patches form grainstones (Plate 2.22). Elsewhere, grainstones do not occur in this facies. The limestones are wholly carbonate except for the presence of a few heavily abraded benthonic foraminifera with infills of glauconite at Nadorello east. Carbonate mud matrix fills 20-60% of the pore space and occasionally fills all pore space.

The allochens are composed almost entirely of bioclasts with the exception of a few Globigerinid wackestone lithoclasts at San Biagio west. Bioclasts are dominated by benthonic foraminifera but coralline algal rhodoliths are significant forming up to 50% of the bulk composition of the rock. Other bioclasts include common echinoid debris, chelstone and fenestrate bryozoan fragments and occasional bivalve fragments.

Coralline red algae form up to 50% of the limestones in the form of rhodoliths. Eight species of algae, with variable abundance, have been described from this facies (see Section 4.1.2), namely: *Archaeolithothamnium saipanense*, *Lithothamnium aggregatum*, *L.* cf. *marianae*, *Lithophyllum ovatum*, *L. personatum*, *Mesophyllum* cf. *vaughanii*, *Lithoporella* cf. *melobesioides* and *Melobesia* cf. *cuboïdes*. *L.* cf. *marianae* and *M.* cf. *vaughanii* are by far the most abundant and, along with few *A. saipanense*, form the cores of many rhodoliths. *L. aggregatum* is a common subsequent encruster where the facies is typically developed but it is not present where the facies is interbedded with the foraminiferal grainstone-packstone facies.

Benthonic foraminifera form up to 75% of these rocks (Plates 2.23-2.25). Eight genera, two subgenera and two species have been recognised. In order of decreasing abundance, these are: *Lepidocyclus* (*Mephrolapidina*), *Lepidocyclus* (*Eulepidina*) *dilatata*, *Amphistegina*, *Botallia*, *Pararotalia*, *Spiroclypeus*, *Heterostegina*, *Operculina*, *Cycloclypeus* and *Micogypsinoïdes complanatus*. The first three listed are common throughout, whilst the others are subordinate in numbers and of equal variable amounts except for *M. complanatus* which is present in very small numbers. *L.* (*Eulepidina*)

dilatata is a distinctive form of this facies, often locally abundant (Plate 2.15) and commonly forming the nucleus of algal rhodoliths.

c) Diagenesis: Diagenesis throughout the Upper Oligocene limestones is described in Section 5.1. Cementation in this facies is more complex than in the foraminiferal grainstone-packstone facies. Four periods of cement (Section 5.1.2) are developed, whereas in the foraminiferal grainstone-packstone facies only two are present. Compaction (Section 5.1.3) is prominent in the packstones where the third period cement is absent and syn-cementation pore fillers (Section 5.1.5) are found only in this facies, at both Nadorello east and San Biago west. Neomorphism is represented by the common formation of microspar in the wackestones and muddy packstones.

2.4.3 Foraminiferal Grainstone-Packstone Facies

a) Macrofacies: This facies is by far the most widespread and is represented by most of the outcrop in the study area. At Carboj (Fig. 2.3; Plate 2.10) and in the outcrops to the west, including La Conca (Fig. 2.4; Plate 2.11), it represents the entire exposed succession. The facies reaches its maximum thickness at the Carboj dam measured section (41 m). At the southern end of the Carboj ravine it has a thickness of 38 m and at La Conca it is 21.5 m thick. Elsewhere, to the west of Carboj, outcrops invariably expose 4-20 m of succession. To the east of Carboj at Contrada Giovanni (Fig. 2.5), San Biago east (Fig. 2.7) and Tombe Sicani (Fig. 2.8) and in the areas around these figured outcrops the facies contains some intercalations of the rhodolithic algal packstone-wackestone facies, albeit a small amount at San Biago east. Where seen, this facies always unconformably overlies Eocene white limestones (Section 2.6.2) and has a poor development of basal phosphatic conglomerate (Section 2.2.2).

The facies is characterised by massive (0.4-2.0 m) to flaggy (40-100 mm) bedded foraminiferal limestones which weather light grey but have a cream to beige colour when fresh. Flaggy bedding pervades the succession in the La Conca area and to its west. Flaggy beds form the lower 28 m of the succession at San Biago east and they comprise the

exposed succession at Mt Gargalupo (6.5 km to the southeast of San Biagio). Elsewhere they are absent or few. Very occasional cross-bedded units (0.4-0.6 m thick) are found in the succession in the west of the study area, in the measured section at Carboj and in one outcrop in the La Conca area. Macrofauna is scarce. Cidaroid spines are common at Carboj and in the La Conca area. Sparse irregular echinoids are found at only three localities. Crushed examples of small *Echinolampas* (determined by Dr E.P.F. Rose) were found in the Carboj measured section and in the outcrops at the southern end of the Carboj ravine. In the La Conca area, in a road cutting next to the Sciacca-Sambuca road two crushed examples of spatangoid echinoids were found.

b) Microfacies: The facies is characterised by benthonic foraminiferal packstones and grainstones (Plates 2.26-2.34)(poorly washed biosparites, unsorted biosparites and sorted biosparites in Folk (1962) terminology) of generally equal proportions. The former, however, contain only small amounts of mud matrix in their pores (5-20% of pore space is filled). They therefore represent slightly lower energy, poorer washed, versions of the grainstones. In general, grainstones are more common in the Carboj and La Conca areas. Packstones are more common in the succession to the east of Carboj. Sorting is found only in the cross-bedded units (Plate 2.31) except where it is caused by a monotypic *L. (Nephrolepidina)* fauna (Plate 2.32) which is seen in the La Conca and Caltabellotta areas. Well rounded grains are not seen. In the grainstones only minor abrasion of the foraminifera is present. Echinoid grains and algal fragments may be sub-rounded to rounded.

The rocks are wholly carbonate except for the presence of small quantities of glauconite pellets in the La Conca area, at the San Biagio east locality, and in outcrops in the Tombe Sicani area. In the western Nadorello area glauconite and glauconitic minerals are common as infills of foraminiferal chambers and pores of echinoid grains in c.12 m of sediments (Section 6.2). These sediments also contain diagenetic feldspars (Section 5.2).

The facies contains nearly all the benthonic foraminifera listed

in the previous section (2.4.2b). It lacks the very large *L. (Eulepidina) dilatata*, but contains, in addition, a restricted occurrence of *Miogypsina* (found in outcrops in the Caltabellotta area). Other bioclasts are represented by rounded echinoid and algal debris (Plate 2.30, 2.34) and fragments of tubular and fenestrate bryozoans. The relative amounts of these bioclasts vary greatly. Most beds contain a bioclast association of common *L. (Nephrolepidina)* and *Amphistegina* (Plate 2.26). Some beds (in particular, the cross bedded units), however, are dominated by *Amphistegina* and *Rotalia* (Plate 2.31), other beds are formed almost exclusively of *L. (Nephrolepidina)* (Plates 2.32, 2.33). Some beds have abundant echinoid debris, others have relatively abundant bryozoans.

c) Diagenesis: Cement diagenesis in this facies is restricted to the poor development of the first and second periods of cement (Section 5.1.2). As a result of this, compaction (Section 5.1.3) is widespread and has had considerable effect, resulting in rotation or redistribution of grains, fracturing of grains and pressure solution between grains. Neomorphism too (Section 5.1.4) is widespread and takes the form of common microspar and occasional pseudospar formation from lime mud. A restricted occurrence of dolomitisation (Section 5.1.6) is seen at San Biagio east and glauconitisation (Section 6.2) of grains is found in western Nadorello.

2.4.4 Facies Distribution

The rhodolithic algal packstone-wackestone facies is represented by a single bed (4-6 m thick) resting unconformably on Upper Cretaceous chalks with a relatively well developed basal phosphatic conglomerate in the central region of the study area, from the Nadorello area in the south to San Biagio west locality in the north. To the east of this area (and to the eastern limit of the study area) the facies no longer rests on the unconformable surface and is represented by minor intercalations in predominantly foraminiferal grainstone-packstone successions. To the west, at Contrada Giovanni, the facies is found interbedded with the foraminiferal grainstone-packstone facies and to the west of Contrada Giovanni, in the Carboj and La Conca areas, the facies is no longer present.

Conversely, the foraminiferal grainstone-packstone facies forms most of the exposed successions to the east of the centrally positioned Nadorello-San Biagio west outcrops. To the west, a transition series between the two facies is seen at Contrada Giovanni whilst further west in the Carboj and La Conca areas the foraminiferal grainstone-packstone facies represents all the outcrop. Where seen, at San Biagio east and at the southern end of the Carboj ravine, this facies rests unconformably on Eocene white limestones with a very poorly developed phosphatic conglomerate at the base. This unconformable relationship can also be inferred in the Tombe Sicani and Carboj dam areas. The only cross bedded units are found at Carboj dam and to the west whilst small amounts of glauconite pellets are found in the northwest (contradas Magaggiari and Finocchio), north (San Biagio east locality only) and the southeast (in the Tombe Sicani area). *In situ* glauconitisation is seen only in western Nadorello in c. 12 m of sediments.

2.4.5 Conclusion

Two facies are recognised in the Upper Oligocene of southwest Sicily in rocks which have been previously mapped as a single limestone unit. These facies are here named the "rhodolithic algal packstone-wackestone facies" and the "foraminiferal grainstone-packstone facies". The former facies differs from the latter in having: a more massive bedform; common coralline red algal rhodoliths; a more abundant more diverse macrofauna; a microfauna which contains common *L. (Eulepidina) dilatata* but no *Miogyssina*; more muddy packstone, sometimes wackestone lithologies; and more periods of cementation. The rhodolithic algal packstone-wackestone facies is always found associated with a well developed basal phosphatic conglomerate resting on Upper Cretaceous chalk whereas the foraminiferal grainstone-packstone facies rests unconformably on Eocene white limestones with only a poor development of phosphatic conglomerate at the base.

The facies distribution is outlined in section 2.4.4 and in essence shows that the rhodolithic algal packstone-wackestone facies outcrops in the centre of the study area on the unconformable surface. To the west, foraminiferal grainstone-packstone facies form the entire

exposed succession. To the east these grainstone-packstones rest on the unconformity surface and form most of the succession with some intercalations of the rhodolithic facies.

This facies distribution is placed in a palaeogeographic context in section 2.6.2 below, incorporating features of the depositional environment inferred in section 2.5.

2.5 Depositional environment

2.5.1 Introduction

The contained fauna and flora, rock type (or texture), glauconite and carbonate diagenesis are all useful indices of depositional environment. The common faunal and floral content of the two facies and their close, sometimes interbedded, relationship suggests that they were both deposited under similar environmental constraints of: oxidation, salinity, temperature, light intensity and depth. The two facies were, however, deposited under different water energies: the rhodolithic algal packstone-wackestone facies formed in a lower energy environment than the foraminiferal grainstone-packstones. The latter contain occasional cross beds, indicative of at least moderately high energy conditions.

2.5.2 Oxidation

The abundance of a more or less *in situ* benthonic fauna precludes anything other than an oxidising environment for overall deposition. However, the presence of *in situ* glauconite in the western Nadorello area indicates that this area at least was temporarily within the oxygen minimum zone. Moreover, the presence of early marine ferroan calcite cements in the same area indicates a reducing environment soon after sediment deposition. It is therefore inferred that this part of the area was sheltered from main currents with consequently reduced circulation.

2.5.3 Salinity

All the fauna and flora of the sediments, together with the glauconite found in western Nadorello, suggest accumulation under normal

marine salinities. Echinoderms and bryozoans lack mechanisms to control internal ionic concentrations in low and high salinities, and are therefore restricted to normal salinities (*circa* 34-37‰) (Schopf, 1980). Coralline red algae prefer normal marine salinities and few species can tolerate low salinities (Adey & McIntyre, 1973).

The ecological preferences of some living benthonic foraminifera are given by Murray (1973). Of those listed, *Amphistegina*, *Rotalia*, *Heterostegina* and *Operculina* are present in the Sicilian Chattian and all are found today in normal marine salinities of 33-37‰. *Heterostegina* can tolerate hypersaline conditions of > 37‰, *Rotalia* is restricted to salinities of 36-38‰, and *Amphistegina* is generally found in salinities > 34‰. In general, however, hyaline calcareous foraminifera dominating the benthonic foraminiferal association (as they do here) represent accumulation under intermediate (normal) salinities (Murray, 1973).

In ancient deposits, in studies of Oligo-Miocene sediments from Australia, Chaproniere (1975) concluded that *Lepidocyclina* (*Eulepidina*), *Heterostegina*, *Cycloclypeus*, *Operculina* and some species of *L.* (*Nephrolepidina*) lived in normal saline environments though at different depths. Bennett (1980) in a study of Upper Oligocene Limestones from the Maltese islands (Coralline Limestone Formation) concluded that an assemblage of *Amphistegina*, *Heterostegina*, *Lepidocyclina*, *Cycloclypeus*, *Spiroclypeus* and *Miogypsina* in sediments associated with coralline red algae and a diverse macrofauna represented accumulation in normal marine conditions.

Finally, glauconite although a diagenetic mineral, forms on, or just below, the sediment water interface and can therefore be used to indicate depositional environment. Where it is marine in occurrence, it is indicative of normal marine salinities (McRae, 1972) or an "open marine environment" (Odin & Letolle, 1980).

2.5.4 Temperature

The coralline red algal assemblage is dominated by the cool water genera *Lithothamnium* and *Mesophyllum* over the warm water genera *Archaeolithothamnium*, *Lithophyllum* and *Lithoporella* and therefore represents

accumulation in cool waters (Section 4.1.4).

Data from Murray (1973) suggest that *Amphistegina* is restricted to bottom water temperatures of 25-26°C, whilst *Rotalia* tolerates temperatures between 14-25°C, and *Heterostegina* and *Operculina* are restricted to tropical waters. Subsequent work by Hallock (1979) would, however, suggest that this narrow 25-26°C temperature range given for *Amphistegina* is wrong since it is found extending to the limit of the photic zone (and therefore to cooler temperatures) around the Caroline islands and Hawaii. Also, Cushman (1970) records common *Amphistegina* from sediments in bottom water temperatures of 7-13°C around the Philippine islands.

Benthonic foraminifera size is correlated with temperature (Haynes, 1981). Within benthic marine species, higher latitude (and therefore cooler water) populations tend to breed at a later age and less often than lower latitude (and warmer water) populations. Consequently, higher latitude populations tend to be older and larger (Schopf, 1980). In marine bivalves, the largest species of a genus (or family) is said to live in the coldest water (Nicol, 1967).

The large size of the Sicilian Chattian fauna, in particular *L. (Eulepidina) dilatata*, the large species of the echinoids *Clypeaster* and *Echinolampas*, and the bivalve *Chlamys*, along with their low diversity and, in the case of the macrofauna, small population may indicate accumulation in cool temperatures. The benthonic foraminifera, although abundant, do not form a thick sequence of sediments. Although the top of the sequence is never seen, their slow accumulation is evidenced by the formation of glauconite (where the conditions are conducive). This slow rate of reproduction is another indication that temperatures are cool (Haynes, 1981, Schopf, 1980).

Finally, in diagenesis, the general lack or poor development of marine cements suggests that we are dealing with cool (deep) (CaCO₃) undersaturated waters rather than warm (shallow) saturated or super-saturated waters. Also, *in situ* glauconite indicates a fairly narrow

range of bottom water temperatures during its formation, of between 7-20°C (Section 6.6.3).

2.5.5 Light Intensity

The presence of well preserved and therefore autochthonous coralline red algae indicates that the deposits formed within the photic zone. However, these algae utilise light from the more penetrative blue-green wave band and can therefore live in very low light intensive (deep) waters. The presence of large benthonic foraminifera may also indicate light penetrated waters. In many living species various algae occur in their endoplasm and ectoplasm with a possible symbiotic relationship (Haynes, 1981). Hallock (1979) lists fifteen species of large foraminifera which are known or suspected to maintain algal symbionts. Of those listed *Amphistegina* and *Heterostegina* are present in the Sicilian Upper Oligocene. If it is assumed that these and other genera of large foraminifera maintained algal symbionts in the geologic past, then this too would suggest that the Sicilian Chattian was deposited in light penetrated waters.

2.5.6 Depth

Given that the position of southwest Sicily was tropical-subtropical in the Upper Oligocene (Smith & Briden, 1977), all criteria point towards deposition on a deep shelf. The mere presence of the coralline red algae *Archaeolithothamnium* and *Lithoporella* would suggest tropical-subtropical latitude, as would the presence of *Heterostegina* and *Operculina* (providing their environmental preferences have not changed significantly from Oligocene to Recent). However, the predominance of the cool water genera *Lithothamnium* and *Mesophyllum* suggests deposition in cooler, deeper waters in a tropical-subtropical environment, and a depth of 80-250 m can be estimated from the coralline algal assemblage (Section 4.1.4).

In general, those features listed above as being indicative of cooler temperatures also suggest deeper shelf environments in tropical-subtropical latitudes. Of the foraminifera present, Cushman (1970) has recorded, from the seas around the Philippine islands, the common

occurrence of *Amphistegina* in depths of 40-100 m *Heterostegina* (20-80 m), *Operculina* (20-80 m) and *Rotalia* (40-100 m, frequently 200 m). Different species have different depth ranges and commonly these genera extend above and below the limits given above. Hallock (1979) shows that species of *Amphistegina* prefer different depth ranges around the Caroline islands and Hawaii, one species extending into waters as shallow as 5 m, whilst another is restricted to water depths > 30 m to the base of the photic zone. Foraminifera, as genera rather than species, are therefore only broadly useful as palaeobathymetric indices. However, the predominance of hyaline calcareous foraminifera along with the absence of any Miliolida (which are indicative of very shallow waters, *vide* Haynes, 1981), absence of Nodosariida, and near absence of Textulariida (both indicative of deeper waters in areas of normal salinities, Haynes, 1981) suggest deposition on a shelf of moderate depth (Murray, 1973).

Finally, McRae (1972) notes that in tropical areas, warm water conditions prevent glauconitisation until cooler waters are attained at depth. Consequently, Porrenga (1967) found that glauconite occurs at depths of 125-250 m off the Niger delta. Above 125 m, chamosite and goethite occur.

2.5.7 Water Turbulence

Evidence from the rhodoliths and lithologies indicates that the rhodolithic algal packstone-wackestone facies is of a lower energy environment than the foraminiferal grainstone-packstone facies. This energy difference, however, does not appear to be great.

Rhodolith formation requires regular gentle movement to allow concentric growth. Too much movement and the algae would become fragmented, with too little movement the algae stabilise and coalesce. Consequently, rhodolith substrates have packstone lithologies with common settling features (umbrella and geopetal structures) produced by their periodic movement. Where the substrate is well developed (at Nadorello east and San Biagio west) it is muddier and the rhodoliths have growth forms indicative of relatively lower energy whereas where

the rhodolith beds are intercalated with the (higher energy) foraminiferal grainstone-packstones they are less muddy and the rhodoliths have massive non-branching growth forms indicative of higher energy environments (Section 4.1.3).

The absence or paucity of matrix in the foraminiferal grainstone-packstones indicates that they formed in a higher energy environment than the rhodolithic packstone-wackestones. However, this energy increase is not excessive since: some matrix is present; the grains of the grainstones are not rounded and are only occasionally sorted; and only two cross bedded units were found throughout the whole study area. Also, the presence of *in situ* glauconite formation in the western Nadorello area in these deposits suggests some, but not excessive, turbulence (Section 6.6.4).

In conclusion, therefore, it is suggested that the foraminiferal grainstone-packstone facies is of only slightly higher water energy than the rhodolithic algal packstone-wackestones. Where the former is found interbedded with the latter, it is possible that *Lepidocyclina* (*Eulepidina*) *dilatata*, found only in the rhodolith facies, was large enough to form a stable substrate which the algae could then colonise (rhodoliths are often found with these foraminifera as their nucleus). Thus formed, the rhodoliths then acted as a baffle to trap mud. In this way, the two facies could form in an environment of very similar water energies.

2.5.8 Summary

The above data indicate deposition of the Upper Oligocene limestones in well oxygenated, normal saline, cool waters within the photic zone at depths of 80-250 m at a tropical-subtropical latitude. Each of the two facies, however, probably accumulated in slightly different water energies: the rhodolithic algal packstone-wackestone facies in a slightly lower water energy environment than the foraminiferal grainstone-packstone facies.

2.6 Palaeogeography of the Saccense Carbonate Platform

2.6.1 General

The palaeogeographic evolution of western Sicily from Triassic to Oligocene times is outlined in section 1.4, and the palaeogeography of western Sicily for Middle Cretaceous to Eocene times is given in Figure 1.4 (after Catalano & D'Argenio, 1978). At that time, the area now represented by western Sicily comprised three carbonate platforms separated by two basins, all with an east-west trend. The Upper Oligocene limestones described here are located on the southernmost platform, the Saccense Carbonate Platform.

Although Catalano & D'Argenio (1978) make no mention of it, evidence from outcrops in the Mt Kronio-Contrada Suvaretto area (just to the east of Sciacca, near the coast) indicates that the platform was bounded to the south by another basin. The Eocene facies of this area is dominated by re-sedimented limestone conglomerates and calcarenites (turbidites) commonly showing grading, sometimes displaying sole structures, and occasionally channels can be seen. These limestones are interbedded with deeper water calcisiltites with flints, representing autochthonous sedimentation in the area. The facies suggests accumulation in a relatively steep, sharp slope environment during Eocene times. This steep slope and presumably sharp shelf break is further suggested by the presence of Lower and Middle Oligocene reefal deposits throughout the Mt Kronio area. The Saccense Carbonate Platform was, in terms of Read's (1982) terminology, an "isolated carbonate platform", for which it shows all the indicative features, including the necessary shallow water carbonates surrounded by deeper water deposits, at least in Eocene-Middle Oligocene times.

Whilst the southern boundary of this platform can be demonstrated to be sharp and steep, there is no evidence for this in the Eocene and possible Oligocene at the northern boundary of the platform. Neither is there evidence (such as the interfingering of deep and shallow water deposits) to suggest that the boundary with the basin to the north was gradual. However, in the Maastrichtian to Palaeocene of the Mt Genuardo area there are "megabreccia" deposits (Catalano & D'Argenio, 1978) -

fault generated conglomerates suggesting that the boundary was tectonically active, steep and probably sharp, at least by the beginning of the Tertiary.

2.6.2 Upper Oligocene

As described above, two facies are recognised in the Upper Oligocene: a rhodolithic algal packstone-wackestone facies and a foraminiferal grainstone-packstone facies. (These facies, located on the Saccense Carbonate Platform, pass northwards into an argillaceous Upper Oligocene sequence situated in the Sicani Basin which underlies the Lower Miocene Limestones described in Chapter 3). The algal facies is best developed at the base of the succession in the centre of the study area where it rests on Upper Cretaceous chalk with a well developed phosphatic conglomerate at the base. The foraminiferal facies is found in the west and east of the area where it rests on Eocene calcilutites with a minimal development of basal phosphatic conglomerate.

Figure 2.9 explains these features in terms of differential subsidence. It is inferred that Lower Tertiary, mainly Eocene (with some Oligocene, *vide* Campisi, 1968), calcilutites were deposited on top of Upper Cretaceous chalks. These Eocene calcilutites were then eroded, forming a channel or elongate trough in the centre of the study area. This trough extended from Nadorello in the south to San Biagio in the north. Its location may have been governed by block faulting in the underlying Cretaceous (Fig. 2.9A). Until this time the Upper Cretaceous - Lower Tertiary succession may not have been, or was only partially, lithified. This is indicated by the burrows at Nadorello east (Section 2.2.1) and may explain the general lack of lower Tertiary clasts in the basal conglomerate.

This trough, when formed (Fig. 2.9B), became the site for minor conglomerate formation and dumping and subsequently low energy rhodolithic algal limestones which were sheltered from currents in the depression (Fig. 2.10). The foraminiferal grainstone-packstones were, however, deposited on the bordering current-swept topographic high areas. Minor developments of the rhodolithic algal facies were able to form in

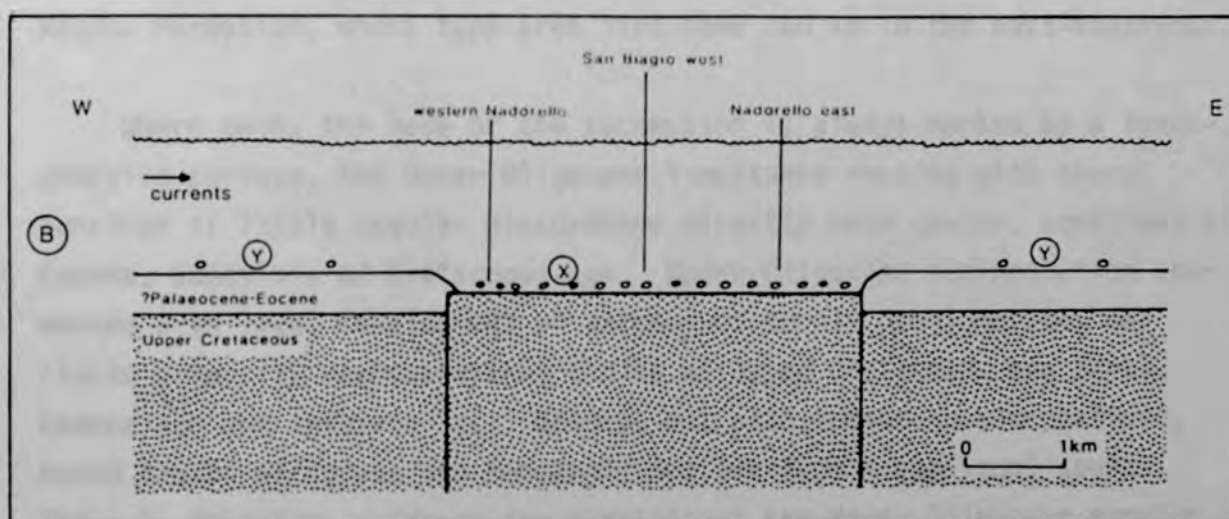
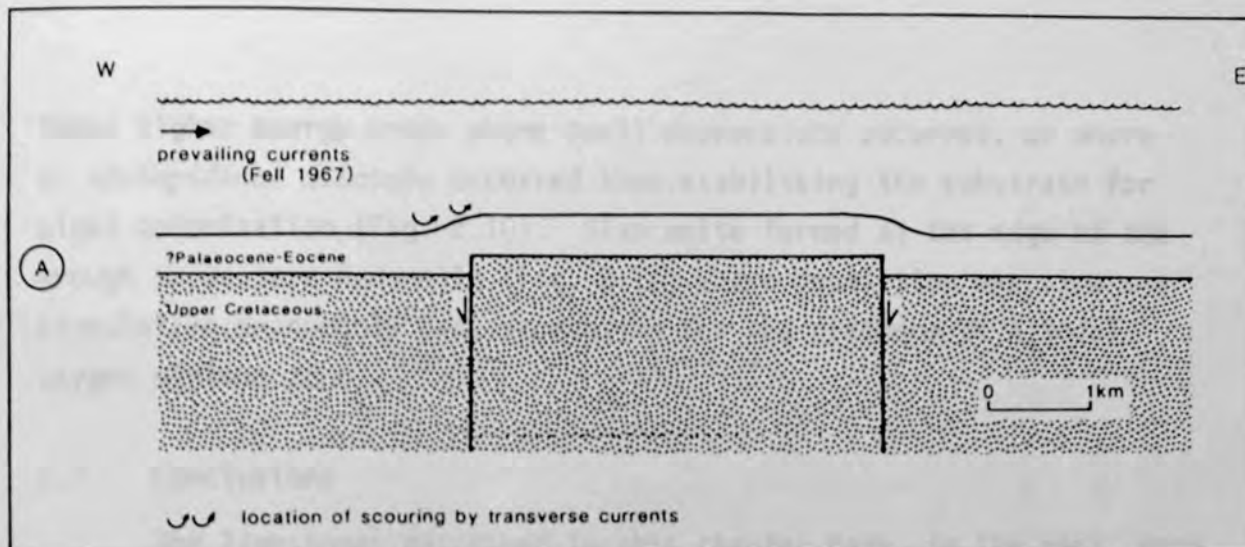


Figure 2.9. Upper Oligocene facies distribution explained by fault control. A: scouring and erosion of the pre-Upper Oligocene substrate is governed by faults in the Upper Cretaceous chalk. B: scouring and erosion completed, the basal Upper Oligocene conglomerate is deposited on the Upper Cretaceous rocks exposed in the trough (x) which is sheltered from the transverse currents and becomes the site for the rhodolithic algal packstone-wackestone facies. The foraminiferal grainstone-packstone facies is deposited on the current swept highs (y) where Palaeogene rocks are exposed.

these higher energy areas where small depressions occurred, or where *L. (Eulepidina) dilatata* occurred thus stabilising the substrate for algal colonisation (Fig. 2.10). Glauconite formed at the edge of the trough in western Nadorello (Fig. 2.10) where deposition was slow and circulation presumably bad, accounting for the presence of a local oxygen minimum zone.

2.7 Conclusions

The limestones described in this chapter have, in the past, been imprecisely or in part incorrectly dated as Upper Oligocene - Lower Miocene in age. They are here ascribed to the Upper Oligocene (Chattian), and correlated as the westward equivalent of the Irminio Member of the Ragusa Formation, whose type area lies some 160 km to the east-southeast.

Where seen, the base of the succession is always marked by a transgressive surface, the Upper Oligocene limestones resting with sharp junction if little angular discordance directly onto chalks, sometimes of Eocene, sometimes of Cretaceous age. Upper Oligocene sedimentation commenced with local development of patches of cobble conglomerate, the clasts primarily unphosphatised chalks of Upper Cretaceous and partly Eocene age and inferred local origin, but also including phosphatised, bored chalks of Eocene age seemingly derived from a non-local source. There is therefore evidence for significant pre-Upper Oligocene erosion, following deformation sufficient to make Cretaceous as well as Eocene rocks accessible to erosion, and evidence too for an Eocene period of phosphatisation of an adjacent area, perhaps reflecting closer proximity than previously recognised of the Cretaceous - Eocene phosphogenic province of North Africa.

The limestones form discrete outcrops, now separated by the effects of Upper Miocene - Pliocene tectonism and later erosion. Although hitherto mapped as a single unit, two major facies may be distinguished: a rhodolithic algal packstone-wackestone facies and a foraminiferal grainstone-packstone facies. From the contained flora, macrofauna and microfauna and authigenic glauconite mineralisation, it is inferred that the limestones were all deposited in cool oxygenated waters of normal

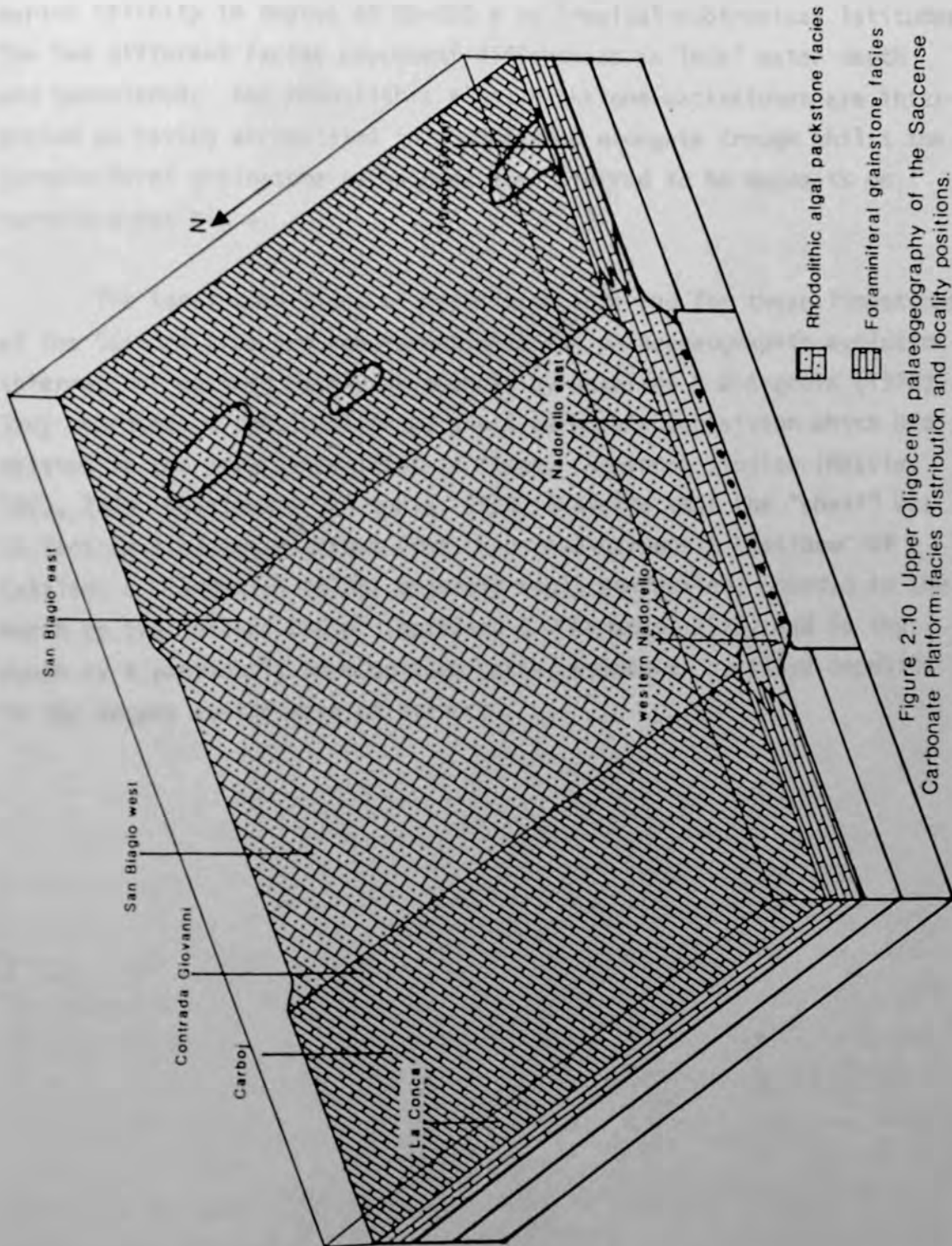


Figure 2.10 Upper Oligocene palaeogeography of the Saccense Carbonate Platform: facies distribution and locality positions.

marine salinity in depths of 80-250 m in tropical-subtropical latitudes. The two different facies represent differences in local water depth and turbulence: the rhodolithic algal packstone-wackestones are interpreted as having accumulated in a sheltered elongate trough whilst the foraminiferal grainstone-packstones are inferred to be deposits on current-swept highs.

The local conditions of deposition inferred for these limestones of the Sciacca area are consistent with the palaeogeographic evolution inferred for western Sicily as a whole by Catalano & D'Argenio (1978). They represent a continuation of shelf carbonate deposition which had existed in the area since Triassic times. Regional studies (Masche, 1973, 1979; Catalano & D'Argenio, 1978) indicate that the "shelf" was in fact an isolated platform (the "Saccense Carbonate Platform" of Catalano & D'Argenio, 1978), arguably fault controlled, bounded in the north by the "Sicani Basin" (Catalano & D'Argenio, 1978) and in the south by a previously unrecognised basin, evidenced by slope deposits in the Eocene to the east of Sciacca.

CHAPTER 3

LOWER MIOCENE LIMESTONES

3.1 Introduction

3.1.1 General

Lower Miocene glauconitic limestones are well known in western Sicily (Section 3.1.2) where they form an extensive though fragmented outcrop. The limestones described here are located in two main areas. Most are found partially encircling the Mesozoic outcrops which form the upland area of Mt Genuardo (situated immediately north of the Upper Oligocene limestones described in Chapter 2) and are bounded by the towns of San Margherita di Belice, Sambuca, Giuliana, Bisacquino and Contessa Entellina (Fig. 1.5). The second area comprises a single comparative section from Mt Cardellia near Corleone, some 18-20 km NNE of Mt Genuardo (Fig. 1.5).

In the Mt Genuardo area these rocks are more poorly exposed than the Upper Oligocene limestones described in the previous chapter. To the west, north and east of Mt Genuardo, they form a series of discrete, mostly grass covered ridges (2-5 km long) with broken outcrop along their length (Plates 3.1, 3.2). These ridges are separated from the Mesozoic rocks of Mt Genuardo by a series of depressions formed by Upper Oligocene mudstones and marls (Section 3.3.2; Mascle, 1973, 1979, map encl.). Bedding in the ridges dips ($20-60^{\circ}$) consistently away from the Mesozoic massif.

To the west of Mt Genuardo the Lower Miocene limestones form the Serra Lunga ridge (Plate 3.1) from UB 319733 to UB 352748. To the north they form the ridge of Costa del Conte (Plate 3.2) (UB 353774 to UB 368768) and the upland areas from Cozzo Parrino (UB 324762) to Bufalo (UB 382760) along with the ridge to the immediate south of Contessa Entellina (between UB 383770 and UB 406771) and the upland areas to its east from UB 415780 to UB 443756. Finally, to the east of Mt Genuardo, the limestones are

poorly exposed, forming a number of poorly defined upland areas to the southwest of Bisacquino and north of Giuliana between UB 446744 to UB 433723.

At Mt Cardellia the limestones are well exposed and form a south facing cliff feature (between UB 532819 and UB 555813) which caps an Upper Oligocene argillaceous sequence (also well exposed) below (Plate 3.5).

3.1.2 Previous Work

There is no work which deals with these particular limestones in any detail. Daina (1965), Blondeau *et al.* (1972) and Mascle (1973, 1979) briefly describe the succession at Mt Cardellia. Mascle (1973, 1979) partially maps the extent of Lower Miocene glauconitic sandy limestones (his "serie greso-glauconieuse") in southwest Sicily and very briefly describes the succession at Battellaro and Serra Lunga. Other works which refer to these rocks generally incorporate more extensive areas and stratigraphy and are usually of a structural interest. They include those works listed under "Previous Work" for the Upper Oligocene limestones (Section 2.1.2), together with Checchia Rispoli (1911) Roccatti (1911) and Castany (1956). Elsewhere in western Sicily, Lower Miocene glauconite bearing rocks have featured, with variable extent, in the works of: G.G. Gemmellaro (1859, 1902), M. Gemmellaro (1912, 1914), Floridia (1931), Jacobacci (1955), Marchetti (1956), Ruggieri (1957, 1959), Accordi (1958), Campisi (1958), Colacicchi (1958), Schmidt di Friedberg (1959, 1962), Schmidt di Friedberg *et al.* (1960), Broquet (1962, 1964, 1968, 1970, 1972), Broquet *et al.* (1963), Duee (1965, 1969), Wezel (1966, 1967, 1969, 1970) and Broquet & Duee (1967).

3.1.3 Stratigraphic Nomenclature

The Lower Miocene glauconitic limestones of western Sicily have been attributed to different formations by different authors. Marchetti (1956) and Flores (1959) place them in the Alia and Tavernola Formations; Colacicchi (1958) and Campisi (1958) put them in the Geraci Formation; Schmidt di Friedberg *et al.* (1960) place them in the Collesano Formation; whilst Schmidt di Friedberg (1962) includes them in the Bonifato Formation.

The deposits are included in the "flysch oligocene-aquitanean" of Accordi (1958), the "inerte argilo-gresuse" of Schmidt di Friedberg (1959), and the "serie greso-glaucouneuse" of Mascle (1973, 1979).

Schmidt di Friedberg (1962) describes and defines the Bonifato Formation (from Mt Bonifato near Alcamo, 40 km to the north-northwest of the study area) to include Upper Oligocene and Lower Miocene limestones, argillaceous limestones and glauconitic limestones. The author then recognised the lateral extension of this formation to include Lower Miocene glauconitic limestones from the Sicani Mountains. This lateral extension was agreed by Blondeau *et al.* (1972) and in subsequent works by Mascle (1973, 1979). Inclusion of the Lower Miocene glauconitic sandy limestones in the Bonifato Formation is therefore accepted here.

3.1.4 Correlation

Previous publications all agree on a Lower Miocene (Aquitanean-Burdigalian) age for these glauconitic sandy limestones though they rarely, if ever, give their reasons for this. At Mt Cardellia there is a thick (*c.* 210 m), continuous, well exposed Upper Oligocene to Lower Miocene succession which has yielded an abundant and diverse planktonic and benthonic foraminiferal fauna useful in dating the succession precisely. Blondeau *et al.* (1972) provide an extensive faunal list from this locality. Their lower 40 m consists of greyish marls that have yielded a fauna of: *Globigerina rohri*, *G. venezuelana*, *G. cf. sellii*, *G. ciproensis angulisuturalis*, *G. ciproensis angustiumbilitata*, *G. cf. praebulloides*, *Globigerina* sp., *Globigerinita dissimilis*, *G. unicava*, *Globorotalia opima opima*, *G. opima nana*, *Pullenia cf. bulloides*, *Stilostomella cf. verneuili*, *Cibicides* sp., *Gyroldina* sp., *Uvigerina cf. rustica*, *U. havanensis*, *Bolivina* sp., *Lenticulina* sp., *Planulina* sp., *Ellipsoglandulina multicostata*, *Pleurostomella* sp. and *P. cf. brevis*. Above are 60 m of grey green grey red sandy marls containing: *Globigerina rohri*, *G. venezuelana*, *G. cf. sellii*, *G. gr. ciproensis*, *G. ciproensis angustiumbilitata*, *Globorotalia opima opima*, *G. opima nana*, *Globigerinita dissimilis*, *G. unicava*, *Pullenia bulloides*, *Sphaeroidina cf. bulloides*, *Planulina cf. renzi*, *Cibicides* sp., *Uvigerina cf. rustica*, *Uvigerina* sp.,

Stilostomella verneuli, *S. verneuli paucistriata* and *Ellipsoglandulina multicostata*. These beds are overlain by 40 m of marls and sands with some beds of glauconitic sandy limestones containing *Globigerina venezuelana*, *G. gr. ciperensis*, *G. cf. praebulloides*, *Globigerinita dissimilis*, *G. unicava*, *Globorotalia gr. opima*, *G. opima nana*, *Pullenia bulloides*, *Sphaeroidina cf. bulloides*, *Planulina cf. renzi*, *Uvigerina cf. rustica*, *Uvigerina sp.*, *Pleurostomella sp.*, *Stilostomella sp.*, *S. verneuli*, *Bolivina sp.*, *Vulvulina spinosa* and *Vulvulina sp.*

The first two associations Blondeau *et al.* (1972) attribute to undifferentiated Oligocene but the third is said to be indicative of an Upper Oligocene - Lower Miocene (Aquitanian) age. The relative abundance of *G. venezuelana*, *G. ciperensis* and *G. rohri* in the lower association may suggest that they too are of Upper Oligocene age (Stainforth *et al.*, 1975). Capping this sequence are massive glauconitic limestones which yielded *Nephrolepidina* and *Miogypsina cf. gwyteri* at the base, and *Nephrolepidina* and *Miolepidocyclina cf. burdigalensis* at the top which indicate a Lower Miocene (middle Aquitanian - lower Burdigalian) age (Blondeau *et al.*, 1972).

In the region of Mt Genuardo neither Blondeau *et al.* (1972) or Mascle (1973, 1979) list any fauna from the grey mudstones and marls in the area although they assign them to the Oligocene. In the overlying glauconitic sandy limestones, however, Mascle records a fauna of *Lepidocyclina (Nephrolepidina) sp.*, *Spiroclypeus sp.*, *Operculina sp.*, *Heterostegina sp.*, *Amphistegina sp.* and *Miogypsina cf. globulina* which he ascribes to the Lower Miocene.

In this work a fauna of common to abundant *Miogypsina* along with (in decreasing proportions) *L. (Nephrolepidina)*, *Amphistegina*, *Heterostegina*, *Operculina*, *Rotalia*, *L. (Eulepidina)*, *Spiroclypeus* and *Sphaerogypsina* has been identified from the glauconitic sandy limestones throughout their outcrop but especially in the Mt Genuardo area. This association differs significantly from that found in the Chattian limestones described in the previous Chapter in containing common to abundant *Miogypsina*. As stated previously (Section 2.1.4), *Miogypsina* is known to

range from Chattian into the Lower Miocene (Beggren, 1971), becoming abundant only in Lower Miocene times. The abundant *Miogypsina* recorded here, therefore, suggests a Lower Miocene age for the sandy glauconitic limestones.

3.2 Stratigraphic Sections

Four sections through the Lower Miocene glauconitic sandy limestones are described and illustrated here to characterise the widespread facies. Figures give descriptions of macrofacies, microfacies and diagenesis; and the positions of samples used in geochemical analysis of glauconites are also indicated. Plates indicate the line of measured section.

Three of the four sections are situated in the Mt Genuardo area (see location map, Fig. 1.5) on the Mt Genuardo structural stratigraphic unit (Section 1.3): Serra Lunga, Costa del Conte and Battellaro. These three localities are representative of the succession in their immediate area; they illustrate variations and/or consistencies in the succession throughout the Mt Genuardo area; have a relatively thick succession; show extensive local exposure with favourable weathering characteristics; they are accessible, both to the locality and through the stratigraphy; and they are widespread in geographic distribution thus giving widespread reference localities for this unit.

The fourth section, Mt Cardellia, is situated 18-20 km to the NNE on the Mt Barracu-Mt Colomba structural stratigraphic unit (Catalano & D'Argenio, 1978, 1981; see also section 1.3). This last stratigraphic section is presented here to facilitate comparison in lithologies between the two structural stratigraphic units supposedly (Catalano & D'Argenio, 1978) situated respectively at the southern edge and in the centre of the Sicani Basin in Lower Miocene times. Moreover, the Mt Cardellia sequence ranges conformably from Oligocene into Lower Miocene and facilitates comparison with the Upper Oligocene strata to the south described in Chapter 2.

The positions of the four localities are indicated on the outcrop

KEY TO FIGURES 2.2 = 2.8 and 3.1 = 3.4

FAUNA



Echinoids



Cidaroid spines



Chlamys



Leptocyclus (Eulepidina)

FLORA



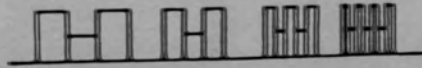
Red algal rhodoliths

LITHOCLASTS



Phosphatised and unphosphatised chalk lithoclasts

LITHOLOGY



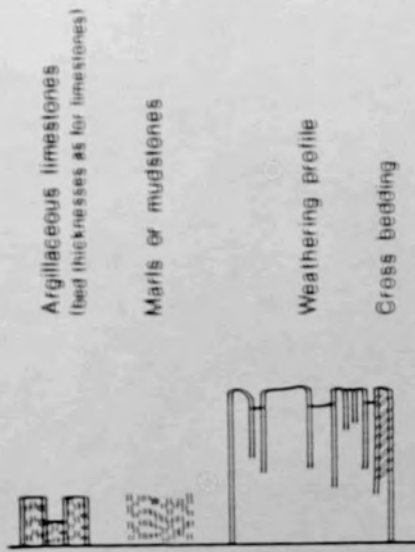
10 - 6.0m beds

0.4 - 1.0m beds

0.1 - 0.4m beds

< 0.1m beds

Limestones



Argillaceous limestones
(bed thicknesses as for limestones)

Marls or mudstones

Weathering profile

Cross bedding

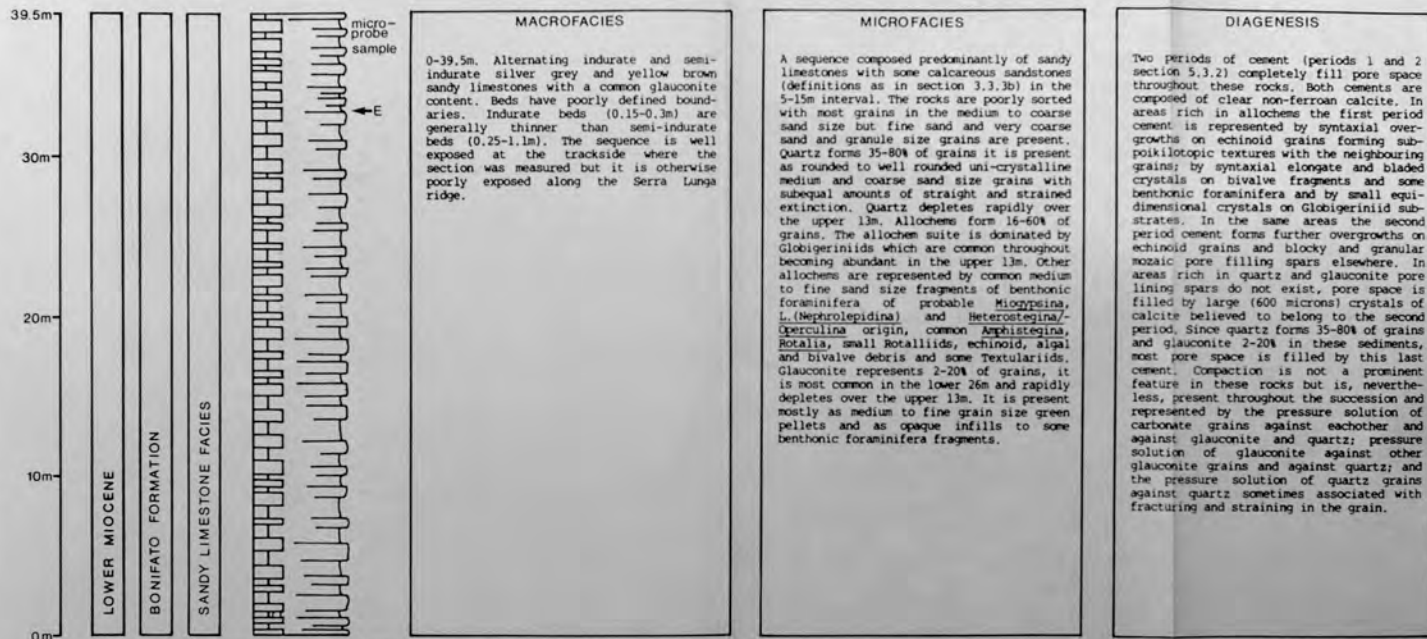


Figure 3.1 Serra Lunga measured stratigraphic section.

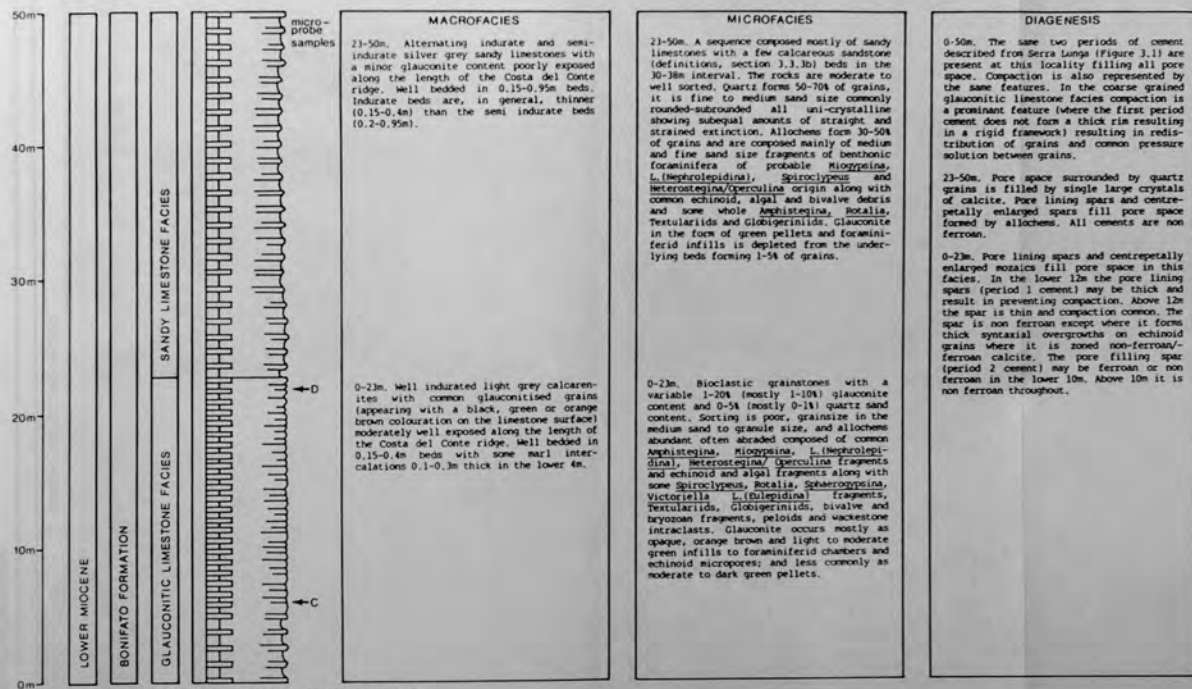


Figure 3.2 Costa Del Conte measured stratigraphic section

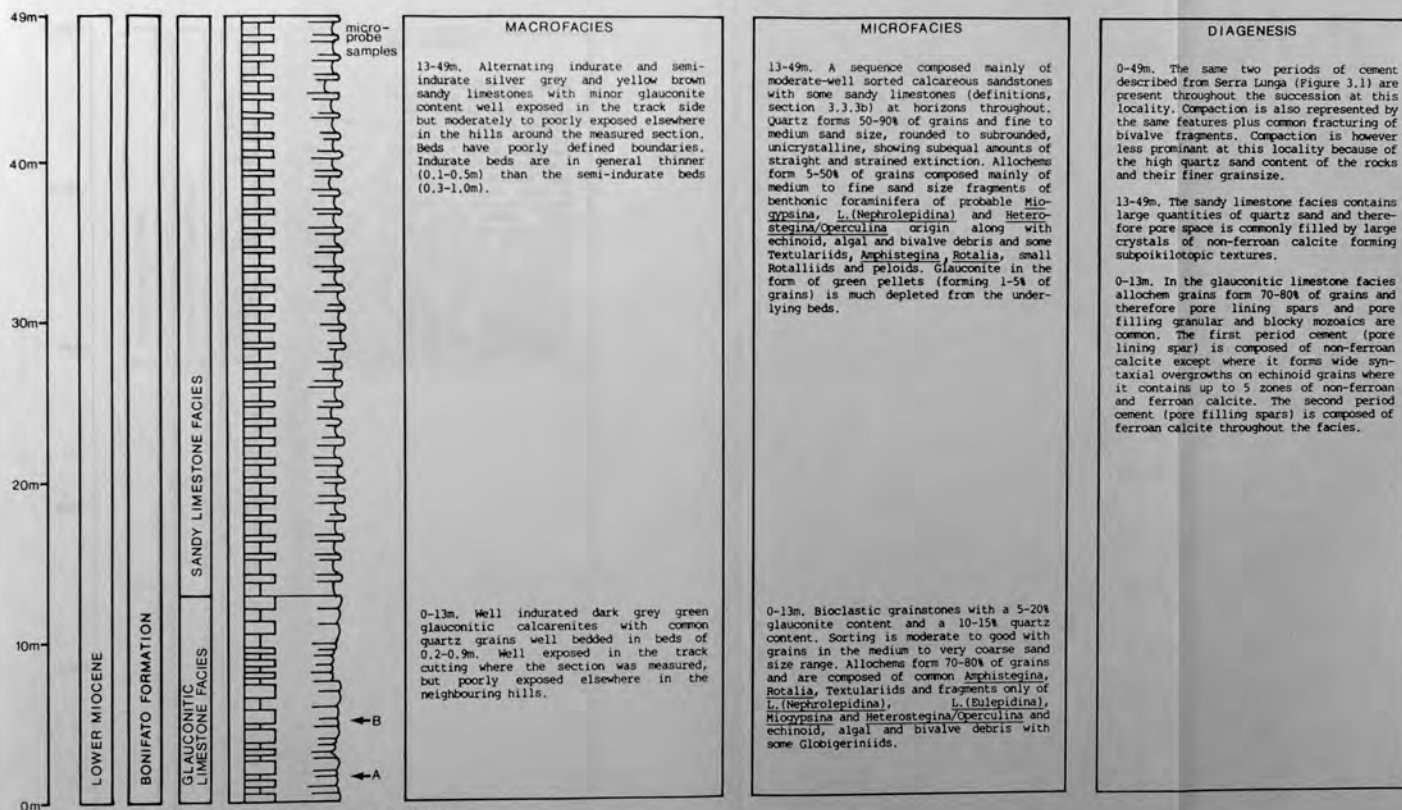


Figure 3.3 Battellaro measured stratigraphic section.

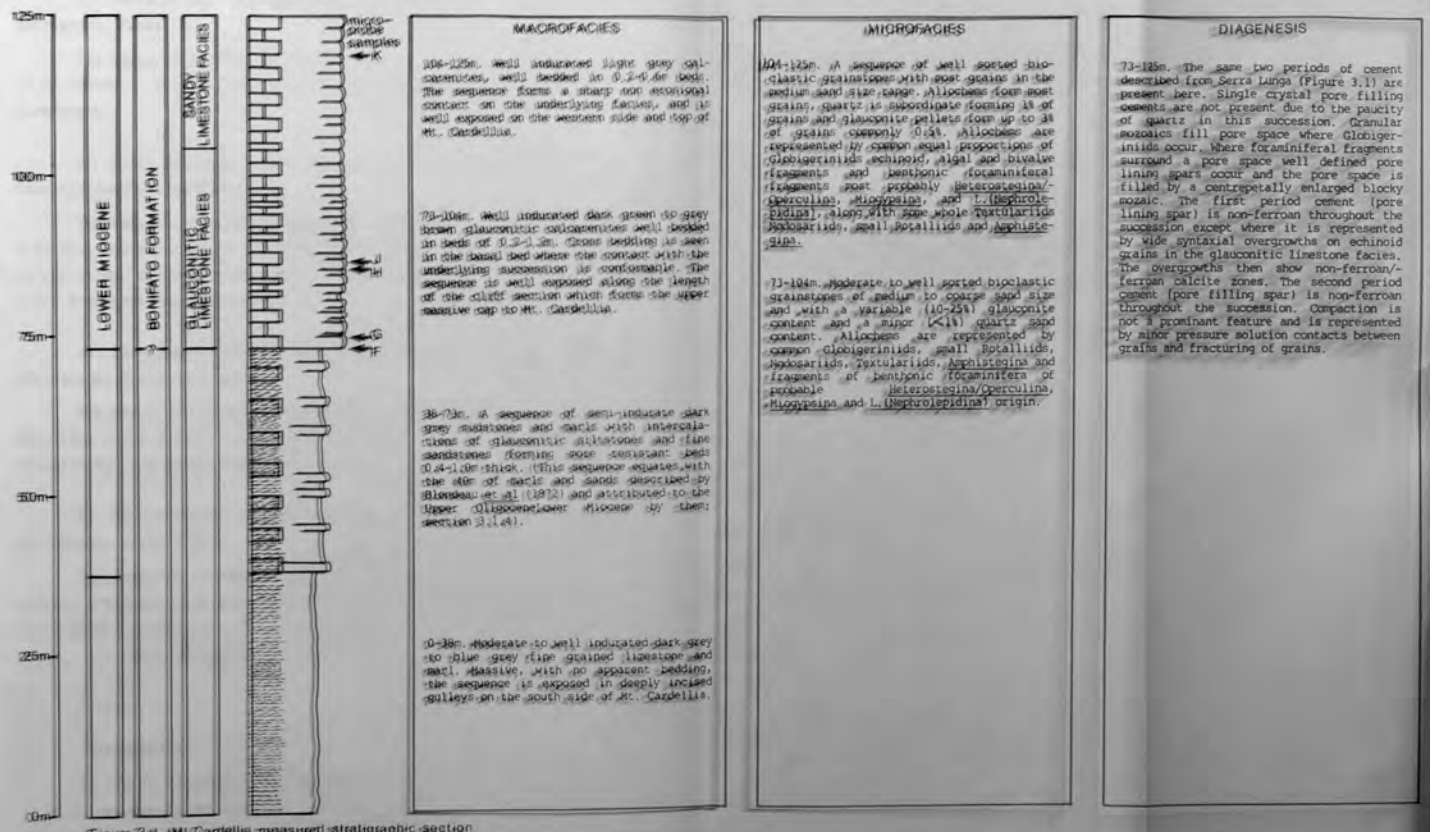


Figure 31A MI Cardellia measured stratigraphic section.

map, Figure 1.5. The localities are, as follows:

1) Serra Lunga. Stratigraphic section, Figure 3.1; locality photograph, Plate 3.1.

The measured section is situated 5.5 km due north of Sambuca at UB 350747. It takes the form of a cutting at the side of a rough farm track.

2) Costa del Conte. Stratigraphic section, Figure 3.2; locality photograph, Plate 3.2.

The measured section is situated 8 km north northeast of Sambuca, 4 km west southwest of Contessa Entellina at UB 358770. It was measured on the steep, south facing, slope of Costa del Conte adjacent to a mule track transgressing this slope.

3) Battellaro. Stratigraphic section, Figure 3.3; locality photograph, Plates 3.3 and 3.4.

The measured section is situated 2 km due east of Contessa Entellina at UB 424774. The section takes the form of a track cutting immediately west of the Battellaro fortress.

4) Mt Cardellia. Stratigraphic section, Figure 3.4; locality photograph, Plate 3.5.

The measured section is situated 17 km northeast of Mt Genuardo (around which sections 1-3 are positioned), 6 km southeast of Corleone at UB 539813 (lower part of the succession) and at UB 533818 (upper part). The measured section is dog-legged as indicated in Plate 3.5.

3.3 Facies

3.3.1 Introduction

In the Mt Genuardo area, two facies, recognisable in the field, in rocks previously regarded as a single unit (Masclé, 1973, 1979; Catalano & D'Argenio, 1978), are distinguished by their glauconite and quartz sand content respectively. They are termed here the "glauconitic

limestone facies" and the "sandy limestone facies". The former characterises the lower part and the latter the upper part of the succession. The facies differ in grain size, allochem assemblage and diagenesis, as well as in their glauconite and quartz sand content.

At Mt Cardellia, the sandy limestone facies is not seen. There the glauconitic limestone facies is overlain by limestones which in other respects (allochems, low glauconite content, and diagenesis), are similar to the sandy limestone facies but they contain little or no quartz sand. Because of their similarity, they are considered together with the sandy limestone facies here.

3.3.2 Glauconitic Limestone Facies

a) Macrofacies: In the Mt Genuardo area the facies has a thickness of 13-27 m and is found in all the Lower Miocene outcrops (except the Serra Lunga ridge) where it forms the lower part of the succession. The facies rests with apparent conformity on dark grey mudstones, siltstones and marls of Upper Oligocene age (see Section 3.1.4) as can be seen at an inaccessible cliff in the Costa del Conte ridge, and which can be inferred by the proximity of Upper Oligocene marl outcrops in the Battellaro area. The facies is, in turn, conformably overlain by sediments of the sandy limestone facies.

At Mt Cardellia the facies is 31 m thick and rests conformably on a sequence of dark grey mudstones and marls with intercalations of glauconitic siltstones and fine sandstones, all of Upper Oligocene - Lower Miocene (Aquitania) age (see Section 3.1.4). The facies is conformably overlain by a non-sandy equivalent of the sandy limestone facies.

At both Mt Genuardo and Mt Cardellia the limestones are dark green, grey brown in colour, well bedded in beds 0.1-1.2 m but most commonly 0.2-0.6 m thick. At Costa del Conte and Mt Cardellia the lower beds are separated by intercalations of soft marls 0.02-0.3 m thick; in the upper parts and elsewhere the intercalations are absent. Cross bedding is seen in only the one bed which marks the base of the

glaucopit limestone facies at Mt Cardellia. No macrofauna has been found. Trace fossils (burrows) have been found and illustrated, but only from Mt Cardellia (by Daina, 1965).

b) Microfacies: The facies (Plates 3.6-3.19) is represented by bioclastic grainstones with a variable (1-70%, mostly 10-25% of grains) glauconite content and minor (0-15%, mostly < 1%) quartz content. Sorting varies from good to poor (see Figs 3.2 to 3.4) and roundness varies with grain type as described below. Where sorting is good grain size lies within the medium and coarse sand sizes, sometimes extending into very coarse sand size (Plate 3.16). Where sorting is poor bioclasts are only slightly abraded and the grain size of the rock is dictated by the fauna present (Plate 3.6). However, grain size rarely extends beyond granule (4 mm) size. Usually, glauconite occurs evenly dispersed in the sediment but at Mt Cardellia, on a few occasions, it is concentrated in 10-30 mm horizons where it can form 90% of the grains.

Microfacies is similar at the three localities where the facies is recognised. However, variation in the glauconite and quartz sand content, and in the type of allochems, does occur between localities (compare Figs 3.2 to 3.4) and especially between the localities in the Mt Genuardo area and Mt Cardellia.

The occurrence and petrography of glauconite found in this facies is described in Sections 6.2 and 6.3. Glauconite pellets are most abundant at Mt Cardellia, where they consistently form 10-25% of grains, (Plates 3.18, 3.19), sometimes concentrated to 50-70% in thin 10-30 mm horizons (Plate 3.16). In the Mt Genuardo area, at Battellaro, glauconite forms 5-20% of grains (Plate 3.13), and at Costa del Conte 1-20% mostly 1-10% and mostly as infillings to benthonic foraminiferid chambers (Plate 3.8).

Quartz is most common in the succession in the Mt Genuardo area. At Battellaro it consistently forms 10-15% of grains (Plates 3.10, 3.11) whereas at Costa del Conte it forms 0-5% mostly 0-1%. At Mt Cardellia

however, quartz is very uncommon forming less than 1%, usually much less than 1%, of grains. Quartz throughout the facies is always present as uniaxial grains showing almost equal amounts of strained and straight extinction. Shape and grain size, however, vary between localities. At Costa del Conte most quartz is fine sand size and rounded-subrounded, some is subangular. At Battellaro most quartz is medium to coarse sand size, some is very coarse (up to 1.2 mm); it is mostly rounded-subrounded, some is subangular (Plates 3.10-3.13). Finally at Cardellia where quartz is scarce it is very fine to fine sand size and angular-subangular.

Figures 3.2 to 3.4 indicate the relative abundances of the allochems at each measured section. At Costa del Conte sorting is poor and allochems are at their most abundant (Plates 3.6-3.9) and represented by common, often abraded, *Amphistegina*, *Miogypsina*, *Nephrolepidina*, echinoid and algal fragments and *Heterostegina/Operculina* fragments, along with some bivalve fragments, Textulariids, *Rotalia*, *Spiroolypeus*, *Eulepidina* fragments, fenestrate bryozoans, Globigeriniids and rare *Sphaerogypsina*, peloids and wackestone intra-clasts. At Battellaro (Plates 3.10-3.13), however, *Rotalia*, *Amphistegina* and Textulariids are prominent members of a similar assemblage and the larger benthonics such as *Nephrolepidina*, *Eulepidina*, *Miogypsina* and *Heterostegina/Operculina* are represented by fragments only. At Mt Cardellia (Plates 3.14-3.19) Globigeriniids, small Rotalliids, Nodosariids and Textulariids are more common and the larger benthonics are represented mostly by fragments.

c) Diagenesis: carbonate diagenesis throughout the Lower Miocene limestones is described in Section 5.3. It is the same at all localities and represented by cementation and compaction. Two periods of cement are developed and these differ from the sandy limestone facies in being commonly formed of ferroan calcite. Compaction is common and represented by grain redistribution or rotation grain fracture and pressure solution between grains. As well as carbonate diagenesis, widespread glauconitisation of carbonate grains is present in this facies, and dealt with more fully in Chapter 6.

3.3.3 Sandy Limestone Facies

a) Macrofacies: This facies is found in the Mt Genuardo area but not at Mt Cardellia. It forms the entire ridge and measured section at Serra Lunga and the upper part of the succession at Costa del Conte and in the Battellaro area. In the other upland areas to the north and east of Mt Genuardo, the facies is present but poorly exposed. At Serra Lunga the facies reaches its greatest thickness - 39 m. Elsewhere, at Battellaro and Costa del Conte it is 36 m and 27 m thick respectively. Where seen (Costa del Conte and Battellaro), the contact with the underlying glauconitic facies is sharp and non-erosional. The change from one facies to the other is abrupt without transition beds.

The facies is represented by alternating indurate and semi-indurate 0.15-1.1 m beds of silver to yellow brown coloured sandy limestones (Plate 3.4). Bed boundaries are poorly defined but straight. Cross bedding is seen in four beds at Serra Lunga. Macrofauna and trace fossils are absent.

At Mt Cardellia, on top of the glauconitic limestone facies, are 21 m of well bedded (0.2-0.6 m beds) grey coloured calcarenite limestones, which also have a sharp non-erosional contact with the glauconitic facies, contain no cross beds and no macrofauna or trace fossils.

b) Microfacies: The facies is characterised by sandy limestones (where combined quartz and glauconite is equal to less than 50% bulk composition of the rock) and calcareous sandstones (quartz plus glauconite more than 50%). The first represent most of the succession at Serra Lunga and Costa del Conte, whilst the latter predominate at Battellaro. Both sediments contain no matrix and are grain supported. Generally, the microfacies at Costa del Conte and Battellaro are similar, but these two differ from that found at Serra Lunga.

At Costa del Conte (Plates 3.20, 3.21) and Battellaro (Plates 3.22-3.24), the sediments are moderate to well sorted. Quartz forms 50-70% of grains at Costa del Conte and 50-90% at Battellaro. The facies is represented throughout by mainly fine, sometimes medium sand

size, rounded to subrounded, sometimes subangular grains, all unicrystalline with subequal proportions showing strained and straight extinction (Plates 3.20-3.24). Allochems form 30-50% of grains at Costa del Conte and 5-50% at Battellaro. At both localities they are represented by small (medium to fine sand size) fragments of benthonic foraminifera of probable *Miogypsina*, *Nephrolepidina* and *Heterostegina/Operculina* origin, along with algal and echinoid debris, bivalve fragments and some Textulariids with occasional *Amphistegina*, Globigeriniids, small Rotalliids and peloids. Glauconite forms 1-5% of grains at both localities. It is represented by pellets only, of fine to medium sand size (Sections 6.2 and 6.3).

In contrast, at Serra Lunga (Plates 3.25-3.27) the sediments have moderate to poor sorting and are coarser grained. Quartz forms 35-80% of grains. It is represented mostly by medium to coarse sand size rounded to well rounded grains, all unicrystalline with equal proportions of strained and straight extinction (Plates 3.25-3.27). Allochems form 16-60% of grains. Globigeriniids are the predominant feature of the allochem suite: they are common throughout the succession and become abundant in the upper 13 m. Other allochems include those listed for Costa del Conte and Battellaro, present in similar proportions. Glauconite forms 2-20% of grains. It is represented mostly by pellets of fine to medium sand size, along with some benthonic foraminiferid infills (Sections 6.2 and 6.3).

The limestones present at Cardellia (Plates 3.28-3.30) are grainstones throughout, well sorted and of medium sand size grains. Quartz forms less than 1% of grains, represented by fine sand size angular to subangular-subrounded unicrystalline straight extinction grains. Glauconite pellets form 0.5-3% mostly 0.5% of grains. Allochems are represented by common, equal proportions of Globigeriniids, echinoid fragments, bivalve fragments, red algal fragments and foraminiferid fragments most probably of *Heterostegina/Operculina*, *Miogypsina* and *Nephrolepidina* origin along with some small Rotalliids, Textulariids, Nodosariids, and *Amphistegina*.

The relative abundance of Globigeriniids and the fragmentary

nature of the larger benthonic foraminifera present in these well sorted rocks, which contain little glauconite, show more similarities with the sandy limestone facies than the glauconitic limestone facies. They also show similar diagenesis to the sandy limestone facies but both differ from the glauconitic limestone facies. Because of their similarity, the limestones are taken to represent a non-sandy equivalent to the sandy limestone facies.

c) Diagenesis: Cementation and compaction are common and widespread. Two periods of cement, as found in the glauconitic limestones, are present here. Unlike the glauconitic limestones, however, they are always formed of non-ferroan calcite. By virtue of the greater amount of quartz in this facies, first period pore lining cements are rare and pore spaces are commonly filled by a single crystal of second period cement. Compaction is represented by the same features as the glauconitic limestone facies but it is less prominent, probably as a result of its finer grain size (fine to medium sand size) or in some cases its predominant quartz grain composition offering resistance to pressure solution (Section 5.3.3).

3.3.4 Conclusion

In the Mt Genuardo area, two facies are distinguished in the field by their glauconite and quartz sand content. They are here termed the glauconitic limestone facies and the sandy limestone facies, and respectively occupy the lower and upper parts of the succession. At Mt Cardellia the sandy limestone facies is not seen but a non-sandy equivalent to this facies overlies the glauconitic limestone facies there.

The glauconitic limestone facies rests conformably on Upper Oligocene argillaceous rocks. The microfacies differs in the Mt Genuardo area to that found at Mt Cardellia. Around Mt Genuardo quartz is more common and glauconite less common and represented by both pellets and benthonic foraminiferid infills. The allochem suite in this area is dominated by whole and fragmentary larger benthonic foraminifera. At Mt Cardellia quartz is present in only minor proportions (< 1%) and glauconite, present in only pellet form, is much more abundant (up to

70% of grains). The allochem suite, in contrast, contains common Globigeriniids, small Rotaliids, Nodosariids and Textulariids which are seen in only minor quantities in the Mt Genuardo area. At both Mt Genuardo and Mt Cardellia the limestones are grainstones of medium to coarse sand size. Diagenesis is similar, represented by two periods of cementation, plus compaction and glauconitisation of carbonate grains.

The sandy limestone facies rests with sharp non-erosional contact on the glauconitic limestone facies without intermediate transition beds. The facies is found only in the Mt Genuardo area and comprises grain supported rocks with 50-90% quartz grains which are mainly fine sand size and rounded to subrounded in shape. Glauconite is much less common than in the underlying facies. It is not authigenic, and is probably reworked from underneath. The allochem suite is similar to that found in the glauconitic limestone facies. However, Globigeriniids are more common (especially at Serra Lunga) and other foraminifera are represented in a more fragmentary form by medium to fine sand size grains. Diagenesis is represented by cementation and compaction the same as in the underlying facies but ferroan calcite cements are not seen. At Mt Cardellia, limestones with a similar glauconite content, allochem suite and diagenesis represent a non-sandy equivalent to this facies.

3.4 Depositional Environment

3.4.1 Glauconitic Limestone Facies

Moderate water turbulence in these sediments is evidenced by: the abraded and fragmentary form of the allochems in grain supported rocks which lack matrix; the general moderate sorting and non-rounding of allochems; the light abrasion of some allochems and preservation of the delicate tests of Globigeriniids, Nodosariids and Textulariids; and the presence of only one cross bedded unit in the whole study area.

Normal salinities are indicated by the general predominance of hyaline calcareous foraminifera (Section 2.5.3) especially in the Mt Genuardo area. A more open marine environment than that inferred for

the Upper Oligocene limestones (Chapter 2) is indicated by the presence of Globigeriniids (Funnell, 1967; Haynes, 1981).

Cool bottom temperatures are suggested by common *Amphistegina* and *Rotalia* and by the poor development of a marine pore-lining cement (Section 2.5.4). Deposition near the oxygen minimum zone is indicated by alternating ferroan calcite/calcite zones in echinoid overgrowths of such cement (Section 5.3.2).

Shelf water depths of 80-250 m are indicated by the predominance of hyaline calcareous foraminifera composed of a similar association (containing *Miogypsina*, *Nephrolepidina*, *Heterostegina*, *Operculina*, *Amphistegina*, *Rotalia*, *Spiroclypeus* and *Eulepidina*) to that found in the Upper Oligocene limestones (Section 2.4.2b). However, the more common presence of Textulariids along with some Nodosariids as well as Globigeriniids might suggest (Funnell, 1967; Haynes, 1981) that the environment was situated at the deeper end of this 80-250 m depth range and that the area was in an outer shelf position. Furthermore, the greater abundance of Nodosariids, Textulariids and Globigeriniids at Mt Cardellia relative to Mt Genuardo suggests that water depths are greater in the former area and indicates a deepening trend towards the northeast.

Finally, slow sedimentation rate is indicated by the deposition of, at the most, 60-80 m glauconitic limestones in the Lower Miocene (Blondeau *et al.* (1972) record a maximum thickness of 75 m in the Corleone area), whereas the Numidian Flysch of the same age is up to 2500 m thick (Wezel, 1975b).

Evidence from the sediments, therefore, is in agreement with the environment inferred from the glauconite (discussed at length in Section 6.6): moderately turbulent, normal saline cool waters around the oxygen minimum zone at depths of 80-250 m, with slow sedimentation rate.

3.4.2 Sandy Limestone Facies

The sandy limestone facies (including the non-sandy equivalent in the Mt Cardellia succession) represents a general deepening of the

environment in the area. This is suggested by: the relative abundance of Globigeriniids in this facies compared with the glauconitic limestone facies; and by the generally smaller size of the allochems, which are on average medium to fine sand size. The general fine sand size of the quartz grains cannot be used as an environmental index since this is probably inherited from the source rock (see following Section).

The relative abundance of Globigeriniids (in comparison with benthonic foraminifera) is dependent on a number of factors as Haynes (1981) points out, and abundance need not increase proportionately with depth. However, when taken in account with other factors, it is possible to associate their abundance with depth. Consequently the common presence of Textulariids and some Nodosariids along with the smaller grain size of the sediment possibly suggest greater depths, though none of these features would if they were considered in isolation. Furthermore, the overall similarities between the allochem suites of the two facies (compare Figures 3.1 to 3.4) suggests that the amount of deepening was not great, and outer shelf water depths were still maintained.

Moderate water turbulence in this facies is indicated by the presence of moderately sorted, abraded and fragmentary but non-rounded allochems in grain-supported rocks which lack matrix and which also show the preservation of delicate tests of Globigeriniids, Nodosariids and Textulariids. The texture of the quartz sand, which is abundant in this facies in the Mt Genuardo area cannot be used as an index of depositional environment since it is believed to be inherited from the source rock (see following Section).

The temperature, salinity and oxidation of the environment cannot be precisely inferred because of the rarity of whole benthonic fauna. The environment, however, must have been oxidising since some unabraded, and apparently *in situ* benthonic foraminifera are present. The sparsity of this fauna may be due to depressed temperatures and/or salinities as a result of the increased water depth.

Glauconite in this facies is derived, and presumably reworked from

the underlying facies where it is authigenic. The cessation of glauconite formation may be the result of strongly oxidising conditions or depressed temperatures and/or salinities. Increased sedimentation rate associated with the influx of quartz sand is not the cause since the glauconitisation process does not continue into the upper part of the Mt Cardellia succession where little quartz sand is found.

3.4.3 Conclusions

Evidence from the sediments of the glauconitic limestone facies suggests an environment in agreement with that required for the glauconitisation process (Section 6.6): moderately turbulent, normal saline, cool waters around the oxygen minimum zone with slow sedimentation rates at the deeper end of the 80-250 m depth range. The sediments also indicate a general northeasterly deepening trend from Mt Genuardo to Mt Cardellia.

The overlying sandy limestone facies represents greater water depths in the area in an environment which is otherwise moderately turbulent, oxidising with slow sedimentation rates and possibly depressed temperatures and salinities. The cessation of the glauconitisation process in this facies may be due to strongly oxidising conditions or depressed temperatures and/or salinities.

Finally, the general deepening trend recorded in the succession may be the result of the Lower Miocene transgression well documented in the central Mediterranean area from southern Italy (Selli, 1957; Afchain, 1966; Bonardi *et al.*, 1971; Ogniben, 1973), southeast Sicily (Colacicchi, 1963), Malta (Bennett, 1979, 1980), and Tunisia (Castany, 1955). A Lower Miocene transgression is also known worldwide (Hallam, 1963).

3.5 Regional Setting

The glauconitic sandy limestones described here lie within the confines of the Sicani trough (Section 1.4). Mt Genuardo is situated at the southern margin of this trough (Catalano & D'Argenio, 1978) and has had a history from late Triassic times, of shelf, slope and basinal sedimentation. Mt Cardellia, however, is situated towards the centre of the

trough and has been the site of pelagic/hemipelagic deposition from the Middle Triassic onwards. Both areas were the site of deep water (pelagic) argillaceous rocks in Upper Oligocene times (Masclé, 1973, 1979; Catalano & D'Argenio, 1978, 1981). The trough is bounded to the south by the Saccense Carbonate Platform and to the north by the Trapanese Carbonate Platform (Fig. 1.4).

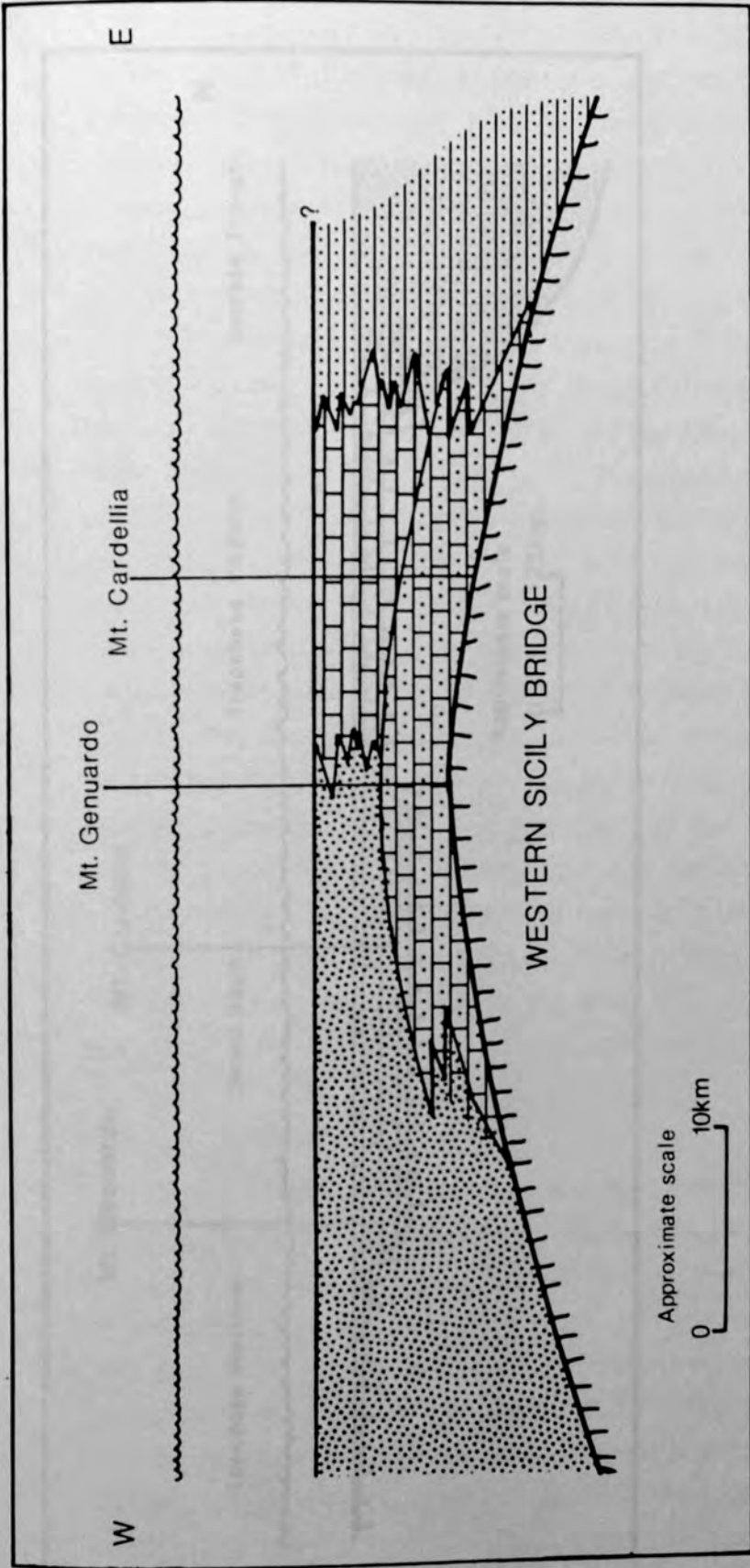
Lower Miocene glauconitic sandy limestones form a blanket of sediment over these three palaeogeographic units and pass northwards into the Upper Oligocene - Lower Miocene Numidian or Nebrodean Flysch of the Imerese Basin (Wezel, 1966, 1969, 1970, 1975a; Broquet, 1968, 1970, 1972; Masclé 1970, 1973, 1979; Catalano & D'Argenio, 1978). Southwards, the sediments presumably eventually pass into the carbonates of the North African Platform as seen in southeast Sicily (Rigo & Barbieri, 1959; Colacicchi, 1963; Di Grande *et al.*, 1977; Pedley, 1981) and the Maltese islands (Pedley, 1975, 1978; Pedley *et al.*, 1976; Bennett, 1979, 1980); or into shelf facies sandstones as seen in Tunisia (Wezel, 1968, 1970). In Tunisia continental sandstone facies in the south pass northwards into shelf sandstone facies, the outer part of which contains glauconite, and which passes still northwards into slope facies Numidian Flysch (Wezel, 1968, 1970). The Lower Miocene glauconitic limestones described here occupy a similar position between shelf (Maltese islands) and slope (Numidian Flysch) facies and show influences of both a carbonate shelf (the lower glauconitic limestone facies) and a terrigenous clastic slope (the upper sandy limestone facies).

There is a difference of opinion on the source area for the Numidian Flysch. Broquet (1968, 1970, 1972), Caire (1970) and Masclé (1970, 1973, 1979) claim that the flysch was derived from the north, with its source in a hypothetical outcrop of sandstones of the Permo-Triassic Verrucano Formation. This source explains the high mineralogical and textural maturity of the flysch which is represented by orthoquartzites or quartz arenites and which are unlikely to be formed by the direct erosion of crystalline basement present in the area as represented by the Peloritani mountains. Both Broquet and Masclé suggest that the Trapani Platform (their Vicari Zone) acted as a barrier to the southward transport of this sand except when it was occasionally allowed to spill over

into the Sicani Basin (their Cammarata Zone) where glauconitic limestones were being deposited.

In contrast, Wezel (1970, 1975a & b) claims that the flysch had its source area in the south, in continental sandstones of the Saharan Platform, and that it represents grainflow, slump and turbidity current deposits at the base of the African continental rise. Wezel argues that the mineralogical and textural maturity of the flysch sands (which are composed of 90-95% uniaxial rounded quartz grains mostly of fine sand size and with frosted textures and some of coarse sand to granule size with only 5-10% matrix) is inherited from a source of dune and interdune sands in the Nubian Sandstone of the Saharan cratonic landmass. This southerly source is also suggested by palaeocurrent directions towards the north and by a northward transition in northern Sicily from very coarse proximal sandstones through fine proximal sandstones of submarine fan origin into distal graded sandstones of near-axis trough deposition (Wezel, 1970, 1975a & b). Furthermore, Wezel (1970) rules out the hypothetical Verrucano source since such sandstones characteristically contain metamorphic rock fragments and feldspars likely to be preserved in the resedimented flysch; and Wezel (1975a) points out that there was probably a palaeo-high between the flysch and the proposed location of the Verrucano source, thus inhibiting a southward transportation of the sediment.

The sandy limestones described in this work show many features typical of the sands of the Numidian flysch. The quartz throughout is composed of uniaxial grains of fine sand size and rounded-sub-rounded shapes with some well rounded coarse sand. There are no rock fragments, feldspars or matrix. Moreover, their outcrop only in the Mt Genuardo area passing northeastwards into a limestone equivalent at Mt Cardellia suggests that the source of the sand was in the south to southwest and therefore agrees with Wezel's (1970, 1975a & b) Saharan source. Furthermore, the presence of glauconitic limestones with authigenic glauconite requires slow sedimentation rates unlikely to be produced if the passage of the flysch into the Imerese Basin was directly from the south.



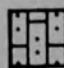

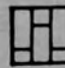


-  Glauconitic limestone facies
-  Sandy limestone facies and Nummidian Flysch
-  Sandy limestone facies (non-sandy equivalent)
-  Deep water deposits of the proto-Caltanissetta Basin
-  Basal Miocene substrate

Figure 3.5A. Distribution of Lower Miocene facies relative to the Western Sicily Bridge.

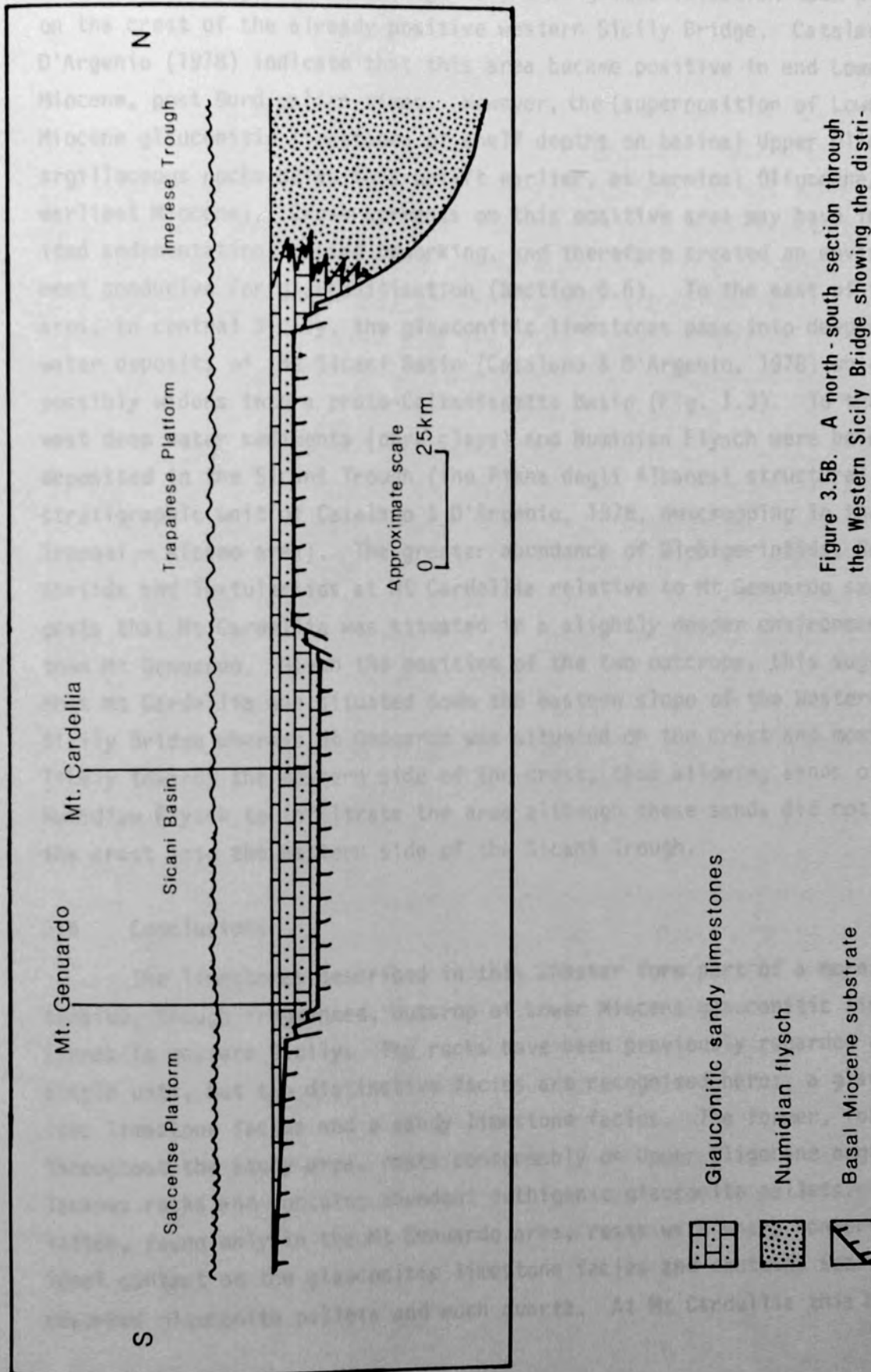


Figure 3.5B. A north-south section through the Western Sicily Bridge showing the distribution of the glauconitic sandy limestones, relative to the established palaeogeographic domains, along its length.

It is suggested here (Fig. 3.5) that glauconitisation took place on the crest of the already positive western Sicily Bridge. Catalano & D'Argenio (1978) indicate that this area became positive in end Lower Miocene, post Burdigalian times. However, the (superposition of Lower Miocene glauconitic limestones of shelf depths on basinal Upper Oligocene argillaceous rocks dates this uplift earlier, as terminal Oligocene/earliest Miocene). Cross currents on this positive area may have inhibited sedimentation, caused reworking, and therefore created an environment conducive for glauconitisation (Section 6.6). To the east of the area, in central Sicily, the glauconitic limestones pass into deeper water deposits of the Sicani Basin (Catalano & D'Argenio, 1978) which possibly widens into a proto-Caltanissetta Basin (Fig. 1.3). To the west deep water sediments (dark clays) and Numidian Flysch were being deposited in the Sicani Trough (the Piana degli Albanesi structural stratigraphic unit of Catalano & D'Argenio, 1978, outcropping in the Trapani - Alcamo area). The greater abundance of Globigeriniids, Nodosariids and Textulariids at Mt Cardellia relative to Mt Genuardo suggests that Mt Cardellia was situated in a slightly deeper environment than Mt Genuardo. Given the position of the two outcrops, this suggests that Mt Cardellia was situated down the eastern slope of the Western Sicily Bridge whereas Mt Genuardo was situated on the crest and most likely towards the western side of the crest, thus allowing sands of the Numidian Flysch to infiltrate the area although these sands did not cross the crest into the eastern side of the Sicani Trough.

3.6 Conclusions

The limestones described in this Chapter form part of a more extensive, though fragmented, outcrop of Lower Miocene glauconitic limestones in western Sicily. The rocks have been previously regarded as a single unit, but two distinctive facies are recognised here: a glauconitic limestone facies and a sandy limestone facies. The former, found throughout the study area, rests conformably on Upper Oligocene argillaceous rocks and contains abundant authigenic glauconite pellets. The latter, found only in the Mt Genuardo area, rests with sharp non-erosional contact on the glauconitic limestone facies and contains sparse reworked glauconite pellets and much quartz. At Mt Cardellia this facies

is represented by limestones with sparse reworked glauconite but little to no quartz.

In the glauconitic limestone facies the sediments indicate a depositional environment in agreement with that concluded from the authigenic glauconite (Chapter 6): moderately turbulent, normal saline, cool waters around the oxygen minimum zone with slow sedimentation rate in the deeper part of the 80-250 m depth range. Furthermore, the greater abundance of Globigeriniids, Nodosariids and Textulariids at Mt Cardellia relative to the Mt Genuardo area indicates a slight increase in water depth in that area, and therefore a northeasterly deepening trend.

The overlying sandy limestone facies represents greater water depths in the area, possibly the result of the well-documented, arguably world-wide, Lower Miocene transgression. The environment is otherwise moderately turbulent, oxidising, with slow sedimentation rates and possibly depressed temperatures and salinities. The cessation of authigenic glauconite growth may be due to strongly oxidising conditions or depressed temperatures and/or salinities.

This succession, which overlies Upper Oligocene deep water argillaceous deposits, dates uplift of the Western Sicily Bridge as terminal Oligocene - earliest Miocene. Previously, earliest uplift was recorded as Lower Miocene, post Burdigalian age. When considered in a regional context, it is envisaged that the glauconitic limestones formed a blanket of sediment on the crest of the palaeo-high forming the Western Sicily Bridge, covering the palaeogeographic units of the Saccense Carbonate Platform, Sicani Basin and Trapanese Carbonate Platform. Cross currents sweeping over this palaeo-high reduced sedimentation, caused reworking, and so created an environment conducive for glauconitisation. Northwards, the sediments grade into the Numidian Flysch of the Imerese Trough (Fig. 3.5B); southwards they presumably pass into carbonates or sandstones of the North African shelf, and therefore the sediments occupy an outer shelf position. Eastwards, down the slope of the Western Sicily Bridge the sediments grade into deep water deposits. Westwards they pass into deposits of the Numidian Flysch.

Finally, the quartz of the sandy limestone facies is similar, in grain size, roundness and crystal composition, to sands described from the Numidian Flysch by Wezel (1970), which suggests that it has the same source. The presence of sand at Mt Genuardo but not at Mt Cardellia agrees with the southern derivation of the flysch from the Saharan Platform, proposed by Wezel (1970, 1975a & b).

4.1.3. Introduction

Coraline red algae (Rhodophyta), represented by members of the Rhodocystales, form a significant part (20-50%) of the algal rhodoliths found described in Chapter 2. Despite their common occurrence, algae from this area have not previously been described or illustrated. Blodgett et al. (1972) and Masole (1973, 1979) use only the general term "Rhodocystales" (Wray & McIntyre, 1973) or identify some algae as *Chlorocystis* (Blodgett, a distinctive form (Elliott, 1957) not identified here).

This study adopts the palaeontological framework used by Johnson (1962) and adopted by Wray (1977), classifying the Family Rhodocystaceae into two subfamilies: Corallinaceae (articulating forms, all found in southwest Sicily) and Rhodocystaceae (non-articulating forms). Because of the lack of knowledge for the Rhodocystales, the terms are defined (Johnson, Wray (1977) and Blodgett (1979) and the terms are defined.

Johnson (1962) level of classification is used to identify fossil corals. This is because Wray (1977) classification is species level requires high resolution material, accurate or fortuitous sectioning, observations of the internal form and architecture of the skeleton, and accurate measure of cell and reproductive structure dimensions. There is no comprehensive reference catalogue and taxonomic descriptions are scattered in the literature. However, factors used to distinguish species may be primarily or predominantly controlled (Johnson & Wray, 1965; Wray, 1977; Blodgett, 1979). Practical taxonomic classification is therefore difficult and often subjective.

The classification of the subfamily Rhodocystales is based on

CHAPTER 4

DESCRIPTIVE PALAEOBIOLOGY

4.1 Coralline Red Algae

4.1.1 Introduction

Coralline red algae (Rhodophycophyta), represented by members of the Melobesioidea, form a significant part (20-50%) of the algal rhodolith facies described in Chapter 2. Despite their common occurrence, algae from this area have not previously been described or illustrated. Blondeau *et al.* (1972) and Mascle (1973, 1979) use only the general term "Lithothamnées" (Adey & MacIntyre, 1973) or identify some algae as *Subterraneaniphylum thomasi*, a distinctive form (Elliott, 1957) not identified here.

This study adopts the palaeobotanic taxonomic framework used by Johnson (1961a) and outlined by Wray (1977), classifying the Family Corallinaceae into two subfamilies: Corallinoidea (articulating forms, not found in southwest Sicily) and Melobesioidea (crustose forms). Descriptive terminology for the thallus is taken from the works of Johnson (1961a), Wray (1977) and Poignant (1979) where the terms are defined.

Diagnostic generic-level criteria used to identify fossil corallines are listed by Wray (1977). Identification to species level requires well preserved material, accurate or fortuitous sectioning, observations on the growth form and architecture of the thallus, and accurate measurements of cell and reproductive structure dimensions. There is no comprehensive reference monograph and taxonomic descriptions are scattered in the literature. Moreover, features used to characterise species may frequently be environmentally controlled (Johnson & Adey, 1965; Wray, 1977; Poignant, 1980). Precise taxonomic identification is therefore difficult and often uncertain.

Identification of the southwest Sicily Melobesioidea is based on

comparison with published descriptions of Tertiary material; shape and architecture of the thallus; dimensions of the hypothallic and perithallic cells; and shape and size of the reproductive structures. Species level identification is restricted to the best preserved material, displaying most, if not all, the morphological features necessary for precise identification. Nevertheless, eight species of Melobesioidea are described and illustrated, for the first time, from the Upper Oligocene of southwest Sicily,

Major descriptive accounts of Tertiary Corallinaceae used for comparison include: Johnson (1957, 1961b, 1962a & b, 1963, 1964, 1965a & b), Johnson & Adey (1965), Johnson & Ferris (1949), Johnson & Kaska (1965) and Johnson & Tafur (1952).

4.1.2 Systematic Palaeontology

Phylum RHODOPHYCOPHYTA Papenfuss 1946

Syn. RHODOPHYTA Wettstein 1901

Class RHODOPHYCEAE Ruprecht 1851

Order CRYPTONEMIALES Schmitz, in Eugler 1892

Family CORALLINACEAE (Lamouroux) Harvey 1849

Subfamily MELOBESIOIDEA in Johnson 1957

Genus ARCHAEOLITHOTHAMNIUM Rothpletz 1891

Archaeolithothamnium saipanense Johnson

Plates 4.1-4.6

- 1957 *Archaeolithothamnium saipanense* Johnson, pp. 217,220, pl. 38, figs 1-4, 6.
 1965b *Archaeolithothamnium saipanense* Johnson; Johnson, p. 265, pl. 2, fig. 1.
 1980 *Archaeolithothamnium saipanense* Johnson; Bennett, pp. 77,78, pls 2.28. 1-2, 2.29. 1-2.

Diagnosis (Compiled from Johnson 1957, 1965b). A species of *Archaeolithothamnium* characterised by nearly square perithallic cells regularly arranged to form a boxwork pattern, and by relatively large closely packed narrow ellipsoidal sporangia arranged in (commonly repeated) layers.

Description. Thallus 0.5-7 mm (commonly 0.5-1.5 mm) thick with frequently developed protuberances or branches (up to 5 mm long and 1-2 mm dia.). Hypothallus thin (15-30 μ), simple multi-layered type formed of 3-5 rows of cells (12-17 μ tall, by 10-12 μ wide). Perithallic tissue regularly ordered, both vertically and horizontally though preferred calcification of the vertical walls often gives a threaded appearance. The cells are rectangular to square (8-16 μ tall, by 8-12 μ wide). Sporangia frequently numerous, concentrated in protuberances, closely packed in layers and often repeated vertically. They are ellipsoidal, may be narrow or bulbous and are 80-120 μ tall by 45-70 μ diameter.

Remarks. The general appearance of the tissue and growth habit of this alga is very similar to *A. intermedium* (Raineri, 1923; described and illustrated in Johnson, 1965b) and *A. nummululiticum* ((Gumbel) Rothpletz, 1891; described and illustrated in Johnson, 1961b, 1962a; Johnson & Kaska, 1965), but it differs in smaller cell size and dimensions of sporangia. The tissue is similar (in cell and sporangia dimensions and boxwork form) to *A. sociabile* (Lemoine, 1939; described and illustrated in Johnson, 1965b) but differs in the presence of protuberances and multiple layers of closely packed sporangia seen in *A. saipanense* to which it is ascribed.

A. saipanense has previously been described from the Eocene of Saipan (Johnson, 1957; the Upper Eocene to Middle Oligocene of Borneo (Johnson, 1965b); and the Upper Oligocene of the Maltese islands (Bennett, 1980).

Occurrence. Common in seventeen thin sections from Nadorello east as the initial alga of a rhodolith, or encrusting *Lithoporella melobesioides* and often encrusted by *Lithothamnium aggregatum* or *Mesophyllum vaughanii* sometimes after fragmentation.

Genus LITHOTHAMNIUM Philippi 1837

Lithothamnium aggregatum Lemoine

Plates 4.7-4.10

1939 *Lithothamnium aggregatum* Lemoine, pp. 66,67, pl. 1, fig. 12,
pl. 3, figs 3,4, text-fig. 27.

1957 *Lithothamnium* cf. *aggregatum* Lemoine; Johnson, pp. 220,221,
pl. 40, figs 2,4.

1965b *Lithomnium aggregatum* Lemoine; Johnson, p. 266.

Diagnosis (compiled from Lemoine, 1939; and Johnson, 1965b). A species of *Lithothamnium* characterised by (commonly superimposed) thin thalli 300 to 600 μ thick, composed of a prominent hypothallus and threaded perithallus with cell dimensions of: (hypothallus) 15-22 μ long by 9-13 μ wide and (perithallus) 10-22 μ tall by 8-13 μ wide. Conceptacles as yet undescribed.

Description. Thalli, 200-600 μ thick. Hypothallus multilayered, 50-80 μ thick formed of cells 15-22 μ long by 10-12 μ wide. Perithallus is threaded with cells 10-21 μ tall by 9-14 μ wide. Conceptacles (350 μ dia. by 110-130 μ tall) are uncommon and form a relief on the surface of the perithallus.

Remarks. The alga is similar in growth habit to other thin, non-branching, simple crustose forms listed in Johnson (1957, 1961b) and Johnson & Kaska (1965) (namely: *L. abrardi*, *L. andrusovi*, *L. bourcarti*, *L. caravellense*, *L. crispithallus*, *L. cymbicrusta*, *L. engelhartii*, *L. exiguum*, *L. fumigatum*, *L. funafutiense*, *L. grahami*, *L. ladronicum*, *L. leptum*, *L. lichenoides*, *L. peleense*, *L. saipanense*, *L. subtile*, *L. tagpochaense*, *L. tanapagense* and *L. toltecensum*) but differs in hypothallic and perithallic cell and conceptacle dimensions. It is ascribed to *L. aggregatum* in having all the features diagnostic of this species.

L. aggregatum has previously been described from the Oligocene of Algeria (Lemoine, 1939) and Borneo (Johnson, 1965b). *L. cf. aggregatum* is described from the Upper Eocene of Saipan (Johnson, 1957).

Occurrence. *L. aggregatum* is positively identified in only three thin sections from Nadorello east but may be present in many more where it is represented by thin infertile thalli with multi-layered hypothallus. It is found as multiple encrustations on rhodoliths of *L. cf. marianae* and *M. cf. vaughanii*.

Lithothamnium cf. marianae Johnson

Plates 4.11-4.14

1957 *Lithothamnium marianae* Johnson, pp. 220,226, pl. 41, figs 1-3.

1962a *Lithothamnium marianae* Johnson; Johnson, p. 156, pl. 2, figs 2, 3.

Diagnosis (compiled from Johnson, 1957, 1962a). A species of *Lithothamnium* characterised by a branching thallus with lensoid growth in the perithallic tissue. Hypothallus absent or poorly developed composed of cells 13-20 μ long by 10-12 μ wide. Perithallic cells 10-24 μ tall by 7-13 μ wide. Conceptacles (270-686 μ dia. by 135-190 μ high) abundant.

Description. Thick branches (up to 7 mm long by 5 mm dia.; commonly 4-6 mm long by 2-3.5 mm dia.) closely spaced (5-6 mm apart) on a crustose thallus of 0.5-1.5 mm thickness. The perithallus tissue is threaded. Lensoid growth zones are infrequently developed, located in fertile branches, not present where these are infertile. Hypothallus multi-layered, commonly thin, formed of 3-4 rows of cells, sometimes relatively thick formed of 8-12 rows of cells (13-21 μ long by 10-12 μ wide). Perithallic cells 10-22 μ tall by 8-13 μ wide. Conceptacles abundant (located in branches), 350-650 μ dia. by 120-205 μ high.

Remarks. In its branching habit, lensoid tissue growth, subordinate hypothallus, cell sizes, and conceptacle size this alga is similar to *L. marianae*. It differs, however, in not possessing the pronounced lensoid tissue growth described and illustrated by Johnson (1957, 1962a) but does show lensoid tissue growth that is remarkably similar to the tissue illustrated by Johnson (1962a, pl. 2, fig. 3) for *L. marianae*. For these reasons it is identified as *L. cf. marianae* and distinguished from other branching species of *Lithothamnium* with lensoid tissue growth (*L. lacroixi*, Lemoine, 1917; *L. wallisium*, Johnson & Tafur, 1952) by cell and conceptacle dimensions.

L. marianae has previously been described from the Upper Eocene of Saipan (Johnson, 1957) and Sarawak (Johnson, 1962a).

Occurrence. Common in 32 thin sections from Nadorello east and probably present but not positively identifiable in a similar number more. Found as whole rhodoliths and fragmented branches and on few occasions can be seen to encrust *Archaeolithothamnium saipanense*.

Genus LITHOPHYLLUM Philippi 1837

Lithophyllum ovatum (Capeder)

Plates 4.15-4.16

- 1900 *Lithothamnium ovatum* Capeder, p. 177, pl. 6, figs 5a,b.
 1926 *Lithophyllum ovatum* (Capeder); Lemoine, pp. 245-246, text-fig. 3.
 1933 *Lithophyllum ovatum* (Capeder) Lemoine; Airoidi, p. 70, pl. 10.
 1957 *Lithophyllum ovatum* (Capeder) Lemoine; Johnson, p.228, pl. 43, figs 4, 8.
 1965b *Lithophyllum* cf. *ovatum* (Capeder) Lemoine; Johnson, p. 271, (cum. syn.).

Diagnosis (compiled from Lemoine, 1926; Airoidi, 1933; & Johnson, 1957). A species of *Lithophyllum* characterised by the development of thin crusts up to 800 μ thick containing a prominent co-axial hypothallus 75-320 μ thick of cells 15-40 μ long by 7-14 μ thick. Perithallus is layered with cells 8-15 μ tall by 7-11 μ wide and contains flat roofed conceptacles 210-330 μ dia. by 95-130 μ high.

Description. Thin crust 200-250 μ thick. Coaxial hypothallus 80-100 μ thick, cells 22-30 μ long by 10-15 μ thick. Perithallus layered, cells 10-15 μ tall by 8-12 μ wide, containing one single pored flat roofed conceptacle 340 μ diameter by 130 μ high.

Remarks. The alga is similar in growth habit to other non-branching thin crustose forms of *Lithophyllum* listed and described in Johnson (1957, 1961b) (namely: *L. linguisticum*, *L. prelichenoides*, *L. quadratum*, *L. racemus*, *L. samosense*, *L. stefanini*, and *L. yendoii*) but differs in conceptacle and hypothallic and perithallic cell dimensions and in the development and type of hypothallus. It is ascribed to *L. ovatum* in having all the features diagnostic of this species.

L. ovatum has been previously described from the Oligocene of northern Italy (Lemoine, 1926; Airoidi, 1933), and Borneo (Johnson, 1965b) and the Upper Eocene of Saipan (Johnson, 1957).

Occurrence. Found in only one thin section from Nadorello east as the final encrustation on a rhodolith.

Lithophyllum personatum Airoidi

Plates 4.17-4.21

1933 *Lithophyllum personatum* Airoidi, pp. 73,74, pl. 11, fig. 4.

Diagnosis. A species of *Lithophyllum* characterised by very large conceptacles 430-760 μ dia. by 200-220 μ high in a layered perithallus of rectangular cells 10-18 μ tall by 8-14 μ wide (except above conceptacles, where the layering is undulose and the cells 23 by 18 μ dimension) resting on a simple multi-layered to very poorly co-axial hypothallus 55-200 μ thick formed of rectangular cells 18-28 μ tall by 8-14 μ wide.

Description. Thick closely spaced protuberances 1-4 mm tall by 1-2.25 mm wide (at the base) developed in a thallus 1-7 mm thick. Hypothallus multi-layered to sub-plumose, 70-130 μ thick formed of rectangular cells 10-23 μ long by 8-14 μ wide. Perithallus layered and sometimes lensoid (in fertile protuberances only) formed of rectangular cells 10-15 μ tall by 8-13 μ wide. Layering absent, cells 12-18 μ tall by 10-14 μ wide for 5-8 cells thickness immediately above the conceptacles, which are single pored with a flat base and convex roof, and 530-720 μ dia. by 180-230 μ high.

Remarks. The large size of the conceptacles of this alga allows the exclusion of most species of *Lithophyllum* and its subsequent identification as *L. ovatum*. *L. johnsoni* (Johnson, 1961b; Johnson & Kaska, 1965) and *L. racemus* (Johnson, 1957) have conceptacles of large diameter (400-560 μ) but differ in their development of co-axial hypothallus and flattened conceptacle form (130-150 μ high) respectively. Airoidi (1933), in his original description of *L. personatum* from the Upper Oligocene (Rupelian) of northern Italy, made no comment on the general growth form of the thallus (e.g. thin crust or branching) except that it is nodular. Features of the general form of the thallus therefore cannot be used in identification.

Occurrence. Positively identified in only four thin sections from Nadorello east, but infertile specimens may be present in a further four.

On one occasion *L. personatum* is seen to encrust *Archaeolithothamnium*, and on another, to be encrusted by *Lithothamnium*.

Genus MESOPHYLLUM Lemoine 1928

Mesophyllum cf. *vaughanii* (Howe)

Plates 4.22-4.26

- 1918 *Lithothamnium vaughanii* Howe, pp. 6,7, pls 7, 8.
 1939 *Mesophyllum vaughanii* (Howe); Lemoine, p. 89, pl. 1, figs 2, 8, 11, 15.
 1962a *Mesophyllum vaughanii* (Howe) Lemoine; Johnson, p. 157, pl. 3, figs 1, 2.
 1965a *Mesophyllum vaughanii* (Howe) Lemoine; Johnson, p. 809, pl. 98, figs 1, 2.
 1965a *Mesophyllum* cf. *vaughanii* (Howe) Lemoine; Johnson, p. 809.
 1965b *Mesophyllum vaughanii* (Howe) Lemoine; Johnson, p. 268, pl. 4, fig. 3, pl. 5, fig. 5.
 1980 *Mesophyllum* cf. *vaughanii* (Howe) Lemoine; Bennett, p. 80, pls 2.31.3, 2.32.

Diagnosis (compiled from Lemoine, 1939; Johnson, 1962a, 1965a,b). A species of *Mesophyllum* characterised by a simple multi-layered hypothallus, a perithallus with pronounced lenticular growth zones and numerous conceptacles often containing sporangia. Hypothallic cells, 13-32 μ long by 8-19 μ thick; perithallic cells, 7-21 μ tall by 8-15 μ wide; conceptacles multipored, 350-600 μ dia. by 140-220 μ high.

Description. Crustose form. Common thick protuberances (< 8 mm dia. by 8 mm high) and slender branches (< 3 mm dia. by 8-10 mm long). Pronounced growth zones (5-7 cells deep) in perithallus with cells 10-25 μ tall by 8-12 μ wide. Growth zones are lenticular in the region of the protuberances. Conceptacles, numerous, commonly contain sporangia, are concentrated in protuberances and measure 450-1100 μ dia. by 140-200 μ high. Hypothallus, well defined, 90-200 μ thick, cells 10-25 μ long by 8-18 μ thick.

Remarks. The general growth habit, appearance, cell sizes of the tissue and multi-layered hypothallus suggest that this alga is *Mesophyllum vaughanii*. The conceptacle size range overlaps but is generally greater

than that accepted for *M. vaughanii*. For this reason, along with the absence of any described alga with similar tissue to *M. vaughanii* but larger conceptacle size (Johnson, 1962a), the alga is ascribed to *M. cf. vaughanii*.

M. vaughanii is a widely distributed Upper Eocene - Lower Oligocene form (Johnson, 1965b), but has also been described from the Middle Oligocene of Sarawak (Johnson, 1965b); the undifferentiated Oligocene of Algeria (Lemoine, 1939) and the Upper Oligocene of Malta (Bennett, 1980).

Occurrence. *M. vaughanii* is of common occurrence in 20 thin sections from Nadorello east in the form of whole rhodoliths and fragmented branches and protuberances. In the rhodoliths it is commonly mutually exclusive from all other species of algae; on rare occasions it may encrust *Lithothamnium cf. marianae*.

Genus LITHOPORELLA Foslíe 1909

Lithoporella cf. melobesioides (Foslíe)

Plates 4.27-4.29

- 1903 *Mastophora melobesioides* Foslíe, pp. 23-25.
 1904 *Mastophora (Lithoporella) melobesioides* (Foslíe); Foslíe, in Weber van Bosse & Foslíe, p. 73.
 1909 *Lithoporella melobesioides* (Foslíe) Foslíe; Foslíe, pp. 58,59.
 1928 *Melobesia (Lithoporella) melobesioides* (Foslíe) Foslíe; Lemoine, p. 104.
 1949 *Lithoporella (Melobesia) melobesioides* (Foslíe) Foslíe; Johnson & Ferris, p. 196, pl. 39, figs 1, 2.
 1961b *Lithoporella melobesioides* (Foslíe) Foslíe; Johnson, p. 936 (cum. syn.).
 1962a *Lithoporella melobesioides* (Foslíe) Foslíe; Johnson, pp. 163,164, pl. 3, fig. 3.
 1963 *Lithoporella melobesioides* (Foslíe) Foslíe; Souaya, p. 250, pl. 7, fig. 6.
 1964 *Lithoporella melobesioides* (Foslíe) Foslíe; Johnson, pp. 482-484, pl. 3, fig. 4.
 1965a *Lithoporella melobesioides* (Foslíe) Foslíe; Johnson, p. 811.
 1965b *Lithoporella melobesioides* (Foslíe) Foslíe; Johnson, pp. 271,272, pl. 2, fig. 6.

- 1965 *Lithoporella melobesioides* (Foslie) Foslie; Johnson & Kaska, pp. 50,51, pl. 44, fig. 3.
 1980 *Lithoporella melobesioides* (Foslie) Foslie; Bennett, pp. 81,82, pls 2.28.3-6, 2.33.3, 2.34.1-3.

Diagnosis (compiled from Johnson, 1957, 1961b, 1962a, 1964, 1965a,b). A species of *Lithoporella* characterised by a cell size variation within the range 22-99 μ tall by 9-41 μ wide, found between and within thalli; monoporate conceptacles of 600-1000 μ dia. by 200-290 μ high; and frequent superimposition of thalli.

Description. Monostromatic thallus formed of large cells elongate normal (or at a high angle) to the substrate. Cell size varies greatly (30-85 μ tall by 15-35 μ wide) even within a single thallus. Commonly 2 to 6 thalli are found superimposed. Conceptacles are absent.

Remarks. Without a large sample size of fertile specimens commonly sectioned through the centres of conceptacles, it is not possible to separate *L. melobesioides* from the species *L. crassa* (Ishijima in Johnson, 1961b), *L. atlantica* (Foslie in Johnson, 1957), *L. conjuncta* (Foslie in Johnson, 1957), *L. antiquitas* (Johnson, 1961b) and *L. longicella* (Johnson, 1961b) all of which have restricted cell size ranges within that of *L. melobesioides*. The cells, however, are too large to cause confusion with *L. minus* (Johnson, 1964). The alga is ascribed to *L. cf. melobesioides* since it shows the cellular features common to this species but positive identification cannot be made without a larger sample size of fertile specimens.

L. melobesioides has a known age range from Eocene to Recent within which it is ubiquitous (Johnson, 1962a). Within the Mediterranean area it has been recorded from the Oligocene of Algeria (Lemoine, 1939), northern Italy (Airoldi, 1933) and the Maltese islands (Bennett, 1980); from the Miocene of northern Italy (Conti, 1943); and from the Middle Miocene of Egypt (Souaya, 1963).

Occurrence. Found in seven thin sections from Nadorello east as initial encrustations on *Lepidocyclina* (*Eulepidina*) foraminifera and eroded

rhodolithic fragments, and as single thalli often interleaved with *Melobesia* cf. *cuboides* in *Lithothamnium* cf. *marianae* and *Mesophyllum* cf. *vaughanii* rhodoliths.

Genus MELOBESIA Lamouroux 1812

Melobesia cf. *cuboides* Johnson

Plates 4.30-4.32

- 1957 *Melobesia?* *cuboides* Johnson, pp. 234,235, pl. 43, fig. 6, 7.
 1962a *Melobesia cuboides* Johnson; Johnson, p.164, pl. 5, fig. 6.
 1962a *Melobesia* cf. *cuboides* Johnson; Johnson, p. 164.
 1965b *Melobesia* cf. *cuboides* Johnson; Johnson, p. 273.
 1965 *Melobesia?* *cuboides* Johnson; Johnson & Kaska, pp. 51,52, pl. 34,
 fig. 2.
 1980 *Melobesia cuboides* Johnson; Bennett, p. 82, pl. 2.35.

Diagnosis (compiled from Johnson, 1957, 1962a). A species of *Melobesia* characterised by a monostromatic thallus consisting of square or slightly horizontally elongate cells 10-30 μ long by 10-23 μ tall. Commonly several thalli are superimposed. Conceptacles as yet undescribed.

Description. Monostromatic thallus consisting of horizontally elongate, sometimes square, cells 30-45 μ long by 20-30 μ tall. Up to 4 thalli superimposed. Conceptacles not present.

Remarks. The monostromatic thallus and horizontally elongate aspect of the cells of this alga characterise it as *Melobesia*. The size of the cells, however, is larger than accepted for *M. cuboides* but similar in dimension (19-43 μ long by 9-17 μ tall) to that accepted for *M. cf. cuboides* by Johnson (1962a) and for this reason the alga is ascribed to *M. cf. cuboides* here.

M. cuboides has previously been described from the Eocene of Saipan (Johnson, 1957) Sarawak (Johnson, 1962a) and Guatemala (Johnson & Kaska, 1965); and the Upper Oligocene of Malta (Bennett, 1980). *M. cf. cuboides* has been described from the Eocene (Johnson, 1962a) and Lower Miocene (Johnson, 1965b) of Sarawak. The *Melobesia* sp. described by Airoidi (1933) from the Upper Oligocene of northern Italy has cell dimensions

similar to those of *M. cuboides* and therefore may be this species.

Occurrence. The alga is of minor occurrence in 12 thin sections from Nadorello east, usually forming the first encrustation on large *Lepidocyclina* (*Eulepidina*) foraminifera; sometimes interleaved with *Lithoporella melobesioides*, or as single thalli within *Lithothamnium* cf. *marianae* and *Mesophyllum* cf. *vaughanii* rhodoliths.

4.1.3 Rhodolithic Growth Form

The coralline red algae from southwest Sicily are present in the form of rhodoliths (*sensu* Adey & MacIntyre, 1973): free living crustose forms which nucleate on particulate matter and show concentric growth forms around it. At the Nadorello east locality three morphologically different types of rhodolith can be recognised in field outcrop. Two of these types (1 & 2) are abundant, the third (3) is common to infrequent. A fourth morphological type (4) is found at the Contrada Giovanni locality and in the Mt Gargalupo area.

1) Compact Branching Growth Form

Plates: 4.33, 4.34

Rhodoliths with good sphericity measuring 20-30 mm diameter, formed of compact massive algal thallus with closely spaced, relatively thick and short (4-5 mm dia. by 5-6 mm long) branches. Nuclei are formed of fragments of the same or other algae.

2) Compact-Laminar and Laminar Growth Forms

Plates: 4.35, 4.36

Rhodoliths with good sphericity measuring 40-70 mm diameter. Centres commonly composed of compact branching forms later encrusted by algae with thin thalli, thus forming a laminar exterior. Some rhodoliths are formed of thin thalli throughout. In both cases, subsequent encrustations of thalli are not in contact everywhere, but are commonly separated by lenticular voids later infilled with sediment (a feature recorded previously by Bosellini & Ginsburg, 1971), or by encrustations of cheilostome bryozoans.

3) Open Branching Growth Form

Plates: 4.37, 4.38

Rhodoliths with poor sphericity commonly encrusting lepidocycline foraminifera. They are formed of thin thalli (0.5-1.5 mm thick) with widely spaced (10-15 mm) relatively long narrow branches (1-2 mm dia. by 3-6 mm long).

4) Compact Non-Branching Growth Form

Plates: 4.39, 4.40

Rhodoliths with poor sphericity measuring 35-55 mm maximum diameter formed of compact massive thallus 2-5 mm thick. No branches. Nuclei commonly *Lepidocyclina* (*Eulepidina*) foraminifera.

Rhodoliths, in general, owe their growth form to formation in quite particular energy regimes additional to the parameters listed in section 4.1.4 which control the growth and distribution of coralline algae in general. A delicate balance must exist between water movement and light intensity, resulting in concentric growth (Wray, 1977). Excessively strong water motion prevents the relatively light and fragile rhodoliths from forming, whereas weak wave or current action leads either to their stabilisation through growth and coalescence of crusts or to burial by fine sediment (Adey & MacIntyre, 1973).

Rhodoliths which are densely branched or which have concentric (laminar) structure are thought to represent growth in environments with considerably more water movement than those with open branching forms which represent growth in quiescent conditions (Bosellini & Ginsburg, 1971; Wray, 1971; Adey & MacIntyre, 1973). Bosellini & Ginsburg (1971) found that the former occupied positions in current swept channels whilst the latter represented growth in the protected environment of sea grasses.

In southwest Sicily, the growth form of the rhodoliths is primarily governed by the algal species present. Certain species are known to have particular growth habits (Johnson, 1957, 1961b; Johnson & Kaska, 1965). Of the rhodoliths examined in thin section the compact branching form (type 1) and non-branching form (type 4) were composed of *Lithothamnium* cf. *marianae* and *Mesophyllum* cf. *vaughanii*. These species may

be subsequently repeatedly encrusted by thin thalli of *L. aggregatum* to give a compact-laminar form (type 2). Those type 2 rhodoliths with laminar growth throughout have thin thalli of *Archaeolithothamnium saipanense* or *L. cf. marianae* in the centres and are subsequently encrusted by *L. aggregatum*. *L. aggregatum* is present always as a late stage encrustation when rhodoliths are relatively large. Rhodoliths with an open branching form (type 3) are always formed of *A. saipanense*.

However, the rhodolith growth forms may also be related, secondarily, to environment. The delicate open branching forms (type 3) may represent growth in quiescent conditions, possibly in the shelter of hollows or sea grasses. In contrast, the compact branching forms may represent growth in higher energy conditions (as found by Bosellini & Ginsburg, 1971; and Bosence, 1976), possibly in open current swept areas. The subsequent encrustation of these forms by thin crusts of *L. aggregatum* may reflect the need for a large particle size to allow this species to encrust. The encrustation of other species of *Lithothamnium* is governed by the particle size of the substrate (Adey, 1970a & b). Grain size, rather than energy conditions, is therefore thought to control the presence of *L. aggregatum*.

At the Contrada Giovanni locality and in the Mt Gargalupo area the rhodoliths are almost entirely represented by compact non-branching forms, and the assemblage shows a complete absence of open branching forms. This feature may reflect higher energy conditions at these localities than at the Nadorello east locality. This is consistent with the inter-bedding of the algal rhodolithic facies with grainstones in the Contrada Giovanni and Mt Gargalupo successions; and with the position of the Contrada Giovanni succession on the boundary between grainstone facies to the west and algal wackestones, packstones to the east (Section 2.4.4).

Present day rhodoliths are recorded from a variety of latitudes and depths: from Bermudan lagoons in depths of 2-5 m (Bosellini & Ginsburg, 1971); from 5-30 m in the Skagerrak (Alexandersson, 1974); and from depths of over 50 m on the forereef of the Bermuda Platform (Focke & Gebelin, 1978). Adey & MacIntyre (1973) conclude that

rhodoliths can form in clear tropical waters in offshore banks and in exposed localities in depths of 50-250 m and yet also occur in protected shallow lagoons. The southwest Sicily algal assemblage is thought to represent accumulation in depths of 80-250 m (following Section) and therefore is consistent with these findings.

4.1.4 Palaeoecology

The red algae are potentially sensitive environmental indicators. Work on Recent representatives (Adey, 1966, 1968, 1970a, 1970b, 1971; Bosellini & Ginsburg, 1971; Adey & MacIntyre, 1973) has indicated that the major factors controlling their distribution are: light intensity, water temperature, salinity, substrate and water energy. Their distribution can be related to depth but this is usually a reflection of the above factors especially light intensity (Adey, 1966, 1971; Adey & Adey, 1973; Adey & MacIntyre, 1973). As a group they occur in most seas from intertidal depths to 200-250 m (Adey & MacIntyre, 1973). This lower limit is largely governed by light intensity and the ability of the red algae to utilize light from the more penetrative blue green wavelengths.

The southwest Sicilian mid-Tertiary red algal genera have proven long time ranges from Jurassic (*Archaeolithothamnium*, *Lithothamnium*, *Lithoporella*, *Lithophyllum*) and early Tertiary (*Mesophyllum*, *Melobesia*) through to Recent. Their slow development makes them of little use in stratigraphic correlation but gives them enhanced palaeoenvironmental value. Indeed, Wray (1977) considers that the present genera of the Hawaiian archipelago exist under much the same conditions as they did during the Tertiary.

Listed below in order of decreasing abundance and with their associated ecological preferences are the red algal genera from the Mid-Tertiary of southwest Sicily.

Lithothamnium: All seas, almost always subtidal. A prominent element of the flora in shallow water at cooler, primarily northern, latitudes (Adey, 1966). In the tropics it becomes a prominent element

of the flora in deeper (cooler) water, occurring at depths > 50 m in the Hawaiian archipelago (Wray, 1977).

Mesophyllum: All seas, from subtidal to deep water. A prominent element of the flora in shallow water at cooler, primarily southern, latitudes but predominates in deeper environments (> 50 m; Wray, 1977) within the tropics.

Archaeolithothamnium: This genus is considered to be almost exclusively subtidal and virtually restricted to tropical - subtropical waters where it has been recorded from depths down to 250 m (Adey & MacIntyre, 1973; Wray, 1977).

Lithophyllum: All seas, but greatest development within the tropics (Johnson, 1961a). Known to be intertidal to depths of 80 m (Wray, 1977).

Lithoporella: Virtually restricted to tropical - subtropical waters (Adey & MacIntyre, 1973). It is a predominant coralline component of tropical reefs and common in waters of < 10 m (Wray, 1977). It is strictly a hard substrate encruster and commonly the initial colonizer.

Melobesia: Temperate and tropical seas where it is commonly intertidal (Johnson, 1961a).

A tropical - subtropical environment for the southwest Sicily limestones is evidenced by the mere presence of *Archaeolithothamnium* and *Lithoporella*. Accumulation in cooler, deeper water is suggested by the predominance of the cool water genera, *Lithothamnium* and *Mesophyllum*, over the warm water genera *Archaeolithothamnium*, *Lithophyllum* and *Lithoporella*. By comparison with the work of Adey & Boykins (in Wray, 1977), it is suggested that this association represents accumulation in water depths > 80 m because of the similar relative abundances of the genera present to the association recorded for 80 m depth in the Hawaiian archipelago. Above 80 m depth *Archaeolithothamnium* and *Lithophyllum* become relatively much more abundant. Below 80 m no data are given for the relative abundances of the algal association. The southwest Sicily limestones therefore accumulated in water depths > 80 m with a lower limit set

at 250 m, governed by the photic zone and by the greatest depth to which rhodoliths are known to occur.

4.1.5 Conclusions

The mere presence of red algae suggests that the enclosing limestones formed under normal marine conditions in light penetrated water. The presence of the warm water genera *Archaeolithothamnium*, *Lithophyllum* and *Lithoporella* is evidence of deposition in a tropical/sub-tropical environment. However, the predominance of the cool water genera (*Lithothamnium* and *Mesophyllum*) over these warm water genera suggests accumulation in cooler, therefore deeper 80-250 m waters.

The formation of rhodoliths implies regular gentle movement of the bottom. The formation of these rhodoliths by *Lithothamnium* cf. *marianae*, *Mesophyllum* cf. *vaughanii* and *Archaeolithothamnium saipanense* is consistent with the branching growth form typical of rhodolith forming algae (Adey & MacIntyre, 1973). The subsequent encrustation by *L. aggregatum* may represent the ability of this alga to encrust only large size clasts. Its ability to encrust larger areas faster allows it to become the predominant encruster.

Four different growth forms of rhodoliths are recognised in the southwest Sicily limestones. These are related in the first instance to the species forming the rhodoliths and in the second instance to the environments within which they are formed. The abundance of compact non-branching growth forms along with the absence of open branching forms at the Contrada Giovanni locality and in the Mt Gargalupo area suggests that the deposits accumulated under higher energy conditions than at Nadorello east.

The algae are thus consistent with the palaeoenvironment inferred for the limestones in Section 2.5; and the species identifications are consistent both with a Palaeogene age for the limestones, and with their Indo-West Pacific affinities as found elsewhere for fauna and flora in the Mediterranean (Zammit-Maempel, 1979; Bennett, 1980).

4.2 Trace Fossils

4.2.1 Introduction

Trace fossils are present, but not common, in the mid-Tertiary successions of both southwest and southeast Sicily. (The latter are described here to complement the phosphorite study of Chapter 7 and to expand the description of the phosphorite and hardground occurrence in SE Sicily). In southwest Sicily, Mascle (1973, 1979) records their presence but does not identify or describe them. Those from southeast Sicily have no previous record or description.

Burrows (into soft sediment) and borings (into hard substrates) are here classified to generic level on their gross morphology, following Häntzschel (1975) and Bromley (1972) respectively. Identification to species level has been made where widely used, unambiguous names are available. New species have not been designated despite minor variations in burrow or bore diameter, or sedimentary infill, because of the doubtful specific value of these criteria.

4.2.2 Systematic Palaeontology

Ichnogenus THALASSINOIDES Ehrenberg 1944

Thalassinoides paradoxica (Woodward)

Plates 4.41-4.43; text-figs 2.1, 2.2

- 1830 *Spongia paradoxica* Woodward, p. 5.
 1869 *Siphonia paradoxica* (Woodward); Wiltshire, p. 176.
 1967 *Thalassinoides paradoxica* (Woodward); Kennedy, pp. 142-148, pls 3, 4, 8, figs 5, 9, fig. 2; text-figs 4, 5A + B, (cum. syn.)
 1975 *Thalassinoides paradoxicus* (Woodward); Bromley, p. 411.
 1980 *Thalassinoides paradoxica* (Woodward); Bennett, pp. 177-179, pl. 3.13.1.

Diagnosis (after Kennedy, 1967). A species of *Thalassinoides* characterised by an irregular, very extensive horizontal burrow network, occurring at several levels, connected by vertical shafts. Diameter of tunnels variable, between 7 and 60 mm, short blind tunnels very common.

Surface covered with longitudinal ridges. Generally occurs associated with erosion surfaces.

Description. Burrow system with both vertical and horizontal components extending to some 0.25-0.3 m depth. Tunnel sizes 15-60 mm (commonly 20-35 mm) diameter. Non-branching vertical components located in the upper region of the system. Horizontal to sub-horizontal components frequently bifurcating at angles of 40° to 90° and at irregular intervals of 30 to 300 mm. Swelling up to twice normal burrow diameters occurs at junction points. Short blind tunnels present but not common. Burrow walls generally smooth, very rarely with fine striations sub-parallel to burrow axis.

Remarks. The genus has characteristic gross morphology and is distinguished from *Ophiomorpha* by lack of tuberculate wall structure. The species is distinguished from the three other recognised species (Kennedy, 1967; Häntzschel, 1975): by its smaller burrow dimensions from *T. saxonicus*; by its lack of reticulate burrow surface ornament from *T. ornatus*; and by its more irregular branching pattern from *T. suevicus*.

The Sicilian burrows are ascribed to *T. paradoxica* since they resemble this species as described by Kennedy (1967) from the Lower Chalk of southern England in possessing vertical connecting shafts, irregular horizontal networks, some burrows terminating blindly and some showing a surface ornament of longitudinal striations. *T. paradoxica* is considered to be the stenomorphic variety of *T. suevicus*, its formation being restricted by the progressive lithification of the enclosing sediment (Bromley, 1975). *Thalassinoides* may be the work of burrowing crustaceans (Frey, 1975b).

Occurrence. *T. paradoxica* is restricted to two localities within the study area: Upper Cretaceous - Upper Oligocene unconformity at Nadorello east (Fig. 2.2) in southwest Sicily (where the burrows are thought to have formed in Upper Oligocene times since they are absent from the underlying Cretaceous sequence), and within the Lower Miocene of Donnalucata in southeast Sicily (Fig. 7.1). Horizontal components predominate whilst

vertical components are subordinate in the southwestern Sicily example, and vice-versa in southeast Sicily. At Donnalucata, the burrows are associated with a hardground (Section 7.2.2); at Nadorello east, this can only be inferred from their presence.

Stratigraphic Range. *Thalassinoides* has a known minimum range from Triassic to Tertiary (Häntzschel, 1975). *T. paradoxica* has been described from the Upper Cretaceous of England (Kennedy, 1967, 1970a) and the USA (Frey & Howard, 1970). Bromley (1970) notes that the species is probably associated with the Upper Cretaceous hardgrounds throughout Europe, southwest Asia and north Africa. Bennett (1980) records *T. paradoxica* from the Lower Miocene of the Maltese islands.

Geographic distribution. *Thalassinoides* has been widely recorded from Euro-Asia and Australia (Häntzschel, 1975), and from the western USA by Frey & Howard (1970), but descriptions from the Mediterranean area are few (notably Bennett, 1980). There is no previous record of *Thalassinoides* in Sicily. In the Mediterranean area *T. paradoxica* has so far only been recorded from the Maltese islands.

Thalassinoides suevicus (Rieth)

Plates 4.44-4.47

- 1932 *Spongites suevicus quenstedti* Rieth, p. 274.
- 1932 *Spongites suevicus* Quenstedt; Rieth, p. 292.
- 1932 *Cylindrites suevicus* (Quenstedt); Rieth, pl. 13a,b.
- 1964 *Thalassinoides suevicus* (Rieth); Häntzschel, p. 302.
- 1967 *Thalassinoides* cf. *suevicus* (Rieth); Kennedy, pp. 140-141,
pl. 1, fig. 2, (*cum. syn.*).
- 1980 *Thalassinoides suevicus* (Rieth); Bennett, pp. 179-181,
pl. 3.31.2, 3.

Diagnosis (compiled from Häntzschel, 1964, Bennett, 1980). A species of *Thalassinoides* characterised by extensive branching burrow systems in the horizontal sub-horizontal plane, vertical burrows few or absent. Tunnel diameters 20-50 mm.

Description. Extensive branching burrow system of predominantly horizontal sub-horizontal bifurcating burrows with some vertical components. Tubes 10-35 mm (commonly 15-30 mm) diameter, branching at angles of 40° - 90° , at regular intervals of 150-250 mm, with minor swelling at the branch points. Burrow walls smooth and unornamented. The system is exposed mostly as imprints on extensive weathered surfaces oblique and sub-parallel to bedding.

Remarks. *T. suevicus* is distinguished by its much smaller burrow dimensions from *T. saxonicus*, by its lack of reticulate ornament from *T. ornatus*, and by its regular branching pattern from *T. paradoxica*.

The burrows are ascribed to *T. suevicus* in that they resemble this species as described by Häntzschel (1964) from the Campanian of Westphalia, in possessing extensive bifurcating burrows which are horizontal sub-horizontal in aspect with few vertical components.

Occurrence. Found in the Lower Miocene shelf limestones of southeast Sicily, *T. suevicus* is extensive in two beds (0.5-1 m thick) immediately above and below the hardground at Donnalucata (Section 7.2.2). It is also restricted in exposure at Pizzo Capra d'Oro (Fig. 7.1) where it occurs as small (10-20 mm dia.) burrows in a horizon (0.5-1 m thick) located immediately below a phosphorite conglomerate.

Stratigraphic range. The known minimum range of *Thalassinoides* is Triassic to Tertiary. Many unspecified records of the genus may, in fact, be *T. suevicus* since the specific burrow dimensions (20-50 mm) are those most commonly occurring, and unlike *T. paradoxica*, *T. suevicus* is not restricted to hardground associations.

T. suevicus has been described from the Upper Cretaceous of Westphalia (Häntzschel, 1964) and the Lower Miocene of the Maltese islands (Bennett, 1980) and *T. cf. suevicus* from the Upper Cretaceous of southern England (Kennedy, 1967).

Geographic distribution. *T. suevicus* has been identified from England and Germany, but the only reported Mediterranean occurrence is that by Bennett

(1980) from Malta. It may, however, be as widespread as the genus, which is widely recorded from the USA, Europe, Asia and Australia (Häntzschel, 1975).

Ichnogenus TRYPANITES Mägdefrau 1932

Trypanites weisei Mägdefrau

Plate 4.48

1932 *Trypanites weisei* Mägdefrau, p. 152.

1972 *Trypanites weisei* Mägdefrau; Bromley, p. 95, text-fig. 1,
(*cum. syn.*).

Diagnosis (after Bromley, 1972). A species of *Trypanites* characterised by simple unbranched cylindrical borings 1-2 mm diameter, perpendicular to the substrate.

Description. Straight or slightly sinuous cylindrical borings perpendicular to the substrate and of almost constant diameter (0.8-1.5 mm) in any one bore. Penetrating 5-10 mm, they do not branch and have no wall lining or ornament.

Remarks. The bores are ascribed to *Trypanites* (*sensu* Bromley, 1972) in that they possess a single opening and unbranched tube. They are ascribed to *T. weisei* since they are perpendicular to the substrate and are *c.* 1 mm in diameter.

T. weisei is distinguished from *T. cretacea*, *T. biforans* and *T. clavatus* by its circular cylindrical form; *T. solitarius* by its perpendicular orientation to the substrate; and from *T. vadaszi* which is restricted to wood substrates.

Occurrence. Common in phosphatic clasts in the phosphorite conglomerates of Lower Miocene age from Contrada le Serre, Pizzo Capra d'Oro and Donnalucata (where they are also found penetrating the hardground surface) in southeast Sicily. The bores are also found penetrating phosphatised and non-phosphatised chalk clasts in the basal conglomerate of the Upper Oligocene at Nadorello east and San Biagio in southwest Sicily.

Stratigraphic range. *Trypanites* as defined by Mägdefrau (1932) has a known range from Triassic to Miocene. Bromley's (1972) definition would extend this to the Recent. *T. weisei* was originally described from the Middle Triassic of Germany.

Geographic distribution. The genus is known from USSR, Germany and Poland (Häntzschel, 1975). Bennett (1980) describes *Trypanites* sp. from the phosphatic hardgrounds and clasts from the Maltese Lower Miocene.

Trypanites sp.

Plates 4.42, 4.49

Description. Straight cylindrical, or flask shaped borings perpendicular or at high angles to the substrate. Straight bores have openings 3-8 mm diameter and range in depth from 15-60 mm to unknown depths. Flask shaped bores have openings 3-4 mm diameter widening to 10-12 mm in the chamber of the bore which penetrates 30-45 mm depth.

Remarks. These borings are ascribed to *Trypanites* since they possess a single opening and are unbranched. They are distinguished from *T. weisei* by their larger diameter, and from *T. solitarius* by their sub-perpendicular orientation to the substrate.

Bore openings are clearly exposed on extensive surfaces. Exposure in vertical section is, however, poor. The straight bores may be of sipunculid annelid origin (Bromley, 1970) whilst the flask shaped bores may be of bivalve origin (Kelley, 1980). Poor exposure coupled with the classification of ichnofossils on pure morphologic (and not genetic) grounds necessitates their incorporation under one species here.

Occurrence. The straight bores are found in profusion on the hardground surface in the Lower Miocene at Donnalucata in southeast Sicily. Flask shaped bores are also present, but less common. The openings to bores of this dimension are also found on the surface of a fissure cutting the Upper Oligocene and Cretaceous at Nadorello east in southwest Sicily, where they are infilled with Lower Miocene glauconitic limestone.

Shallow (10-20 mm) straight bores also penetrate phosphatised and non-phosphatised chalk clasts in the basal conglomerate at Nadorello east and San Biagio, southwest Sicily.

"*Stratigraphic range*" and "*Geographic distribution*": see *T. weisei*.

4.2.3 Palaeoenvironments

That trace fossils are potentially significant palaeoenvironmental indices is evidenced by a substantial, relatively recent literature, well represented by the symposium volumes edited by Crimes & Harper (1970, 1977) and by Frey (1975a). Although but two species of burrows and two of borings are represented in the Sicilian mid-Tertiary, together they are sufficient to indicate normal marine salinities; relatively low energy conditions; moderate (50-300 m) depth of sedimentation; local variable rates in sedimentation and lithification; and the presence of lithified substrates.

Shallow horizontal burrow systems (such as *Thalassinoides*) with poorly developed walls are characteristic of shelf seas (Seilacher, 1964, 1967). Moreover, they represent excavation under normal marine salinities in low energy conditions (Rhoads, 1975) since fluctuating salinities and high energy conditions resulting in shifting substrates, necessitate the formation of deep vertical burrows. *Thalassinoides* is ubiquitous in shallow water (50-300 m) shelf sea deposits, to which it is restricted.

The irregular branching pattern of *T. paradoxica* is caused by the excavation of these burrows during the lithification of the enclosing sediment (*vide* Bromley, 1975; Kennedy, 1970b, 1975). Both Bromley (1967b) and Kennedy (1967) note the exclusive occurrence of this species with recognised hardgrounds. The presence of *T. paradoxica* in the southwest Sicily deposits may therefore indicate significant lithification of the burrowed substrate and incipient hardground formation even though a hardground as such is not evidenced by a bored or mineralised surface. In southeast Sicily, however, *T. paradoxica* underlies a mineralised and bored

hardground surface.

In shelf sea deposits, the number of burrows reflects the rate of sedimentation: slow rates of deposition result in the addition of more burrows. Thus sediments with an abundance of burrows are not indicative of a frenzy of activity but of prolonged sea floor exposure due to slow rates of sedimentation (Howard, 1975). The greater number of burrows in the beds immediately below and above the hardground in southeast Sicily (Section 7.2.2) relative to beds elsewhere in the succession therefore indicates slower sedimentation, a feature which might be expected since the hardground itself represents a pause in sedimentation.

The presence of borings indicates a lithified substrate. Borings are commonly associated with submarine hardgrounds and often cited as proof of submarine lithification (Bromley, 1968, 1970, 1972, 1975; Kennedy, 1975; Warne, 1975, 1977). The quantity of borings is unlikely to reflect the duration of sedimentary omission (Bromley, 1975) since, given a favourable environment, a community of sponges and bivalves can completely break down a limestone surface to a depth of several centimetres in a few years. The absence of boring activity to this degree in the southeast Sicily hardground suggests that the optimum conditions for colonisation by borers were not attained and that the limiting factors listed by Bromley (1975) had an effect. However, since all extant boring organisms dominate the littoral and reefal environments, and since hardgrounds can form in a variety of depths (Fischer & Garrison, 1967) it is suggested that the southeast Sicily hardground may have formed in depths too great for optimum colonisation by boring organisms.

4.2.4 Conclusions

Although burrow systems from the mid-Tertiary of Sicily have seldom been recognised let alone described or identified, two species of the burrow system *Thalassinoides* (*T. paradoxica*, *T. suevicus*) and the boring *Trypanites* (*T. weisei*, *T. sp.*) are widely developed in association with carbonates of Upper Oligocene and Lower Miocene age in both southwest and southeast Sicily.

The morphology of *Thalassinoides* burrows in Sicily is closely similar to that of burrows excavated in Cretaceous, chalky lithologies in England and Germany. In Sicily, however, the age of burrow formation appears to be Upper Oligocene - Lower Miocene rather than Cretaceous. Extension of the species range from Upper Cretaceous to Lower Miocene is consistent with Bennett's (1980) identification of both *T. paradoxica* and *T. suevicus* from the Lower Miocene shelf carbonates of the Maltese islands.

Differences in burrow morphology between *T. paradoxica* and *T. suevicus* can be ascribed to the mechanical difficulties of burrow excavation during hardground lithification of the sediment, as argued by Bromley (1975) and Kennedy (1975). *T. paradoxica* is considered to be the stenomorphic equivalent of *T. suevicus* and indicates the presence of an associated hardground. A hardground is further evidenced at Donnalucata in southeast Sicily by the presence of common *Trypanites* bores on a mineralised surface.

The profusion of *T. suevicus* burrows in the beds below and above the hardground in southeast Sicily suggest a slow depositional rate immediately before and after hardground formation. *Trypanites* borings on the hardground surface, although common, are not abundant, and have caused only a small amount of bioerosion. The hardground may therefore have formed in waters too deep for optimum colonisation by boring organisms (which mostly occupy the littoral and reefal environments).

By analogy with other reported occurrences of *T. paradoxica* and *T. suevicus*, their environment of formation is inferred to be open shelf in water depths of 50-300 m under normal saline conditions. This is consistent with the environment inferred from: coralline red algae (this Chapter), facies associations (Chapter 2), and phosphorites (Chapter 7).

CHAPTER 5

DIAGENESIS

5.1 Carbonate diagenesis: Upper Oligocene Limestones

5.1.1 Introduction

Widespread post depositional diagenetic alteration of the limestones is present in three forms: cementation, compaction and neomorphism. The first two have had considerable effect; neomorphism, although widespread, is minimal. In addition, syn-cementation muds, and crystal and pelletal silts, plus dolomitisation are present but only locally developed. Non-carbonate diagenesis takes the form of glauconitisation of foraminiferal chamber infills and the formation of early diagenetic pore-filling feldspars, both found in the western Nadorello area and dealt with in Chapter 6 and Section 5.2 respectively.

The features of carbonate diagenesis are described and discussed below. Four periods of cementation are recognised. The first three periods are early, pre-compaction and of marine origin. The fourth period is late, post-compaction and of a fresh water origin. Compaction is represented by grain redistribution or rotation, grain fracture and pressure solution between grains. Neomorphism is represented by the common formation of microspar and occasionally pseudospar. Neomorphic syntaxial overgrowths on echinoid grains are also recognised but they are of limited occurrence as are the syn-cementation pore-fillers and dolomitisation. The latter is found only at San Biagio east where it is inferred to be of metasomatic origin unrelated to the general depositional and diagenetic environments of the area.

5.1.2 Cementation

a) Introduction

Four periods of cementation (referred to here by number from first (earliest) to fourth (latest) period) are easily recognisable*. All cements, except where associated with glauconitic sediments, are non-ferroan

* SEE PLATE 5.3

low magnesian calcite (determined by staining as outlined in Appendix I). Where glauconitic sediments are involved (in western Nadorello only) the associated cements show phases of ferroan and non-ferroan calcite.

The criteria used for recognition of cement spar in this work were most of those listed by Bathurst (1975, p.417-419), namely:

- 1) There are two or more generations of spar.
- 2) There are no relict structures such as seen in neomorphic spar.
- 3) Particles composed of micrite are not altered to spar.
- 4) Mechanically deposited micrite is present but unaltered.
- 5) Contacts between spar and particles are sharp.
- 6) The margins of the sparry mosaic coincide with surfaces that were once free, such as surfaces of skeletal particles.
- 7) The spar lines a cavity which it fills incompletely.
- 8) The sparry mosaic occupies the upper part of a cavity whose lower part is occupied by a more or less flat topped internal (geopetal) sediment.
- 9) The intercrystalline boundaries in the mosaic are made up of plane interfaces.
- 10) The size of the crystals increases away from the initial substrate of the mosaic.
- 11) The crystals of the sparry mosaic have a preferred shape orientation with longest axes normal or at a high angle to the initial substrate of the mosaic.
- 12) The mosaics are characterised by a greater percentage of en-facial junctions than would be expected for neomorphic spar.

In addition to these criteria, the presence of alternating zones of ferroan and non-ferroan calcite seen in syntaxial echinoid overgrowths are believed to be indicative of cement rather than neomorphic overgrowths (Evamy & Shearman, 1965).

b) First Period

The first period of cement is represented by syntaxial overgrowths,

seen only on some echinoid grains but from all localities except San Biagio east and west. It is dusty in appearance and occurs as thin (10-30 μ) jagged coatings with peaks extended parallel to the c-direction of the crystal (echinoid grain) (Plates 5.1-5.4).

c) Second Period

The second period of cementation is widespread. It occurs at all the figured localities (Section 2.3) in a pore-lining position and fills some of the smaller pores. It is generally poorly developed and only at the San Biagio west locality does it form a substantial pore-lining cement (Plate 5.28). It is represented by a clear spar (when viewed under the petrological microscope) forming syntaxial overgrowths on echinoid grains and scalenohedra and equant spar on other substrates (Plates 5.1-5.5).

It is thickest (up to 300 μ) on echinoid grains and shows preferential growth in the c-direction of the crystals (Plate 5.3). On other substrates it shows a variable development (Plate 5.2). *Amphistegina*, *Spiroclypeus*, *Heterostegina*, *Operculina* and bivalve fragments commonly show rims of scalenohedra up to 80 μ long visibly syntaxial on their substrates. Fenestrate bryozoan fragments are also good sites for cementation (Plate 2.27), their chambers are commonly filled by the second period of cement. Algal and mud substrates are poor sites: cement is commonly not present or is represented by occasional equidimensional crystals up to 40 μ size. Lepidocycline foraminifera can either show their chambers completely filled by the second period of cement or the cement may be represented by only a few thin scalenohedra if any at all.

In the glauconitic limestones of western Nadorello (Section 6.2) this second period of cement forms, on echinoid grains, up to seven zones of alternating ferroan (stained blue with potassium ferricyanide) and non-ferroan calcite. These zones, with sharp and gradational boundaries, are serrated in appearance with apices extended in the c-direction of the crystal (Plate 5.6).

d) Third Period

The third period of cement is found only at Nadorello east (Plates 5.3, 5.4, 5.7-5.9) and in blocks of breccia (formed by Mio-Pliocene faulting) in the San Biagio area (Plate 5.10) at UB 372679 and UB 392673. At Nadorello east it is present in the upper part of the succession at locality B (Fig. 2.1) but it is not seen at A and C. The spar is therefore local in its development. At both Nadorello and San Biagio it forms a pore-lining (Plates 5.3, 5.7, 5.8) and fills some of the smaller pores (Plate 5.4). It is dusty in appearance, caused by an abundance of inclusions 2-5 μ in size, the larger of which are less frequent and opaque (Plate 5.9). Where the spar nucleates on echinoid grains it is syntaxial. On other substrates it is bladed, sometimes acicular in appearance forming rims 100-140 μ thick on *L. (Eulepidina)*, *Amphistegina*, *Spiroclypeus*, *Heterostegina* and *Operculina* foraminifera where it can often be seen to be syntaxial; and rims 60-80 μ thick on algal and mud substrates (Plate 5.7).

e) Fourth Period

The fourth period of cement is found only in the Nadorello area (Plates 5.3-5.9), the San Biagio west locality and in breccia blocks from the San Biagio area (Plate 5.10). The spar is clear, pore filling and forms centripetally enlarged blocky mosaics (Plate 5.7) or wide syntaxial overgrowths on echinoid cement substrates (Plate 5.3). In the western Nadorello area where this cement is associated with glauconitic limestones it is of ferroan calcite throughout and shows none of the zones seen in the second period (Plate 5.6).

f) Relative Timing

Timing of the cements relative to each other is evidenced by their superimposition on echinoid grains. Thus the first period is coated by the second period which is subsequently coated by the third period and, in turn, coated by the fourth period (Plate 5.3). The cements can also be timed relative to compaction. Thus the first, second and third periods pre-date compaction and the fourth post-dates it.

The pre-compaction timing of the second period cement (and

therefore, by inference, the first period) is demonstrated by its presence on fractured foraminifera, but never on the fracture surfaces; and by its preservation of the original grain distribution and point contacts between grains where they are enclosed, or partially enclosed, in echinoid overgrowths of the cement (Plates 5.11, 5.12). Elsewhere in the same rocks areal pressure solution contacts (notably around the boundary of the echinoid overgrowths, Plates 5.1, 5.2) prevail (Plate 5.11) since the second period cement does not form a substantial rim to produce a rigid framework except at San Biagio west (Plate 5.27). The pre-compaction timing of the third period cement is presumed, since, in the rocks where it occurs, there are no compaction features and point contacts prevail throughout (Plates 2.22, 5.10).

The post-compaction timing of the fourth period of cement is evidenced by its deposition on fracture surfaces; its fill of fractures in bioclasts; and by its presence as a pore-filling cement in rocks which show common pressure solution contacts between grains.

g) Discussion

Carbonate sediments may be cemented in both submarine and sub-aerial environments. However, distinction between cements formed in these two environments on the basis of crystal morphology alone is often far from easy, as is the distinction of neomorphic spar from cement spar. Mineralogy, oxygen isotope values and trace element (notably Sr and U) concentrations within the cementing mineral are better indices of origin than crystal morphology. However, late stage diagenetic alteration associated with final subaerial exposure frequently destroys earlier mineralogies. Aragonite is either dissolved or inverted to calcite, and Mg^{2+} is lost from high magnesian calcites, converting them to low magnesian calcite. In consequence, original trace element concentrations are also lost. In practice, therefore, the morphology and sequence of cement generations are the most readily available and useful guides for distinguishing between submarine and subaerial cements.

Marine cements frequently have a dusty appearance whereas fresh-water cements are clear (Bathurst, 1975; Wilson, 1975). According to

Folk (1974) and Bathurst (1975) marine cements are thought to be restricted to a micritic, fibrous or bladed scalenohedral form whereas freshwater cements commonly form blocky mosaics. The elongate habit is typical of marine cements; sideways growth of the crystals is inhibited by incorporating Mg^{2+} , and to a lesser extent, Na^+ in the lattice (Folk, 1974; Bathurst, 1975). Conversely, in a freshwater environment poisoning of the lattice by Mg^{2+} and Na^+ does not occur and therefore blocky, equant crystals can form. However, these features of marine and freshwater cements are not hard and fast rules. Consequently, clear, blocky aragonitic cement has been described from the marine environment (Land & Moore, 1980).

The first three periods of cementation described above are early, pre-compaction and are inferred to be of marine origin. The first and third periods are both dusty and the latter also shows common bladed scalenohedral, sometimes acicular growth form - all features of marine cements. The second period of cement is clear, composed of pore-lining scalenohedra, equant crystals and relatively thick syntaxial overgrowths on echinoid grains. Where the spar is associated with authigenic glauconite bearing deposits the syntaxial overgrowths show seven zones of alternating ferroan and non-ferroan calcite. Ferroan calcite represents precipitation in reducing conditions whereas iron free calcite forms in oxidising conditions (Evamy, 1969). The echinoid overgrowths therefore record alternating reducing/oxidising conditions, an environment which is closely similar to the environment evidenced by glauconite formation (oxygen minimum zone, Section 6.6.2) and therefore the cement is inferred to be syn-glaucinitisation, early marine in origin. This inference is substantiated by the exclusive presence of these zoned cements in glauconitic sediments (here, and in the Lower Miocene limestones) when ferroan calcites could conceivably form in any environment below the water table (Evamy, 1969).

The mineralogy of marine cement is apparently largely controlled by temperature and the relative supersaturation of the polymorphs of $CaCO_3$ in seawater (Bricker, 1971; Folk, 1974; Bathurst, 1975). Aragonite is generally precipitated in relatively warmer, shallower water

whilst magnesian calcite is usually found in cooler, deeper water. However, in detail, the situation is far more complex since at shallow depths seawater is supersaturated with respect to all three polymorphs of Ca CO_3 . Consequently, both aragonite and magnesian calcite can, and do, precipitate, in some cases together (Alexandersson, 1972, 1974; Moberley, 1973; Schroeder, 1974).

Within the Chattian limestones the bladed scalenohedral form, indicative of an original high magnesian calcite mineralogy, dominates in the third period cement and in consequence implies that it was precipitated in relatively deeper or cooler water than that in which aragonite would be expected to occur. The restricted development of this spar and more so, that of the first period cement and the poor to moderate, but widespread development of the second period cement may also indicate crystallisation in cooler deeper environments which are likely to be less saturated with Ca CO_3 relative to shallow warm water environments.

The fourth and final period of cementation is a late, post compaction, clear, equant, blocky calcite spar. Such spar is characteristic of cement precipitated from meteoric water and its large crystal size would suggest crystallisation below the water table in the phreatic environment (Folk, 1974). Equant spar is able to grow once meteoric water has flushed Mg^{2+} from the sediment-pore fluid system, the Mg : Ca ratio being reduced from about 3 : 1 to 1 : 3. Once this prime inhibitor to equant cement growth is removed, then large calcite crystals can form perfect rhombohedra, subhedral and anhedral crystal mosaics, with the largest crystals representing the slowest growth rates (Folk, 1974). It is possible that the same crystal mosaics could be produced by deep burial of the sediment, where pore fluids have an Mg : Ca ratio of 1 : 2 to 1 : 4 due to capture of Mg by dolomite and clays (Folk, 1974). However, this is not the case in the Upper Oligocene since the area, and the "Western Sicily Bridge" in general has a history of uplift from Upper Oligocene onwards (Section 3.5).

This fourth period of cement is found only in the rhodolithic algal packstone-wackestone facies in the central part of the study area

been protected from compaction by the third period cement (Plates 5.7, 5.8). The second and third features are self evident when the rocks are examined in thin section. Pressure solution is by far the most common feature.

Most contacts between grains are accommodatory (i.e. one grain goes into solution in preference to its neighbour). Microstylolites (Plate 5.14) are rare but do occasionally occur at contacts between grains of *Heterostegina*, *Operculina*, *Spiroclypeus* and *Amphistegina* foraminifera. Finer grained rocks (coarse sand size grains) tend to show less effects of pressure solution than their coarser grained counterparts at the same locality (compare Plate 2.31 with Plate 5.15). This is likely to be the result of the greater amount of grain contacts in the finer grained rocks thus dissipating the pressure.

The various grains present have reacted differently to the excessive pressure. Echinoid grains with their overgrowths rarely, if ever, go into solution (it is always their neighbours which take preferential solution; Plates 5.1, 5.2) and they never fracture. Algae are the most susceptible to fracture and pressure solution and commonly go into solution in preference to their neighbours. Occasionally pressure solution of an algal clast may be so extensive that it appears "interstitial" to the other grains (Plate 5.15). Where lepidocycline foraminifera (and in particular *L. (Nephrolepidina)*) are abundant and subjected to excessive pressure their outer chamber walls and septa preferentially go into solution and with probable local reprecipitation of this calcium carbonate, it results in a massive calcite boundary between grains (Plate 2.32) (pressure welding of Bathurst, 1975). *Heterostegina*, *Operculina* and *Spiroclypeus* have reacted to the excessive pressure by common fracturing of the test (Plate 5.16), solution of the thinner internal septal walls (Plate 5.17) and occasional apparent ductile deformation. Ductile deformation also occurs in some *L. (Eulepidina)* bearing rocks (Plate 5.18). Rock fragments vary in their reaction to the excessive pressure, some go into solution in preference to their neighbours, others do not (Plate 5.19).

(Section 2.4.4). It is not seen in the foraminiferal grainstone-packstones found to the east and west. The cement records probably the final period of uplift into the phreatic environment. Its absence from the foraminiferal grainstone-packstones could suggest that these limestones were carried still higher into the vadose environment, possibly consistent with their situation on different structural units to the rhodolithic algal packstone-wackestones (Section 2.6).

In general, these late stage freshwater cements have a local source for their calcite, usually aragonitic bioclasts within the same limestone. Thus Friedman (1964), Bathurst (1966), Land *et al.* (1967), Bennett (1980) and Buchbinder & Friedman (1980) all concluded that dissolved aragonite is locally precipitated as calcite. Pingitore (1970) found that almost all (80%) calcite precipitated in Pleistocene limestones of Barbados was derived from the local dissolution of aragonite. The general lack of late stage blocky cement in the Upper Oligocene of southwest Sicily along with the lack of any aragonitic fauna adds further weight to this local source theory. A possible source for the fourth period cement could be local Upper Miocene - Quaternary limestones which have an abundant leached gastropod/bivalve fauna. This proposed semi-autochthonous source may explain why the spar is restricted in occurrence since much of the dissolved calcium carbonate may have been reprecipitated before reaching the Upper Oligocene.

5.1.3 Compaction

a) Observations

Compaction is widespread. It is found in all porous rocks except where the third period cement is found (Section 5.1.2d) or where the second period has formed a substantial rim (San Biagio west only). It has had considerable effect and has resulted in: the rotation and redistribution of grains, fracture of grains and pressure solution between grains. The first is evidenced by an interlocking texture and bedding parallel orientation of *Nephrolepidina* (Plates 2.32, 5.12) in a rock dominated by that genus. It is also inferred from the lack of any large pore space in rocks which have undergone compaction (Plates 5.11, 5.13). Such pore space is preserved in similar rocks which have

b) Discussion

Most limestones show little evidence of compaction (Pray, 1960; Zanol, 1969) and for this reason, it is usually inferred that an early phase of cementation has taken place to give the sediment rigidity (Bathurst, 1975). Meyers (1980), however, describes skeletal limestones from the Carboniferous of New Mexico in which intergranular porosities are commonly reduced by 50% and more rarely by up to 75%, accomplished by both mechanical (rotation and breakage) and chemical (pressure solution) processes.

In sediments containing ostracods, thin shelled brachiopods, abundant fenestrate bryozoans and echinoid debris Meyers found that deformation progressed from breakage of brachiopods and ostracods accompanied by grain repacking (rotation and redistribution) into rocks showing increasing breakage, plastic deformation and pressure solution of bryozoans. The most compacted rocks show common pressure solution and occasional breakage of echinoderm fragments. Overburden, skeletal architecture, pre-compaction diagenesis, clay mineral presence and pore fluid chemistry all had an influence on the degree of compaction, but Meyers concluded that shell architecture and pore fluid chemistry were the most important in promoting compaction. Microcrystalline grains (mostly bryozoans) were more susceptible to mechanical and chemical compaction than single crystal echinoderms of the same order of size. This was explained by slippage of neighbouring crystals in microcrystalline grains allowing breakage and plastic deformation whilst higher susceptibility to pressure solution was explained by a higher surface area to volume of skeletal calcite in bryozoans to that in echinoderms.

In the situation described by Meyers, pore fluid chemistry was of prime importance in chemical compaction (as implied by the theoretical work of Weyl, 1959). Qualitatively, the greater degree of undersaturation with respect to CaCO_3 , the lesser the amount of overburden needed to cause intergranular and intragranular pressure solution. Meyers concludes that fresh water phreatic lenses invaded the sediments (geologically) soon after deposition in response to sea level changes and that this fresh water enhanced chemical compaction.

Compaction in the Upper Oligocene limestones of southwest Sicily is enhanced by a poorly developed pore-lining spar, but it shows similarities to that described by Meyers (1980). Microcrystalline grains (especially coralline red algae) break and go into solution more readily; on occasions *Operculina/Heterostegina* and rarely *L. (Eulepidina)* deform in a plastic manner. In comparison, echinoid fragments never fracture and never enter pressure solution. Repacking of grains has occurred throughout except where the dusty marine third period of cement occurs preventing compaction and preserving grain distribution (compare Plate 5.8 with Plate 5.19). The amount of compaction is, however, less than that described by Meyers. This may be due to a combination of a number of reasons including:

- (1) Absence or low quantities of clay minerals (none have been found in the limestones).
- (2) The presence of pore solutions which did not become grossly undersaturated with respect to CaCO_3 until overburden was lifted (undersaturation must, however, have occurred since some pressure solution is present).
- (3) A relatively small amount of overburden. This is possible since the limestones are situated on a topographic high, which is unlikely to be the site of thick successions.
- (4) Near monomineralic sediments, they are composed mainly of benthonic foraminifera, echinoid and red algal debris all of which were originally high magnesian calcite. Had the sediment been polymineralic, then aragonite might be expected to go into solution before magnesian calcite, and magnesian calcite into solution before non-magnesian calcite, provided that the pore solution was not supersaturated with respect to all three polymorphs.
- (5) The presence of different microcrystalline grains, than those encountered by Meyers (1980). The benthonic foraminifera present here may be more resistant to pressure solution and breakage.

Finally, an interesting feature common to both of these compacted limestones (described here, and by Meyers, 1980) is that they both contain relatively common echinoderm fragments (possibly abundant in some

of Meyers' rocks). Echinoid plates form the best hosts for cementation; they are single crystals of calcite with suppressed growth in the c-direction. Consequently, when released from the echinoid test, they readily accept CaCO_3 from solution. In deep cool marine environments where the water is not supersaturated with respect to CaCO_3 , precipitation will preferentially occur at the echinoid fragment forming wide overgrowths there at the expense of a substantial pore-lining spar. When buried this sediment will be susceptible to compaction.

5.1.4 Neomorphism

a) Introduction

Neomorphism is represented by the common formation of microspar (seen at all localities, Plates 5.20, 5.21) and occasionally pseudospar from carbonate mud. It is also represented by syntaxial overgrowths on echinoid grains, some foraminifera and bivalve fragments. In all cases carbonate mud is replaced. Usually mud matrix is replaced but on some occasions the mud in peloids is partially replaced to give a granuleuse structure. Bioclasts and lithoclasts (other than contemporaneous intraclasts) show no signs of neomorphism.

The criteria used for the recognition of neomorphic spar were those given by Bathurst (1975, p.484-491) namely: a gradational junction between unaltered micrite and spar crystals; crystal diameters commonly 5-10 μ and occasionally up to 50 μ ; irregular variations in spar crystal size from place to place, and lack of the more uniform vectoral size change found in cement spar; relics of primary micrite frequently found within areas of spar; and, the spar lacks the features normally attributed to cement spar (Section 5.1.2a).

b) Syntaxial Overgrowths

Neomorphic syntaxial overgrowths on echinoid grains are not common and were identified only from the Tombe Sicani and Nadorello east localities. At Tombe Sicani (Fig. 2.8) the overgrowths are found in wackestones whilst at Nadorello east (Fig. 2.2) they are found in fully cemented packstones. Different criteria are used to distinguish the overgrowths

from cement overgrowths in each case.

In the wackestones (Plates 5.22, 5.23) the overgrowths are distinguished from their cement counterparts in that: they commonly have indistinct boundaries with the adjacent microspar or mud; they are often thinner than cement overgrowths, commonly less than half the thickness; and they are found in rocks with wackestone, matrix supported textures. The grains are thought not to be derived complete with overgrowths since the delicate structures of the overgrowths are preserved and since the enclosed grains are themselves rounded to subrounded.

In the cemented packstones (Plates 5.20, 5.21) neomorphic overgrowths are recognised by their replacement of microspar. The overgrowths are large, filling all the neighbouring interclast space which, elsewhere in the same rock, is commonly partially filled by mud subsequently altered to microspar. In the region occupied by the overgrowths, however, mud or microspar is never seen; it is presumably replaced by the overgrowth. Since the rocks in which these overgrowths are found are fully cemented (by fourth period cement) it seems likely that the overgrowths are part cement, part neomorphic and that this might account for their large size.

Syntaxial neomorphic overgrowths found on bivalves and some foraminifera (*Heterostegina/Operculina* fragments) are found only in the wackestones of the Tombe Sicani locality. Their identification as neomorphic in origin rests on the fact that they are found in rocks with wackestone textures (Plate 5.23), and that their delicate structures are unlikely to survive transport.

c) Discussion

In general, the precise timing of neomorphic alteration in relation to cement precipitation is not wholly known. Cullis (1904) and Schlanger (1964) thought that the process could be initiated early in an unconsolidated sediment. Folk (1974) considered neomorphism to be a subaerial phenomenon, possibly linked to the flushing of Mg^{2+} from the sediment. Bathurst (1975) stated that it operated at normal temperature

and pressure. Both authors agreed that the flow of meteoric water was important. Buchbinder & Friedman (1980) found the process to be indicative of the vadose environment, whereas Mazzullo (1980) found it to be representative of freshwater vadose and burial environments.

Neomorphism of lime mud to microspar and occasionally pseudo-spar is found throughout the Upper Oligocene limestones. It is probably the result of uplift into the vadose and phreatic environments (and therefore it is contemporaneous with fourth period cement) since fresh water is apparently required for the process to occur. It is most evident in highly porous packstones, mostly in the foraminiferal grainstone packstone facies, where they have not been cemented by the dusty marine spar of the third period of cement. This location in porous rocks supports inferences that neomorphism is dependent on the circulation of pore fluid. Its lesser effect in rocks cemented by the third period of cement could be the result of: closure of many of the smaller pores by this cement; protection of the mud from the pore fluids by the thick cement coat; or lithification of the mud which may have taken place at the time of cementation.

Apart from the occasional development of pseudospar, aggrading neomorphism is not present. Even in the case of the pseudospar, it is still only carbonate mud that is neomorphosed. Aggrading neomorphism is thought to be dependent on a source of unstable or supersoluble carbonate crystals (aragonite or high magnesian calcite) which act as nuclei for the initial, heterogeneous process (Folk, 1974) (the nucleation stage of Bathurst, 1975). The lack of aragonitic bioclasts and the conversion of magnesian calcite to calcite upon contact with meteoric water may explain why aggrading neomorphism has had little effect on the Chattian limestones.

5.1.5 Syn-cementation Pore Fillers

a) Observations

Syn-cementation partial and complete pore fill is present at two localities: Nadorello east (Fig. 2.2) and San Biagio west (Fig. 2.6). At both localities the deposits are not common. They post-date the

second and predate the fourth period of cement. At Nadorello east the relationship with the third period cannot be seen.

At Nadorello east pelletal silts are found. They are geopetal in position, they rarely completely fill pore space, and their depositional surfaces can be curved or at several different angles to the sedimentary bedding (Plates 5.24-5.26). Pellets are 7-20 μ size, formed of fine micritic carbonate, and are round with diffuse boundaries. Commonly pellets coalesce to form mud masses with some detectable pellet boundaries (Plate 5.26).

At San Biagio west mixtures of mud, crystals and opaque pellets are found (Plates 5.27, 5.28). They commonly completely fill pore space; or where partial fill is present their depositional surfaces are flat and parallel to sedimentary bedding. Both crystals (5-15 μ size) and opaque pellets (10-40 μ size) are common and mixed evenly in the mud. This secondary pore fill is different to any matrix deposited with the original sediment, which is composed of mud with small algal and foraminiferal fragments.

These two types of secondary pore fill described above are petrographically different, occur at separate localities and may represent two unrelated periods of generation. They are, however, similar in that they both occupy a post-second, pre-fourth period of cement position.

b) Discussion

Geopetal silts similar in appearance to those seen at Nadorello east and syn-cementation in position have been described from a Permian wackestone mound in New Mexico by Dunham (1969) who interpreted them to be of vadose environment deposition. Dunham argued that only in that environment would pore water velocities be fast enough to carry the silt size particles. The absence of clay size material is explained by the preferential solution of these particles in the meteoric water due to their large surface area to volume ratio whereas sand size material is absent because it is too big to pass in the pore system. Dunham was unsure about the source for the particles but concluded that they were

derived from the primary sediments of the mound.

The pelletal silts found at Nadorello east, for the reasons set out by Dunham, are also likely to be of vadose environment origin. This suggests that the area under study was uplifted into the vadose environment after cement period two (and most likely after period three) and then subsided back into the phreatic environment to allow fourth period cement precipitation. A more plausible explanation, however, would be that the area was uplifted into a position where a fluctuating water table could provide the two required (vadose and phreatic) environments.

At San Biagio west these diagenetic sediments are different in appearance: they contain a large quantity of mud. However, it is inferred here that they are of a similar vadose environment origin since they occupy the same post second cement position and since they are also different from primary matrix in the sediment and therefore could not be considered to be of primary origin. The large amount of mud could be explained by rapid transportation to, and burial in, a pore space and therefore not giving solution time to take place.

5.1.6 Dolomitisation

Dolomite, identified by its lack of stain with Alizarin red-S, is present only in the lower 22 m of the San Biagio east succession. It occurs as equant anhedral and subhedral crystals and as euhedral rhombs (50-100 μ size) replacing mud matrix, textularids and algae (Plate 5.29). It is not common, forming at most 2-3% of the rock.

This restricted occurrence, not associated in any way with a change in facies in the Upper Oligocene, suggests that the dolomite is not early diagenetic, since dolomite of this type is associated with shallow marine and supratidal deposits (Ginsburg, 1975), whereas the Upper Oligocene has an interpreted shelf environment (Sections 2.5 & 2.6) in waters of 80-250 m depth. Neither is the dolomite likely to be of deep burial genesis since this would produce widespread massive dolomites (Mattes & Mountjoy, 1980).

Dolomitisation, similar in aspect, is found in Cretaceous to Middle Oligocene limestones at Mt Kronio (3 km to the east of Sciacca) to the south of the study area, reported by Mascle (1973, 1979), and believed to be the result of hot springs and fumeroles known there. The restricted occurrence at San Biagio may be of similar metasomatic origin since its presence is not consistent with the regional depositional and diagenetic patterns.

5.1.7 Conclusion

Four periods of cementation are identified and described. The first three are early, pre-compaction and of marine origin whilst the fourth is late, post-compaction and of a freshwater phreatic origin. All are either restricted in occurrence or are poorly developed. Although the second period cement is clear and therefore might be thought of as fresh water in origin, the occurrence of ferroan calcite/calcite zoning in echinoid overgrowths where the cement is associated with authigenic glauconite sediments suggests that the cement is syn-glauconitisation in origin and therefore marine. The common bladed scalenohedral habit of the dusty third period cement suggests that it was probably precipitated as high magnesian calcite. This, along with the restricted or poor development of the first three periods of cement, suggests precipitation in deeper, cooler less saturated (with respect to CaCO_3) waters and would agree with the water depth of 80-250 m suggested by the sediments (Section 2.5.6).

The late fourth period cement probably reflects final uplift of the sediments into the realm of fresh water. It is of phreatic origin and is pre-dated by a period of vadose pore-fillers found only in the rhodolithical algal packstone - wackestone facies. Calcium carbonate for this late cement is possibly derived from the semi-autochthonous dissolution of aragonitic molluscs in nearby Upper Miocene - Quaternary limestones. Such late cements often have a source within the host limestone. The poor development of the spar here probably reflects the absence of aragonitic bioclasts in the Upper Oligocene limestones.

Compaction, timed as post third pre fourth period of cement, is

widespread and has had considerable effect resulting in rotation or redistribution of grains, fracture of grains and pressure solution between grains. Coralline red algal clasts are found to be the most susceptible to fracture and pressure solution whereas echinoid grains are the most resistant. Compaction is enhanced by the poor marine cementation in echinoid bearing rocks but it is probably inhibited by the near monomineralic sediment and the skeletal architecture of the abundant benthonic foraminifera present.

Finally, neomorphism is widespread and is represented by the common formation of microspar and occasionally pseudospar from carbonate mud. It also takes the more restricted form as syntaxial overgrowths on echinoid grains, bivalve fragments and some foraminifera. The general absence of aggrading neomorphism is attributed to the lack of aragonitic material in these near monomineralic sediments. Neomorphism is generally related to freshwater environments and therefore in southwest Sicily, it is probably contemporaneous with uplift into the vadose and phreatic environments and with fourth period cementation.

5.2 Diagenetic Feldspars: Upper Oligocene Limestones

5.2.1 Introduction

Unweathered euhedral and subhedral crystals of feldspar (Plates 5.30, 5.31), 100-400 μ in length, forming some 2-3% bulk composition of the rock, occur evenly distributed in the lower 3-4 m of Upper Oligocene succession in southwestern Nadorello. The beds are located 6-8 m above Cretaceous chalk outcrops but the unconformity between the two is not exposed and the precise position cannot be ascertained. The crystals are clear and lack inclusions indicating that they are early, pre-compaction, pore-fillers rather than late replacement in origin. They embay bioclasts as a result of compaction and pressure solution.

Twelve separate feldspar grains from two thin sections were analysed using an electron microprobe housed at the Department of Earth Sciences, University of Cambridge. The absolute abundances of the element oxides are given in Table 5.1 whilst the Na:K:Ca ionic ratios are plotted in Figure 5.1.

5.2.2 Microprobe Results

In Table 5.1 the analyses of feldspar cores (C) are distinguished from rims (R). From the analyses it can be seen that, with two exceptions, there is little change in composition from core to rim. Two analyses were made of adjacent areas in the core of FEL 1 to illustrate the amount of chemical variation in a single core (which ideally should be homogeneous). Comparison of these results with the analyses of cores and rims of other grains suggests that all the grains except FEL 6 and FEL 11 are homogeneous. There is, however, a variation in the chemistry between grains (discussed below). FEL 6 and FEL 11 are zoned with K enriched/Na depleted cores relative to their rims. The variation of K, however, is not apparent until plotted against Na and Ca in Figure 5.1.

In Figure 5.1 feldspar cores are identified from rims by symbol. The analyses plot in the anorthoclase and oligoclase feldspar fields (as defined in Deer *et al.*, 1963, Vol. 4, Fig. 1) and may be referred to as calcic anorthoclase and sodic oligoclase. With the exception of two points (the cores of both zoned crystals) all the analyses plot on a line with little scatter. The cores and rims of individual crystals plot close to each other on the line.

This line may record a diagenetic evolution from feldspars which are K enriched/Na depleted to those which are K depleted/Na enriched. The two zoned crystals show just this trend. Their cores plot outside the linear group of analyses but their rims plot within the group. The cores may represent an earlier period of feldspar formation when pore solutions were even more K enriched/Na depleted. The rims, however, have formed during the main period of feldspar formation. In the same manner, it is suggested that crystals which form early during this main period of feldspar formation plot towards the K enriched/Na depleted end of the line, whilst those which form late plot towards the K depleted/Na enriched end.

5.2.3 Discussion

Diagenetic feldspars may be either sodic or potassic, although the former are most common in carbonate rocks (Kastner, 1971; Kastner &

| Sample Element | FEL-1C | FEL-1C | FEL-2C | FEL-2C | FEL-2R | FEL-3C | FEL-3R | FEL-4C | FEL-4R | FEL-5C | FEL-5R | FEL-6C | FEL-6R |
|--------------------------------|--------|--------|--------|--------|--------|--------|--------|--------|--------|--------|--------|--------|--------|
| Na ₂ O | 7.62 | 7.61 | 7.11 | 7.15 | 8.03 | 7.98 | 6.80 | 6.50 | 7.63 | 7.42 | 1.41 | 6.44 | |
| Al ₂ O ₃ | 21.01 | 21.25 | 19.92 | 19.64 | 22.44 | 22.74 | 19.58 | 19.45 | 21.65 | 20.80 | 20.61 | 19.15 | |
| SiO ₂ | 64.70 | 65.08 | 65.73 | 65.46 | 63.72 | 63.40 | 66.28 | 66.50 | 63.57 | 65.32 | 72.30 | 66.04 | |
| K ₂ O | 3.80 | 3.88 | 5.90 | 5.60 | 2.99 | 2.86 | 6.97 | 7.23 | 3.37 | 4.75 | 4.72 | 7.20 | |
| CaO | 2.59 | 2.68 | 1.46 | 1.62 | 3.67 | 4.03 | 1.21 | 0.81 | 3.28 | 2.40 | 1.04 | 0.99 | |
| Fe ₂ O ₃ | 0.19 | 0.18 | 0.15 | 0.14 | 0.18 | 0.21 | 0.18 | 0.18 | 0.13 | 0.18 | - | 0.28 | |
| BaO | 0.36 | 0.38 | - | - | 0.41 | 0.50 | - | - | 0.52 | 0.34 | - | - | |
| Total | 100.27 | 101.06 | 100.27 | 99.61 | 101.44 | 101.72 | 101.02 | 100.67 | 100.15 | 101.21 | 100.08 | 100.10 | |

| Sample Element | FEL-7C | FEL-8C | FEL-9C | FEL-10C | FEL-10R | FEL-11C | FEL-11R | FEL-12C | FEL-12R |
|--------------------------------|--------|--------|--------|---------|---------|---------|---------|---------|---------|
| Na ₂ O | 6.90 | 7.35 | 7.13 | 6.51 | 6.61 | 4.48 | 7.43 | 7.77 | 7.31 |
| Al ₂ O ₃ | 19.99 | 20.47 | 19.24 | 19.30 | 19.17 | 19.99 | 19.93 | 21.60 | 20.64 |
| SiO ₂ | 65.47 | 65.27 | 66.85 | 66.98 | 66.51 | 68.27 | 65.76 | 63.52 | 65.05 |
| K ₂ O | 6.22 | 5.24 | 7.15 | 7.21 | 7.10 | 7.20 | 5.50 | 3.26 | 5.02 |
| CaO | 1.45 | 2.01 | 0.85 | 0.87 | 0.96 | 0.87 | 1.63 | 3.41 | 2.12 |
| Fe ₂ O ₃ | 0.12 | 0.17 | 0.15 | 0.19 | 0.25 | 0.15 | 0.16 | 0.20 | 0.21 |
| BaO | 0.21 | 0.43 | - | - | - | - | - | 0.40 | 0.36 |
| Total | 100.36 | 100.94 | 101.37 | 101.06 | 100.60 | 100.96 | 100.41 | 100.16 | 100.71 |

Table 5.1 Feldspar geochemistry. Microprobe analyses of cores (C) and rims (R) of twelve feldspar grains

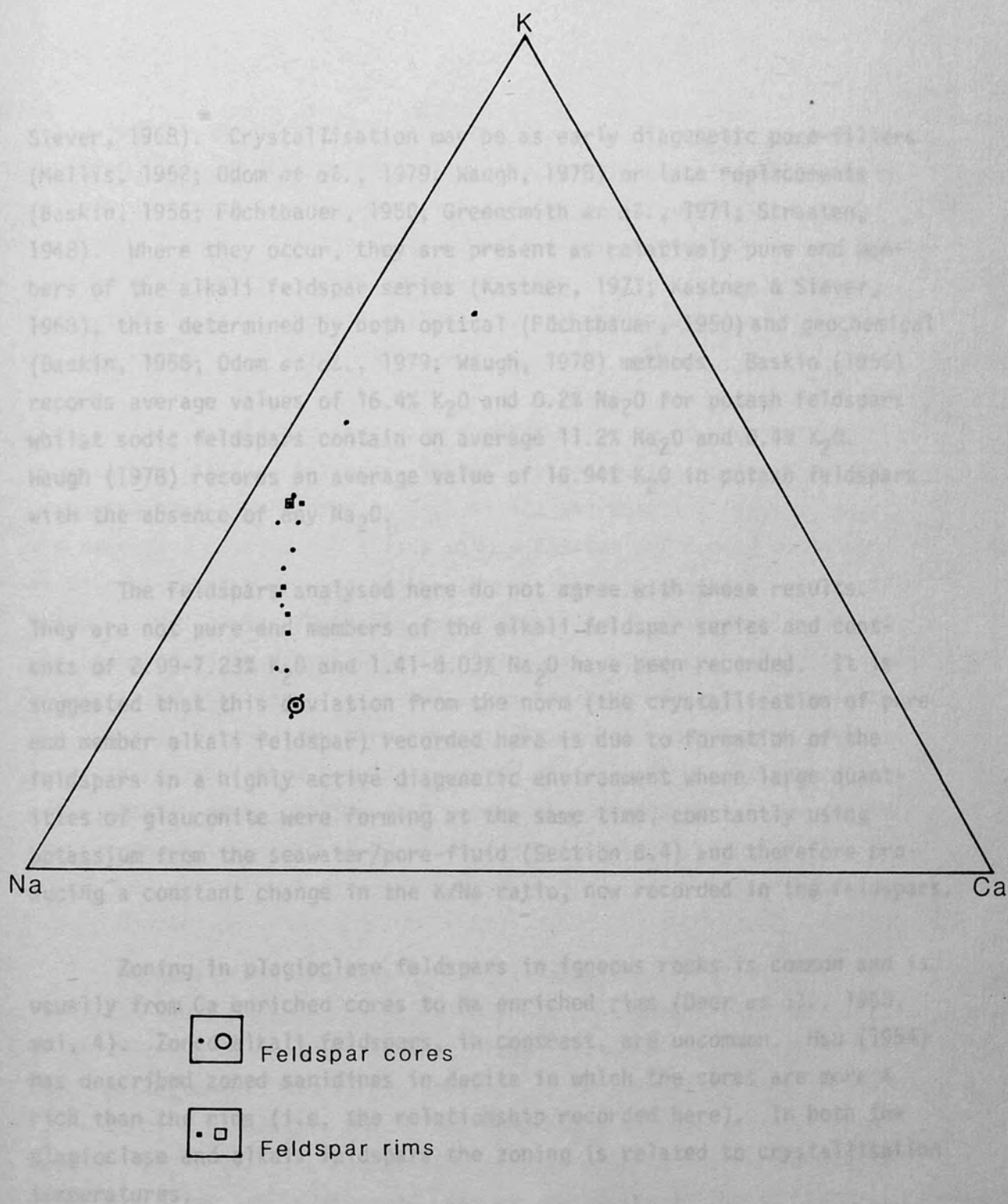


Figure 5.1 Feldspar geochemistry. Plot of K:Na:Ca ratio for cores and rims from 12 grains.

Siever, 1968). Crystallisation may be as early diagenetic pore-fillers (Mellis, 1952; Odom *et al.*, 1979; Waugh, 1978) or late replacements (Baskin, 1956; Fùchtbauer, 1950; Greensmith *et al.*, 1971; Straaten, 1948). Where they occur, they are present as relatively pure end members of the alkali feldspar series (Kastner, 1971; Kastner & Siever, 1968), this determined by both optical (Fùchtbauer, 1950) and geochemical (Baskin, 1956; Odom *et al.*, 1979; Waugh, 1978) methods. Baskin (1956) records average values of 16.4% K_2O and 0.2% Na_2O for potash feldspars whilst sodic feldspars contain on average 11.2% Na_2O and 0.4% K_2O . Waugh (1978) records an average value of 16.94% K_2O in potash feldspars with the absence of any Na_2O .

The feldspars analysed here do not agree with these results. They are not pure end members of the alkali feldspar series and contents of 2.99-7.23% K_2O and 1.41-8.03% Na_2O have been recorded. It is suggested that this deviation from the norm (the crystallisation of pure end member alkali feldspar) recorded here is due to formation of the feldspars in a highly active diagenetic environment where large quantities of glauconite were forming at the same time, constantly using potassium from the seawater/pore-fluid (Section 6.4) and therefore producing a constant change in the K/Na ratio, now recorded in the feldspars.

Zoning in plagioclase feldspars in igneous rocks is common and is usually from Ca enriched cores to Na enriched rims (Deer *et al.*, 1963, vol. 4). Zoned alkali feldspars, in contrast, are uncommon. Hsu (1954) has described zoned sanidines in dacite in which the cores are more K rich than the rims (i.e. the relationship recorded here). In both the plagioclase and alkali feldspars the zoning is related to crystallisation temperatures.

In the feldspars described here, zoning and evolution towards more sodic feldspars traces a change in the chemistry of the pore-fluids. A change in chemistry from K enriched/Na depleted to K depleted/Na enriched pore-fluids is suggested. This feature could be caused by the crystallisation of the feldspars themselves but this is unlikely since they are not abundant. The enclosing limestones, however, contain abundant examples of glauconitised foraminiferal infills, the formation of which

would deplete the pore-fluids in K but leave Na virtually untouched (section 6.4) and thus cause its relative enrichment. If this is the method for K depletion/Na enrichment of the pore-fluids in which the feldspars formed, then the feldspars are syn-glaucanisation and therefore early diagenetic. This agrees with their clear optical properties without inclusions suggesting that they are early diagenetic pore-fillers rather than late replacements.

Early diagenetic feldspars form in a low temperature diagenetic environment (Kastner & Siever, 1968). In marine sediments it has been suggested that clay minerals, free silica and detrital feldspar supply the necessary alumina and silica with potassium and sodium being derived from seawater or pore-fluids (Berg, 1952; Kastner & Siever, 1968; Kastner, 1971). Baskin (1956) concludes that diagenetic feldspars of replacement origin crystallise from meteoric waters and are often found with small quantities of diagenetic quartz, tourmaline and muscovite. The association recorded here between glauconite and feldspar suggests that the feldspar here formed under the constraints of the glauconite environment: normal saline cool waters of moderate turbulence around the oxygen minimum zone at 80-250 m depth (Section 6.6).

5.2.4 Conclusion

Diagenetic feldspars are found associated with glauconitic limestones in the southwestern Nadorello area. Petrographic evidence suggests that the feldspars are early diagenetic pore-fillers rather than late replacements. Microprobe analyses of twelve grains show the feldspars to have a variable calcic anorthoclase - sodic oligoclase composition rather than the composition of pure end members of the alkali feldspar series (as is recorded, without exception in the literature). Zoning in two grains from K enriched/Na depleted cores to K depleted/Na enriched rims is recorded. Other grains are not zoned but their variable compositions suggest the same K/Na trend. This change in chemistry reflects a change in chemistry of the pore-fluids which is attributed to local glauconitisation of foraminiferal chamber infills. Crystallisation of the feldspars is therefore early diagenetic and contemporaneous with glauconitisation under the constraints of the glauconite environment (Section 6.6)

5.3 Carbonate Diagenesis: Lower Miocene Limestones

5.3.1 Introduction

Apart from glauconitisation (Chapter 6) cementation and compaction are the only two diagenetic features of significance in the Lower Miocene limestones. Neomorphism is insignificant since almost all the rocks have a grainstone texture, and mud matrix (neomorphosed to microspar) is found in only two thin sections from Mt Cardellia.

Features of cementation and compaction are described and discussed below. Two periods of cement are recognised: the first is early, pre-compaction and of a marine origin; the second is late, post-compaction and of a freshwater phreatic origin. Compaction is represented by grain redistribution or rotation, grain fracture and pressure solution between grains.

5.3.2 Cementation

a) Introduction

Two periods of cement (referred to here as the first (i.e. earliest) and second (i.e. latest) periods) can be recognised at all localities and in both facies in the Lower Miocene. However, positive recognition of both periods, which are respectively pre and post compaction, is not possible in all thin sections. All the cement is clear and it shows a range of textures which can be related to particular substrates. In the glauconitic limestone facies ferroan calcite cements are common whereas in the sandy limestone facies the cements, with the same textures, are all of non-ferroan calcite.

b) First period

The cement is widespread but generally poorly developed. It is pore-lining in position and possibly fills some of the smaller intragranular pore-space such as benthonic foraminiferal chambers. Where it can be positively identified it is represented by wide syntaxial overgrowths on echinoid grains (Plates 5.32, 5.33); by slightly elongate to bladed scalenohedral crystals and syntaxial overgrowths on bivalve fragments and *Amphistegina*, *Heterostegina/Operculina*, and *Spiroclypeus*

foraminiferal substrates (Plates 5.34, 5.35); and by equidimensional crystals on other substrates (Plates 5.33, 5.34, 5.36-5.39).

Syntaxial echinoid overgrowths up to 600 μ wide show preferential growth in the c-direction of the crystal (Plate 5.32). They form sub-poikilotopic textures and show preservation of original grain distribution with point contacts between grains within the overgrowth. In contrast, elsewhere in the same sediment compaction features such as areal pressure solution contacts between grains are common. The overgrowths are therefore pre-compaction - a timing which is confirmed by the occasional presence of pressure solution contacts between the cement overgrowth and neighbouring grains. Where this cement is found in the sandy limestone facies it is composed of non-ferroan calcite. In the glauconitic limestone facies, however, as in the Upper Oligocene glauconitic limestones of western Nadorello (Section 5.1.2c), the cement has serrated zones (5 in all) of ferroan and non-ferroan calcite with apices extended in the c-direction of the crystal.

Slightly elongate to bladed scalenohedral crystals are syntaxial on, and perpendicular to, their substrates and vary from 30 μ to 70 μ long, most commonly 30-50 μ long. Their pre-compaction time of formation is evidenced by their presence on grains which have been broken but their absence from the fracture surfaces of such grains. The cement is composed of non-ferroan calcite throughout the Lower Miocene succession.

Equidimensional crystals of 10-30 μ size are found on all other substrates except quartz and glauconite but particularly on Globigerinids, *Nephrolepidina* and *Miogypsina* (Plates 5.38, 5.39). There are no grain fracture textures present to indicate that the cement is first period generation but its pore-lining position suggests this. The cement is non-ferroan throughout.

c) Second Period

This cement is widespread and fills all the remaining pore-space. Except in the case of the bladed crystals (Plate 5.34) a junction between this and the previous cement cannot be readily identified. The recognition

of this second period cement rests on the fact that it is post-compaction in timing, infilling fractures and pore-space (Plates 5.46, 3.7). If pore space had been filled pre-compaction, then the features described in Section 5.3.3a would not be seen.

The cement is represented: by further syntaxial growths on echinoid grains which fill fractures in neighbouring grains; by granular mosaics of equidimensional crystals 10-30 μ size found mostly in and around Glyceriniids but also in the smaller pore-spaces in the sediment (Plates 5.34, 5.36); and by blocky mosaics of crystals 30-150 μ size found in some of the larger pore-spaces (Plates 5.38, 5.39). Both the mosaics show vague vectoral increase in size towards the centre of the pore-space. In areas of sediment rich in quartz and glauconite each pore-space is commonly filled by a solitary large (up to 600 μ) crystal of calcite, and sometimes poikilotopic and sub-poikilotopic textures are formed (Plates 5.34, 5.37, 5.40, 5.41). Never, in these areas, are pore-lining spars and centripetally enlarged spars, typical of pure carbonates, seen.

Where this second period cement is found in the sandy limestone facies it is always composed of non-ferroan calcite. In the glauconitic limestone facies, however, it can be of either ferroan (Plate 5.42) or non-ferroan calcite, and only one type will occur in any one rock. Zoning, of the type described for the first period cement, is never seen. The ferroan calcite cements are most common in the basal part of the glauconitic limestone facies. Other than this, and the fact that they are not found in the sandy limestone facies, no other pattern for their occurrence was observed. They may be present or absent from glauconite rich sediments.

d) Discussion

The first period of cement is early, pre-compaction and inferred to be of marine origin since it has, in part, a bladed scalenohedral form and contains ferroan calcite - calcite zoning in the echinoid overgrowths where they are associated with glauconitic sediments (Section 5.1.2g explains the significance of these features). The scalenohedral form is

more typical of precipitation as high magnesian calcite rather than aragonite and would suggest precipitation in deeper cooler water as would the general poor development of the cement (Section 5.1.2g).

The second period cement is a late, post-compaction, clear, equant, blocky calcite spar inferred to be of freshwater origin for the reasons set out in Section 5.1.2g. Furthermore, its large size (where associated with quartz and glauconite grains) and its, sometimes, ferroan calcite mineralogy would suggest that it crystallised below the water table in the phreatic environment. The cement is not the result of precipitation from deep connate waters for the same reason that the fourth period cement in the Upper Oligocene limestones is not: that is, the area has a history of uplift from Upper Oligocene onwards.

Ferroan calcite forming this cement in some rocks implies two features of the environment: that the environment was reducing and that the pore-fluids contained free iron in sufficient abundance to form the ferroan calcites. The absence of ferroan calcites in other rocks suggests the absence of at least one of these features in the diagenetic environment.

Two explanations are possible for the occurrence of ferroan calcite:

- 1) When iron solutions pervade the complete Lower Miocene succession, the presence of ferroan calcites in the glauconitic limestone facies only could be explained by reducing environments forming locally in that facies. Such local development of reducing environments could be caused by decaying organic matter originally associated with the authigenic glauconite growth (Rech-Frollo, 1963).

- 2) When reducing environments pervade the complete Lower Miocene succession, the presence of ferroan calcites in the glauconitic limestone facies only might suggest that the source of the iron is from the glauconite itself. Since glauconite formation does not necessarily require the presence of organic matter (McRae, 1972; Odin & Letolle, 1980; Odin & Matter, 1981), the latter explanation for the distribution of ferroan calcites may be the correct one.

The presence of large cement crystals in pores surrounded by quartz and glauconite grains bears comment. Such crystals preclude any thought that the granular mosaics and the smaller blocky mosaics often in the same sediment are of a neomorphic origin since it is unlikely that neomorphism would form different size crystals around different grain types. Only cements do this because they are syntaxial on their substrate. Furthermore, pores surrounded by carbonate grains provide many sites for syntaxial nucleation of carbonate cements and so rim spars and granular mosaics form. Pores surrounded by quartz and glauconite grains need provide no sites for syntaxial nucleation of cement. Either cementation begins by nucleation on the most minute of carbonate grains adhering to the surface of the quartz or glauconite, or a completely new lattice is formed by precipitation at a random site on the surface of the detrital grains. Whatever the case, nucleation sites are few and therefore cement crystals are large.

Finally, the second period cement represents uplift of the sediments into the phreatic environment and could quite conceivably be of the same period of generation as the fourth period cement in the Upper Oligocene limestones. The source of the CaCO_3 for the cement may be the same source postulated for the Upper Oligocene limestones since these Upper Miocene - Quaternary limestones are common in western Sicily and since no source within the Lower Miocene glauconitic sandy limestones can be seen.

5.3.3 Compaction

a) Observations

Compaction is widespread and is found throughout the succession at all localities. In general, it is not as prominent as in the Upper Oligocene limestones (Section 5.1.3) most likely because the Lower Miocene rocks are finer grained. Nevertheless, it has resulted in redistribution or rotation of grains, fracture of grains and pressure solution between grains.

The first (Plate 5.32) is evidenced by the smaller intergranular pore-spaces in the compacted sediment than the original pore-space

between grains preserved where there is a first period syntaxial echinoid cement. Fracturing of grains in these rocks is much less common than in the Upper Oligocene limestones, probably because the large platy grains formed by *Heterostegina*, *Operculina* and *Spiroclypeus* which are prone to fracture, are represented here by small fragments only. However, fracturing is present and found in some *Nephrolepidina* and *Miogypsina*. It is common in algal fragments in coarser grained rocks, and it is present in some quartz grains where they are abundant and abut each other.

Pressure solution between grains is common and present everywhere. Contacts are accommodatory with allochems going into solution in preference to glauconite and quartz (Plates 3.16, 5.43-5.45) and glauconite going into solution in preference to quartz (Plate 5.43). Occasionally quartz - quartz contacts will be of a flat areal pressure solution nature, and this is sometimes accompanied by fracture of the quartz and straining of its lattice at the point of contact (Plates 5.44, 5.46, 5.47). At Costa del Conte, where *Nephrolepidina* and *Miogypsina* are common, a pressure welded texture (Section 5.1.3) forms between these grains. Echinoid grains and their first period cement overgrowths again, never go into solution in preference to other allochems, but are preferentially dissolved against glauconite and quartz grains (Plate 5.45).

b) Discussion

Compaction in the Lower Miocene limestones, enhanced by the poor development of an early pore-lining cement, has produced features similar to those seen in the Upper Oligocene limestones. The same grains react in the same manner, though in general compaction is less prominent, a feature attributable to smaller grain size and to a combination of the variables listed in section 5.1.3b. The Lower Miocene limestones differ in containing common quartz and glauconite grains and these have reacted to compaction in a manner which would be expected. All grains (carbonate and glauconite) go into solution in preference to the harder and more mechanically durable quartz which will go into solution or fracture only when it is in contact with other quartz grains. Allochems go into solution in preference to glauconite presumably for the reasons set out

by Meyers (1980) in that the microcrystalline grains of which they are composed offer a higher surface area to volume ratio.

5.3.4 Conclusions

Two periods of cementation are identified and described. The first is early, pre-compaction and represented by a poorly developed pore-lining spar. Ferroan calcite/calcite zoning in the echinoid overgrowths only where the cement is associated with sediments containing authigenic glauconite (glauconitic sandy facies) suggests that the cement is syn-glauconitisation and therefore marine. Furthermore, the bladed scalenohedral habit of some of the cement suggests that it was precipitated as high magnesian calcite. This, along with the general poor development of the spar, suggests precipitation in deeper, cooler waters and agrees with a water depth of 80-250 m suggested by the glauconite (Section 6.6.5) and the sediments (Section 3.4.1).

The second period cement is late, post-compaction and results in infill of the remaining pore space. The sometimes large size of crystals in this cement along with its sometimes ferroan calcite mineralogy suggests that it formed in the phreatic environment and probably represents final uplift of the limestones. The presence of ferroan calcites only in the glauconitic limestone facies suggests that the source of the iron was in the glauconite itself. Different textures in this cement are related to substrate. Thus granular and blocky mosaics are located in pore spaces surrounded by allochems which provide numerous sites for syntaxial cement growth; whilst in pore space surrounded by quartz and glauconite grains single crystals of calcite are found because no sites for syntaxial cement growth are provided. Finally, it is suggested that the cement is probably of the same period of generation as the fourth period in the Upper Oligocene limestones and that the calcium carbonate for the cement probably has the same source in the Upper Miocene - Quaternary limestones.

Compaction, enhanced by the poor development of an early pore-lining spar, is widespread. It shows all the features seen in the Upper Oligocene limestones (namely rotation or redistribution of grains,

fracture of grains and pressure solution between grains), but it is generally less prominent probably due to its smaller grain size. A pressure solution hierarchy in the grains can be seen in which quartz is the most resistant to solution followed by glauconite, followed by the allochems, which are the least resistant.

6.1 Introduction

As noted by McRee (1972) and Odin & Matten (1987), the term "glauconite" has been used in two senses: most commonly as a morphological term to designate sand-sized, greenish coloured grains found in sedimentary rocks; less commonly as the name of a mineral species or family of hydrated iron rich micaceous clay minerals. "Glauconite" is used here, as in previous works which record it in southwest Sicily (section 3.1.2), in the morphological sense. However, analyses are presented to prove that most southwest Sicily glauconite grains are truly of the mineral glauconite, and that others represent early stages in the glauconitisation process. Glauconite formation suggests slow sedimentary accumulation in normal saline cool waters at depths of 80-250 m in a tropical-subtropical latitude. This environment is consistent with that concluded from the enclosing sediments (Chapters 2 & 3).

6.2 Occurrence

Glauconite occurs in both Upper (Oligocene limestones (Chapter 2) and Lower Miocene limestones (Chapter 3) in southwest Sicily. In the Upper Oligocene limestones it occurs in only minor quantities, and is very restricted in its stratigraphic and geographic occurrence. In the Lower Miocene, glauconite is abundant and widespread.

In the Upper Oligocene limestones, authigenic glauconite was recorded only in some 12 m of foraminiferal grainstone - packstones in western Madonia to the northeast of a mapped road track at US 335577. It occurs as infill within benthonic foraminiferal chambers and as infill to the pores of echinoid stems, occasionally replacing the echinoid calcite (Plates 5.1, 5.2). Glauconitisation is not species restricted, for all genera of foraminifera present at this horizon are affected. However, only 50% to 80% of foraminifera are glauconitised.

CHAPTER 6

GLAUCONITE

6.1 Introduction

As noted by McRae (1972) and Odin & Matter (1981), the term "glaucouite" has been used in two senses: most commonly as a morphological term to designate sand-sized, greenish coloured grains found in sedimentary rocks; less commonly as the name of a mineral species or family of hydrated iron rich micaceous clay minerals. "Glaucouite" is used here, as in previous works which record it in southwest Sicily (Section 3.1.2), in the morphological sense. However, analyses are presented to prove that most southwest Sicily glaucouite grains are truly of the mineral glaucouite, and that others represent early stages in the glaucouitisation process. Glaucouite formation suggests slow sedimentary accumulation in normal saline cool waters at depths of 80-250 m in a tropical-subtropical latitude. This environment is consistent with that concluded from the enclosing sediments (Chapters 2 & 3).

6.2 Occurrence

Glaucouite occurs in both Upper Oligocene limestones (Chapter 2) and Lower Miocene limestones (Chapter 3) in southwest Sicily. In the Upper Oligocene limestones it occurs in only minor quantities, and is very restricted in its stratigraphic and geographic occurrence. In the Lower Miocene, glaucouite is abundant and widespread.

In the Upper Oligocene limestones, authigenic glaucouite was recognised only in some 12 m of foraminiferal grainstone - packstones in western Nadorello to the northeast of a mapped rough track at UB 335597. It occurs as infills within benthonic foraminiferal chambers and as infills to the pores of echinoid stereom, occasionally replacing the echinoid calcite (Plates 6.1, 6.2). Glaucouitisation is not species restricted, for all genera of foraminifera present at this horizon may be affected. However, only 50% to 10% of foraminifera are glaucouitised,

the percentage decreasing up the succession. The commonly occurring coralline red algal fragments in the same facies are not glauconitised, nor are the rarer fenestrate bryozoans. The authigenic nature of the glauconite at this locality is proved by the presence of ferroan calcite cements (Section 5.1.2) and is indicated by the variable chemistry of early diagenetic feldspars also found here (Section 5.2).

Derived glauconite is found in the Upper Oligocene limestones of Nadorello east (Fig. 2.2) as rare foraminiferal infills. It also occurs in the Caltabellotta area (Between Caltabellotta and Rocca San Crispino to the west) and in Contradas Finocchio and Genovese (Fig. 1.6), but as very sparse pellets. The detrital origin of this glauconite is evidenced by its occurrence as very sparse, often well abraded, grains and by the absence of any ferroan calcite cements in sediments which indicate well oxygenated bottom conditions not conducive for glauconite formation.

In the Lower Miocene limestones glauconite occurs as ubiquitous sand size pellets (Plates 3.16-3.19) characterising the limestones at all four localities studied in detail (Figs. 3.1-3.4). It is most abundant in the glauconitic limestone facies (Section 3.3.2) where it consistently forms 10-25% (sometimes 50-70%) of grains at Mt Cardellia, 5-20% of grains at Battellaro and 1-20% (mostly 1-10%) of grains at Costa del Conte. At this last locality glauconite is commonly represented by infills of benthonic foraminiferal chambers (Plates 3.6, 3.7) and micropores of echinoid clasts as well as pellet form. As in the Upper Oligocene limestones, glauconitisation affects all genera of foraminifera present. In the sandy limestone facies (Section 3.3.3) glauconite, present in pellet form only, is much less abundant and forms 0.5-3% (mostly 0.5%) of grains at Mt Cardellia, 1-5% of grains at both Battellaro and Costa del Conte, and 2-20% of grains at Serra Lunga. The authigenic nature of the glauconite in the glauconitic limestone facies is indicated by its abundance and by the common occurrence of early marine ferroan calcite cements in this facies (Section 5.3.2). In contrast, in the sandy limestone facies the detrital or derived nature of the glauconite is suggested by its sparsity, and evidenced by the absence of ferroan calcite cements.

6.3 Petrography

Glaucanite occurs in two quite distinct morphological forms: as pellets, and as infills to foraminiferal chambers and echinoid stereom micropores. Pellets are sub-spherical to capsule shaped, usually with smooth surfaces but they occasionally show a transverse or irregular cracking pattern. They are moderate to dark green (opaque in thick sections), formed of aggregates of minute crystals with no preferred orientation and therefore show aggregate polarisation and extinction. Pellets range in size from 100 μ to 1 mm but are generally in the 150-500 μ size range.

Where glauconite infills foraminifera chambers and micropores of echinoid stereom it is more variable in appearance (agreeing with its variable geochemistry, Section 6.4.2). It is generally opaque but may commonly be orange-brown in colour and occasionally light to moderate green. All three colour varieties can be found within a single test infilling different chambers and can occur alongside apparently unaltered lime mud (orange-brown and light to moderate green varieties only) in the same test. Occasionally the foraminifera tests and the echinoid clasts are themselves altered, in part, to glauconite. Foraminiferal tests commonly show signs of abrasion.

6.4 Geochemistry

6.4.1 Analysis

Twelve rock samples (A to M) were analysed by use of an electron microprobe housed at the Department of Earth Sciences, University of Cambridge. Preparation of the samples was standard, and by staff of the department.

Ten samples were chosen as representative of all four Lower Miocene localities (A & B from Battellaro, C & D from Costa del Conte, E from Serra Lunga and F, G, H, J & K from Cardellia) together with two samples representative of the single Upper Oligocene locality yielding authigenic glauconite (L & M are from western Nadorello). The Lower Miocene samples are representative of both the glauconitic limestone facies and the sandy

limestone facies (E & K only). The precise collecting horizons are indicated on the stratigraphic sections, Figures 3.1 to 3.4. The Upper Oligocene samples were collected low in the glauconite sequence at western Nadorello, from horizons yielding diagenetic feldspars (Section 5.2).

Analyses are presented in Tables 6.1 to 6.9 below. Individual analyses are distinguished by a three or four digit reference number:

- 1) First digit (letter A to M) designates the rock sample/locality, as noted above.
- 2) Second digit (number 1 to 7) designates a particular pellet, foraminifera or echinoid clast within the rock sample.
- 3) Third digit (letter C or R) designates whether, in the case of pellets, a core or rim respectively is analysed, or letter A to E designates analysis of different parts of the same foraminifera or echinoid clast.
- 4) Fourth digit (number 1 to 3) designates, in the case of pellets only, analyses made on different parts of the pellet core or rim.

All samples were analysed for the thirteen elements Na, Mg, Al, Si, P, S, Cl, K, Ca, Cr, Mn, Fe and Ba. Tables 6.1 to 6.9 record 151 analyses of 46 pellets, 16 foraminifera and 2 echinoid clasts. A further 65 duplicate analyses were made to check the reproducibility of results and variation of geochemistry within grains. These analyses were consistent with those presented here, and are therefore not included.

Tables group analyses by grain type, locality and age. Thus the first Tables present analyses on Lower Miocene pellets from Battellaro (Table 6.1), Costa del Conte (6.2), Serra Lunga (6.3) and Mt Cardellia (6.4). Analyses of Lower Miocene partially glauconitised pellets from three of the four localities are given in Table 6.5 and analyses of foraminiferal chamber infills from Costa del Conte and Battellaro are given in Table 6.6. Analyses of foraminiferal chamber infills from Upper Oligocene samples are recorded in Table 6.7. Table 6.8 (Upper

| Sample Element | A-1C | A-1R | A-2C | A-3C | B-1C | B-1R | B-2C | B-2R | B-3C | B-3R | B-4C | B-4R | B-5C | B-5R |
|--------------------------------|-------|-------|-------|-------|-------|-------|-------|-------|-------|-------|-------|-------|-------|-------|
| Na ₂ O | - | - | - | - | - | - | - | - | - | - | - | - | - | - |
| MgO | 4.45 | 4.38 | 4.07 | 3.55 | 4.34 | 4.52 | 4.44 | 4.82 | 4.18 | 4.15 | 4.13 | 3.95 | 4.33 | 3.94 |
| Al ₂ O ₃ | 4.16 | 4.84 | 6.22 | 5.63 | 5.07 | 6.74 | 4.19 | 5.13 | 4.72 | 4.87 | 4.36 | 4.50 | 3.85 | 5.03 |
| SiO ₂ | 51.73 | 51.87 | 50.32 | 48.53 | 52.05 | 53.86 | 51.88 | 53.08 | 49.82 | 50.84 | 50.12 | 49.06 | 52.35 | 51.13 |
| P ₂ O ₅ | - | - | 0.26 | - | - | - | - | - | - | - | - | - | - | - |
| S | - | - | - | 0.17 | - | - | - | - | 0.16 | 0.26 | - | - | - | - |
| Cl | - | - | - | - | - | - | - | - | - | - | - | - | - | - |
| K ₂ O | 8.39 | 8.22 | 8.25 | 7.73 | 8.10 | 8.13 | 8.43 | 8.48 | 7.79 | 7.40 | 7.31 | 7.18 | 8.03 | 8.18 |
| CaO | 1.08 | 1.20 | 1.46 | 1.16 | 1.25 | 1.43 | 1.13 | 1.33 | 1.24 | 1.41 | 1.01 | 1.28 | 1.26 | 1.09 |
| CrO ₂ | - | - | - | - | 0.11 | 0.13 | - | - | - | - | - | - | - | - |
| MnO | - | - | - | - | - | - | - | - | - | - | - | - | - | - |
| Fe ₂ O ₃ | 25.13 | 23.92 | 22.20 | 23.93 | 25.11 | 23.30 | 24.30 | 23.68 | 24.70 | 23.74 | 24.70 | 23.96 | 25.09 | 24.82 |
| BaO | - | - | - | - | - | - | - | - | - | - | - | - | - | - |
| Total | 94.94 | 94.43 | 92.78 | 90.70 | 96.03 | 98.11 | 94.37 | 96.52 | 92.61 | 92.67 | 91.63 | 89.93 | 94.91 | 94.19 |

Table 6.1 Battellaro, Lower Miocene glauconite pellets: microprobe geochemistry. Relative proportions of elements and element oxides expressed as percentages. For explanation of sample numbers see section 6.4.1

| Sample Element | C-1C | C-1R | C-2C | C-2R | C-3C | C-3R | C-4C | C-4R |
|--------------------------------|-------|-------|-------|-------|-------|-------|-------|-------|
| Na ₂ O | - | - | - | - | - | - | - | - |
| MgO | 4.20 | 4.44 | 5.68 | 5.92 | 5.58 | 6.01 | 5.17 | 5.41 |
| Al ₂ O ₃ | 7.35 | 6.09 | 4.37 | 4.89 | 4.91 | 5.42 | 5.09 | 5.06 |
| SiO ₂ | 49.28 | 51.70 | 51.85 | 53.24 | 51.89 | 53.09 | 52.46 | 54.19 |
| P ₂ O ₅ | - | 0.17 | 0.20 | 0.19 | 0.30 | 0.72 | - | - |
| S | - | - | - | - | - | - | 0.17 | - |
| Cl | - | - | - | - | - | - | - | - |
| K ₂ O | 7.12 | 7.28 | 7.69 | 7.97 | 7.84 | 7.49 | 7.95 | 8.09 |
| CaO | 4.35 | 1.59 | 1.42 | 1.56 | 1.65 | 2.24 | 2.48 | 1.41 |
| CrO ₂ | - | 0.14 | - | - | - | - | - | - |
| MnO | - | - | - | - | - | - | - | - |
| Fe ₂ O ₃ | 20.50 | 20.49 | 21.20 | 21.12 | 21.33 | 19.69 | 22.61 | 22.16 |
| BaO | - | - | - | - | - | 0.41 | - | - |
| Total | 92.80 | 91.90 | 92.41 | 94.89 | 93.50 | 95.07 | 95.93 | 96.32 |

Table 6.2 Costa del Conte, Lower Miocene glauconite pellets: microprobe geochemistry (c.p. Table 6.1)

| Sample Element | E-1C | E-1R | E-2C | E-3C | E-3R |
|--------------------------------|-------|-------|-------|-------|-------|
| Na ₂ O | - | - | - | - | - |
| MgO | 4.46 | 4.06 | 4.49 | 4.14 | 4.10 |
| Al ₂ O ₃ | 4.83 | 5.03 | 4.57 | 3.84 | 3.43 |
| SiO ₂ | 54.20 | 53.53 | 53.62 | 51.67 | 53.90 |
| P ₂ O ₅ | - | 0.21 | - | - | - |
| S | - | - | - | - | - |
| Cl | - | - | - | - | - |
| K ₂ O | 7.33 | 7.11 | 7.63 | 8.41 | 8.37 |
| CaO | 1.17 | 1.21 | 0.99 | 0.77 | 0.69 |
| CrO ₂ | - | - | - | - | 0.12 |
| MnO | - | - | - | - | - |
| Fe ₂ O ₃ | 23.38 | 23.05 | 23.12 | 25.94 | 25.34 |
| BaO | - | 0.29 | - | - | - |
| Total | 95.37 | 94.49 | 94.42 | 94.77 | 95.95 |

Table 6.3 Serra Lunga, Lower Miocene glauconite pellets:
microprobe geochemistry (c.p. Table 6.1)

| Sample Element | F-1C | F-1R | F-2C | F-2R | F-3C | F-3R | F-4C | F-4R |
|--------------------------------|-------|-------|-------|-------|-------|-------|-------|-------|
| Na ₂ O | - | - | - | - | - | - | - | - |
| MgO | 4.65 | 4.42 | 4.99 | 4.48 | 4.07 | 4.00 | 4.81 | 4.51 |
| Al ₂ O ₃ | 5.90 | 6.70 | 5.75 | 5.28 | 5.96 | 5.52 | 6.54 | 4.88 |
| SiO ₂ | 54.21 | 53.95 | 55.38 | 53.10 | 55.11 | 52.66 | 56.64 | 54.59 |
| P ₂ O ₅ | - | - | - | - | - | - | - | - |
| S | - | - | - | - | - | - | - | - |
| Cl | - | - | - | - | - | - | - | 0.09 |
| K ₂ O | 7.36 | 7.02 | 7.57 | 7.61 | 6.97 | 7.01 | 7.53 | 8.15 |
| CaO | 1.17 | 1.29 | 1.25 | 1.44 | 1.15 | 1.18 | 1.35 | 1.25 |
| CrO ₂ | - | - | - | - | - | - | - | - |
| MnO | - | - | - | - | - | - | - | - |
| Fe ₂ O ₃ | 21.87 | 20.57 | 21.46 | 20.58 | 21.46 | 21.89 | 21.32 | 22.99 |
| BaO | - | 0.27 | - | - | - | - | - | - |
| Total | 95.16 | 94.22 | 96.40 | 92.49 | 94.72 | 92.26 | 98.19 | 96.46 |

Table 6.4 Cardellia, Lower Miocene glauconite pellets microprobe geochemistry (c.p. Table 6.1)

| Sample Element | G-1C | G-1R | G-2C | G-2R | G-3C | G-3R | G-4C | G-4R | G-5C | G-5R |
|--------------------------------|-------|-------|-------|-------|-------|-------|-------|-------|-------|-------|
| Na ₂ O | - | - | - | - | - | - | - | - | - | - |
| MgO | 4.91 | 4.71 | 4.53 | 5.05 | 4.88 | 4.70 | 5.14 | 5.12 | 5.03 | 5.04 |
| Al ₂ O ₃ | 5.85 | 5.53 | 5.24 | 5.31 | 10.41 | 13.48 | 5.11 | 6.41 | 5.06 | 5.03 |
| SiO ₂ | 53.49 | 51.29 | 51.39 | 54.18 | 52.75 | 53.55 | 54.47 | 56.06 | 51.98 | 51.87 |
| P ₂ O ₅ | - | - | - | - | - | - | - | - | - | 0.20 |
| S | - | - | - | - | - | - | - | - | - | - |
| Cl | 0.07 | - | - | - | - | 0.07 | - | - | - | - |
| K ₂ O | 7.90 | 7.74 | 7.49 | 7.75 | 5.26 | 5.44 | 8.12 | 7.78 | 8.54 | 8.44 |
| CaO | 1.29 | 1.14 | 1.21 | 1.12 | 1.78 | 1.61 | 1.07 | 1.10 | 0.90 | 1.02 |
| CrO ₂ | - | - | - | - | 0.13 | - | - | - | - | - |
| MnO | - | - | - | - | - | - | - | - | - | - |
| Fe ₂ O ₃ | 22.88 | 22.46 | 20.52 | 20.86 | 16.29 | 16.00 | 20.93 | 20.01 | 23.11 | 23.36 |
| BaO | - | - | - | - | - | - | - | - | - | - |
| Total | 96.39 | 92.87 | 90.38 | 94.27 | 91.50 | 94.85 | 94.84 | 96.48 | 94.62 | 94.96 |

Table 6.4 contd

| Sample Element | H-1C | H-1R | H-2C | H-2R | H-3C | H-3R | H-4C | H-4R | H-5C | H-5R |
|--------------------------------|-------|-------|-------|-------|-------|-------|-------|-------|-------|-------|
| Na ₂ O | - | - | - | - | - | - | - | - | - | - |
| MgO | 3.75 | 3.84 | 3.77 | 4.04 | 4.01 | 4.15 | 4.62 | 4.55 | 4.22 | 4.28 |
| Al ₂ O ₃ | 4.16 | 5.18 | 3.71 | 5.01 | 3.60 | 4.00 | 5.29 | 6.00 | 2.34 | 2.93 |
| SiO ₂ | 50.04 | 51.80 | 51.62 | 52.57 | 51.70 | 51.62 | 53.10 | 53.80 | 50.58 | 51.07 |
| P ₂ O ₅ | 0.19 | - | - | - | - | - | - | 0.18 | 0.23 | 0.17 |
| S | - | - | - | - | - | - | - | - | - | - |
| Cl | - | - | - | - | - | - | - | 0.07 | - | - |
| K ₂ O | 7.69 | 7.82 | 7.63 | 7.35 | 7.21 | 7.17 | 7.89 | 7.42 | 7.84 | 7.70 |
| CaO | 1.02 | 1.05 | 1.03 | 1.22 | 1.09 | 1.23 | 1.00 | 1.46 | 1.33 | 1.05 |
| CrO ₂ | - | 0.15 | - | - | - | - | - | 0.12 | - | - |
| Fe ₂ O ₃ | 23.59 | 24.01 | 24.74 | 23.09 | 24.53 | 23.33 | 20.76 | 19.15 | 26.71 | 26.34 |
| BaO | - | - | - | - | - | - | - | - | - | - |
| Total | 90.44 | 93.85 | 92.50 | 93.28 | 92.14 | 91.50 | 92.67 | 93.10 | 93.25 | 93.54 |

Table 6.4 contd.

| Sample Element | J-1C | J-1R | J-2C | J-2R | J-3C | J-3R | J-4C | J-4R | J-5C | J-5R | K-1C | K-1R | K-2C | K-2R |
|--------------------------------|-------|-------|-------|-------|-------|-------|-------|-------|-------|-------|-------|-------|-------|-------|
| Na ₂ O | - | - | - | - | - | - | - | - | - | - | - | - | - | - |
| MgO | 4.88 | 5.00 | 4.94 | 4.68 | 4.61 | 4.66 | 4.76 | 4.71 | 4.49 | 4.50 | 4.80 | 5.15 | 4.89 | 4.95 |
| Al ₂ O ₃ | 3.69 | 3.99 | 3.86 | 4.28 | 3.74 | 4.34 | 4.16 | 4.34 | 3.30 | 3.24 | 4.73 | 5.25 | 4.47 | 4.86 |
| SiO ₂ | 50.88 | 51.06 | 49.99 | 49.65 | 51.32 | 51.27 | 51.09 | 49.83 | 50.87 | 50.55 | 53.31 | 53.03 | 51.02 | 51.97 |
| P ₂ O ₅ | - | - | 0.24 | - | - | - | - | 1.51 | - | - | 0.27 | 0.22 | - | 0.19 |
| S | - | - | - | - | - | - | - | - | - | - | - | - | - | - |
| Cl | - | - | - | - | - | - | - | - | - | - | - | - | - | - |
| K ₂ O | 8.34 | 8.31 | 8.18 | 8.14 | 8.23 | 8.25 | 7.96 | 7.53 | 7.78 | 7.71 | 7.99 | 7.72 | 7.71 | 7.69 |
| CaO | 0.90 | 1.01 | 1.42 | 1.12 | 0.92 | 1.08 | 1.04 | 3.16 | 1.14 | 1.09 | 1.35 | 1.51 | 1.15 | 1.27 |
| CrO ₂ | - | - | - | - | - | - | - | - | - | - | 0.11 | - | - | - |
| MnO | - | - | - | - | - | - | - | - | - | - | - | - | - | - |
| Fe ₂ O ₃ | 23.53 | 22.58 | 22.83 | 21.90 | 22.99 | 22.03 | 21.68 | 19.74 | 23.18 | 23.34 | 21.82 | 20.75 | 20.81 | 20.63 |
| BaO | - | - | - | - | - | - | - | - | - | - | - | - | - | - |
| Total | 92.22 | 91.95 | 91.46 | 89.77 | 91.81 | 91.63 | 90.69 | 90.82 | 90.76 | 90.43 | 94.38 | 93.63 | 90.05 | 91.56 |

Table 6.4 contd.

| Sample Element | A-4C | A-4R | B-6C1 | B-6R1 | B-6R2 | B-6C2 | B-6R3 | B-7C | B-7R1 | B-7R2 | F-5C | F-5R1 | F-5R2 | K-3C | K-3R |
|--------------------------------|-------|-------|-------|-------|-------|-------|-------|-------|-------|-------|-------|-------|-------|-------|-------|
| Na ₂ O | - | 0.38 | - | - | - | - | - | - | - | - | - | - | - | - | - |
| MgO | 1.13 | 0.54 | 0.46 | 1.25 | 2.05 | 0.96 | 0.56 | 1.03 | 0.48 | 0.46 | 0.60 | 0.28 | 0.82 | 1.12 | 0.89 |
| Al ₂ O ₃ | 0.25 | 0.14 | - | 1.74 | 1.61 | 6.14 | 0.92 | 3.76 | 1.91 | 1.32 | 0.75 | - | 3.62 | 0.66 | - |
| SiO ₂ | 4.05 | 0.55 | 0.30 | 8.57 | 6.95 | 12.07 | 3.70 | 11.43 | 6.56 | 4.90 | 8.09 | 0.21 | 17.90 | 4.73 | 0.16 |
| P ₂ O ₅ | - | - | - | 2.71 | 1.90 | 1.18 | 0.45 | 0.16 | 0.16 | - | - | - | - | - | - |
| S | - | 0.34 | - | - | - | 0.46 | - | 0.22 | - | - | 0.21 | - | - | - | - |
| Cl | - | 0.32 | - | - | - | 0.06 | - | - | - | - | - | - | - | - | - |
| K ₂ O | 0.40 | 0.20 | - | 0.36 | 0.25 | 1.22 | 0.13 | 0.76 | 0.31 | 0.21 | 0.07 | - | 0.28 | 0.53 | - |
| CaO | 50.72 | 50.82 | 62.47 | 47.89 | 50.09 | 36.37 | 54.96 | 41.32 | 46.80 | 48.56 | 52.77 | 62.99 | 41.78 | 50.70 | 57.44 |
| CrO ₂ | - | - | - | - | - | - | - | 0.13 | - | - | - | - | - | - | - |
| MnO | - | - | - | - | - | - | - | - | 0.14 | 0.19 | - | - | - | - | - |
| Fe ₂ O ₃ | 1.77 | 0.39 | - | 1.73 | 1.55 | 3.66 | 0.97 | 3.50 | 2.24 | 1.92 | 0.33 | 0.16 | 1.89 | 1.67 | 0.13 |
| BaO | - | - | - | - | - | 0.24 | - | - | - | - | - | - | - | - | - |
| Total | 58.32 | 53.68 | 63.23 | 64.25 | 64.40 | 62.36 | 61.69 | 62.31 | 58.60 | 57.56 | 62.82 | 63.64 | 66.29 | 59.41 | 58.62 |

Table 6.5A Lower Miocene glauconitised pellets (Early Stage): microprobe geochemistry (c.p. Table 6.1). Pellets from Battellaro (prefix A & B) and Cardellia (F & K)

| Sample Element | A-5C | A-5R | E-4C | E-4R | G-6C | G-6R1 | G-6R2 | H-6C1 | H-6R1 | H-6R2 | H-6C2 | K-4R1 | K-4C | K-4R2 |
|--------------------------------|-------|-------|-------|-------|-------|-------|-------|-------|-------|-------|-------|-------|-------|-------|
| Na ₂ O | - | - | - | - | - | - | - | - | - | - | - | - | - | - |
| MgO | 3.66 | 3.92 | 2.08 | 0.91 | 4.96 | 4.60 | 4.59 | 4.22 | 3.50 | 3.24 | 4.15 | 3.77 | 3.37 | 4.67 |
| Al ₂ O ₃ | 4.00 | 4.57 | 9.77 | 6.01 | 4.58 | 5.93 | 4.58 | 2.34 | 3.82 | 2.70 | 2.82 | 5.17 | 9.15 | 5.82 |
| SiO ₂ | 42.43 | 52.01 | 32.41 | 20.08 | 35.13 | 53.46 | 53.19 | 50.58 | 41.21 | 41.87 | 50.59 | 45.51 | 44.46 | 52.71 |
| P ₂ O ₅ | - | - | - | - | - | - | - | 0.23 | - | - | - | 0.18 | 0.20 | 0.64 |
| S | - | - | 0.60 | - | - | - | - | - | - | - | - | - | 0.28 | - |
| Cl | 0.07 | - | - | - | - | - | - | - | - | - | - | 0.07 | - | - |
| K ₂ O | 5.65 | 7.55 | 1.32 | 1.64 | 4.88 | 7.77 | 7.72 | 7.84 | 5.10 | 6.60 | 7.75 | 5.86 | 6.21 | 7.24 |
| CaO | 10.72 | 1.21 | 18.25 | 16.64 | 15.20 | 1.13 | 1.24 | 1.33 | 1.29 | 1.26 | 0.95 | 2.17 | 6.40 | 2.45 |
| CrO ₂ | - | - | - | - | - | 0.13 | - | - | - | - | - | - | 0.11 | - |
| MnO | - | - | - | - | - | - | - | - | - | - | - | - | - | - |
| Fe ₂ O ₃ | 20.11 | 24.03 | 6.90 | 9.01 | 16.75 | 21.29 | 20.75 | 26.71 | 33.98 | 30.50 | 26.47 | 17.81 | 18.45 | 21.79 |
| BaO | - | - | - | - | - | - | - | - | - | - | - | - | - | - |
| Total | 86.64 | 93.29 | 71.33 | 54.29 | 81.50 | 94.31 | 93.27 | 93.25 | 88.90 | 86.17 | 92.73 | 80.54 | 88.63 | 95.32 |

Table 6.5B Lower Miocene glauconitised pellets (Late Stage): microprobe geochemistry (c.p. Table 6.1). Pellets from Battellaro (A), Serra Lunga (E) and Cardellia (G, H & K)

| Sample Element | D-1 | D-2A | D-2B | D-3A | D-3B | D-3C | D-3D | D-4A | D-4B | D-5A | D-5B | A-6A | A-6B | A-6C |
|--------------------------------|-------|-------|-------|-------|-------|-------|-------|-------|-------|-------|-------|-------|-------|-------|
| Na ₂ O | - | - | - | - | 0.37 | - | - | - | - | - | - | - | - | - |
| MgO | - | 4.63 | 5.06 | 3.93 | 2.85 | 3.44 | 3.76 | 3.91 | 3.78 | 3.17 | 3.69 | 2.45 | 3.67 | 1.52 |
| Al ₂ O ₃ | 0.21 | 6.47 | 6.22 | 6.97 | 7.58 | 8.76 | 9.85 | 7.12 | 11.39 | 5.06 | 7.37 | 5.89 | 7.87 | 2.65 |
| SiO ₂ | 20.58 | 53.88 | 54.78 | 48.68 | 41.19 | 43.21 | 60.96 | 54.32 | 51.26 | 40.32 | 46.47 | 31.68 | 48.15 | 12.12 |
| P ₂ O ₅ | - | - | - | - | - | - | 0.18 | - | - | - | - | 10.19 | - | 4.85 |
| S | 1.35 | - | - | - | - | - | 0.16 | - | - | 0.16 | 0.44 | 0.26 | - | - |
| Cl | - | - | - | - | - | - | - | - | - | - | - | - | - | - |
| K ₂ O | - | 5.04 | 5.63 | 3.58 | 3.82 | 3.74 | 2.91 | 3.08 | 3.03 | 4.54 | 4.63 | 4.35 | 6.78 | 1.46 |
| CaO | 3.34 | 2.64 | 3.13 | 3.23 | 2.68 | 2.59 | 3.36 | 3.17 | 2.86 | 4.49 | 5.69 | 17.93 | 1.76 | 39.42 |
| CrO ₂ | - | - | - | - | - | - | - | - | - | - | - | - | - | 0.14 |
| MnO | - | - | - | - | - | - | - | - | - | - | - | - | - | - |
| Fe ₂ O ₃ | 61.05 | 17.88 | 18.61 | 17.07 | 15.88 | 16.46 | 11.23 | 19.27 | 16.79 | 16.92 | 15.87 | 12.99 | 21.25 | 4.60 |
| BaO | - | - | - | - | 0.26 | - | - | - | - | - | 0.28 | - | - | - |
| Total | 86.53 | 90.54 | 93.43 | 83.46 | 74.63 | 78.20 | 92.41 | 90.87 | 89.11 | 74.66 | 84.44 | 85.74 | 89.48 | 66.76 |

Table 6.6 Lower Miocene glauconitised foraminiferid chamber infills: microprobe geochemistry (c.p. Table 6.1). Foraminifera from Costa del Conte (prefix D) and Battellaro (A)

| Sample Element | L-1A | L-1B | L-1C | L-1D | L-1E | L-2A | L-2B | L-2C | L-3A | L-3B | L-3C | L-3D | L-4A | L-4B | L-4C |
|--------------------------------|-------|-------|-------|-------|-------|-------|-------|-------|-------|-------|-------|-------|-------|-------|-------|
| Na ₂ O | - | - | - | - | - | - | - | - | - | 0.59 | 0.47 | 0.43 | - | - | - |
| MgO | 2.09 | 2.21 | 1.94 | 1.42 | 1.90 | 2.70 | 2.75 | 2.54 | 1.14 | 1.21 | 0.91 | 0.99 | 2.61 | 3.23 | 2.51 |
| Al ₂ O ₃ | 7.57 | 7.05 | 4.36 | 3.70 | 5.12 | 8.85 | 7.57 | 6.64 | 3.67 | 3.39 | 2.84 | 3.18 | 7.10 | 10.34 | 6.37 |
| SiO ₂ | 21.14 | 19.09 | 8.73 | 8.09 | 12.72 | 32.56 | 34.38 | 26.81 | 10.40 | 10.23 | 8.10 | 10.81 | 37.24 | 44.38 | 31.15 |
| P ₂ O ₅ | 2.28 | 2.26 | 1.93 | 2.00 | 1.44 | 1.78 | 0.96 | 2.80 | 13.39 | 17.45 | 15.05 | 14.44 | 0.55 | 0.24 | 0.68 |
| S | 0.15 | - | - | - | - | - | - | - | 0.80 | 1.04 | 0.92 | 0.89 | - | - | - |
| Cl | 0.08 | 0.12 | - | 0.10 | 0.08 | 0.12 | 0.07 | 0.08 | - | - | - | 0.10 | - | 0.09 | 0.10 |
| K ₂ O | 1.71 | 1.55 | 0.58 | 0.46 | 0.84 | 2.97 | 3.33 | 2.64 | 0.82 | 0.77 | 0.68 | 0.99 | 3.36 | 3.47 | 2.88 |
| CaO | 4.67 | 5.12 | 3.46 | 4.17 | 2.75 | 4.16 | 3.05 | 8.13 | 23.34 | 29.23 | 23.42 | 23.31 | 6.18 | 2.20 | 2.43 |
| CrO ₂ | 0.21 | - | 0.12 | - | 0.18 | - | - | - | - | - | - | - | - | - | - |
| MnO | 0.12 | - | - | - | - | - | - | - | - | - | - | - | - | - | - |
| Fe ₂ O ₃ | 29.69 | 33.87 | 50.09 | 40.76 | 40.91 | 25.56 | 22.89 | 25.86 | 20.07 | 16.23 | 16.12 | 15.07 | 23.05 | 23.93 | 25.46 |
| BaO | 0.80 | 0.89 | 0.81 | 0.82 | 0.73 | 0.74 | 0.69 | 0.66 | 0.61 | 0.45 | 0.32 | 0.31 | - | 0.53 | 0.30 |
| Total | 70.51 | 72.16 | 72.02 | 61.52 | 66.67 | 79.44 | 75.69 | 76.16 | 74.24 | 80.59 | 68.83 | 70.52 | 80.09 | 88.41 | 71.88 |

Table 6.7 Western Nadorello, Upper Oligocene glauconitised foraminiferid chamber infills: microprobe geochemistry (c.p. Table 6.1)

| Sample Element | L-5A | L-5B | L-5C | L-6A | L-6B | L-6C | M-1A | M-1B | M-1C | M-2A | M-2B | M-3A | M-3B | M-4A | M-4B |
|--------------------------------|-------|-------|-------|-------|-------|-------|-------|-------|-------|-------|-------|-------|-------|-------|-------|
| Na ₂ O | - | - | - | 0.44 | - | - | - | - | - | - | - | 0.58 | 0.49 | - | - |
| MgO | 2.18 | 1.49 | 2.31 | 1.83 | 1.73 | 1.67 | 2.78 | 2.32 | 3.04 | 2.12 | 3.23 | 1.68 | 0.69 | 2.95 | 2.82 |
| Al ₂ O ₃ | 7.27 | 4.79 | 7.93 | 7.32 | 5.90 | 7.61 | 10.93 | 10.13 | 10.16 | 5.57 | 7.61 | 6.55 | 4.51 | 5.64 | 6.90 |
| SiO ₂ | 21.35 | 14.27 | 23.77 | 16.83 | 15.35 | 17.49 | 33.91 | 36.04 | 34.51 | 19.03 | 39.06 | 19.88 | 9.45 | 43.73 | 39.41 |
| P ₂ O ₅ | 0.79 | 0.72 | 1.01 | 7.91 | 10.95 | 9.06 | 0.80 | 0.48 | 0.75 | 1.39 | 0.71 | 12.57 | 18.95 | 2.24 | 0.28 |
| S | - | - | - | 0.34 | 0.72 | 0.34 | - | - | 0.20 | - | - | 0.83 | 1.05 | - | - |
| Cl | - | 0.10 | - | - | 0.12 | 0.06 | 0.14 | 0.08 | 0.12 | 0.09 | 0.15 | 0.15 | 0.10 | 0.11 | 0.09 |
| K ₂ O | 1.27 | 0.94 | 1.33 | 1.24 | 1.15 | 1.45 | 2.30 | 3.83 | 3.15 | 1.72 | 4.59 | 1.48 | 0.74 | 6.08 | 4.96 |
| CaO | 2.13 | 2.30 | 2.05 | 12.21 | 19.94 | 15.04 | 2.96 | 2.50 | 3.69 | 2.98 | 2.17 | 22.19 | 33.20 | 5.20 | 2.54 |
| CrO ₂ | 0.12 | - | - | - | - | - | 0.13 | - | - | - | 0.15 | 0.11 | - | 0.13 | - |
| MnO | 0.13 | - | 0.12 | 0.13 | - | - | 0.16 | - | 0.15 | - | - | - | - | - | - |
| Fe ₂ O ₃ | 37.56 | 31.71 | 37.99 | 31.31 | 22.47 | 23.96 | 29.73 | 25.35 | 29.42 | 41.01 | 27.31 | 13.63 | 8.94 | 23.45 | 20.40 |
| BaO | 1.14 | 0.68 | 0.99 | 0.71 | 0.66 | 0.58 | 0.79 | 0.48 | 0.78 | 0.81 | 0.42 | 0.41 | - | - | - |
| Total | 73.94 | 57.00 | 77.50 | 80.27 | 78.99 | 77.26 | 84.63 | 81.21 | 85.97 | 74.72 | 85.40 | 80.06 | 78.12 | 89.53 | 77.40 |

Table 6.7 contd.

| Sample | M-5A | M-5B | M-5C | M-5D | M-5E |
|--------------------------------|-------|-------|-------|-------|-------|
| Element | | | | | |
| Na ₂ O | 0.52 | 0.47 | - | - | 0.42 |
| MgO | 1.17 | 0.56 | 2.85 | 1.85 | 0.60 |
| Al ₂ O ₃ | 2.50 | 1.31 | 8.47 | 4.91 | 1.32 |
| SiO ₂ | 12.29 | 13.26 | 44.72 | 17.35 | 6.68 |
| P ₂ O ₅ | 18.55 | 16.09 | 0.20 | 1.14 | 14.44 |
| S | 0.88 | 0.95 | - | - | 0.75 |
| Cl | - | - | 0.07 | - | 0.12 |
| K ₂ O | 1.30 | 0.81 | 4.98 | 1.64 | 0.71 |
| CaO | 29.53 | 36.25 | 1.84 | 2.22 | 39.44 |
| CrO ₂ | - | - | 0.14 | - | - |
| MnO | - | - | - | - | - |
| Fe ₂ O ₃ | 20.36 | 10.58 | 24.05 | 49.39 | 11.77 |
| BaO | 0.33 | - | 0.43 | 0.92 | - |
| Total | 87.43 | 80.28 | 87.75 | 79.42 | 76.25 |

Table 6.8 Western Nadorello, Upper Oligocene mineralised echinoid grain: microprobe geochemistry (c.p. Table 6.1)

Oligocene samples) and 6.9 (Lower Miocene samples) record data on echinoid pellets, *Dicrinera* and *Paracrinera* and *Paracrinera* pellets, the latter are included for comparative purposes).

| Sample | C-5A | C-5B | C-5C | C-5D |
|--------------------------------|-------|-------|-------|-------|
| Element | | | | |
| MgO | 0.89 | 0.97 | 0.72 | 0.79 |
| Al ₂ O ₃ | 0.26 | 0.14 | - | - |
| SiO ₂ | 0.97 | 0.55 | - | - |
| CaO | 57.85 | 59.42 | 58.73 | 58.35 |
| Fe ₂ O ₃ | 0.13 | - | - | - |
| Total | 60.10 | 61.08 | 59.45 | 59.14 |

Table 6.9 Costa del Conte, Lower Miocene unmineralised echinoid grain (C-5A & C-5B) and its cement overgrowth (C-5C & C-5D): microprobe geochemistry (c.p. Table 6.1)

Tables 6.1 to 6.4 indicate that there is not a great difference between the chemistry of pellet cores and their surrounding rims. However, there is a slight general trend for cores to show enrichment in Fe₂O₃ (82% of analyses) and K₂O (61% of analyses) and depletion in Al₂O₃ (73% of analyses) and CaO (64% of analyses) relative to the rims. SiO₂ and MgO show no constant enrichment or depletion trend. In all cases, the variation is slight, in the order of 2-3% for Fe₂O₃ and correspondingly less for the other elements.

Table 6.5A records analyses on grey carbonate pellets (some of which may be dense, rounded coralline red algal clasts) inferred, despite their lack of green colouration to be partly glauconitised pellets. Table 6.5B records analyses on typical green pellets. Overall, Table 6.5 records a continuous range of composition confirming that the pellets represent arrested stages from early (Table 6.5A) to late (Table 6.5B) in the glauconitization process, although most analyses tend to cluster at the extremes of the range. Three features of the process are apparent:

1) Glauconite pellets are formed from a calcium carbonate precursor. Grains inferred to be the earliest stages in the process are

Oligocene samples) and 6.9 (Lower Miocene samples) record data on echinoid clasts, both mineralised and unmineralised (the latter are included purely for comparative purposes).

6.4.2 Results

Comparison of Tables 6.1 to 6.4 indicates that the pellets have an almost constant chemistry. Major components have the ranges: SiO_2 48-56%, but mostly 50-54%; Fe_2O_3 16-27%, mostly 20-25%; K_2O all between 7-8.5% except pellet G-3 (Table 6.4) with *c.* 5.4%; Al_2O_3 2-10%, mostly 4-6%; and MgO 3-6%, mostly 3.5-5%. The oxide total ranges from 90-98% but most analyses lie within 91-96%. In contrast, the analyses presented in Tables 6.5-6.8 have totals ranging from 54-93% with correspondingly different ranges for each element. Notably, the ranges tend to be greater, and in general, abundances of SiO_2 , Fe_2O_3 , K_2O , Al_2O_3 and MgO are less whereas CaO and P_2O_5 are significantly greater.

Tables 6.1 to 6.4 indicate that there is not a great difference between the chemistry of pellet cores and their surrounding rims. However, there is a slight general trend for cores to show enrichment in Fe_2O_3 (82% of analyses) and K_2O (61% of analyses) and depletion in Al_2O_3 (73% of analyses) and CaO (64% of analyses) relative to the rims. SiO_2 and MgO show no constant enrichment or depletion trend. In all cases, the variation is slight, in the order of 2-3% for Fe_2O_3 and correspondingly less for the other elements.

Table 6.5A records analyses on grey carbonate peloids (some of which may be dense, rounded coralline red algal clasts) inferred, despite their lack of green colouration to be partly glauconitised pellets. Table 6.5B records analyses on typical green pellets. Overall, Table 6.5 records a continuous range of composition confirming that the pellets represent arrested stages from early (Table 6.5A) to late (Table 6.5B) in the glauconitisation process, although most analyses tend to cluster at the extremes of the range. Three features of the process are apparent:

- 1) Glauconite pellets are formed from a calcium carbonate precursor. Grains inferred to be the earliest stages in the process are

almost wholly calcium carbonate (see analyses B-6C1 and F-5R1, Table 6.5A), and calcium carbonate similar in composition to that of calcite cement (analyses C-5C & D in Table 6.9).

2) Glauconitisation, in its early stages, in any single grain, is not uniform and shows no obvious chemical zonation from core to rim. Rather, glauconitisation appears to develop randomly throughout a grain (analyses of Table 6.5). Enrichment and depletion of some of the oxides in the core relative to the rim (as mentioned previously) is seen only in late stage glauconitised pellets.

3) Si, Al and Fe are introduced early in the glauconitisation process, whereas K is mainly introduced in the later stages. K is apparently introduced in a process unrelated to the addition of Fe (e.g. compare analysis of pellet E-4 with the more mature pellet G-6: in E-4C the ratio of Fe : K is 5.2 : 1; whereas in the more mature G-6C the ratio of Fe : K is 3.4 : 1 indicating that K is incorporated more quickly late in the process).

Table 6.6 indicates that the glauconite in foraminiferal chamber infills of Lower Miocene samples contains significant quantities (2.5-5.7%) of CaO. Additionally, the analyses show similar, if variable chemistries both between different chambers of the same foraminifera and between different foraminifera (except for analyses of A.6 which contains large quantities of P_2O_5 and CaO). The early introduction of Si, Al and Fe and late introduction of K, seen in the pellets is also seen in the chamber infills.

Tables 6.7 and 6.8 indicate that the foraminiferal chamber infills and the mineralised echinoid grains from Upper Oligocene samples contain not only glauconite (evidenced by the relative abundances of Fe_2O_3 , SiO_2 , Al_2O_3 and K_2O), but commonly also show significant quantities of carbonate - apatite evidenced by the relative abundances of P_2O_5 (0.5-19%) and CaO (2.5-33%) along with traces of S, Cl, CrO_2 , MnO and BaO.

6.4.3 Discussion

The geochemical data presented in Tables 6.1 to 6.4 characterise

the mineral forming the green pellets as glauconite. The mineral can be distinguished from chamosite which contains larger quantities of Fe_2O_3 (45%) and Al_2O_3 (23%) and smaller quantities of SiO_2 (25%) (Deer *et al.*, 1962). It cannot be distinguished from the closely similar celadonite on chemistry alone, but since the latter mineral is known only from volcanic rocks (Deer *et al.*, 1962; Wise & Eugster, 1964; Foster, 1969; McRae, 1972, Odin & Matter, 1981) its presence as an authigenic mineral in sediments is unlikely. Data presented in Tables 6.1 to 6.4 are fully consistent with the range of glauconite compositions estimated by similar microprobe analysis and published in recent years (e.g. Birch *et al.*, 1976; Velde, 1976; Loveland, 1981; Odin & Matter, 1981).

Significantly high quantities of P_2O_5 and CaO in association with glauconite, as shown in the Upper Oligocene samples of Tables 6.7 and 6.8 and the Lower Miocene sample A.6 in Table 6.6, have been described elsewhere (Birch *et al.*, 1976). They have been interpreted as phosphatisation contemporaneous with glauconitisation, giving rise to carbonate apatite. The traces of S, Cl, CrO_2 and MnO along with some of the BaO probably have the same source. Some of the CaO is also likely due to the presence of unaltered calcite which must be present in at least minor quantities throughout all the glauconite (Tables 6.1-6.8) to account for the generally > 1% CaO recorded.

The early introduction of Fe along with the late fixation of K has been recorded by many workers (Burst, 1958b, Ehlman *et al.*, 1963; Bentor & Kastner, 1965; Seed, 1965; Foster, 1969; McRae, 1972; Birch *et al.*, 1976; Velde, 1976; Odin & Matter, 1981). Its occurrence here is, therefore, not remarkable. The early introduction of Si and Al, however, has not been previously noted. It was thought, until recently, that glauconite originated from a high alumina smectite, an illite or degraded mica (the "layer lattice theory" of Burst, 1958a,b; Hower, 1961) and therefore introduction of Si and Al was not needed. Odin & Letolle (1980) and Odin & Matter (1981), however, describe how glauconite forms from a calcium carbonate precursory grain which involves the precipitation of minute crystals of "glauconitic smectites" in micropores (5-10 μ size) within the grain, these smectites eventually pervading the whole grain. This

process would account for the early introduction of Si, Al and Fe observed in the data here and is therefore favoured as an explanation for glauconite formation (Section 6.5).

The variation from Fe enriched/Al depleted cores to Fe depleted/Al enriched rims recorded here has been recorded previously by Velde (1976).

Birch *et al.* (1976) consider that glauconite containing > 7% K₂O is "mature" whilst grains with < 7% are "immature". This being so, then the pellets of Tables 6.1-6.4 can be considered as mature whilst all other analyses (Tables 6.5-6.8) are of immature glauconite. The almost homogeneous nature (indicated by core and rim analyses) of the green pellets in Tables 6.1-6.4 and the heterogeneity of the pellets (and other glauconite modes of occurrence) in Tables 6.5-6.8 agrees with maturity and immaturity respectively (Burst, 1958b; Ehlmann *et al.*, 1963). Velde (1976) found that as K content increased towards its maximum of 8-9% then the grains in the bulk sample tended towards chemical homogeneity. Since the bulk of the pellets in the Lower Miocene deposits (both from the glauconitic limestone facies and the sandy limestone facies) can be considered as chemically mature (they contain 7-8% K₂O) and chemically homogeneous within grains (indicated by core and rim analyses) and between grains (they agree with the chemical limits set out by Birch *et al.*, 1976, and Odin & Matter, 1981), they represent a mature glauconite substrate or environment. In contrast, the chemical immaturity and heterogeneity of the Upper Oligocene glauconite occurrence suggests that this substrate was immature.

In summary, the microprobe data presented here identify, for the first time, the green pellets present in the Lower Miocene of southwest Sicily as the mineral glauconite. The range of geochemical analyses agrees with recently published microprobe data for glauconite. P₂O₅ and much of the CaO content along with the traces of S, Cl, CrO₂, MnO and BaO are due to the presence of carbonate-apatite whilst some of the CaO is due to unaltered calcium carbonate. The early fixation of Si, Al and Fe agrees with Odin & Matter's (1981) mechanism for the formation of glauconite from a calcium carbonate precursor. The late fixation of much

of the K confirms an observation commonly recorded in the literature. Finally, the absolute chemistry and the chemical homogeneity within and between pellets in the Lower Miocene deposits suggests that most of the pellets are composed of mature glauconite and that the Lower Miocene glauconite substrate/environment of the glauconitic limestone facies (where the glauconite is authigenic in occurrence), was a mature one. The chemistry of the Upper Oligocene glauconite, however, suggests that the glauconite is immature and that the Upper Oligocene glauconite substrate/environment was immature.

6.5 Origin of Glauconite

Given that the environment is conducive, three different origins for glauconite have been proposed in the literature.

1) As a gel, of Mg, Fe, Al and Si to which K was later added. This origin, favoured 1891-1939 (Murray & Renard, 1891; Collet, 1908; Takahashi, 1939), was discarded when Burst (1958a,b) presented the "layer lattice theory" only on the grounds that Burst's theory appeared more likely for a process that was poorly understood anyway.

2) By ionic exchange introducing Fe and K into the lattice of a detrital layer silicate of either a clay mineral or a degraded mica (the "layer lattice theory" of Burst, 1958a,b). This process was widely accepted until recently (McRae, 1972). Its deficiency is that it cannot account for the glauconitisation of anything other than a layer lattice substrate.

3) By the precipitation of minute crystals of glauconitic smectite in the micropore system of a carbonate grain with subsequent dissolution of the calcium carbonate and eventual replacement of the grain. This origin for glauconite grains was proposed by Odin & Matter (1981) who cited as evidence the presence of glauconitic smectite crystals in detrital micas (Odin, 1972) and in limestone hardgrounds (Aubry & Odin, 1973). Once all the grain has been replaced the K₂O content is 4.5-6.6%. Subsequent evolution follows the growth of larger and better shaped crystallites with the introduction of more K to form glauconitic mica.

As noted above (Section 6.4), geochemical variation documented in

Tables 6.1 to 6.8 is consistent with the origin of both pellets and foraminiferal chamber/echinoid stereom infills by glauconitisation of a calcium carbonate precursor rather than of a degraded silicate lattice. Moreover, the early introduction of Si, Al and Fe along with later addition of K would agree with Odin & Matter's (1981) theory for glauconitisation and cannot be explained by the formation of glauconite from a degraded layer silicate lattice.

6.6 Environment of Glauconite Formation

Glauconite, although a diagenetic mineral, forms, at the present day, on a marine sediment surface or just below the sediment/water interface (Odin & Letolle, 1980). It is a useful index of palaeoenvironmental conditions, where it can be proved to be *in situ* and not derived, since its formation is controlled by physico-chemical parameters such as salinity, acidity, oxidation, temperature, water turbulence, water depth and sedimentation rate.

6.6.1 Salinity & Acidity

Typically, glauconite forms in "normal marine" (McRae, 1972) or "open marine" (Odin & Letolle, 1980) waters which are slightly alkaline (pH 7-8) (Dapples, 1967; Fairbridge, 1967). Glauconite from lacustrine and other continental deposits has, however, been recorded (McRae, 1972).

That the southwest Sicily glauconites formed under normal marine conditions is evidenced by the associated algal flora (in the Upper Oligocene limestones, Section 4.1.4), microfauna of large benthonic foraminifera and echinoid macrofauna (Sections 2.5.3 & 3.4.1), since these forms are all abundant and strictly stenohaline. These associations, however, provide no clue to the acidity of the enclosing aqueous solution.

6.6.2 Oxidation

Modern glauconite most commonly occurs in waters of Eh 0 (McRae, 1972; Burnett, 1980) with a range from slightly oxidising (Eh +50 to +400 mV, Larsen & Chilingar, 1967) to slightly reducing (Eh 0 to -200 mV) (Cloud, 1955; Burst 1958a,b; Dapples, 1967; Fairbridge, 1967).

That the southwest Sicily glauconite formed near the oxygen minimum

zone is indicated by their association with early (marine) ferroan calcite cements (Sections 5.1.2, 5.3.2) since these reflect an environment of alternating oxidising and reducing conditions. The presence of small quantities of carbonate-apatite occurring alongside some of the glauconite (mainly the Upper Oligocene foraminiferal occurrence) suggests that the environment was weakly reducing (Section 7.8.3).

6.6.3 Temperature

Temperature of formation ranges from 7-20°C. Individual authors disagree on the extent of the range. Porrenga (1967) found glauconite restricted to bottom temperatures of 10-15°C off the Niger Delta. McRae (1972) quotes a general range of 15-20°C whilst Odin & Letolle (1980) quote temperatures of 7-15°C as general for glauconite formation.

In southwest Sicily, relatively cool bottom temperatures are indicated by the coralline red algal assemblage and by the low diversity and large size of individuals of both macrofauna and microfauna in the associated sediments (Section 2.5.4 & 3.4.1). More precisely, *Rotalia* and *Amphistegina* may indicate bottom temperatures of 14-25°C and 7-13°C respectively (Section 2.5.4). The poor development of marine cement also indicates cool seawater poorly saturated with CaCO₃ (Sections 5.1.2 & 5.3.2).

6.6.4 Water Turbulence

Glauconite is commonly preserved in sediments which show evidence of turbulence (Cloud, 1955; McRae, 1972). Continued marked water flow and agitation would, however, be incompatible with the particularly narrow range of oxygenation conditions required, but some turbulence is needed to introduce the required ions and to carry away any fine sediment which might otherwise be deposited.

In southwest Sicily abrasion of foraminifera in grainstone/packstone sediments and the presence of nearby algal rhodolith beds in the Upper Oligocene along with moderate sorting and occasional cross beds in the Lower Miocene all indicate the presence of moderately turbulent conditions.

6.6.5 Water Depth

Modern glauconite forms in 30-500 m water depths (McRae, 1972; Odin & Letolle, 1980; Odin & Matter, 1981) but it is most common at 60-350 m. It is found in inner shelf, outer shelf and upper slope positions. This parameter is generally a function of temperature and water turbulence. Thus, in tropical latitudes glauconite occurs in cooler waters at depth, whereas in temperate latitudes it occurs in shallower water limited by excessive water turbulence producing oxidising conditions at the shallowest depths.

In southwest Sicily water depths 80-250 m (probably < 200 m) are inferred from the coralline red algal assemblage (Section 4.1.4) and generally from the Upper Oligocene (Section 2.5.6) and Lower Miocene (Section 3.4.1) sediments. This agrees with the probable tropical-subtropical position of Sicily in Upper Oligocene/Lower Miocene times (Smith & Briden, 1977) where cool bottom temperatures would be found at depth.

6.6.6 Sedimentation Rate

Glauconite formation is favoured by low, or even negative sedimentation rate (McRae, 1972): a condition which is often provided by a marine transgression, and with which glauconitisation on a wide scale commonly occurs (Odin & Matter, 1981).

In southwest Sicily slow sedimentation rate is indicated by the limited thickness (c. 100 m maximum) of the Upper Oligocene - Lower Miocene succession. Also, a Lower Miocene transgression is well documented throughout the central Mediterranean area (Section 3.4.3). The widespread Lower Miocene glauconitic limestones of southwest Sicily and those found in western Sicily in general (Section 3.1.2) could be a result of this transgression. In the central Mediterranean area in general slow sedimentation rates in the Lower Miocene are indicated by the presence of heavily bioturbated beds and common hardgrounds in southeast Sicily (Section 4.2.3) and the Maltese islands (Bennett, 1979, 1980).

6.6.7 Summary

The conditions of formation of glauconite in southwest Sicily are

consistent with those of glauconite formation in general. Moreover, the presence of glauconite confirms that the Upper Oligocene - Lower Miocene carbonates of southwest Sicily were deposited in normal saline cool waters of moderate turbulence around the oxygen minimum zone at depths of 80-250 m with a slow sedimentation rate in a tropical-sub-tropical latitude. The abundance of glauconite in the Lower Miocene limestones relative to the Upper Oligocene limestones is inferred to reflect the widespread transgression recorded in the Lower Miocene of the Mediterranean area.

6.7 Conclusions

Glauconite occurs as green pellets and as green, orange-brown and opaque infillings to benthonic foraminifera and the micropores of echinoid clasts. In the Upper Oligocene limestones glauconite is restricted in occurrence and occurs in minor quantities as foraminifera and echinoid clast infills. In the Lower Miocene limestones glauconite, in the form of pellets, is ubiquitous and abundant whilst foraminiferid and echinoid infills are found in abundance at only one of the four localities studied.

The results of 151 microprobe analyses, from samples in Upper Oligocene and Lower Miocene limestones and from both the glauconitic limestone facies and the sandy limestone facies in the Lower Miocene, are presented in Tables 6.1-6.9. The analyses identify for the first time the green mineral present as the mineral glauconite. The geochemical analyses indicate that all forms of glauconite (pellets, foraminifera and echinoid infills) have formed from a calcium carbonate precursor. The early fixation of Si, Al and Fe along with the late fixation of K agrees with Odin & Matter's (1981) theory of glauconite formation from a calcium carbonate grain. The P_2O_5 content and much of the CaO content, along with the traces of S, Cl, CrO_2 , MnO and BaO, seen most commonly in the Upper Oligocene glauconites, represent the presence of small quantities of carbonate - apatite, whilst some of the CaO represents unaltered calcium carbonate. The absolute chemistry, and the chemical homogeneity within and between most of the Lower Miocene pellets suggests that these pellets are mature, and that the Lower Miocene

glaucinite environment/substrate of the glauconitic limestone facies was a mature one. The contrary is so for the Upper Oligocene environment/substrate.

PHOSPHORITES OF SICILY AND MALTA

Finally, evidence from both the Upper Oligocene and Lower Miocene glauconite occurrence suggests that the environment of glauconite formation was the same, and in agreement with that already recorded for glauconite in the literature. In southwest Sicily, glauconite formed in normal saline conditions in cool waters of moderate turbulence around the oxygen minimum zone at depths of 80-250 m with a slow sedimentation rate in a tropical-subtropical latitude. The abundance and widespread occurrence of glauconite in the Lower Miocene of western Sicily in general is inferred to reflect the well documented and widespread transgression in the Lower Miocene of the Mediterranean area.

The term phosphorite is applied to phosphate-rich rocks of marine sedimentary origin. Denton takes the boundary between phosphorites and phosphatic sediments at $>0.1\% \text{P}_2\text{O}_5$ accepting as phosphorite any phosphate-enriched sediment, but authors generally (e.g. Plant et al., 1979; Lucas, Powell & Roberts, 1980) regard a phosphorite as a sediment containing more than 15-20% P_2O_5 . The phosphorites described here sometimes contain up to 16% P_2O_5 , but the term phosphorite applied to them is consistent with the definitions of both Denton (1960) and Lucas et al. (1980).

Phosphorites have great economic significance. They form the basis of a major mineral industry of worldwide importance (Denton, 1979; Roberts, 1973; Siansky, 1980), ranking second to iron ore in terms of value, tonnage produced and volume of international trade. Their economic importance resides in the fact that, together with phosphate deposits of igneous origin, they are the only suitable source of phosphorus for the manufacture of phosphate fertilisers and some phosphorus-based chemicals (Roberts, 1980b). In 1978, phosphorites contributed 84% of the total production of 125 million tonnes of phosphate raw material.

Wide recent interest in the occurrence, geochemistry and geology of phosphorites is evidenced by the symposium volumes of Cook & Sengupta (1978), Denton (1980) and Notholt et al. (1980a). Also by participation in 1977 of International Geological Correlation Programme Project

CHAPTER 7

PHOSPHORITES OF SICILY AND MALTA

7.1 Introduction

The term phosphorite has been variously interpreted. Tooms *et al.* (1969) define a phosphorite as "a marine authigenic mineral deposit composed mainly of carbonate apatite". In contrast, Emigh (1967) considers that the term should be restricted, used only to designate a phosphatic mineral deposit of economic significance. Bushinski (1969) and Slansky (1979) both rigidly define a phosphorite as a rock containing more than 18% P_2O_5 by weight. More recently, Bentor (1980) confines the term phosphorite to phosphate-rich rocks of marine sedimentary origin. Bentor takes the boundary between phosphorites and phosphatic sediments at "0.x% P_2O_5 " accepting as phosphorite any phosphate-enriched sediment, but authors generally (e.g. Plant *et al.*, 1979; Lucas, Prevot & Trompette, 1980) regard a phosphorite as a sediment containing more than 15-20% P_2O_5 . The phosphorites described here sometimes contain less than 15% P_2O_5 , but the term phosphorite applied to them is consistent with the definitions of both Bentor (1980) and Tooms *et al.* (1969).

Phosphorites have great economic significance. They form the basis of a major mineral industry of worldwide importance (Emigh, 1975; Notholt, 1975; Slansky, 1980), ranking second to iron ore in terms of gross tonnage produced and volume of international trade. Their economic value resides in the fact that, together with phosphate deposits of igneous origin, they are the only suitable source of phosphorus for the manufacture of phosphate fertilisers and some phosphorus-based chemicals (Notholt, 1980b). In 1978, phosphorites contributed 84% of the total world production of 125 million tonnes of phosphate raw material.

Wide recent interest in the occurrence, geochemistry and genesis of phosphorites is evidenced by the symposium volumes of Cook & Shergold (1979), Bentor (1980) and Notholt *et seq.* (1980a). Also by establishment in 1977 of International Geological Correlation Programme Project

156: Proterozoic - Cambrian phosphogenic provinces in Asia and Australia, to determine the extent of, and prevailing concepts of, deposition for phosphorites of this time and area (Notholt, 1978). This project has subsequently broadened into a multidisciplinary research programme to investigate the nature and distribution of all phosphorite deposits, re-titled "Phosphorites", stimulating development of an International Phosphate Resource Data Base (Cook, 1980).

Phosphorites from the circum-Mediterranean countries, especially those of Morocco and Tunisia, are well known for their economic significance. The major deposits, however, are all of Cretaceous to Eocene age (Sheldon, 1964; British Sulphur Corporation, 1973; Lucas, Prevot & Trompette, 1980). The Oligocene apparently marks a hiatus in phosphate deposition worldwide (Cook & McElhinny, 1979; Notholt, 1980b), and although Miocene phosphorites are known from offshore western Morocco (Summerhayes, 1970; McArthur, 1980), the most extensive and best known Miocene deposits are from Florida, U.S.A. (Riggs & Freas, 1965; Riggs 1979a,b, 1980).

This Chapter describes phosphorites from the Upper Oligocene of southwest Sicily, and the Lower Miocene of southeast Sicily and Malta. The presence of mid-Tertiary phosphate in southwest Sicily has hitherto been recorded only as "nodules phosphates" (Masclé, 1973, 1979), with no details of nature, occurrence or geochemistry. The phosphates of southeast Sicily are somewhat better documented, in that they have been mapped and briefly described (Ruggieri, 1961 Bommarito & La Rosa, 1962) and redescribed and analysed for major elements by Di Grande *et al.* (1978). Similarly, the stratigraphic occurrence of phosphorites on the Maltese islands is well known, but their conglomeratic nature has only recently been established (Felix, 1973) and detailed work on their genesis and geochemistry is as yet unpublished (Bennett, 1980). "Noduletti fosfateri" have been recorded more widely though sparsely in the Middle to Upper Miocene of Sicily by Ruggieri (1957, 1959) and Colacicchi (1963), but no other significant deposits of central Mediterranean position and mid-Tertiary age are known.

This account details the geographic and stratigraphic occurrence

of phosphorites in the three areas (southwest Sicily, southeast Sicily, Maltese islands); describes the phosphorite mineralogy and petrography; and records details of analyses for major, trace and rare earth elements so as to elucidate the local environments of phosphorite genesis and deposition.

7.2 Geographic, Stratigraphic and Facies Occurrence

7.2.1 Southwest Sicily

In southwest Sicily a single phosphorite is known, forming part of the basal Upper Oligocene conglomerate (fully described in Section 2.2.2). The most extensive outcrops are at Nadorello east (Figs 1.5, 2.1, 2.2; Plates 2.5, 4.41) and San Biagio west (Fig. 2.6; Plates 2.8, 2.9). Light to dark brown coloured phosphatic clasts < 5 mm to 150 mm in size are set in a matrix of rhodolithic algal foraminiferal packstone-wackestones. Although the age of the matrix is Upper Oligocene (Section 2.1.4), the phosphatised clasts are all chalks of Eocene age (Section 2.2.2).

A further phosphorite is found at the top of the exposed Upper Oligocene succession at the Tombe Sicani locality (Fig. 2.8) where it is represented by sparse rounded phosphatised calcareous siltstone pebbles (up to 20 mm dia.) and fragments of fish teeth distributed in the upper 0.2 m of foraminiferal grainstone packstones.

7.2.2 Southeast Sicily

In southeast Sicily, at least five phosphorite horizons are known from the southwestern limits of the Iblean Plateau (Fig. 1.3). Their occurrence is briefly documented by Di Grande (1975) and Di Grande *et al.* (1978), and mapped by Bommarito & La Rosa (1962) who also identified an associated macrofauna of fish teeth: *Carcharodon auriculatus*, *Oxyrhina desori*, *O. hastalis*, *Odontaspis contortidens*, *O. cuspidata*, and *Hemipristis serra*. The most extensive and accessible exposures occur at Donnalucata where a phosphatised hardground is also found (VA 661 692 to VA 667 691; Fig. 7.1; Plates 4.42, 7.1) on the south coast, and in the Contrada le Serre valley (VA 752 930; Fig. 7.1; Plates 7.2, 7.3) some 6 km to the north of Ragusa.

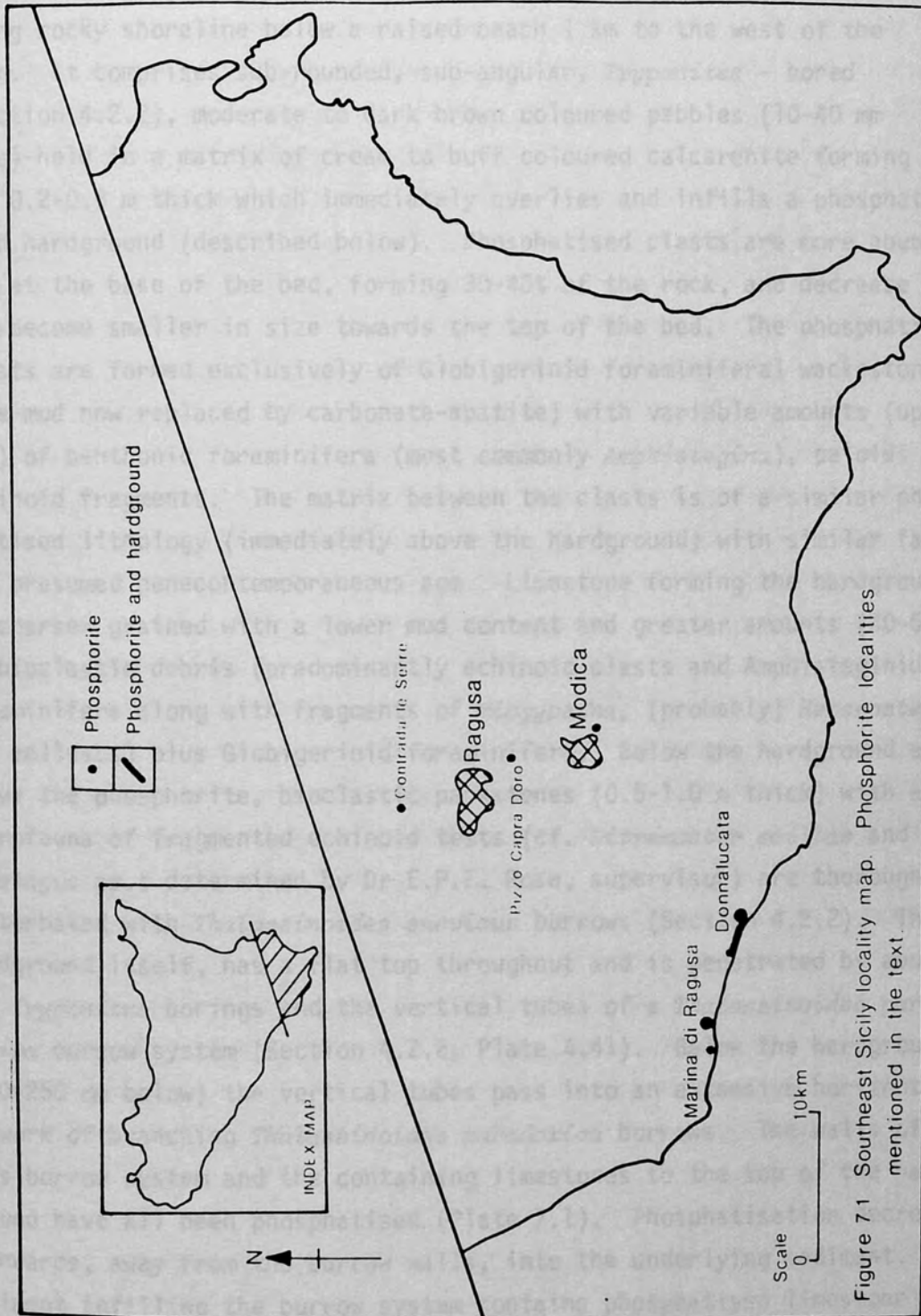


Figure 7.1 Southeast Sicily locality map. Phosphorite localities mentioned in the text.

At Donnalucata, phosphorite forms part of a 1.5 to 3 m bedded sequence dipping gently to the south (2-10°S 088) and exposed in a low lying rocky shoreline below a raised beach 1 km to the west of the town. It comprises sub-rounded, sub-angular, *Trypanites* - bored (Section 4.2.2), moderate to dark brown coloured pebbles (10-40 mm size) held in a matrix of cream to buff coloured calcarenite forming a bed 0.2-0.3 m thick which immediately overlies and infills a phosphatised hardground (described below). Phosphatised clasts are more abundant at the base of the bed, forming 30-40% of the rock, and decrease and become smaller in size towards the top of the bed. The phosphatised clasts are formed exclusively of Globigerinid foraminiferal wackestones (the mud now replaced by carbonate-apatite) with variable amounts (up to 15%) of benthonic foraminifera (most commonly *Amphistegina*), peloids and echinoid fragments. The matrix between the clasts is of a similar phosphatised lithology (immediately above the hardground) with similar fauna and presumed penecontemporaneous age. Limestone forming the hardground is coarser grained with a lower mud content and greater amounts (40-60%) of bioclastic debris (predominantly echinoid clasts and Amphisteginid foraminifera along with fragments of *Miogypsina*, (probably) *Heterostegina* and molluscs) plus Globigerinid foraminifera. Below the hardground and above the phosphorite, bioclastic packstones (0.5-1.0 m thick) with a macrofauna of fragmented echinoid tests (cf. *Ditremaster scillae* and *Eupatagus* sp.; determined by Dr E.P.F. Rose, supervisor) are thoroughly bioturbated with *Thalassinoides suevicus* burrows (Section 4.2.2). The hardground itself, has a flat top throughout and is penetrated by abundant *Trypanites* borings and the vertical tubes of a *Thalassinoides paradoxica* burrow system (Section 4.2.2; Plate 4.41). Below the hardground (150-250 mm below) the vertical tubes pass into an extensive horizontal network of branching *Thalassinoides paradoxica* burrows. The walls of this burrow system and the containing limestones to the top of the hardground have all been phosphatised (Plate 7.1). Phosphatisation decreases downwards, away from the burrow walls, into the underlying sediment. The sediment infilling the burrow system contains phosphatised limestone clasts (as described above) and is itself phosphatised.

At Contrada le Serre, phosphorite occurs as two conglomeratic horizons some 0.75-1.0 m apart in a sequence of buff (light grey weathered)

colour foraminiferal echinoid bioclastic packstones and grainstones (Plates 7.2, 7.3). Each horizon is some 50-120 mm thick, formed of loosely packed, moderate to dark brown-coloured, sub-rounded to sub-angular, commonly *Trypanites*-bored, poorly sorted, phosphatised Globigerinid foraminiferal wackestone clasts (5-30 mm size). These horizons are well exposed on both valley sides for some 1-2 km. Phosphorites with similar appearance and lithology can be seen at Pizzo Capra D'Oro (Fig. 7.1, 2 km south of Ragusa Ibla, at VA 782 854) and in a road cutting 2 km to the southeast of Modica (Fig. 7.1) at VA 802 786). Burrows of *T. suevicus* are sparse but present throughout the calcarenites above, below, and between the phosphorites at Contrada le Serre; abundant below the phosphorites at Pizzo Capra D'Oro (Plate 4.47); and sparse below the phosphorite exposed southeast of Modica. The enclosing limestones are of a different facies and contain abundant foraminifera, *Miogypsina* with subordinate amounts of *Amphistegina*, and echinoid debris. Elsewhere (to the east of Ragusa), they have yielded a benthonic foraminiferal fauna of *Amphistegina*, *Miogypsina*, *Heterostegina*, and *Elphidium*, identified by Di Grande (1975) and Di Grande *et al.* (1977) and dated as Lower Miocene in age by their relationship to planktonic foraminifera collected from soft marly beds in the sequence above and below the phosphorite-containing calcarenites. Di Grande *et al.* (1978) correlate the phosphorite horizons with the upper reaches of the "livello a banchi calcarenitici" (of Di Grande *et al.*, 1977) (Plate 7.2), cited as a mappable unit throughout the Iblean Plateau within the Irminio Member of the Ragusa Formation of Rigo & Barbieri (1959). Di Grande *et al.* (1977) correlate the calcarenites with zones N4 to N7 of Blow (1969), and the position of the phosphorites near the top of the calcarenite unit may therefore indicate a possible Burdigalian age for phosphorite deposition, since no major period of non-deposition is recorded for this time in this area (Pedley, 1981).

Phosphorites at Donnalucata, Pizzo Capra D'Oro, Modica and Contrada le Serre are similar in gross lithology, with regard to both clasts and their containing matrix, and their close association with *T. suevicus*-burrowed horizons. They are also broadly similar in late Lower Miocene (Burdigalian) age, and may represent but a single phosphogenic event.

7.2.3 Maltese Islands

In the islands of Malta and Gozo (Fig. 1.2), two major and several minor phosphorite horizons occur within the Lower Miocene Globigerina Limestone Formation. These have long been recorded as "nodule" beds, but their conglomeratic nature has recently been recognised by Felix (1973) and confirmed by Pedley *et al.* (1976). General features of the two main phosphorite beds have been recorded by Pedley *et al.* (1976), Pedley (1978), and Bosence *et al.* (1981), and in much further detail by Bennett (1980 unpublished).

The lower main phosphorite bed (C₁ of Pedley, Qammieh Conglomerate Bed of Bennett), found at the base of the Middle Globigerina Limestone, outcrops throughout Malta and Gozo, being thickest (up to 0.6 m) and containing the largest cobbles in the west, and thinnest (< 0.2 m) at Benghisa Point (586 634) in southeast Malta. Everywhere (except Benghisa Point where only partial hardground formation has occurred) it is underlain by a well developed mineralised hardground. Most complete, extensive and accessible exposures for both features are to be found at Qammieh Peninsula (square 39 81) in northwest Malta (Fig. 7.2) and west from Xwieni Bay (324 932) along the north coast of Gozo to Reqqa Point (313 935), (Fig. 7.2; Plates 7.4, 7.5).

The conglomerate comprises poorly sorted, phosphatised lithoclasts ranging from cobble (> 120 mm) to sand size (< 1 mm) with both phosphatised and unphosphatised bioclasts held in a non-phosphatised foraminiferal coccolith wackestone matrix, the foraminifera consisting of equal amounts of benthonic, mainly Rotaliid, and planktonic Globigeriniid foraminifera (Bennett, 1980). This rests on and infills the hardground and underlying burrow systems, thus allowing the conglomerate to extend for a thickness of 2-3 m down into the Lower Globigerina Limestone (Plates 7.4, 7.5).

A detailed study of the conglomerate enabled Bennett (1980) to distinguish three types of lithoclasts, an autochthonous non-phosphatised fauna, and an allochthonous phosphatised fauna (Plate 7.6). Lithoclasts were divisible into: glauconite-phosphate pebbles (phosphatised clasts with no internal structure but commonly a glauconitised rim) which occur

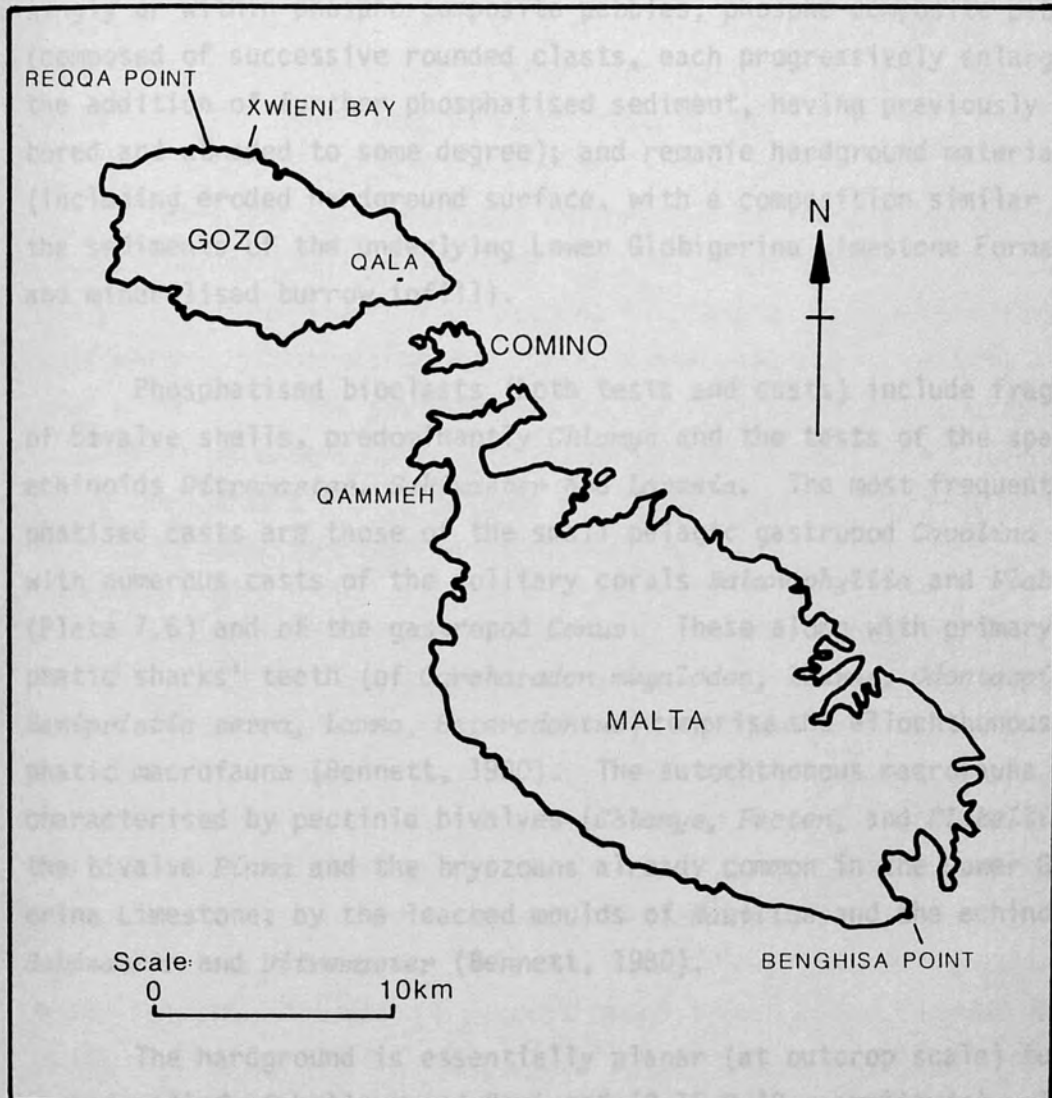


Figure 7.2 Maltese islands locality map. Phosphorite localities mentioned in the text.

singly or within phospho-composite pebbles; phospho-composite pebbles (composed of successive rounded clasts, each progressively enlarged by the addition of further phosphatised sediment, having previously been bored and abraded to some degree); and remanie hardground material (including eroded hardground surface, with a composition similar to the sediments of the underlying Lower Globigerina Limestone Formation, and mineralised burrow infill).

Phosphatised bioclasts (both tests and casts) include fragments of bivalve shells, predominantly *Chlamys* and the tests of the spatangoid echinoids *Ditremaster*, *Schizaster* and *Lovenia*. The most frequent phosphatised casts are those of the small pelagic gastropod *Cavolina* along with numerous casts of the solitary corals *Balanophyllia* and *Flabellum* (Plate 7.6) and of the gastropod *Conus*. These along with primary phosphatic sharks' teeth (of *Carcharodon megalodon*, *Isurus*, *Odontaspis*, *Hemipristis serra*, *Lamna*, *Heterodontus*) comprise the allochthonous phosphatic macrofauna (Bennett, 1980). The autochthonous macrofauna is characterised by pectinid bivalves (*Chlamys*, *Pecten*, and *Flabellipecten*), the bivalve *Pinna* and the bryozoans already common in the Lower Globigerina Limestone; by the leached moulds of *Nautilus* and the echinoids *Schizaster* and *Ditremaster* (Bennett, 1980).

The hardground is essentially planar (at outcrop scale) but has a rugged relief of hollows and "spines" (0.15-0.40 m amplitude). Its upper surface is characterised by intense replacement of lime mud by carbonate apatite and common glauconite impregnation. Mineralisation extends down thalassinoidean burrow systems some 0.4 m to 0.5 m into the underlying sediment. Burrow systems associated with the hardground and underlying sediment range from the stenomorphic thalassinoidean form *Thalassinoides paradoxica* found only within the lithified sediment forming the hardground and passing down into the non-restricted form *Thalassinoides suevicus* found in association with *Planolites* and *Chondrites* which are common throughout the Lower Globigerina Limestone.

The phosphorite horizon has been included in the Lower Globigerina Limestone Formation, dated as Aquitanian-Burdigalian (Lower Miocene, Blow, 1969, zones ?N4-N5) by Felix (1973), and apparently in the Middle

Globigerina Limestone, dated as Aquitanian-Burdigalian (Blow, 1969, zones ?N4, N6-N7) by Gianelli & Salvatorini (1972). The phosphorite is therefore of a controversial Lower Miocene age.

There are no significant differences in lithofacies and microfaunas between the limestones of the clasts and those of the underlying and enclosing Globigerina Limestone, so phosphatisation is inferred to have been penecontemporaneous, Lower Miocene in age. However, since some elements of the phosphatised macrofauna (notably *Balanophyllia* and *Flabellum*) have no counterpart in the unphosphatised surrounding limestone sequence, a source outside the present geographic area of the Maltese islands is inferred (Bennett, 1980).

The upper main phosphorite bed (C₂ of Pedley, Xwieni Conglomerate Bed of Bennett), found at the base of the Upper Globigerina Limestone, outcrops throughout the islands of Malta and Gozo but the most extensive and accessible exposure is found on the northern coast of Gozo between Xwieni Bay and Reqqa Point (Fig. 7.2, Plates 7.7, 7.8). At this locality Bennett (1980) recognises five individual conglomeratic pulses to constitute the bed. The thickness and number of the pulses decrease rapidly to the southeast. Only two pulses occur in northwestern and central Malta. Everywhere (except in southeast Gozo at Hondoq ir-Rummien, south of Qala at 386 873, Fig. 7.2) the conglomerate is held in a non-phosphatised matrix of foraminiferal wackestone similar to the overlying Upper Globigerina Limestone. At Hondoq ir-Rummien the conglomerate is concentrated into one bed (0.18 m thick) without non-phosphatised matrix resting above a hardground on top of the Qammieh Conglomerate indicating non-deposition of the Middle Globigerina Limestone in this area (Bennett, 1980).

The general compositional features of the bed are similar to those of the Qammieh Conglomerate, except that large cobbles are lacking and the smaller (20-50 mm size) phospho-composite pebbles dominate with subordinate amounts of finer (1-30 mm size) glauconite phosphate clasts, all composed of phosphatised foraminiferal limestones (Bennett, 1980). Macrofossils amongst the clasts include all but *Heterodontus* listed for the sharks' teeth present in the Qammieh Conglomerate, plus the

phosphatised tests and casts of *Conus*, *Cypraea*, *Cavolina*, *Flabellum*, *Caryophyllia*, *Cyathoceras*, *Cladocera*, *Ceratotrochus*, *Ostraea*, and, in particular the echinoids *Pliolampas vassali* and *Ditremaster scillae* (Bennett, 1980). The non-phosphatised clasts are dominated by a rich echinoid fauna: *Schizaster eurynotus*, *Ditremaster scillae*, *Pericosmus latus*, *Echinoecyamus stellatus*, *Spatangus marmorae*, *Lovenia anteroalta*, *Echinolampas scutiformis*, *Brissospis duciei* and *Brissospis crescenticus* (Challis, 1979).

The conglomerate infills a burrow system extending some 0.3-0.4 m down into the Middle Globigerina Limestone (Plates 7.8, 7.9). The system comprises burrows of *Thalassinoides suevicus*, *Planolites* and *Chondrites* (Bennett, 1980) of variable amounts from almost complete bioturbation (Plate 7.8) to only a few tunnels.

The upper main phosphorite horizon is included within the Upper Globigerina Limestone by Felix (1973) and therefore dated as Langhian (Blow, 1969, zone N9), but although included within the Upper Globigerina Limestone by Gianelli & Salvatorini (1972), is dated as Blow (1969) zone N8 within the Langhian.

There are no significant differences in the lithofacies and microfaunas between the limestones of the clasts and those of the enclosing Upper Globigerina Limestone suggesting that phosphatisation was penecontemporaneous. However, the diverse phosphatised fauna and lack of cobble size clasts at this level led Bennett (1980) to conclude that the phosphorite was derived from a source outside the present geographic area of the Maltese islands.

The two main conglomerate beds differ in that the lower bed is a single unit, clearly associated with a major hardground, whereas the upper bed is a multiple unit without an extensive underlying hardground. However, they are similar in clast lithology; in matrix; in their presence throughout Malta and Gozo; and in their general decrease in bed thickness from northwest to southeast.

7.3 Petrography

7.3.1 Observations

Forty thin sections (10 each from southwest and southeast Sicily, and 20 from the Maltese islands) were examined under a polarising microscope to determine the mode of phosphate occurrence in these rocks. The mineral francolite (identified as indicated in Section 7.4) was observed to occur in two readily distinguishable forms (identified by comparison with already published data on optics and textures in Kerr, 1959; Cook, 1972; and Manheim *et al.*, 1980):

1) Dark brown to opaque francolite

(Plates: 7.10-7.13)

Dark brown to opaque cryptocrystalline francolite occurs as round to irregularly shaped spots and areas generally 50 to 100 μ but occasionally 200 μ across (Plate 7.10); as discontinuous laminae some 50-100 μ thick and commonly 0.4-1.0 mm, occasionally 2-3 mm in length (Plate 7.11); as irregular shaped areas 100-300 μ size (Plate 7.12) and as rounded pellets 0.2-1.0 mm in diameter (Plate 7.13).

Spots show a diffuse boundary with the surrounding carbonate mud, so indicating that they may form by alteration of the mud. Where spots occur inside foraminiferal chambers, it is possible to recognise a sequence whereby increasingly larger spots progressively fill the chambers, then the pores in the surrounding test wall, before the test itself and the enclosing carbonate mud are altered to francolite (Plate 7.10).

Laminae were observed parallel to some clast and bore surfaces (Plate 7.11). They often cap broader laminae of the pale yellow francolite, and alternate with it. On some occasions they can be seen to contain rounded spots (Plate 7.11). This, along with the diffuse nature of the boundaries of the laminae, might suggest that they form as a secondary replacement.

Pellets (Plate 7.13) are round to oval in shape, show no internal structure, and are formed of very dense opaque francolite. Their very sharp boundaries with the adjacent sediment suggest that they may be

transported grains or that they are preferentially phosphatised relative to their surrounding matrix.

2) Light yellow, yellow orange, to orange brown francolite

(Plates: 7.14-7.17)

This paler coloured francolite is isotropic to sub-isotropic, often granular (with grains 5-10 μ across); sometimes amorphous; sometimes speckled with opaque irregular spots 10-30 μ in size. It occurs: in foraminiferal chambers and enclosing matrix, where it appears to replace carbonate mud (Plates 7.14,7.15); within the calcite intergranular cement, where it forms a carious texture with the calcite crystals, either replacing, or being replaced by them (Plate 7.16); paralleling some clast margins (and fracture surfaces) forming rims 50 μ to 2 mm thick with sharp outer, and diffuse inner boundaries (Plate 7.10), suggesting that it progressively replaced the carbonate mud towards the interior; as alternating laminae of yellow brown and opaque francolite in bore infills; as pore-lining cement; and as coatings, sometimes multiple (thus forming a sub-oolitic texture), on surfaces and clasts (in the Maltese phosphorites only), showing sharp boundaries with the substrate (Plate 7.17) therefore suggesting primary precipitate rather than secondary replacement.

7.3.2 Variation with Locality

In southwest Sicily, the dark francolites predominate, occurring as spots within clasts, as laminae paralleling the perimeter of clasts at the exterior, and as spots and laminae within the sediment infilling bores within the clasts. Paler yellow brown francolite is subordinate, but common, impregnating the outer surfaces of the clasts and lining borings which penetrate the clasts, commonly alternating with laminae of opaque francolite.

Only one major period of phosphatisation can be inferred from the textures observed. Furthermore, since both the clasts and the bore infills have been phosphatised, it is inferred that phosphatisation took place below the sediment water interface. Phosphatisation took the form

of alteration of the interior of the clast and bore infill at randomly spaced isolated nuclei forming opaque aggrading spots; progressive alteration of the exterior of the clast towards the interior forming yellow brown francolite rims; and alteration of the bore infills and clast enclosing sediment in zones parallel to the bore/clast walls forming alternating poorly defined laminae of yellow brown and opaque francolite (Plate 7.11).

No cross-cutting relationships can be identified between these modes of francolite occurrence to suggest separate periods of phosphatisation.

In southeast Sicily, dark francolite occurs as irregularly shaped areas and as poorly defined discontinuous laminae at the outer surfaces of clasts. It also occurs in pellet form. However, the dominant francolite is that of the paler light yellow to yellow orange optical type which occurs as replacement of carbonate mud in foraminiferal chambers; in the intergranular matrix of the hardground, where it possibly replaces calcite crystals or is replaced by them (a feature of common occurrence (Kerr, 1959) and recorded by Hewitt (1980) and Horton *et al.*, 1980); and in the clasts and matrix of the overlying conglomerate. Only one period of phosphatisation can be inferred since cross-cutting relationships, of the various modes of carbonate apatite, are not observed.

On Malta and Gozo, pale yellow orange francolite predominates, replacing carbonate mud in the hardground and in the clasts of both the Qammieh and Xwieni Conglomerates where the mud is progressively replaced towards the interior. It also occurs as primary precipitated coatings on clasts and hardground surfaces (Plate 7.17, and Bennett, 1980, Plate 3.16.2) in the Qammieh Conglomerate, and as a pore-lining cement in the Xwieni Conglomerate at Qala (Bennett, 1980, Plate 3.22.1-3). Opaque francolite is subordinate, but common, occurring as irregular areas, sometimes coalescing, within the hardground below the Qammieh Conglomerate; within clasts of both the Qammieh and Xwieni Conglomerates; and as impregnated coatings on the surfaces of the hardground and clasts.

Bennett (1980) notes that complex cycles of sedimentation, boring,

encrustation, glauconitisation, phosphatisation and erosion are apparent in many of the clasts. Up to six periods of boring and phosphatisation were identified (Plate 7.18) in the thin sections studied. Bennett (1980) suggests that glauconite impregnation of surfaces is often a precursor to phosphatisation. This however, was not recognised in this study. Rather, glauconitisation appears to take a parallel role, occurring replacing infills of foraminiferal chambers; and as impregnations of hardground and clast surfaces. It can be seen to predate and post-date francolite.

7.3.3 Discussion

Although the authigenic francolite described here varies from opaque to pale yellow in appearance, and from small spots to larger areas or to laminae in occurrence, its textures are predominantly those of replacement and less commonly those of primary precipitates.

The replacement of lime mud and foraminiferal tests by francolite is of common occurrence, and has already been recorded by Ames (1959, 1960), D'Angeljan (1967, 1968), McConnell (1973), Bennett (1980) and Manheim *et al.* (1980). In particular, Manheim *et al.* include colour photomicrographs of opaque and light yellow francolite both of which replace carbonate mud, and the latter foraminiferal tests.

Primary precipitates of phosphate have been described from the Maltese islands by Bennett (1980), who identified them as dahllite. Bennett's thin sections were re-examined during the present study, and his interpretation of pore-lining cement and encrusting laminae, sometimes forming sub-oolitic texture, as primary is confirmed. However, the identification of these as dahllite is not confirmed for the reasons set out in the following Section.

Direct precipitation of dahllite has been recorded by Braithwaite (1968) and Trueman (1971) for Recent terrestrial phosphatic deposits on Remire island in the Indian Ocean. Precipitation of (undifferentiated) carbonate apatite in the marine environment has been recorded by Burnett (1977) and Birch (1980) as cement, and by Cook (1972), Birch (1978) and

Horton *et al.* (1980) as oolitic grains. The recognition of these features in the Maltese phosphorites is therefore not remarkable.

Francolite in opaque pellet form has been recognised only from Donnalucata (southeast Sicily) within the study area. It is however, of common occurrence and has been recorded: from the Permian Phosphoria Formation by Emigh (1958, 1967); from the Cambrian of Queensland, Australia by Cook (1972); from the Miocene of Florida by Riggs (1980); and from the Recent, off the west coast of Peru (Burnett, 1980) and South Africa (Birch, 1980). Emigh showed that the pellets had calcitic precursors and suggested that they formed by the phosphatisation of them. Cook (1972) suggested that some of the structureless pellets formed by the phosphatisation of rounded biogenic calcareous fragments or by the reworking of collophane mud (as proposed by Russell and Trueman, 1971). Non-phosphatised rounded pellets are present in a single partially phosphatised conglomerate clast from Contrada le Serre, southeast Sicily. In the absence of any collophane mud deposit in the area it is possible that these may be the precursors of the opaque francolite pellets found at Donnalucata.

In conclusion, phosphorites from southwest Sicily and southeast Sicily are formed exclusively by francolite replacing pre-existing limestone in a single identifiable phase in an environment below the sediment water interface. Those of the Maltese islands are predominantly replacement francolites with minor amounts of primary cements and films (identified as dahllite by Bennett, 1980), in sediments with a complex diagenetic history.

7.4 Mineralogy

7.4.1 Analyses

Twenty powder samples together comprising ten rocks from southwest Sicily, and five from Malta and Gozo were prepared and analysed by X-Ray Diffraction (XRD) using the technique described in Appendix I. Descriptions of the samples and their stratigraphic and geographic sources are included in Table A2.1 of Appendix II.

The ten samples from southwest Sicily were collected at Nadorello east, since this is the largest and least weathered phosphorite outcrop. Several whole pebbles were analysed to assess any variation of phosphate mineralogy between pebbles. Additionally, separate analyses were made of pebble coatings and pebble interiors to test for variation within pebbles.

In southeast Sicily, the five samples were collected from Donnalucata, and represent both the phosphorite clasts and the surface of the underlying hardground. Those from the Maltese islands were collected from the Qammieh Conglomerate and its underlying hardground at Qammieh and from the Xwieni Conglomerate bed to the west of Xwieni Bay. These two localities were sampled by Bennett (1980) and direct comparison is therefore possible with his more extensive analyses of Maltese phosphorites.

Samples were chosen from rocks with known fluorine values (Section 7.5) so that sample range might extend from high (1.96%) to low (0.57%) fluorine value. This was done to test for the presence of both the high fluorine carbonate-apatite "carbonate-fluorapatite" (francolite) and the fluorine depleted "carbonate-hydroxyapatite" (dahllite) since both minerals have been reported in sedimentary apatite (McConnell, 1973; Bennett, 1980).

7.4.2 Results

Measurements of lattice "d-spacings" for all twenty samples are given in Table A2.2 of Appendix II. These data are all consistent with the range of values recorded for francolite (Berry, 1974; Jarvis, 1980), and sufficiently different from those of dahllite (Berry, 1974) to be able to distinguish the mineral as francolite. Mean value XRD data for the samples from southwest Sicily, southeast Sicily and the Maltese islands are given in Table 7.1. There is no significant difference between mean values from the different localities. Moreover, comparison with published data for both synthetic francolite (Berry, 1974) and other sedimentary francolites (Jarvis, 1980) (Table 7.2) indicates no significant difference in mineralogy.

| hk1 | (a) | | (b) | | (c) | |
|-----|-------------------|------------------|-------------------|------------------|-------------------|------------------|
| | d(\AA) | I/I ₀ | d(\AA) | I/I ₀ | d(\AA) | I/I ₀ |
| 100 | 8.111 | 7 | 8.109 | 7 | 8.111 | 6 |
| 200 | 4.048 | 7 | 4.047 | 7 | 4.048 | 6 |
| 111 | 3.862 | 6 | 3.868 | 7 | 3.866 | 7 |
| 002 | 3.439 | 39 | 3.439 | 41 | 3.439 | 39 |
| 102 | 3.165 | 15 | 3.168 | 16 | 3.163 | 15 |
| 210 | - | - | - | - | - | - |
| 211 | 2.787 | 100 | 2.789 | 100 | 2.784 | 100 |
| 112 | 2.771 | 54 | 2.773 | 55 | 2.769 | 54 |
| 300 | 2.686 | 50 | 2.680 | 50 | 2.679 | 51 |
| 202 | 2.618 | 29 | 2.619 | 29 | 2.618 | 31 |
| 301 | 2.505 | 7 | 2.507 | 7 | 2.507 | 7 |
| 212 | 2.282 | - | 2.283 | - | 2.281 | - |
| 310 | 2.238 | 24 | 2.238 | 22 | 2.236 | 24 |
| 221 | 2.209 | 5 | 2.208 | 5 | 2.212 | 5 |
| 311 | - | - | - | - | - | - |
| 302 | 2.125 | 6 | 2.125 | 6 | 2.125 | 6 |
| 113 | 2.058 | 8 | 2.059 | 7 | 2.059 | 6 |
| 400 | - | - | - | - | - | - |
| 203 | 1.996 | 6 | 1.996 | 6 | 1.995 | 6 |
| 222 | 1.928 | 27 | 1.930 | 28 | 1.927 | 27 |
| 312 | 1.876 | - | 1.874 | - | 1.875 | - |
| 320 | 1.853 | 6 | 1.852 | 6 | 1.852 | 5 |
| 213 | 1.834 | 30 | 1.835 | 31 | 1.833 | 30 |
| 321 | 1.786 | 12 | 1.785 | 12 | 1.785 | 12 |
| 410 | 1.760 | 12 | 1.759 | 12 | 1.760 | 12 |
| 402 | 1.740 | 12 | 1.740 | 12 | 1.740 | 13 |
| 004 | 1.723 | 14 | 1.722 | 14 | 1.722 | 14 |
| 322 | 1.628 | - | 1.627 | - | 1.627 | - |
| 313 | 1.602 | - | 1.601 | - | 1.602 | - |

TABLE 7.1 XRD analysis. Mean values of d-spacings (d(\AA)) and peak intensity (I/I₀) for phosphorite samples from (a) southwest Sicily (n = 10), (b) southeast Sicily (n = 5), and (c) Malta (n = 5). For techniques and raw data see appendices.

| hk1 | (a) | | (b) | |
|-----|-------|------------------|-------|------------------|
| | d(Å) | I/I ₀ | d(Å) | I/I ₀ |
| 100 | 8.12 | 8 | 8.08 | 6 |
| 200 | 4.055 | 8 | 4.04 | 6 |
| 111 | 3.872 | 8 | 3.87 | 6 |
| 002 | 3.442 | 40 | 3.45 | 45 |
| 102 | 3.167 | 14 | 3.17 | 16 |
| 210 | 3.067 | 18 | 3.05 | 18 |
| 211 | 2.800 | 100 | 2.79 | 100 |
| 112 | 2.772 | 55 | 2.77 | 55 |
| 300 | 2.702 | 60 | 2.69 | 50 |
| 202 | 2.624 | 30 | 2.62 | 30 |
| 301 | 2.517 | 6 | 2.51 | 4 |
| 212 | 2.289 | 8 | 2.28 | 8 |
| 310 | 2.250 | 20 | 2.24 | 20 |
| 221 | 2.218 | 4 | - | - |
| 311 | 2.140 | 6 | 2.13 | 6 |
| 302 | 2.128 | 4 | - | - |
| 113 | 2.061 | 6 | 2.06 | 6 |
| 400 | 2.028 | 2 | 2.02 | 2 |
| 203 | 1.997 | 4 | 1.998 | 4 |
| 222 | 1.937 | 25 | 1.931 | 25 |
| 312 | 1.884 | 14 | 1.878 | 12 |
| 320 | 1.862 | 4 | - | - |
| 213 | 1.837 | 30 | 1.836 | 30 |
| 321 | 1.797 | 16 | 1.789 | 12 |
| 410 | 1.771 | 14 | 1.762 | 10 |
| 402 | 1.748 | 14 | 1.742 | 10 |
| 004 | 1.722 | 16 | 1.724 | 16 |
| 322 | 1.637 | 6 | 1.632 | 4 |
| 313 | 1.607 | 4 | 1.604 | 2 |

TABLE 7.2 XRD data. Values of d-spacings (d(Å)) and peak intensity (I/I₀) of (a) synthetic fluorapatite standard (from Berry, 1974) and (b) French Cretaceous carbonate-fluorapatite (from Jarvis, 1980).

Samples from Nadorello east (southwest Sicily) show no distinction in mineralogy between phosphate coating the pebbles and that within the pebble interiors (compare XRD data for RTB 19A with RTB 19B, Table A2.2).

All twenty samples were found to be composite, containing both francolite and calcite (along with a small amount of free quartz in the southeast Sicily and Maltese samples). The presence of these other mineral phases was detected by their respective XRD patterns. In samples low in fluorine (e.g. M12) and therefore expected to contain dahllite, it was the calcite which had the effect of reducing the weight % of fluorine in the sample, and therefore giving a misleading impression of dahllite. The actual phosphate mineral, however, was always francolite (compare Table A2.2, with Table 7.2).

The sample richest in fluorine (sample RTB 19A with 1.96% F) has relative proportions of some 82% francolite and 18% calcite. These were calculated by comparing the peak sizes of the calcite 100 intensity peak (at 3.035 \AA d-spacing) of a pure limestone from southwest Sicily with that of phosphorite sample RTB 19A. The proportion of calcite in sample RTB 19A could therefore be estimated, leaving a residue attributable to francolite. (This estimate, however, is only approximate since a statistical population of peak sizes on XRD graphs of both the sample and the comparative limestone should be studied and the factors listed in Zussman, 1977, taken into account). The value of 82% francolite, however, does appear reasonably accurate in that it is consistent with other analyses (see below).

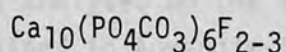
The amount of P_2O_5 in sample RTB 19A was determined by plasma analysis (Section 7.5) as 28.04%. If this represents 82% francolite in the sample, and assuming that a small amount (0.1%) of P_2O_5 was present in the original unphosphatised limestone (since similar values were analysed in the pure limestones, Table 7.8), the P_2O_5 value may be calculated for pure francolite as approximately 34%, a value similar to that (35.01%) obtained by Deer *et al.* (1966) for francolite from an altered lava. In support of this observation the fluorine value for the francolite in RTB 19A is calculated as 2.32%. A similar value (2.30%) is

obtained from Fig. 7.10 (P_2O_5 v F) for a francolite with 34% P_2O_5 .

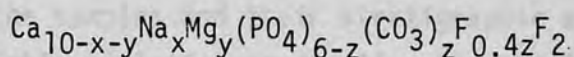
7.4.3 Discussion

The major phosphate mineral in phosphorites is carbonate apatite with variable quantities of substituent fluorine (McConnell, 1973). Consequently, it is possible to distinguish (*vide* Deer *et al.*, 1966) a relatively high (> 1% F) fluorine carbonate apatite (carbonate-fluorapatite, francolite) from a low (< 1% F) fluorine carbonate apatite (carbonate-hydroxyapatite, dahllite).

Deer *et al.* (1962, 1966) note that there is an isomorphous series between the end members fluorapatite ($Ca_{10}(PO_4)_6F_2$) and hydroxyapatite ($Ca_{10}(PO_4)_6OH_2$). This is likely to occur in the carbonate apatites also. The chemical composition of carbonate apatites is approximated by D'Angeljan (1967) and Tooms *et al.* (1969) as:



McClellan (1980) gives the francolite formula as:



This range in composition is presumed to account for the slight variation in d-Å spacing recorded in Tables A2.2 and 7.2, variation which is not great enough to characterise a mineral other than francolite.

Francolite is by far the most common sedimentary carbonate apatite mineral (McConnell, 1973), so its occurrence in these samples is unremarkable. Dahllite, a less frequent mineral, has an affinity for fluorine (McConnell, 1973) which ultimately results in its conversion to francolite.

Bennett (1980) distinguished dahllite as a mineral forming coatings by direct precipitation in contrast to francolite as a replacement mineral in clasts and hardgrounds of the Maltese islands. His observations are consistent with those of Braithwaite (1968) and Trueman (1971) who recorded the precipitation of dahllite albeit in a freshwater environment in Recent phosphatic deposits from Remire island (Indian Ocean); also with Ames (1959, 1960), D'Angeljan (1967, 1968) and McConnell (1973), who describe replacement of limestone by francolite. However, analyses tabulated

here do not confirm Bennett's findings. In the case of the Maltese samples, this may be a result of limited sampling, because examples of the dahllite coatings described by Bennett (1980) were not obtained during the author's field season on Malta. However, in the case of the western Sicily phosphorite, both coatings and clast interiors were observed and sampled, and francolite is the only phosphate mineral present. This is consistent with petrographic evidence (Section 7.3) that the Sicilian phosphorite coatings are secondary replacements rather than primary precipitates.

7.5 Major Element Geochemistry

7.5.1 Introduction

Fifty-two powder samples of phosphorites and limestones (collected from southwest Sicily, southeast Sicily and the Maltese islands) were analysed on the inductively coupled plasma (ICP) spectrometer, as outlined in Appendix I, to determine the relative concentrations of ten major elements (P, Ca, Si, Fe, Al, Mg, Na, K, Ti and Mn). Descriptions of the samples and their stratigraphic and geographic sources are given in Table A2.1 of Appendix II. The absolute abundances of these element oxides are given in Tables 7.3 to 7.8.

Additionally, fluorine content was determined by calorimetric method as outlined in Appendix I. An attempt was also made to analyse for H₂O and CO₂ using the method proposed by Groves (1937). Results were inconsistent, and since XRD analyses had shown that the phosphorite samples were composite in containing both francolite and calcite (Section 7.4), values for CO₂ content in the francolite were masked by CO₂ derived from the calcite. Alternative techniques for separate CO₂ and H₂O analyses were therefore not attempted, but their combined value is approximated to in the Tables as the "loss on ignition", in the manner adopted by Deshmukh (1979) and Lucas, Prevot & Trompette (1980).

Values for each of the metal oxides (except MnO, since it is present in very small amounts and shows little variation in abundance) are plotted (along with F) against P₂O₅ or CaO in Figs 7.3 to 7.19.

| Sample Element | RTA 7A | RTA 7B | RTA 7C | RTA 7D | RTA 11A | RTA 11B | RTA 13A | RTA 13B | RTA 13C | RTB 19A | RTB 19B | Mean |
|--------------------------------|--------|--------|--------|--------|---------|---------|---------|---------|---------|---------|---------|-------|
| P ₂ O ₅ | 23.32 | 19.70 | 20.98 | 23.16 | 13.94 | 19.70 | 14.27 | 21.22 | 19.27 | 28.04 | 29.11 | 21.16 |
| CaO | 54.64 | 55.91 | 55.85 | 50.74 | 52.38 | 51.29 | 51.23 | 52.04 | 51.52 | 55.27 | 56.08 | 53.36 |
| SiO ₂ | 2.25 | 2.01 | 1.84 | 2.95 | 2.09 | 1.93 | 2.15 | 1.74 | 1.73 | 3.60 | 3.47 | 2.34 |
| Fe ₂ O ₃ | 3.30 | 0.86 | 0.95 | 1.19 | 1.15 | 2.55 | 2.75 | 2.26 | 2.13 | 3.40 | 2.19 | 2.06 |
| Al ₂ O ₃ | 0.87 | 0.79 | 0.78 | 1.20 | 0.81 | 0.76 | 0.72 | 0.45 | 0.45 | 1.25 | 1.25 | 0.85 |
| MgO | 0.58 | 0.63 | 0.61 | 0.81 | 0.44 | 0.53 | 0.46 | 0.43 | 0.43 | 0.44 | 0.43 | 0.53 |
| TiO ₂ | 1.02 | 0.88 | 0.99 | 1.17 | 0.77 | 1.02 | 0.64 | 0.93 | 0.82 | 0.78 | 0.83 | 0.90 |
| K ₂ O | 0.23 | 0.16 | 0.16 | 0.26 | 0.17 | 0.16 | 0.21 | 0.12 | 0.11 | 0.32 | 0.28 | 0.20 |
| TiO ₂ | 0.15 | 0.05 | 0.09 | 0.08 | 0.06 | 0.12 | 0.05 | 0.05 | 0.04 | 0.18 | 0.11 | 0.09 |
| MnO | <0.01 | 0.01 | <0.01 | <0.01 | 0.01 | <0.01 | <0.01 | 0.01 | 0.02 | <0.01 | <0.01 | 0.01 |
| F | 1.49 | 1.14 | 1.21 | 1.52 | 0.91 | 1.18 | 0.91 | 1.29 | 1.23 | 1.96 | 1.92 | 1.34 |
| LOI | 13.17 | 17.66 | 17.80 | 13.72 | 24.92 | 18.32 | 24.03 | 17.21 | 20.31 | 4.05 | 2.37 | 15.77 |
| Total | 100.03 | 99.80 | 100.27 | 97.53 | 97.65 | 97.57 | 97.43 | 97.67 | 98.06 | 99.30 | 98.32 | 98.61 |
| Sc | 44 | 44 | 45 | 47 | 46 | 49 | 45 | 46 | 45 | 38 | 37 | 44 |
| V | 74 | 29 | 32 | 36 | 39 | 68 | 73 | 57 | 53 | 75 | 53 | 54 |
| Ni | 100 | 56 | 106 | 96 | 49 | 100 | 80 | 122 | 115 | 103 | 86 | 92 |
| Cu | 19 | 36 | 3 | 22 | 18 | 46 | 64 | 48 | 88 | 33 | 25 | 37 |
| Sr | 1365 | 1186 | 1318 | 1152 | 1178 | 1329 | 1000 | 1077 | 975 | 1269 | 1261 | 1192 |
| Y | 183 | 167 | 186 | 112 | 97 | 211 | 88 | 106 | 91 | 304 | 197 | 158 |
| Zr | 90 | 63 | 73 | 60 | 33 | 79 | 31 | 46 | 39 | 130 | 99 | 68 |
| Ba | 41 | 26 | 54 | 55 | 47 | 33 | 49 | 27 | 22 | 74 | 64 | 45 |

TABLE 7.3 Southwest Sicily phosphorite: major and trace element geochemistry. Relative proportions of major element oxides, the element fluorine and loss on ignition (LOI, corrected for fluorine content) expressed as weight per cent; trace element abundance expressed as parts per million. Samples are all from Nadorello east and comprise whole clasts (RTA 7A - RTA 13A), clast interiors (RTA 13C, RTP 19B), and clast exteriors (RTA 13B, RTB 19A). See appendices for details of sources and techniques.

| Sample Element | 2.9A | 11.4 | 6.3 | 45M | 36.1A | 36.1B | 97.2A | 119 | Mean |
|--------------------------------|-------|-------|--------|-------|-------|-------|--------|--------|-------|
| P ₂ O ₅ | 20.39 | 18.57 | 17.06 | 28.54 | 12.11 | 34.16 | 17.81 | 9.96 | 20.93 |
| CaO | 54.09 | 53.93 | 54.32 | 56.42 | 27.20 | 55.36 | 55.29 | 52.64 | 54.58 |
| SiO ₂ | 1.91 | 1.89 | 1.70 | 1.95 | 28.68 | 0.42 | 2.75 | 4.11 | 2.10 |
| Fe ₂ O ₃ | 0.65 | 1.47 | 0.83 | 1.17 | 3.68 | 0.38 | 1.67 | 4.97 | 1.59 |
| Al ₂ O ₃ | 0.77 | 0.71 | 0.70 | 0.82 | 9.10 | 0.21 | 1.07 | 1.47 | 0.82 |
| MgO | 0.39 | 0.41 | 0.48 | 0.33 | 0.80 | 0.50 | 0.39 | 0.68 | 0.45 |
| Na ₂ O | 0.73 | 0.76 | 0.65 | 0.95 | 0.73 | 0.97 | 0.41 | 0.37 | 0.69 |
| K ₂ O | 0.17 | 0.18 | 0.16 | 0.19 | 5.25 | 0.04 | 0.30 | 0.23 | 0.18 |
| TiO ₂ | 0.04 | 0.09 | 0.07 | 0.10 | 1.15 | 0.01 | 0.06 | 0.08 | 0.06 |
| MnO | <0.01 | <0.01 | 0.01 | <0.01 | <0.01 | <0.01 | 0.01 | 0.01 | <0.01 |
| F | 1.24 | 1.11 | 1.03 | 1.84 | 0.28 | 1.79 | 1.05 | 0.64 | 1.24 |
| LOI | 17.67 | 18.94 | 23.10 | 6.50 | 9.91 | 4.06 | 19.60 | 26.62 | 16.64 |
| Total | 98.06 | 98.07 | 100.11 | 98.82 | 98.90 | 97.91 | 100.41 | 101.78 | 99.29 |
| Sc | 43 | 44 | 39 | 43 | 29 | 38 | 38 | 36 | 40 |
| V | 29 | 69 | 28 | 50 | 87 | 26 | 56 | 89 | 50 |
| Ni | 58 | 54 | 70 | 50 | 66 | 26 | 31 | 40 | 47 |
| Cu | 6 | 25 | 8 | 13 | 40 | 6 | 13 | 27 | 14 |
| Sr | 950 | 1147 | 1089 | 1278 | 775 | 1803 | 636 | 1203 | 1158 |
| Y | 121 | 144 | 131 | 232 | 19 | 9 | 227 | 15 | 126 |
| Zr | 38 | 62 | 59 | 70 | 0 | 0 | 27 | 14 | 39 |
| Ba | 47 | 29 | 47 | 58 | 191 | 93 | 36 | 38 | 50 |

TABLE 7.4 Southwest Sicily phosphorite: major and trace element geochemistry (c.p. TABLE 7.3). Samples all whole clasts, from Porcarria (2.9A), Nadorello east (11.4, 6.3), San Biagio west (45M), Caltabellotta (36.1A,B),

| Sample Element | 187.2 | 187.5 | 193.2 B | 187.3 | 187.15 | 188 M | 191 M | 192.8 A | Mean |
|--------------------------------|-------|--------|---------|--------|--------|-------|-------|---------|--------|
| P ₂ O ₅ | 11.29 | 8.50 | 14.35 | 11.90 | 15.78 | 20.45 | 13.84 | 14.29 | 13.80 |
| CaO | 54.91 | 55.36 | 49.90 | 53.25 | 49.88 | 50.16 | 47.95 | 48.11 | 51.69 |
| SiO ₂ | 1.20 | 1.64 | 2.86 | 2.80 | 4.26 | 3.01 | 4.07 | 4.11 | 2.99 |
| Fe ₂ O ₃ | 0.50 | 0.49 | 2.19 | 1.73 | 2.70 | 2.88 | 2.83 | 2.75 | 2.01 |
| Al ₂ O ₃ | 0.32 | 0.43 | 0.56 | 0.52 | 0.92 | 0.76 | 0.75 | 0.97 | 0.65 |
| MgO | 0.65 | 0.74 | 1.01 | 0.88 | 0.97 | 0.65 | 1.52 | 0.84 | 0.91 |
| Na ₂ O | 0.71 | 0.50 | 1.61 | 0.78 | 0.99 | 0.96 | 1.74 | 0.87 | 1.02 |
| K ₂ O | 0.13 | 0.14 | 0.34 | 0.26 | 0.39 | 0.24 | 0.42 | 0.32 | 0.28 |
| TiO ₂ | 0.02 | 0.02 | 0.04 | 0.03 | 0.05 | 0.04 | 0.03 | 0.06 | 0.04 |
| MnO | 0.01 | 0.01 | <0.01 | <0.01 | <0.01 | 0.01 | <0.01 | <0.01 | 0.01 |
| F | 0.73 | 0.60 | 0.89 | 0.74 | 0.95 | 1.20 | 0.88 | 0.94 | 0.87 |
| LOI | 29.07 | 32.30 | 24.85 | 27.87 | 21.87 | 19.31 | 25.70 | 25.07 | 25.75 |
| Total | 99.55 | 100.73 | 98.61 | 100.77 | 98.77 | 99.67 | 99.74 | 98.34 | 100.02 |
| Sc | 41 | 40 | 41 | 36 | 38 | 41 | 39 | 41 | 40 |
| V | 69 | 61 | 118 | 97 | 106 | 99 | 74 | 96 | 90 |
| Ni | 33 | 24 | 55 | 33 | 66 | 48 | 43 | 55 | 45 |
| Cu | 15 | 0 | 40 | 5 | 37 | 0 | 20 | 40 | 20 |
| Sr | 1864 | 1698 | 1760 | 1506 | 1896 | 1901 | 2013 | 2055 | 1837 |
| Y | 11 | 15 | 21 | 17 | 19 | 33 | 36 | 40 | 24 |
| Zr | 0 | 3 | 8 | 5 | 19 | 25 | 11 | 25 | 12 |
| Ba | 48 | 52 | 53 | 37 | 63 | 62 | 59 | 66 | 55 |

TABLE 7.5 Southeast Sicily phosphorites: major and trace element geochemistry (c.p. TABLE 7.3). Samples from hardground at Donnalucata (187.2, 187.5, 193.2 B) and whole clasts from phosphorite conglomerates at Donnalucata (187.3, 187.15), Modica (188 M), Marina di Ragusa (191 M), and Contrada le Serre (192.8 A).

| Sample Element | M1 | M2 | M3 | M12 | M11 | M13 | M8 | M9 | M10 | M4 | M5 | M6 | M7 | M14 | M15 | Mean |
|--------------------------------|--------|-------|--------|--------|--------|-------|--------|--------|--------|-------|--------|-------|--------|-------|--------|--------|
| P ₂ O ₅ | 16.23 | 14.13 | 10.51 | 12.55 | 14.60 | 15.48 | 15.78 | 16.76 | 13.03 | 14.48 | 13.29 | 17.75 | 18.46 | 20.46 | 21.68 | 15.67 |
| CaO | 54.77 | 53.16 | 53.90 | 52.35 | 54.36 | 52.29 | 55.90 | 56.25 | 55.67 | 51.30 | 51.13 | 54.38 | 55.29 | 53.94 | 54.71 | 53.96 |
| SiO ₂ | 2.57 | 2.79 | 4.37 | 4.19 | 3.40 | 2.83 | 2.62 | 2.23 | 2.59 | 4.07 | 4.17 | 3.27 | 3.32 | 3.17 | 3.11 | 3.25 |
| Fe ₂ O ₃ | 1.62 | 1.09 | 0.78 | 1.19 | 0.81 | 0.89 | 0.68 | 0.34 | 0.77 | 1.49 | 1.44 | 0.95 | 0.89 | 0.94 | 1.49 | 1.02 |
| Al ₂ O ₃ | 0.62 | 0.66 | 0.96 | 0.86 | 0.84 | 0.62 | 0.63 | 0.53 | 0.55 | 0.93 | 0.86 | 0.68 | 0.75 | 0.87 | 0.71 | 0.74 |
| MgO | 0.86 | 0.85 | 1.17 | 1.09 | 0.80 | 0.84 | 0.81 | 0.76 | 0.82 | 0.97 | 0.97 | 1.00 | 1.00 | 0.87 | 0.82 | 0.91 |
| Na ₂ O | 1.08 | 0.99 | 1.09 | 1.21 | 1.18 | 1.28 | 0.98 | 1.02 | 0.83 | 1.29 | 1.10 | 1.32 | 1.22 | 1.06 | 1.10 | 1.12 |
| K ₂ O | 0.19 | 0.23 | 0.25 | 0.38 | 0.25 | 0.29 | 0.16 | 0.12 | 0.20 | 0.36 | 0.38 | 0.26 | 0.20 | 0.24 | 0.26 | 0.25 |
| TiO ₂ | 0.06 | 0.06 | 0.09 | 0.05 | 0.06 | 0.04 | 0.06 | 0.06 | 0.05 | 0.05 | 0.05 | 0.05 | 0.06 | 0.05 | 0.05 | 0.06 |
| MnO | <0.01 | <0.01 | <0.01 | 0.02 | <0.01 | <0.01 | <0.01 | 0.01 | 0.01 | 0.02 | <0.01 | <0.01 | <0.01 | 0.01 | <0.01 | 0.01 |
| F | 0.96 | 0.87 | 0.67 | 0.57 | 0.83 | 0.94 | 0.94 | 0.98 | 0.81 | 0.91 | 0.83 | 1.01 | 1.10 | 1.10 | 1.34 | 0.92 |
| LOI | 21.19 | 24.14 | 26.88 | 26.51 | 23.33 | 23.58 | 22.41 | 21.46 | 26.01 | 23.15 | 25.80 | 18.60 | 17.93 | 16.45 | 14.96 | 22.16 |
| Total | 100.16 | 98.98 | 100.68 | 100.97 | 100.47 | 99.09 | 100.98 | 100.52 | 101.34 | 99.02 | 100.03 | 99.28 | 100.23 | 99.16 | 100.28 | 100.07 |
| Sc | 36 | 35 | 36 | 39 | 39 | 41 | 37 | 38 | 38 | 39 | 39 | 38 | 37 | 40 | 37 | 38 |
| V | 55 | 37 | 75 | 53 | 71 | 46 | 43 | 43 | 37 | 60 | 44 | 31 | 33 | 51 | 40 | 48 |
| Ni | 50 | 38 | 33 | 40 | 38 | 33 | 27 | 22 | 33 | 41 | 48 | 33 | 34 | 29 | 37 | 36 |
| Cu | 23 | 3 | 0 | 16 | 6 | 0 | 1 | 1 | 16 | 50 | 24 | 18 | 8 | 7 | 6 | 12 |
| Sr | 1419 | 1299 | 833 | 1035 | 1119 | 1207 | 1344 | 1323 | 1110 | 1220 | 1191 | 1419 | 1445 | 1553 | 1620 | 1276 |
| Y | 31 | 22 | 10 | 21 | 22 | 19 | 18 | 20 | 13 | 37 | 37 | 26 | 29 | 18 | 28 | 23 |
| Zr | 17 | 13 | 25 | 15 | 17 | 8 | 17 | 21 | 15 | 17 | 15 | 11 | 13 | 9 | 10 | 15 |
| Ba | 40 | 40 | 42 | 37 | 37 | 37 | 40 | 39 | 36 | 43 | 43 | 46 | 44 | 45 | 52 | 41 |

TABLE 7.6 Maltese phosphorites: major and trace element geochemistry (c.p. TABLE 7.3). Samples from terminal Lower Globigerina Limestone hardground (M3, M12), whole clasts of lower main (C1) Globigerina Limestone phosphorite conglomerate (M1, M2, M11, M13, M8, M9, M10) and upper main (C2) Globigerina Limestone phosphorite conglomerate (M4, M5, M6, M7, M14, M15), from north Gozo (cols. 1-3, 10-13), west Gozo (7-9), and northwest Malta (4-6, 14-15).

| Sample Element | M16 | M17 | M18 | Mean |
|--------------------------------|--------|--------|--------|--------|
| P ₂ O ₅ | 0.92 | 0.61 | 1.30 | 0.94 |
| CaO | 57.49 | 57.73 | 56.97 | 57.39 |
| SiO ₂ | 1.36 | 1.41 | 1.33 | 1.37 |
| Fe ₂ O ₃ | 1.11 | 0.81 | 0.55 | 0.82 |
| Al ₂ O ₃ | 0.27 | 0.28 | 0.28 | 0.28 |
| MgO | 0.80 | 0.84 | 1.03 | 0.89 |
| Na ₂ O | 0.32 | 0.15 | 0.20 | 0.22 |
| K ₂ O | 0.13 | 0.14 | 0.13 | 0.13 |
| TiO ₂ | 0.03 | 0.02 | 0.02 | 0.02 |
| MnO | <0.01 | <0.01 | <0.01 | <0.01 |
| F | 0.03 | 0.03 | 0.04 | 0.03 |
| LOI | 38.27 | 38.95 | 39.05 | 38.76 |
| Total | 100.74 | 100.98 | 100.91 | 100.86 |
| Sc | 38 | 40 | 45 | 41 |
| V | 25 | 25 | 27 | 26 |
| Ni | 33 | 27 | 25 | 28 |
| Cu | 1 | 2 | 1 | 1 |
| Sr | 348 | 329 | 350 | 342 |
| Y | 10 | 10 | 12 | 11 |
| Zr | 0 | 0 | 0 | 0 |
| Ba | 36 | 32 | 37 | 35 |

TABLE 7.7 Maltese phosphorites: major and trace element geochemistry (c.p. TABLE 7.3). Samples from terminal Lower Coralline Limestone hardground (M16) and whole clasts from its infilling conglomerate (M17, M18) from Qammieh, north-west Malta.

| Sample Element | JTA 3 | JTA 5A | JTB 5 | RTB 12 | RTB 18 | RTB 20 | RTC 2 | Mean |
|--------------------------------|-------|--------|--------|--------|--------|--------|--------|--------|
| P ₂ O ₅ | 0.06 | 0.54 | 0.13 | 0.32 | 0.09 | 0.15 | 0.12 | 0.20 |
| CaO | 56.37 | 58.06 | 56.55 | 58.17 | 58.05 | 57.75 | 57.28 | 57.46 |
| SiO ₂ | 0.66 | 1.21 | 0.91 | 0.39 | 0.56 | 0.56 | 0.92 | 0.74 |
| Fe ₂ O ₃ | 0.07 | 0.24 | 0.33 | 0.15 | 0.06 | 0.40 | 0.27 | 0.22 |
| Al ₂ O ₃ | 0.27 | 0.47 | 0.39 | 0.18 | 0.24 | 0.23 | 0.36 | 0.31 |
| MgO | 0.33 | 0.47 | 0.59 | 0.66 | 0.54 | 0.56 | 0.52 | 0.52 |
| Na ₂ O | 0.06 | 0.15 | 0.03 | 0.03 | 0.02 | 0.02 | 0.05 | 0.05 |
| K ₂ O | 0.06 | 0.15 | 0.07 | 0.05 | 0.08 | 0.07 | 0.08 | 0.08 |
| TiO ₂ | 0.02 | 0.02 | 0.03 | 0.02 | 0.02 | 0.02 | 0.02 | 0.02 |
| MnO | 0.01 | <0.01 | <0.01 | 0.01 | <0.01 | <0.01 | <0.01 | <0.01 |
| F | 0.04 | 0.03 | 0.01 | 0.01 | 0.01 | 0.02 | 0.01 | 0.02 |
| LOI | 41.82 | 40.05 | 40.95 | 40.51 | 39.98 | 41.03 | 40.93 | 40.75 |
| Total | 99.77 | 101.40 | 100.00 | 100.50 | 99.66 | 100.82 | 100.57 | 100.38 |
| Sc | 44 | 42 | 42 | 35 | 34 | 35 | 38 | 39 |
| V | 13 | 16 | 19 | 35 | 19 | 26 | 17 | 21 |
| Ni | 18 | 22 | 18 | 21 | 18 | 25 | 22 | 21 |
| Cu | 0 | 2 | 0 | 0 | 0 | 0 | 0 | 0 |
| Sr | 207 | 362 | 219 | 283 | 212 | 214 | 288 | 255 |
| Y | 6 | 7 | 6 | 4 | 5 | 5 | 6 | 6 |
| Zr | 0 | 0 | 0 | 0 | 0 | 0 | 0 | 0 |
| Ba | 30 | 38 | 7 | 30 | 29 | 6 | 37 | 25 |

TABLE 7.8 Southwest Sicily limestones: major and trace element geochemistry (c.p. TABLE 7.3). Samples of unmineralised Cretaceous chalk (JTA 3, JTA 5A) and Oligo-Miocene algal foraminiferal limestones (JTB 5 - RTC 2).

The abundances of Fe_2O_3 and Al_2O_3 are, in turn, plotted against Na_2O and K_2O in Figs 7.20 to 7.23 to demonstrate any possible dichotic relationships between the trivalent and univalent cations which all possibly replace the Ca^{2+} ion.

7.5.2 Variation in Abundance of P_2O_5 and SiO_2

Values for P_2O_5 are generally high ($> 10\%$) in all Tables except Tables 7.7 and 7.8. From Table 7.7 it can be seen that the limestone forming the terminal Lower Coralline Limestone hardground and its overlying conglomerate is not significantly phosphatic. The limestone does, however, contain slightly higher abundances of P_2O_5 (and Fe_2O_3 and Na_2O) than the pure limestones from southwest Sicily (Table 7.8), suggesting that some mineralisation has taken place. Furthermore, Bennett (1980) records a P_2O_5 content of 5.38% from the hardground elsewhere (Is sika) on Malta indicating that significant mineralisation does occur at this time and level. The very high (34%) P_2O_5 content of sample 36.1B (Table 7.4) reflects the fish tooth debris composition of this sample which is therefore probably pure carbonate apatite.

Values for SiO_2 are generally low ($< 4\%$, most commonly $< 3\%$) except in some samples from southeast Sicily and the Maltese islands. The higher values of SiO_2 in these samples correlate with the presence of small amounts of free quartz detected in the phosphatised limestones of these areas by thin section petrography and XRD. The very high SiO_2 value of 36.1A (Table 7.4) is due to the phosphatised silty limestone composition of this sample.

7.5.3 Variation of Major Elements relative to P_2O_5

Figures 7.3 to 7.10 are separate bivariate plots of element (oxide) against P_2O_5 . Except for MgO (Fig. 7.6) all the elements show an enrichment in the phosphorites relative to the limestones; and to some extent show positive correlations (with high variance) with P_2O_5 abundance. (MgO shows an enrichment in the Maltese and southeast Sicily phosphorites only). This enrichment, seen in all the phosphorites, suggests that the elements are introduced in the phosphatisation process and that they are held in the francolite lattice.

Key to symbols used in Figures 7.3 to 7.37

- Southwest Sicily phosphorite (Nadorello east locality only).
- ▼ Southwest Sicily phosphorite (various localities).
- Southeast Sicily phosphorites and hardground.
- Maltese islands phosphorites (from within the Globigerina Limestone Formation).
- Maltese islands phosphorites (at the terminal Lower Coralline Limestone hardground).
- ▲ Southwest Sicily Limestones (Upper Cretaceous and Upper Oligocene).

Figures 7.3 to 7.11 Variation of the major elements relative to P_2O_5 : bivariate plots of weight% P_2O_5 against weight% major element (oxide).

- Figure 7.3 P_2O_5 v SiO_2
Figure 7.4 P_2O_5 v Fe_2O_3
Figure 7.5 P_2O_5 v Al_2O_3
Figure 7.6 P_2O_5 v MgO
Figure 7.7 P_2O_5 v Na_2O
Figure 7.8 P_2O_5 v K_2O
Figure 7.9 P_2O_5 v TiO_2
Figure 7.10 P_2O_5 v F
Figure 7.11 P_2O_5 v 'X'

$\%P_2O_5$

196

30

20

10

Figure 7.3

1

2

3

4

$\%SiO_2$

$\%P_2O_5$

30

20

10

Figure 7.4

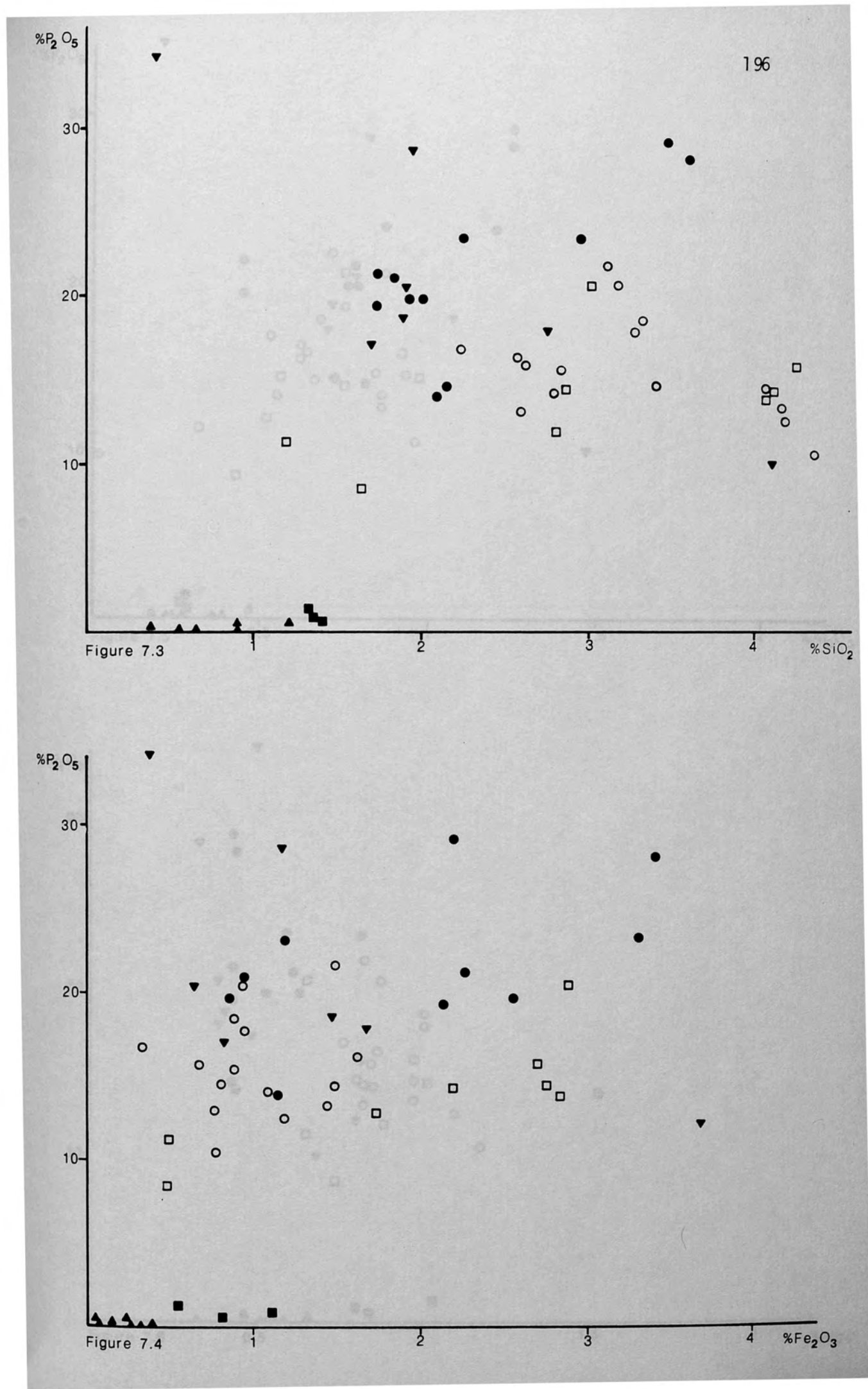
1

2

3

4

$\%Fe_2O_3$



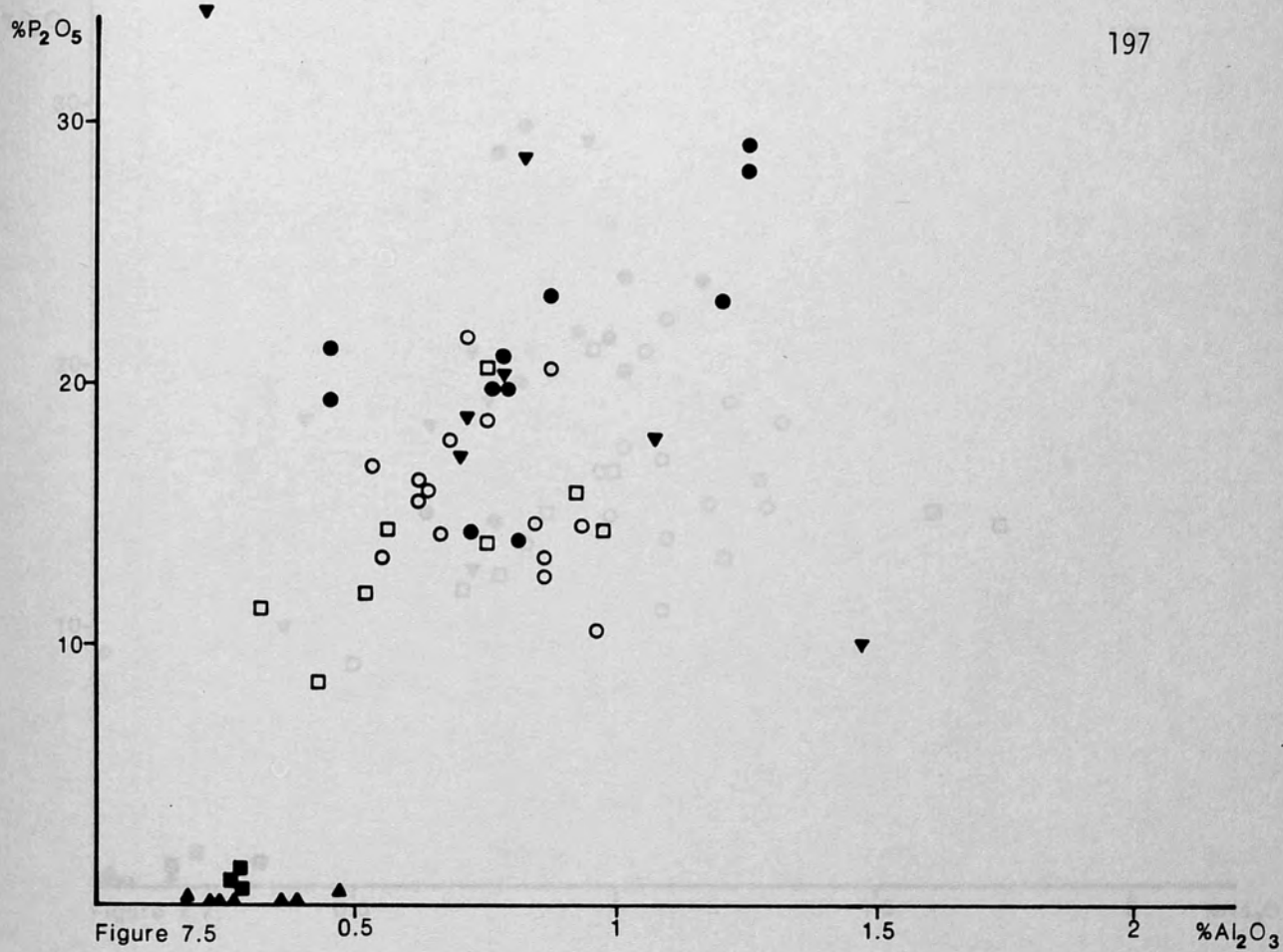


Figure 7.5

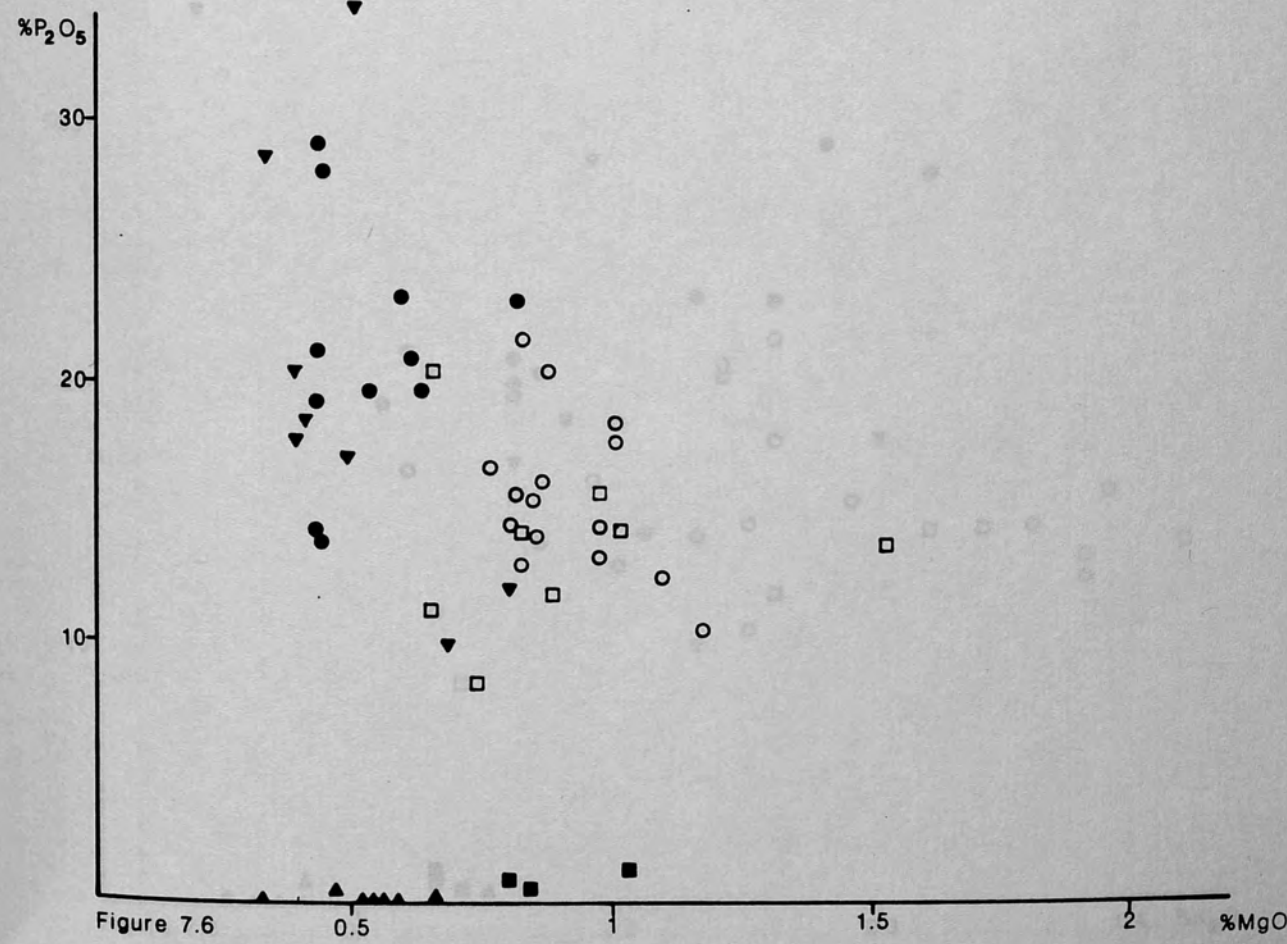
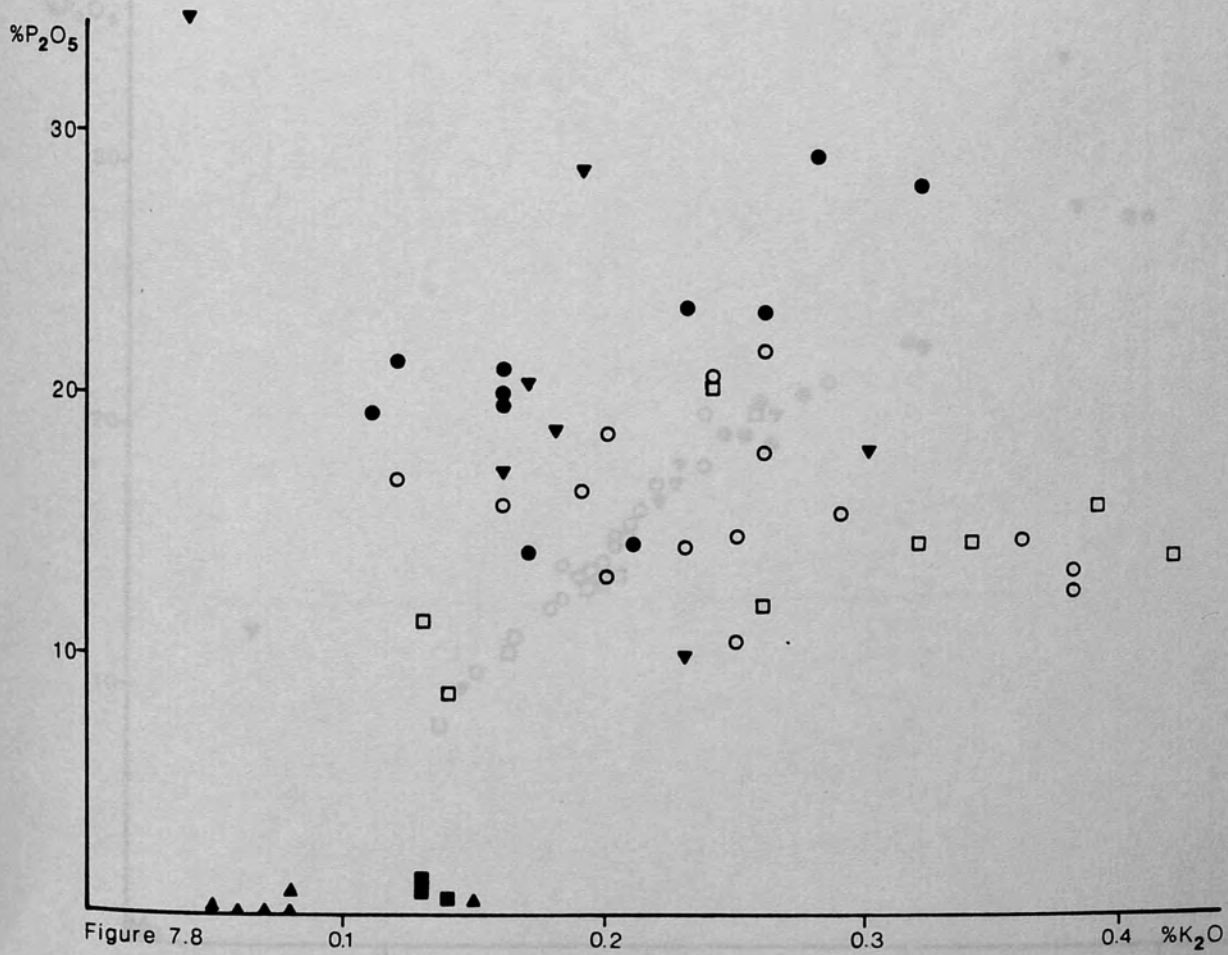
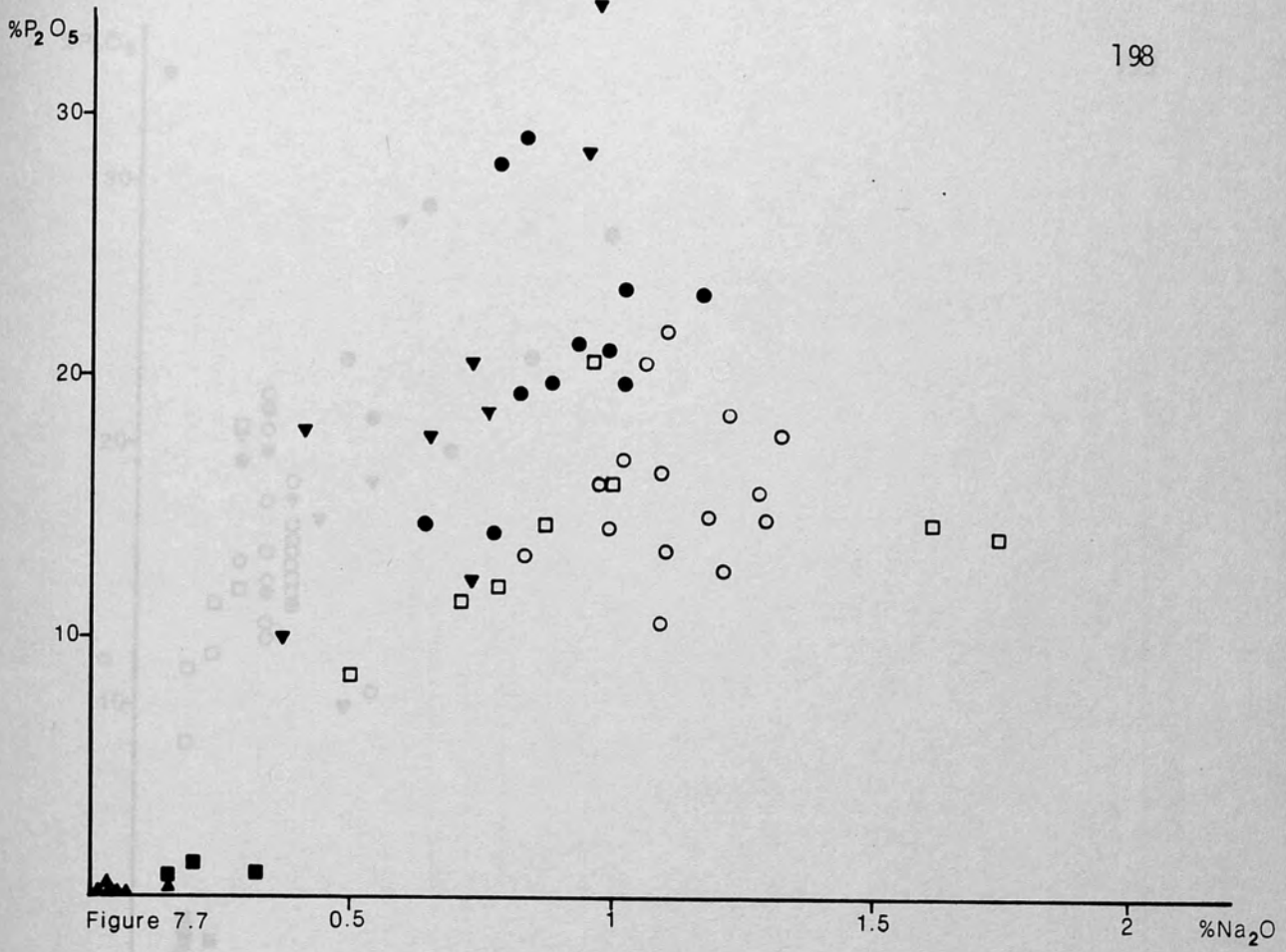


Figure 7.6



%P₂O₅

199

30

20

10

Figure 7.9

0.1

0.2

0.3

0.4 %TiO₂

%P₂O₅

30

20

10

Figure 7.10

0.5

1

1.5

2 %F

The form of these graphs is shown in Fig. 7.11, a hypothetical graph, which plots P_2O_5 against element (oxide) X. Pure francolite plots within ellipse A. The length of 'a' and its position along the (element) X axis is dependent on many factors including: the ability of francolite to incorporate X in its lattice; availability of X; availability of other elements substituting in the same sites as X; and weathering effect. Pure limestone plots within ellipse B. The length of 'b' is shorter since limestone does not incorporate as many substitutions, its length is mainly governed by impurities within the limestone. The vertical axes of the ellipses are short and their position along the P_2O_5 axis is governed by the amount of P_2O_5 found in francolites and limestones. Deposite specimens of limestone and francolite plot anywhere in the zone delimited by the two ellipses.

The positive correlations with P_2O_5 found in Figs 7.3 to 7.10 are therefore due to the progressive replacement of calcite by francolite. The high variance about the regression mixing axis (in Figs 7.3 to 7.9) is an effect of the factors controlling the lengths of 'a' and 'b', listed above. The low variance present in the X vs P_2O_5 regression (Fig. 7.10) may be an effect of the limited substitution at the X site in the francolite lattice. F^{2+} is thought to substitute for Ca^{2+} and CO_3^{2-} in the carbonate apatite lattice (see Gieseler, 1984).

7.5.4 Variation of Major Elements relative to CaO

Figures 7.12 to 7.19 are separate bivariate plots of element (oxide) against CaO. All oxides except P_2O_5 and TiO_2 show a negative correlation with CaO abundance. This effect is again probably due to progressive replacement of calcite by francolite. In all graphs phosphatised limestones plot towards the top left whilst increasingly more francolite plot progressively towards the bottom right. The high variance about the axes of regression/mixing reflects the substitution of the Ca²⁺ by all the elements.

The absence of a negative correlation with TiO_2 (Fig. 7.19) may be due to the very low abundances of this oxide, so that any relationship with CaO is masked by other elements substituting for the Ca²⁺ ion, or by the composite nature of the samples. The absence of any correlation

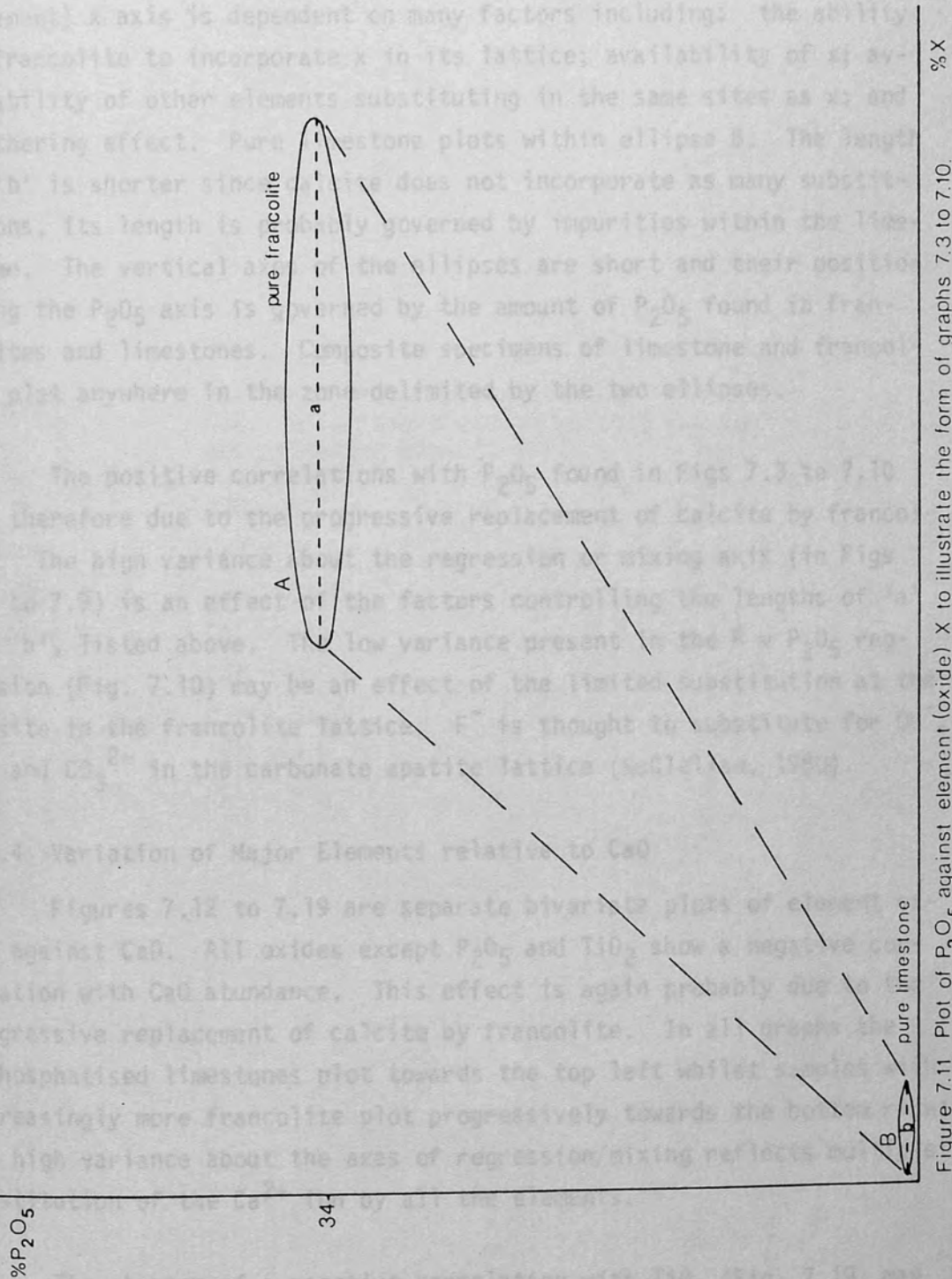


Figure 7.11 Plot of P_2O_5 against element (oxide) X to illustrate the form of graphs 7.3 to 7.10. See text for explanation.

The form of these graphs is shown in Fig. 7.11, a hypothetical graph, which plots P_2O_5 against element (oxide) x . Pure francolite plots within ellipse A. The length of 'a' and its position along the (element) x axis is dependent on many factors including: the ability of francolite to incorporate x in its lattice; availability of x ; availability of other elements substituting in the same sites as x ; and weathering effect. Pure limestone plots within ellipse B. The length of 'b' is shorter since calcite does not incorporate as many substitutions, its length is probably governed by impurities within the limestone. The vertical axes of the ellipses are short and their position along the P_2O_5 axis is governed by the amount of P_2O_5 found in francolites and limestones. Composite specimens of limestone and francolite plot anywhere in the zone delimited by the two ellipses.

The positive correlations with P_2O_5 found in Figs 7.3 to 7.10 are therefore due to the progressive replacement of calcite by francolite. The high variance about the regression or mixing axis (in Figs 7.3 to 7.9) is an effect of the factors controlling the lengths of 'a' and 'b', listed above. The low variance present in the F v P_2O_5 regression (Fig. 7.10) may be an effect of the limited substitution at the F^- site in the francolite lattice. F^- is thought to substitute for OH^- , Cl^- and CO_3^{2-} in the carbonate apatite lattice (McClellan, 1980).

7.5.4 Variation of Major Elements relative to CaO

Figures 7.12 to 7.19 are separate bivariate plots of element oxide against CaO. All oxides except P_2O_5 and TiO_2 show a negative correlation with CaO abundance. This effect is again probably due to the progressive replacement of calcite by francolite. In all graphs the unphosphatised limestones plot towards the top left whilst samples with increasingly more francolite plot progressively towards the bottom right. The high variance about the axes of regression/mixing reflects multiple substitution of the Ca^{2+} ion by all the elements.

The absence of a negative correlation with TiO_2 (Fig. 7.19) may be due to the very low abundances of this oxide, so that any relationship with CaO is masked by other elements substituting for the Ca^{2+} ion, or by the composite nature of the samples. The absence of any correlation

Figures 7.12 to 7.19 Variation of the major elements relative to CaO: bivariate plots of weight% CaO against weight% major element oxide.

- | | |
|-------------|-----------------|
| Figure 7.12 | CaO v P_2O_5 |
| Figure 7.13 | CaO v SiO_2 |
| Figure 7.14 | CaO v Fe_2O_3 |
| Figure 7.15 | CaO v Al_2O_3 |
| Figure 7.16 | CaO v MgO |
| Figure 7.17 | CaO v Na_2O |
| Figure 7.18 | CaO v K_2O |
| Figure 7.19 | CaO v TiO_2 |

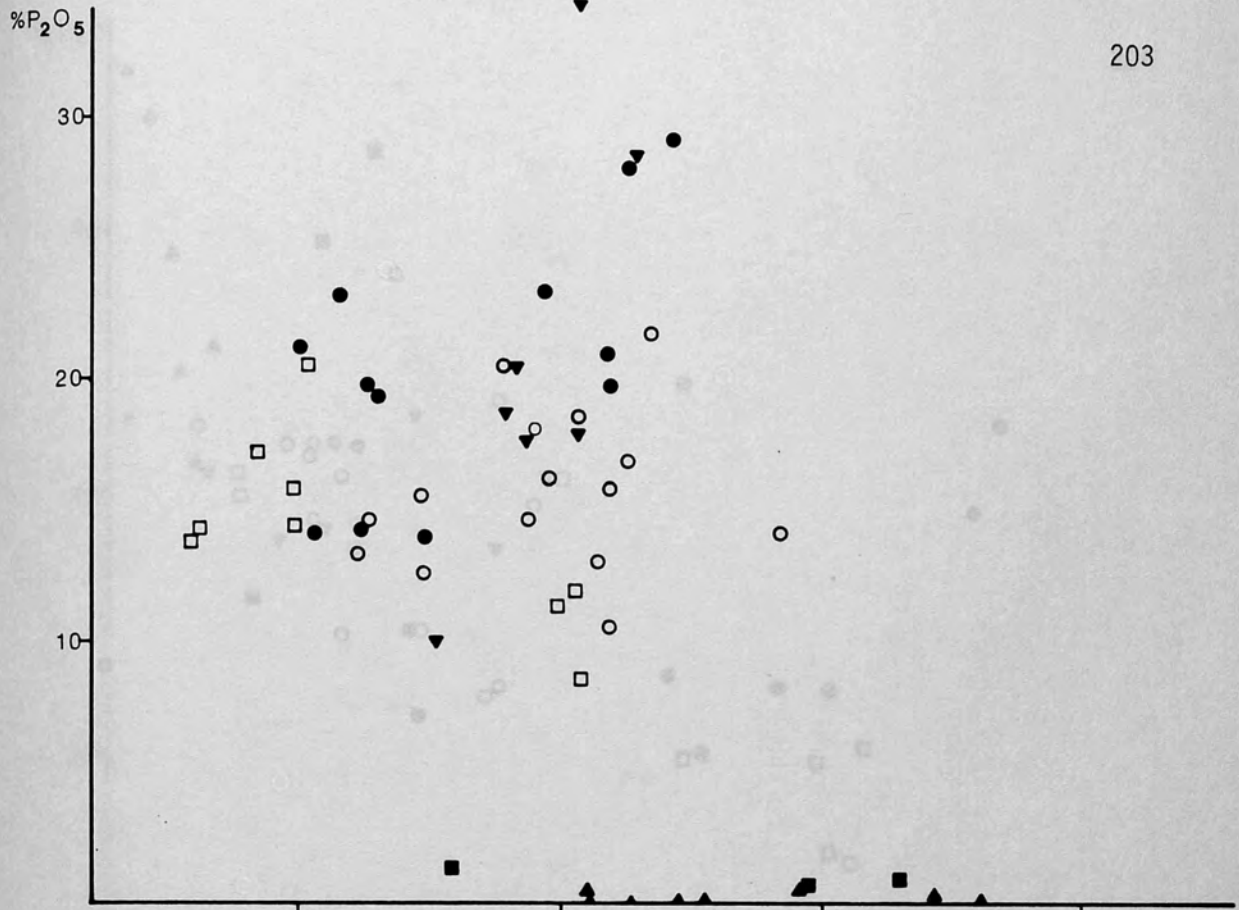


Figure 7.12

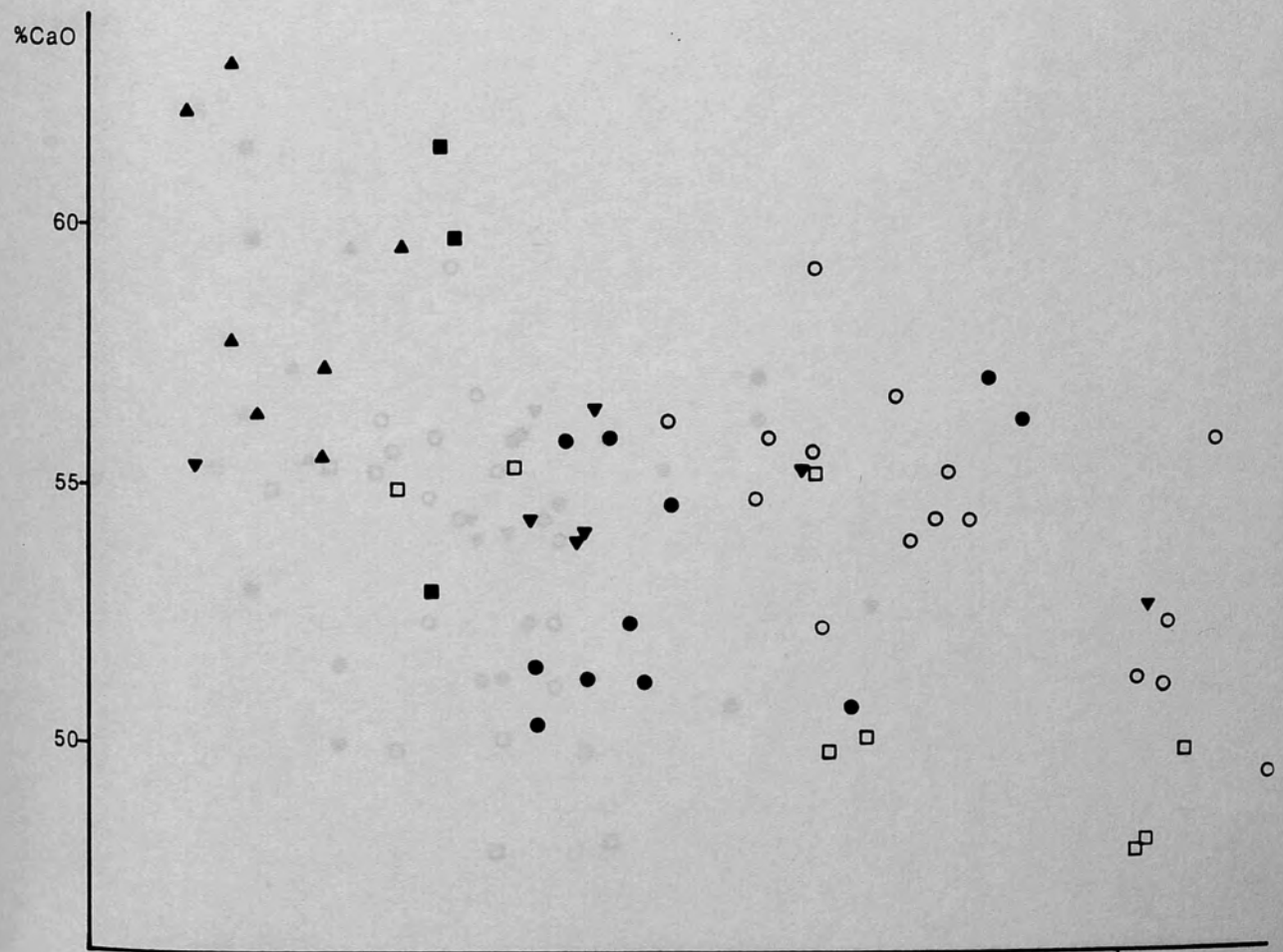


Figure 7.13

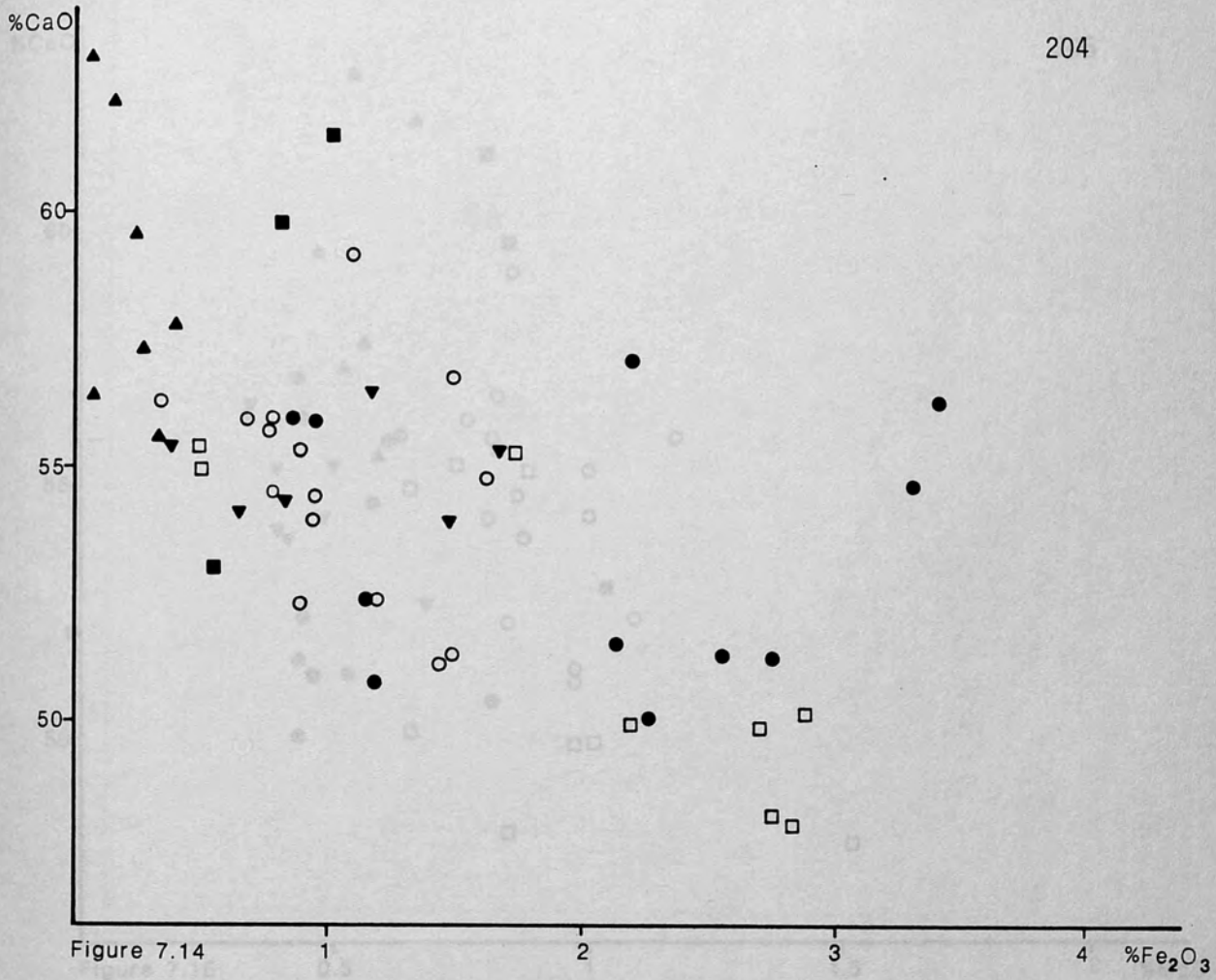


Figure 7.14

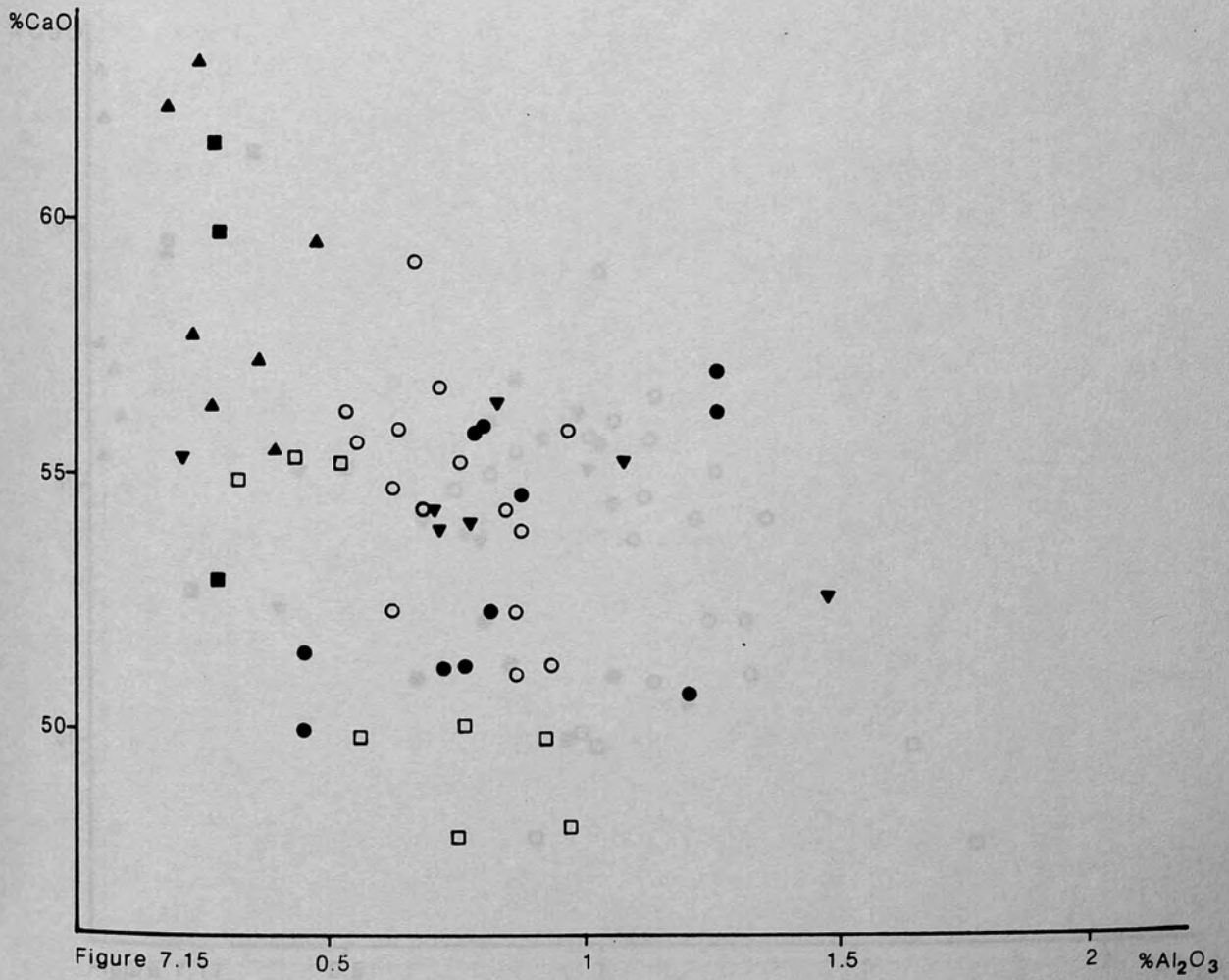


Figure 7.15

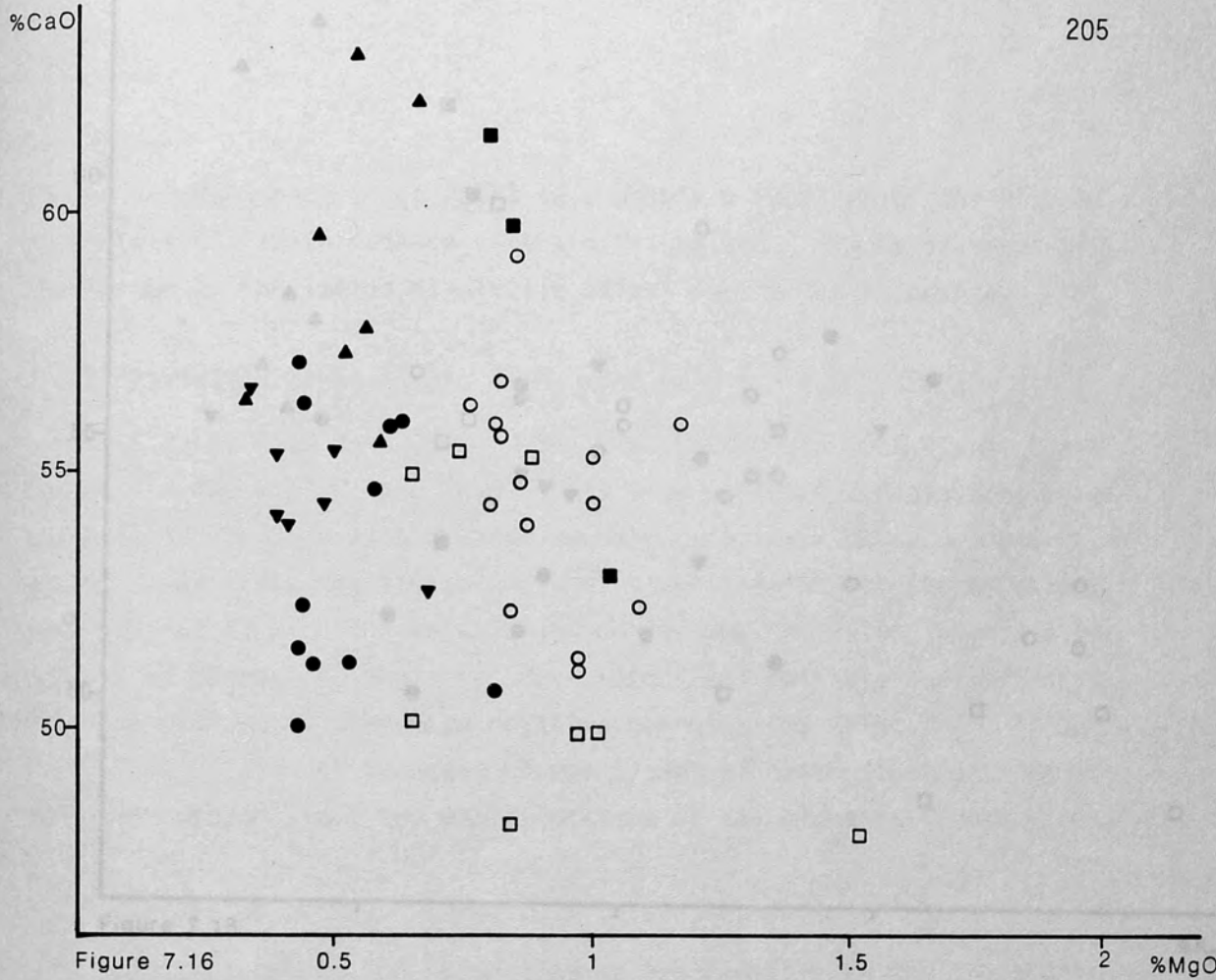


Figure 7.16

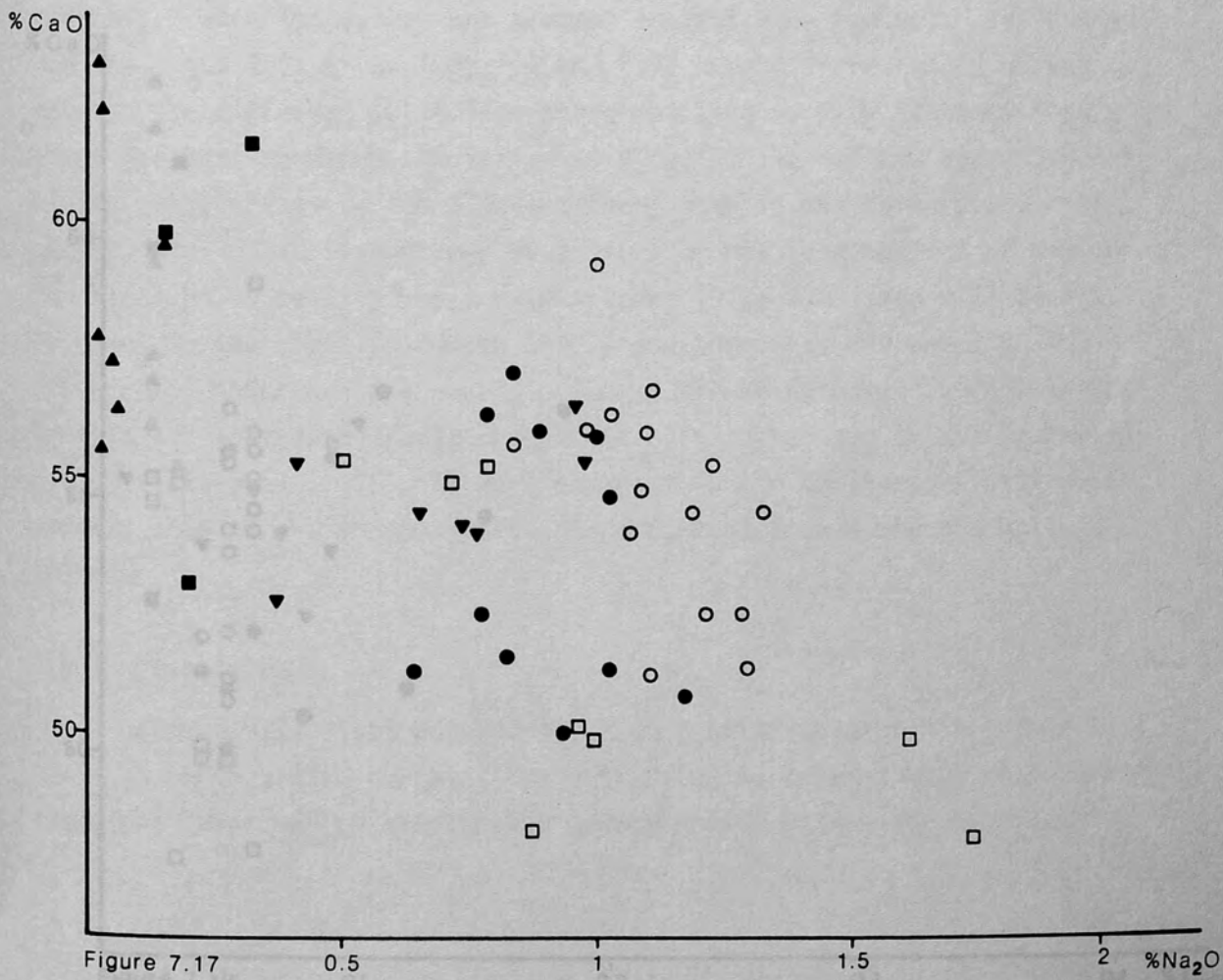


Figure 7.17

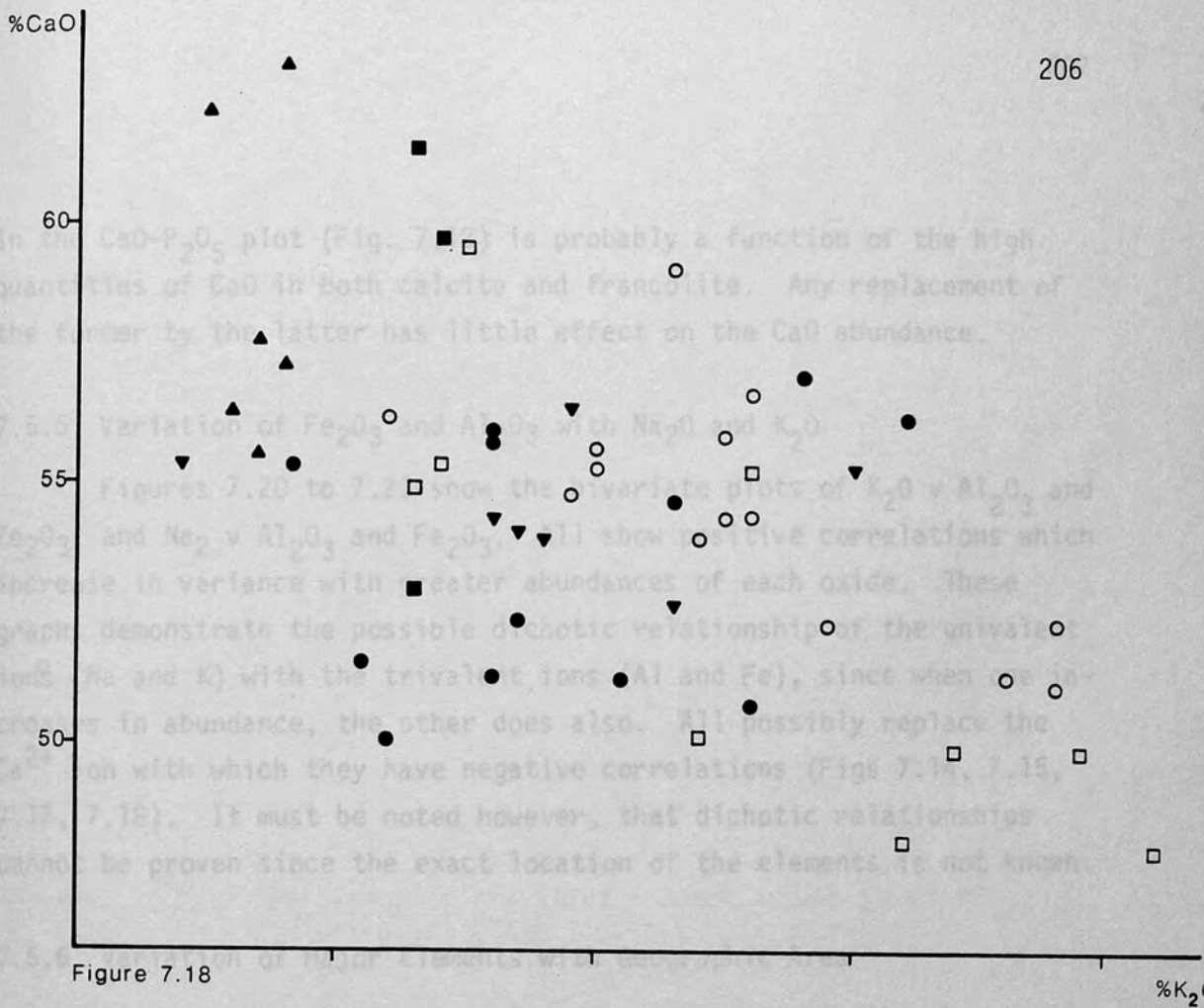


Figure 7.18

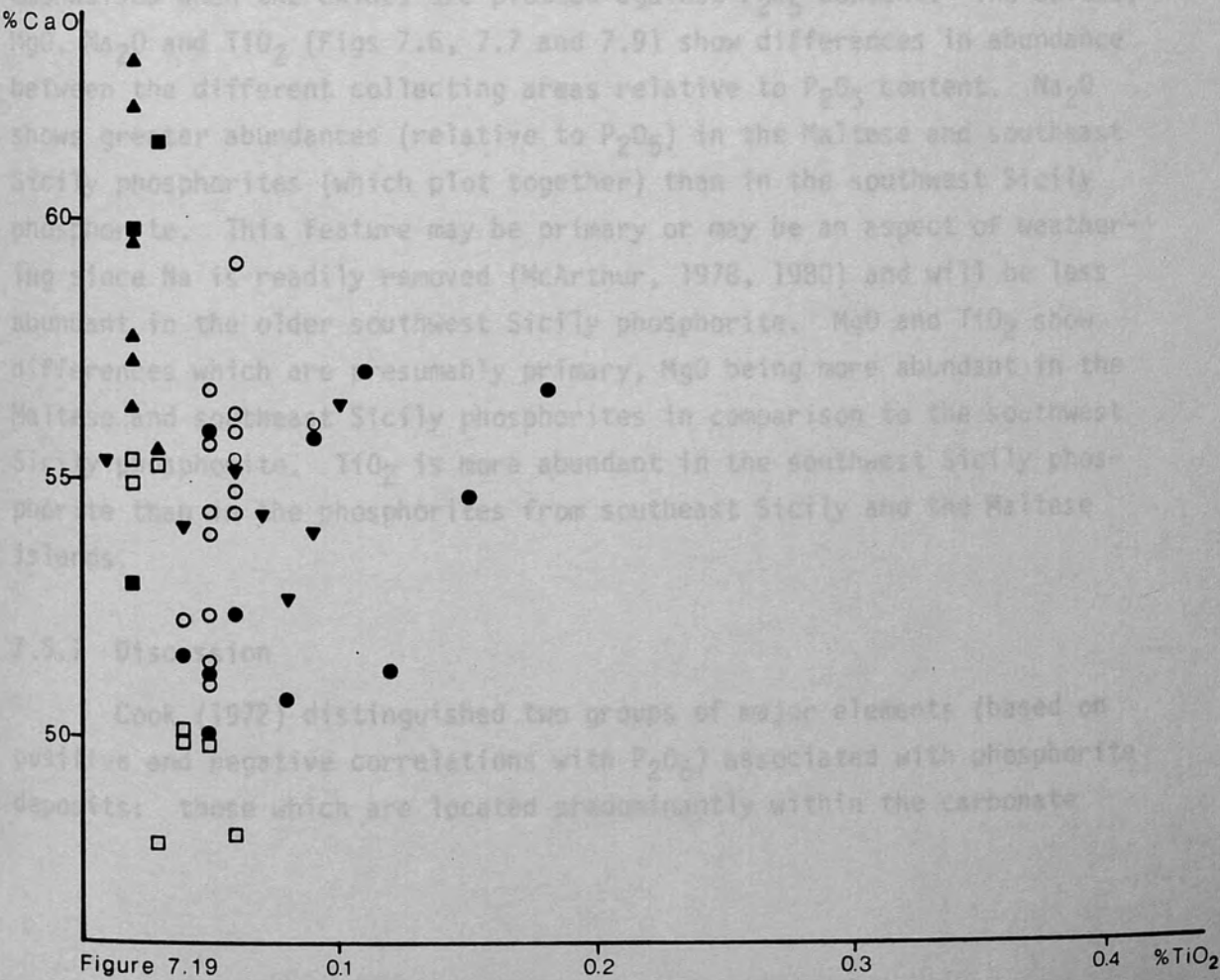


Figure 7.19

in the CaO-P₂O₅ plot (Fig. 7.12) is probably a function of the high quantities of CaO in both calcite and francolite. Any replacement of the former by the latter has little effect on the CaO abundance.

7.5.5 Variation of Fe₂O₃ and Al₂O₃ with Na₂O and K₂O

Figures 7.20 to 7.23 show the bivariate plots of K₂O v Al₂O₃ and Fe₂O₃; and Na₂ v Al₂O₃ and Fe₂O₃. All show positive correlations which increase in variance with greater abundances of each oxide. These graphs demonstrate the possible dichotic relationship of the univalent ions (Na and K) with the trivalent ions (Al and Fe), since when one increases in abundance, the other does also. All possibly replace the Ca²⁺ ion with which they have negative correlations (Figs 7.14, 7.15, 7.17, 7.18). It must be noted however, that dichotic relationships cannot be proven since the exact location of the elements is not known.

7.5.6 Variation of Major Elements with Geographic Area

Differences in the major element geochemistry in the phosphorites from southwest Sicily, southeast Sicily and the Maltese islands are best emphasised when the oxides are plotted against P₂O₅ content. The oxides, MgO, Na₂O and TiO₂ (Figs 7.6, 7.7 and 7.9) show differences in abundance between the different collecting areas relative to P₂O₅ content. Na₂O shows greater abundances (relative to P₂O₅) in the Maltese and southeast Sicily phosphorites (which plot together) than in the southwest Sicily phosphorite. This feature may be primary or may be an aspect of weathering since Na is readily removed (McArthur, 1978, 1980) and will be less abundant in the older southwest Sicily phosphorite. MgO and TiO₂ show differences which are presumably primary, MgO being more abundant in the Maltese and southeast Sicily phosphorites in comparison to the southwest Sicily phosphorite. TiO₂ is more abundant in the southwest Sicily phosphorite than in the phosphorites from southeast Sicily and the Maltese islands.

7.5.7 Discussion

Cook (1972) distinguished two groups of major elements (based on positive and negative correlations with P₂O₅) associated with phosphorite deposits: those which are located predominantly within the carbonate

Figures 7.20 to 7.23 Variation of trivalent element oxides relative to univalent element oxides (all expressed in weight%).

- Figure 7.20 Al_2O_3 v K_2O
 Figure 7.21 Fe_2O_3 v K_2O
 Figure 7.22 Al_2O_3 v Na_2O
 Figure 7.23 Fe_2O_3 v Na_2O

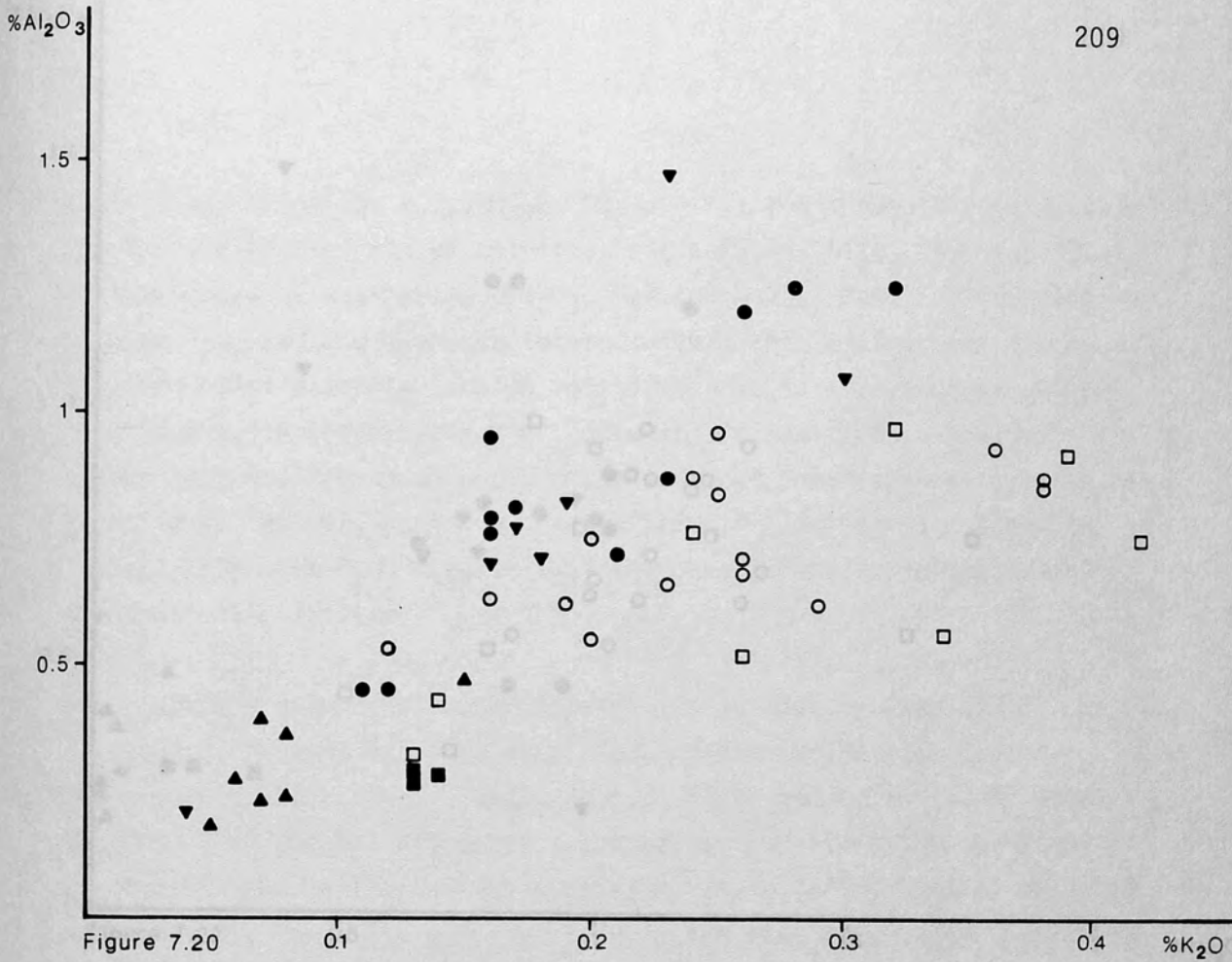


Figure 7.20

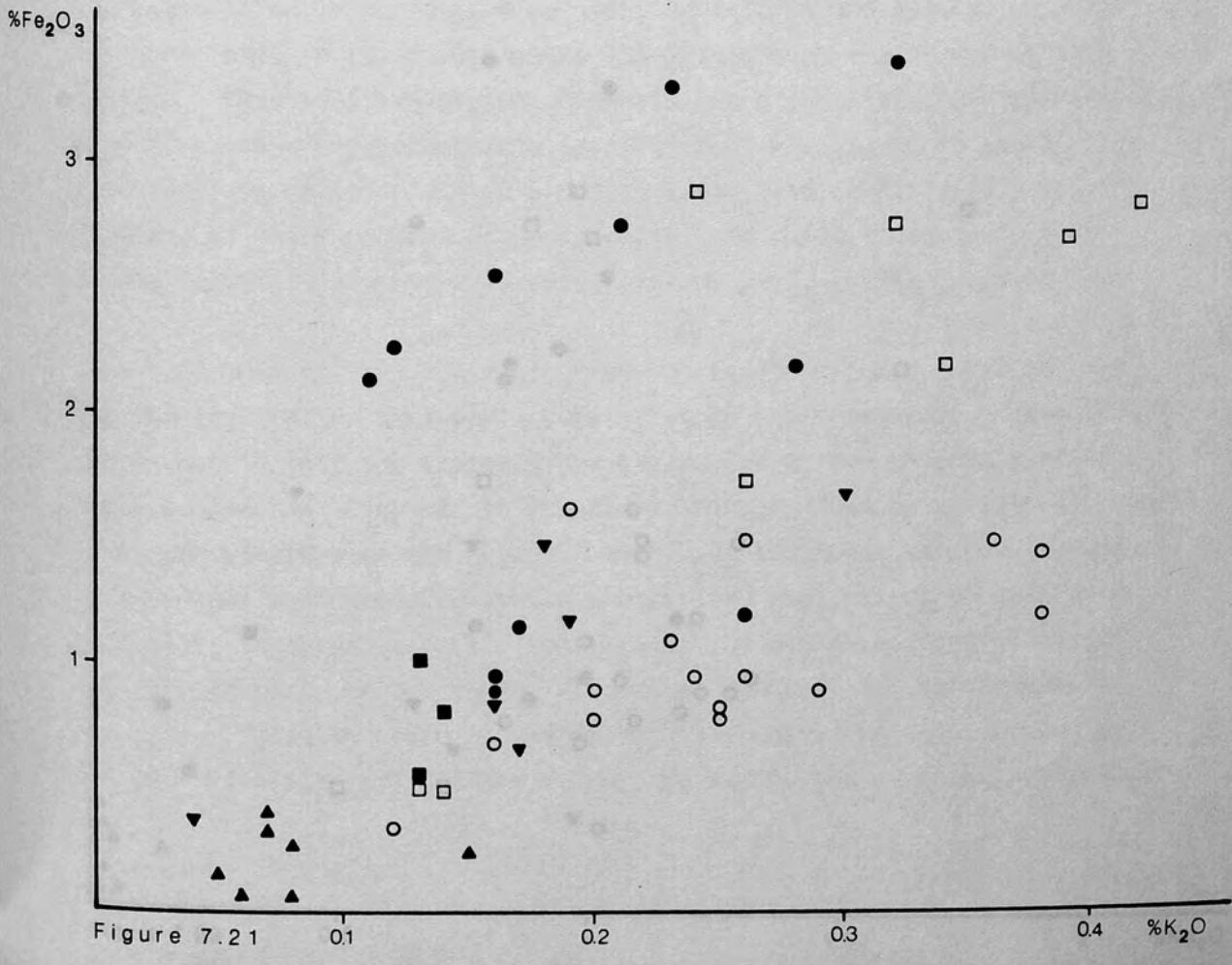


Figure 7.21

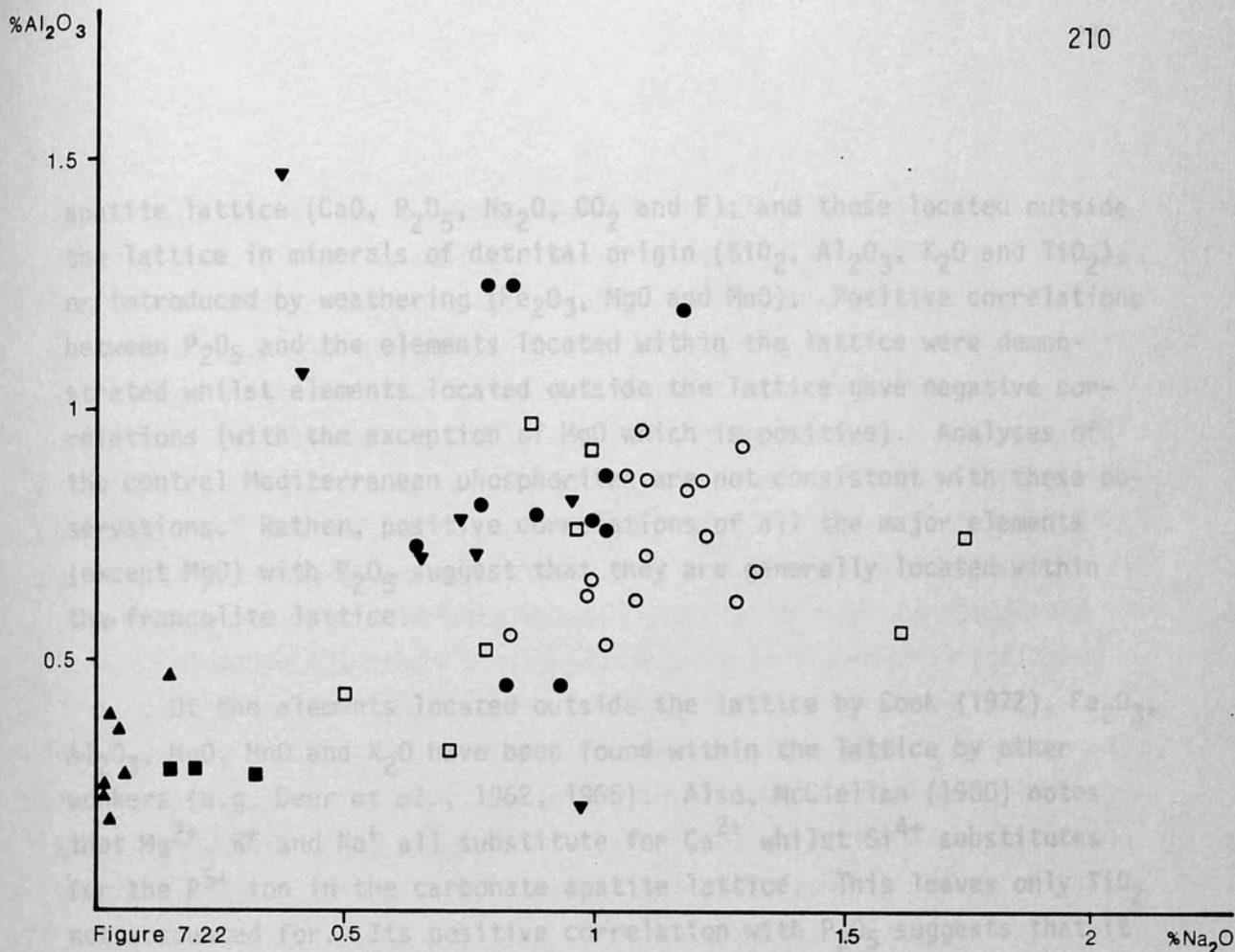


Figure 7.22

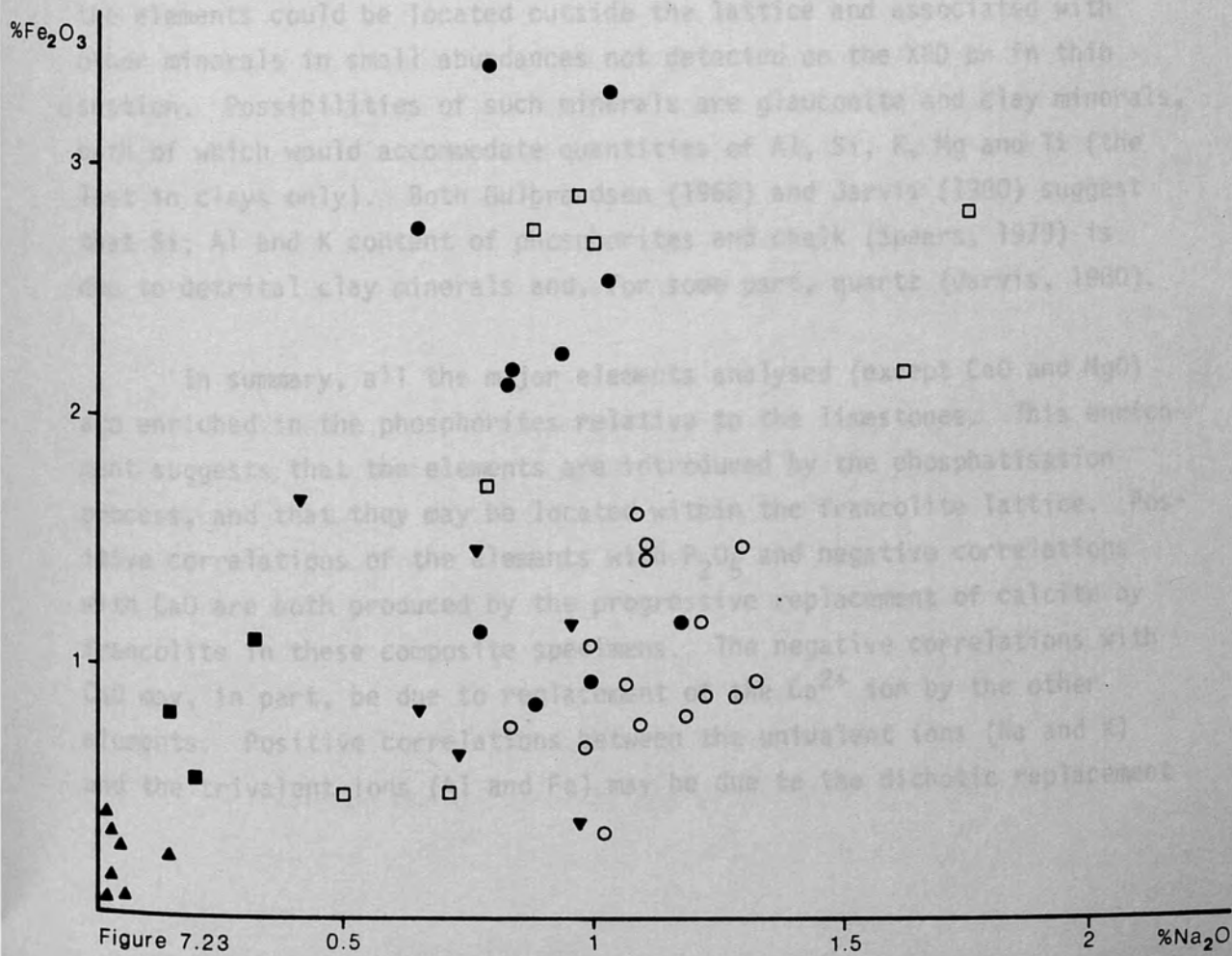


Figure 7.23

apatite lattice (CaO , P_2O_5 , Na_2O , CO_2 and F); and those located outside the lattice in minerals of detrital origin (SiO_2 , Al_2O_3 , K_2O and TiO_2), or introduced by weathering (Fe_2O_3 , MgO and MnO). Positive correlations between P_2O_5 and the elements located within the lattice were demonstrated whilst elements located outside the lattice gave negative correlations (with the exception of MgO which is positive). Analyses of the central Mediterranean phosphorites are not consistent with these observations. Rather, positive correlations of all the major elements (except MgO) with P_2O_5 suggest that they are generally located within the francolite lattice.

Of the elements located outside the lattice by Cook (1972), Fe_2O_3 , Al_2O_3 , MgO , MnO and K_2O have been found within the lattice by other workers (e.g. Deer *et al.*, 1962, 1966). Also, McClellan (1980) notes that Mg^{2+} , K^+ and Na^+ all substitute for Ca^{2+} whilst Si^{4+} substitutes for the P^{5+} ion in the carbonate apatite lattice. This leaves only TiO_2 not accounted for. Its positive correlation with P_2O_5 suggests that it is located within the carbonate apatite lattice. However, the high variance shown by TiO_2 and other plots might suggest that a proportion of the elements could be located outside the lattice and associated with other minerals in small abundances not detected on the XRD or in thin section. Possibilities of such minerals are glauconite and clay minerals, both of which would accommodate quantities of Al, Si, K, Mg and Ti (the last in clays only). Both Gulbrandsen (1966) and Jarvis (1980) suggest that Si, Al and K content of phosphorites and chalk (Spears, 1979) is due to detrital clay minerals and, for some part, quartz (Jarvis, 1980).

In summary, all the major elements analysed (except CaO and MgO) are enriched in the phosphorites relative to the limestones. This enrichment suggests that the elements are introduced by the phosphatisation process, and that they may be located within the francolite lattice. Positive correlations of the elements with P_2O_5 and negative correlations with CaO are both produced by the progressive replacement of calcite by francolite in these composite specimens. The negative correlations with CaO may, in part, be due to replacement of the Ca^{2+} ion by the other elements. Positive correlations between the univalent ions (Na and K) and the trivalent ions (Al and Fe) may be due to the dichotic replacement

of the Ca^{2+} ion by these ions. High variance in all except the F v P_2O_5 plot is probably due to multiple substitutions in the francolite lattice, and in part due to the presence of other mineral phases such as quartz, glauconite and clay minerals. Quartz only is present in sufficient quantities to be detected by XRD and light microscope petrography. F content of the francolite can be estimated from the P_2O_5 v F graph (and from XRD graphs). Assuming a P_2O_5 content of 34% for a pure francolite sample, the F content, which is the same for all samples from all localities, is estimated as approximately 2.3%. Finally, differences in the major element geochemistry between geographic areas do occur, and suggest that the southwest Sicily phosphorite is essentially different from those found in southeast Sicily and the Maltese islands. This is indicated by MgO , Na_2O and TiO_2 abundances relative to P_2O_5 (though the Na_2O abundances may be affected by different amounts of removal by weathering) and by the presence of free quartz (raising the SiO_2 values) in the southeast Sicily and Maltese phosphorites only.

7.6 Trace Element Geochemistry

7.6.1 Introduction

Analyses were made for the seven trace elements Sc, V, Ni, Cu, Sr, Zr and Ba at the same time as for major elements using the ICP technique (see Appendix I). The same samples were used for both major and trace element analyses, without further preparation for the latter. Values were obtained for additional trace elements (Li, Cr, Co, Zn, Ga, Nb and Pb), but these have been disregarded for the reasons set out in Appendix I.

The absolute trace element abundances are given in Tables 7.3 to 7.8 and plotted against percentage of P_2O_5 and CaO in Figs 7.24 to 7.37. Distinction is made by symbol between samples collected from the three different areas (southwest Sicily, southeast Sicily, Maltese islands) so as to reveal differences or similarities in their trace element composition.

7.6.2 Variation in Trace Element Absolute Abundances

Comparison of the phosphorite analyses (Tables 7.3 to 7.6) with

the analyses of the terminal Lower Coralline Limestone hardground and overlying conglomerate (Table 7.7) shows that the latter is appreciably depleted in all the trace elements except Sc. Indeed, Sc is essentially invariable throughout the analyses and need not be considered further. Comparison of Table 7.7 with the pure limestone analyses (Table 7.8) shows that the hardground and its overlying conglomerate are slightly enriched in all the trace elements suggesting a minor amount of mineralisation at this level, and agreeing with the major element analyses (Section 7.5).

Comparison of the phosphorite analyses (Tables 7.3 to 7.6) with the pure limestone analyses (Table 7.8) shows that the former are enriched in all the trace elements.

7.6.3 Variation of Trace Elements with P_2O_5

Figures 7.24 to 7.30 are bivariate plots of trace element abundance relative to P_2O_5 . There is a general enrichment in the trace elements in the phosphorite samples relative to the non-phosphatised limestones. Ni, Sr and Zr (Figs 7.26, 7.28, 7.29) show positive correlation despite high variance. For V, Cu and Ba (Figs 7.25, 7.27, 7.30) the variance is high and relationships are not so apparent.

7.6.4 Variation of Trace Elements with CaO

Figures 7.31 to 7.37 are separate bivariate plots of trace element abundance relative to CaO. All elements show a negative correlation with CaO abundance. V and Sr (Figs 7.32 and 7.35) appear to show the strongest negative correlation although with high variance. Ni, Cu, Zr and Ba (Figs 7.33, 7.34, 7.36 and 7.37) have too high a variance for negative correlation with CaO to be immediately apparent. Generally, however, samples with low concentrations of CaO (the phosphorites) show high values for trace element abundance (and vice versa for limestones).

7.6.5 Variation of Trace Elements with Geographical Areas

In Figures 7.24 to 7.37 samples from southwest Sicily, southeast Sicily and the Maltese islands are distinguished by symbol. Graphs which plot trace element abundance against that for CaO show wide overlap of

Figures 7.24 to 7.30 Variation of trace elements relative to P_2O_5 : bivariate plots of weight% P_2O_5 against ppm trace element.

- Figure 7.24 P_2O_5 v Sc
 Figure 7.25 P_2O_5 v V
 Figure 7.26 P_2O_5 v Ni
 Figure 7.27 P_2O_5 v Cu
 Figure 7.28 P_2O_5 v Sr
 Figure 7.29 P_2O_5 v Zr
 Figure 7.30 P_2O_5 v Ba

100 150 200 ppm Sc

Figure 7.25 30 100 150 200 ppm V

%P₂O₅

30

20

10

Figure 7.24

50

100

150

200 ppm Sc

%P₂O₅

30

20

10

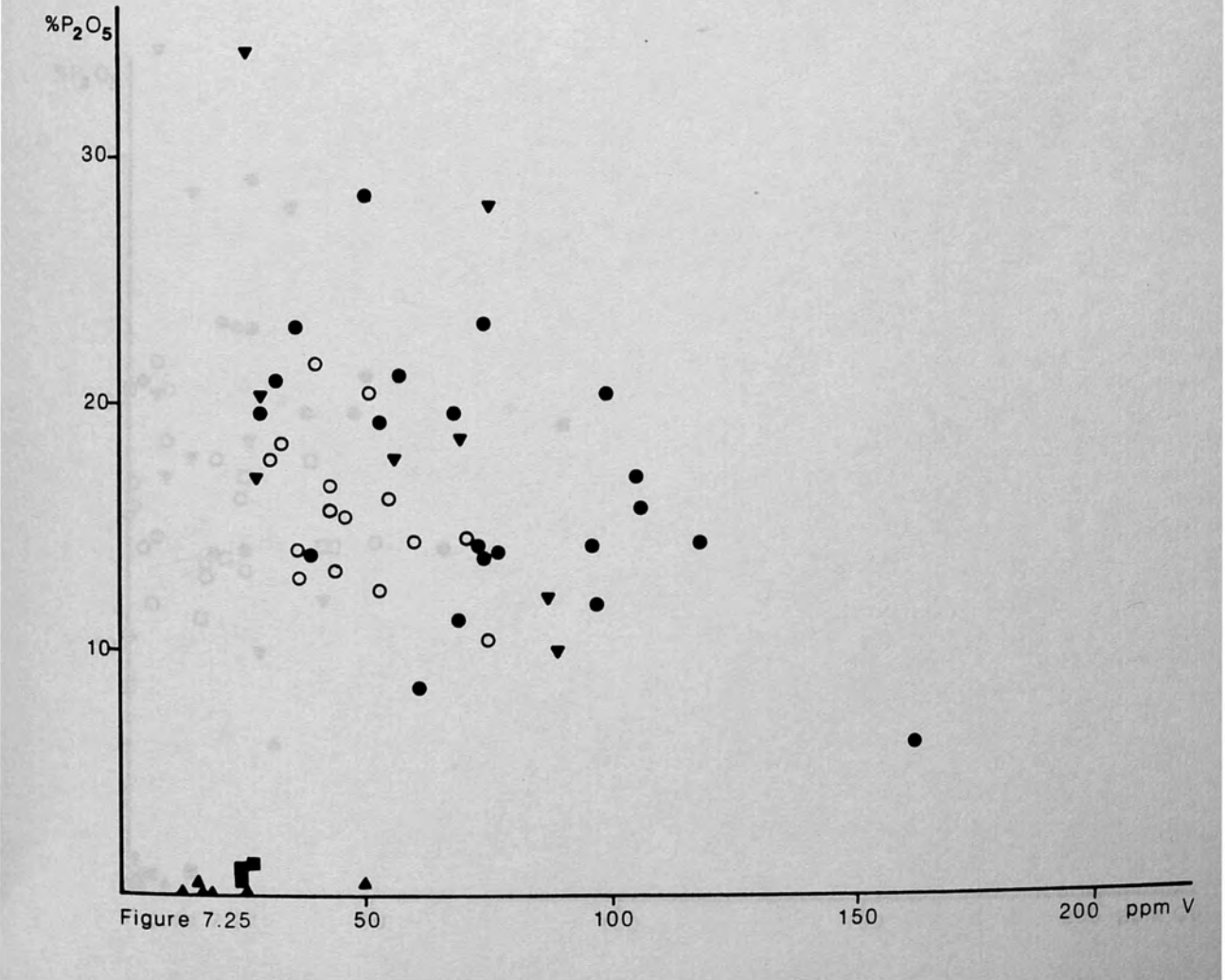
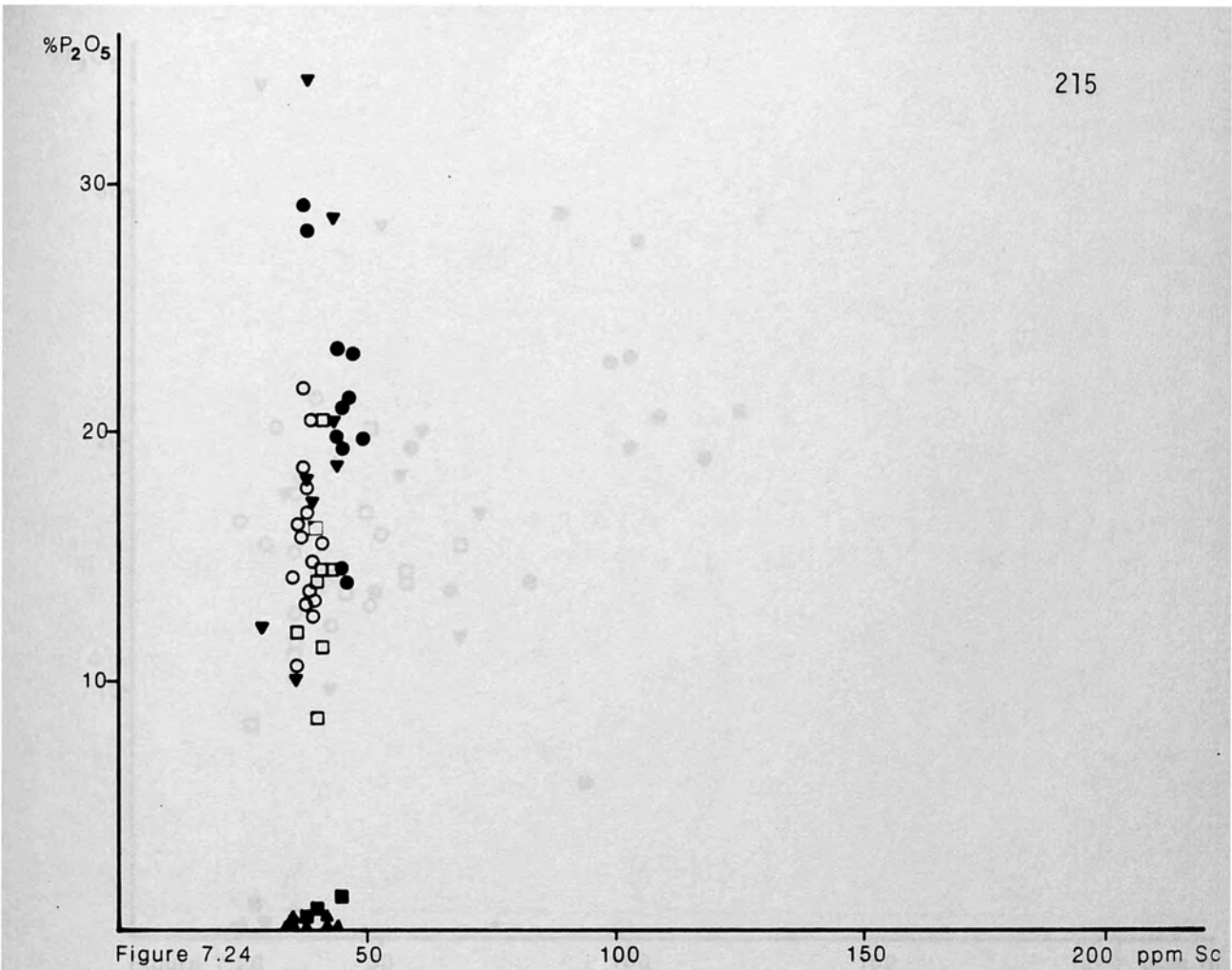
Figure 7.25

50

100

150

200 ppm V



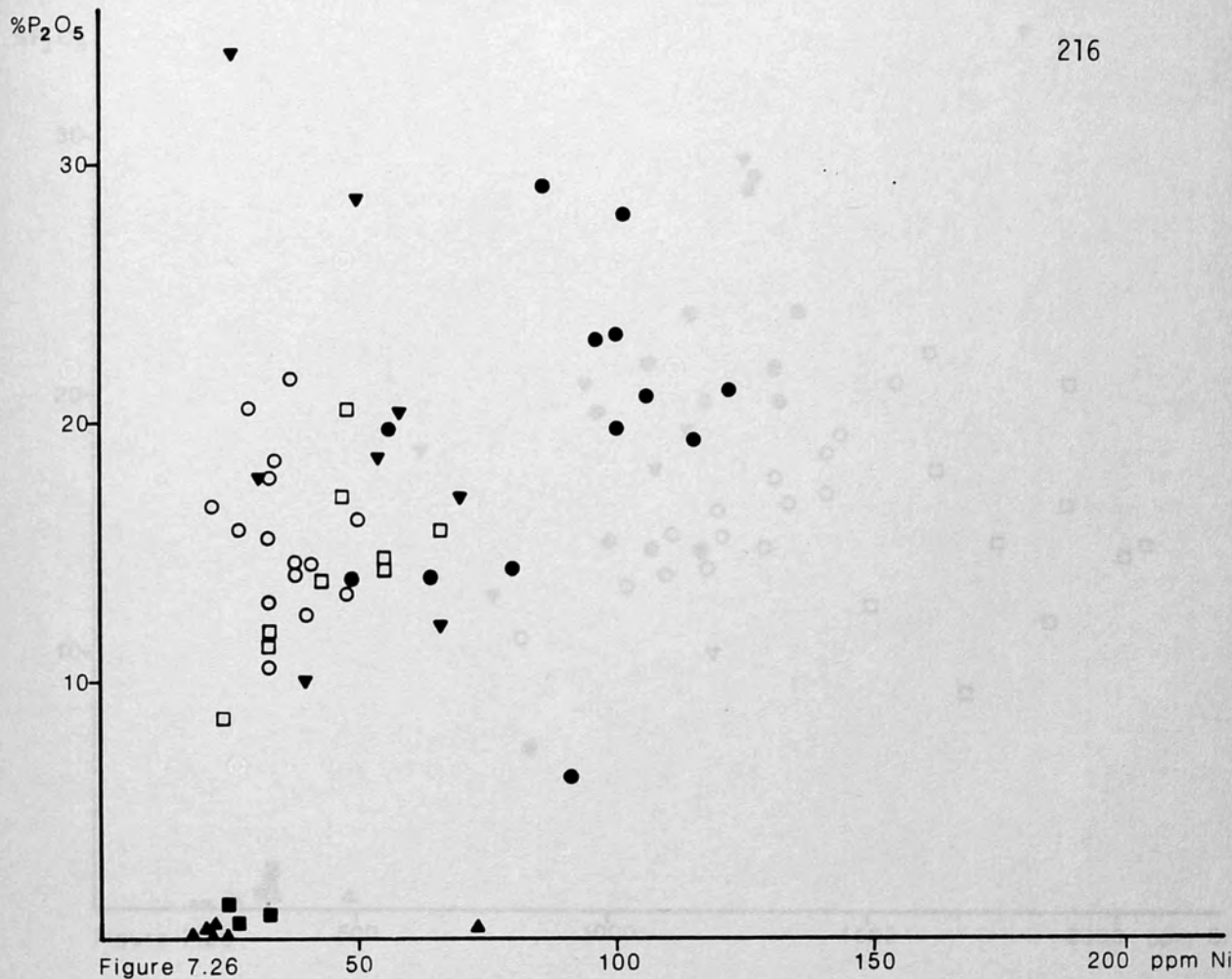


Figure 7.26

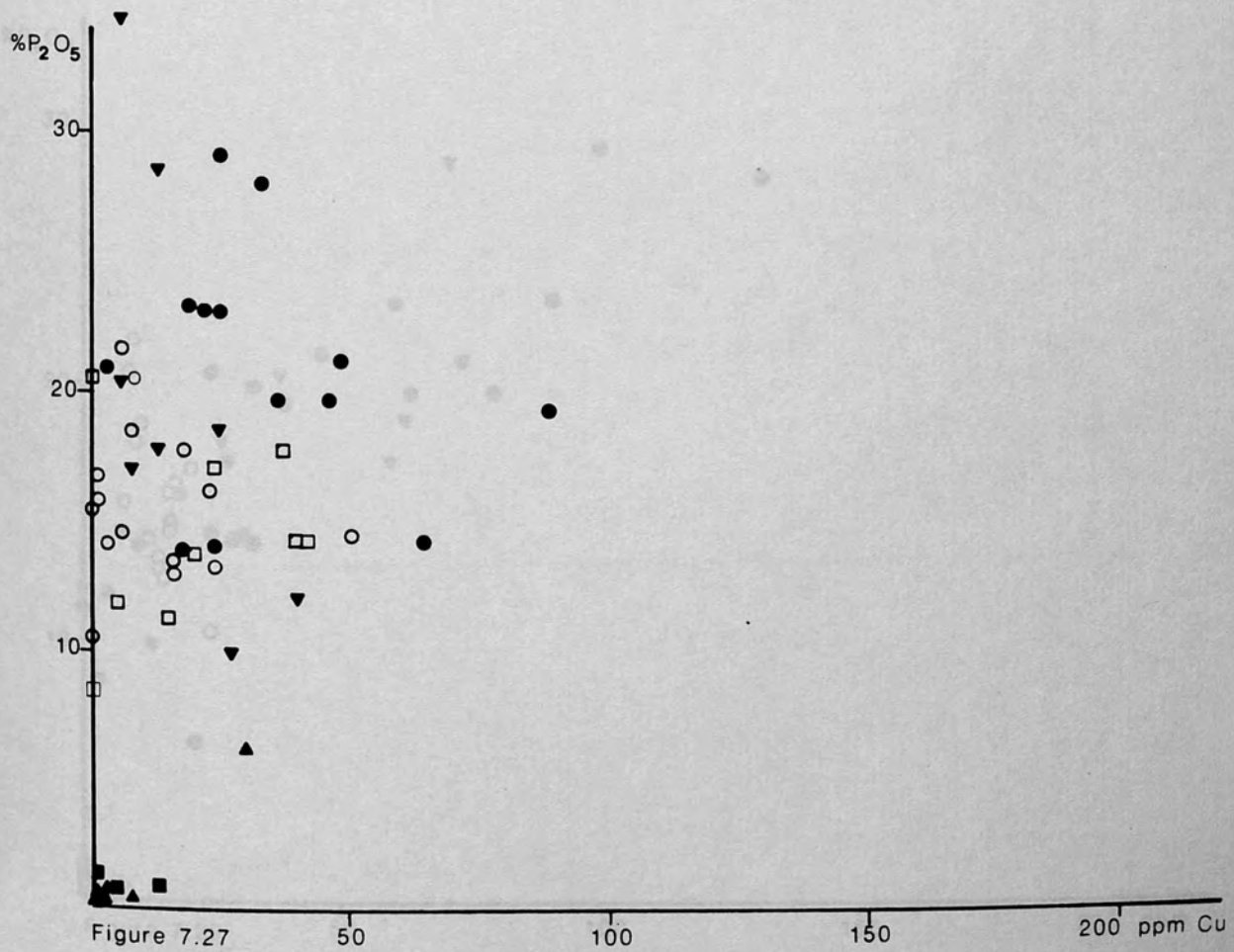
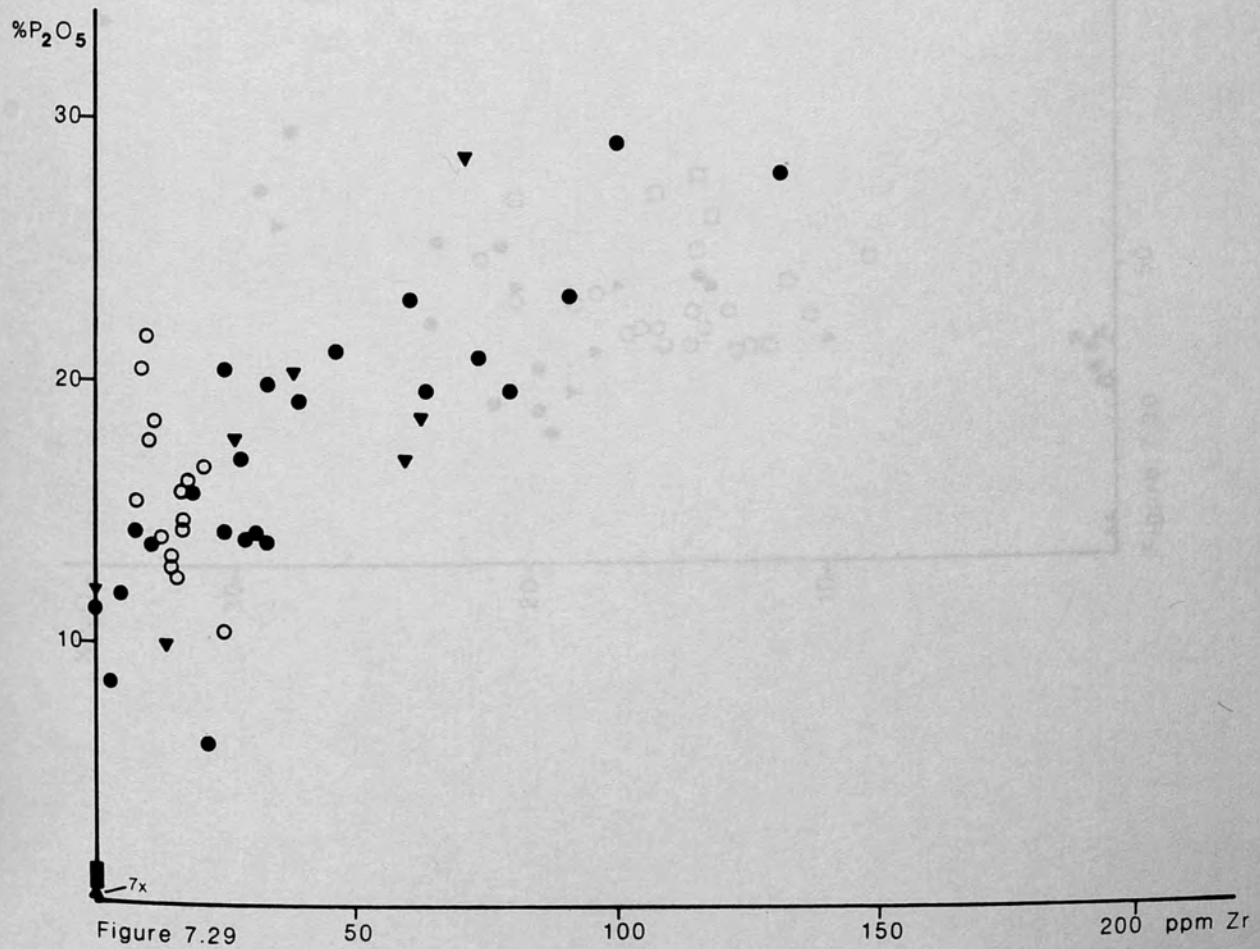
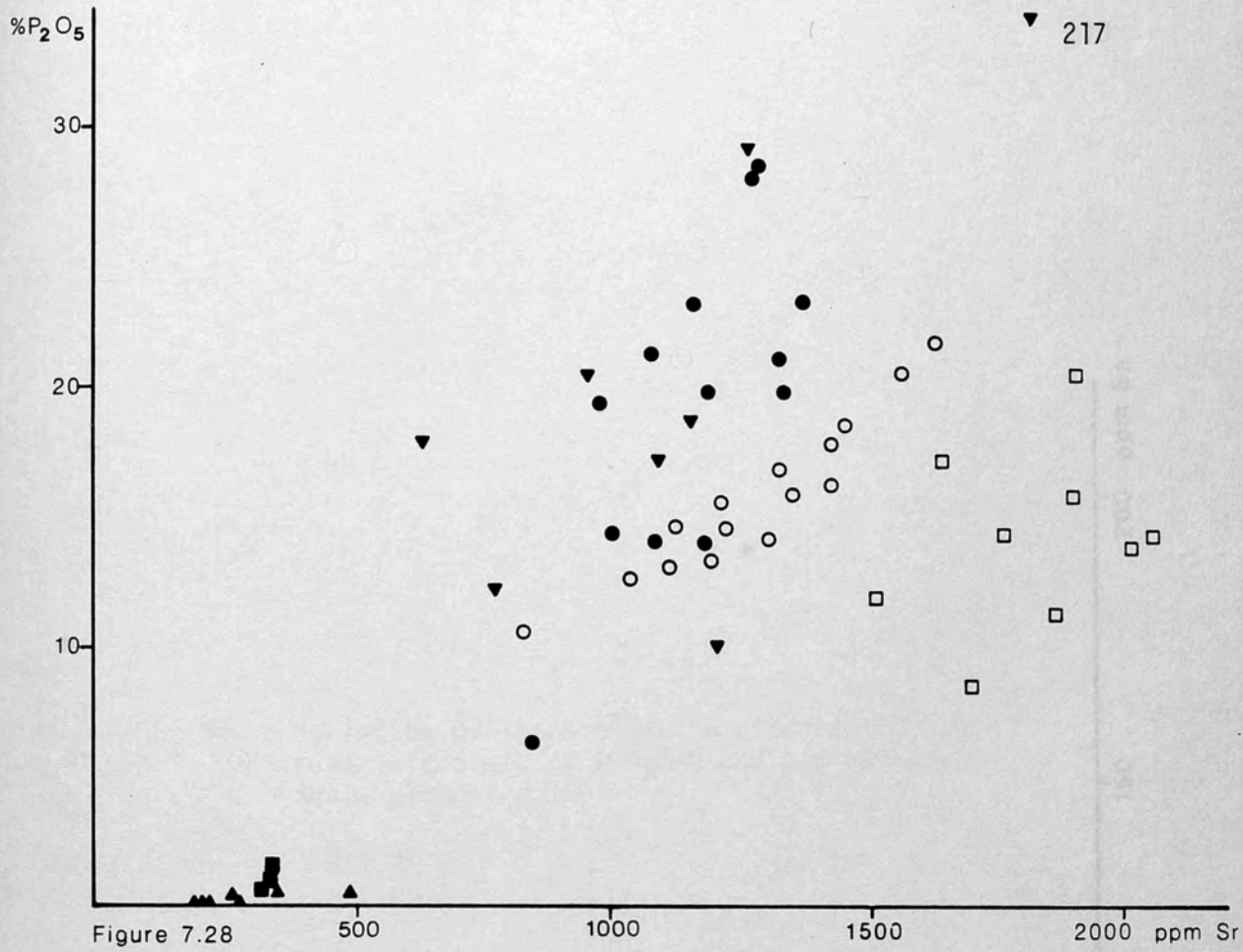


Figure 7.27



Figures 7.31 to 7.37 Variation of trace elements relative to CaO; bivariate plots of weight% CaO against ppm trace element.

Figure 7.31 CaO v Sc

Figure 7.32 CaO v V

Figure 7.33 CaO v Ni

Figure 7.34 CaO v Cu

Figure 7.35 CaO v Sr

Figure 7.36 CaO v Zr

Figure 7.37 CaO v Ba

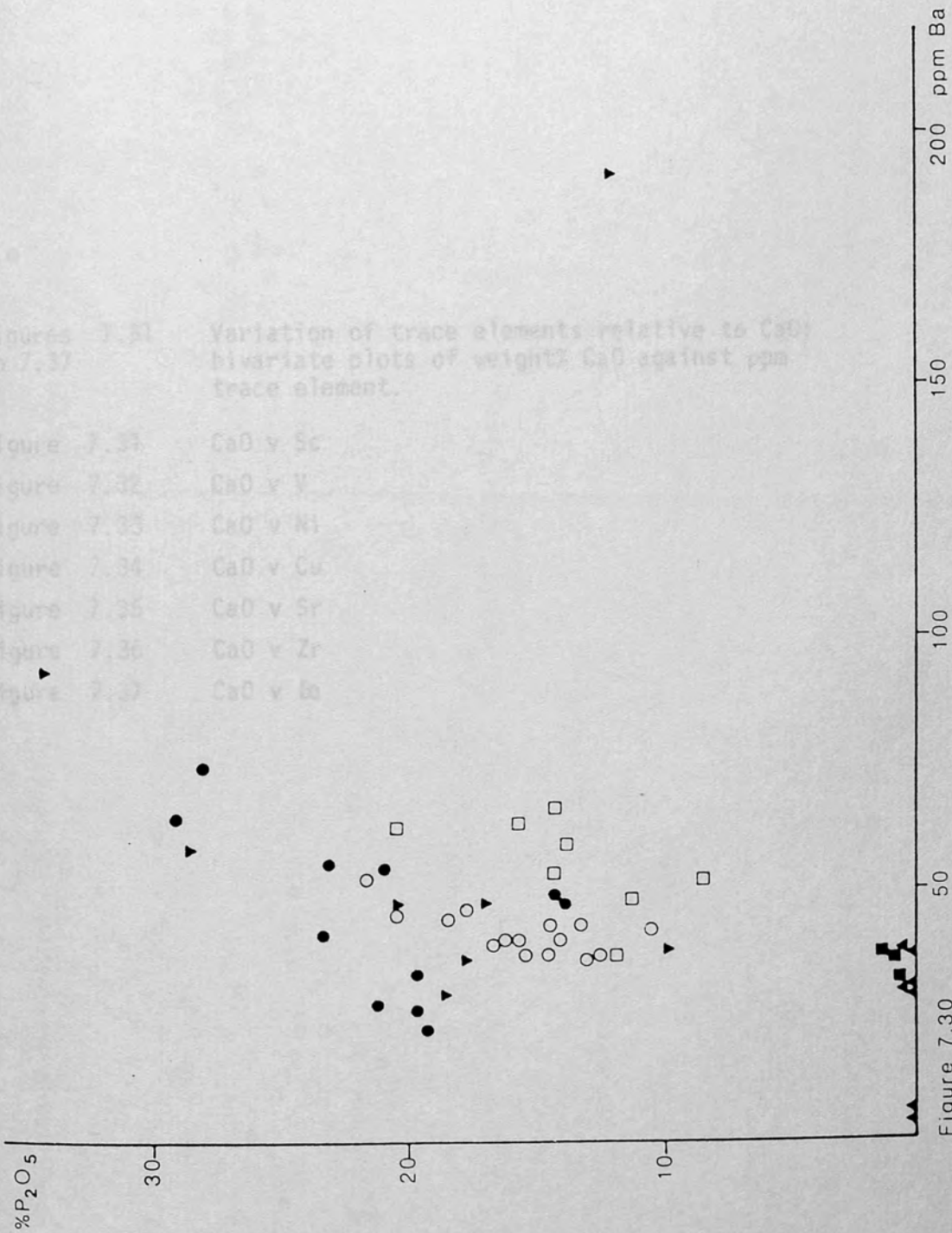


Figure 7.30

Figures 7.31 to 7.37 Variation of trace elements relative to CaO: bivariate plots of weight% CaO against ppm trace element.

- Figure 7.31 CaO v Sc
Figure 7.32 CaO v V
Figure 7.33 CaO v Ni
Figure 7.34 CaO v Cu
Figure 7.35 CaO v Sr
Figure 7.36 CaO v Zr
Figure 7.37 CaO v Ba

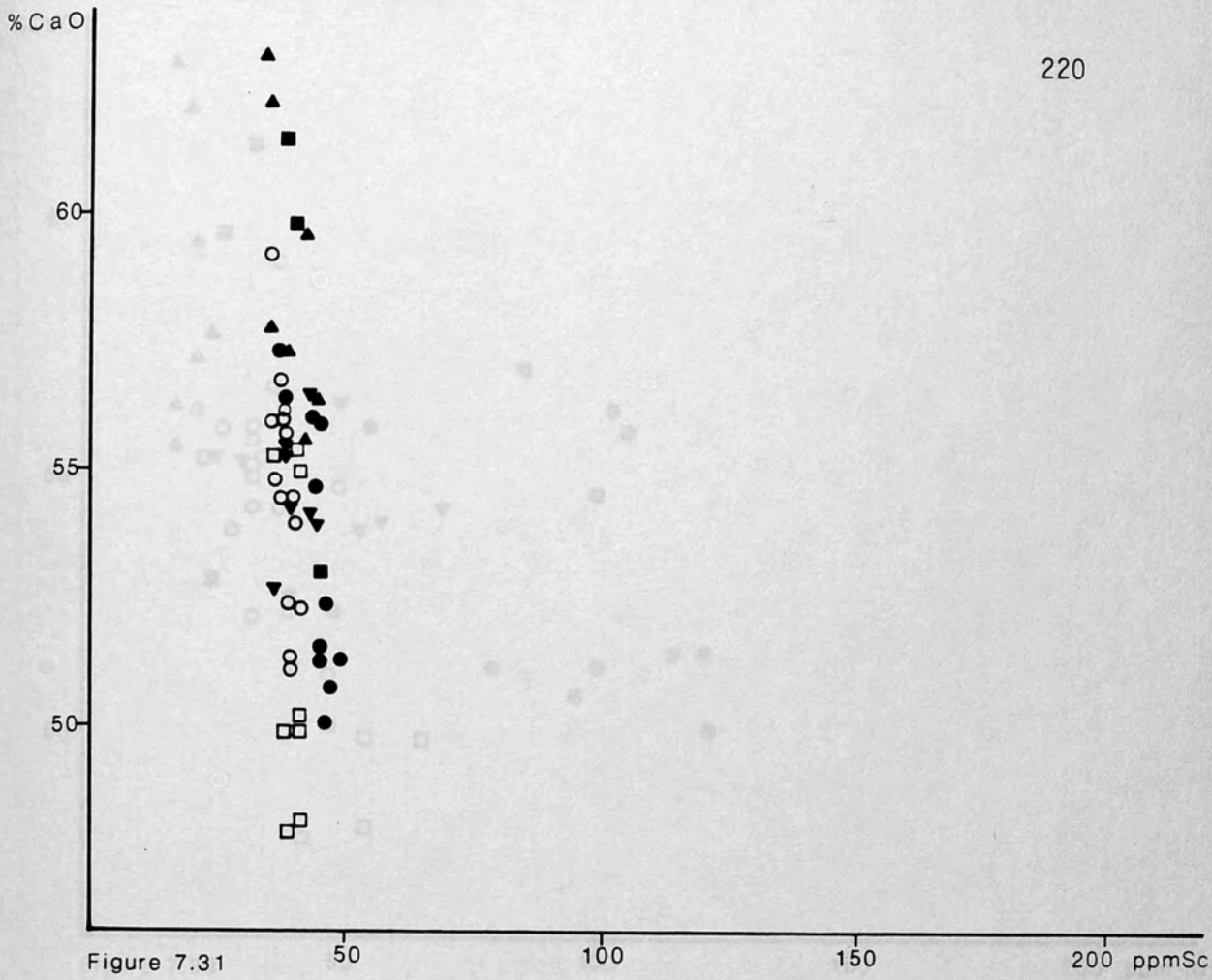


Figure 7.31

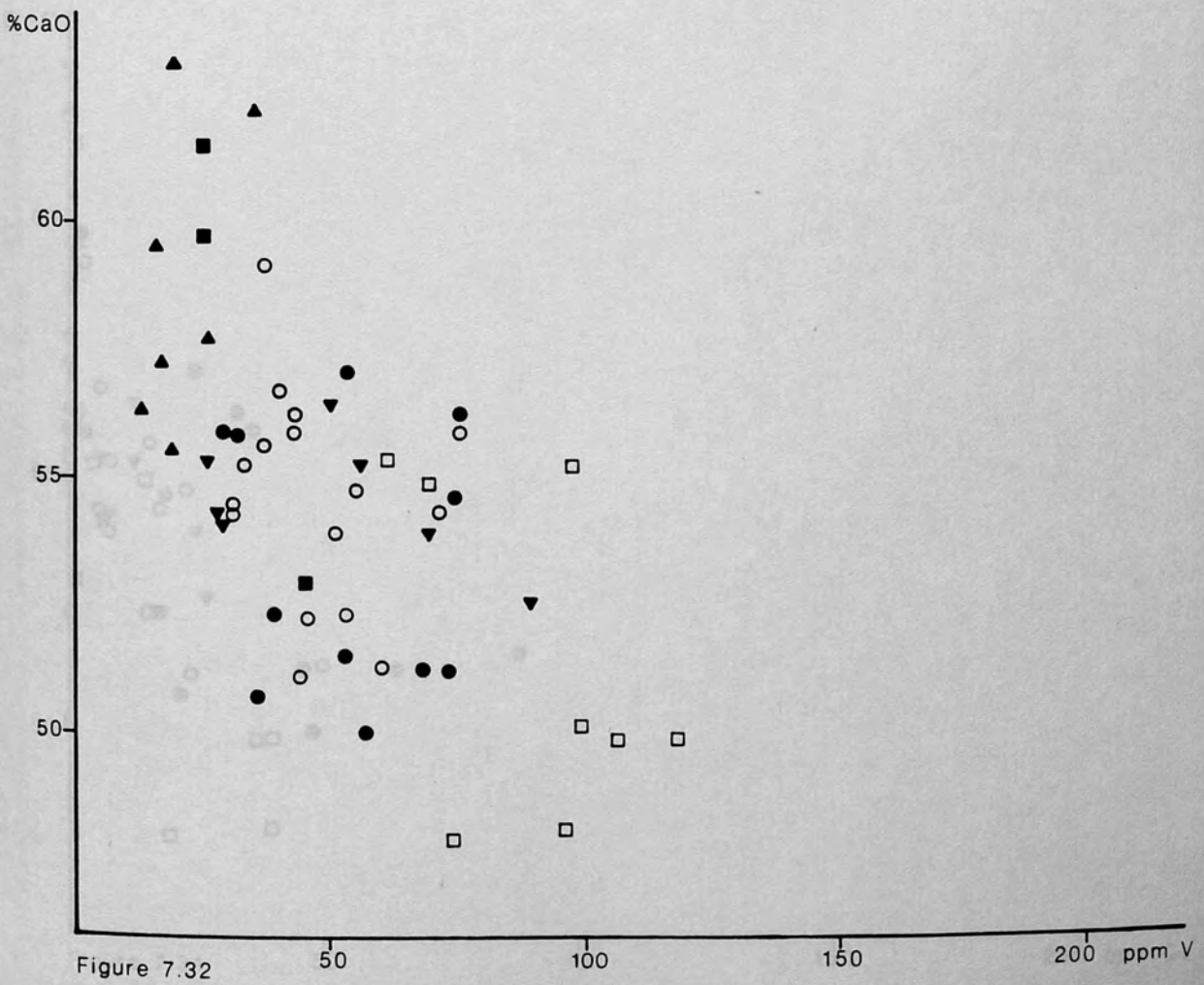


Figure 7.32

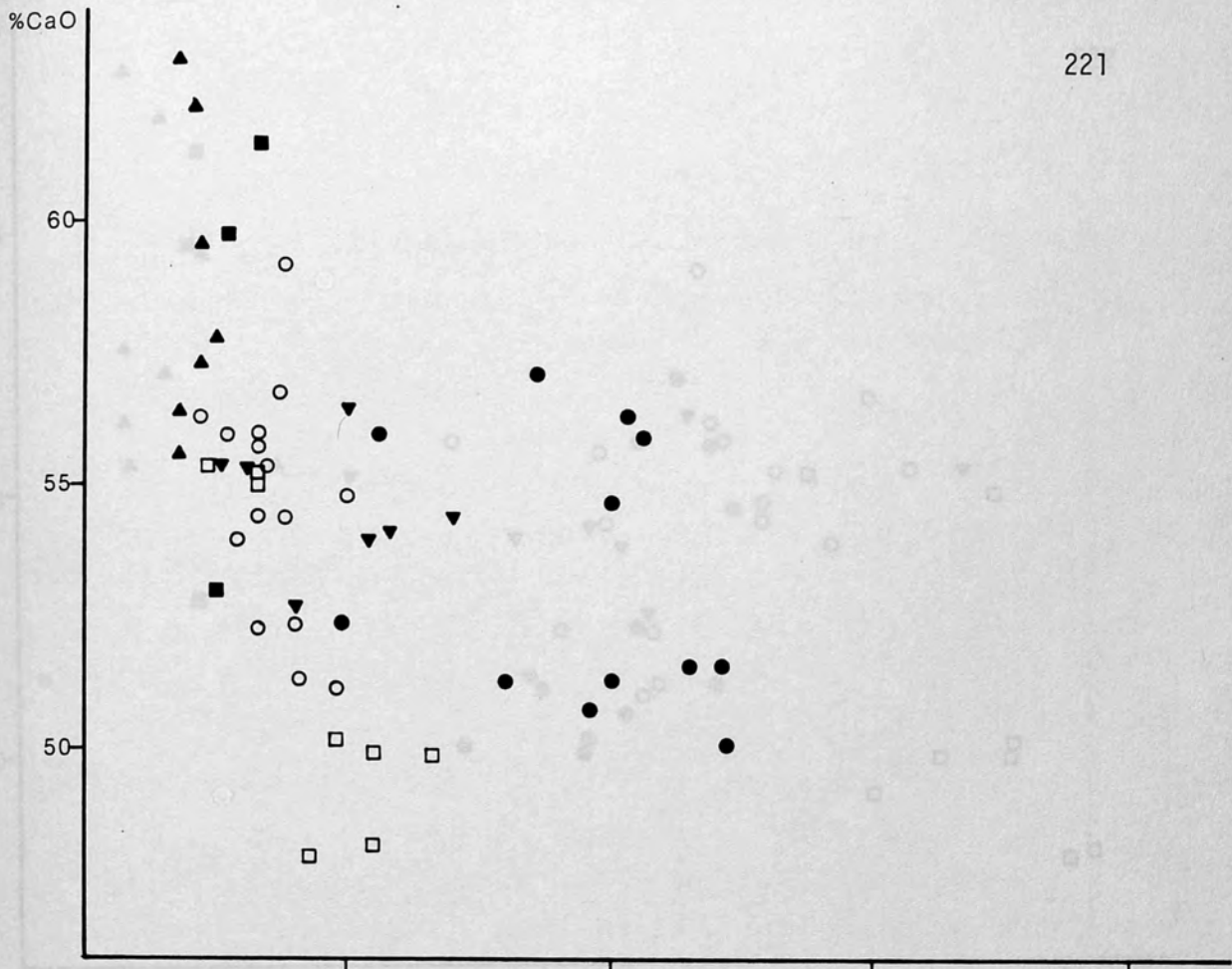


Figure 7.33

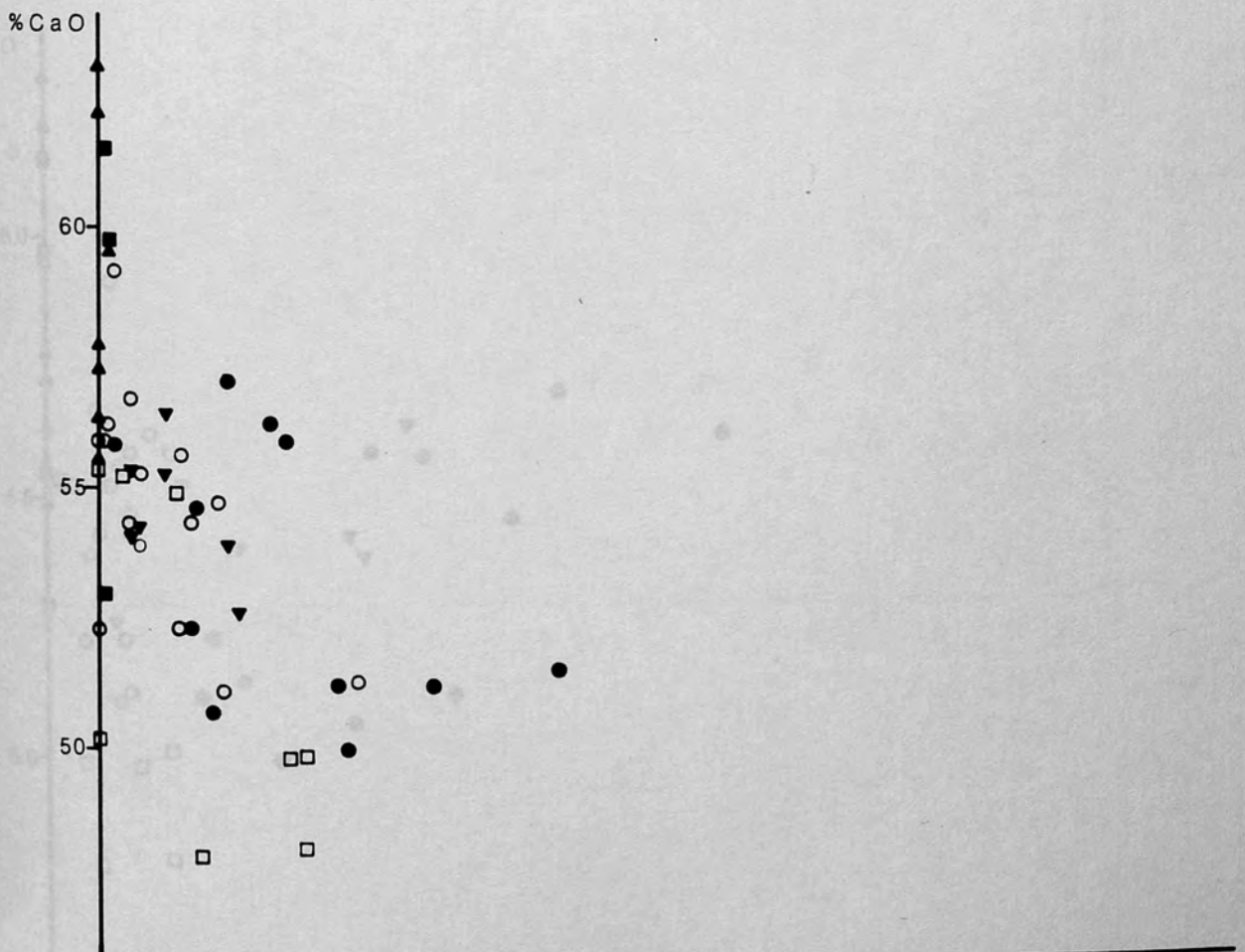


Figure 7.34

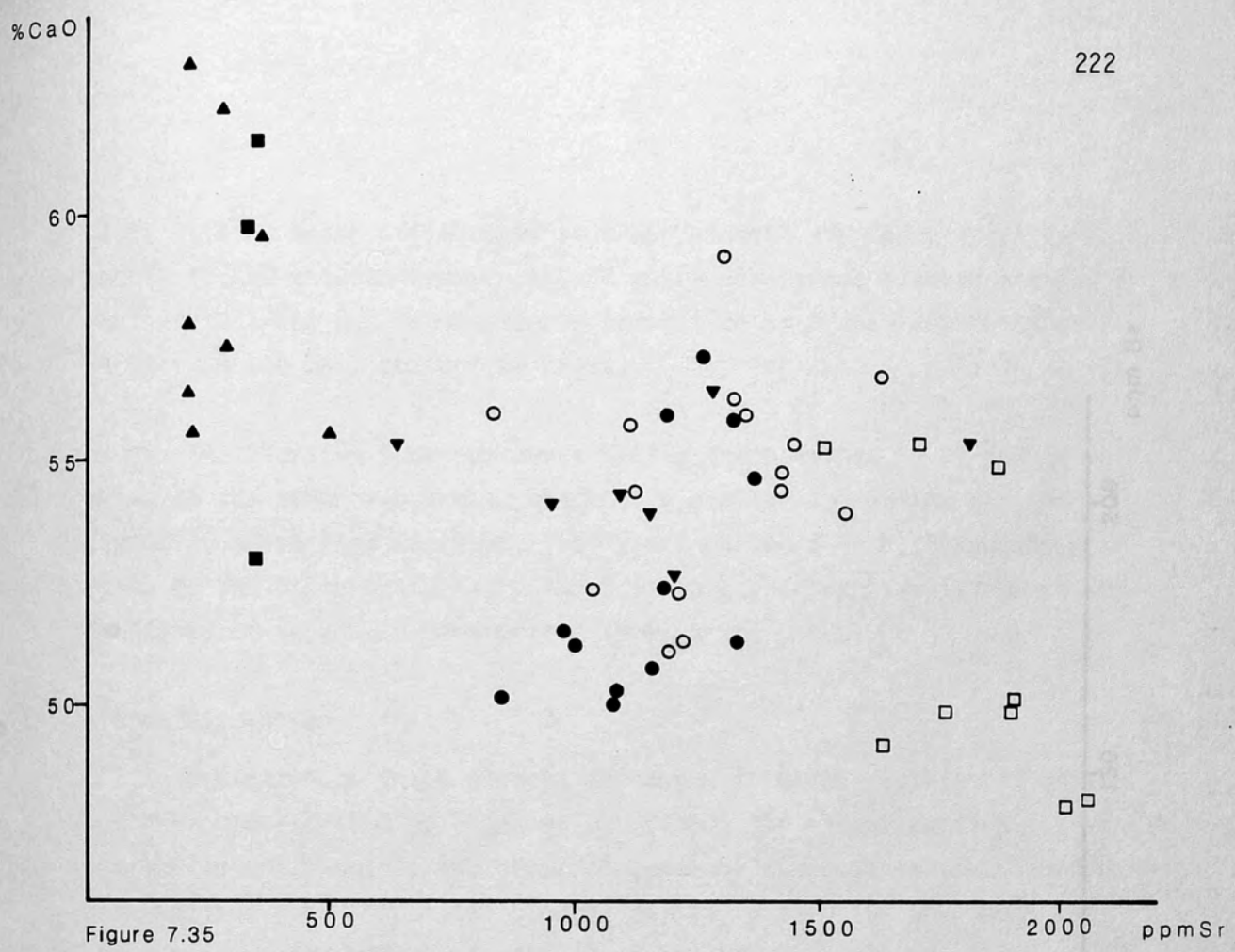


Figure 7.35

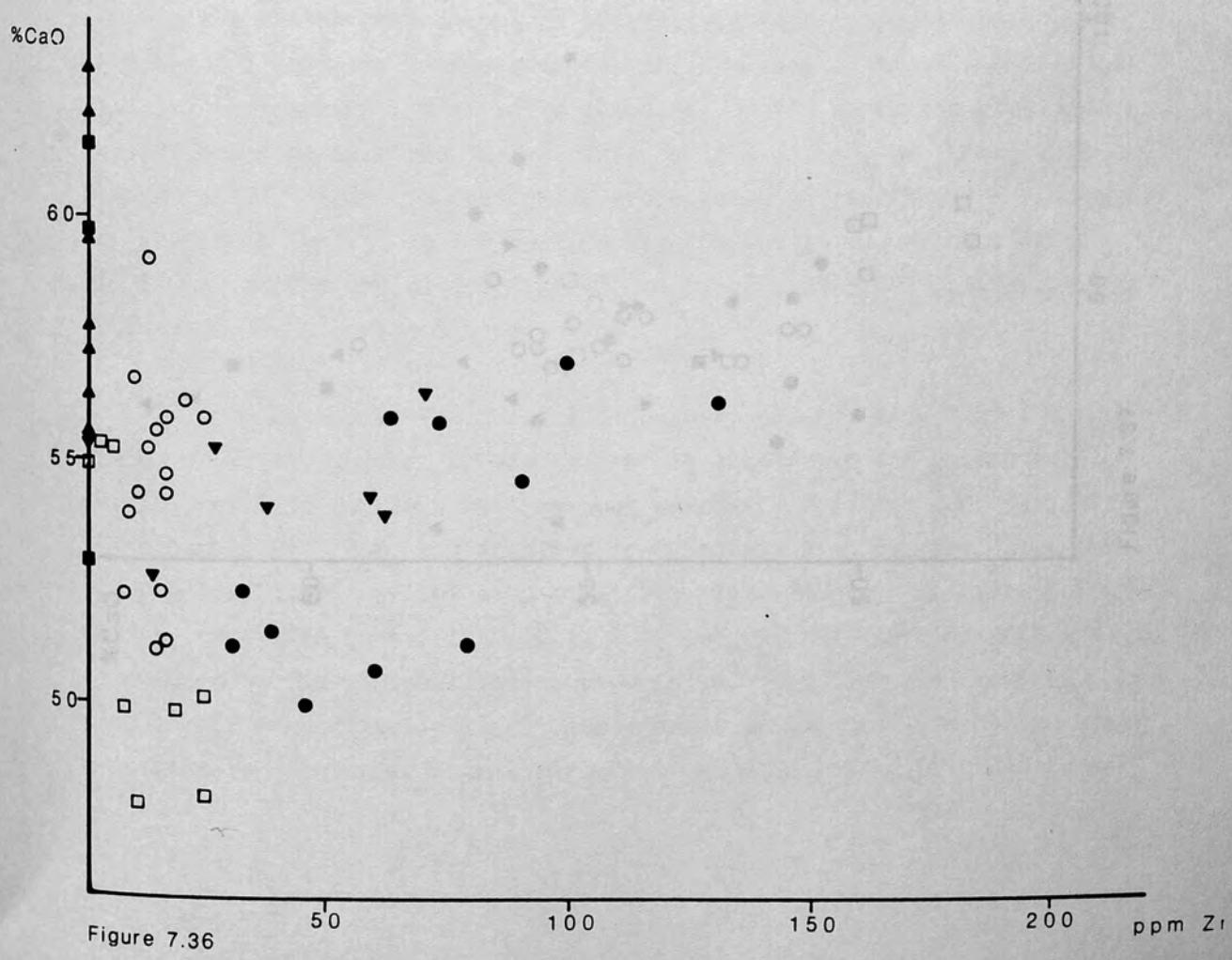


Figure 7.36

phats with no major differences in trace element abundance relative to amount of CaO between areas. Graphs which plot trace element abundance against that for P_2O_5 show clearer separation with some overlap of plots from the main collecting areas.

Phosphorites from southwest Sicily are enriched in Ni and Zr relative to the other two areas, which have similar abundances for these elements; those from southeast Sicily are enriched in V, Sr and Ba relative to the other two areas. There is no significant variation in the abundance of Sc and Cu between the three areas.

7.6.6 Discussion

Variation in trace element abundance in marine authigenic minerals has been ascribed by Tooms et al. (1959) to: their availability in the marine environment; the crystallochemical characteristics of carbonate apatites and associated mineral phases; adsorption phenomena and the concentrating effect of organisms; and the chemical character of the environment. In phosphorites, they consider that availability of elements in the marine environment is of greatest importance, since elements enriched and depleted in phosphorites are the same as those enriched and depleted in seawater (relative to abundance in the Earth's crust). Minor variations can be ascribed to the other factors listed, or (Cook, 1971; Warburton, 1973, 1980) to weathering processes. In general, P^{5+} is thought to substitute for P^{3+} in the apatite lattice whilst Ni, Sr, Zr and Ba may occupy the Ca positions (Tooms et al. 1959; Altschier, 1962; Jan, 1968; Provot & Lucas, 1973).

Sections 7.6.2, 7.6.3 and 7.6.4 above, clearly show that the levels of V, Ni, Cu, Sr, Zr and Ba are all greater in the phosphorite samples relative to the pure limestone samples. Positive correlations with P_2O_5 and negative correlations with CaO are also observed. Positive correlations with P_2O_5 suggest that the elements are introduced by the phosphatization process and that they are probably located in the francolite lattice. Replacement of the Ca^{2+} ion by the elements can be inferred from their negative correlations with CaO trace

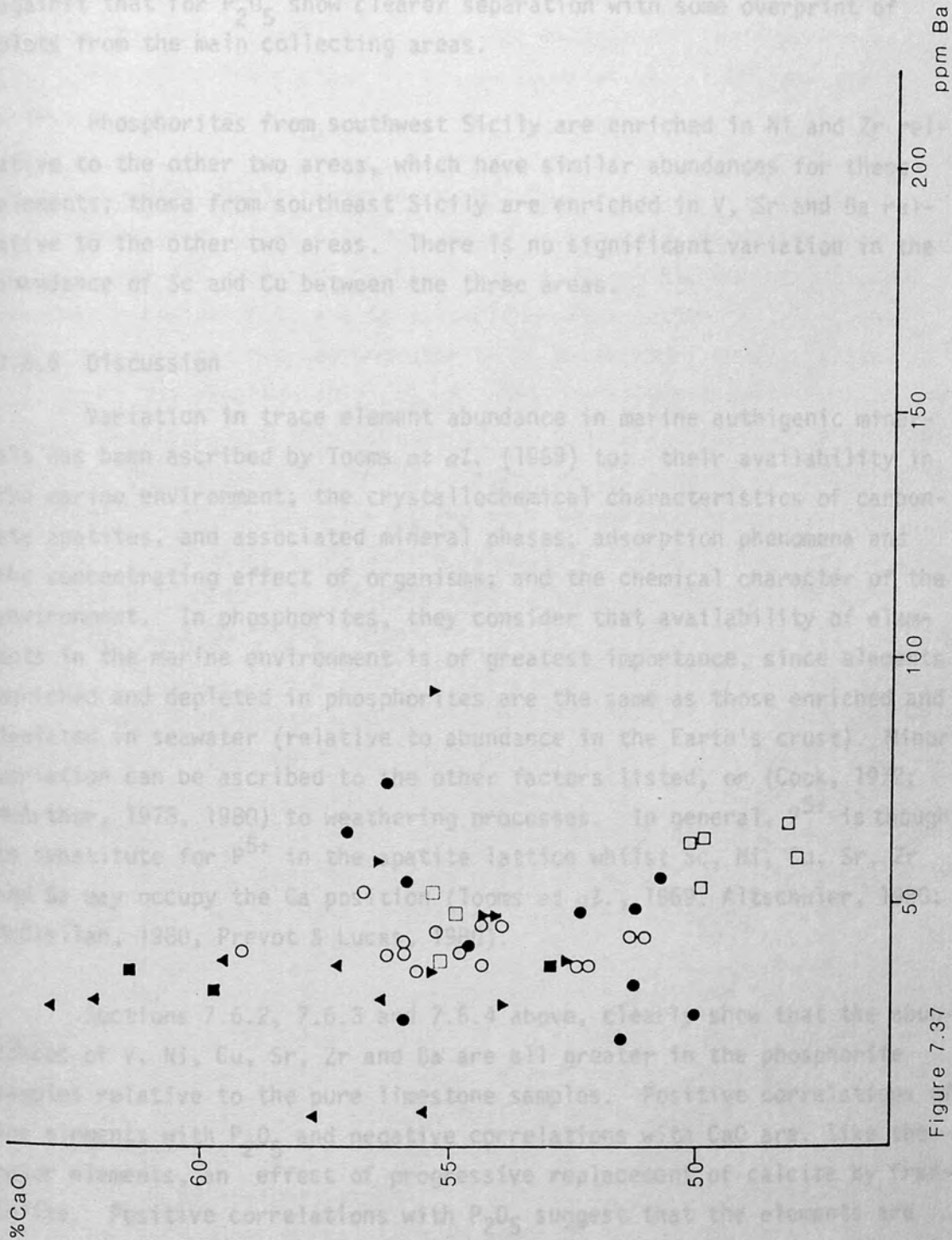


Figure 7.37

plots with no major differences in trace element abundance relative to amount of CaO between areas. Graphs which plot trace element abundance against that for P_2O_5 show clearer separation with some overprint of plots from the main collecting areas.

Phosphorites from southwest Sicily are enriched in Ni and Zr relative to the other two areas, which have similar abundances for these elements; those from southeast Sicily are enriched in V, Sr and Ba relative to the other two areas. There is no significant variation in the abundance of Sc and Cu between the three areas.

7.6.6 Discussion

Variation in trace element abundance in marine authigenic minerals has been ascribed by Tooms *et al.* (1969) to: their availability in the marine environment; the crystallochemical characteristics of carbonate apatites, and associated mineral phases; adsorption phenomena and the concentrating effect of organisms; and the chemical character of the environment. In phosphorites, they consider that availability of elements in the marine environment is of greatest importance, since elements enriched and depleted in phosphorites are the same as those enriched and depleted in seawater (relative to abundance in the Earth's crust). Minor variation can be ascribed to the other factors listed, or (Cook, 1972; McArthur, 1978, 1980) to weathering processes. In general, V^{5+} is thought to substitute for P^{5+} in the apatite lattice whilst Sc, Ni, Cu, Sr, Zr and Ba may occupy the Ca position (Tooms *et al.*, 1969; Altschuler, 1980; McClellan, 1980, Prevot & Lucas, 1980).

Sections 7.6.2, 7.6.3 and 7.6.4 above, clearly show that the abundances of V, Ni, Cu, Sr, Zr and Ba are all greater in the phosphorite samples relative to the pure limestone samples. Positive correlations of the elements with P_2O_5 and negative correlations with CaO are, like the major elements, an effect of progressive replacement of calcite by francolite. Positive correlations with P_2O_5 suggest that the elements are introduced by the phosphatisation process and that they are probably located in the francolite lattice. Replacement of the Ca^{2+} ion by the elements cannot be inferred from their negative correlations with CaO since

they are present in such small abundances. The very high variance present in these plots is due to the same controlling factors as in the major elements (Section 7.5.3) but it is greater in the trace elements because they are present in much smaller amounts and their presence is also affected by the factors listed in Tooms *et al.* (1969) and given above.

Of the elements analysed, V, Ni, Cu, Sr and Zr have abundances within the ranges given for the average phosphorite (based on 18 regional averages and 224 analyses) by Altschuler (1980). Ba, however, is depleted by a factor of 10 and Sc is enriched by a factor of 3-4. Since composition of the average phosphorite is estimated from data collected throughout the stratigraphic column, then the observed deviations in the central Mediterranean phosphorites may be due to a particular enrichment of Sc and depletion of Ba in the seawater at the time of their formation. The chemistry of the seawater is the most important factor affecting trace element abundances in marine authigenic minerals (Tooms *et al.*, 1969) and differences in their relative abundances do occur throughout geological time (Notholt, 1980b).

There may, however, be an alternative chemical reason for the depletion of Ba in the central Mediterranean phosphorites. The Ba^{2+} ion has an ionic radius very much larger than the Ca^{2+} ion making substitution difficult. If there are ions available with an ionic radius closer to that of the Ca^{2+} ion, and the valences are suitable, then substitution with these ions may be made in preference to the Ba^{2+} ion.

Of the elements normal in abundance in comparison to the average phosphorite Sr is worthy of comment. The southwest Sicily phosphorite which is of Eocene origin shows lower abundances of Sr relative to P_2O_5 (Fig. 7.28) than the Lower Miocene Maltese and southeast Sicily phosphorites. This may be due to the metastable character of Sr which is often removed by weathering (McArthur, 1978, 1980). This feature (depletion of Sr in older rocks) is also apparent in Altschuler's (1980, Table 1) listing of Sr contents in phosphorites of Precambrian to Pliocene age.

7.7 Yttrium and Rare Earth Element Geochemistry

7.7.1 Introduction

The Rare Earth Elements (REE) are a group ranging from La (Atomic no. 57) to Lu (Atomic no. 71). Along with Y (Atomic no. 39) they exhibit many chemical similarities: where one is found, in nature the others are likely to occur (Haskin & Gehl, 1962). They are therefore considered together here. Despite the chemical similarities of Y and the REE, fractionation is common, having been demonstrated by many authors for both igneous and sedimentary rocks (summarised by Herrmann, 1970), and also seawater (Goldberg *et al.*, 1963; Høgdahl *et al.*, 1968).

Under normal conditions the oxidation state of the group is trivalent. Ce, Pr and Tb can be oxidised to 4⁺ and Eu, Sm and Yb reduced to 2⁺. However, Herrmann (1970) notes that whereas some REE distributions may show anomalous behaviour of Ce and Eu, no similar anomalies are observed for Pr, Sm, Tb and Yb in naturally formed minerals and rocks.

Analyses were carried out (using the ICP spectrometer and the sample and data preparation techniques outlined in Appendix I) on nineteen powdered samples (comprising 10 phosphorite and limestone samples from southwest Sicily, four phosphorite samples from southeast Sicily, and five phosphorite samples from the Maltese islands, with sources of origin as specified in Table A2.1, Appendix II) to determine the abundance and distribution of Y and the REE and to detect any fractionation and/or anomalies in their distribution with geographic area. Fractionation may reflect the depth of formation of the enclosing mineral, whereas Ce and Eu anomalies may reflect the chemical properties of the depositional environment (Piper, 1974).

The absolute concentrations of REE in naturally occurring materials produce a saw-tooth pattern when plotted against atomic number (the Oddo-Harkins rule of Haskins *et al.*, 1966). Consequently the detail of the distribution and the relationship of one element to its neighbour is masked. This problem is overcome by dividing each element in the distribution by the same element in another distribution (normalisation). Theoretically, normalisation to any distribution is possible. In

practice it is convenient for comparison to use an accurate set of widely available data and to present results in a graphic form. Normalisation to chondrite was undertaken to allow comparison with a wide range of published data in this form. Normalisation to limestone RTB 18, mean Maltese phosphorite and average sediment (Herrmann, 1970) allowed the respective detection of: the introduction of Y and REE through the phosphatisation process; differences in distribution between geographic area; and differences in the phosphorite Y and REE distribution in comparison to average sediment.

The concentrations used in the normalisation procedure are given in Table A2.3, Appendix II. The standards NIM G (granite) and MT 2 (basalt) were analysed, and their data published here (Table 7.11), to allow comparison of the results obtained by the ICP technique. Florida phosphorite standard 120B was analysed to allow comparison of the central Mediterranean phosphorites with a more distal collecting area.

7.7.2 Results

Tables 7.9 and 7.10 list the absolute concentrations of Y and the REE for phosphorites from southwest Sicily and from southeast Sicily and the Maltese islands respectively. Table 7.11 lists the concentrations for the igneous standards NIM G and MT 2 along with phosphorite standard 120B and limestones JTA 5A (Upper Cretaceous chalk) and RTB 18 (Upper Oligocene foraminiferal grainstone - packstone) both from southwest Sicily.

Figures 7.38 to 7.40 show chondrite-normalised values plotted on a log scale against atomic number for individual specimens from southwest Sicily, southeast Sicily and the Maltese islands, and for mean distributions from each of these areas. From these graphs it can be seen that the Y and REE distribution patterns are similar for each sample and each area collectively. All show an enrichment of the light REE (La-Eu) relative to the heavy REE (Gd-Lu), negative Ce and Eu anomalies, and positive Y anomaly. However, the Ce anomaly is smaller and the Eu anomaly larger in the southwest Sicily specimens in comparison to the other two areas (most apparent in the mean phosphorite graphs, Fig. 7.40A,B). The distribution pattern for the phosphorite standard 120B (Fig. 7.41A) shows

| Sample Element | RTA 7A | RTA 7B | RTA 11B | RTA 13A | RTA 13B | RTA 13C | RTB 19A | RTB 19B | Mean |
|----------------|--------|--------|---------|---------|---------|---------|---------|---------|--------|
| La | 117.78 | 103.05 | 118.94 | 48.98 | 58.58 | 50.63 | 185.11 | 118.94 | 100.25 |
| Ce | 171.52 | 21.71 | 184.48 | 36.95 | 30.86 | 24.48 | 132.16 | 65.39 | 83.44 |
| Nd | 80.77 | 57.39 | 93.26 | 40.01 | 37.31 | 32.82 | 121.80 | 69.55 | 66.61 |
| Sm | 15.22 | 10.24 | 18.44 | 8.10 | 6.73 | 5.95 | 22.13 | 12.38 | 12.40 |
| Eu | 3.88 | 2.63 | 4.66 | 2.05 | 1.79 | 1.57 | 5.56 | 3.14 | 3.16 |
| Gd | 18.80 | 13.54 | 22.06 | 9.14 | 7.99 | 7.22 | 28.48 | 16.42 | 15.46 |
| Dy | 18.91 | 13.89 | 22.69 | 9.38 | 9.18 | 8.02 | 29.58 | 17.32 | 16.12 |
| Ho | 4.61 | 3.55 | 5.17 | 2.16 | 2.25 | 2.05 | 7.65 | 4.33 | 3.97 |
| Er | 12.08 | 10.00 | 14.18 | 6.10 | 6.24 | 5.45 | 19.76 | 11.79 | 10.70 |
| Yb | 12.52 | 9.88 | 14.28 | 6.37 | 6.19 | 5.70 | 19.35 | 11.70 | 10.75 |
| Lu | 1.98 | 1.59 | 2.26 | 1.01 | 1.04 | 0.88 | 3.25 | 1.94 | 1.74 |
| ΣREE | 458.41 | 247.47 | 500.36 | 170.24 | 168.16 | 144.76 | 574.83 | 332.90 | 324.64 |
| Y | 183.05 | 167.24 | 210.83 | 87.52 | 106.05 | 91.05 | 303.84 | 197.24 | 168.35 |

TABLE 7.9 Southwest Sicily phosphorite: ppm of Yttrium and REE. Samples are all from Nadorello east and comprise whole clasts (RTA 7A - RTA 13A), clast interiors (RTA 13C, RTB 19B), and clast exteriors (RTA 13B, RTB 19A). See appendices for details of sources and techniques.

| Sample Element | 187.2 | 187.3 | 187.5 | 187.15 | Mean | M1 | M3 | M11 | M12 | M14 | Mean |
|----------------|-------|-------|-------|--------|-------|-------|-------|-------|-------|-------|-------|
| La | 4.70 | 7.65 | 6.94 | 12.08 | 7.84 | 17.35 | 5.66 | 14.55 | 13.05 | 9.87 | 12.10 |
| Ce | 3.50 | 4.92 | 4.50 | 9.20 | 5.53 | 14.61 | 7.13 | 12.87 | 11.30 | 9.04 | 10.99 |
| Nd | 3.98 | 5.61 | 5.04 | 10.24 | 6.22 | 15.59 | 5.69 | 12.92 | 10.64 | 10.54 | 11.08 |
| Sm | 0.74 | 1.20 | 0.92 | 2.13 | 1.25 | 2.86 | 1.05 | 2.48 | 2.19 | 1.52 | 2.02 |
| Eu | 0.21 | 0.29 | 0.25 | 0.52 | 0.32 | 0.75 | 0.23 | 0.61 | 0.53 | 0.14 | 0.46 |
| Gd | 0.40 | 1.20 | 0.93 | 2.47 | 1.25 | 3.02 | 0.86 | 2.56 | 2.19 | 1.68 | 2.06 |
| Dy | 0.97 | 1.57 | 1.37 | 2.63 | 1.64 | 3.64 | 0.96 | 2.86 | 2.42 | 1.92 | 2.36 |
| Ho | 0.26 | 0.38 | 0.39 | 0.67 | 0.43 | 0.88 | 0.26 | 0.69 | 0.59 | 0.50 | 0.58 |
| Er | 0.74 | 1.09 | 1.11 | 1.78 | 1.18 | 2.54 | 0.68 | 1.93 | 1.64 | 1.25 | 1.61 |
| Yb | 0.79 | 1.20 | 1.14 | 1.83 | 1.24 | 2.58 | 0.69 | 1.97 | 1.65 | 1.36 | 1.65 |
| Lu | 0.13 | 0.19 | 0.18 | 0.29 | 0.20 | 0.41 | 0.11 | 0.32 | 0.27 | 0.22 | 0.27 |
| ΣREE | 16.42 | 25.30 | 22.77 | 43.84 | 27.08 | 64.23 | 23.32 | 53.76 | 46.47 | 38.31 | 45.22 |
| Y | 8.19 | 16.97 | 14.20 | 24.50 | 15.97 | 30.82 | 5.32 | 21.63 | 20.60 | 18.11 | 19.30 |

TABLE 7.10 Southeast Sicily and Maltese phosphorites: ppm of Yttrium and REE. Samples are hardground (187.2, 187.5) and whole clasts (187.3, 187.15) from Donnalucata, southeast Sicily; and hardground (M3, M12), C1 conglomerate (M1, M11), and C2 conglomerate (M14) from Malta. See appendices for details of sources and techniques.

| Sample Element | 120 B | NIM G | MT 2 | JTA 5A | RTB 18 |
|----------------|--------|--------|-------|--------|--------|
| La | 75.80 | 96.77 | 7.35 | 5.24 | 3.00 |
| Ce | 91.39 | 155.83 | 20.87 | 5.67 | 2.92 |
| Nd | 71.27 | 67.14 | 22.94 | 4.85 | 2.54 |
| Sm | 13.21 | 12.92 | 5.85 | 1.01 | 0.65 |
| Eu | 3.00 | 0.39 | 1.96 | 0.24 | 0.17 |
| Gd | 13.91 | 12.23 | 5.35 | 0.67 | 0.49 |
| Dy | 15.11 | 16.48 | 4.59 | 0.98 | 0.60 |
| Ho | 3.61 | 3.69 | 0.83 | 0.23 | 0.15 |
| Er | 10.27 | 11.43 | 2.31 | 0.63 | 0.41 |
| Yb | 10.14 | 11.71 | 1.69 | 0.63 | 0.40 |
| Lu | 1.67 | 1.69 | 0.25 | 0.10 | 0.07 |
| ΣREE | 309.38 | 390.28 | 74.35 | 20.25 | 11.40 |
| Y | 124.40 | 106.69 | 18.47 | 7.30 | 4.55 |

TABLE 7.11

Standards and Limestones: ppm of Yttrium and REE.
 Samples are United States Geological Survey Florida phosphorite (120 B), granite (NIM G), and basalt (MT 2); plus samples of Cretaceous chalk (JTA 5A) and Oligo-Miocene limestone (RTB 18) from Nadorello east, southwest Sicily.

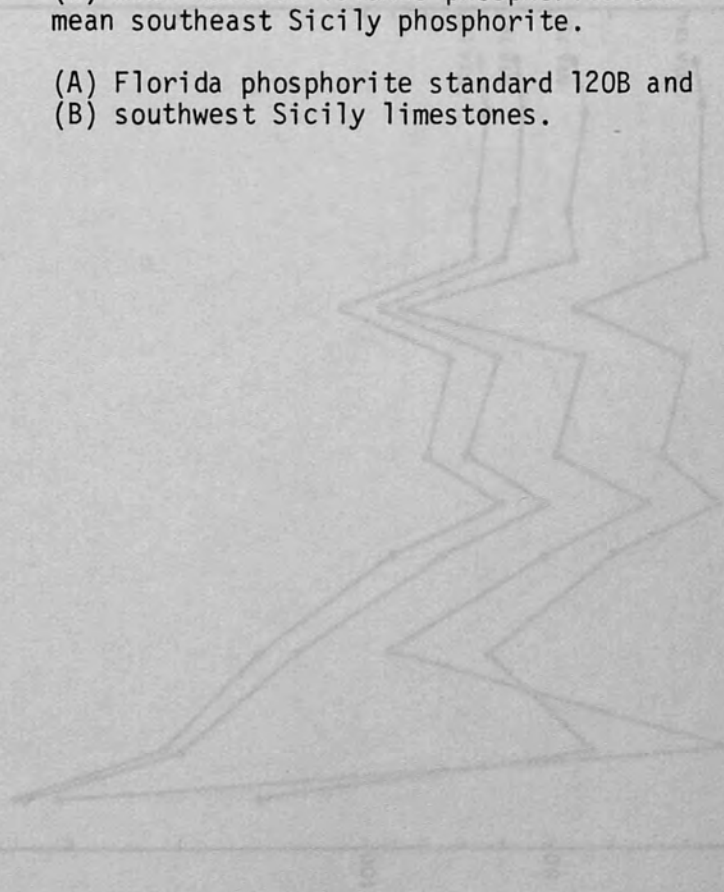
Figures 7.38 to 7.41 Chondrite normalised concentrations of Y and REE plotted on a log scale against element atomic number for:

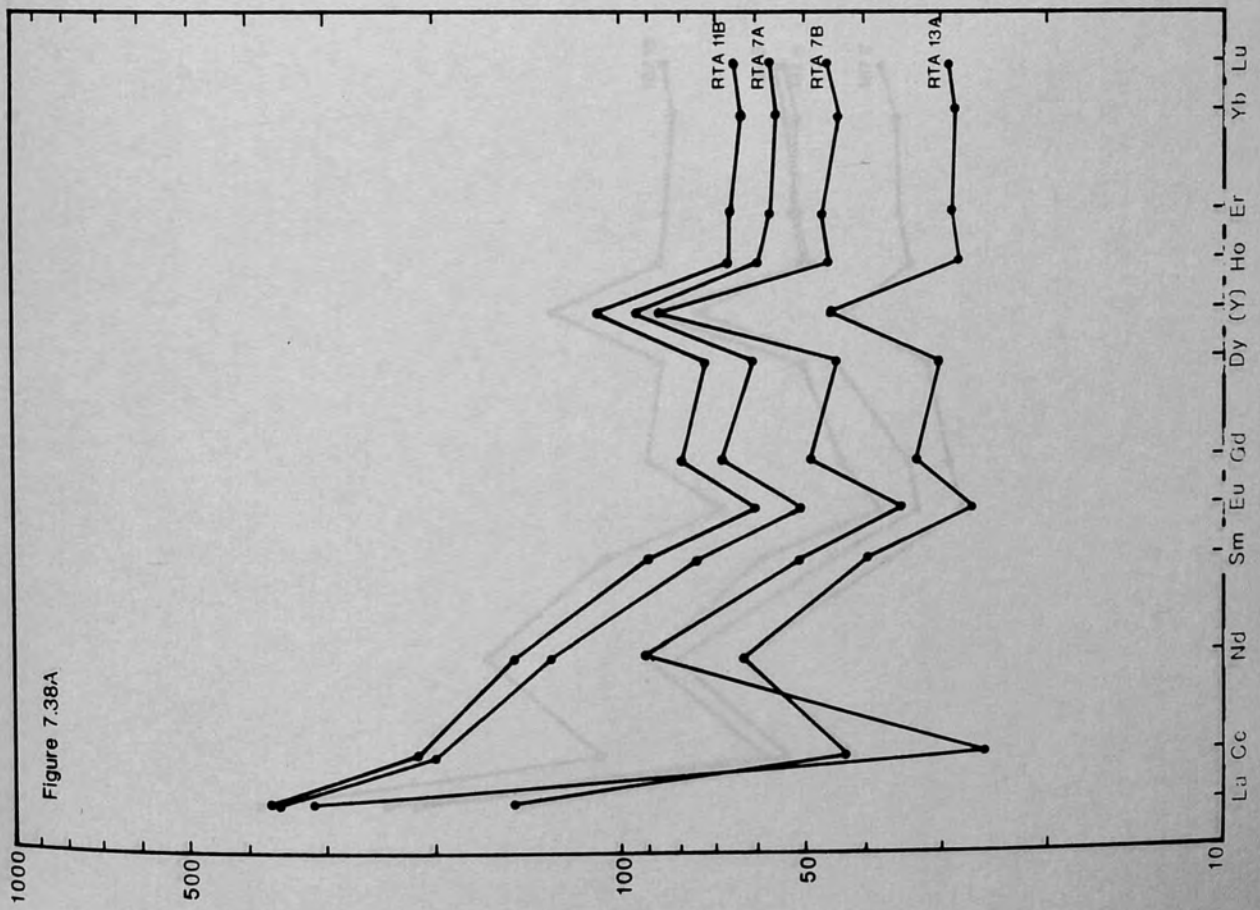
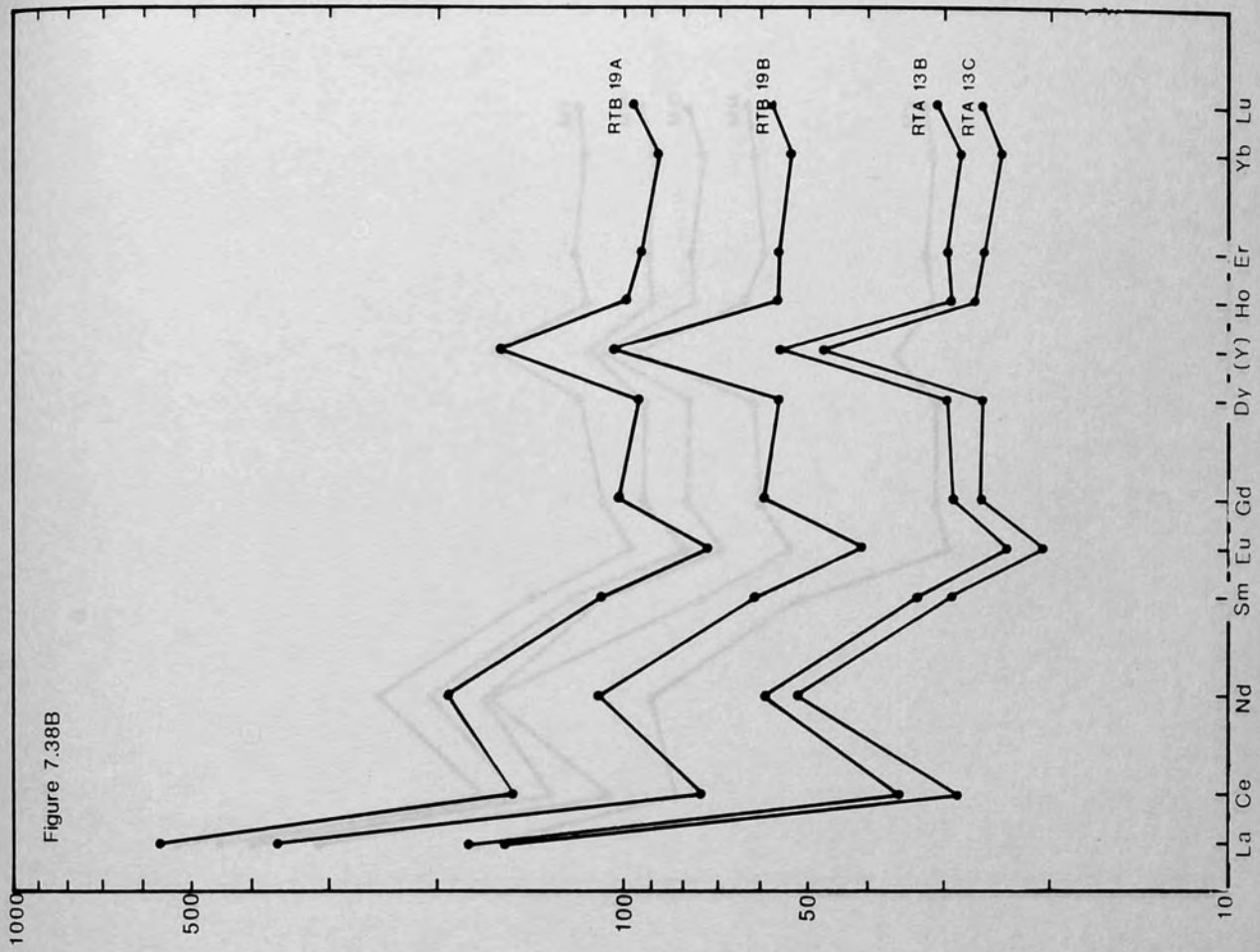
Figure 7.38 Phosphatic clasts from southwest Sicily.
A & B

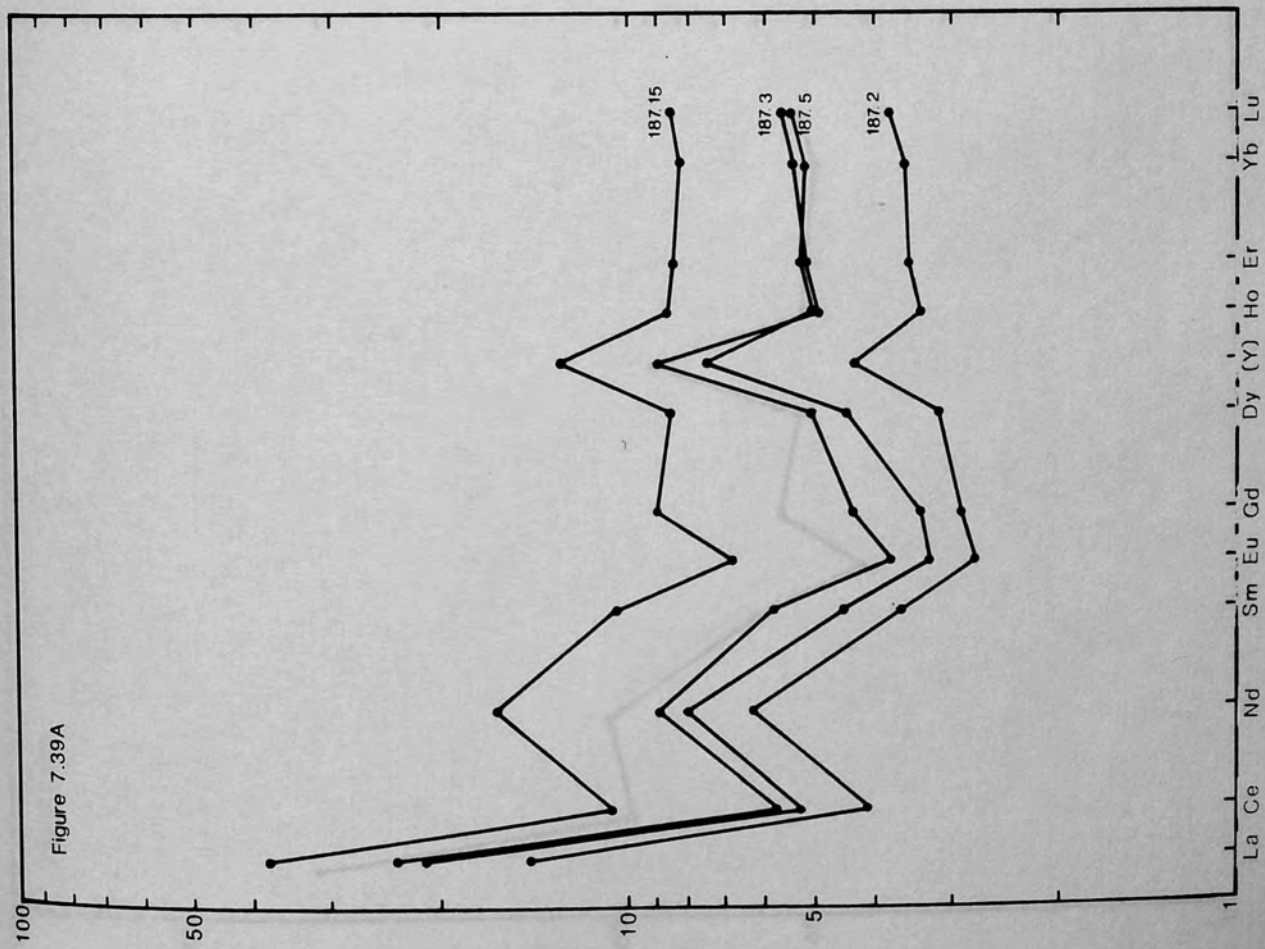
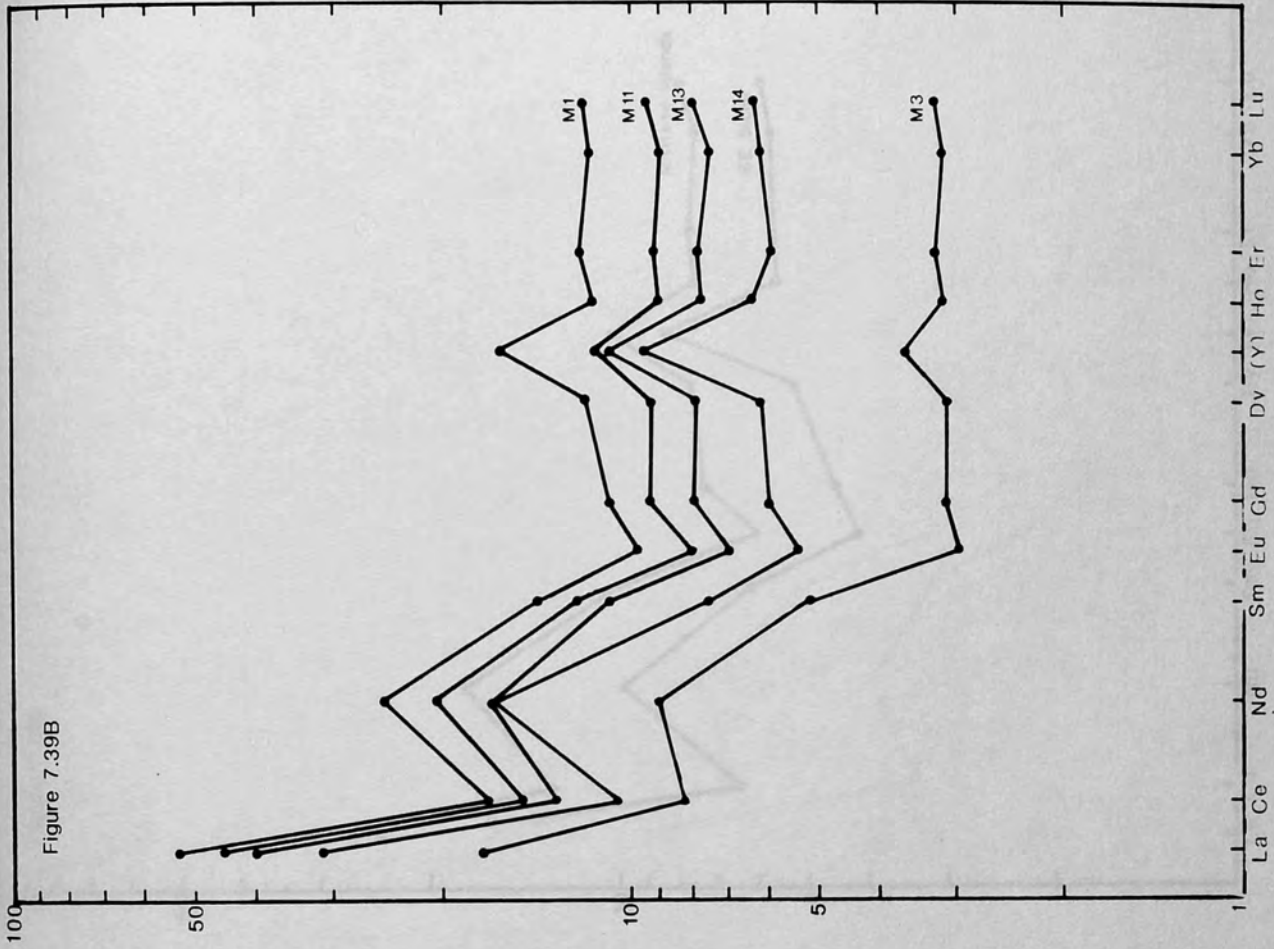
Figure 7.39 Phosphatic clasts from (A) southeast Sicily and (B) Maltese islands.

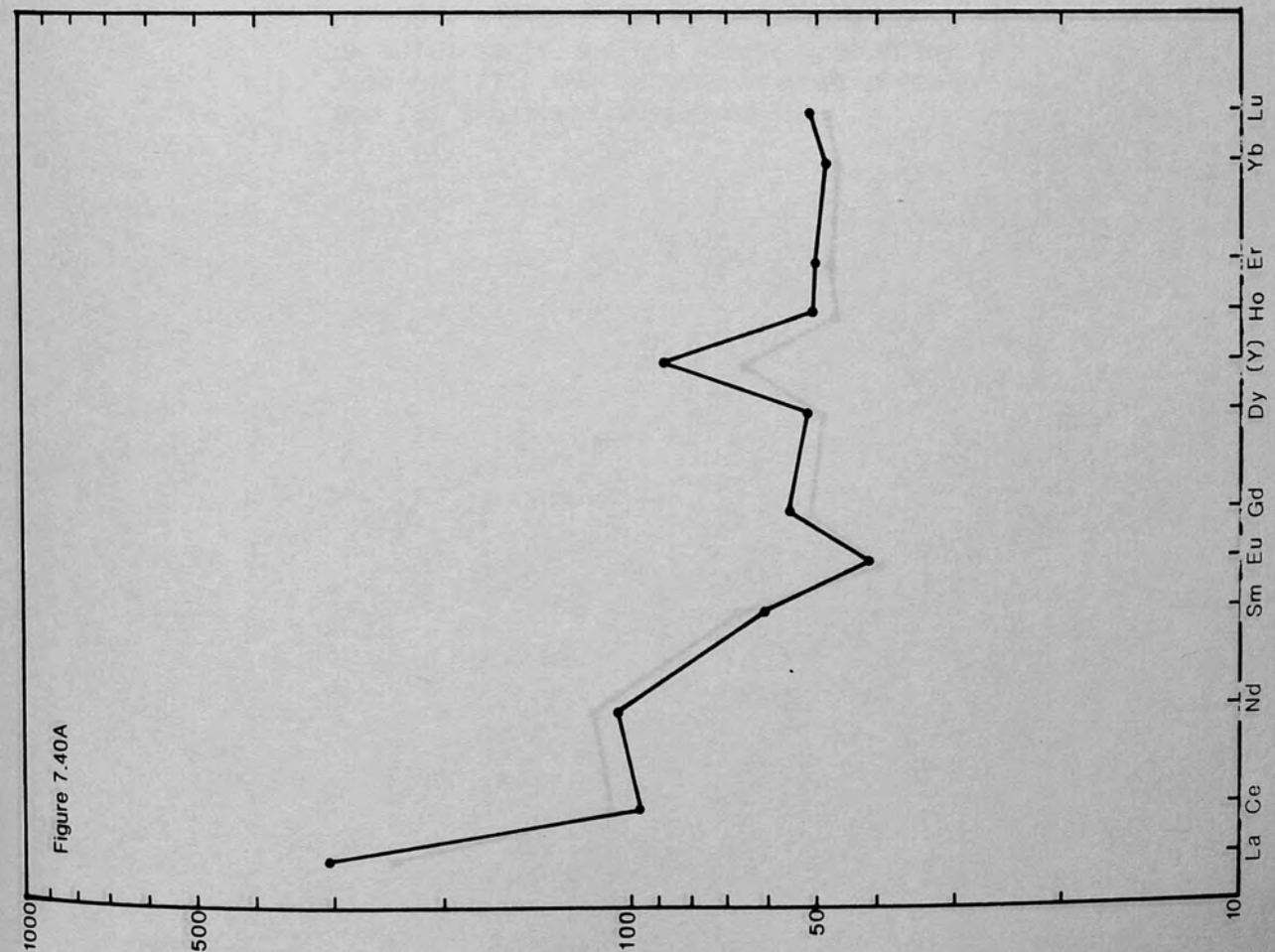
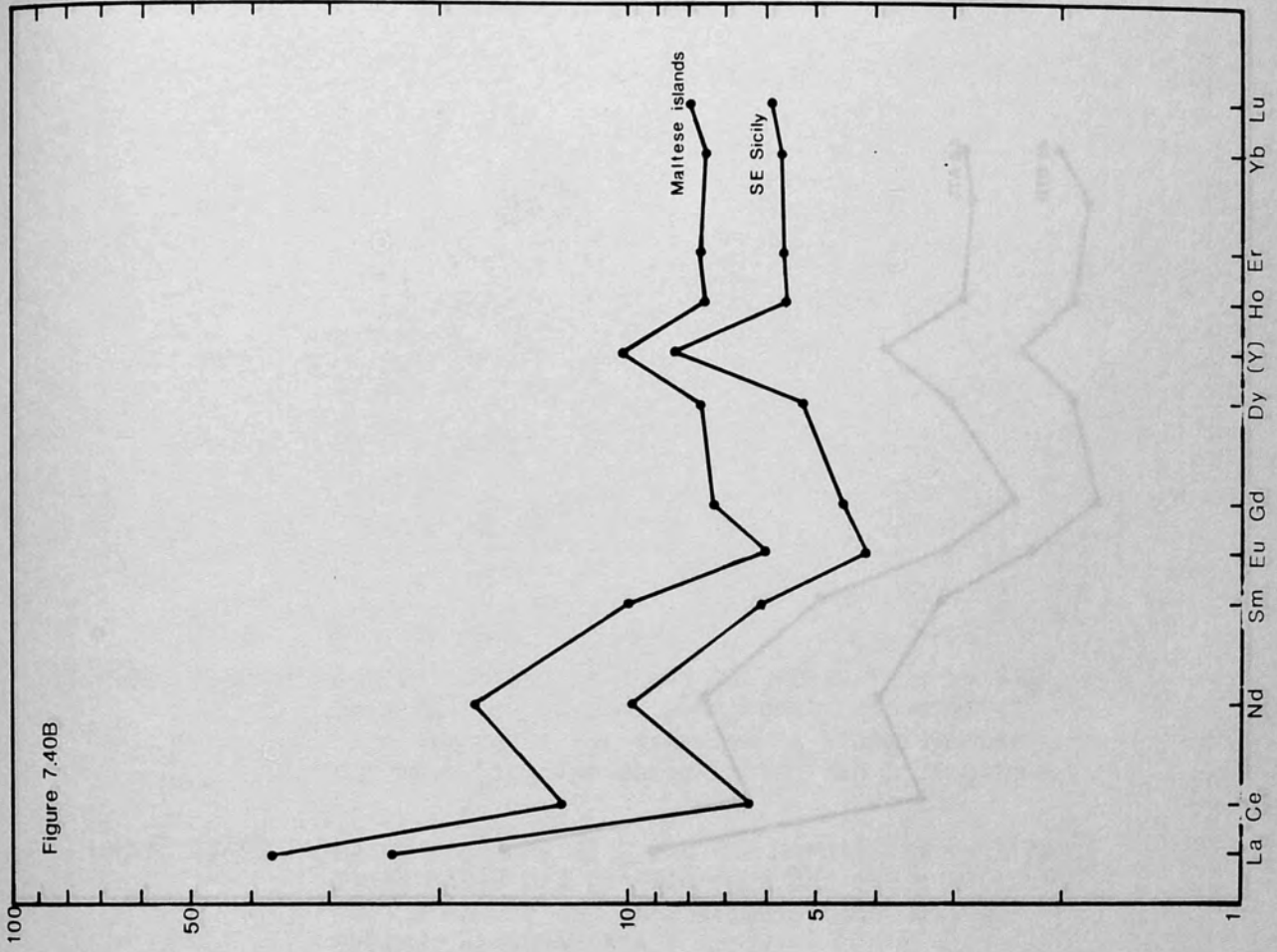
Figure 7.40 (A) mean southwest Sicily phosphorite and (B) mean Maltese islands phosphorite and mean southeast Sicily phosphorite.

Figure 7.41 (A) Florida phosphorite standard 120B and (B) southwest Sicily limestones.









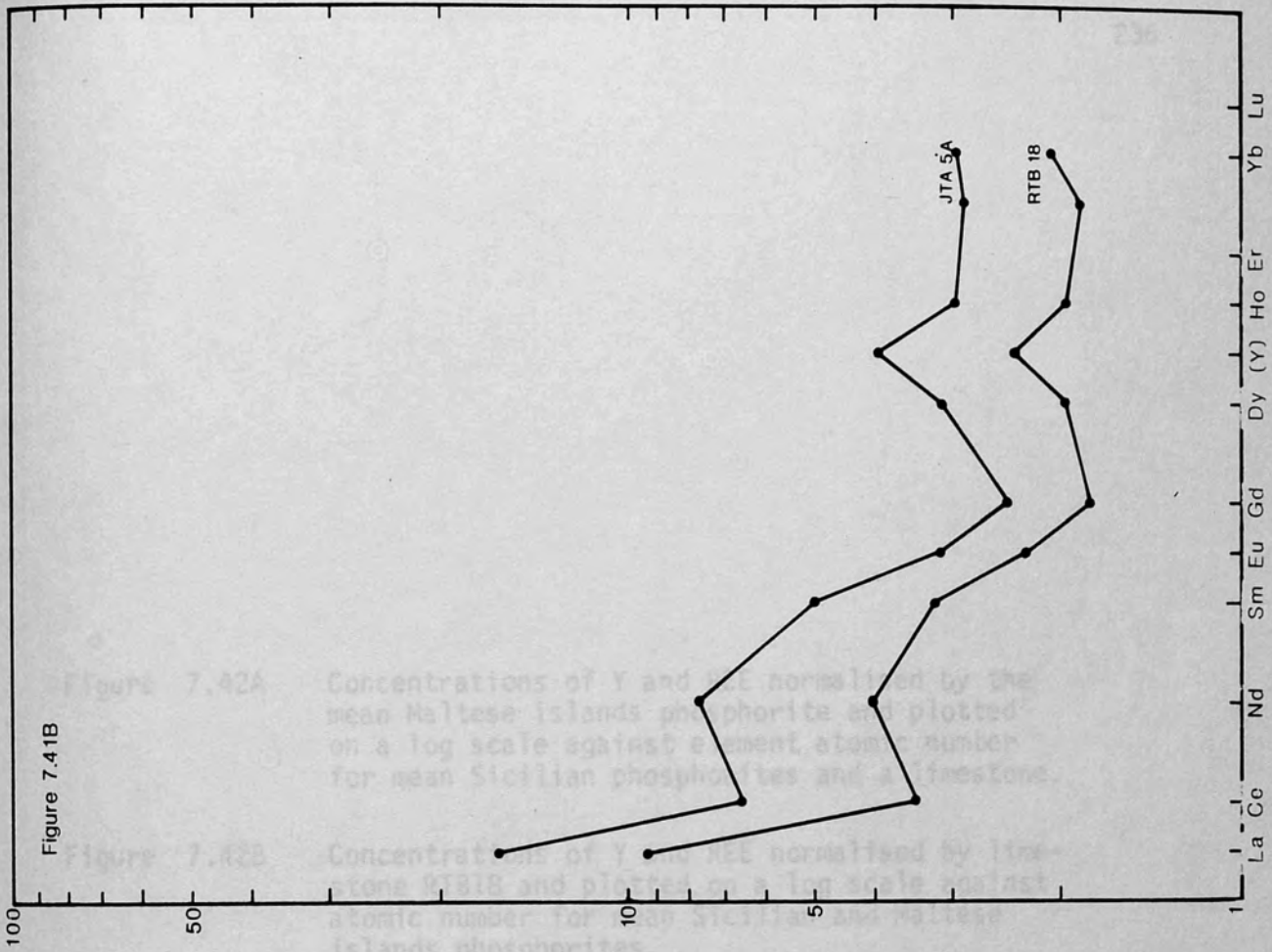


Figure 7.41B

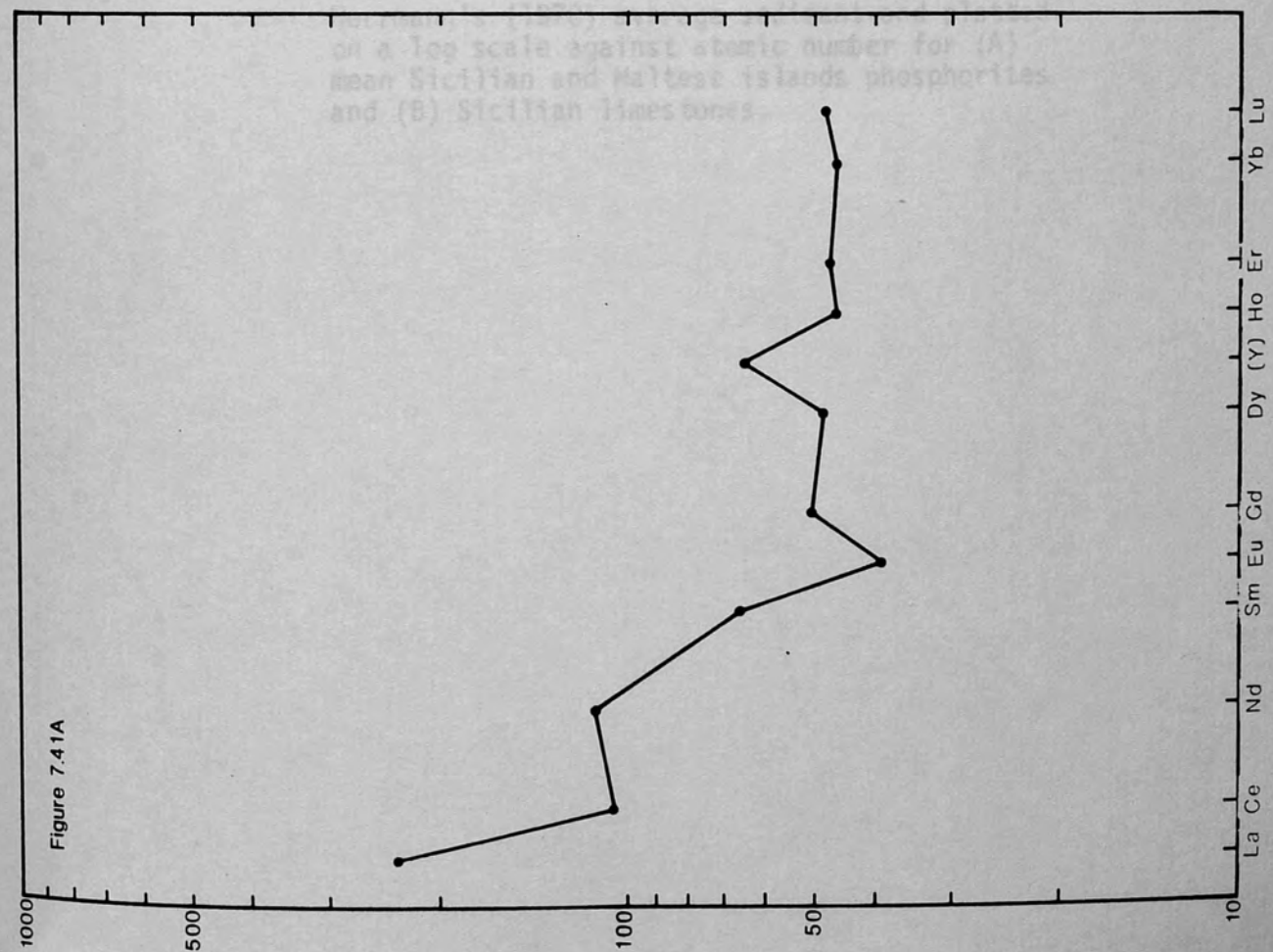


Figure 7.41A

Figure 7.42A Concentrations of Y and REE normalised by the mean Maltese islands phosphorite and plotted on a log scale against element atomic number for mean Sicilian phosphorites and a limestone.

Figure 7.42B Concentrations of Y and REE normalised by limestone RTB18 and plotted on a log scale against atomic number for mean Sicilian and Maltese islands phosphorites.

Figure 7.43 Concentrations of Y and REE normalised by Herrmann's (1970) average sediment and plotted on a log scale against atomic number for (A) mean Sicilian and Maltese islands phosphorites and (B) Sicilian limestones.

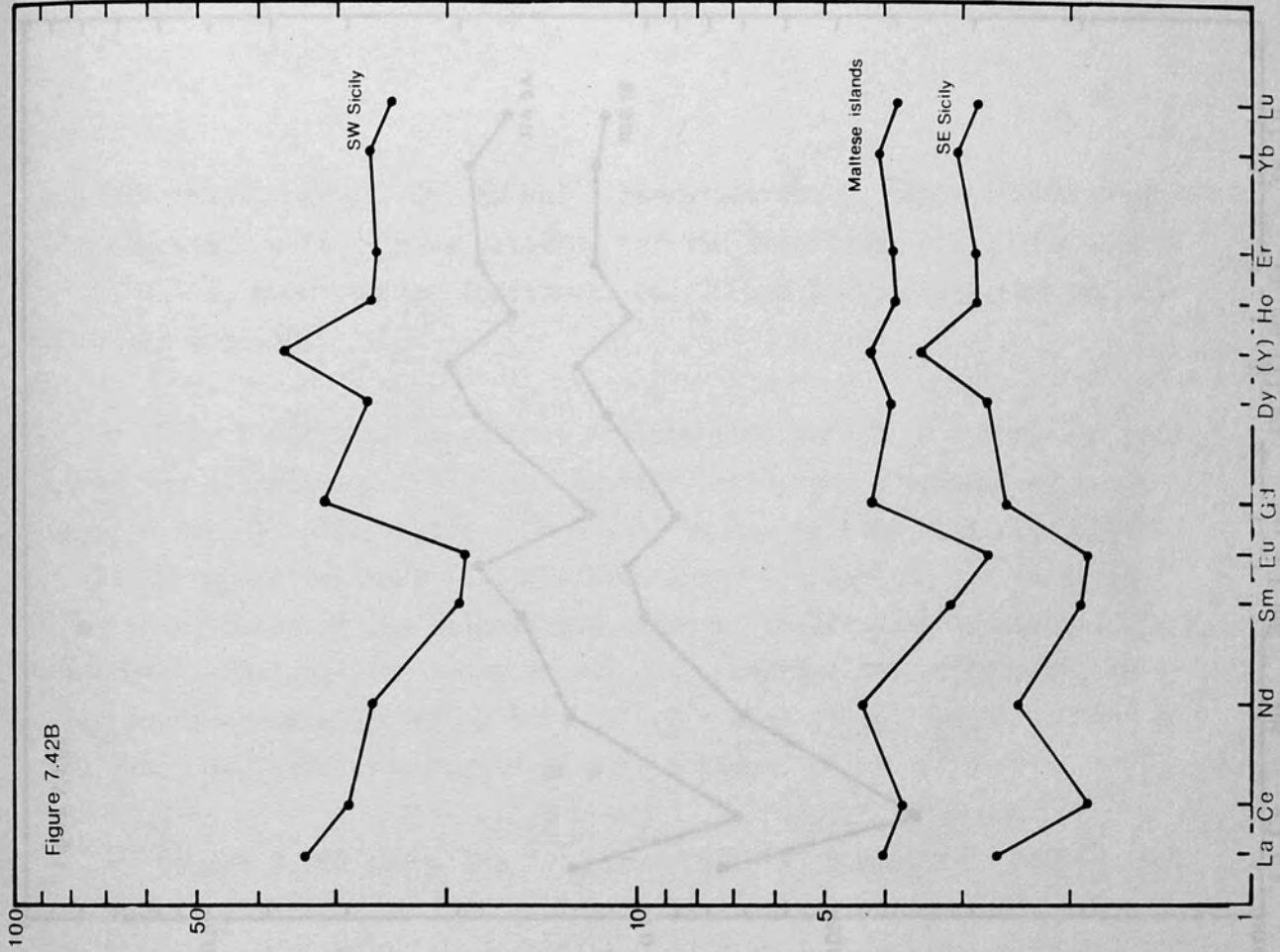


Figure 7.42B

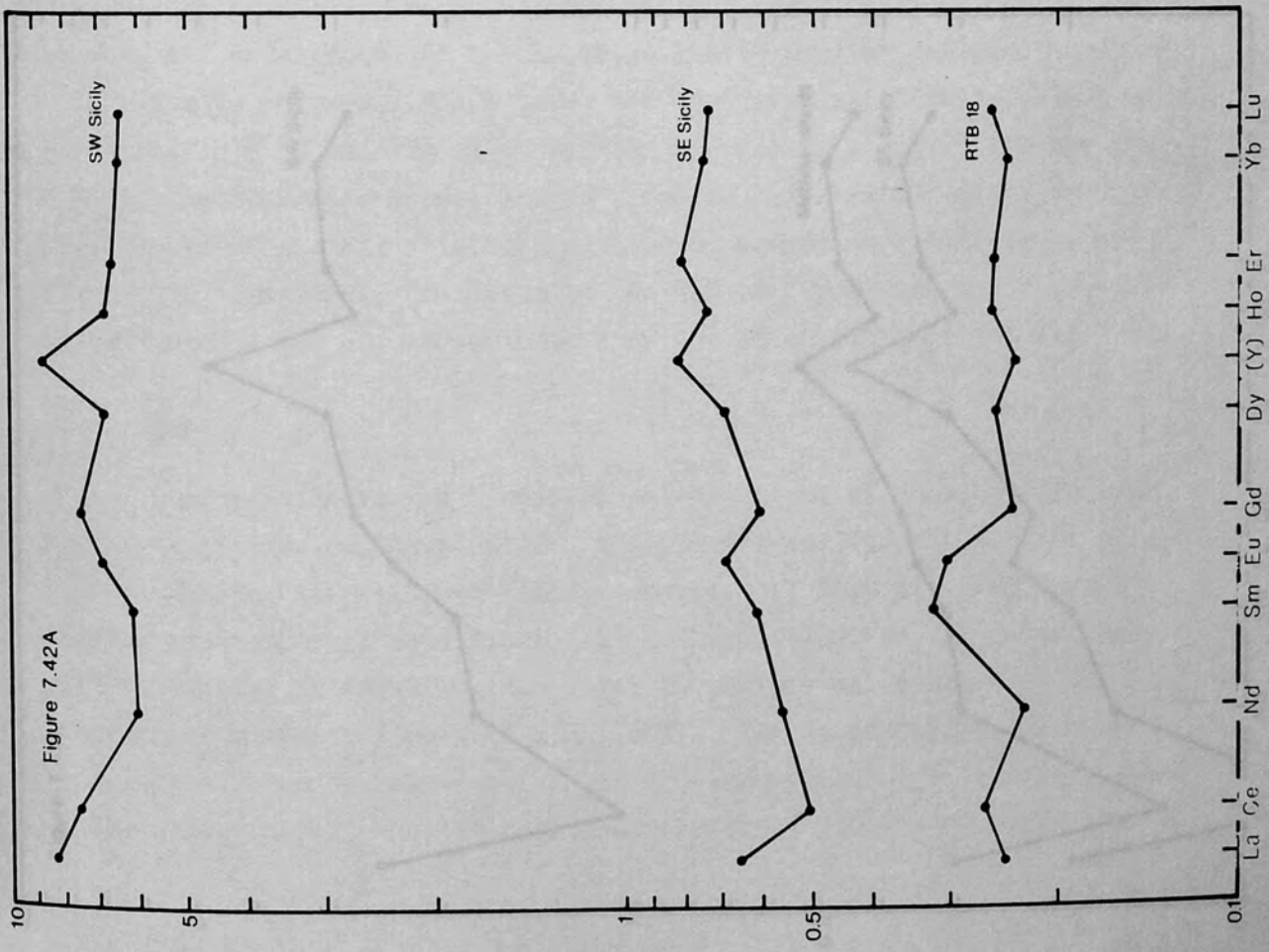


Figure 7.42A

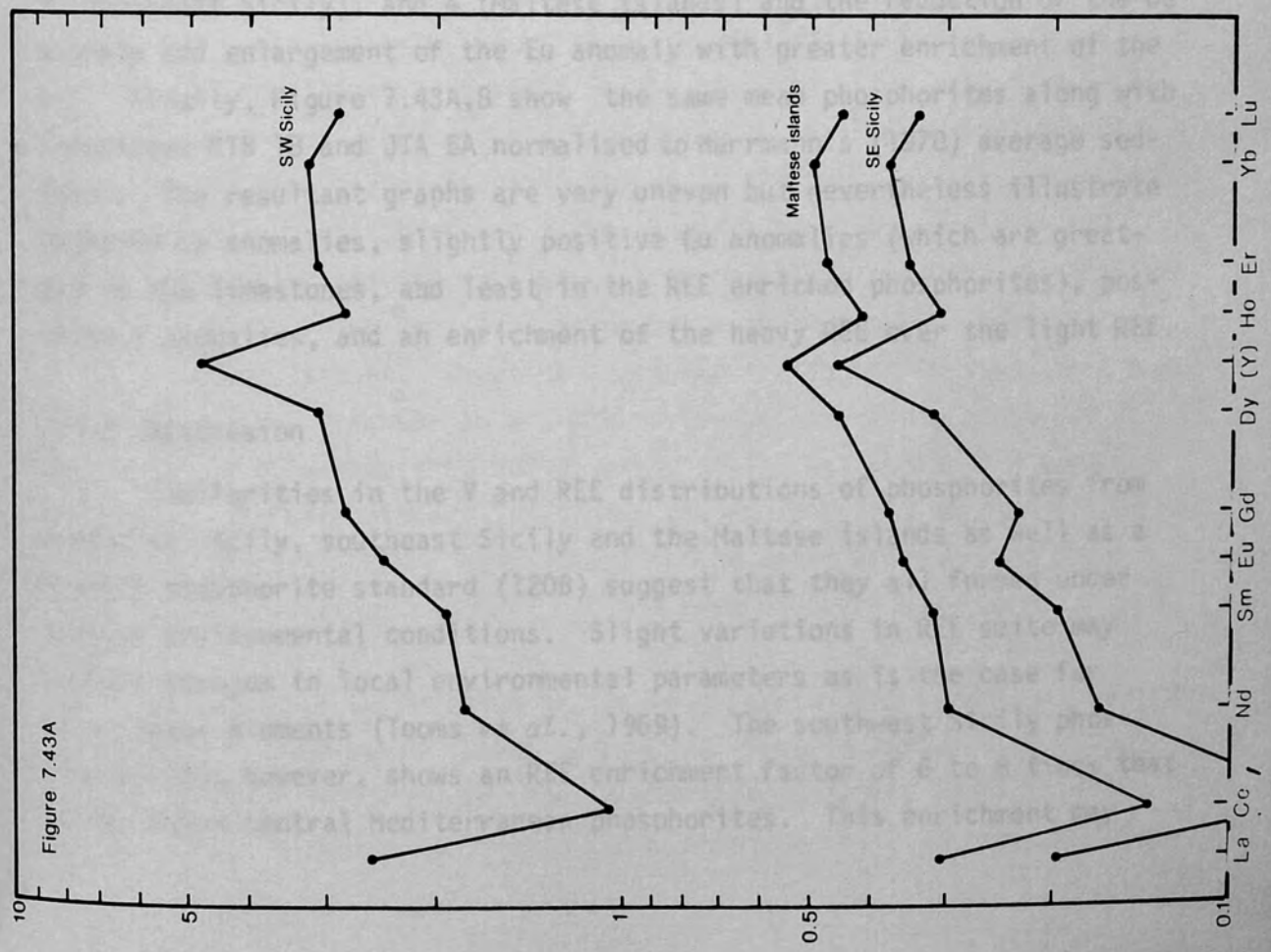
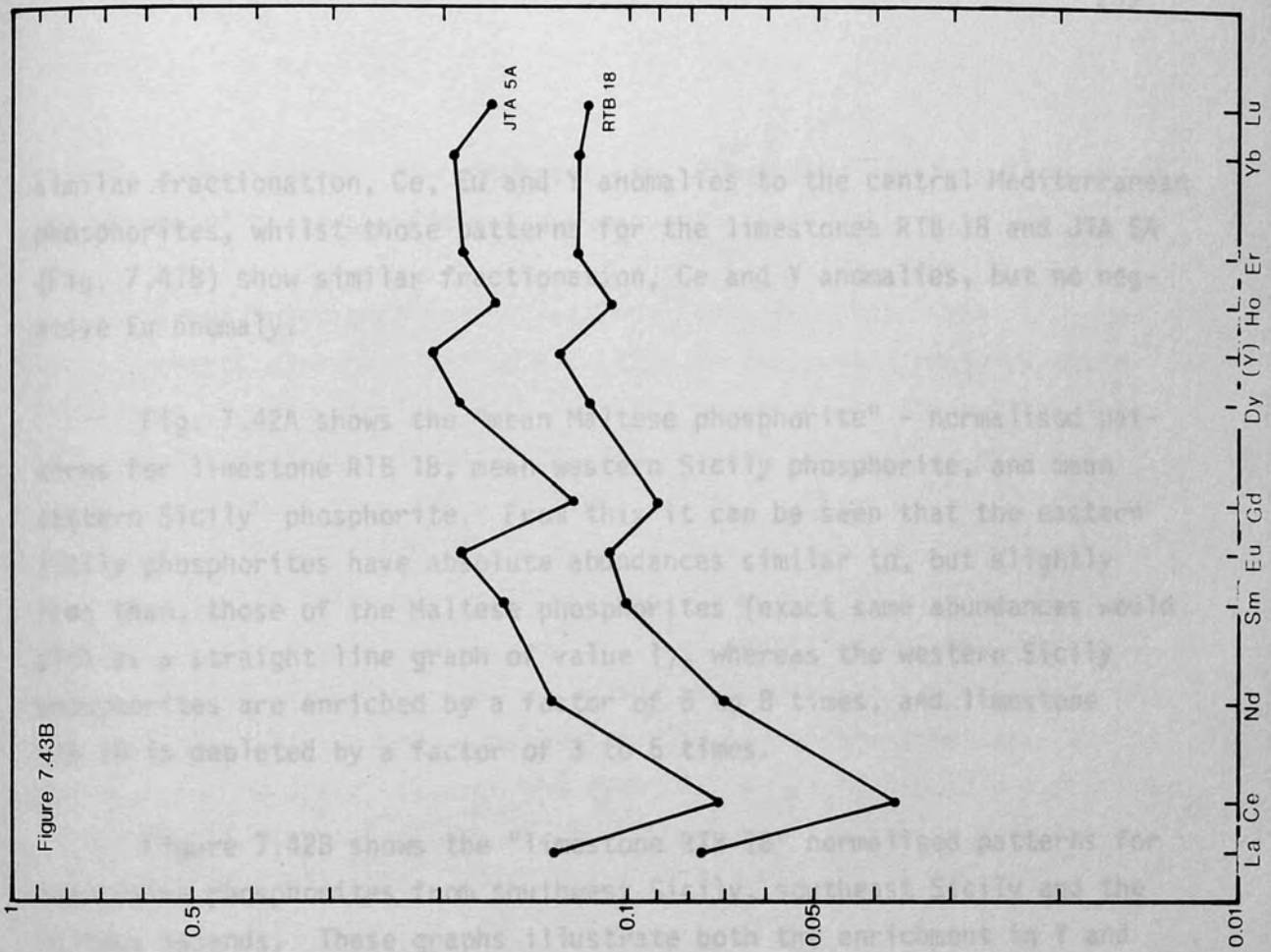


Figure 7.43B

Figure 7.43A

similar fractionation, Ce, Eu and Y anomalies to the central Mediterranean phosphorites, whilst those patterns for the limestones RTB 18 and JTA 5A (Fig. 7.41B) show similar fractionation, Ce and Y anomalies, but no negative Eu anomaly.

Fig. 7.42A shows the "mean Maltese phosphorite" - normalised patterns for limestone RTB 18, mean western Sicily phosphorite, and mean eastern Sicily phosphorite. From this it can be seen that the eastern Sicily phosphorites have absolute abundances similar to, but slightly less than, those of the Maltese phosphorites (exact same abundances would plot as a straight line graph of value 1), whereas the western Sicily phosphorites are enriched by a factor of 6 to 8 times, and limestone RTB 18 is depleted by a factor of 3 to 5 times.

Figure 7.42B shows the "limestone RTB 18" normalised patterns for mean value phosphorites from southwest Sicily, southeast Sicily and the Maltese islands. These graphs illustrate both the enrichment in Y and the REE relative to limestone RTB 18 by factors of 30 (southwest Sicily), 2 (southeast Sicily), and 4 (Maltese islands) and the reduction of the Ce anomaly and enlargement of the Eu anomaly with greater enrichment of the REE. Finally, Figure 7.43A,B show the same mean phosphorites along with limestones RTB 18 and JTA 5A normalised to Herrmann's (1970) average sediment. The resultant graphs are very uneven but nevertheless illustrate negative Ce anomalies, slightly positive Eu anomalies (which are greatest in the limestones, and least in the REE enriched phosphorites), positive Y anomalies, and an enrichment of the heavy REE over the light REE.

7.7.3 Discussion

Similarities in the Y and REE distributions of phosphorites from southwest Sicily, southeast Sicily and the Maltese islands as well as a Florida phosphorite standard (120B) suggest that they all formed under similar environmental conditions. Slight variations in REE suite may reflect changes in local environmental parameters as is the case for other trace elements (Tooms *et al.*, 1969). The southwest Sicily phosphorite, however, shows an REE enrichment factor of 6 to 8 times that of the other central Mediterranean phosphorites. This enrichment may

reflect longer periods of phosphatisation (see below) or formation of the phosphorites at a different geologic time (see Notholt, 1980b).

Strong fractionation and relative light REE enrichment is of common occurrence elsewhere and no exception in the central Mediterranean limestones and phosphorites. It has been recorded for the average granitic and intermediate igneous rocks and average sediment by Herrmann (1970), and for average shale by Piper (1974). REE in marine waters are considered by Piper (1974) to be derived from the weathering of continental rocks with subsequent transport to the oceans by surface run off. The bulk of continental rocks are relatively enriched in the light REE, and this is inherited by river water and in turn by shallow oceanic water (Piper, 1974). Deep ocean waters, however, show a relative enrichment in the heavy REE over the light REE which is probably a function of the longer residence times of the former over the latter (Goldberg *et al.*, 1963; Høgdahl *et al.*, 1968; Piper, 1974).

The light REE/heavy REE fractionation seen in the central Mediterranean phosphorites and limestones is probably due to availability (as is true for trace elements, Tooms *et al.*, 1969) and is inherited from the original fractionation present in the seawater. The predominance of light REE over heavy REE suggests deposition in shallow rather than deep water and the slight enrichment in the heavy REE relative to average sediment may reflect enrichment in these elements from the upwelling of deeper ocean waters or the ease of ability for limestones and phosphorites (rather than other sediments) to incorporate these elements in the calcite or apatite lattice. Previous light REE enrichment in limestones has been recorded for Precambrian and Carboniferous limestones by Haskin & Gehl (1962) for Recent coral and assorted shells by Schofield & Haskin (1964); and for mid-Tertiary limestones and phosphorites on the Maltese islands by Bennett (1980). Enrichment in the heavy REE over the light REE relative to average sediment has not been recorded elsewhere.

Depletion of Ce relative to its neighbouring REE is well documented in the marine environment (Goldberg *et al.*, 1963; Høgdahl *et al.*, 1968; Piper, 1974) and in marine authigenic minerals (Goldberg *et al.*, 1963; Bennett, 1980; Fleet *et al.*, 1980). Depletion of Ce in the phosphorites

may be, in part, inherited from that already present in the limestones (concluded by Bennett, 1980), but, for the greater part, it is inherited from the seawater. This can be said for two reasons:

1) The absolute REE abundances for the phosphorites are greater than those for the limestones. This introduction of REE must be from the seawater with subsequent incorporation in the authigenic francolite.

2) There is a reduction in the size of anomaly with an increase in the absolute abundances of the elements (Fig. 7.42B). This may be a function of the lower residence time of Ce in seawater (recorded by Goldberg *et al.*, 1963) along with longer periods of phosphatisation, allowing relatively more Ce along with greater absolute abundances of REE to be incorporated in the carbonate apatite lattice.

Negative Eu anomalies have previously been recorded in phosphorites by Semenov *et al.* (1962) and by Bennett (1980); in glauconites by Fleet *et al.* (1980), and it is present in the average sediment of Herrmann (1970). However, depletions of Eu are not always associated with marine phosphorites (Goldberg *et al.*, 1963). Under normal conditions Eu exists in a trivalent state, but it can be reduced to 2^+ . In the marine environment Eu will occur in concentrations conformable with those of its adjacent REE (Goldberg *et al.*, 1963; Høgdahl *et al.*, 1968). Its depletion in the phosphorites may therefore reflect its reduction to the bivalent state. Present day phosphorites are known to form in mildly reducing conditions (Baturin, 1969; Veeh *et al.*, 1973; Burnett, 1980; Odin & Letolle, 1980) which would be likely to reduce only some of the Eu present. Depletion of Eu in the phosphorites may therefore reflect its partial reduction and incorporation of one fraction (either the reduced Eu^{2+} or the normal Eu^{3+}) in the carbonate apatite lattice, or uptake of all Eu with subsequent loss of the less tightly held Eu^{2+} by weathering. The observed Eu deficiency in the phosphorites therefore supports inferences that phosphorites form under mildly reducing conditions (Bennett, 1980; Odin & Letolle, 1980).

Y enrichment (relative to the heavy REE) has previously been recorded in seawater by Høgdahl *et al.* (1968) but has never been recorded in marine authigenic or biogenic minerals. The anomaly is not present in

the NIM G (granite) distribution (analysed at the same time as the phosphorites) suggesting that it is not due to analytical error. It is however, present in both limestones and phosphorites. Its presence in the Florida phosphorite standard 120B (Fig. 7.41A) precludes any suggestion that the anomaly in the central Mediterranean phosphorites is due to an enrichment in the Tethys sea. It may, however, be explained by Y^{3+} replacing the abundant Ca^{2+} ion (a feature of common occurrence, Howlett, pers. comm. 1981) in the limestones and phosphorites but which is much less abundant in the NIM G granite standard. There is no positive regression correlation between Y and CaO to suggest that the former is replacing the latter, but this relationship could be masked by the composite form of the samples and by other elements replacing Ca^{2+} .

In summary therefore, it appears that the similarities in REE distribution including Ce depletion reflects a pattern inherited by the phosphorite from seawater, and to a lesser extent, from the limestone precursor. Eu depletion reflects formation in a mildly reducing environment and Y enrichment reflects the ease of ability for the Y^{3+} ion to replace the Ca^{2+} ion. Phosphatisation has resulted in the enrichment of all the REE. Similarities in the distribution of the REE from the phosphorites of the three main collecting localities in the central Mediterranean area and including the Florida phosphorite standard (120B) suggests that they formed under the same physico-chemical conditions.

7.8 Phosphorite Palaeogeography, Formation and Environments

7.8.1 Palaeogeography

Kasakov (1937) was the first to propose the now widely accepted concept that the upwelling of cold ocean waters, rich in nutrients including phosphate, onto coastal shelves, could bring about the formation of phosphorite deposits. Conditions conducive to upwelling are given in Freas & Eckstrom (1968) and include: situations where ocean currents flow parallel to the coast, or just offshore, and are enhanced by prevailing winds in the same direction; where ocean currents flow over topographic highs; in the trade wind belts ($0-40^{\circ}$ north and south); along the north and west coasts of continents in the northern hemisphere, and

the south and west coasts in the southern hemisphere; along the coasts of continents with arid climates; along coasts in the belt of westerlies (20-40° north and south); and in large open basins with unrestricted circulation and open connection to the polar seas.

An estuarine source and depositional environment was proposed by Bushinski (1964) and Pevear (1966) to account for the formation of phosphorites in the western U.S.A. This, however, would only be possible if deposition occurred under an arid environment, preferable off a landmass of limestone terrain (Pevear, 1966) since estuaries are areas of rapid clastic sedimentation which would inhibit phosphate accumulation.

However, McKelvey *et al.* (1959) suggest that the mechanism of upwelling is more than adequate to account for the considerable quantities of phosphate found in phosphorites. Care should be taken, however, to stress that upwelling does not supply phosphate-rich water (Bentor, 1980). Rather, its effect is to counteract P-depletion of surface water by biological activity by providing a continuous or seasonal, although dilute (70-100 ppb), supply of P and other nutrients.

The central Mediterranean phosphorites are consistent with the constraints set out by Freas & Eckstrom (1968) and confirmed, to some extent, by Cook & McElhinny (1979). They are deposited in a tropical-subtropical environment (Section 4.1.4, and Bennett, 1980) on topographically high areas. Burollet (1967) shows southwest Sicily, southeast Sicily and Malta to be situated on positive areas within and bordering Lower Miocene subsiding troughs. Bennett (1980) further suggests that the Maltese phosphorites were formed on local topographic high areas.

7.8.2 Phosphate Mineral Formation

Two quite different models have been proposed for the deposition of marine phosphate minerals: direct inorganic precipitation, and phosphatisation of a pre-existing limestone.

Kasakov's (1937) original hypothesis stated that upwelling of cold ocean currents led to the direct inorganic precipitation of apatite onto

the sea-floor. Although the idea of upwelling being an important factor in phosphogenesis has been accepted, Kasakov's dominantly inorganic mechanism for precipitation has now been abandoned for a number of reasons (listed in Bentor, 1980).

Phosphatisation of a pre-existing limestone was first inferred by Emigh (1958, 1967) who noted that pelletal phosphorites often had limestone precursors. Ames (1959, 1960) revealed through laboratory experiments that calcite powder through which a dilute phosphate solution is percolated at room temperature easily converts to apatite. There is ample evidence that this process - phosphatisation - occurs in nature: Dietz *et al.* (1942), Hamilton & Rex (1959), and D'Angeljan (1967, 1968) have all discovered phosphatised foraminiferal tests and micritic lime mud. Pevear (1966) stated that the inorganic replacement of CaCO_3 was the only reasonable method of phosphorite formation.

However, studies of Recent phosphorites off southwest Africa by Baturin (1969), Romankevitch & Baturin (1972), Baturin & Bezrukow (1979) and Birch (1980) have documented precipitation of, and replacement by, carbonate-apatite, occurring at the present day below the sediment water interface. Manheim *et al.* (1975) reported the replacement of Pleistocene foraminiferal tests off Peru whilst Burnett (1977) described, from the same deposit, free growth of apatite crystals. It appears, therefore, that marine phosphorites may be formed by both precipitation of, and replacement by, carbonate-apatite. Furthermore, Bentor (1980) and others would suggest that there is some little understood organic control on both events since Recent phosphorites are often associated with organic matter-rich sediments.

The central Mediterranean phosphorites show petrographic fabrics which suggest both direct precipitation and replacement of pre-existing limestone. The latter is more common and is the dominant form of carbonate apatite in all three collecting areas (southwest Sicily, southeast Sicily, Maltese islands) where it replaces lime mud, foraminifera and (possibly) calcite crystals. Direct precipitation is of restricted occurrence in the Maltese phosphorites only, where it occurs as thin coatings on grains and hardground surfaces, and as pore-lining cement in

some phosphorites.

7.8.3 Phosphorite environments

The formation of carbonate apatite in the marine environment is apparently controlled by a number of physical parameters which include: depth, salinity, Eh, pH, slow deposition, and organic interaction.

Depth: Kasakov (1937) considered that phosphorites formed at depths between 50-200 m; McKelvey *et al.* (1953) suggest depths between 200-1000 m; Veeh *et al.* (1973), 100-400 m; and Burnett (1980), 100-400 m. Cook (1976) regards depth of less than 500 m as optimum for phosphorite formation. The source of upwelling off the Namibian coast is only about 200 m deep (Calvert & Price, 1971).

Salinity: From a study of ancient and present day phosphorites, Cook (1976) concluded that they form in waters of normal salinity. Martens & Harris (1970) have shown, through laboratory experiments, that carbonate-apatite precipitation is critically dependent of the Mg^{2+}/Ca^{2+} ratio in the aqueous solution, and not possible in normal seawater (with a ratio value of 5.3). In Mg free seawater (a situation found in pore-fluids, Bendor, 1980) however, precipitation of carbonate-apatite and phosphatisation of any $CaCO_3$ present is possible.

Eh: Recent phosphorites are forming in reduced sediments and are often associated with glauconite, a mineral considered to form in mildly reducing environments (Bendor, 1980; Odin & Letolle, 1980), though strongly negative values of Eh are not required and probably not conducive to phosphorite formation. Thus Veeh *et al.* (1973), Burnett (1980) and Burnett *et al.* (1980) found that phosphorites form presently on the Peru-Chile continental slope throughout the entire breadth of the oxygen minimum belt: a zone within which minor oscillations between positive and negative Eh occur. Baturin *et al.* (1970) measured an Eh of -210 mV in the phosphorites off Namibia.

pH: Baturin (1969) and Cook (1976) suggest that phosphorites form in mildly alkaline environments, and that this is the primary controlling factor. In areas of Recent phosphorite deposition pH values in the interstitial water of less than 7.5, and between 7.2 and 7.5, have persistently been measured (Bendor, 1980).

Slow deposition: Accumulation of phosphorite is known to occur with sea floor exposure over long periods of time. Thus phosphorites of Pleistocene age are found in active phosphate belts off the coast of Peru today (Manheim *et al.*, 1975; Burnett, 1977). Phosphatisation and phosphorite conglomerates are often found associated with submarine hardgrounds (Bromely, 1975; Bennett, 1980; Jarvis, 1980) which are themselves sites of non-deposition with prolonged exposure on the sea floor.

Organic interaction: The role played by organic material is little understood. Recent phosphorites are found associated with organic rich sediments (Birch, 1980; Burnett, 1980; Notholt, 1980b). Bentor (1980) argues that phosphorus is concentrated by the organic material and is then regenerated to enrich the interstitial pore-fluids in which crystallisation and replacement occur.

There is nothing to suggest that the central Mediterranean phosphorites formed in environments with constraints other than those listed above. They have formed in sediments which are thought to accumulate in water depths of 50-300 m; those of the Maltese islands have a parallel occurrence with glauconite therefore suggesting formation in mildly reducing conditions; and both the southeast Sicily and Maltese phosphorites are associated with submarine hardgrounds. Boring on these hardgrounds and in the phosphatised clasts of the southwest Sicily phosphorite suggests prolonged exposure on the sea floor.

7.8.4 Central Mediterranean Phosphorites

The depositional environment of the southwest Sicily phosphorite is essentially a secondary one since it is inferred that the phosphatic clasts are reworked from an older Eocene deposit. The primary environment, however, can be elucidated by reference to clast rock type, trace fossils, petrography and REE geochemistry.

Variably bored and eroded chalk rock forms the phosphatised clasts. The Cretaceous to Eocene chalks of Europe and north Africa can be interpreted, on general faunal and sedimentological grounds, as being deposited in open shelf seas in depths of 50-300 m (Kennedy, 1975). The bored clast

surfaces indicate prolonged exposure as lithified clasts on the sea floor prior to phosphatisation which occurred below the sediment water interface indicated by the phosphatisation of the infills to the borings together with the clasts themselves. The negative Eu anomaly discovered in the REE distribution may reflect a reducing environment for phosphatisation.

In both southeast Sicily and the Maltese islands there is local formation and phosphatisation of submarine hardgrounds with subsequent erosion and deposition of phosphorite conglomerates. Both areas show the phosphorites enclosed in similar limestone facies which are analogous to previously described ancient shelf sea carbonates (e.g. Kennedy, 1975; Wilson, 1975). The presence of the trace fossil *Thalassinoides suevicus* implies open shelf sea conditions and depths of 50-300 m *vide* Kennedy (1975). Its abundance in the beds below the hardgrounds in both areas indicates slow deposition prior to hardground formation. Hardground formation with extensive boring activity on the hardground surface suggests non-deposition and prolonged exposure on the sea floor. That phosphatisation occurred below the sediment water interface or in restricted microenvironments is evidenced by its replacement of lime mud matrix in the sediment and within foraminiferal chambers. Finally, formation of the phosphate minerals in locally mildly reducing conditions may be indicated by the negative Eu anomaly, but is evidenced by the parallel formation of glauconite in the Maltese phosphorites.

Burollet (1967) shows both southeast Sicily and the Maltese islands to be situated on positive areas bordering Lower Miocene subsiding troughs to the northwest. Inferred current directions for these times are predominantly easterly - southeasterly (Sheldon, 1964; Fell, 1967). The combination of these two factors would result in upwelling and possible phosphorite formation. Slow deposition, and non-deposition recorded in southwest Sicily and the Maltese islands may reflect uplift of these areas and presumably upwelling currents provided the necessary phosphate and subsequent erosion of the hardgrounds to produce the phosphorite conglomerates.

7.9 Conclusion

The analyses presented above have shown that these central Mediterranean phosphorites are composed of only one carbonate-apatite mineral: carbonate fluorapatite (francolite), having an estimated F content of 2.3%. All phosphorite samples are composite containing both francolite and calcite. Francolite is secondary, found replacing lime mud, foraminifera and possibly calcite crystals. It is present as two optically distinguished forms: as dark brown to opaque amorphous spots and laminae, and as light yellow brown to orange brown areas isotropic to sub-isotropic in nature. This second optical type is additionally found forming primary laminar coats on hardground surfaces and multiple coatings on phosphorite conglomerate clasts in the Maltese islands succession. The mineral in this form has been identified as dahllite by Bennett (1980).

Major element analyses have shown that all the elements except Ca and Mg are enriched in the phosphorites relative to the pure limestones. This, along with positive correlation of the elements with P_2O_5 and negative correlation with CaO, suggests that the elements are located in the francolite lattice. High variance in these plots is probably due to multiple substitution of the Ca^{2+} ion by the elements, and to a lesser extent due to location of some of the elements (Si, Al, Fe, K and Ti) within minor quantities of quartz, glauconite and clay minerals within the phosphorites.

Trace element analyses for Sc, V, Ni, Cu, Sr, Zr and Ba have shown that all but Sc are enriched in the phosphorites in comparison to the limestones. For the same reasons as above, the trace elements are thought to be located, for the greater part, in the francolite. Depletion of Ba and the enrichment of Sc in the central Mediterranean phosphorites relative to the average phosphorite (Altschuler, 1980) probably reflects the availabilities of these ions at the time of formation of the phosphorites rather than any physico-chemical factors. Higher relative abundances of Sr in the younger southeast Sicily and Maltese phosphorites in comparison to the older southwest Sicily phosphorite may be a result of weathering loss from the older deposits.

Y and REE analyses have demonstrated the fractionation of the light REE over the heavy REE in both phosphorites and limestones, along with a Ce negative anomaly and a Y positive anomaly, all believed to be inherited features from seawater. An Eu negative anomaly, however, is found only in the phosphorites and may reflect formation in a mildly reducing environment.

Major element, trace element and REE analyses show similarities between the southeast Sicily and Maltese phosphorites but that these differ from the southwest Sicily phosphorite. These differences and similarities are also seen in lithology and age. The southwest Sicily phosphorite comprises phosphatised chalks of Eocene age whilst the southeast Sicily and Maltese phosphorites are phosphatised benthonic and planktonic foraminiferal wackestones of Lower Miocene age, in both cases associated with hardground formation. The geochemical fingerprint of the southwest Sicily phosphorite is significantly different to suggest that it belongs to a different phosphogenic episode than the Lower Miocene southeast Sicily and Maltese phosphorites which have similar geochemistries. The exclusive Eocene date of the phosphatised clasts might suggest that they are in some way associated with the Cretaceous to Eocene phosphorites of north Africa.

The southeast Sicily and Maltese hardgrounds are envisaged as forming on topographic highs with little or no deposition and with subsequent erosion to form phosphorite conglomerates. Upwelling, to produce the phosphatisation, is thought to be from the northwest. Along with the southwest Sicily phosphorite, they are thought to form in water depths of 50-300 m; in mildly reducing environments; and phosphatisation is thought to take place below the sediment water interface.

In conclusion, it is inferred that the continent-ocean configuration, prevailing current direction, sea floor topography, climate of the adjacent continent and latitude were the major features of the palaeo-environment which led to formation of these Tertiary phosphorites in the central Mediterranean area, and that this pattern is consistent with the general pattern of phosphorite palaeoenvironmental origins advocated by Freas & Eckstrom (1968).

CHAPTER 8

CONCLUSION

8.1 Stratigraphy

8.1.1 Upper Oligocene Limestones

The Upper Oligocene limestones are characterised by light grey weathering massive beds of poorly sorted coarse grained bioclastic packstones and grainstones containing abundant *Lepidocyclina* benthonic foraminifera and common algal rhodoliths. These limestones are divisible into two facies which differ in their major constituents, rock type and macrofauna (Section 2.4): a foraminiferal grainstone-packstone facies and a rhodolithic algal packstone-wackestone facies. Apart from foraminifera, only three invertebrates are locally common: a large cassiduloid echinoid, *Echinolampas* cf. *visedoi* Lambert; a moderately large clypeasteroid echinoid of low profile, *Clypeaster* cf. *villaplanae* Cotteau; and isolated valves of a large, strongly ribbed species of the pectinid bivalve *Chlamys*.

Only three formations spanning Upper Oligocene sediments have so far been defined in Sicily: the Ragusa Formation of Middle Eocene to Middle Miocene shelf carbonates (Rigo & Barbieri, 1959); the Bonifato Formation of Upper Oligocene to Lower Miocene deep shelf glauconitic limestones (Schmidt di Friedberg, 1962); and the Numidian Flysch Formation of Upper Oligocene to Lower Miocene siliciclastic sediments (Wezel, 1966). Clearly, the Upper Oligocene shallow water shelf carbonates described here correspond more closely in lithofacies with the Ragusa Formation than either of the other two. Moreover, they correspond more closely with the benthonic foraminiferal calcarenites and calcirudites of its Irminio Member than with the fine grained sometimes nodular bedded limestones of the underlying Leonardo Member. However, since the Irminio Member has been reliably dated as Lower Miocene (Aquitanian to Burdigalian) in age on the basis of contained planktonic foraminifera (especially *Globigerinoides primordius* and *G. sicanus*) (Di Grande *et al.*,

1977), use of this formation/member name for the limestones of southwest Sicily would imply that the Irminio Member is diachronous.

The limestones are characterised by a benthonic foraminiferal association typically of sub-equal abundances of *Lepidocyclina* (*Eulepidina*) *dilatata*, L. (*Nephrolepidina*), *Spiroclypeus*, *Amphistegina*, *Pararotalia*, *Rotalia*, *Cycloclypeus* and *Heterostegina/Operculina* with some *Miogypsinoidea complanatus* and *Miogypsina*. The presence of *Miogypsinoidea complanatus* along with the presence but paucity of *Miogypsina* suggests that the limestones belong to the Chattian Stage of the Upper Oligocene (Section 2.1.4). Closely similar associations are well known from the Upper Oligocene elsewhere in the Tethyan realm, and have been recorded from the: Maltese islands (Felix, 1973; Bennett, 1980), southern Italy (Afchain, 1966) central Italy (Pieroni, 1965), northern Italy (Cita, 1965), Somalia (Azzaroli, 1958) and Australia (Chaproniere, 1975).

8.1.2 Lower Miocene Limestones

The Lower Miocene limestones are represented by well bedded, moderately sorted, sand sized, bioclastic grainstones with a common glauconite and quartz sand content. They are separable into a lower glauconitic limestone facies and an upper sandy limestone facies. Macrofauna has not been found.

The limestones have been previously correlated with the Bonifato Formation (Section 3.1.3) defined by Schmidt di Friedberg (1962) to comprise the Upper Oligocene-Lower Miocene glauconitic limestones of western Sicily. In contrast, the only two other formations spanning mid-Tertiary (Upper Oligocene - Lower Miocene) sediments in Sicily are characterised by non-glauconitic shelf limestones (Ragusa Formation) or siliciclastic deposits (Numidian Flysch Formation).

The benthonic foraminiferal association identified from these limestones is characterised by common to abundant *Miogypsina* along with *L.* (*Nephrolepidina*), *Amphistegina*, *Heterostegina/Operculina*, *Rotalia*, *L.* (*Eulepidina*), *Spiroclypeus*, *Sphaerogypsina* and undifferentiated small Rotaliids, Textulariids and Nodosariids. Correlation with the Lower

Miocene (Aquitanean - Burdigalian) is indicated by the relative abundance of *Miogypsina* (Section 3.1.4) and, according to Blondeau *et al.* (1972) and Mascle (1979), the identification of *Miogypsina cf. gunteri* and *Miolepidocyclina cf. burdigalensis* from some localities. (This Lower Miocene age is also suggested by the presence of Upper Oligocene - Lower Miocene (Aquitanean) argillaceous sediments with a rich planktonic fauna (Section 3.1.4) situated conformably below these glauconitic sandy limestones). Similar *Miogypsina*-rich limestones are known from the Lower Miocene of southeast Sicily (Di Grande *et al.*, 1977), central Italy (Pieroni, 1965) and northern Italy (Cita, 1965) where, in the last case, they are also associated with glauconitic limestones.

8.1.3 Palaeogene-Neogene Boundary

That there is little change in benthonic foraminiferal associations across the Palaeogene - Neogene (Oligocene/Miocene) boundary has been known for some years (Adams, 1973; Senes, 1976). The presence, therefore, of similar foraminiferal associations here, in both Upper Oligocene and Lower Miocene limestones, is unsurprising. The foraminifera, however, are mostly identified only to generic level. Identification to species level may indicate more significant change and facilitate more precise (zonal) correlation and such a study is currently in progress by my colleague John Elliott of Bedford College (University of London) (Elliott, in prep.). The containing sediments do, however, record a marked change in the sedimentary regime: from pure limestones (on the Saccense Carbonate Platform, Chapter 2) and argillaceous deposits (in the Sicani Basin, Section 3.3.2) of Upper Oligocene age, to glauconitic limestones of Lower Miocene age throughout.

On the Saccense Carbonate Platform there is evidence for at least a local break in sedimentation between the Upper Oligocene and Lower Miocene limestones. There, in a restricted exposure at Nadorello east (locality D, Fig. 2.1), the Upper Oligocene is represented by 3-4 m of algal limestones resting unconformably on Upper Cretaceous chinks. These limestones are, in turn, overlain by a single bed (0.3-0.5 m thick) of glauconitic sandy limestones (of probable Burdigalian age *vide* C.G. Adams, pers. comm.). Exposure of the contact between the Upper Oligocene and Lower Miocene sediments is poor but it is irregular with minor erosional

relief. Elsewhere at Nadorello east similar glauconitic limestones infill a fissure in the Upper Oligocene algal limestones (at locality B, Fig. 2.1). The fissure surface is bored by *Trypanites* (Section 4.2.2) indicating that sufficient time had elapsed for lithification of the limestones to occur. These *Trypanites* bores were then infilled by the Lower Miocene glauconitic limestones.

In the Sicani Basin, however, the Upper Oligocene - Lower Miocene succession is apparently continuous. There, the junction between the Upper Oligocene argillaceous deposits and the Lower Miocene glauconitic sandy limestones is arbitrary and transitional, marked by a gradual introduction of glauconitic limestones beds (Section 3.3).

8.2 Depositional History

8.2.1 Upper Oligocene Limestones

The Upper Oligocene limestones rest unconformably, sometimes with slight angular discordance, on chalks of Upper Cretaceous and Eocene age. Prior to deposition, fault controlled differential subsidence (Section 2.6.2), possibly related to the first periods of collision orogeny and southward thrusting which began in northern Sicily in Upper Oligocene - Lower Miocene times (Section 1.3), caused localised erosion to expose Upper Cretaceous chalk in a north-south trending trough in the centre of the area whilst on its adjacent flanks, Eocene and possibly Oligocene (*vide* Campisi, 1968) chalks formed the substrate for Upper Oligocene deposition.

Sedimentation began with the deposition of small quantities of conglomerate in the central trough rather than on the elevated flanks. The conglomerate is composed of (Section 2.2.2): chalk pebbles, cobbles and boulders locally derived from the Upper Cretaceous and Eocene limestones below the unconformity; large echinoids and bivalves of Upper Oligocene age; and phosphatised chalk pebbles and cobbles derived from an allochthonous source. The contained microfauna of the phosphatised chalky limestone clasts indicates that they are exclusively of Eocene age. Geochemical analyses of these phosphatic clasts are presented in Chapter 7 along with analyses of other mid-Tertiary phosphorites from

the central Mediterranean area (southeast Sicily and the Maltese islands). The analyses show that the trace element suite in the Eocene clasts of the southwest Sicily phosphorite (enriched in Ni and Zr) is significantly different from the suites found in the Lower Miocene phosphorites from southeast Sicily and the Maltese islands, which are similar to each other. The southwest Sicily phosphorite is also enriched in the Rare Earth Elements by a factor of six to eight times over the other two areas. This difference in geochemistry suggests that the southwest Sicily phosphorite belongs to a different phosphogenic province (Notholt, 1980b) and that the mid-Tertiary central Mediterranean province, represented by the phosphorites of southeast Sicily and the Maltese islands did not extend into southwest Sicily. Moreover, this difference in geochemistry in the southwest Sicily phosphorite is consistent with a difference in age of the clasts (exclusively Eocene) indicating that they were derived from an Eocene phosphorite, of which the closest known example outcrops in Tunisia (British Sulphur Corporation, 1973).

On top of the basal conglomerate up to c.40 m of Upper Oligocene limestones were deposited in two facies. Rhodolithic algal packstones and wackestones were deposited in the central trough whilst foraminiferal grainstones and packstones were deposited on the bordering high areas (Fig. 2.10). Minor developments of the rhodolithic facies also occur within the eastern high area.

Both facies are dominated by an association of hyaline calcareous foraminifera (listed in Section 8.1.1) which differs only in the presence of *L. (Eulepidina) dilatata* in the rhodolithic facies but its absence in the foraminiferal facies. The rhodolithic facies is characterised by algal rhodoliths of variable growth form (Section 4.1.3) composed of eight species of six genera of crustose coralline red algae (Section 4.1). The algal association is dominated by the cool water genera *Lithothamnium* and *Mesophyllum* over the warm water genera *Archaeolithothamnium*, *Lithophyllum* and *Lithoporella*. From the combined flora, macrofauna and microfauna it is inferred (Section 2.5) that the limestones were deposited in cool, oxygenated waters of normal marine salinity in depths of 80-250 m in a tropical-subtropical latitude. The two facies represent differences in local water depths and turbulence

(Section 2.6.2): the rhodolithic facies representing deposition in the central trough which was sheltered from transverse currents (Fig. 2.9) whilst the foraminiferal grainstones were deposited on the bordering current swept high areas. Minor developments of the rhodolithic facies in the east of the area represent deposition in local depressions or stabilisation of the substrate by the large *L. (Eulepidina) dilatata*, thus allowing algal encrustation.

These Upper Oligocene limestones form part of the Saccense Carbonate Platform (Section 1.4). As described above (Section 2.2.1), their base (which can be seen or inferred at several localities) is unconformable on Upper Cretaceous to Eocene chalks. However, the top of the succession is seen only at Nadorello east, where glauconitic sandy limestones of probable Burdigalian age overlie with erosional contact. Elsewhere, a contact with overlying younger formations is not seen.

Immediately to the north of the Upper Oligocene limestones (Fig. 1.5) the Upper Oligocene situated in the Sicani Basin (Fig. 1.4) is represented by deep water argillaceous deposits (Catalano & D'Argenio, 1978; Section 3.3.2). No interbedding or interfingering of Upper Oligocene limestones and argillaceous deposits can be seen. This, along with the absence of any argillaceous material in the limestones, suggests that the boundary between the Saccense Carbonate Platform and the Sicani Basin was sharp and steep and that the difference in water depth between the two was considerable. Complementary studies on the Upper Oligocene - Lower Miocene foraminifera of the Saccense Platform and the Sicani Basin are intended to elucidate both stratigraphic (zonal) and palaeoenvironmental relationships of the two regions in more detail (Elliott, in prep.).

8.2.2 Lower Miocene Limestones

Two facies are recognised in the Lower Miocene limestones from the Sicani Basin (Section 3.3): a glauconitic limestone facies and a sandy limestone facies. The former, found throughout the outcrop area (Fig. 1.5), rests conformably on Upper Oligocene argillaceous deposits. The latter, found only in the Mt Genuardo area, rests with sharp, non-erosional contact on the glauconitic limestone facies.

Microprobe analyses of the green mineral found in these sediments are presented in Chapter 6. The analyses identify the mineral as glauconite and not chamosite (which can also occur in pelletal form in sedimentary rocks). The authigenic nature of the glauconite pellets in the glauconitic limestone facies is suggested by their abundance and indicated by their association with early marine ferroan calcite cements (Section 6.2). In contrast, in the sandy limestone facies the detrital (reworked) nature of the glauconite is suggested by its relative sparsity and by the absence of any early marine ferroan calcite cements. Microprobe results suggest that the glauconite pellets were formed from calcium carbonate precursory grains (Section 6.4) since the grains analysed have chemistries which indicate intermediate stages in the glauconitisation process, from grains of (near) pure calcite to grains of pure glauconite. This development of glauconite from a calcium carbonate precursor supports the latest theory for glauconite formation proposed by Odin & Matter (1981) and contradicts the earlier "layer lattice theory" which requires an initial substrate of a layer silicate mineral (Sections 6.4.3 and 6.5). The microprobe results presented here also show that most of the glauconite pellets are chemically mature (they contain $K_2O > 7\%$, Section 6.4.3) and therefore the substrate/environment for glauconite formation was a mature one.

Sediments of the glauconitic limestone facies suggest a depositional environment (Section 3.4.1) in agreement with that concluded from the authigenic glauconite (Section 6.6): moderately turbulent, normal saline, cool waters around the oxygen minimum zone with slow sedimentation rate in the deeper part of the 80-250 m depth range. The overlying sandy limestone facies represents greater water depths (still within the 80-250 m range), possibly as a result of the Lower Miocene transgression well known elsewhere in the Mediterranean (Section 3.5). The environment of the facies is otherwise moderately turbulent, oxidising with slow sedimentation rates and possibly depressed temperatures and salinities. The cessation of authigenic glauconite growth in this facies may reflect the introduction of strongly oxidising conditions, or may be due to depressed temperatures and/or salinities.

When viewed in a regional context (Section 3.5), the glauconitic

limestones are interpreted to be a blanket of sediment on the crest of the north-south trending palaeo-high which formed the Western Sicily Bridge (Catalano & D'Argenio, 1978; Section 1.3) covering the palaeogeographic units of the Saccense Carbonate Platform, Sicani Basin and the Trapanese Carbonate Platform (Fig. 3.5). Cross currents (palaeocurrent directions for the time were in a general east-west direction, Fell, 1967) sweeping over this palaeo-high reduced sedimentation, caused reworking, and so created an environment conducive for glauconitisation. Mt Genuardo, in the south, was situated on the crest or slightly to the western side of the palaeo-high whilst Mt Cardellia, to the north, was situated down the eastern slope of the Western Sicily Bridge (Fig. 3.5). These two positions explain the presence of abundant quartz sand in the succession at Mt Genuardo but its near absence at Mt Cardellia (Section 3.5). The quartz sand has a similar texture and petrography to the quartz sands of the Numidian Flysch (described by Wezel, 1970) suggesting that it has the same source. Its presence at Mt Genuardo but not at Mt Cardellia agrees with the southern derivation of the flysch from the Saharan Platform proposed by Wezel (1970, 1975) (Section 3.5).

Finally, this interpretation of facies distribution dates uplift of the Western Sicily Bridge as terminal Oligocene - earliest Miocene, earlier than the post-Burdigalian timing previously proposed by Catalano & D'Argenio (1978).

8.3 Diagenetic History

8.3.1 Upper Oligocene Limestones

The diagenetic features of the Upper Oligocene limestones are described and discussed fully in Sections 5.1 and 5.2. The widespread features of diagenesis are: cementation (four periods, Section 5.1.2), compaction (Section 5.1.3) and neomorphism (Section 5.1.4). Localised diagenetic features include: syn-cementation pore sediments (Section 5.1.5), dolomitisation (Section 5.1.6), and feldspar formation (Section 5.2).

The time relationships of all these diagenetic events (except dolomitisation, which is present at only one locality and is of unknown timing) are as follows:

- 1) Precipitation of the first period of cement (Section 5.1.2b) in a marine environment at or below the sediment/water interface.
- 2) Precipitation of the second period of cement (Section 5.1.2c) at or below the sediment/water interface. Where this cement is associated with the glauconitic sediments in western Nadorello it contains alternating zones of ferroan and non-ferroan calcite indicating that it formed in the same environment as the glauconite and at the same time, and therefore it is early diagenetic in origin (Section 5.1.2g).
- 3) Formation of pore-filling feldspars, syn-glauconitisation (Section 5.2) and therefore early diagenetic, marine in origin. Since both feldspar formation and the second period cement are syn-glauconitisation, it is likely that they are contemporaneous with each other.
- 4) Precipitation of the third period of cement (Section 5.1.2d) in a marine environment at or below the sediment water interface.
- 5) Compaction due to progressive burial by younger sediments, resulting in redistribution and fracture of grains and also pressure solution between grains (Section 5.1.3).
- 6) Deposition of pore-filling sediments after uplift into the vadose environment (Section 5.1.5).
- 7) Precipitation of the fourth period cement in a fresh water phreatic environment (Section 5.1.2e). Neomorphism of depositional lime mud to microspar was probably contemporaneous with this cementation period since the process is generally believed to take place in a fresh water environment (Section 5.1.4). Both events 6 and 7 probably took place upon final uplift of the sediments, with vadose and phreatic environments represented in the same rocks by means of a fluctuating water table.

The first three periods of cementation, which are early marine in origin (Section 5.1.2), are also useful indices of depositional environments. Their general poor or localised development suggests precipitation in cool deep waters in a subtropical environment where waters are less saturated with CaCO_3 (Section 5.1.2). Also, the probable high Mg-calcite original mineralogy of these cements suggests the same deep cool water environment (Section 5.1.2g), which agrees with the environment

inferred from the sediments (Section 8.2.1).

8.3.2 Lower Miocene Limestones

Diagenesis in the Lower Miocene limestones is less complex. The features are fully described and discussed in Section 5.3. They include two periods of cementation separated by a period of compaction.

1) First period of cement (Section 5.3.2b), precipitated at or below the sediment/water interface. The cement commonly shows ferroan calcite/calcite zones (in the glauconitic limestone facies) indicating that it is syn-glauconitisation, early marine in origin.

2) Compaction (Section 5.3.3) due to progressive burial by younger sediments and resulting in the same features as found in the Upper Oligocene limestones.

3) Second period of cement (Section 5.3.2c), precipitated in the fresh water phreatic environment after uplift.

Correlation of the diagenetic events found in the Upper Oligocene and Lower Miocene limestones is probably restricted to the last period of cementation. The first three periods of cement found in the Upper Oligocene are early marine and therefore Upper Oligocene in age. These do not correlate with the marine cement found in the Lower Miocene limestones since this is Lower Miocene in age. Compaction in each of the rock units is of similar intensity (i.e. it is represented by grain fracture and grain contact pressure solution throughout) and so it probably relates to the continuing process of burial (rather than the superimposition of thrust sheets) and therefore it is of near penecontemporaneous age. In each occurrence, it post-dates the early marine cement and pre-dates final pore-filling cement. Finally, in both the Upper Oligocene and Lower Miocene limestones the last diagenetic event is that of pore-filling clear blocky spar of fresh water phreatic origin. In both cases this is probably related to (the same period of) final uplift and hence is of presumed Quaternary age (Masclé, 1973, 1979).

8.4 Regional Setting

8.4.1 General

Sicily is situated in the central Mediterranean sea between the

continental masses of Europe and Africa. Geologically, the island is located on the northern edge of the African Plate and it forms an eastern extension of the structural and palaeogeographic zones recognised in northwest Africa (Buroillet, 1967; Durand Delga, 1967; Caire, 1970, 1978; Wezel, 1970; Bemmelen, 1975; Brunn & Buroillet, 1979). Undeformed African carbonate platform is represented by the Eocene to Miocene limestones of the Iblean Plateau (Fig. 1.3) in southeast Sicily, which form part of the "African Promontory" stretching as far north and east as Apulia and the southern Adriatic (Caire, 1978). In southwest Sicily Channel *et al.* (1980) argue, that since palaeomagnetic data from the southernmost "thrust sheet" of the Western Sicily Bridge (on which some of the Upper Oligocene limestones, described here, are situated) are similar to those recorded for the Iblean Plateau and northwest Africa, then this "thrust sheet" must be *in situ* and, like the Iblean Plateau, represent a northern extension of undeformed African Platform. Apart from these two areas, in southwest and southeast Sicily, the pre-Neogene rocks which outcrop on the island are allochthonous and have travelled varying distances in a southerly direction (Catalano & D'Argenio, 1978; Catalano *et al.*, 1978; Channell *et al.*, 1980). The most allochthonous unit is that of the Peloritani Mountains in the northeast of the island which is believed to have travelled from an original position that is now the site of the present day island of Sardinia (Caire, 1978). The rocks of this unit include gneiss and schist of probable Devonian age representing part of the Hercynian basement of the "European Plate" (Duce, 1970; Truillet, 1970; Caire, 1978).

8.4.2 Palaeogeography

The general palaeogeography of the central Mediterranean area in Upper Oligocene - Lower Miocene times is given in Figure 8.1. This work has shown (Section 3.5) from stratigraphic evidence (Upper Oligocene deep water argillaceous rocks overlain by Lower Miocene outer shelf glauconitic limestones) that the Western Sicily Bridge was a positive area in basal Miocene times, effectively separating the Western Sicily Neogene Basin (Castelvetrano Basin) from the Central Sicily Neogene Basin (Caltanissetta Basin). This separation is indicated by the deposition of Numidian Flysch in western Sicily in the Castelvetrano Basin (Catalano & D'Argenio, 1978) and on the western flank of the Western Sicily Bridge (Section 3.5);

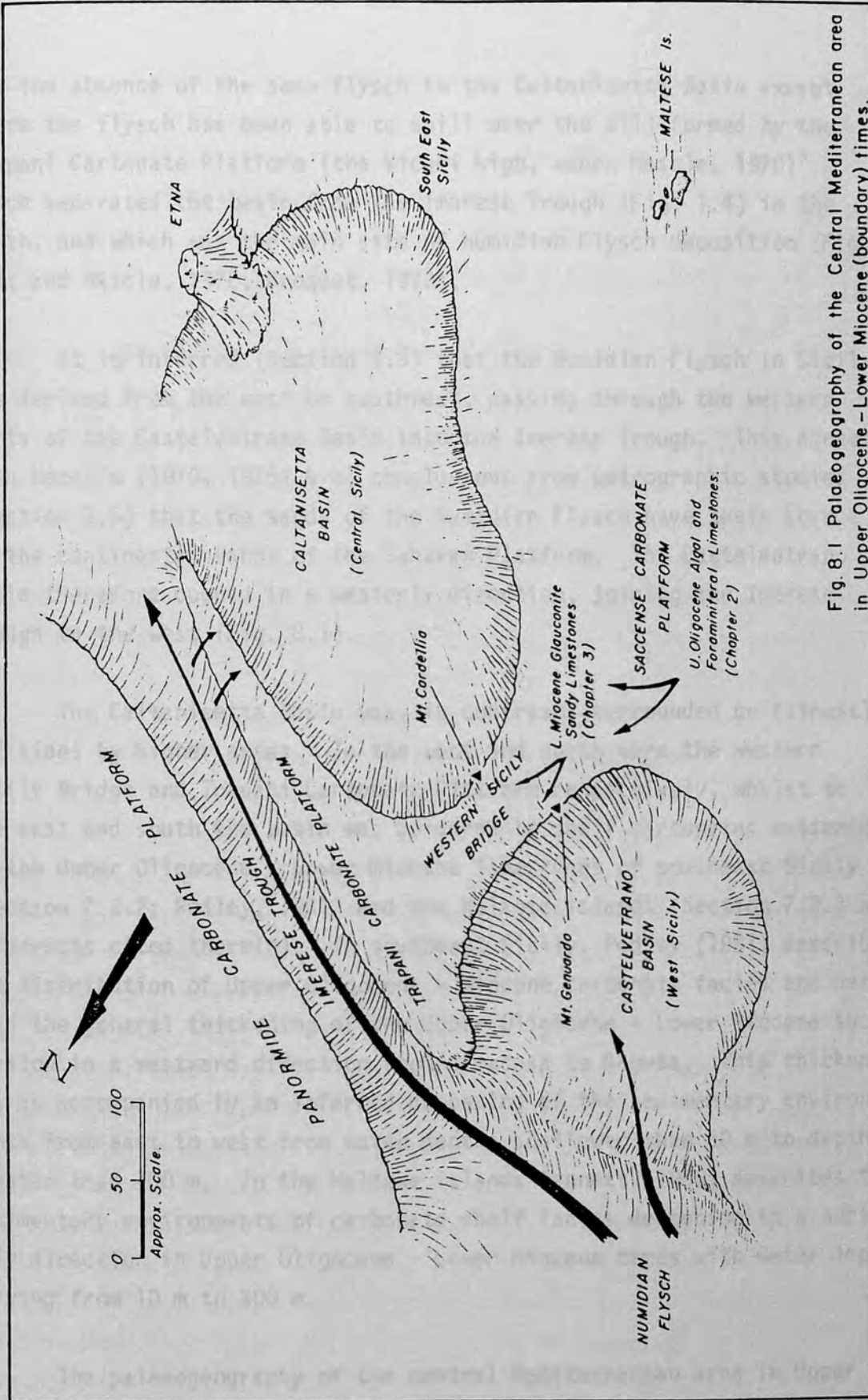


Fig. 8.1 Palaeogeography of the Central Mediterranean area in Upper Oligocene - Lower Miocene (boundary) times.

and the absence of the same flysch in the Caltanissetta Basin except where the flysch has been able to spill over the sill formed by the Trapani Carbonate Platform (the Vicari high, *sensu* Mascle, 1970) which separates the basin from the Imerese Trough (Fig. 1.4) in the north, and which was the main site of Numidian Flysch deposition (Fig. 8.1; and Mascle, 1970; Broquet, 1970).

It is inferred (Section 3.5) that the Numidian Flysch in Sicily was derived from the west or southwest, passing through the western parts of the Castelvetro Basin into the Imerese Trough. This agrees with Wezel's (1970, 1975a & b) conclusions from petrographic studies (Section 3.5) that the sands of the Numidian Flysch have their source in the continental sands of the Saharan Platform. The Castelvetro Basin therefore opened in a westerly direction, joining the Imerese Trough in the west (Fig. 8.1).

The Caltanissetta Basin was, in contrast, surrounded on (almost) all sides by higher areas. To the west and north were the Western Sicily Bridge and Trapani Carbonate Platform respectively, whilst to the east and south the basin was bordered by shelf carbonates evidenced by the Upper Oligocene - Lower Miocene limestones of southeast Sicily (Section 7.2.2; Pedley, 1981) and the Maltese islands (Section 7.2.3 and references cited therein). In southeast Sicily, Pedley (1981) describes the distribution of Upper Oligocene - Miocene carbonate facies and details the general thickening of the Upper Oligocene - Lower Miocene succession in a westward direction from Siracusa to Ragusa. This thickening is accompanied by an inferred deepening of the sedimentary environments from east to west from water depths shallower than 50 m to depths greater than 100 m. In the Maltese islands Bennett (1980) describes the sedimentary environments of carbonate shelf facies deepening in a northerly direction in Upper Oligocene - Lower Miocene times with water depths varying from 10 m to 300 m.

The palaeogeography of the central Mediterranean area in Upper Oligocene - Lower Miocene times is therefore composed of a shelf in the south, (extending as far north as the Sciacca area in southwest Sicily and the Siracusa area in southeast Sicily) passing northwards into the

central and western Sicily basins separated by the positive axis of the Western Sicily Bridge, and still northwards into the east-west trending Trapani Carbonate Platform and Imerese Trough (Fig. 8.1). This distribution of palaeogeographic units agrees with that inferred for the Tunisian Tertiary by Buroillet (1967), who recognises a shelf in the south and a flysch trough in the north with a zone of basins between.

8.4.3 Facies Distribution and Palaeoenvironments

The Upper Oligocene rhodolithic algal limestones and foraminiferal limestones described in Chapter 2 form a limited occurrence of facies which are widespread in western Tethys in Upper Oligocene - Lower Miocene times. (There is, for example, close comparison between these limestones and those found in southeast Sicily and the Maltese islands - my observations). The Lower Miocene glauconitic sandy limestones described in Chapter 3 are also known from elsewhere in the Mediterranean area. These facies, where they occur, may represent similar, if not the same, environments as those outlined for southwest Sicily in Section 8.2 which are, for the algal and foraminiferal limestones, shelf limestones accumulating in cool oxygenated waters of normal marine salinity in depths of 80-250 m in a tropical-subtropical latitude; and, for the glauconitic sandy limestones, outer shelf deposits accumulating in moderately turbulent, normal saline, cool waters around the oxygen minimum zone with slow sedimentation rates in the deeper part of the 80-250 m depth range.

In southeast Sicily, limestones of the Siracusa Limestone (Lower Miocene (Aquitanian) Pedley, 1981) were examined in the large working quarry at San Cusumano (16 km northwest along the coast from Siracusa). The limestones, which are massive and show no well defined beds, contain abundant algal rhodoliths in a benthonic foraminiferal limestone matrix and have a common macrofauna of a single large species of *Clypeaster*. Their similarity with the southwest Sicily limestones is also shown by their algal association which is dominated by *Lithothamnium* and *Mesophyllum* and by their benthonic foraminiferal content which includes common *Nephrolepidina*, *Spiroclypeus* and *Amphistegina* along with local abundances of *Eulepidina*. These limestones form a maximum thickness of 20 m in southeast Sicily and they extend over a

restricted geographic area (Pedley, 1981) in comparison to the age equivalent benthonic foraminiferal grainstones and packstones of the Irminio Member of the Ragusa Formation which outcrop extensively in southeast Sicily (Pedley, 1981) and which reach a maximum thickness of 130 m. These limestones, which are generally well bedded (in 0.20 - 1.5 m beds), were examined at Donnalucata (on the south coast) and in the extensive outcrops around the town of Ragusa. Macrofauna is represented by sparse small echinoids and microfauna by common to abundant *Miogypsina* along with *Nephrolepidina*, *Amphistegina* and *Spiroclypeus*; *Thalassinoides* burrows are locally common. Despite their slight age disparity the southeast Sicily limestones are similar in lithology, macrofauna, microfauna and facies distribution patterns (the rhodolithic facies is subordinate in thickness and extent) to the Upper Oligocene limestones of southwest Sicily and therefore it is likely that they represent similar shelf environments situated on the southeast side of the Central Sicily Basin.

On the Maltese islands the limestones of the Upper Oligocene Lower Coralline Limestone Formation are similar in appearance to the southwest Sicily limestones. They are fully described by Bennett (1980) and main features summarised by Bosence *et al.* (1981). Bennett (1980) recognises four members in the formation of which the middle two, the Attard and Xlendi members, bear the closest comparison with the southwest Sicily succession. The Attard Member is dominantly a rhodolithic algal limestone with the algal association again dominated by *Lithothamnium* and *Mesophyllum* and containing four species (*Mesophyllum* cf. *vaughanii*, *Archaeolithothamnium saipanense*, *Lithoporella* cf. *melobesioides* *Melobesia* cf. *cuboides*) also recognised in southwest Sicily (Section 4.1.2). The Xlendi Member is composed of grainstones with clasts predominantly of foraminifera represented by *Nephrolepidina*, *Amphistegina*, *Spiroclypeus* and *Heterostegina*. Macrofauna is sparse and represented by irregular echinoids. This Maltese succession, however, differs from both the southwest Sicily and southeast Sicily successions in containing features which suggest deposition in much shallower water. For example, the Attard Member contains corals present in concentrations forming small patch reefs (Pedley, 1978) and the Xlendi Member is extensively cross bedded, interpreted as an offshore bar by Bennett (1980). Also, the Maghlok Member (which underlies the Attard Member) is dominated by a

miliolid foraminifera fauna probably representing restricted marine conditions (Haynes, 1981) and interpreted as a very shallow water deposit by Bennett (1980). The Maltese Upper Oligocene limestones, although similar to the Sicilian limestones discussed above, have basic differences and are therefore interpreted as much shallower water deposits.

In North Africa, as a background to the description of the echinoid macrofauna, Rose (1966, 1974) describes rhodolith and foraminiferal limestones from the Upper Oligocene of Libya. Macroscopically, the limestones are similar, they contain common foraminiferal elements (*Nephrolepidina*, *Eulepidina*, *Amphistegina*, *Spiroclypeus*, *Heterostegina* and *Operculina*; see also Lehmann *et al.*, 1967), and, according to Rose (pers. comm. 1980-83), the *Echinolampas* and *Clypeaster* spp. found in the Upper Oligocene of southwest Sicily belong to morphologically similar species groups as those found in the Libyan Upper Oligocene. In Tunisia, glauconitic sandstones, very similar petrographically (Wezel, 1970) to those described from southwest Sicily, are recorded from the Lower Miocene where they are interpreted as outer shelf deposits (Wezel, 1970, Buroillet *et al.*, 1978).

In Europe, rhodolith limestones have been described from the Upper Oligocene of Italy by Airoidi (1933) and Afchain (1966), and one of the algal species described by Airoidi has been identified from the Upper Oligocene of southwest Sicily. Foraminiferal limestones with similar elements to those described from southwest Sicily have been described from the Upper Oligocene of northern Italy by Cita (1965) and Pieroni (1965) and from the Upper Oligocene and Lower Miocene of southern Spain by Coppel & Guillen (1965) and Vera (1969). Lower Miocene glauconitic sandy limestones are described from northern Italy where they rest on Lepidocycline limestones of Upper Oligocene age (Cita, 1965) and from borehole data in the Gulf of Leon (of southern France) Buroillet & Dufaure (1972) record transgressive glauconitic limestones resting on Palaeozoic rocks.

On a wider Tethyan scale, foraminiferal limestones with common foraminiferal elements to those described from southwest Sicily, sometimes associated with algal material, have been described from the Upper

Oligocene and Lower Miocene of Australia (Chaproniere, 1975) and Somalia (Azzaroli, 1958) and from the Upper Oligocene of the west Pacific (Premoli Silva & Brusa, 1981). Similar algal rhodolith and foraminiferal limestones are also known from the Upper Oligocene and Lower Miocene of the Caribbean area (Poddubiuk, pers. comm. 1982), where their echinoid macrofauna is also very similar to that found in southwest Sicily (Rose, pers. comm. 1982).

In conclusion, it has been shown that Upper Oligocene - Lower Miocene shelf carbonates of the types described from southwest Sicily are common in the Tethyan realm at this time and therefore the rocks described here are of more than local interest and should provide useful information for the interpretation of these facies elsewhere in Tethys at the Oligo-Miocene time.

ADEY, W.H., 1970a: The effects of light and temperature on growth rates in boreal-subarctic crustose corallines. *J. Phycol.*, 6: 259-276.

ADEY, W.H., 1970b: Some relationships between crustose corallines and their substrate. *Sci. Islandica*, 21: 21-25.

ADEY, W.H., 1971: The sublittoral distribution of crustose corallines on the Norwegian coast. *Sarsia*, 46: 41-60.

ADEY, W.H. & ADEY, P.J., 1973: Studies of the biosystematics and ecology of the epilithic crustose Corallinaceae of the British Islands. *Br. Phycol.*, 2, 81: 343-407.

ADEY, W.H. & MACINTYRE, I.G., 1973: Crustose coralline algae: a re-evaluation in the geological sciences. *Bull. geol. Soc. Am.*, 84: 883-904.

ARCHAIN, C., 1966: La base de la serie Tertiaire sur le bord oriental de la Calabre Ulteriore (Note preliminaire). *C. r. Somm. Sec. geol. Fr.*, 10: 397-398.

AZZAROLI, M., 1933: Contributo allo studio delle corallinacee del Terziario Italiano. Part I. Corallinacee dell'Oligocene Ligure - Piemontese. *Palaeontogr. Ital.*, 33: 58-85, pls. 9-12.

ALEXANDERSSON, T., 1972: Intracrystalline growth of marine aragonite and Mg-calcite: evidence of precipitation from supersaturated seawater. *J. sediment. Petrol.*, 42: 461-466.

ALEXANDERSSON, T., 1974: Carbonate cementation in coralline algal nodules in the Skagerrak, North Sea: biochemical precipitation in undersaturated waters. *J. sediment. Petrol.*, 44: 7-26.

REFERENCES

- ACCORDI, B., 1958: Il flysch oligocenico-aquitano dei Monti Nebrodi (Sicilia nord-orientale). Eclog. geol. Helv., 51: 827-833.
- ADAMS, C.G., 1973: Some Tertiary Foraminifera. In: HALLAM, A. (ed.), Atlas of Palaeobiogeography. Elsevier Pub. Co., Amsterdam, 453-468.
- ADEY, W.H., 1966: The distribution of saxicolous crustose corallines in the northwestern North Atlantic. J. Phycol., 2: 49-54.
- ADEY, W.H., 1968: The distribution of crustose corallines on the Icelandic coast. Sci. Islandica, 1: 18-30.
- ADEY, W.H., 1970a: The effects of light and temperature on growth rates in boreal-subarctic crustose corallines. J. Phycol., 6: 269-296.
- ADEY, W.H., 1970b: Some relationships between crustose corallines and their substrate. Sci. Islandica, 2: 21-25.
- ADEY, W.H., 1971: The sublittoral distribution of crustose corallines on the Norwegian coast. Sarsia, 46: 41-58.
- ADEY, W.H. & ADEY, P.J., 1973: Studies of the biosystematics and ecology of the epilithic crustose Corallinaceae of the British Islands. Br. Phycol. J., 8: 343-407.
- ADEY, W.H. & MACINTYRE, I.G., 1973: Crustose coralline algae: a re-evaluation in the geological sciences. Bull. geol. Soc. Am., 84: 883-904.
- AFCHAIN, C., 1966: La base de la serie Tertiaire sur le bord oriental de la Calabre Ulteriore (Note preliminaire). C. r. Somm. Soc. geol. Fr., 10: 397-398.
- AIROLDI, M., 1933: Contributo allo studio delle Corallinacee del Tertiario Italiano. Part 1. Corallinacee dell' Oligocene Ligure - Piemontese. Palaeontogr. Ital., 33: 58-83, pls. 9-12.
- ALEXANDERSSON, T., 1972: Intragranular growth of marine aragonite and Mg-calcite: evidence of precipitation from super-saturated seawater. J. sediment. Petrol., 42: 441-460.
- ALEXANDERSSON, T., 1974: Carbonate cementation in coralline algal nodules in the Skagerrak, North Sea: biochemical precipitation in undersaturated waters. J. sediment. Petrol., 44: 7-26.

- ALLMAN, M. & LAWRENCE, D.F., 1973: Geological laboratory techniques. Blandford Press, London, 335pp.
- ALTSCHULER, Z.S., 1980: The geochemistry of trace elements in marine phosphorites part 1. Characteristic abundances and enrichment. In: BENTOR, Y.K. (ed.), Marine phosphorites - geochemistry, occurrence, genesis. Spec. Publ. Soc. econ. Palaeontol. Mineral. Tulsa, n.29, 19-30.
- AMES, L.L., 1959: The genesis of carbonate-apatite. Econ. Geol., 54: 829-841.
- AMES, L.L., 1960: Some cation substitutions during the formation of phosphorite from calcite. Econ. Geol., 55: 354-362.
- AUBRY, M.P. & ODIN, G.S., 1973: Sur la nature mineralogique du verdissiment des craies: formation d'une phyllite apparentee aux glauconies en milieu semi-confine poreux. Bull. Soc. geol. Normandie, 61: 11-22.
- AUZENDE, J.-M. & OLIVET, J.-L., 1974: Structure of the Western Mediterranean Basin. In: BURK, C.A. & DRAKE, C.L. (eds), The Geology of Continental Margins. Springer Verlag, New York, 723-731.
- AZZAROLI, A., 1958: L'Oligocene e il Miocene della Somalia. Palaeontogr. Ital., 52: 1-142.
- BALDACCI, L., 1886: Descrizione geologica dell' isola di Sicilia. Mem. Carta Geol. Italia Roma, 1: 403pp.
- BASKIN, Y., 1956: A study of authigenic feldspars. J. Geol., 64: 132-155.
- BATHURST, R.G.C., 1966: Boring algae, micrite envelopes and lithification of molluscan biosparites. Geol. J., 5: 15-32.
- BATHURST, R.G.C., 1975: Carbonate sediments and their diagenesis. Elsevier Scientific Pub. Co., Amsterdam, 2 ed., 658pp.
- BATURIN, G.N., 1969: Authigenic phosphate concretions in the Recent sediments of the southwest African shelf. Dokl. Acad. Sci. USSR., 189: 1359-1362 (English transl.).
- BATURIN, G.N. & BEZRUKOW, P.L., 1979: Phosphorites on the seafloor and their origin. Mar. Geol., 31: 297-316.
- BATURIN, G.N., KOCHENOV, A.V. & PETELIN, V.P., 1970: Phosphorite formation on the shelf of SW Africa. Lith. and Min. Res., 3: 266-276.
- BENMELEN, R.W. van, 1969: Origin of the western Mediterranean sea. Verh. Kon. Geol. Mijnb. Gen., 26: 13-52.

- BEMMELEN, R.W. van, 1975: Driving forces of Mediterranean Orogeny (Tyrrhenian test case). In: SQUYRES, C.H. (ed.), Geology of Italy. Earth Sci. Soc. Libya, 15 Ann. Field Conf., Tripoli, Vol. 1: 263-292.
- BENNETT, S.M., 1979: A transgressive carbonate sequence spanning the Paleogene-Neogene boundary on the Maltese islands. Ann. Geol. Pays Hellen, Tome hors serie, 1979, fasc. 1: 71-80.
- BENNETT, S.M., 1980: Palaeoenvironmental studies in Maltese mid-Tertiary carbonates. Unpubl. PhD thesis, University of London (Bedford College), 2 vols.
- BENTOR, Y.K. (ed.), 1980a: Marine phosphorites - geochemistry, occurrence, genesis. Spec. Publ. Soc. econ. Palaeontol. Mineral. Tulsa, n.29, 249pp.
- BENTOR, Y.K., 1980b: Phosphorites - the unsolved problems. In: BENTOR, Y.K. (ed.), Marine phosphorites - geochemistry, occurrence, genesis. Spec. Publ. Soc. econ. Palaeontol. Mineral. Tulsa, n.29, 3-18.
- BENTOR, Y.K. & KASTNER, M., 1965: Notes on the mineralogy and origin of glauconite. J. sediment. Petrol., 35: 155-166.
- BERG, R.R., 1952: Feldspathized sandstone. J. sediment. Petrol., 22: 221-223.
- BERGGREN, W.A., 1971: Tertiary boundaries and correlations. In: FUNNELL, B.M. & RIEDEL, W.R. (eds), The micropalaeontology of oceans. Cambridge Univ. Press, 693-809.
- BERRY, L.G. (ed.), 1974: Selected powder diffraction data for minerals. Joint committee on powder diffraction standards, Swarthmore, 833pp.
- BIJU-DUVAL, B., LETOUZEY, J., MONTADERT, L., COURRIER, P., MUGNIOT, J.F. & SANCHO, J., 1974: Geology of the Mediterranean Sea Basins. In: BURK, C.A. & DRAKE, C.L. (eds), The Geology of Continental Margins. Springer-Verlag, New York, 695-721.
- BIRCH, G.F., 1978: Penecontemporaneous phosphatisation by replacement and precipitation mechanisms on the western margin of southern Africa. 10th Intern. Congr. Sediment., Abstracts, 71-72.
- BIRCH, G.F., 1980: A model of penecontemporaneous phosphatization by diagenetic and authigenic mechanisms from the western margin of southern Africa. In: BENTOR, Y.K. (ed.), Marine phosphorites - geochemistry, occurrence, genesis. Spec. Publ. Soc. econ. Palaeontol. Mineral. Tulsa, n.29, 79-100.

- BIRCH, G.F., WILLIS, J.P. & RICKARD, R.S., 1976: An electron microprobe study of glauconites from the continental margin off the west coast of South Africa. Mar. Geol., 22: 271-283.
- BLONDEAU, A., LORENZ, C., MAGNE, J. & MASCLE, G.H., 1972: L'Oligocene et le Miocene inferieur en Sicile centro-occidentale. Bull. Soc. geol. Fr., Ser 7, 14: 137-146.
- BLOW, W.H., 1969: Late middle Eocene to Recent planktonic foraminiferal biostratigraphy. Proc. First Int. Conf. Plank. Microf., Geneva 1967, 1: 199-422.
- BOCCALETTI, M. & GUAZZONE, G., 1975: Plate tectonics in the Mediterranean region. In: SQUYRES, C.H. (ed.), Geology of Italy. Earth Sci. Soc. Libya, 15 Ann. Field Conf., Tripoli, Vol.1: 143-164.
- BOMMARITO, S. & LA ROSA, N., 1962: Ricerche sulla estensione dell'orizzonte fosfatifero nella regione Iblea. Riv. Minerar. Sicilia, 76-78: 184-190.
- BONARDI, G., PESCATORE, T., SCANDONE, P. & TORRE, M., 1971: Problemi paleogeografici connessi con la successione Mesozoico-Terziaria di Stilo (Calabria meridionale). Bull. Soc. Natur. Napoli, 80: 12pp, 2 fig.
- BOSELLINI, A. & GINSBURG, R.N., 1971: Form and internal structure of Recent algal nodules (rhodolites) from Bermuda. J. Geol. 79: 669-682.
- BOSENCE, D.W.J., 1976: Ecological studies on two unattached coralline algae from western Ireland. Palaeontology, London, 19: 365-395.
- BOSENCE, D.W.J., PEDLEY, H.M. & ROSE, E.P.F., 1981: Field guide to mid-Tertiary carbonate facies of the Maltese islands. Palaeontological Assoc. London, guide, 88pp.
- BRAITHWAITE, C.J. R., 1968: Diagenesis of phosphatic carbonate rocks on Remire, Amirantes, Indian Ocean. J. sediment. Petrol., 38: 1194-1212.
- BRICKER, O.P. (ed.), 1971: Carbonate cements. Johns Hopkins Press, Baltimore, 376pp.
- BRITISH SULPHUR CORPORATION, 1973: World survey of phosphate deposits. 3rd ed., British Sulphur Corp., London, 180pp.
- BROMLEY, R.G., 1967a: Marine phosphorites as depth indicators. Mar. Geol., 5: 503-509.
- BROMLEY, R.G., 1967b: Some observations on burrows of thalassinoid Crustacea in chalk hardgrounds. Q.J. geol. Soc. London, 123: 157-182.

- BROMLEY, R.G., 1968: Burrows and borings in hardgrounds. Dansk. Geol. Foren. Meddr., 18: 247-250.
- BROMLEY, R.G., 1970: Borings as trace fossils and *Entobia cretacea* Portlock, as an example. In: CRIMES, T.P. & HARPER, J.C. (eds), Trace fossils. Seel House Press, Liverpool, 49-90.
- BROMLEY, R.G., 1972: On some ichnotaxa in hard substrates, with a redefinition of *Trypanites* MÄGDEFRAU. Palaeontol. Z. Berlin, 46: 93-98.
- BROMLEY, R.G., 1975: Trace fossils at omission surfaces. In: FREY, R.W. (ed.), The study of trace fossils. Springer-Verlag, Berlin, 399-428.
- BROQUET, P., 1962: Serie stratigraphique du Cozzo Cavolino. Bull. Soc. geol. Fr., ser.7, 4: 738-743.
- BROQUET, P., 1964: Observations stratigraphiques, tectoniques et sedimentologiques sur le flysch numidien des Madonies (Sicile). Ann. Soc. geol. Nord., 84: 141-152.
- BROQUET, P., 1968: La provenance du materiel detritique du Numidien des Madonies (Sicile). C.r.Somm. Soc. geol. Fr., 136-138.
- BROQUET, P., 1970: The geology of the Madonie mountains of Sicily. In: ALVAREZ, W. & GOHRBANDT, K.H.A. (eds), Geology and History of Sicily. Petrol. Expl. Soc. Libya, 201-230.
- BROQUET, P., 1972: Etude geologique de la region des Madonies (Sicile) (sedimentologie et tectonique). Geologica Romana, 11: 1-113.
- BROQUET, P., CAIRE, A., DUEE, G. & TRUILLET, R., 1963: Essai de reconstitution paleogeographique du Nord-est sicilian. C.r. Somm. Soc. geol. Fr., 300-302.
- BROQUET, P., CAIRE, A. & MASCLE, G.H., 1966: Structure et evolution de la Sicile occidentale (Madonies et Sicani). Bull. Soc. geol. Fr., Ser.7, 8: 994-1013.
- BROQUET, P. & DUEE, G., 1967: Nouvelles observations sur les flysch de Sicile. C.r. Somm. Soc. geol. Fr., 270-271.
- BRUNN, J.H. & BUROLLET, P.F., 1979: Island arcs and the origin of folded ranges. Geol. Mijnbouw, 58: 117-126.
- BUCHBINDER, L.G. & FRIEDMAN, G.M., 1980: Vadose, phreatic and marine diagenesis of Pleistocene-Holocene carbonates in a borehole: Mediterranean coast of Israel. J. sediment. Petrol., 50: 395-408.

- BURNETT, W.C., 1977: Geochemistry and origin of phosphorite deposits from off Peru and Chile. Bull. geol. Soc. Am., 88: 813-823.
- BURNETT, W.C., 1980: Apatite-glaucinite associations off Peru and Chile: palaeo-oceanographic implications. J. geol. Soc. London, 137: 757-764.
- BURNETT, W.C., VEEH, H.H. & SOUTAR, A., 1980: U-series, oceanographic and sedimentary evidence in support of Recent formation of phosphate nodules off Peru. In: BENTOR, Y.K. (ed.), Marine phosphorites - geochemistry, occurrence, genesis. Spec. Publ. Soc. econ. Palaeontol. Mineral. Tulsa, n.29, 61-72.
- BUROLLET, P.F., 1967: General geology of Tunisia. In: MARTIN, L. (ed.), Guidebook to the geology and history of Tunisia. Petrol. Expl. Soc. Libya, 51-58.
- BUROLLET, P.F. & DUFAURE, Ph., 1972: The Neogene series drilled by the Mistral No.1 well in the Gulf of Lion. In: STANLEY, D.J. (ed.), The Mediterranean sea: A natural sedimentation laboratory. Dowden, Hutchinson & Ross, Stroudsburg, 91-98.
- BUROLLET, P.F. & MUGNIOT, J.M. & SWEENEY, P., 1978: The geology of the Pelagian Block: The margins and basins off Southern Tunisia and Tripolitania. In: NAIRN, A.E.M., KANES, W.H. & STEHLI, F.G. (eds), The Ocean basins and margins, Vol.4B, The western Mediterranean. Plenum Press, New York, 331-360.
- BURST, J.F., 1958a: "Glaucinite" pellets: their mineral nature and applications to stratigraphic interpretations. Bull. Am. Assoc. Petrol. Geol., 42: 310-327.
- BURST, J.F., 1958b: Mineral heterogeneity in "glaucinite" pellets. Am. Mineral., 43: 481-497.
- BUSHINSKI, G.I., 1964: On shallow water origin of phosphorite sediments. In: VAN STRAATEN, L.M.J.V. (ed.), Deltaic and shallow marine deposits. Elsevier, Amsterdam, 62-70.
- BUSHINSKI, G.I., 1969: Old phosphorites of Asia and their genesis. Israel Prog. Sci. Trans., Jerusalem, 266pp.
- CAIRE, A., 1970: Sicily in its Mediterranean setting. In: ALVAREZ, W. & GOHRBANDT, K.H.A. (eds), Geology and history of Sicily. Petrol. Expl. Soc. Libya, 145-170.
- CAIRE, A., 1975: Italy in its Mediterranean setting. In: SQUYRES, C.H. (ed.), Geology of Italy. Earth Sci. Soc. Libya, 15 Ann. Field Conf., Tripoli, Vol.1: 11-74.

- CAIRE, A., 1978: The central Mediterranean mountain chains in the alpine orogenic environment. In: NAIRN, A.E.M., KANES, W.H. & STEHLI, F.G. (eds), The ocean basins and margins, Vol.4B, The Western Mediterranean. Plenum Press, New York, 201-256.
- CAIRE, A. & MASCLE, G., 1964: Existence d'importants mouvements tangentiels Pliocenes dans les Monts Sicani (Sicile). C.r. Somm. Soc. geol. Fr., Fsc.10, 417.
- CALVERT, S.E. & PRICE, N.B., 1971: Upwelling and nutrient regeneration in the Benguela Current, October, 1968. Deep Sea Res. oceanogr. Abstr., 18: 505-523.
- CAMPISI, B., 1958: Note illustrative del rilevamento geologico delle tavolette "Petralia" (p.p.), "Polizzi Generosa" ed "Alimena" (Sicilia settentrionale). Bull. Serv. geol. Ital., 79: 913-928.
- CAMPISI, B., 1968: Microfossili e stratigrafia del Miocene inferiore e medio dei Sicani sud-occidentali. Atti Accad. gioenia Sci. nat. Catania, Ser. 6, 20: 223-324.
- CAPEDER, G., 1900: Contribuzione allo studio dei *Lithothamnion* Tertiari. Malpighia, Genoa, 14: 172-182.
- CASTANY, G., 1956: Essai de synthese geologique du territoire Tunisie-Sicile. Ann. Mines Geol. Tunisie, 16: 101pp.
- CATALANO, R. & D'ARGENIO, B., 1978: An essay of palinspastic restoration across western Sicily. Geologica Romana, 17: 145-159.
- CATALANO, R. & D'ARGENIO, B., 1981: Paleogeographic evolution of a continental margin in Sicily. Guidebook of the field trip in western Sicily. Istituto Geol., Univ. Palermo, 142pp.
- CATALANO, R., D'ARGENIO, B., MONTANARI, L., *et al.*, 1978: Contributi alla conoscenza della struttura della Sicilia occidentale. 1: Il profilo Palermo-Sciacca. Mem. Soc. geol. Ital., 19: 485-493.
- CHALLIS, G.R., 1979: Miocene echinoid biofacies of the Maltese islands. Ann. Geol. Pays Hellen., tome hors series, 1979, fasc. 1: 253-262.
- CHALLIS, G.R., 1980: Palaeoecology and taxonomy of Maltese mid-Tertiary echinoids. Unpub. PhD thesis, Univ. London (Bedford College), 2 vols.
- CHANNELL, J.E.T., CATALANO, R. & D'ARGENIO, B., 1980: Palaeomagnetism and deformation of the Mesozoic continental margin in Sicily. Tectonophysics, 61: 391-407.

- CHAPRONIERE, G.C.H., 1975: Palaeoecology of Oligo-Miocene larger Foraminiferida, Australia. Alcheringa (Assoc. Australas. Palaeontol.), 1: 37-58.
- CHECCHIA-RISPOLI, G., 1911: Sul Miocene di alcune regione della provincia di Palermo e di Girgenti. G. Sci. nat. econ. Palermo, 28: 305-315.
- CHECCHIA-RISPOLI, G., 1918: L'Eocene ed il Miocene di Sciacca. Rend. R. Accad. Lincei, Ser. 5, 27: 252-255.
- CITA, M.B., 1965: Jurassic, Cretaceous and Tertiary microfacies from the southern alps (northern Italy). Internat. Sediment. Petrographical. ser., 8, 99pp, plates 1-117.
- CLOUD, P.E., 1955: Physical limits of glauconite formation. Bull. Am. Assoc. Petrol. Geol., 39: 484-492.
- COLACICCHI, R., 1958: Dicchi sedimentari del flysch oligo-miocenico della Sicilia nordorientale. Eclog. geol. Helv., 51: 901-916.
- COLACICCHI, R., 1963: Geologia del territorio di Pachino (Sicilia meridionale). Geologica Romana, 2: 343-404.
- COLLET, L.W., 1908: Les Depots Marins. Doin, Paris, 320pp.
- CONTI, S., 1943: Contributo allo studio delle Corallinacee del Terziario Italia. Part 2. Corallinacee del Miocene Ligure-Piemontese. Palaeontogr. Ital., 41: 37-61, pls 5-8.
- COOK, P.J., 1972: Petrology and geochemistry of the phosphate deposits of northwest Queensland, Australia. Econ. Geol., 67: 1193-1213.
- COOK, P.J., 1976: Sedimentary phosphate deposits. In: WOLF, K.H. (ed.), Handbook of strata-bound and stratiform ore deposits. Elsevier, New York, 505-535.
- COOK, P.J., 1980: Phosphorites: I.G.C.P. project 156. In: BASSETT, M.G. (ed.), Geological correlation. Int. Geol. Correl. Prog., Paris, 8: 182-184.
- COOK, P.J. & McELHINNY, M.W., 1979: A re-evaluation of the spatial and temporal distribution of phosphorites in the light of plate tectonics. Econ. Geol., 74: 315-330.
- COOK, P.J. & SHERGOLD, J.H. (eds), 1979: Proterozoic-Cambrian phosphorites. Canberra Publishing & Printing Co., 101pp.
- COPPEL, C.F. & GUILLEN, J.C., 1965: Mapa Geologico de Espana : Explicacion de la Hoja no.967, Baena (1 : 50 000). Instituto Geologico y Minero de Espana, 95pp.

- CRIMES, T.P. & HARPER, J.C. (eds), 1970: Trace fossils. Seel House Press, Liverpool, 547pp.
- CRIMES, T.P. & HARPER, J.C. (eds), 1977: Trace fossils 2. Seel House Press, Liverpool, 351pp.
- CULLIS, C.G., 1904: The mineralogical changes observed in the cores of the Funafuti borings. In: BONNEY, T.G. (ed.), The Atol of Funafuti. Roy. Soc. London: 392-420.
- CUSHMAN, J.A., 1970: Foraminifera of the Philippine and adjacent seas. Bull. U.S. natl. Mus., n.100, 608pp.
- DAINA, A., 1965: La serie Mesozoico-Terziaria del Monte Barracu (Sicilia centro-occidentale). Atti Soc. tosc. Sci. nat., 72: 19pp.
- D'ANGLEJAN, B.F., 1967: Origin of marine phosphorites off Baja California, Mexico. Mar. Geol., 5: 15-44.
- D'ANGLEJAN, B.F., 1968: Phosphate diagenesis of carbonate sediments as a mode of *in situ* formation of marine phosphorites observations in a core from the E. Pacific. Can. J. Earth Sci., 5: 81-87.
- DAPPLES, E.C., 1967: Diagenesis of sandstones. In: LARSEN, G. & CHILINGAR, G.V. (eds), Diagenesis in sediments. Elsevier, Amsterdam, 91-125.
- DEER, W.A., HOWIE, R.A. & ZUSSMAN, J., 1962: Rock forming minerals, Vol.5. Longman Group, London, 371pp.
- DEER, W.A., HOWIE, R.A. & ZUSSMAN, J., 1963: Rock forming minerals, Vol.4. Longmans, Green and Co. Ltd, London, 435pp.
- DEER, W.A. HOWIE, R.A. & ZUSSMAN, J., 1966: An introduction to the rock-forming minerals. Longman Group, London, 528pp.
- DEGENS, E.T., WILLIAMS, E.G. & KEITH, M.L., 1957: Environmental studies of Carboniferous sediments, Part 1: Geochemical criteria for differentiating marine from fresh water shales. Bull. Am. Assoc. Petrol. Geol., 41: 2427-2455.
- DESHMUKH, G.P., 1979: Palaeozoic phosphorites, Rajasthan, India. In: COOK, P.J. & SHERGOLD, J.H. (eds), Proterozoic-Cambrian phosphorites. Canberra Publishing & Printing Co.: 36-39.
- DIETZ, R.S., EMERY, K.O. & SHEPARD, F.R., 1942: Phosphorite deposits on the sea floor off S. California. Bull. geol. Soc. Am., 53: 815-847.
- DI GRANDE, A., 1975: Geologia dei dintorni di Scicli (Ragusa, Sicilia). Riv. minerar. Sicilia, 151-153: 15-26.

- DI GRANDE, A., GRASSO, M. & ROMEO, M., 1977: Stratigrafia dei terreni affioranti nei dintorni di Ragusa. Riv. Ital. Paleontol. Stratigr., 83: 137-178.
- DI GRANDE, A., LO GIUDICE, A. & BATTAGLIA, M., 1978: Dati geominalogici preliminari sui livelli Miocenici a fosfati di Scicli-Donnalucata (Sicilia SE). Boll. Soc. geol. Ital., 98: 383-390.
- DUEE, G., 1965: La paleogeographie des monts Nebrodi (Sicile). Bull. Soc. geol. Fr., Ser.7, 7: 889-899.
- DUEE, G., 1969: Etude geologique des monts Nebrodi (Sicile). Unpubl. DSc thesis, Univ. de Paris VI, 369pp.
- DUEE, G., 1970: The geology of the Nebrodi mountains of Sicily. In: ALVAREZ, W. & GOHRBANDT, K.H.A. (eds), Geology and History of Sicily. Petrol. Expl. Soc. Libya., 187-200.
- DUNHAM, R.J., 1962: Classification of carbonate rocks according to depositional texture. In: HAM, W.E. (ed), Classification of carbonate rocks. Mem. Am. Assoc. Petrol. Geol., 1: 108-121.
- DUNHAM, R.J., 1969: Early vadose silt in Townsend mound (reef), New Mexico. In: FRIEDMAN, G.M. (ed), Depositional environments in carbonate rocks: a symposium. Spec. Pub. Soc. econ. Palaeontol. Mineral., 14: 182-191.
- DURAND-DELGA, M., 1967: Structure and geology of the northeast Atlas mountains. In: MARTIN, L. (ed), Guidebook to the geology and history of Tunisia. Petrol. Expl. Soc. Libya, 59-85.
- EHLMANN, A.J., HULINGS, N.C. & GLOVER, E.D., 1963: Stages of glauconite formation in modern foraminiferal sediments. J. sediment. Petrol., 33: 87-96.
- EHRENBERG, K., 1944: Ergänzende Bemerkungen zu den seinerzeit aus dem Miozan von Burgschlinitz beschriebenen Gangerkern und bauten dekapoder krebse. Palaeontol. Z. Berlin, 23: 354-359.
- ELLIOTT, G.F., 1957: Subterraniophyllum, a new Tertiary calcareous alga. Palaeontology, London, 1: 73-75.
- ELLIOTT, J., in prep.: Foraminifera and the Palaeogene/Neogene boundary in western Sicily. Unpub. MPhil/PhD thesis, Univ. London (Bedford College).
- EMIGH, G.D., 1958: Petrography, mineralogy and origin of phosphate pellets in the Phosphoria Formation. Idaho Bur. Mines Geology Pamph., 114, 60pp.

- EMIGH, G.D., 1967: Petrology and origin of phosphorites. In: HALES, L.A. (ed), Anatomy of the western phosphate field. Intermount. Assoc. Geol., 15th Ann. Field Conf., 103-114.
- EMIGH, G.D., 1975: Phosphate rock. In: LEFOND, S.J. (ed), Industrial minerals and rocks. Am. Inst. Mining, Metallurgical and Petroleum Engineers, Inc., New York, 935-962.
- EVAMY, B.D., 1969: The precipitational environment and correlation of some calcite cements deduced from artificial staining. J. sediment. Petrol., 39: 787-793.
- EVAMY, B.D. & SHEARMAN, D.J., 1965: The development of overgrowths from echinoderm fragments. Sedimentology, 5: 211-233.
- EVAMY, B.D. & SHEARMAN, D.J., 1969: Early stages in development of overgrowths on echinoderm fragments in limestones. Sedimentology, 12: 317-322.
- FAIRBRIDGE, R.W., 1967: Phases of diagenesis and authigenesis. In: LARSEN, G. & CHILINGAR, G.V. (eds), Diagenesis in Sediments. Elsevier, Amsterdam, 19-89.
- FANG, J.H. & BLOSS, F.D., 1966: X-Ray diffraction tables. Southern Illinois Univ. Press, Carbondale and Edwardsville, not paginated.
- FELIX, R., 1978: Oligo-Miocene stratigraphy of Malta and Gozo. Meded. Landbouwhooges. Wageningen., Nederland, 73-20, 104pp.
- FELL, H.B., 1967: Cretaceous and Tertiary surface currents of the oceans. Oceanogr. Mar. Biol. Ann. Rev., 5: 317-341.
- FISCHER, A.G. & GARRISON, R.E., 1967: Carbonate lithification on the sea floor. J. Geol. Chicago, 75: 488-496.
- FLEET, A.J., BUCKLEY, H.A. & JOHNSTON, L.R., 1980: The rare earth element geochemistry of glauconites and celadonites. J. geol. Soc. London, 137: 683-688.
- FLORES, G., 1959: Evidence of slump phenomena (olistostromes) in areas of hydrocarbon exploration in Sicily. V World Petrol. Congr., New York, Sect.1, n.13: 259-275.
- FLORIDIA, G.B., 1931: Osservazioni geologiche sul Monte Inici (Trapani). Boll. Soc. geol. Ital., 50: 87-112.
- FOCKE, J.W. & GEBELEIN, C.D., 1978: Marine lithification of reef rock and rhodolites at a fore-reef slope locality (-50 m) off Bermuda. Geol. Mijnbouw, 57: 163-171
- FOLK, R.L., 1962: Classification of Carbonate rocks. Mem. Am. Assoc. Petrol. Geol., 1: 62-84.

- FOLK, R.L., 1974: The natural history of crystalline calcium carbonate: effect of magnesium content and salinity. J. sediment. Petrol., 44: 40-53.
- FOSLIE, M.H., 1903: Den botaniske samling. K. norske vidensk. selsk. Aarsber, 2: 23-25.
- FOSLIE, M.H., 1909: Algologiske Notiser VI. K. norske vidensk. selsk. Skr., 2: 1-63.
- FOSTER, M.D., 1969: Studies of celadonite and glauconite. Prof. Pap. U.S. geol. Surv., 614F: 17pp.
- FREAS, D.H. & ECKSTROM, C.L., 1968: Areas of potential upwelling and phosphorite deposition during Tertiary, Mesozoic and late Palaeozoic times. U.N. Mineral Resour. Develop. Ser., 32: 228-238.
- FREY, R.W. (ed.), 1975a: The study of trace fossils. Springer-Verlag, Berlin, 562pp.
- FREY, R.W., 1975b: The realm of ichnology, its strengths and limitations. In: FREY, R.W. (ed.), The study of trace fossils. Springer-Verlag, Berlin, 13-38.
- FREY, R.W. & HOWARD, J.D., 1970: Comparison of Upper Cretaceous ichnofaunas from siliceous sandstones and chalk, Western Interior Region, U.S.A. In: CRIMES, T.P. & HARPER, J.C. (eds), Trace fossils. Seel House Press, Liverpool, 141-166.
- FRIEDMAN, G.M., 1959: Identification of carbonate minerals by staining methods. J. sediment. Petrol., 29: 87-97.
- FRIEDMAN, G.M., 1964: Early diagenesis and lithification in carbonate sediments. J. sediment. Petrol., 34: 777-813.
- FÜCHTBAUER, H., 1950: Die nicht Karbonatischen Bestandteile des Göttinger Muschelkalkes mit besonderer berücksichtigung der mineralneubildungen. Heid Beitr. zur Min. und Petr., 2: 235-254.
- FUNNELL, B.M., 1967: Foraminifera and Radiolaria as depth indicators in the marine environment. Mar. Geol., 5: 333-347.
- GEMMELLARO, G.G., 1859: Degli squaloidei terziari della Sicilia in rapporto con quelli viventi del Mediterraneo. G. Gab. Lett. Acc. Gioenia Sc. Nat. Catania, 5(4): 231-236.
- GEMMELLARO, G.G., 1902: Sul rinvenimento di un teschio di Squalodontidi nel calcare bituminoso di Ragusa in Sicilia. Atti R. Accad. naz. Lincei Mem. Cl. Sc. Fis. Mat. Nat., 11: 3.

- GEMMELLARO, M., 1912: Ittiodontoliti del Miocene medio di alcune regioni della provincia di Palermo e di Girgenti. G. Sci. nat. econ. Palermo, 29: 117-156.
- GEMMELLARO, M., 1914: Ittiodontoliti del calcare asphaltifero di Ragusa in Sicilia. G. Sci. nat. econ. Palermo, 30: 25-44.
- GIANNELLI, L. & SALVATORINI, G., 1972: I foraminiferi planctonici dei sedimenti Tertiari dell'arcipelago Maltese. I Biostratigrafia del Globigerina Limestone. Atti. Soc. Toscana Sci. Nat., Mem. P.V., Ser.A, 79: 49-74.
- GINSBURG, R.N. (ed.), 1975: Tidal deposits. Springer-Verlag, New York, 428pp.
- GIUNTA, G. & LIGUORI, V., 1973: Evoluzione palaeotettonica della Sicilia nord-occidentale. Boll. Soc. geol. Ital., 92: 903-924.
- GOLDBERG, E.D., KOIDE, M., SCHMITT, R.A. & SMITH, R.H., 1963: Rare earth distributions in the marine environment. J. Geophys. Res., 68: 4209-4217.
- GREENSMITH, J.T., HATCH, F.H. & RASTALL, R.H., 1971: Petrology of the sedimentary rocks. Thomas Murby & Co., London, 5th ed., 502pp.
- GROVES, A.W., 1937: Silicate analyses. Thomas Murby & Co., London, 230pp.
- GULBRANDSEN, R.A., 1966: Chemical composition of phosphorites of the Phosphoria Formation. Geochim. cosmochim. Acta., 30: 769-778.
- HALLAM, A., 1963: Major epirogenic and eustatic changes since the Cretaceous and their possible relationship to crustal structure. Am. J. Sci., 261: 397-423.
- HALLOCK, P., 1979: Trends in test shape with depth in large, symbiont-bearing foraminifera. J. foramin. Res., 9: 61-69.
- HAMILTON, E.L. & REX, R.W., 1959: Lower Eocene *globigerina* ooze from Sylvania Guyor. U.S. geol. Surv., Prof. Papers, 260-W: 785-798.
- HÄNTZSCHEL, W., 1964: Spurenfossilien und Problematika im Campan von Beckum (Westf.). Fortschr. Geol. Rheinl. Westfalen., 7: 295-308.
- HÄNTZSCHEL, W., 1975: Trace fossils and Problematika. In: TEICHERT, C. (ed.), Treatise on invertebrate palaeontology, part W, Miscellanea. Geol. Soc. Am. Inc. and the Univ. Kansas, 269pp.

- HASKIN, L.A., FREY, F.A., SCHMITT, R.A. & SMITH, R.H., 1966: Meteoritic, solar, and terrestrial rare-earth distributions. In: ARHENS, L.H., PRESS, F., RUNCORN, S.K. & UREY, H.C. (eds), Physics and chemistry of the Earth, Vol.7, Pergamon, New York, 167-321.
- HASKIN, L. & GEHL, M.A., 1962: The rare earth distribution in sediments. J. Geophys. Res., 67: 2537-2541.
- HAYNES, J., 1981: Foraminifera. MacMillan Publishers Ltd, 433pp.
- HERRMANN, A.G., 1970: Yttrium and the Lanthanides. In: WEDEPOHL, K.H. (ed.), Handbook of geochemistry Vol.II/5. Springer-Verlag, Berlin.
- HEWITT, R.A., 1980: Microstructural contrasts between some sedimentary francolites. J. geol. Soc. London, 137: 661-667.
- HØGDAHL, O.T., MELSOM, S. & BOWEN, V.T., 1968: Neutron activation analysis of lanthanide elements in sea water. Adv. Chem. Ser., 73: 308-325.
- HORTON, A., IVIMEY-COOK, H.C., HARRISON, R.K. & YOUNG, B.R., 1980: Phosphatic ooids in the Upper Lias (Lower Jurassic) of central England. J. geol. Soc. London, 137: 731-740.
- HOWARD, J.D., 1975: The sedimentological significance of trace fossils. In: FREY, R.W. (ed.), The study of trace fossils. Springer-Verlag, Berlin, 131-146.
- HOWE, M.A., 1918: Contributions to the geology and palaeontology of the canal zone Panama.... On some fossil and Recent Lithothamnieae of the Panama canal zone. Bull. U.S. natl. Mus., 103: 1-13, pls.1-11.
- HOWER, J., 1961: Some factors concerning the nature and origin of glauconite. Am. Mineral., 46: 313-334.
- HSU, K.J., 1954: A study of the optic properties and petrologic significance of zoned sanidines. Am. J. Sci., 252: 441-443.
- JACOBACCI, A., 1955: Escursione Palermo-Vicari-Palermo. Boll. Soc. geol. Ital., 72: 78-82.
- JARVIS, I., 1980: Geochemistry of phosphatic chalks and hardgrounds from the Santonian to early Campanian (Cretaceous) of northern France. J. geol. Soc. London, 137: 705-721.
- JOHNSON, J.H., 1957: Geology of Saipan, Mariana Islands: calcareous algae. U.S. Geol. Surv. Profess. Papers, 280E: 209-246, pls 37-60.
- JOHNSON, J.H., 1961a: Limestone building algae and algal limestones. Colorado School of Mines, Boulder, 297pp.

- JOHNSON, J.H., 1961b: Fossil algae from Eniwetok, Funafuti and Kita-Daito-Jima. U.S. Geol. Surv. Profess. Papers, 260Z: 907-950, pls 267-280.
- JOHNSON, J.H., 1962a: Calcareous algae from Sarawak. Mem. Br. Borneo Geol. Surv., 13: 151-168.
- JOHNSON, J.H., 1962b: The algal genus *Lithothamnium* and its fossil representatives. Q. Colorado Sch. Mines, 57(1): 111pp.
- JOHNSON, J.H., 1963: The algal genus *Archaeolithothamnium* and its fossil representatives. J. Palaeontol., 37: 175-211.
- JOHNSON, J.H., 1964: Palaeocene calcareous red algae from northern Iraq. Micropalaeontology, 10: 207-216.
- JOHNSON, J.H., 1965a: Coralline algae from the Cretaceous and early Tertiary of Greece. J. Palaeontol., 39: 802-814.
- JOHNSON, J.H., 1965b: Tertiary red algae from Borneo. Bull. Br. Mus. nat. Hist., 11: 255-280, pls 1-6.
- JOHNSON, J.H. & ADEY, W.H., 1965: Studies of *Lithophyllum* and related algal genera. Q. Colorado Sch. Mines, 60(2): 105pp.
- JOHNSON, J.H. & FERRIS, B.J., 1949: Tertiary coralline algae from the Dutch East Indies. J. Paleontol., 23: 193-198.
- JOHNSON, J.H. & KASKA, H.V., 1965: Fossil algae from Guatemala. Prof. Contrib. Colorado Sch. Mines, 1: 152pp.
- JOHNSON, J.H. & TAFUR, I.A., 1952: Coralline algae from the Eocene Atascadero Limestone. J. Paleontol., 26: 537-543.
- KASTNER, M., 1971: Authigenic feldspars in carbonate rocks. Am. Miner., 56: 1403-1442.
- KASTNER, M. & SIEVER, R., 1968: Origin of authigenic feldspars in carbonate rocks. Spec. Pap. geol. Soc. Am., 121: 155-156.
- KATZ, A. & FRIEDMAN, G.M., 1965: The preparation of stained acetate peels for the study of carbonate rocks. J. Sediment. Petrol., 35: 248-249.
- KAZAKOV, A.V., 1937: The phosphorite facies and the genesis of phosphorites. In: Geological investigation of agricultural ores USSR. Sci. Inst. Fertilizers and insectofungicides, Trans., 142: 65-113.
- KELLEY, S.R.A., 1980: *Hiatella* - A Jurassic bivalve squatter? Palaeontology, London, 23: 769-781.

- KENNEDY, W.J., 1967: Burrows and surface traces from the Lower Chalk of southern England. Bull. Br. Mus. nat. Hist., 15: 127-167, pl. 1-9.
- KENNEDY, W.J., 1970a: A correlation of the uppermost Albian and the Cenomanian of southwest England. Proc. Geol. Assoc. London, 81: 613-677.
- KENNEDY, W.J., 1970b: Trace fossils in the chalk environment. In: CRIMES, T.P. & HARPER, J.C. (eds), Trace fossils, Seel House Press, Liverpool, 263-282.
- KENNEDY, W.J., 1975: Trace fossils in carbonate rocks. In: FREY, R.W. (ed.), The study of trace fossils. Springer-Verlag, Berlin, 377-398.
- KERR, P.F., 1959: Optical mineralogy. McGraw-Hill, New York, 3rd ed., 442pp.
- KOLODNY, Y., 1981: Phosphorites. In: EMILIANI, C. (ed.), The oceanic lithosphere: The sea, vol.7. John Wiley & sons, New York, 981-1023.
- KRAUSKOPF, K.B., 1956: Factors controlling the concentrations of thirteen rare metals in sea-water. Geochim. cosmochim. Acta., 9: 1-32.
- LAMBSCHER, H. & BERNOULLI, D., 1977: Mediterranean and Tethys. In: BIJU-DUVAL, B. & MONTADERT, L. (eds), International symposium on the structural history of the Mediterranean basins. Editions technips., Paris, 129-132.
- LAMOUREUX, J.V.F., 1812: Extrait d'un memoire sur la class des polypiers coralligenes non etierement pierreux. Nouv. Bull. Soc. Sci. Phil. Paris, 3: 181-188.
- LAND, L.S. & MOORE, C.H., 1980: Lithification micritization and syndepositional diagenesis of biolithites on the Jamaican island slope. J. sediment. Petrol., 50: 357-370.
- LAND, L.S., MACKENZIE, F.T. & GOULD, S.J., 1967: Pleistocene history of Bermuda. Bull. geol. Soc. Am., 78: 993-1006.
- LARSEN, G. & CHILINGAR, G.V., 1967: Introduction (Chapter 1). In: LARSEN, G. & CHILINGAR, G.V. (eds), Diagenesis in sediments. Elsevier, Amsterdam, 1-17.
- LEHMANN, E.P., ROZEBOOM, J.J., WALLER, H.O. & CONLEY, C.D., 1967: Microfacies of Libya. Petrol. Expl. Soc. Libya, 80pp.
- LEMOINE, Mme P., 1917: Corallinacees fossiles de la Martinique. 1. Algues du Miocene Inferieur. Bull. Soc. geol. Fr., (4) 17: 256-279.

- LEMOINE, Mme. P., 1926: Revision des Melobesies Tertiaires d'Italia decrites par M. Capeder. C.r. Socs. sav. Paris & Dep., 1925: 241-259.
- LEMOINE, Mme. P., 1928: Corallinacees fossiles de Catalogne et de Valence recueillies par M. l'Abbe Bataller. Bull. Inst. catal. Hist. nat., (2) 8: 92-107.
- LEMOINE, Mme. P., 1939: Les algues calcaires fossiles de L'Algerie. Bull. carte geol. Alger., (1) 9: 1-128.
- LOVELAND, P.J., 1981: Weathering of soil glauconite in southern England. Geoderma, 25: 35-54.
- LUCAS, J., PREVOT, L. & TROMPETTE, R., 1980: Petrology, mineralogy and geochemistry of the late Precambrian phosphate deposits of Upper Volta (W. Africa). J. geol. Soc. London, 137: 787-792.
- MÄGDEFRAU, K., 1932: Über einige Bohrgänge aus dem Unteren Muschelkalk von Jena. Palaeontol. Z. Berlin, 14: 150-160.
- MANHEIM, F.T., PRATT, R.M. & McFARLIN, P.F., 1980: Composition and origin of phosphorite deposits of the Blake plateau. In: BENTOR, Y.K. (ed.), Marine phosphorites-geochemistry, occurrence, genesis. Spec. Publ. Soc. econ. Palaeontol. Mineral. Tulsa, n.29: 117-138.
- MANHEIM, F.T., ROWE, G.T. & JIPA, D., 1975: Marine phosphorite formation off Peru. J. sediment. Petrol., 45: 243-251.
- MARCHETTI, M.P., 1956: The occurrence of slide and flowage materials (Olistostromes) in the tertiary series of Sicily. Int. geol. Congr. Mexico, 209-225.
- MARTENS, C.S. & HARRIS, R.C., 1970: Inhibition of apatite precipitation in the marine environment by Mg-ions. Geochim. cosmochim. Acta., 34: 621-625.
- MARTINSSON, A., 1970: Toponomy of trace fossils. In: CRIMES, T.P. & HARPER, J.C. (eds), Trace fossils. Seel House Press, Liverpool, 323-330.
- MASCLE, G.H., 1967a: Remarques stratigraphiques et structurales sur la region de Palazzo-Ardriano, Monts Sicani (Sicile). Bull. Soc. geol. Fr., Ser.7, 9: 104-110.
- MASCLE, G.H., 1967b: Relations entre les zones de Sciacca, Campofiorito-Cammarata et Vicari (Sicile occidentale). C.r. Somm. Soc. geol. Fr., Fsc.8: 369-370.

- MASCLE, G.H., 1968: Structure et morphologie de la region de Montevago (Sicile occidentale). Bull. Soc. geol. Fr., Ser.7, 653-657.
- MASCLE, G.H., 1970: Geological sketch of western Sicily. In: ALVAREZ, W. & GOHRBANDT, K.H.A. (eds), Geology and History of Sicily. Petrol. Expl. Soc. Libya, 231-244.
- MASCLE, G.H., 1973: Etude geologique des Monts Sicani. Unpubl. DSc thesis, Univ. de Paris VI.
- MASCLE, G.H., 1974: Les grands traits de l'evolution geologique des Monts Sicani (Sicile). Bull. Soc. geol. Fr., Ser.7, 16: 161-170.
- MASCLE, G.H., 1979: Etude geologique des Monts Sicani. Riv. Ital. Paleontol. Stratigr., Mem. 16, 430pp., folded map.
- MATTES, B.W. & MOUNTJOY, E.W., 1980: Burial dolomitisation of the Upper Devonian Miette Build-up, Jasper National Park, Alberta. In: ZENGER, D.H., DUNHAM, J.B. & ETHINGTON, R.L. (eds), Concepts and models of dolomitisation. Spec. Publ. Soc. econ. Palaeontol. Mineral. Tulsa, n.28: 259-297.
- MAZZULLO, S.J., 1980: Calcite pseudospar replacive of marine acicular aragonite, and implications for aragonite cement diagenesis. J. sediment. Petrol., 50: 409-422.
- McARTHUR, J.M., 1978: Systematic variation in the contents of Na, Sr, CO₃, and SO₄ in marine carbonate fluorapatite and their relationship to weathering. Chem. Geol., 21: 89-112.
- McARTHUR, J.M., 1980: Post-depositional alteration of the carbonate-fluorapatite phase of Moroccan phosphates. In: BENTOR, Y.K. (ed.), Marine phosphorites - geochemistry, occurrence, genesis. Spec. Publ. Soc. econ. Palaeontol. Mineral. Tulsa, n.29: 53-60.
- McCLELLAN, G.H., 1980: Mineralogy of carbonate fluorapatites. J. geol. Soc. London, 137: 741-748.
- McCONNELL, D., 1973: Apatite: its crystal chemistry, mineralogy, utilisation, and geologic and biologic occurrence. Springer-Verlag, Berlin, 111pp.
- McKELVEY, V.E., SWANSON, R.W. & SHELDON, R.P., 1953: The Permian phosphorite deposits of the western United States. In: SAINT GUILHEM, P.L.R. (ed.), Origine des gisements de phosphates de chaux. 19th. Internat. Geol. Cong., Algiers, 1952, Comptes rendus, sec.11, fasc.11, 45-64.

- McKELVEY, V.E., WILLIAMS, J.S., SHELDON, R.P., CRESSMAN, E.R. & CHESNEY, T.M., 1959: The Phosphoria, Shedhorn and Park City Formations in the western phosphate field. U.S. geol. Surv. Prof. Paper, 313A: 1-47.
- McRAE, S.G., 1972: Glauconite. Earth Sci. Rev., 8: 397-440.
- MELLIS, O., 1952: Replacement of plagioclase by orthoclase in deep-sea deposits. Nature, London, 169: 624.
- MEYERS, W.J., 1980: Compaction in Mississippian skeletal limestones, southwestern New Mexico. J. sediment. Petrol., 50: 457-474.
- MOBERLY, R., 1973: Rapid chamber-filling growth of marine aragonite and Mg-calcite. J. sediment. Petrol., 43: 634-635.
- MURRAY, J.W., 1973: Distribution and ecology of living benthic foraminiferids. Heinemann Educational Books Ltd, London, 274pp.
- MURRAY, J. & RENARD, A.F., 1891: Report on the deep sea deposits based on the specimens collected during the voyage of HMS Challenger in the years 1872-1876. In: The Challenger Reports. HMSO, Edinburgh, 525pp.
- NAIRN, A.E.M., KANES, W.H. & STEHLI, F.G. (eds), 1977: The Ocean Basins and Margins. Vol.4A. The Eastern Mediterranean. Plenum Press, New York, 503pp.
- NAIRN, A.E.M., KANES, W.H. & STEHLI, F.G. (eds), 1978: The Ocean Basins and Margins. Vol. 4B. The Western Mediterranean. Plenum Press, New York, 447pp.
- NICOL, D., 1967: Some aspects of coldwater marine pelecypods. J. Paleontol., 41: 1330-1340.
- NOTHOLT, A.J.G., 1975: Phosphate rock: world production, trade and resources. In: FLEMING, R.F.S. (ed.), Proceedings of the first "Industrial Minerals" international congress. Metal Bulletin Ltd, London, 104-119.
- NOTHOLT, A.J.G., 1978: Proterozoic-Cambrian phosphogenic provinces in Asia and Australia: IGCP project 156. In: United Kingdom contribution to the International Geological Correlation Programme. The Royal Society, London, 115-117.
- NOTHOLT, A.J.G., 1980a: Phosphatic and glauconitic sediments. J. geol. Soc. London, 137: 657-659, introduction to pages 661-805.
- NOTHOLT, A.J.G., 1980b: Economic phosphatic sediments: mode of occurrence and stratigraphical distribution. J. geol. Soc. London, 137: 793-805.

- ODIN, G.S., 1972, Observations nouvelles sur la structure de la glauconie en accordéon; description du processus de genese par neof ormation. Sedimentology, 19: 285-294.
- ODIN, G.S. & LETOLLE, R., 1980: Glauconitization and phosphatization environments: A tentative comparison. In: BENTOR, Y.K. (ed.), Marine phosphorites-geochemistry, occurrence, genesis. Spec. Publ. Soc. econ. Palaeontol. Mineral. Tulsa, n.29: 227-238.
- ODIN, G.S. & MATTER, A., 1981: De glauconiarum origine. Sedimentology, 28: 611-641.
- ODOM, I.E., WILLAND, T.N. & LASSIN, R.J., 1979: Paragenesis of diagenetic minerals in the St Peter Sandstone (Ordovician) Wisconsin and Illinois. In: SCHOLLE, P.A. & SCHLUGER, P.R. (eds), Aspects of Diagenesis. Spec. Publ. Soc. econ. Palaeontol. Mineral. Tulsa, n.27: 425-443.
- OGNIBEN, L., 1971: Tettonica della Sicilia e della Calabria. Boll. Acc. Gioenia Sc. Nat. Catania, S4, 11: 14-26.
- OGNIBEN, L., 1973: Schema geologico della Calabria in base ai dati odierni. Geologica Romana, 12: 243-585.
- OGNIBEN, L., 1975: Lithostratigraphic complexes and evidence for tectonic phases in Sicily and Calabria. In: OGNIBEN, L., PAROTTO, M. & PRATURLON, A. (eds), Structural model of Italy. Quad. Ric. Scient., 90: 365-408.
- PEDLEY, H.M., 1975: Oligocene-Miocene stratigraphy of the Maltese islands. Unpub. PhD thesis, Univ. of Hull.
- PEDLEY, H.M., 1978: A new lithostratigraphical and palaeoenvironmental interpretation for the coralline limestone formations (Miocene) of the Maltese islands. Overseas Geol. miner. Resour. London, n.54, 17pp.
- PEDLEY, H.M., 1981: Sedimentology and palaeoenvironment of the southeast Sicilian Tertiary platform carbonates. Sediment. Geol., 28: 273-291.
- PEDLEY, H.M., HOUSE, M.R. & WAUGH, B., 1976: The geology of Malta and Gozo. Proc. Geol. Assoc. London, 87: 325-341.
- PEVEAR, D.R., 1966: The estuarine formation of United States Atlantic coastal plain phosphorites. Econ. Geol., 61: 251-256.
- PHILIPPI, R.A., 1837: Beweis das die Nulliporon Pflanzen sind. Arch. F. nat. ter. Dr Wiegmann, 3 I: 387-393.

- PIERONI, P.G., 1965: *Lepidocyclina* and *Miogypsina* from Opi, Sangro valley (central Apennines). Geologica Romana, 4: 161-180.
- PINGITORE, N.E., 1970: Diagenesis and porosity modification in *Aeropora palmata*, Pleistocene of Barbados, West Indies. J. sediment. Petrol., 40: 712-721.
- PIPER, D.Z., 1974: Rare earth elements in the sedimentary cycle: A summary. Chem. Geol., 14: 285-304.
- PLANT, A., DAYAL, B., JAIN, S.C. & CHAKRAVARTY, T.K., 1979: Status of phosphorite investigation in Uttar Pradesh, India, and approach for future work. In: COOK, P.J. & SHERGOLD, J.H. (eds), Proterozoic - Cambrian phosphorites. Canberra Publishing Printing Co., 35-36.
- POIGNANT, A.F., 1979: Determination generique des corallinacees Mesozoiques et Cenozoiques. Bull. Cent. Rech. Explor.-Prod. Elf-Aquitaine, 3: 757-765.
- POIGNANT, A.F., 1980: Criteres de determination specifiques des Corallinacees fossiles. C.r. Acad. Sc. Paris, 291(D): 389-391.
- PORRENGA, D.H., 1967: Glauconite and chamosite as depth indicators in the marine environment. Mar. Geol., 5: 495-501.
- PRAY, L.C., 1960: Compaction in calcilutites. Bull. geol. Soc. Am., 71: 1946.
- PREMOLI SILVA, I. & BRUSA, C., 1981: Shallow-water skeletal debris and larger foraminifers from deep sea drilling project site 462, Nauru Basin, western equatorial Pacific. In: LARSON, R.L., SCHLANGER, S.O., *et al.*, Init. Repts. DSDP, 61, Washington (U.S. Govt. Printing Office), 439-473.
- PREVOT, L. & LUCAS, J., 1980: Behavior of some trace elements in phosphatic sedimentary formations. In: BENTON, Y.K. (ed.), Marine phosphorites-geochemistry, occurrence, genesis. Spec. Publ. Soc. econ. Palaeontol. Mineral. Tulsa, n.29: 31-40.
- RAINERI, R., 1923: Alge fossili Mioceniche di Cirenaica. Nuova Notarisa, Padova, 35: 5-23.
- READ, J.F., 1982: Carbonate platforms of passive (extensional) continental margins: types, characteristics and evolution. Tectonophysics, 81: 195-212.
- RECH-FROLLO, M.M., 1963: Les conditions de formation de la glauconie en relation avec le flysch. C.r. Acad. Sci., 257: 3011-3013.

- RHOADS, D.C., 1975, The palaeoecological and environmental significance of trace fossils. In: FREY, R.W. (ed.), The study of trace fossils. Springer-Verlag, Berlin, 147-160.
- RIETH, A., 1932: Neue funde spongeliomorpher fucoiden aus dem Jura Schwabens. Geol. palaeontol. Abh., 19: 257-294.
- RIGGS, S.R., 1979a: Petrology of the Tertiary phosphorite system of Florida. Econ. Geol., 74: 195-220.
- RIGGS, S.R., 1979b: Phosphorite sedimentation in Florida - A model phosphogenic system. Econ. Geol., 74: 285-314.
- RIGGS, S.R., 1980: Intraclast and pellet phosphorite sedimentation in the Miocene of Florida. J. geol. Soc. London, 137: 741-748.
- RIGGS, S.R. & FREAS, D.H., 1965: Stratigraphy and sedimentation of phosphorite in the central Florida phosphate district. Amer. Inst. Mining Eng., Preprint 65-H-84, 13pp.
- RIGO, M. & BARBIERI, F., 1959: Stratigrafia pratica applicata in Sicilia. Boll. Serv. geol. Ital., 80: 351-441.
- RIGO DE RIGHI, M., 1954: Notizie sulla geologia di una zona a nord di Menfi (Sicilia sud-occidentale). Riv. minerar. Sicilia, 26: 73-77.
- ROCCATI, A., 1911: Glauconite della ficuzza e di Corleone (Palermo). G. Sci. nat. econ. Palermo, 28: 247-262.
- ROMANKEVICH, Y.A. & BATURIN, G.N., 1972: Composition of the organic matter in phosphorites from the continental shelf off S.W. Africa. Geochem. Int., 9: 464-470 (English transl.).
- RONOV., A.B., BALASHOV, Y.A. & MIGDISOV, A.A., 1967: Geochemistry of the rare earths in the sedimentary cycle. Geochem. Int., 4: 1-17.
- ROSE, E.P.F., 1966: The functional significance of variations in some Tertiary echinoids. Unpub. D.Phil. Thesis, Univ. of Oxford, 439pp.
- ROSE, E.P.F., 1974: Miocene Echinoidea of Libya: a summary and review of their stratigraphical distribution. Mem. Bur. Rech. Minerres, 78: 341-347.
- ROTHPLETZ, A., 1891: Fossile Kalkalgen aus den familien der Codiaceen und der Corallineen. Z. Deutsch. geol. Ges., 43: 295-322.
- RUGGIERI, G., 1957: Aspetti della trasgressione Langhiana nella zona del Monte Pispisa (Segesta). Riv. minerar. Sicilia, 48: 264-267.

- RUGGIERI, G., 1959: Il Paleogene e il Miocene del Monte Bonifato presso Alcamo. Riv. minerar. Sicilia, 57: 3-11, plates 1-6.
- RUGGIERI, G., 1961: Frammenti di stratigrafia Siciliana. Riv. minerar. Sicilia, 70-72: 170-175.
- RUSSELL, R.T. & TRUEMAN, N.A., 1972: The geology of the Duchess phosphate deposits, N.W. Queensland, Australia. Econ. Geol., 66: 1186-1214.
- SCANDONE, P., GIUNTA, G. & LIGUORI, V., 1974: The connection between the Apulia and the Sahara continental margins in the southern Apennines and in Sicily. 67th Congr. Soc. geol. Ital., Parma; Mem. Soc. Geol. Ital., 13: 317-323.
- SCHLANGER, S.O., 1964: Petrology of the limestones of Guam. Prof. Pap. U.S. geol. Surv., 403D: 1-52.
- SCHMIDT DI FRIEDBERG, P., 1959: La geologia del gruppo montuoso delle Madonie in relazione alle possibilita petrolifere della Sicilia centro-settentrionale. Atti II Congr. Petrol. Sicil. Gela, 12pp.
- SCHMIDT DI FRIEDBERG, P., 1962: Introduction a la geologie petroliere de la Sicile. Rev. Inst. Fr. Pet. Paris, 17: 635-668.
- SCHMIDT DI FRIEDBERG, P., BARBIERI, F. & GIANNINI, G., 1960: La geologia del gruppo montuoso delle Madonie (Sicilia centro-settentrionale). Boll. Serv. geol. Ital., 81: 73-107.
- SCHOFIELD, A. & HASKIN, L., 1964: Rare earth distribution patterns in eight terrestrial materials. Geochim. cosmochim. Acta., 28: 437-446.
- SCHOPF, T.J.M., 1980: Palaeoceanography. Harvard Univ. Press, Cambridge, 341pp.
- SCHROEDER, J.H., 1974: Carbonate cements in Recent reefs of the Bermudas and Bahamas: Keys to the past? Ann. Soc. geol. Belg., 97: 153-158.
- SEED, D.P., 1965: The formation of vermicular pellets in New Zealand glauconites. Am. Mineral., 50: 1097-1106.
- SEILACHER, A., 1964: Biogenic sedimentary structures. In: IMBRIE, J. & NEWELL, N. (eds.), Approaches to palaeoecology. J. Wiley & Sons, New York, 296-315.
- SEILACHER, A., 1967: Bathymetry of trace fossils. Mar. Geol., 5: 413-428.

- SELLI, R., 1957: Sulla transgressione del Miocene nell' Italia meridionale. J. Geol., 26: 1-54.
- SELLWOOD, B.W., 1971: A *Thalassinoides* burrow containing the crustacean *Glyphaea udressieri* (Meyer) from the Bathonian of Oxfordshire. Palaeontology, London, 14: 589-591.
- SEMENOV., E.I., KHOLODOV, V.N., BARINSKII, R.L., 1962: Rare earths in phosphorites. Geokhimiya, n.5: 501-507 (English transl.).
- SENES, J. (ed.), 1976: Proceedings of the sixth congress, Bratislava, International Union of Geological Sciences Commission on Stratigraphy, Veda, Bratislava, 70pp.
- SHELDON, R.P., 1964: Exploration for phosphorite in Turkey - a case history. Econ. Geol., 59: 1159-1175.
- SHELDON, R.P., 1980: Episodicity of phosphate deposition and deep ocean circulation - an hypothesis. In: BENTOR, Y.K. (ed.), Marine phosphorites - geochemistry, occurrence, genesis. Spec. Publ. Soc. econ. Palaeontol. Mineral. Tulsa, n.29: 239-248.
- SLANSKY, M., 1979: Proposals for nomenclature and classification of sedimentary phosphate rocks. In: COOK, P.J. & SHERGOLD, J.H. (eds), Proterozoic - Cambrian phosphorites. Canberra Publishing & Printing Co., 60-63.
- SLANSKY, M., 1980: Geologie des phosphates sedimentaires. Mem. Bur. Rech. geol. minieres, n.114, 92pp.
- SMITH, A.G. & BRIDEN, J.C., 1977: Mesozoic and Cenozoic palaeocontinental maps. Cambridge University Press, Cambridge, 63pp.
- SMITH, J.P. & LEHR, J.R., 1966: An X-ray investigation of carbonate -apatites. J. Agric. Food Chem., 14: 342-349.
- SOUAYA, F.J., 1963: Micropalaeontology of four sections south of Qoseit, Egypt. Micropalaeontology, 9: 233-266.
- SPEARS, D.A., 1979: Geochemical aspects of the Santonian Chalk of Ramsgate, England and the origin of the chert and clay minerals. Mineralog. Mag. London, 43: 159-164.
- STAINFORTH, R.M., LAMB, J.L., LUTERBACHER, H., *et al.*, 1975: Cenozoic planktonic foraminiferal zonation and characteristics of index forms. Contr. Paleont. Univ. Kansas, Art. 62: 13-425.
- STRAATEN, L.M.J.U. van, 1948: Note on the occurrence of authigenic feldspar in non-metamorphic sediments. Am. J. Sci., 246: 569-572.

- SUMMERHAYES, C.P., 1970: Phosphate deposits on the northwestern African continental shelf and slope. Unpub. Ph.D. thesis, Univ. of London (Imperial College).
- TAKAHASHI, J., 1939: Synopsis of glauconitisation. In: TRASK, P.D. (ed.), Recent Marine Sediments. Mem. Am. Assoc. Petrol. Geol., 502-512.
- TOOMS, J.S., SUMMERHAYES, C.P. & CRONAN, D.S., 1969: Geochemistry of marine phosphate and manganese deposits. Oceogr. Mar. Biol. Ann. Rev., 7: 49-100.
- TRUEMAN, N.A., 1971: A petrological study of some sedimentary phosphorite deposits. Aust. Miner. Develop. Lab. Bull., 11: 1-71.
- TRUILLET, R., 1970: The geology of the eastern Peloritani mountains of Sicily. In: ALVAREZ, W. & GOHRBANDT, K.H.A. (eds), Geology and history of Sicily. Petrol. Expl. Soc. Libya, 171-186.
- VEEH, H.H., BURNETT, W.C. & SOUTAR, A., 1973: Contemporary phosphorite on the continental margin of Peru. Science, 181: 845-847.
- VELDE, B., 1976: The chemical evolution of glauconite pellets as seen by microprobe determinations. Mineralog. Mag. London, 40: 753-760.
- VERA, J.A., 1969: Estudio geológico de la zona Subbética en la transversal de Loja y sectores adyacentes. Pub. Departamentos Geol., Estrat., Palaeont., Univ. de Granada, Ser. B, n.75: 187pp, plates 1-16.
- WAGNER, C.W. & TOGT, C. van der, 1973: Holocene sediment types and their distribution in the southern Persian Gulf. In: PURSER, B.H. (ed.), The Persian Gulf. Springer-Verlag, Berlin, 123-155.
- WALSH, J.N. & HOWIE, R.A., 1980: An evaluation of the performance of an inductively coupled plasma source spectrometer for the determination of the major and trace constituents of silicate rocks and minerals. Mineralog. Mag. London, 43: 967-974.
- WALSH, J.N., BUCKLEY, F. & BARKER, J., 1981: The simultaneous determination of the Rare Earth Elements in rocks using inductively coupled plasma source spectrometry. Chem. Geol., 33: 141-153.
- WARME, J.E., 1970: Traces and significance of marine rock borers. In: CRIMES, T.P. & HARPER, J.C. (eds), Trace fossils. Seel House Press, Liverpool, 515-526.

- WARME, J.E., 1975: Borings as trace fossils, and the processes of marine bioerosion. In: FREY, R.W. (ed.). The study of trace fossils. Springer-Verlag, Berlin, 181-228.
- WARME, J.E., 1977: Carbonate borers - their roles in reef ecology and preservation. In: FROST, S.H. WEISS, M.P. & SAUNDERS, J.B. (eds), Reefs and related carbonates - ecology and sedimentology. Am. Ass. Petrol. Geol., Studies in Geology, 4: 261-280.
- WAUGH, B., 1978: Authigenic K-feldspar in British Permo-Triassic sandstones. J. geol. Soc. Lond., 135: 51-56.
- WEBER van BOSSE, A. & FOSLIE, M.H., 1904: The corallinaceae of the Siboga-expedition. Siboga-Expedite Mon., 41: 73-75.
- WEYL, P.K., 1959: Pressure solution and the force of crystallization - a phenomenological theory. J. geophys. Res., 64: 2001-2025.
- WEZEL, F.C., 1966: La sezione tipo del Flysch Numidico: stratigrafia preliminare della parte sottostante al Complesso Panormide (Membro di Portella Colla). Atti Accad. gioenia Sci. nat. Catania, 18: 71-92.
- WEZEL, F.C., 1967: Sedimentological characteristics of some Italian turbidites: Numidian flysch "Reitano flysch". Geologica Romana, 6: 396-403.
- WEZEL, F.C., 1968: Osservazioni sui sedimenti dell' Oligocene - Miocene inferiore della Tunisia settentrionale. Mem. Soc. geol. Ital., 7: 417-439.
- WEZEL, F.C., 1969: Prossimalita, distalita e analisi dei bacini dei flysch: un punto di vista attualistico. Mem. Soc. Natur. Napoli, 78: 8pp.
- WEZEL, F.C., 1970: Numidian Flysch: an Oligocene - early Miocene continental rise deposit off the African Platform. Nature, London, 228: 275-276.
- WEZEL, F.C., 1975a: Flysch successions and the tectonic evolution of Sicily during the Oligocene and early Miocene. In: SQUYRES, C. (ed.), Geology of Italy. Petrol. Expl. Soc. Libya: 105-127.
- WEZEL, F.C., 1975b: Diachronism of depositional and diastrophic events. Nature, London, 253: 255-257.
- WILSON, J.L., 1975: Carbonate facies in geologic history. Springer-Verlag, New York, 471pp.

- WILTSHIRE, T., 1869: On the Red Chalk of Hunstanton. Q.J. geol. Soc. London, 25: 185-192.
- WISE, W.S. & EUGSTER, H.P., 1964: Celadonite: synthesis, thermal stability and occurrence. Am. Mineral., 49: 1031-1083.
- WOODWARD, S., 1830: A synoptic table of British organic remains. London & Norwich, 50pp.
- WRAY, J.L., 1971: Ecology and geologic distribution. In: GINSBURG, R.N., REZAK, R. & WRAY, J.L., Geology of calcareous algae (notes for a short course). Comparative sediment. Lab., Univ. Miami, 64pp.
- WRAY, J.L., 1977: Calcareous algae. Elsevier Scientific Pub. Co., 185pp.
- ZAMMIT-MAEMPEL, G., 1979: The Indo-Pacific affinity of some Maltese Tertiary fossils. Centr. Med. Nat., 1: 1-12.
- ZANCL, H., 1969: Structural and textural evidence of early lithification in fine grained carbonate rocks. Sedimentology, 12: 241-256.
- ZUSSMAN, J., 1977: X-Ray diffraction. In: ZUSSMAN, J. (ed.), Physical methods in determinative mineralogy. Academic Press, London, 391-474.

APPENDIX I

TECHNIQUES

A.1.1 Petrology

In total 380 standard thin sections were prepared for microscopic study: 250 from the Upper Oligocene limestones and 100 from the Lower Miocene glauconitic sandy limestones of southwest Sicily, plus 30 from the phosphorite, hardground and associated limestones of southeast Sicily. Additionally, 40 thin sections of Maltese phosphorites prepared for Bennett (1980) were also used. All thin sections are now preserved in the Department of Geology, Bedford College. Microscopic studies were made using a Wild M5 stereomicroscope with rotating polarising stage (no. 368078) and mechanical stage (CP 383130), since these provided excellent optics combined with strong magnification and a wide field of view.

Some 80 acetate peels were taken from cut, polished and etched specimens following the technique described by Allman & Lawrence (1973, p.290). Peels were more easily obtained from non-porous, well-cemented rocks. Porous rocks formed poor peels because acetone "reservoirs" formed in their pores and subsequently dissolved the acetate sheet used for the peel.

Samples used to make acetate peels were stained first to detect aragonite (using Feigl's solution), then to detect high Mg calcite (using Alizarin red S in 30% NaOH solution) after the technique described by Friedman (1959) although results were negative. A modification of the technique described by Katz & Friedman (1965) was used to test for iron free calcite, ferroan calcite and dolomite. Surfaces to be examined were first polished with 400 then 600 grade carborundum powder. Stains were prepared as described by Katz & Friedman (1965). Etching prior to staining was varied from one minute (for well-cemented strongly indurated rocks) to 30 seconds (for poorly cemented porous rocks). Specimens were stained for three minutes in Alizarin red S and five to six minutes in

potassium ferricyanide solution. Alizarin red S solution imparted a deep red to calcite, while dolomite (when present) remained unstained. Potassium ferricyanide solution imparted a blue colour to ferroan calcite (the deepness of colour being dependent on the amount of ferrous iron present) whilst iron free calcite did not stain.

Photomicrographs were taken at magnifications of 12.5x, 32x and 125x. Subsequent printing at 120 mm x 80 mm involved a further 3.3-fold increase in magnification, resulting in total magnifications of 41x, 105x and 410x respectively. All photomicrographs were taken on a Zeiss photomicroscope III which incorporates an automatic exposure meter. Ilford FP4 (ASA 125) and Kodak Panatomic X (ASA 32) monochrome were used. A green filter was used where it was necessary to subdue differences in contrast (e.g. the juxtaposition of clear calcite cement and dense, dark algal material). The colour photomicrographs presented here were printed from colour slides taken on Ektachrome 50 professional film (ASA 50) at the same magnifications with only a slightly larger printing size.

A.1.2 Powder Sample Preparation

Phosphorite and limestone samples were prepared for mineral and geochemical analysis using the following procedure:

- 1) Sediment adhering to phosphorite clasts was removed using a wire brush. Samples were then washed in distilled water and left to dry.

- 2) Large phosphatic clasts were broken using a hammer. The fragments and smaller clasts were reduced in size to 5-10 mm in a jaw crusher. At this point, in some samples, outer coatings of phosphatic clasts were separated from the interiors for preparation for separate geochemical analysis.

- 3) Fragments were reduced to talc in a tungsten carbide tema, operated for periods up to five minutes. This powder was then stored in labelled glass jars. (Previous to steps 2 and 3 care was always taken to ensure that the apparatus was properly cleaned after the previous specimen and especially previous to the first sample of a crushing period).

A.1.3 X-Ray Diffraction Analysis

Graphs of diffraction patterns of powder samples were obtained using a Phillips 1010 diffractometer, housed at Bedford College. The technique is standard. The resultant graphs were compared with standard reference data recorded in a powder diffraction file for minerals (Berry, 1974), after first converting the 2θ angles into $d(\text{\AA})$ spacings using the tables of Fang & Bloss (1966) for Cu $K\alpha$ radiation. All phosphorite samples had diffraction patterns typical of carbonate-fluorapatite (data given in Table A2.2) with varying quantities of calcite present. Slight differences in peak positions were interpreted, following Smith & Lehr (1966), as changes in cell parameters caused by ionic substitutions.

A.1.4 Inductively Coupled Plasma Spectrometry

Inductively coupled plasma (ICP) spectrometry and associated sample preparation were carried out in the Geology Department of King's College, University of London, under the supervision of Dr J.N. Walsh. Analysis was made for major, trace and Rare Earth Elements. The apparatus and the analytical process are described by Walsh & Howie (1980).

a) Major and Trace Elements

Solutions for the combined analysis of major and trace elements were prepared using the technique described by Walsh & Howie (1980) for the preparation of solutions for major element analysis. Further preparation of solutions specifically for trace element analysis as described by Walsh & Howie (1980) was not adopted. The process is designed to remove silicon from silicate rocks so as to concentrate the other major and trace elements, but since silicon is present in only small abundances (< 1-4%) in the limestones and phosphorites analysed here, this concentration process was deemed unnecessary.

Analysis for major (Si, Al, Fe, Mg, Ca, Na, K, Ti, P and Mn) and trace elements (Sc, V, Ni, Cu, Sr, Y, Zr and Ba) was carried out on the ICP spectrometer in the manner described by Walsh & Howie (1980). Analysis was also made for the trace elements Li, Zn, Pb, Cr and Co but the results were disregarded: Li because of contamination by LiBO_2 used as

a flux in sample preparation; Zn and Pb because of spectral interference of other elements on their detection spectra; and Cr and Co because of inconsistent results which may reflect their very low values in phosphorites and limestones, and which, in the case of Cr, may be linked with the very high values of Ca in the samples causing interference on the Cr spectrum which is close to one of those of Ca (Walsh, pers. comm. 1981).

Standard rock samples, used to construct calibration curves from which to estimate the element oxide and trace element composition of each sample, comprised four known standard rocks (Table A.2.4) and three spiked standards. Spiked standards were made by mixing controlled quantities of the known standards together (in the proportions 120B/1C, 1:1; 120B/1C, 1:4; KC11/120B, 1:1) thus forming a stepped increase in element concentration. Four solutions of each standard (known and spiked) were prepared and then analysed along with four blank solutions which were prepared in the same manner as set out above, but the rock powder was not added to the LiBO_2 flux. Their analyses therefore represent the "background" counts for each element oxide and trace element. One solution from each standard and from the blanks which showed consistent intensity counts with the others was then chosen to be analysed together with the samples. In addition, a further ten known standards (Table A2.5), previously prepared by the technical staff at King's College, were analysed to provide more data points to construct calibration curves for the trace elements (not listed in the 120B and 1C standard rocks). All these standards were run after every sixth sample to keep a close check on machine drift.

Results from the ICP were given as intensity counts. These were then corrected for machine drift and background specimen counts (blanks) before converting them into percentages or ppm using the gradients from the calibration curves.

b) Rare Earth Elements

Solutions for Rare Earth Element (REE) analysis were prepared wholly in the manner described by Walsh *et al.* (1981). The technique takes four days for any one sample to be processed from start to finish. However, the apparatus set up at King's College allows a batch of five

samples to be processed together. Throughout the process, care should always be taken to wash the sample containers into the next container required in the process to avoid any loss of REE.

The ICP computerised system is fully calibrated for quantities of REEs likely to be found in phosphorites. Intensities are automatically fed into a computer programme and the printout is given in ppm element within two minutes of running a sample. Three standards (Table 4.11) and two blanks were run along with the phosphorites from the central Mediterranean. The standards allow comparison of the results on the ICP with the same standards and therefore other rocks elsewhere using different or the same techniques. The blanks allow subtraction of any "background" abundances of REE, incorporated in the process. A composite standard, already prepared at King's College, was also run every sixth sample to monitor machine drift. The printout was then corrected for background and drift to obtain the true REE values.

The normalisation of absolute concentrations of REEs in the phosphorites, limestones and standard rocks to chondrite and in some cases average sediment, southwest Sicily limestone and mean Maltese phosphorite follow the principles discussed by Haskin *et al.* (1966). The values of these REEs concentrations and the sources of the data are given in Table A.2.3.

TABLE 42.1 Index to samples used in monazite study, indicating locality and horizon of origin, type of analysis (other than major and trace element analyses for which all samples listed were used), and description of sample.

Locality abbreviations: A(1), Madorello east (grid ref. UB 34598); A(2), Madorello east (UB 351598); A(3), Madorello east (UB 349575); Fo, Rocca Portoria (UB 388597); S8, San Stagio west (UB 363676); C, Calabellotta Tombe Sicani exposure (UB 421601); M6, Monte Gargalupo (UB 420650); Pa, Contrada Pasqualetto (UB 212646); D(1), Donnalucata (VA 667691); D(2), Donnalucata (VA 661691); M, Modica (VA 803785); MR, Marina di Ragusa (VA 592716); CS, Contrade le Serre (VA 752928); M5, North Gozo Maltese islands grid ref. 316934); Dv, Dureira, west Gozo (274897); Q, Qamnet, northwest Malta (396811). Strigraphic abbreviations: T, Turonian, Upper Cretaceous; UC, Upper Oligocene; LM, Lower Miocene.

APPENDIX II

ADDITIONAL TABLES

TABLE A2.1

Index to samples used in phosphorite study, indicating locality and horizon of origin, type of analysis (other than major and trace element analyses for which all samples listed were used), and description of sample.

Locality abbreviations: N(1), Nadorello east (grid ref. UB 349598); N(2), Nadorello east (UB 351598); N(3), Nadorello east (UB 349595); Po, Rocca Porcaria (UB 358597); SB, San Biagio west (UB 363676); C, Caltabellotta Tombe Sicani exposure (UB 421601); MG, Monte Gargalupo (UB 420650); Pa, Contrada Pasqualetto (UB 312646); D(1), Donnalucata (VA 667691); D(2), Donnalucata (VA 661691); M, Modica (VA 803785); MR, Marina di Ragusa (VA 592710); CS, Contrada le Serre (VA 752928); NG, North Gozo (Maltese islands grid ref. 316934); Dw, Durejra, west Gozo (274897); Q, Qammieh, northwest Malta (396811). Stratigraphic abbreviations: T, Turonian, Upper Cretaceous; UO, Upper Oligocene; LM, Lower Miocene.

| XRD/REF | Description |
|---------|--|
| XRD+REF | Phosphatised clast: outer coating |
| XRD+REF | Phosphatised whole clast |
| XRD | Phosphatised whole clast |
| XRD | Phosphatised whole clast |
| XRD | Phosphatised whole clast |
| XRD+REF | 3 (20-30 mm size) phosphatised whole clast |
| XRD+REF | Phosphatised whole clast |
| XRD+REF | Phosphatised clast: outer coating |
| XRD+REF | Phosphatised clast: interior |
| XRD+REF | Phosphatised clast: outer coating |
| XRD+REF | Phosphatised clast: interior |
| XRD | Phosphatised whole clast |
| XRD | Phosphatised whole clast |
| XRD | Phosphatised whole clast |
| XRD | Phosphatised whole clast |
| XRD | Phosphatised silty limestone clast |
| XRD | 3 large (10 mm) fragments of fish teeth |
| XRD | Phosphatised whole clast |
| XRD | Phosphatised whole clast |
| XRD | Chalk (unconformity surface) |
| REF | Chalk (30 cm below unconformity surface) |
| REF | Foraminiferal limestone, burrow infill |
| REF | Rhodolith algal foraminiferal limestone |
| REF | Foraminiferal limestone, burrow infill |
| REF | Rhodolith algal foraminiferal limestone |
| REF | Rhodolith algal foraminiferal limestone |

| Sample No. | Locality | Stratigraphic horizon | XRD/REE | Description |
|------------|----------|-----------------------|---------|---|
| RTA 7A | N(1) | UO | XRD+REE | Phosphatised clast: outer coating |
| RTA 7B | N(1) | UO | XRD+REE | Phosphatised whole clast |
| RTA 7C | N(1) | UO | XRD | Phosphatised whole clast |
| RTA 7D | N(1) | UO | - | Phosphatised whole clast |
| RTA 11A | N(1) | UO | XRD | Phosphatised whole clast |
| RTA 11B | N(1) | UO | XRD+REE | 3 (20-30 mm size) phosphatised whole clasts |
| RTA 13A | N(1) | UO | XRD+REE | Phosphatised whole clast |
| RTA 13B | N(1) | UO | XRD+REE | Phosphatised clast: outer coating |
| RTA 13C | N(1) | UO | XRD+REE | Phosphatised clast: interior |
| RTB 19A | N(2) | UO | XRD+REE | Phosphatised clast: outer coating |
| RTB 19B | N(2) | UO | XRD+REE | Phosphatised clast: interior |
| 11.4 | N(3) | UO | - | Phosphatised whole clast |
| 6.3 | N(1) | UO | - | Phosphatised whole clast |
| 2.9A | Po | UO | - | Phosphatised whole clast |
| 45M | SB | UO | - | Phosphatised whole clast |
| 36.1A | C | UO | - | Phosphatised silty limestone clast |
| 36.1B | C | UO | - | 5 large (10 mm) fragments of fish teeth |
| 97.2A | MG | UO | - | Phosphatised whole clast |
| 119M | Pa | UO | - | Phosphatised whole clast |
| JTA 3 | N(1) | T | - | Chalk (unconformity surface) |
| JTA 5A | N(1) | T | REE | Chalk (30 cm below unconformity surface) |
| JTB 5 | N(2) | UO | - | Foraminiferal limestone: burrow infill |
| RTB 12 | N(2) | UO | - | Rhodolithic algal foraminiferal limestone |
| RTB 18 | N(2) | UO | REE | Foraminiferal limestone: burrow infill |
| RTB 20 | N(2) | UO | - | Rhodolithic algal foraminiferal limestone |
| RTC 2 | N(2) | UO | - | Rhodolithic algal foraminiferal limestone |

| Sample No. | Locality | Stratigraphic horizon | XRD/REE | Description |
|------------|----------|-----------------------|---------|--|
| 187.2 | D(1) | LM | XRD+REE | Phosphatised hardground |
| 187.3 | D(1) | LM | XRD+REE | Phosphatised clast |
| 187.5 | D(1) | LM | XRD+REE | Phosphatised hardground |
| 187.15 | D(1) | LM | XRD+REE | Phosphatised clast |
| 188 M | M | LM | - | 6 small (<10 mm) phosphatised clasts |
| 191 M | MR | LM | - | 9 small (<10 mm) phosphatised clasts |
| 192.8A | CS | LM | - | 4 small (10-25 mm) phosphatised clasts |
| 193.2B | D(2) | LM | XRD | Phosphatised hardground |
| M1 | NG | LM(C1) | XRD+REE | Phosphatised clast |
| M2 | NG | LM(C1) | - | Phosphatised clast |
| M3 | NG | LM(Hg) | REE | Phosphatised hardground |
| M4 | NG | LM(C2) | XRD | Phosphatised clast |
| M5 | NG | LM(C2) | - | Phosphatised clast |
| M6 | NG | LM(C2) | - | Phosphatised clast |
| M7 | NG | LM(C2) | - | Phosphatised clast |
| M8 | Dw | LM(C1) | - | Phosphatised clast |
| M9 | Dw | LM(C1) | - | Phosphatised clast |
| M10 | Dw | LM(C1) | - | Phosphatised clast |
| M11 | Q | LM(C1) | XRD+REE | Phosphatised clast |
| M12 | Q | LM(Hg) | XRD+REE | Phosphatised hardground |
| M13 | Q | LM(C1) | - | Phosphatised echinoid |
| M14 | Q | LM(C2) | XRD+REE | Phosphatised clast |
| M15 | Q | LM(C2) | - | Phosphatised clast |
| M16 | Q | UO(Hg) | - | Lower Coralline Limestone hardground (L.C.L.H) |
| M17 | Q | ?UO | - | Clast from overlying conglomerate of L.C.L.H. |
| M18 | Q | ?UO | - | Clast from overlying conglomerate of L.C.L.H. |

| hkl | RTA 7A | | RTA 7B | | RTA 7C | | RTA 7E | |
|-----|--------|------------------|--------|------------------|--------|------------------|--------|------------------|
| | d(A) | I/I ₀ | d(A) | I/I ₀ | d(A) | I/I ₀ | d(A) | I/I ₀ |
| 100 | 8.102 | 4 | 8.117 | 7 | 8.117 | 7 | 8.109 | 6 |
| 200 | 4.049 | 6 | 4.049 | 6 | 4.046 | 7 | 4.049 | 7 |
| 111 | 3.858 | 6 | 3.853 | 7 | 3.862 | 6 | 3.872 | 6 |
| 002 | 3.439 | 38 | 3.440 | 42 | 3.440 | 40 | 3.437 | 34 |
| 102 | 3.159 | 16 | 3.165 | 15 | 3.173 | 16 | 3.171 | 14 |
| 210 | - | - | - | - | - | - | - | - |
| 211 | 2.793 | 100 | 2.789 | 100 | 2.782 | 100 | 2.786 | 100 |
| 112 | 2.773 | 53 | 2.767 | 56 | 2.776 | 55 | 2.778 | 49 |
| 300 | 2.689 | 48 | 2.684 | 52 | 2.683 | 51 | 2.684 | 47 |
| 202 | 2.620 | 27 | 2.622 | 31 | 2.615 | 30 | 2.616 | 26 |
| 301 | - | - | - | - | - | - | - | - |
| 212 | 2.284 | - | - | - | - | - | - | - |
| 310 | 2.233 | - | - | - | - | - | - | - |
| 221 | 2.202 | - | - | - | - | - | - | - |
| 311 | - | - | - | - | - | - | - | - |
| 302 | 2.122 | - | - | - | - | - | - | - |
| 213 | 2.058 | - | - | - | - | - | - | - |
| 400 | - | - | - | - | - | - | - | - |
| 203 | 1.997 | 6 | 1.993 | 5 | 1.996 | 6 | 1.997 | 7 |
| 222 | 1.929 | 25 | 1.931 | 26 | 1.928 | 27 | 1.925 | 29 |
| 312 | 1.873 | - | 1.870 | - | 1.880 | - | 1.877 | - |
| 320 | 1.852 | 6 | 1.851 | 6 | 1.852 | 7 | 1.858 | 5 |
| 213 | 1.833 | 30 | 1.833 | 31 | 1.834 | 29 | 1.836 | 30 |
| 321 | 1.783 | 14 | 1.785 | 12 | 1.789 | 12 | 1.786 | 11 |
| 410 | 1.759 | 12 | 1.762 | 12 | 1.762 | 12 | 1.759 | 14 |
| 402 | 1.742 | 12 | 1.741 | 12 | 1.741 | 14 | 1.740 | 12 |
| 004 | 1.723 | 12 | 1.721 | 14 | 1.724 | 13 | 1.723 | 16 |
| 322 | 1.676 | - | 1.678 | - | 1.679 | - | 1.677 | - |
| 311 | 1.600 | - | 1.602 | - | 1.602 | - | 1.600 | - |

TABLE A2.2

Values for d-spacing ($d(\text{\AA})$) and peak intensity (I/I_0) obtained by XRD analysis of twenty samples. See TABLE A2.1 for details of sources of samples. No data are given for crystal face 210 since this was obscured by the calcite 100 peak at 3.035. No intensities are given for the 212, 312, 322 and 313 crystal faces, since the peak sizes represented the combined intensities of francolite and calcite at the respective d-spacings.

| hk1 | RTA 7A | | RTA 7B | | RTA 7C | | RTA 11A | |
|-----|-----------------|------------------|-----------------|------------------|-----------------|------------------|-----------------|------------------|
| | $d(\text{\AA})$ | I/I ₀ | $d(\text{\AA})$ | I/I ₀ | $d(\text{\AA})$ | I/I ₀ | $d(\text{\AA})$ | I/I ₀ |
| 100 | 8.102 | 4 | 8.117 | 7 | 8.117 | 7 | 8.109 | 6 |
| 200 | 4.049 | 6 | 4.049 | 6 | 4.046 | 7 | 4.049 | 7 |
| 111 | 3.858 | 6 | 3.863 | 7 | 3.862 | 6 | 3.873 | 6 |
| 002 | 3.439 | 38 | 3.440 | 42 | 3.440 | 40 | 3.437 | 34 |
| 102 | 3.159 | 16 | 3.165 | 15 | 3.173 | 16 | 3.171 | 14 |
| 210 | - | - | - | - | - | - | - | - |
| 211 | 2.793 | 100 | 2.789 | 100 | 2.782 | 100 | 2.785 | 100 |
| 112 | 2.773 | 53 | 2.767 | 56 | 2.776 | 55 | 2.770 | 49 |
| 300 | 2.689 | 48 | 2.684 | 52 | 2.683 | 51 | 2.694 | 47 |
| 202 | 2.620 | 27 | 2.622 | 31 | 2.615 | 30 | 2.616 | 26 |
| 301 | 2.501 | 6 | 2.505 | 8 | 2.508 | 9 | 2.510 | 7 |
| 212 | 2.284 | - | 2.280 | - | 2.279 | - | 2.283 | - |
| 310 | 2.233 | 21 | 2.237 | 23 | 2.239 | 23 | 2.234 | 25 |
| 221 | 2.207 | 4 | 2.204 | 6 | 2.212 | 6 | 2.209 | 6 |
| 311 | - | - | - | - | - | - | - | - |
| 302 | 2.122 | 5 | 2.127 | 6 | 2.123 | 6 | 2.127 | 8 |
| 113 | 2.058 | 7 | 2.056 | 8 | 2.061 | 8 | 2.056 | 6 |
| 400 | - | - | - | - | - | - | - | - |
| 203 | 1.997 | 6 | 1.993 | 5 | 1.996 | 6 | 1.997 | 7 |
| 222 | 1.929 | 25 | 1.931 | 26 | 1.926 | 27 | 1.926 | 29 |
| 312 | 1.873 | - | 1.878 | - | 1.880 | - | 1.872 | - |
| 320 | 1.852 | 6 | 1.854 | 6 | 1.852 | 7 | 1.859 | 5 |
| 213 | 1.833 | 30 | 1.833 | 31 | 1.834 | 29 | 1.836 | 30 |
| 321 | 1.785 | 13 | 1.786 | 12 | 1.789 | 12 | 1.786 | 11 |
| 410 | 1.758 | 12 | 1.762 | 12 | 1.762 | 12 | 1.759 | 14 |
| 402 | 1.742 | 12 | 1.741 | 12 | 1.741 | 14 | 1.740 | 12 |
| 004 | 1.722 | 12 | 1.721 | 14 | 1.724 | 13 | 1.723 | 16 |
| 322 | 1.628 | - | 1.628 | - | 1.629 | - | 1.627 | - |
| 313 | 1.600 | - | 1.602 | - | 1.602 | - | 1.600 | - |

| hk1 | RTA 11B | | RTA 13A | | RTA 13B | | RTA 13C | |
|-----|-----------------|------------------|-----------------|------------------|-----------------|------------------|-----------------|------------------|
| | $d(\text{\AA})$ | I/I ₀ | $d(\text{\AA})$ | I/I ₀ | $d(\text{\AA})$ | I/I ₀ | $d(\text{\AA})$ | I/I ₀ |
| 100 | 8.117 | 6 | 8.117 | 5 | 8.102 | 8 | 8.109 | 9 |
| 200 | 4.046 | 5 | 4.049 | 5 | 4.049 | 7 | 4.047 | 8 |
| 111 | 3.058 | 5 | 3.858 | 4 | 3.867 | 8 | 3.862 | 8 |
| 002 | 3.437 | 43 | 3.437 | 37 | 3.440 | 36 | 3.439 | 41 |
| 102 | 3.169 | 17 | 3.162 | 14 | 3.169 | 13 | 3.159 | 15 |
| 210 | - | - | - | - | - | - | - | - |
| 211 | 2.782 | 100 | 2.781 | 100 | 2.793 | 100 | 2.789 | 100 |
| 112 | 2.767 | 56 | 2.776 | 53 | 2.770 | 52 | 2.769 | 58 |
| 300 | 2.679 | 52 | 2.683 | 50 | 2.693 | 48 | 2.685 | 55 |
| 202 | 2.617 | 29 | 2.614 | 28 | 2.622 | 26 | 2.619 | 33 |
| 301 | 2.503 | 6 | 2.491 | 6 | 2.510 | 7 | 2.505 | 10 |
| 212 | 2.284 | - | 2.279 | - | 2.284 | - | 2.283 | - |
| 310 | 2.235 | 23 | 2.233 | 24 | 2.244 | 25 | 2.241 | 26 |
| 221 | 2.207 | 5 | 2.204 | 5 | 2.215 | 6 | 2.207 | 6 |
| 311 | - | - | - | - | - | - | - | - |
| 302 | 2.124 | 6 | 2.122 | 7 | 2.127 | 7 | 2.127 | 7 |
| 113 | 2.061 | 7 | 2.056 | 8 | 2.056 | 9 | 2.058 | 8 |
| 400 | - | - | - | - | - | - | - | - |
| 203 | 1.998 | 5 | 1.994 | 6 | 1.995 | 7 | 1.998 | 7 |
| 222 | 1.931 | 27 | 1.926 | 28 | 1.929 | 28 | 1.926 | 28 |
| 312 | 1.872 | - | 1.870 | - | 1.880 | - | 1.877 | - |
| 320 | 1.851 | 7 | 1.850 | 6 | 1.852 | 6 | 1.859 | 4 |
| 213 | 1.834 | 28 | 1.833 | 32 | 1.836 | 31 | 1.834 | 30 |
| 321 | 1.789 | 12 | 1.784 | 12 | 1.784 | 13 | 1.786 | 14 |
| 410 | 1.758 | 11 | 1.759 | 11 | 1.758 | 12 | 1.761 | 12 |
| 402 | 1.738 | 12 | 1.739 | 11 | 1.741 | 12 | 1.741 | 13 |
| 004 | 1.721 | 15 | 1.724 | 15 | 1.722 | 14 | 1.724 | 16 |
| 322 | 1.626 | - | 1.631 | - | 1.627 | - | 1.628 | - |
| 313 | 1.600 | - | 1.600 | - | 1.601 | - | 1.604 | - |

| RTB 19A | | RTB 19B | | 187.2 | | 187.3 | |
|---------------|------------------|---------------|------------------|---------------|------------------|---------------|------------------|
| $d(\text{Å})$ | I/I ₀ | $d(\text{Å})$ | I/I ₀ | $d(\text{Å})$ | I/I ₀ | $d(\text{Å})$ | I/I ₀ |
| 8.117 | 9 | 8.102 | 8 | 8.109 | 7 | 8.109 | 7 |
| 4.049 | 9 | 4.046 | 8 | 4.049 | 7 | 4.049 | 7 |
| 3.860 | 7 | 3.860 | 6 | 3.868 | 6 | 3.870 | 6 |
| 3.439 | 39 | 3.439 | 41 | 3.437 | 40 | 3.439 | 38 |
| 3.161 | 15 | 3.166 | 16 | 3.170 | 17 | 3.164 | 15 |
| - | - | - | - | - | - | - | - |
| 2.782 | 100 | 2.793 | 100 | 2.789 | 100 | 2.788 | 100 |
| 2.771 | 52 | 2.775 | 54 | 2.767 | 55 | 2.776 | 53 |
| 2.680 | 48 | 2.683 | 50 | 2.673 | 50 | 2.677 | 49 |
| 2.619 | 28 | 2.620 | 29 | 2.617 | 27 | 2.618 | 26 |
| 2.510 | 7 | 2.505 | 7 | 2.503 | 6 | 2.507 | 6 |
| 2.281 | - | 2.279 | - | 2.281 | - | 2.284 | - |
| 2.238 | 22 | 2.244 | 23 | 2.241 | 20 | 2.239 | 21 |
| 2.212 | 4 | 2.215 | 5 | 2.204 | 4 | 2.209 | 5 |
| - | - | - | - | - | - | - | - |
| 2.122 | 4 | 2.125 | 5 | 2.123 | 6 | 2.127 | 6 |
| 2.061 | 7 | 2.058 | 8 | 2.063 | 8 | 2.056 | 8 |
| - | - | - | - | - | - | - | - |
| 1.997 | 4 | 1.993 | 5 | 1.995 | 6 | 1.998 | 4 |
| 1.926 | 23 | 1.929 | 28 | 1.931 | 28 | 1.927 | 29 |
| 1.880 | - | 1.873 | - | 1.877 | - | 1.880 | - |
| 1.850 | 6 | 1.850 | 6 | 1.853 | 7 | 1.852 | 4 |
| 1.833 | 29 | 1.834 | 29 | 1.834 | 30 | 1.836 | 30 |
| 1.789 | 11 | 1.784 | 12 | 1.786 | 12 | 1.785 | 11 |
| 1.761 | 13 | 1.758 | 14 | 1.758 | 13 | 1.760 | 12 |
| 1.738 | 12 | 1.738 | 14 | 1.740 | 12 | 1.738 | 12 |
| 1.723 | 15 | 1.724 | 15 | 1.721 | 15 | 1.721 | 14 |
| 1.626 | - | 1.627 | - | 1.628 | - | 1.626 | - |
| 1.601 | - | 1.604 | - | 1.600 | - | 1.600 | - |

| hk1 | 187.5 | | 187.15 | | 193.2B | | M1 | |
|-----|-----------------|------------------|-----------------|------------------|-----------------|------------------|-----------------|------------------|
| | $d(\text{\AA})$ | I/I ₀ | $d(\text{\AA})$ | I/I ₀ | $d(\text{\AA})$ | I/I ₀ | $d(\text{\AA})$ | I/I ₀ |
| 100 | 8.109 | 6 | 8.102 | 7 | 8.117 | 7 | 8.109 | 7 |
| 200 | 4.046 | 6 | 4.046 | 8 | 4.046 | 7 | 4.049 | 7 |
| 111 | 3.858 | 8 | 3.873 | 6 | 3.870 | 9 | 3.865 | 9 |
| 002 | 3.440 | 45 | 3.440 | 43 | 3.439 | 41 | 3.439 | 35 |
| 102 | 3.163 | 16 | 3.170 | 15 | 3.172 | 16 | 3.159 | 13 |
| 210 | - | - | - | - | - | - | - | - |
| 211 | 2.785 | 100 | 2.788 | 100 | 2.793 | 100 | 2.780 | 100 |
| 112 | 2.769 | 56 | 2.776 | 55 | 2.776 | 54 | 2.767 | 50 |
| 300 | 2.683 | 50 | 2.689 | 50 | 2.679 | 49 | 2.683 | 47 |
| 202 | 2.622 | 30 | 2.621 | 31 | 2.615 | 29 | 2.614 | 28 |
| 301 | 2.503 | 8 | 2.501 | 8 | 2.507 | 6 | 2.501 | 6 |
| 212 | 2.279 | - | 2.281 | - | 2.284 | - | 2.279 | - |
| 310 | 2.238 | 24 | 2.238 | 24 | 2.233 | 23 | 2.233 | 22 |
| 221 | 2.209 | 6 | 2.204 | 6 | 2.212 | 5 | 2.212 | 4 |
| 311 | - | - | - | - | - | - | - | - |
| 302 | 2.122 | 6 | 2.127 | 6 | 2.124 | 6 | 2.123 | 4 |
| 113 | 2.063 | 7 | 2.058 | 7 | 2.056 | 6 | 2.058 | 5 |
| 400 | - | - | - | - | - | - | - | - |
| 203 | 1.993 | 5 | 1.994 | 6 | 1.998 | 6 | 1.993 | 5 |
| 222 | 1.931 | 28 | 1.931 | 28 | 1.931 | 26 | 1.929 | 24 |
| 312 | 1.870 | - | 1.873 | - | 1.872 | - | 1.872 | - |
| 320 | 1.850 | 6 | 1.851 | 7 | 1.856 | 7 | 1.859 | 5 |
| 213 | 1.833 | 33 | 1.836 | 31 | 1.834 | 30 | 1.833 | 30 |
| 321 | 1.784 | 10 | 1.787 | 13 | 1.785 | 12 | 1.785 | 12 |
| 410 | 1.758 | 12 | 1.762 | 12 | 1.759 | 12 | 1.758 | 12 |
| 402 | 1.739 | 13 | 1.742 | 12 | 1.740 | 12 | 1.738 | 12 |
| 004 | 1.721 | 13 | 1.722 | 14 | 1.724 | 16 | 1.721 | 15 |
| 322 | 1.626 | - | 1.626 | - | 1.627 | - | 1.629 | - |
| 313 | 1.600 | - | 1.603 | - | 1.601 | - | 1.602 | - |

| M4 | | M11 | | M12 | | M14 | |
|-----------------|------------------|-----------------|------------------|-----------------|------------------|-----------------|------------------|
| $d(\text{\AA})$ | I/I ₀ | $d(\text{\AA})$ | I/I ₀ | $d(\text{\AA})$ | I/I ₀ | $d(\text{\AA})$ | I/I ₀ |
| 8.117 | 6 | 8.117 | 4 | 8.102 | 8 | 8.109 | 5 |
| 4.049 | 7 | 4.046 | 5 | 4.049 | 7 | 4.047 | 6 |
| 3.873 | 8 | 3.858 | 6 | 3.865 | 7 | 3.870 | 6 |
| 3.440 | 39 | 3.439 | 36 | 3.437 | 44 | 3.440 | 43 |
| 3.159 | 16 | 3.160 | 14 | 3.172 | 17 | 3.164 | 16 |
| - | - | - | - | - | - | - | - |
| 2.782 | 100 | 2.785 | 100 | 2.788 | 100 | 2.784 | 100 |
| 2.769 | 57 | 2.772 | 50 | 2.770 | 58 | 2.769 | 55 |
| 2.679 | 53 | 2.674 | 48 | 2.680 | 55 | 2.681 | 52 |
| 2.615 | 31 | 2.622 | 32 | 2.617 | 32 | 2.620 | 33 |
| 2.508 | 6 | 2.510 | 6 | 2.501 | 7 | 2.502 | 8 |
| 2.279 | - | 2.281 | - | 2.284 | - | 2.282 | - |
| 2.233 | 25 | 2.235 | 24 | 2.239 | 25 | 2.241 | 24 |
| 2.204 | 6 | 2.212 | 6 | 2.217 | 5 | 2.215 | 6 |
| - | - | - | - | - | - | - | - |
| 2.126 | 7 | 2.122 | 7 | 2.125 | 6 | 2.127 | 7 |
| 2.056 | 6 | 2.063 | 6 | 2.058 | 7 | 2.061 | 7 |
| - | - | - | - | - | - | - | - |
| 1.993 | 5 | 1.996 | 7 | 1.994 | 6 | 1.998 | 6 |
| 1.926 | 29 | 1.931 | 27 | 1.921 | 28 | 1.926 | 26 |
| 1.873 | - | 1.877 | - | 1.873 | - | 1.880 | - |
| 1.851 | 5 | 1.852 | 4 | 1.854 | 6 | 1.859 | 6 |
| 1.834 | 31 | 1.835 | 31 | 1.834 | 28 | 1.833 | 30 |
| 1.787 | 13 | 1.785 | 13 | 1.785 | 12 | 1.784 | 12 |
| 1.758 | 12 | 1.762 | 11 | 1.761 | 12 | 1.761 | 12 |
| 1.742 | 12 | 1.742 | 14 | 1.738 | 12 | 1.739 | 13 |
| 1.721 | 16 | 1.722 | 14 | 1.721 | 12 | 1.724 | 14 |
| 1.626 | - | 1.627 | - | 1.626 | - | 1.628 | - |
| 1.602 | - | 1.601 | - | 1.600 | - | 1.604 | - |

| Sample | 120 B | 10 | KC 11 | KC 13 |
|--------------------------------|--------|--------|----------|----------|
| Element | | | | |
| P ₂ O ₅ | 34.57 | 0.04 | 6.32 | 0.00 |
| CaO | 49.40 | 50.30 | 6.86 | 0.21 |
| SiO ₂ | 4.55 | 6.04 | 55.55 | 77.20 |
| Fe ₂ O ₃ | 1.10 | 0.55 | 8.71 | 1.68 |
| Al ₂ O ₃ | (a) 76 | (b) 30 | (c) 6.51 | (d) 1.50 |
| H ₂ O | 0.25 | 0.47 | 3.99 | 0.01 |
| La | .328 | 40 | 12.10 | 3.00 |
| Ce | .865 | 80 | 10.99 | 2.92 |
| Nd | .630 | 37 | 11.08 | 2.54 |
| Sm | .203 | 6.4 | 2.02 | 0.65 |
| Eu | .077 | 1.3 | 0.46 | 0.17 |
| Gd | .276 | 5.5 | 2.06 | 0.49 |
| Dy | .310 | 5.2 | 2.36 | 0.60 |
| Ho | .077 | 1.4 | 0.58 | 0.15 |
| Er | .210 | 3.4 | 1.61 | 0.41 |
| Yb | .220 | 3.3 | 1.65 | 0.40 |
| Lu | .0339 | 0.6 | 0.27 | 0.07 |
| Y | 1.900 | 35 | 19.30 | 4.55 |

TABLE A2.3 Abundances (in ppm) of Yttrium and REE used in normalisation procedures: (a) chondrite (Bedford College), (b) average sediment (Herrmann, 1970), (c) mean Maltese phosphorite, and (d) limestone RTB 18.

Table A2.4 Published compositions of four standard rocks: two from United States Geological Survey Bureau of Analyzed Samples (120 B, 10) and two from King's College, London (KC 11, KC 13).

* Abundances determined by this study

** Not used for calibration

| Sample Element | 120 B | 1C | KC 11 | KC 13 |
|--------------------------------|-------|--------|-------|-------|
| P ₂ O ₅ | 34.57 | 0.04 | 0.32 | 0.00 |
| CaO | 49.40 | 50.30 | 6.86 | 0.21 |
| SiO ₂ | 4.68 | 6.84 | 55.55 | 77.20 |
| Fe ₂ O ₃ | 1.10 | 0.55 | 8.71 | 1.68 |
| Al ₂ O ₃ | 1.06 | 1.30 | 16.51 | 11.60 |
| MgO | 0.28 | 0.42 | 3.99 | 0.01 |
| Na ₂ O | 0.35 | 0.02 | 3.30 | 3.78 |
| K ₂ O | 0.12 | 0.28 | 2.15 | 4.78 |
| TiO ₂ | 0.15 | 0.07 | 1.10 | 0.13 |
| MnO | 0.032 | 0.025 | 0.14 | 0.02 |
| CdO | 0.002 | - | - | - |
| CO ₂ | 2.79 | - | - | - |
| F | 3.84 | - | - | - |
| L.O.I. | - | 39.90 | - | - |
| Sc | 45* | - | 24 | <1 |
| V | 88* | - | 210 | <5 |
| Ni | 33* | - | 280 | <5 |
| Cu | 3* | - | 108 | 2 |
| Sr | 716* | 30 000 | 370 | 8 |
| Zr | 113* | - | 145 | 420 |
| Ba | 56* | - | 491 | 112 |
| γ** | 145* | - | 28 | 130 |

Table A.2.4 Published compositions of four standard rocks: two from United States Geological Survey Bureau of Analysed samples (120 B, 1C) and two from King's College, London (KC 11, KC 13).

* Abundances determined by this study

** Not used for calibration

| Sample Element | W1 | G2 | GSP 1 | AGV 1 | PCC 1 |
|----------------|-------|-------|--------|--------|--------|
| Sc | 35 | 4 | 7 | 13 | 7 |
| V | 264 | 35 | 53 | 125 | 30 |
| Ni | 76 | 5 | 13 | 19 | 2339 |
| Cu | 110 | 12 | 33 | 60 | 11 |
| Sr | 190 | 479 | 233 | 657 | 0.41 |
| Zr | 105 | 300 | 500 | 225 | 7 |
| Ba | 160 | 1870 | 1300 | 1208 | 1 |
| Y* | 25 | 12 | 30 | 21 | - |
| | DTS 1 | BCR 1 | NIM'D' | NIM'G' | NIM'P' |
| Sc | 4 | 33 | - | - | - |
| V | 10 | 399 | 65 | 2 | 225 |
| Ni | 2269 | 16 | 2120 | 11 | 470 |
| Cu | 7 | 18 | 8 | 15 | 17 |
| Sr | 0.35 | 330 | 5 | 13 | 40 |
| Zr | 3 | 190 | 50 | 300 | 20 |
| Ba | 2.4 | 675 | 20 | 179 | 56 |
| Y* | - | 37 | - | 100 | <5 |

Table A.2.5 Trace element concentrations of ten standard rocks determined by ICP at King's College, London, used in the construction of calibration curves

* Not used for calibration

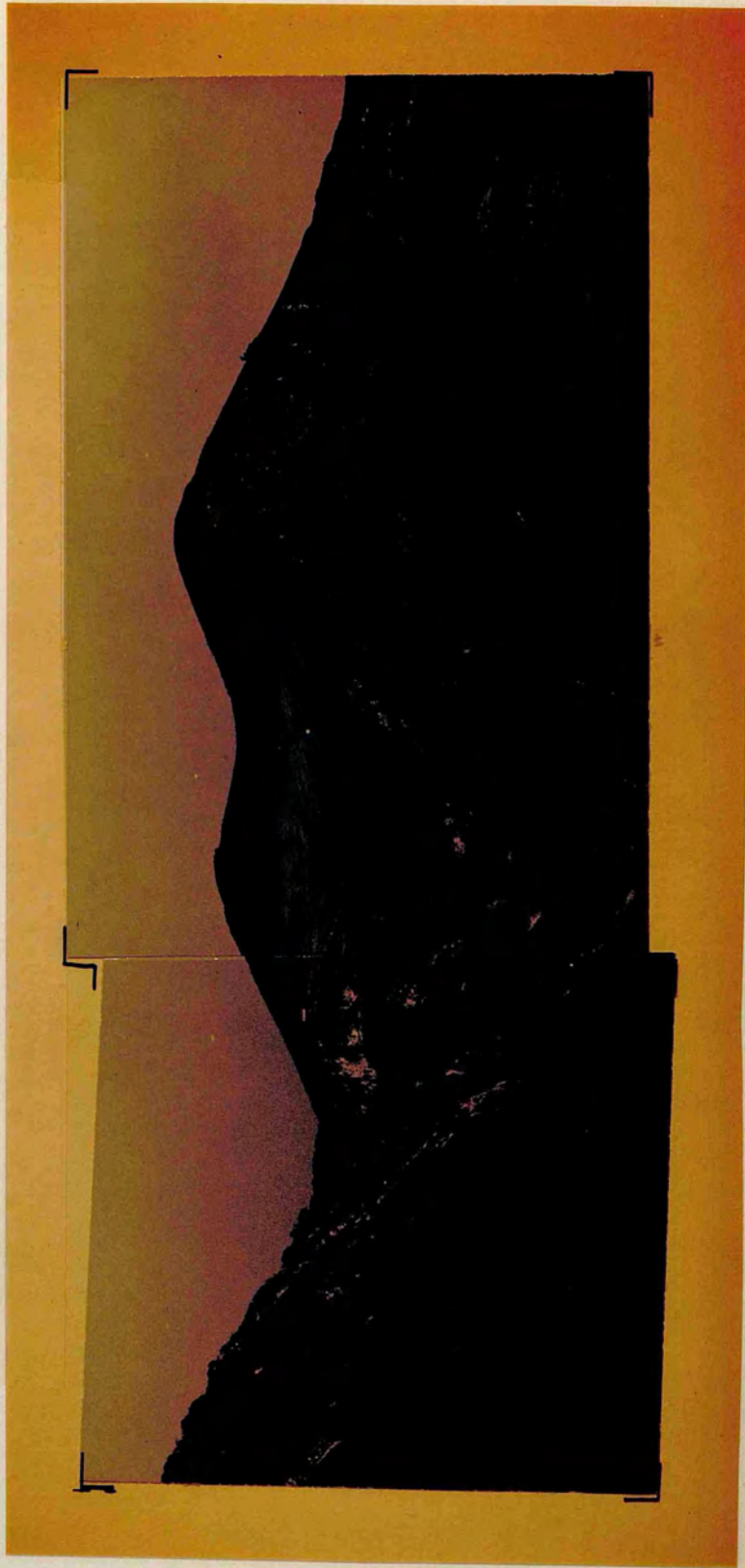
Plates

UPPER OLIGOCENE LIMESTONES: FIELD VIEWS

Plate 2.1 Western Nadorello (UB326 600), view looking east. The light grey Upper Oligocene limestones in the foreground are deformed into two antiforms and a synform. Both antiforms verge south, having gently dipping northern limbs and vertical-sub-vertical southern limbs. Minor southward thrusting has occurred in the intermediate synform (see overlay).

UPPER OLIGOCENE LIMESTONES: FIELD VIEWS

Plate 2.1 Western Nadorello (UB326 600), view looking east. The light grey Upper Oligocene limestones in the foreground are deformed into two antiforms and a synform. Both antiforms verge south, having gently dipping northern limbs and vertical-sub-vertical southern limbs. Minor southward thrusting has occurred in the intermediate synform (see overlay).



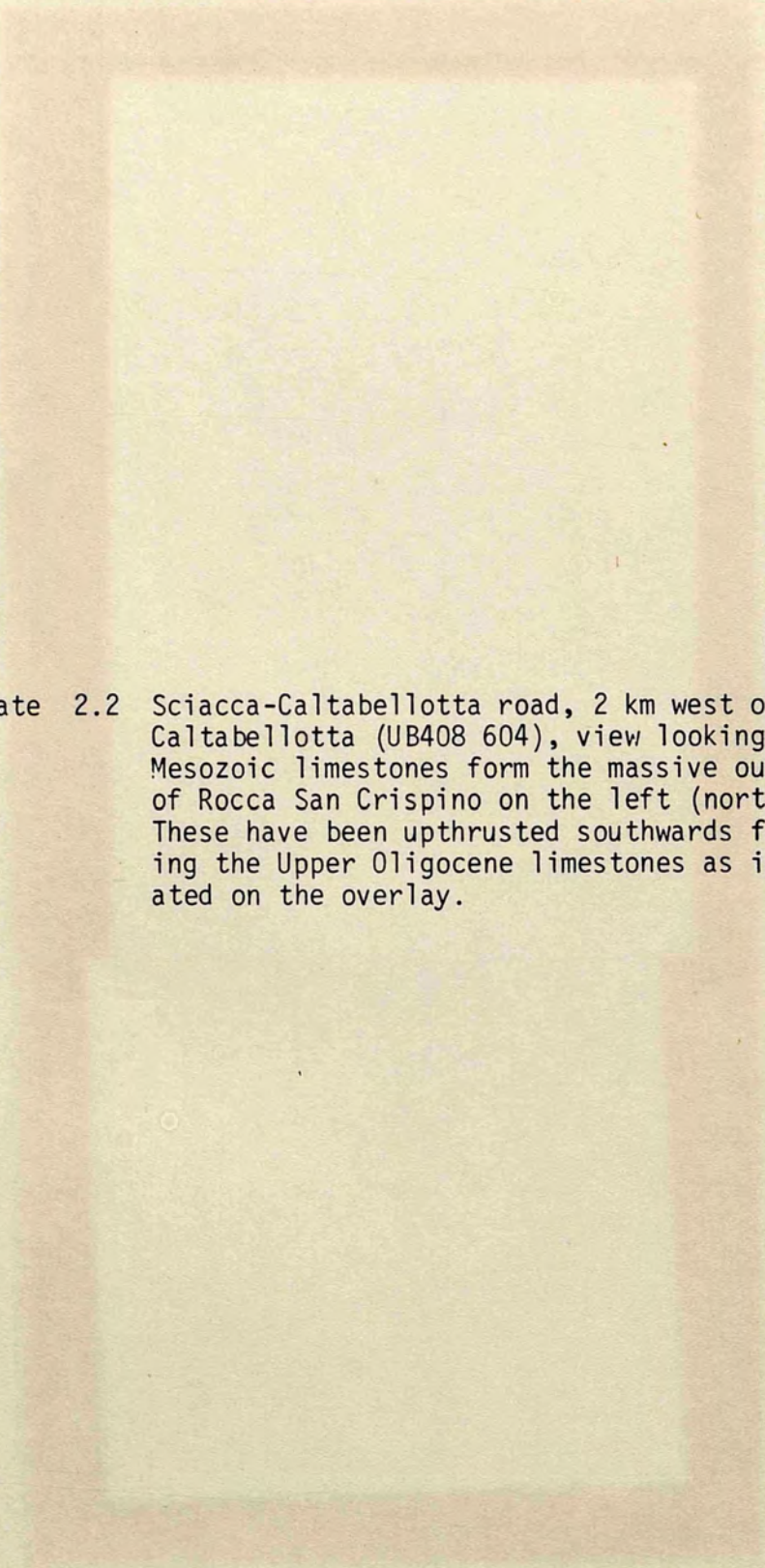


Plate 2.2 Sciacca-Caltabellotta road, 2 km west of Caltabellotta (UB408 604), view looking east. Mesozoic limestones form the massive outcrop of Rocca San Crispino on the left (north). These have been upthrust southwards folding the Upper Oligocene limestones as indicated on the overlay.



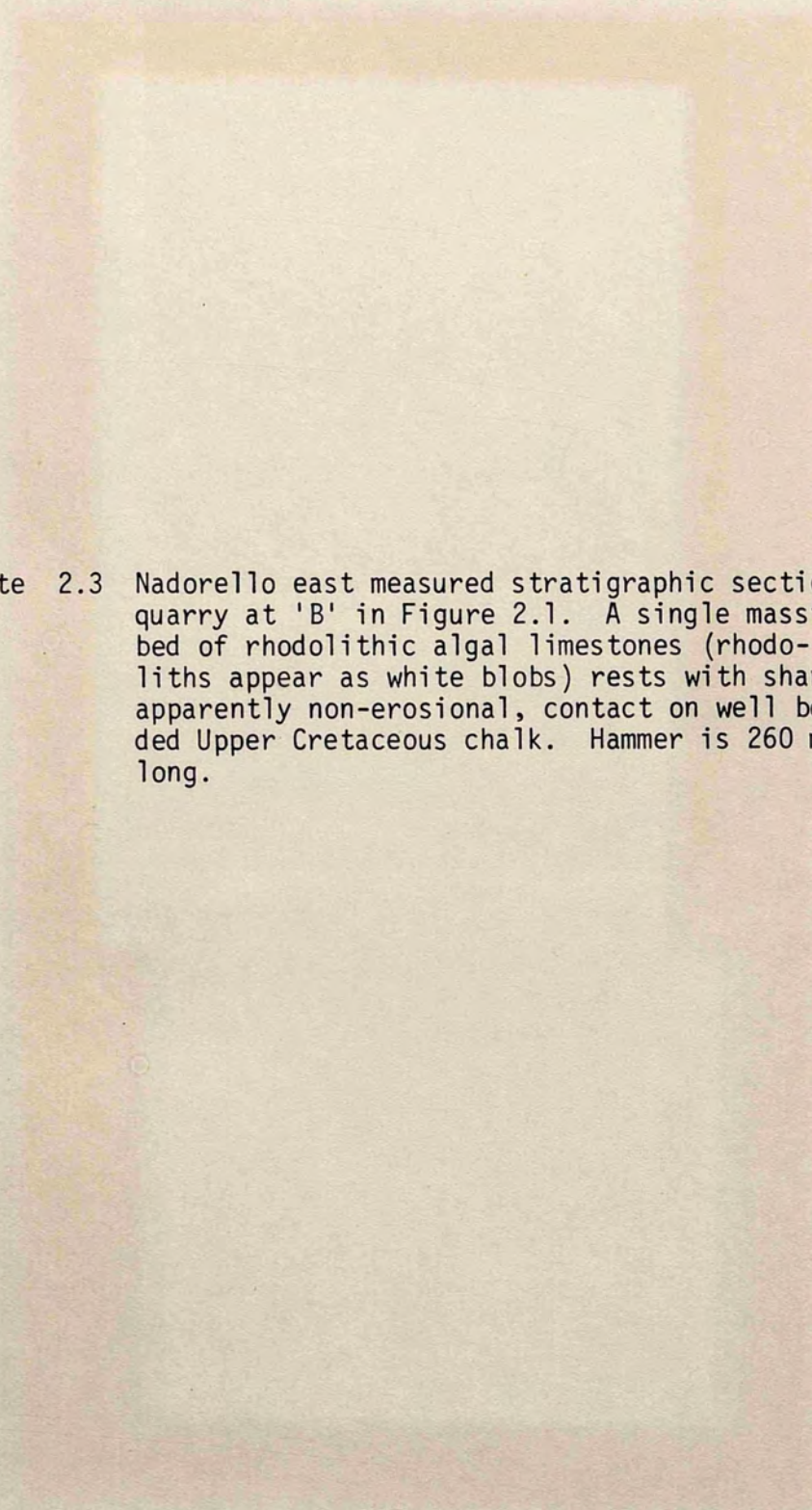


Plate 2.3 Nadorello east measured stratigraphic section, quarry at 'B' in Figure 2.1. A single massive bed of rhodolithic algal limestones (rhodoliths appear as white blobs) rests with sharp, apparently non-erosional, contact on well bedded Upper Cretaceous chalk. Hammer is 260 mm long.

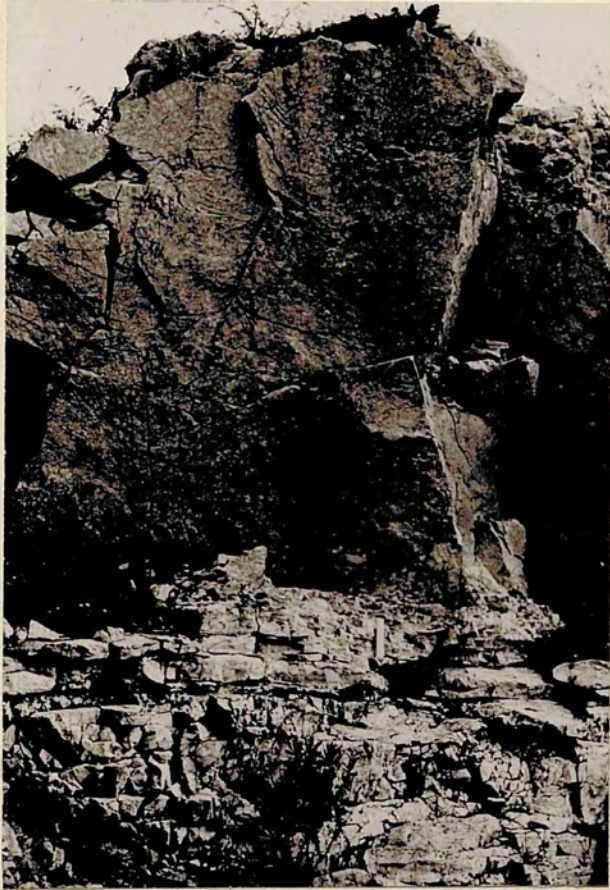


Plate 2.4 Nadorello east, view looking south (towards 'A' in Figure 2.1, UB349 599). A single bed of massive Upper Oligocene grey rhodolithic algal limestones, up to 6 m thick, rests with sharp, erosional contact on Upper Cretaceous chalk.



Plate 2.5 Nadorello east, view of the unconformity at the point indicated in Plate 2.4. The white Upper Cretaceous chalk contains burrows of *Thalassinoides paradoxica* infilled with grey-beige Upper Oligocene foraminiferal limestones. The overlying Upper Oligocene basal conglomerate is formed mostly of locally derived unbored chalks and partly of bored phosphatised chalk clasts (dark grey-black colour). The rule is 150 mm long.

Plate 2.6 Carboj area, view of the unconformity between the Upper Oligocene foraminiferal limestones and white Eocene chalk (UB277 650). The unconformity shows minor erosional relief and is step faulted with small downthrows to the north (right). The Upper Oligocene has a poorly developed basal conglomerate composed of small (< 30 mm) clasts of unbored chalk and phosphatic chalk (dark grey-black colour). The lens cap is 55 mm dia.

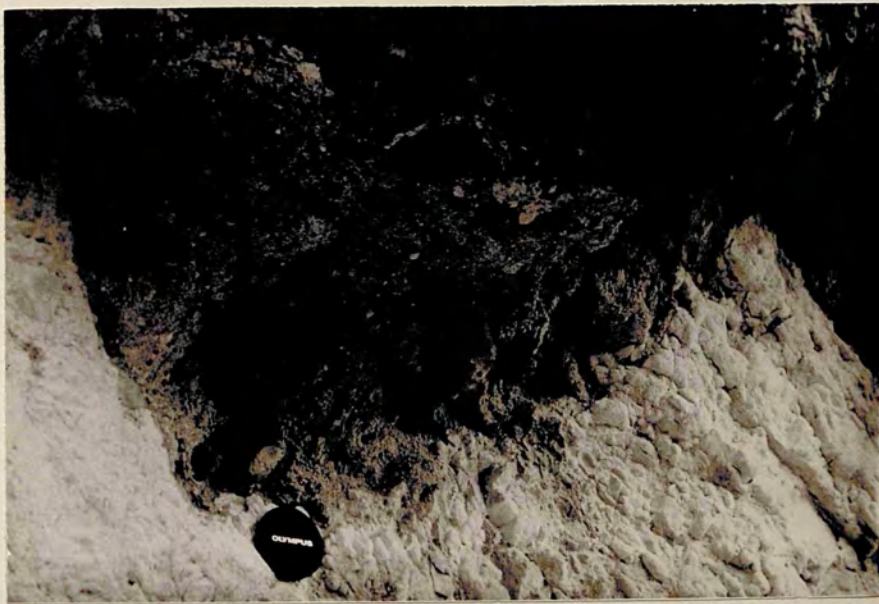
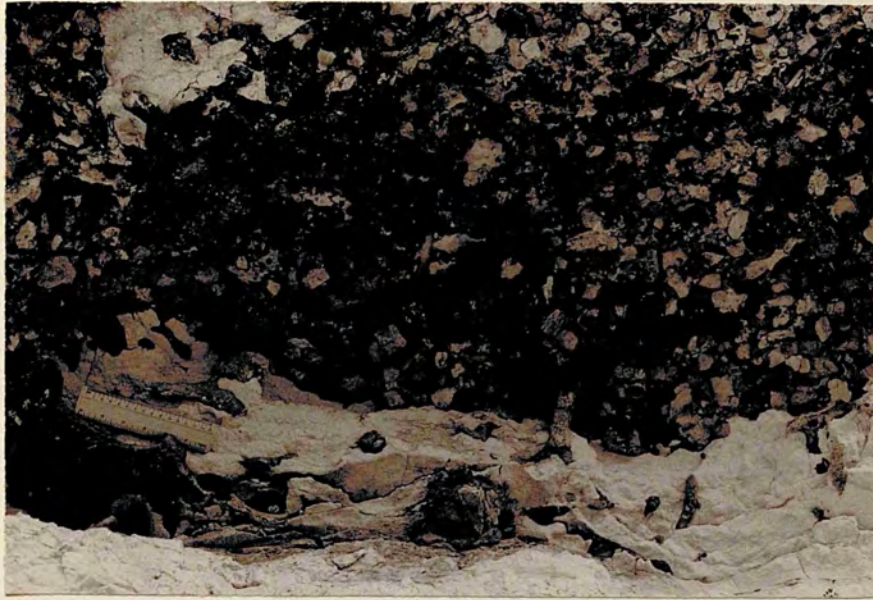


Plate 2.7 San Biagio west measured stratigraphic section.
A single massive bed of grey Upper Oligocene
rhodolithic algal limestones, 4-6 m thick, rests
with erosional unconformity on Upper Cretaceous
chalk (bottom left).



Plate 2.8 San Biagio west. Close view of the unconformity (in Plate 2.7) showing its rugged relief at this locality. Upper Cretaceous chalk occupies the lower half of the photograph overlain by the Upper Oligocene basal conglomerate in the upper half. The conglomerate is composed of abundant unbored chalk clasts and a single large (140 mm long) bored phosphatised chalk clast (arrowed). The lens cap is 55 mm dia.

Plate 2.9 San Biagio west. Close view of the Upper Oligocene basal conglomerate which is composed mainly of small angular and subangular chalk fragments and two bored phosphatised chalk clasts (top left and right). The lens cap is 55 mm dia.



Plate 2.10 Carboj Dam measured stratigraphic section, view looking west. Light grey Upper Oligocene foraminiferal limestones on the right (north) are downfaulted against dark grey Mesozoic limestones on the left (south). Eocene chalks form minor exposures along the track passing through the centre of the view. The section was measured along the line indicated.



Plate 2.11 La Conca measured stratigraphic section. A succession of flaggy bedded foraminiferal limestones measured along the line indicated.



Plate 2.12 Contrada Giovanni measured stratigraphic section, view looking north. A large isolated outcrop of rhodolithic algal limestones and foraminiferal limestones with the section measured along the line indicated. The town of Sambuca is in the background.



Plate 2.13 San Biagio east measured stratigraphic section, view looking northeast. Light grey Upper Oligocene foraminiferal limestones form the upper crags on the left and right, Eocene chinks form the outcrops in the centre. The section was measured along the line indicated.



Plate 2.14 Tombe Sicani measured stratigraphic section, view looking northwest. Massive Upper Oligocene algal and foraminiferal limestones with a sub-vertical dip (centre) form the upper part of the measured section. The lower part of the section, which is poorly exposed, is located in the sporadic outcrops in the hillside to the left of the row of houses.

Plate 2.15 Abundant *Lepidocyclina* (*Eulepidina*) seen in algal packstones in the upper part of the succession at Nadorello east. Small algal rhodoliths form the white areas in the photograph. The lens cap is 55 mm dia.



UPPER OLIGOCENE LIMESTONES: MICROFACIES OF THE
RHODOLITHIC ALGAL PACKSTONE-WACKESTONE FACIES

Plate 2.16 Nadorello east. Compacted algal foraminiferal packstone with a single large fragment of *Mesophyllum* cf. *vaughanii* (left centre), other scattered fragments of algae and foraminifera (whole and fragmentary) including *Amphistegina* (right centre), *Nephrolepidina* (left centre, top) *Spiroclypeus* (bottom centre) and a fragment of *Heterostegina/Operculina* (bottom left). Scale 41 x

Plate 2.17 Nadorello east. Foraminiferal packstone showing poor sorting of grains and abrasion and partial rounding of *Eulepidina* (centre and right centre). Pore space is partly filled with depositional matrix and partly with 2 periods of cement (Periods 3 and 4). Way up is indicated by mud settling on the upper surfaces of grains. Scale 41 x

Plate 2.18 Nadorello east. Foraminiferal packstone with a large *Eulepidina* (left) and *Spiroclypeus* (right centre). The latter forms an umbrella, sheltering the pore space beneath, which has been infilled by two periods of cement (Periods 3 and 4). Scale 41 x

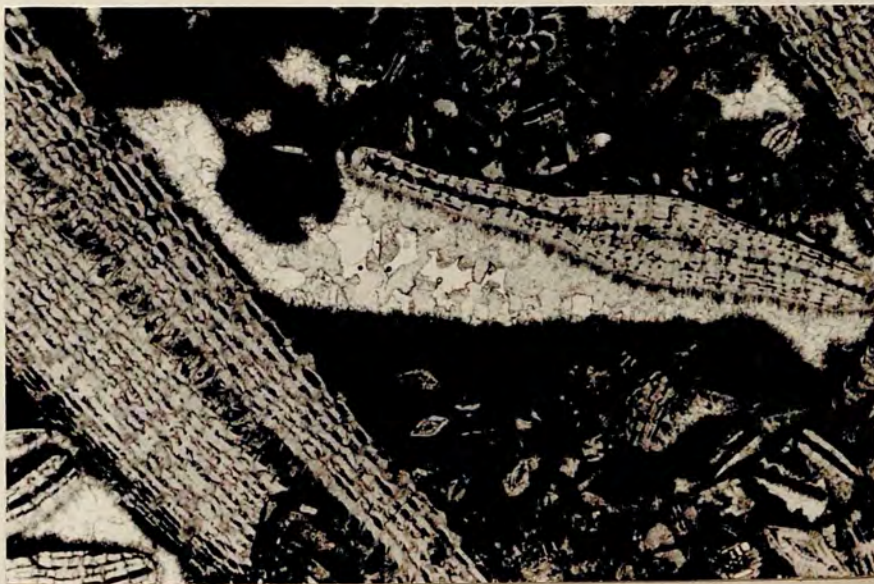
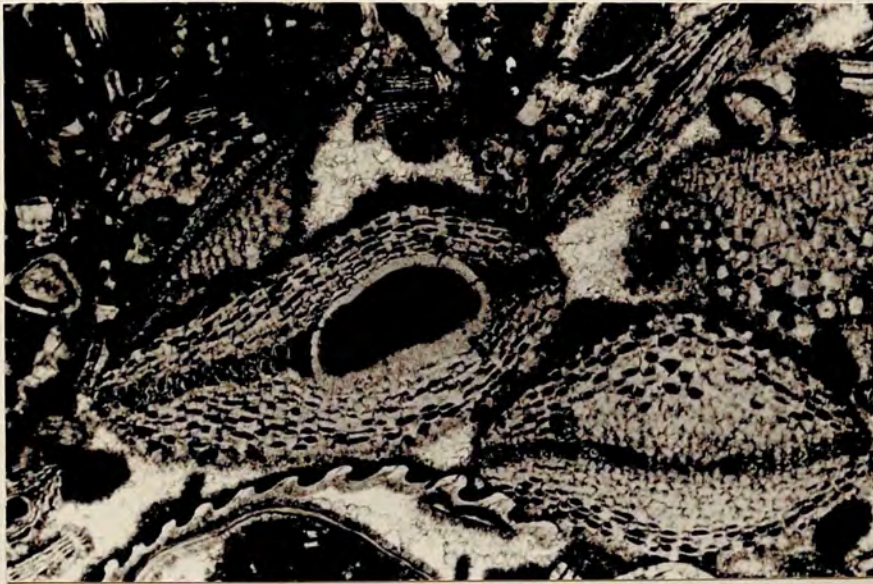
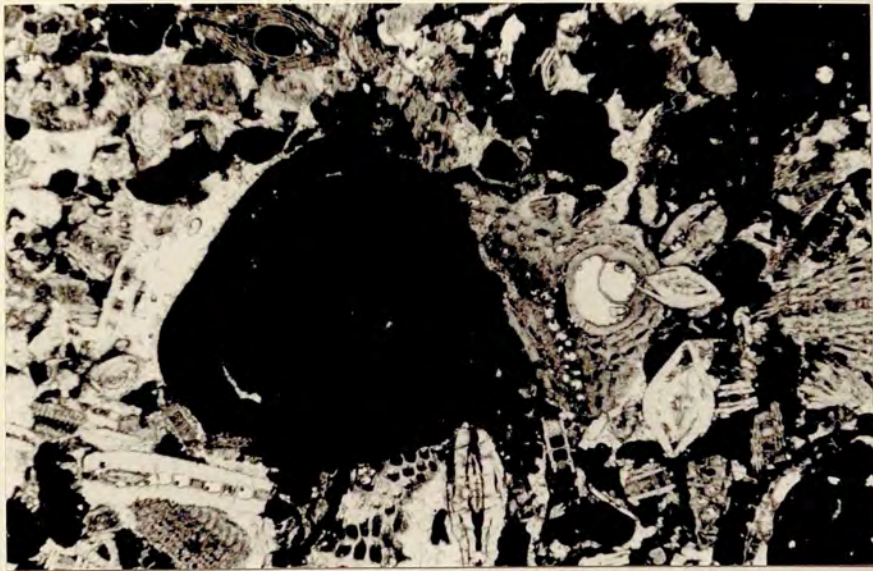


Plate 2.19 Nadorello east. Foraminiferal packstone with almost all pore space filled with depositional lime mud. Foraminifera are represented by *Amphistegina* and *Heterostegina/Operculina*. Scale 105 x

Plate 2.20 Nadorello east. Foraminiferal packstone with pore space partially filled with depositional matrix. The large *Eulepidina* (centre) acts as an umbrella sheltering the pore space below from matrix infill. This pore space is now infilled by two periods of cement (Periods 3 and 4). Scale 41 x

Plate 2.21 Nadorello east. Foraminiferal packstone with pore space partially filled with depositional matrix. The large *Eulepidina* (right) shelters the underlying pore space from matrix fill. This pore space is now infilled with 2 periods of cement (Periods 3 and 4). (Way up is to the right of the photograph). Scale 41 x

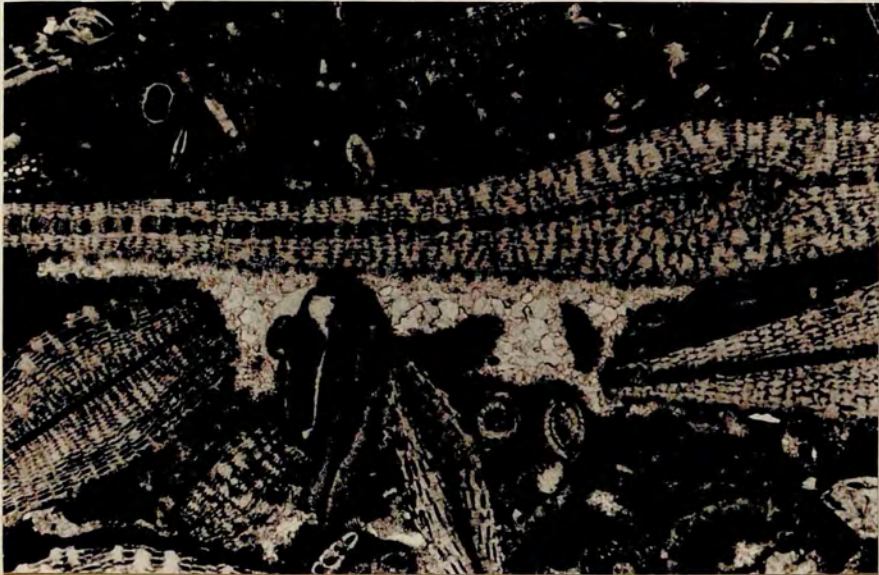


Plate 2.22 Nadorello east. Foraminiferal grainstone. Foraminifera with mud adhering to their surfaces are re-worked from the packstone below. Pore space is filled with two periods of cement (Periods 3 and 4). Foraminifera include *Eulepidina* (top left), *Amphistegina* (top centre), *Spiroclypeus* and *Rotalia* (bottom centre). Scale 41 x

Plate 2.23 Nadorello east. Compacted foraminiferal packstone with *Eulepidina* (centre) and *Spiroclypeus* (right and top centre). Scale 41 x

Plate 2.24 Nadorello east. Foraminiferal packstone with pore space filled partly with depositional matrix and partly with two periods of cement (Periods 3 and 4). Foraminifera include *Eulepidina* (4 examples), *Nephrolepidina* (left centre), *Spiroclypeus* (centre) and *Heterostegina/Operculina* (top centre). (Way up is to top right, given by numerous umbrella structures). Scale 41 x

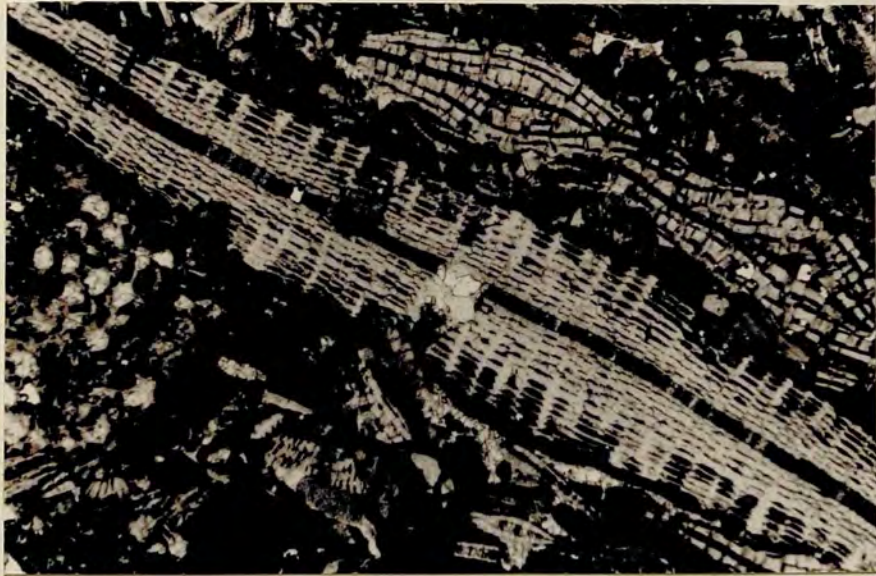


Plate 2.25 Nadorello east. Foraminiferal packstone with pore space partially filled with depositional matrix and partly with two periods of cement (periods 3 and 4). Foraminifera are represented by common *Spiroclypeus* and fragments of *Eulepidina* and a single *Amphistegina* (right centre). (Photograph is the correct way up, given by numerous umbrella structures).
Scale 41 x



UPPER OLIGOCENE LIMESTONES : MICROFACIES OF THE
FORAMINIFERAL GRAINSTONE-PACKSTONE FACIES

Plate 2.26 La Conca. Compacted foraminiferal grainstone with common *Nephrolepidina* and some *Amphistegina* (top centre and left centre), *Heterostegina/Operculina* algal debris (left centre, top) and echinoid debris (right centre). Pressure solution contacts prevail throughout the rock. The algae (black material) are most prone to pressure solution and now occupy "interstitial" positions, the *Heterostegina/Operculina* (top left) preferentially fracture. (Way up is to the right). Scale 41 x

Plate 2.27 Carboj Dam. Compacted foraminiferal grainstone with common bryozoans (centre) echinoid debris and algal debris (black material). Foraminifera include common *Nephrolepidina* and *Amphistegina*. Pressure solution contacts prevail throughout the rock, the echinoid debris and bryozoans act as preferential sites for cement precipitation (Period 2) filling some pore space. Scale 41 x

Plate 2.28 Contrada Giovanni. Poorly sorted compacted foraminiferal packstone with common *Nephrolepidina* (centre and right centre), *Amphistegina* (right centre, top) *Heterostegina/Operculina* (bottom centre and right centre), echinoid and algal (black material) debris and some bryozoans (centre). Depositional matrix and echinoid cements (Period 2) fill some pore space, pressure solution contacts are common. Scale 41 x

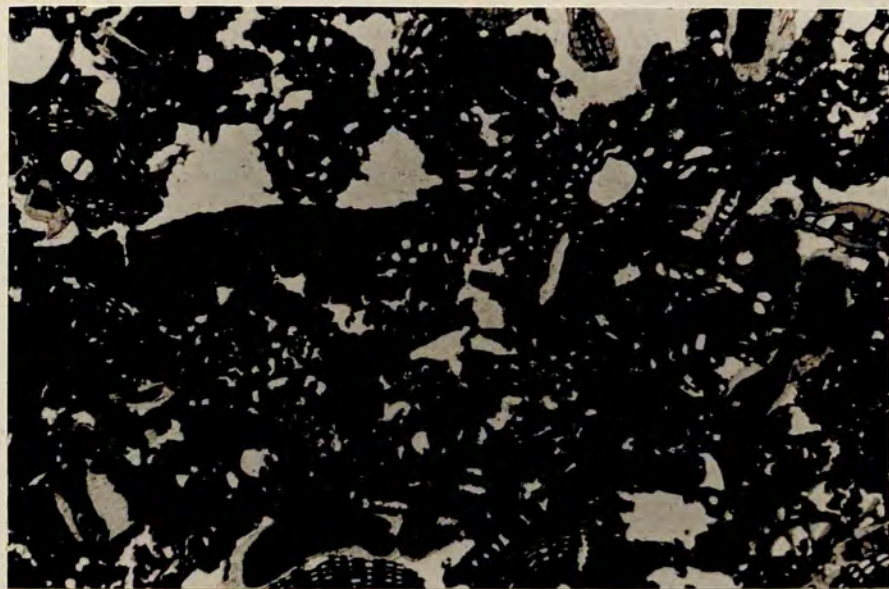
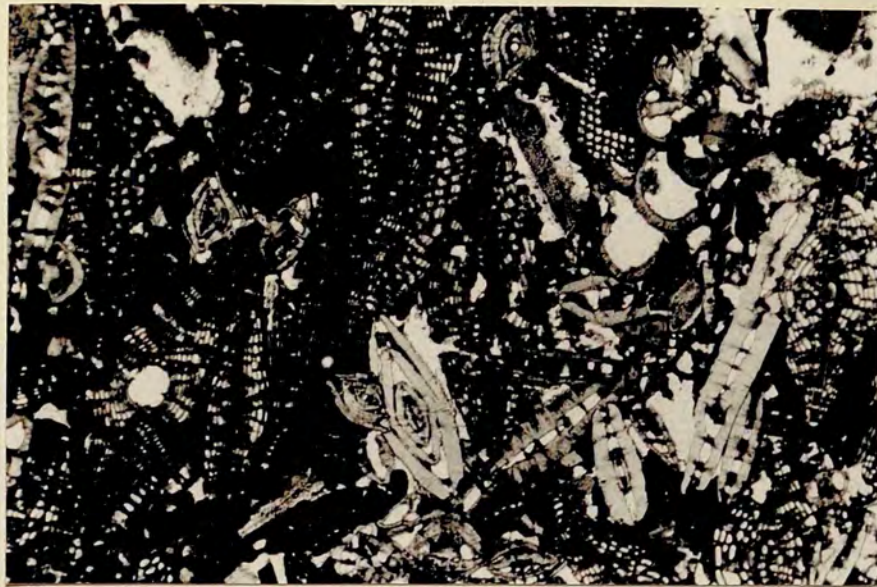


Plate 2.29 Contrada Giovanni. Poorly sorted foraminiferal packstone with common *Nephrolepidina*, *Heterostegina/Operculina* and echinoid and algal debris. Pore space is partly filled by depositional matrix and partly by echinoid cement (Period 2) but mostly remains empty. Compaction features are less pronounced compared to 2.26 to 2.28 but represented by common pressure solution contacts and common fracturing in the *Heterostegina/Operculina*. Scale 41 x

Plate 2.30 San Biagio east. Foraminiferal grainstone with common algal debris (black material) and echinoid debris. Foraminifera are represented by equal proportions of *Nephrolepidina*, *Amphistegina* and *Heterostegina/Operculina*. Pressure solution contacts are common and pore space is partly filled by echinoid cement (Period 2) but mostly remains empty. Scale 41 x

Plate 2.31 Carboj Dam. Foraminiferal grainstone from a cross-bedded unit is dominated by an *Amphistegina* and *Rotalia* fauna. Algal (black material) and echinoid debris are also common. Pore space is partly filled by echinoid cement (Period 2) but mostly remains empty. Minor areal pressure solution contacts prevail throughout the rock. Scale 41 x

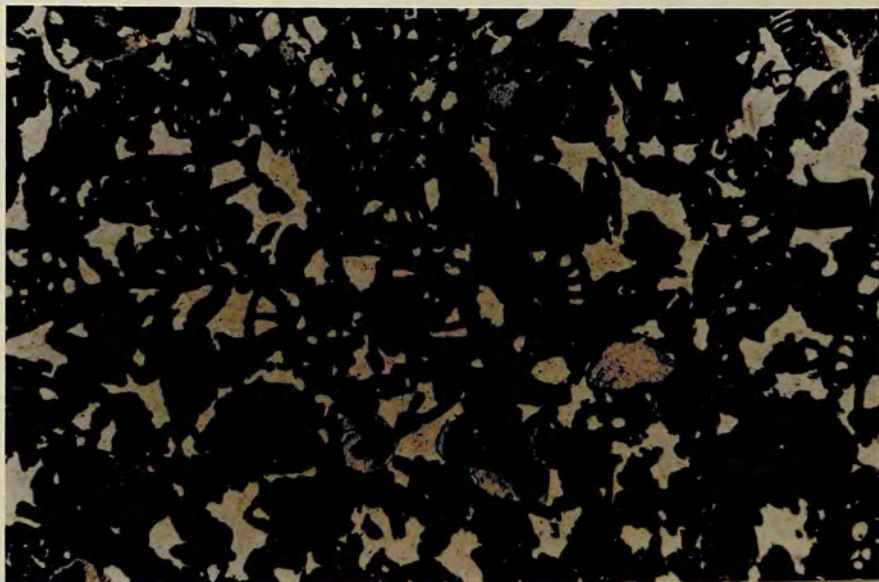
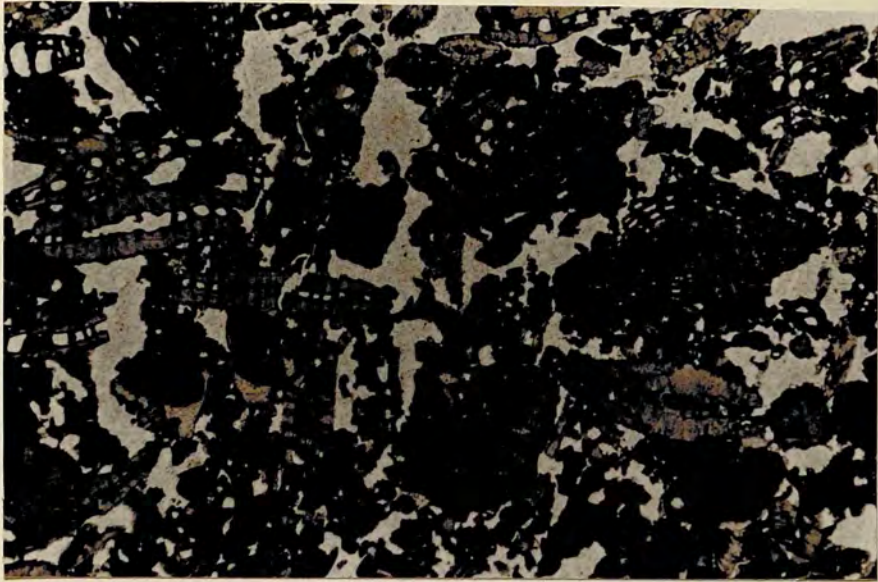
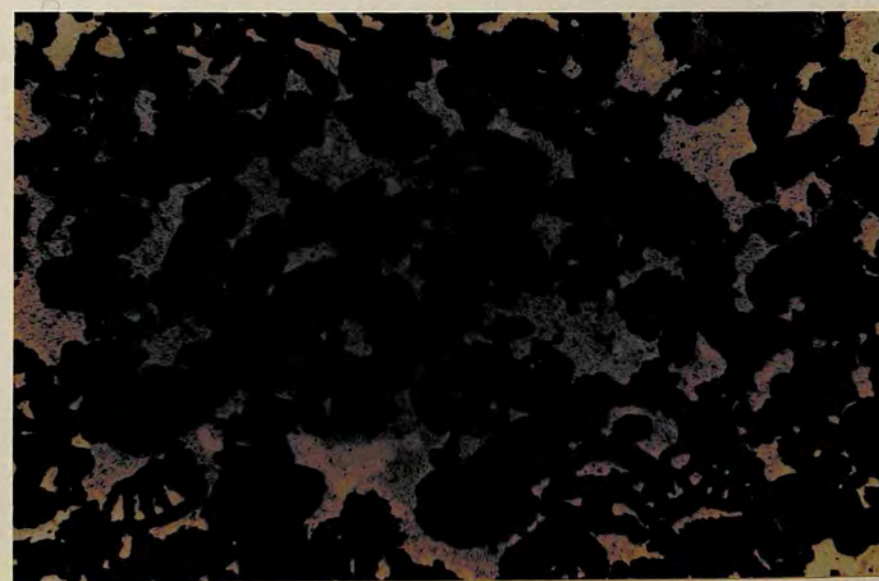
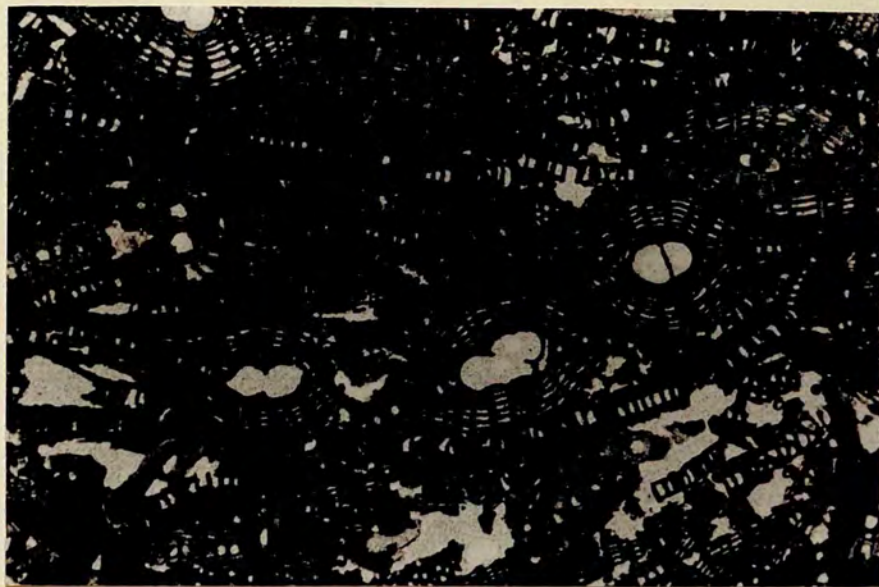


Plate 2.32 La Conca. Foraminiferal grainstone with abundant *Nephrolepidina* foraminifera and some algal debris (black material, right). Compaction has resulted in the rotation of grains into parallel alignment producing an interlocking pressure welded texture between the *Nephrolepidina*. Cementation is minimal, most pore space remains empty. Scale 41 x

Plate 2.33 Carboj Dam. Foraminiferal grainstone with abundant *Nephrolepidina*, some *Amphistegina* (right centre, bottom), *Heterostegina/Operculina* (centre), algal (black material) and echinoid debris. Areal pressure solution contacts prevail throughout the rock. Algae are most prone to pressure solution and occupy "interstitial" positions (top), the *Heterostegina/Operculina* (centre) preferentially fracture. Cement fills some foraminifera chambers and some intergranular pore space, but most remain empty. Scale 41 x

Plate 2.34 Carboj Dam. Grainstone with common algal (black material) and echinoid debris and common *Amphistegina*. Two periods of cement (Periods 1 and 2) on echinoid debris fill some pore space. Scale 41 x



LOWER MIOCENE LIMESTONES: FIELD VIEWS

Plate 3.1 Serra Lunga measured stratigraphic section, view looking northwest. Lower Miocene glauconitic sandy limestones form the Serra Lunga ridge in the left of the view. Upper Oligocene clays and marls are poorly exposed in the low cultivated land in the foreground. The section was measured along the line indicated, where the track traverses the ridge.



Plate 3.2 Costa del Conte measured stratigraphic section, view looking north. Lower Miocene glauconitic and sandy limestones form the length of this, the Costa del Conte ridge. Upper Oligocene clays and marls form poor outcrops at the base of the ridge and in the valley in the foreground. The section was measured along the line indicated.

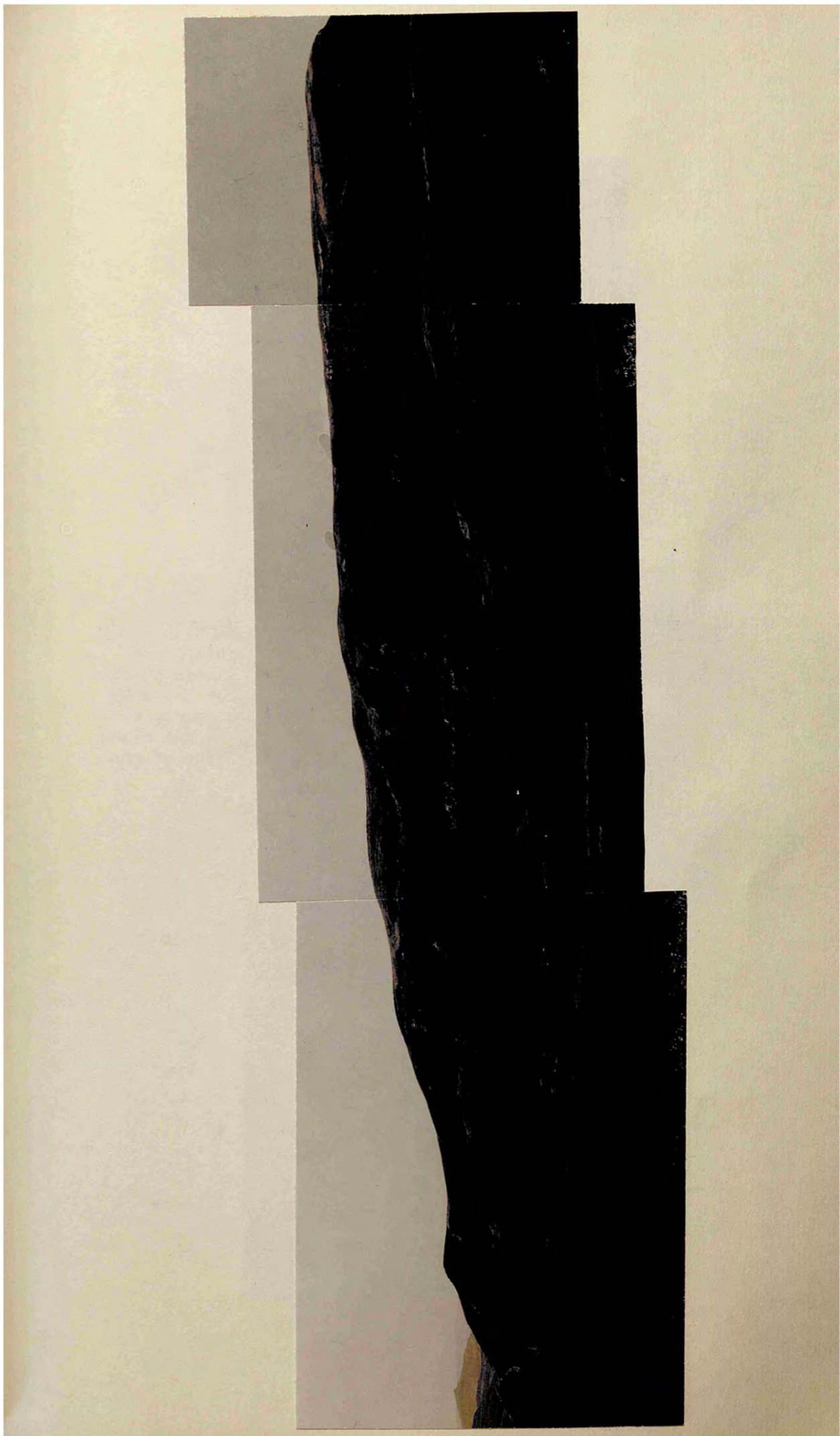


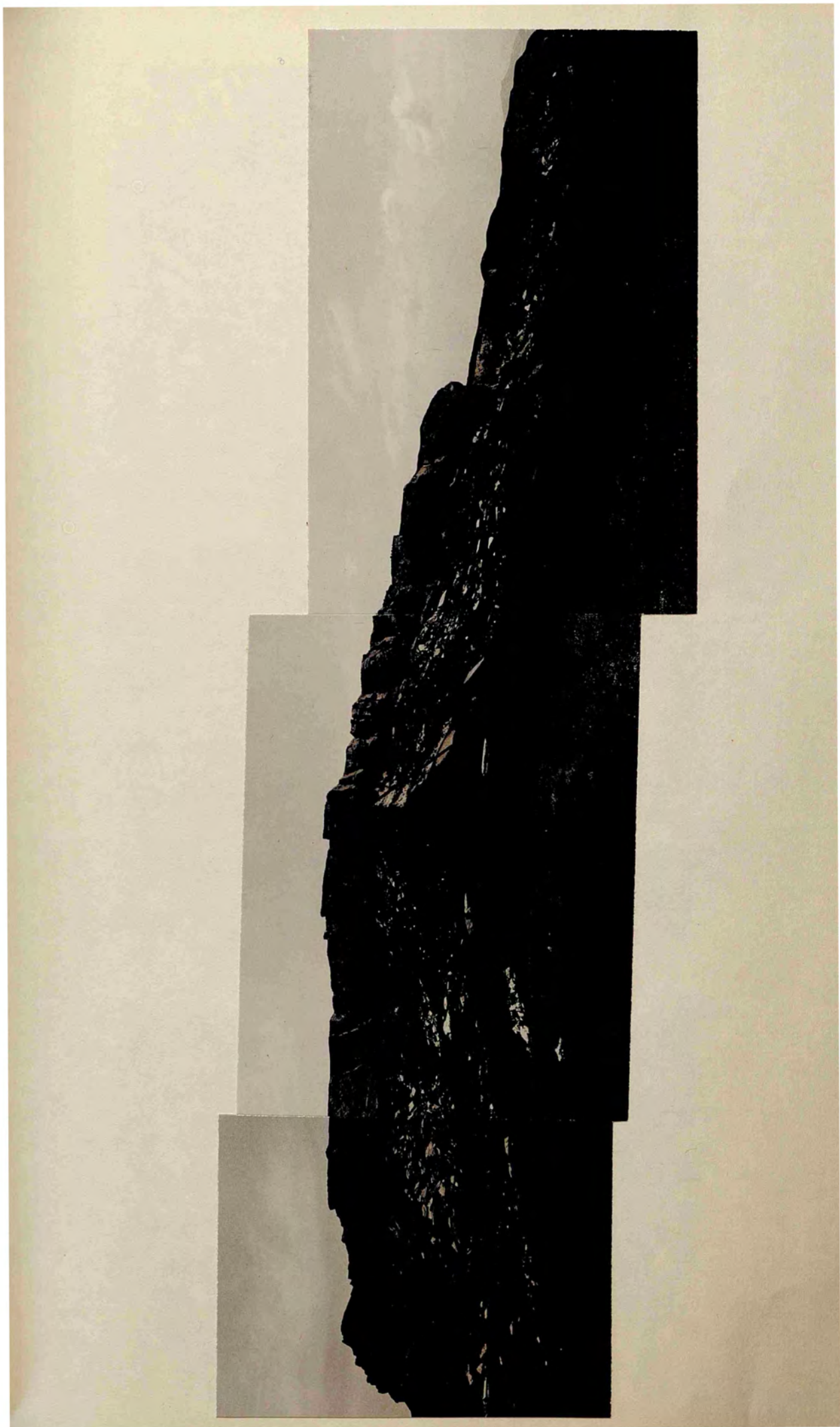
Plate 3.3 Battellaro measured stratigraphic section, view looking east. Lower Miocene glauconitic and sandy limestones form the bedded succession outcropping in the centre to the left of the view. Upper Oligocene clays and marls are poorly exposed below this bedded succession to the right. The section was measured along the line of continuous outcrop.



Plate 3.4 Battellaro. Close view of the beds at the top (left) of the succession seen in Plate 3.3. The more indurate beds (weathering out) contain more carbonate material than the less indurate beds which contain more quartz sand.



Plate 3.5 Mt Cardellia measured stratigraphic section, view looking north. Lower Miocene glauconitic and sandy limestones form the massive crags on the skyline. Uper Oligocene clays and marls form the light grey outcrops below the crags in the middle of the view. The section was measured along the lines indicated.



LOWER MIOCENE LIMESTONES: MICROFACIES OF
THE GLAUCONITIC LIMESTONE FACIES

Plate 3.6 Costa del Conte. Compacted foraminiferal grainstone with abundant *Miogypsina* and some *Nephrolepidina* (left and bottom right), *Amphistegina* (centre), *Spiroclypeus* (right), *Eulepidina* fragments (right centre and left centre) algal (black material) and echinoid debris. Compaction has resulted in the reduction of intergranular pore space and the subsequent formation of areal pressure solution contacts. The remaining intergranular pore space is cement filled. Glauconite is present as opaque fillings to some foraminifera (arrowed). Scale 41 x

Plate 3.7 Costa del Conte. Compacted foraminiferal grainstone with common *Miogypsina* and *Nephrolepidina* and some *Heterostegina/Operculina* (centre and bottom centre), *Amphistegina* (bottom centre), *Spiroclypeus* (left centre) and algal (black material) and echinoid debris. Areal pressure solution contacts prevail throughout the rock, cement fills the remaining (post compaction) intergranular pore space. Glauconite is present as opaque fillings to some foraminifera chambers (arrowed). Scale 41 x

Plate 3.8 Costa del Conte. Foraminiferal grainstone better sorted and finer grained than in Plates 3.6 and 3.7 and showing less effects of compaction nevertheless, still evident in a fully cemented rock. Foraminifera include common *Amphistegina* with *Nephrolepidina* and some *Miogypsina*, *Eulepidina* fragments, *Heterostegina/Operculina* fragments and algal and echinoid debris. Glauconite is present as opaque fillings to some foraminifera (arrowed). Scale 41 x

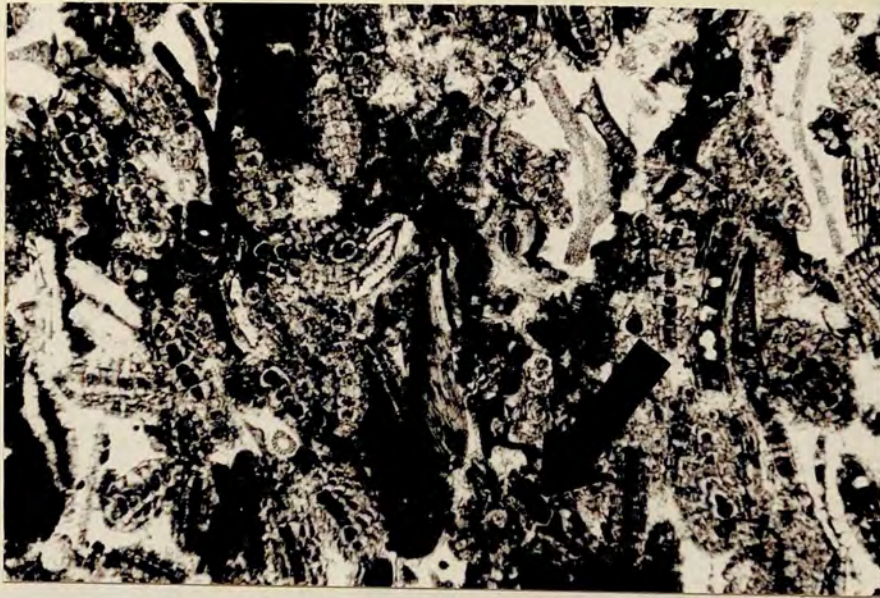


Plate 3.9 Costa del Conte. Compacted grainstone with common *Amphistegina*, fragments of other foraminifera, algal and echinoid debris and some glauconite pellets (well rounded black grains which resist pressure solution). Glauconite is also present as opaque fillings to some *Amphistegina* and as fillings to the pores of echinoid grains. Compaction has resulted in the formation of areal pressure solution contacts between grains; the remaining intergranular pore space is cement filled. Scale 41 x

Plate 3.10 Battellaro, peel photomicrograph. Foraminiferal grainstone with common sub-rounded quartz grains (bottom right), common *Rotalia* (bottom centre), fragments of other benthonic foraminifera and a single abraded *Nephrolepidina* (left). Compaction is minimal and represented by areal pressure solution contacts between some grains. Intergranular pore space is cement filled. Glauconite is represented by opaque fills to some foraminiferid chambers, especially the *Nephrolepidina* (left). Scale 105 x

Plate 3.11 Battellaro, peel photomicrograph. Foraminiferal grainstone with common sub-rounded quartz grains, common Globigeriniids, fragments of benthonic foraminifera and a single Nodosariid (centre). Compaction is minimal, but represented by areal pressure solution contacts between grains. All intergranular pore space is cement filled. Glauconite is represented by opaque material associated with some foraminifera, and by rounded pellets, one of which is embedded in an echinoid grain (centre top). Scale 105 x

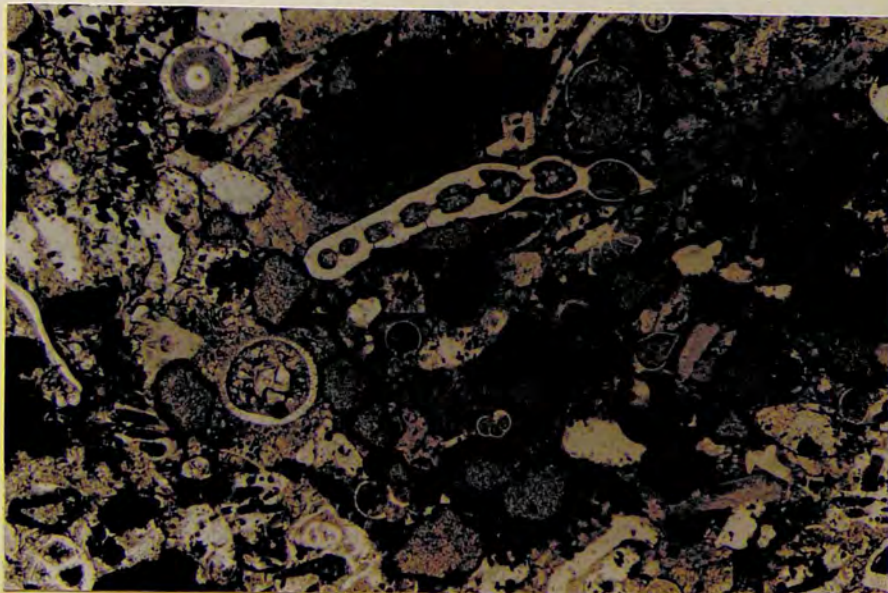
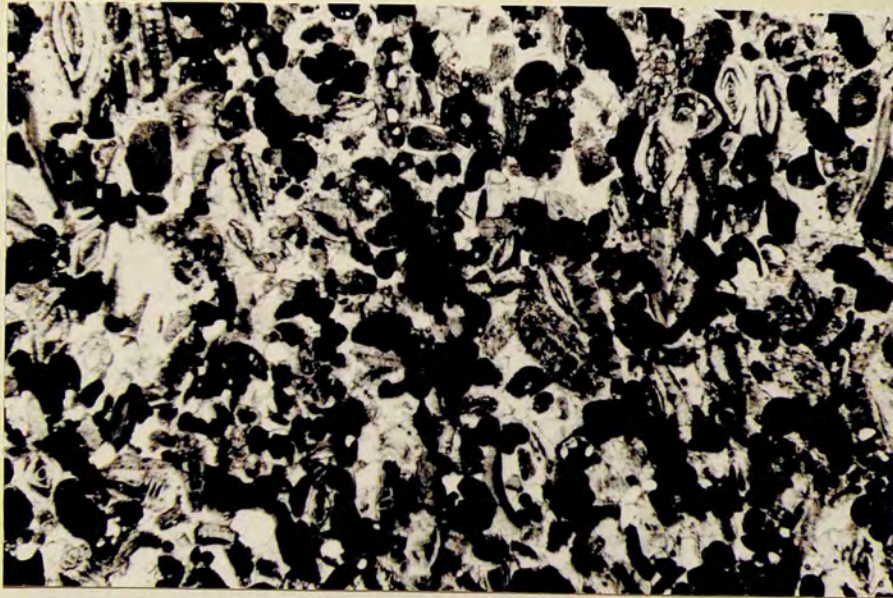


Plate 3.12 Battellaro, peel photomicrograph. Foraminiferal grainstone with common sub-rounded quartz grains, common Globigeriniids, *Rotalia* and fragments of other benthonic foraminifera including a single large fragment of *Heterostegina/Operculina* (centre). Cement fills the intergranular pore space. Glauconite is represented by rounded pellets and opaque and dark infills to some foraminifera. Scale 105 x

Plate 3.13 Battellaro. Grainstone with common quartz grains, glauconite pellets, *Amphistegina*, *Rotalia* and small Rotaliids. Compaction is minimal but represented by areal pressure solution contacts between some grains. Pore space is cement filled. Scale 105 x

Plate 3.14 Cardellia, peel photomicrograph. Grainstone with common Globigeriniids, small Rotaliids and fragments of benthonic foraminifera. Glauconite is present as pellets (black grains) and infills to some foraminifera. Pore space is cement filled. Scale 41 x

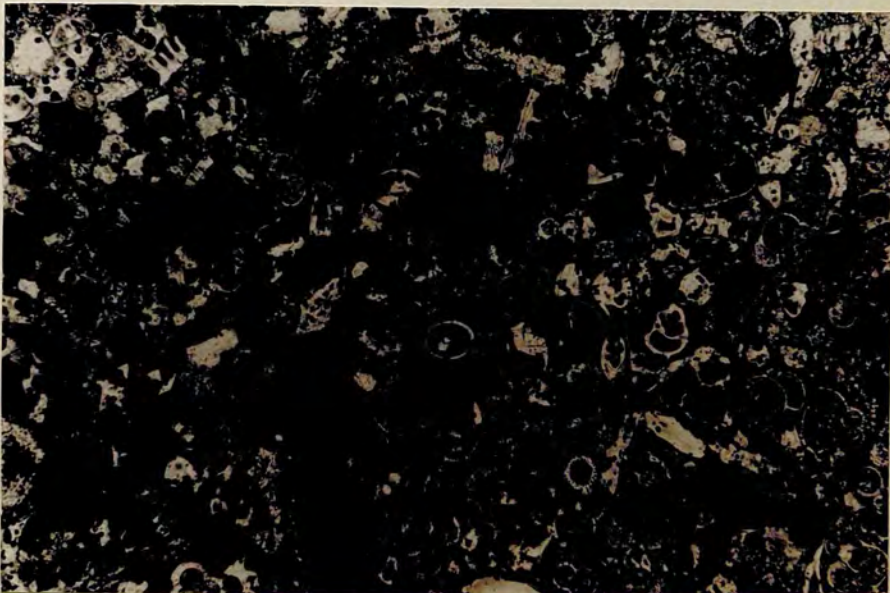


Plate 3.15 Cardellia. Poorly sorted grainstone with *Amphistegina*, Globigeriniids, fragments of benthonic foraminifera and a single Nodosariid (centre). Compaction is represented by pressure solution contacts between some grains. Intergranular pore space is cement filled. Scale 105 x

Plate 3.16 Cardellia. A horizon of a bioclastic grainstone rich in glauconite pellets. Other clasts include fragments of echinoids and foraminifera and a few grains of quartz. Compaction is represented by areal pressure solution contacts between grains. Echinoid material preferentially goes into solution to accommodate the glauconite grain (top right). Intergranular pore space is cement filled. Scale 105 x

Plate 3.17 Cardellia. Bioclastic grainstone with glauconite pellets, Globigeriniids and fragments of echinoids and benthonic foraminiferids. Intergranular pore space is cement filled. Scale 105 x

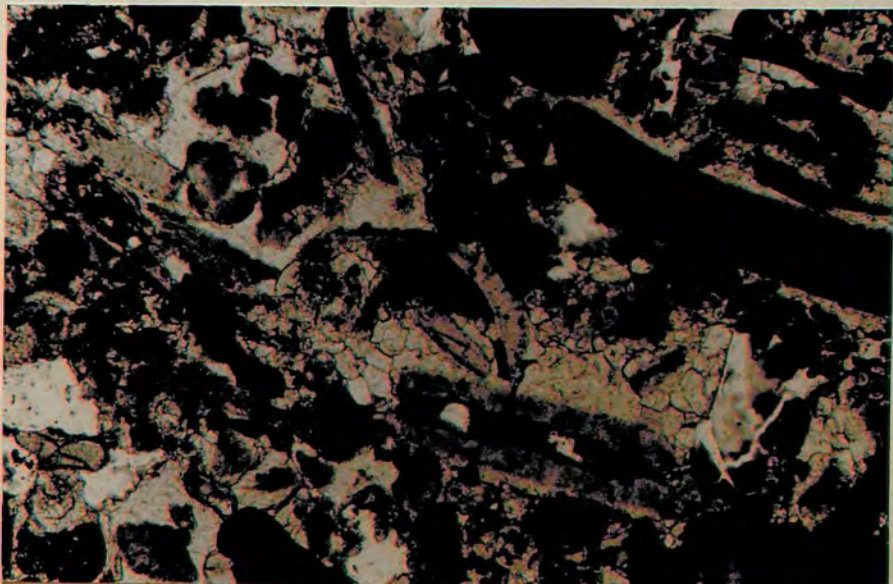
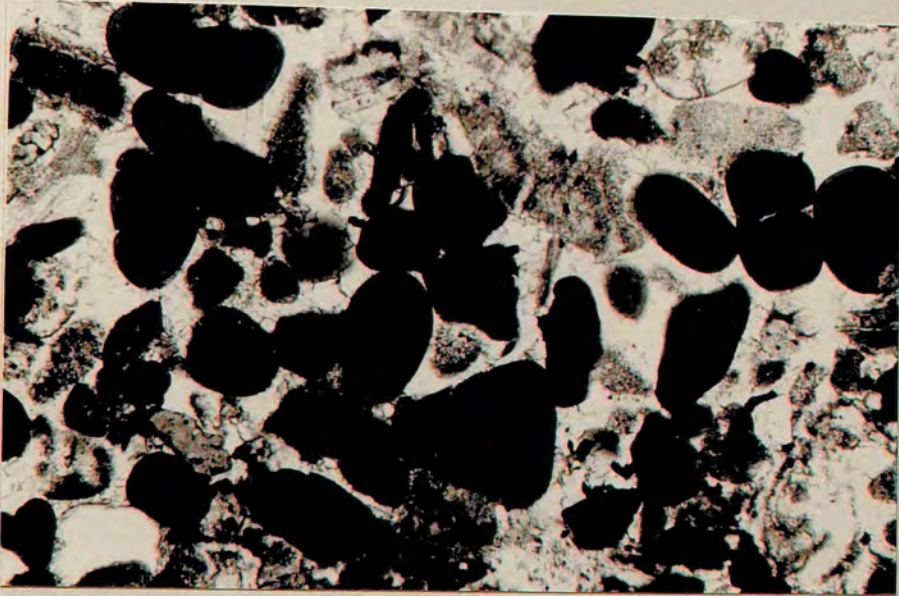
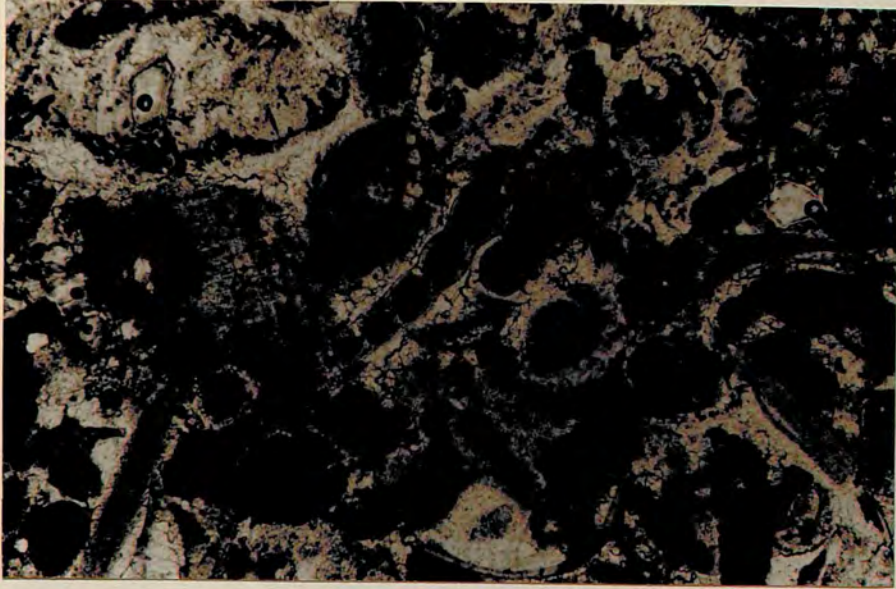
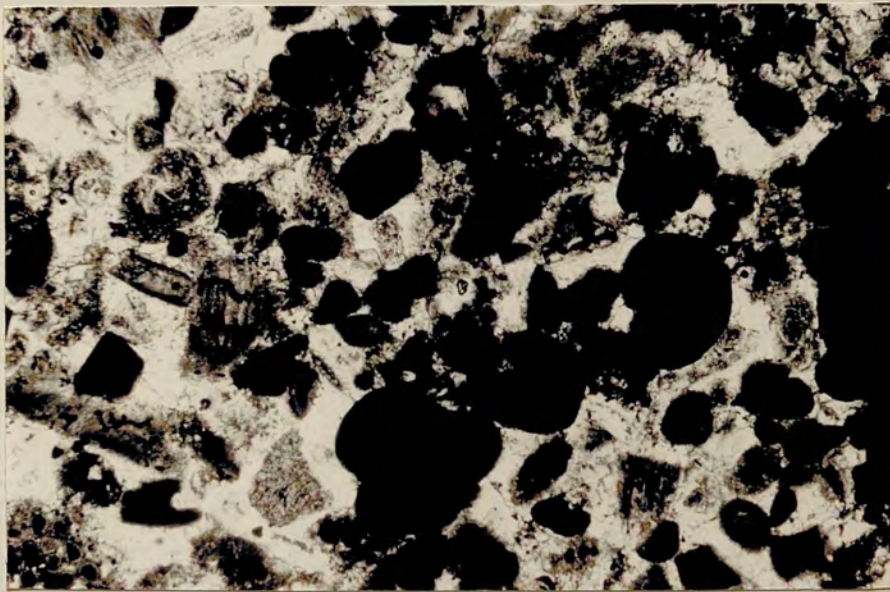


Plate 3.18 Cardellia. Bioclastic grainstone with glauconite pellets, Globigeriniids, small Rotaliids, and fragments of echinoids, benthonic foraminifera and bivalves. Compaction is represented by real pressure solution contacts between some grains. Intergranular pore space is cement filled. Scale 105 x

Plate 3.19 Cardellia. Bioclastic grainstone with abundant glauconite pellets and fragments of echinoids and benthonic foraminifera. Compaction is represented by real pressure solution contacts between some grains. Intergranular pore space is cement filled. Scale 105 x



LOWER MIOCENE LIMESTONES: MICROFACIES OF
THE SANDY LIMESTONE FACIES

Plate 3.20 Costa del Conte. Sandy limestone with common rounded to subangular grains of fine sand size quartz. Allochems are represented by Globigeriniid and small Rotaliid foraminifera and by fragments of echinoid and algal debris. Intergranular pore space is cement filled. Scale 41 x

Plate 3.21 Costa del Conte. Sandy limestone with common rounded to angular grains of fine sand size quartz. Glauconite pellets are present and allochems are represented by Globigeriniids, small Rotaliids, a single *Amphistegina* (top, right) and fragments of echinoid and bivalve. Compaction is represented by areal pressure solution contacts between some grains. Intergranular pore space is cement filled. Scale 105 x

Plate 3.22 Battellaro. Sandy limestone with common rounded to subangular fine sand size quartz grains and with allochems represented by Globigeriniids and bivalve fragments. Intergranular pore space is cement filled. Scale 105 x

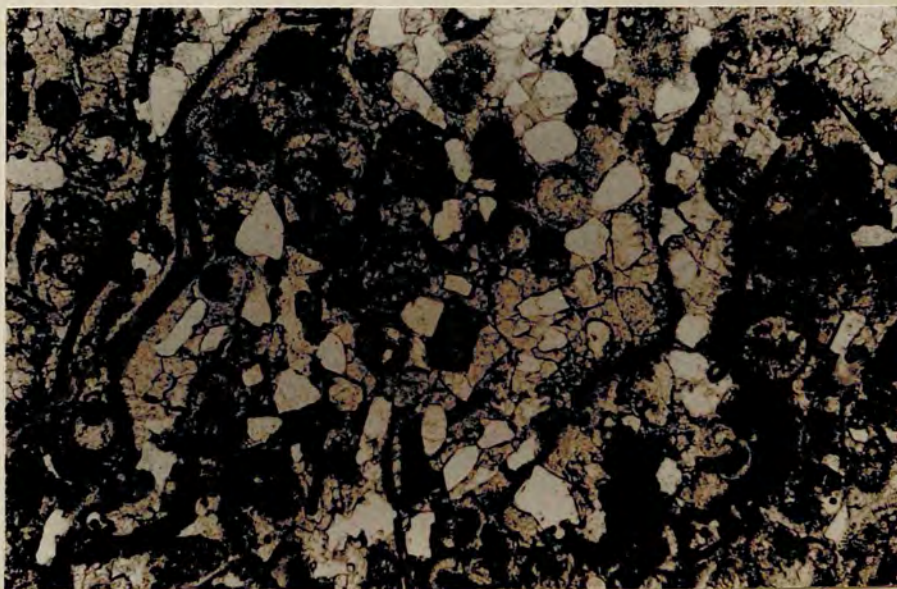
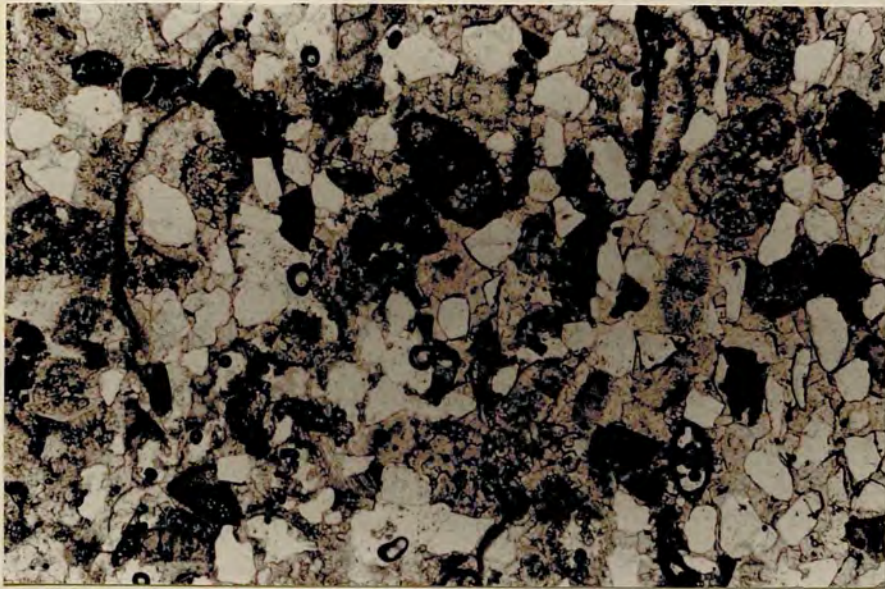


Plate 3.23 Battellaro. Calcareous sandstone with abundant well sorted rounded to angular fine sand size quartz grains. Other grains are represented by a few glauconite pellets and some small echinoid and algal debris. Pore space is cement filled. Scale 41 x

Plate 3.24 Battellaro. Sandy limestone with a calcareous sandstone horizon within it. Quartz grains are well sorted, rounded to subangular, of fine sand size. Allochems are represented by small Rotaliids, Globigeriniids and algal and bivalve debris. Pore space is cement filled: sub-poikilotopic cement in the calcareous sandstone and granular cement in the sandy limestone. Scale 41 x

Plate 3.25 Serra Lunga. Sandy limestone, coarser grained than those in Plates 3.20-3.24, containing medium to coarse sand size rounded to well rounded quartz grains. Other grains are represented by rounded opaque glauconite pellets, Globigeriniids and fragments of benthonic foraminifera, algae and echinoids. Pore space is cement filled. Scale 105 x

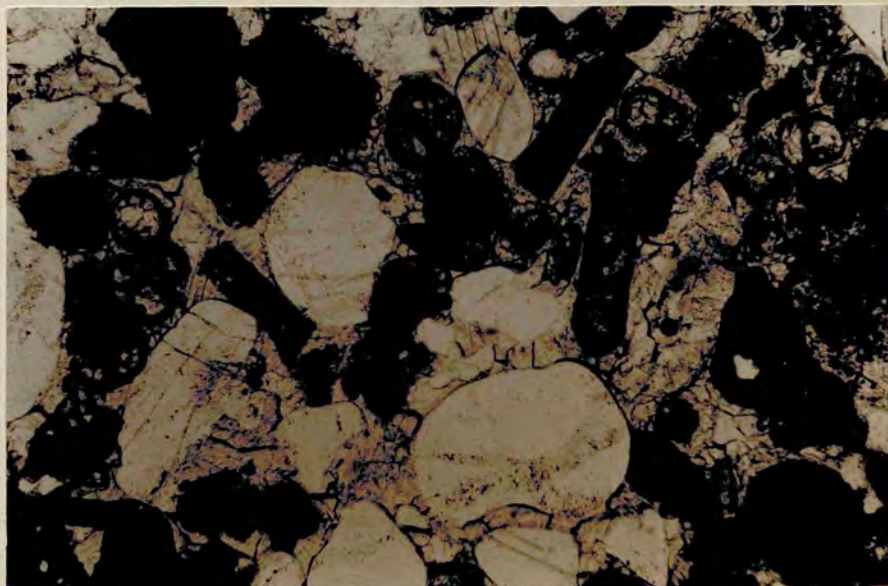
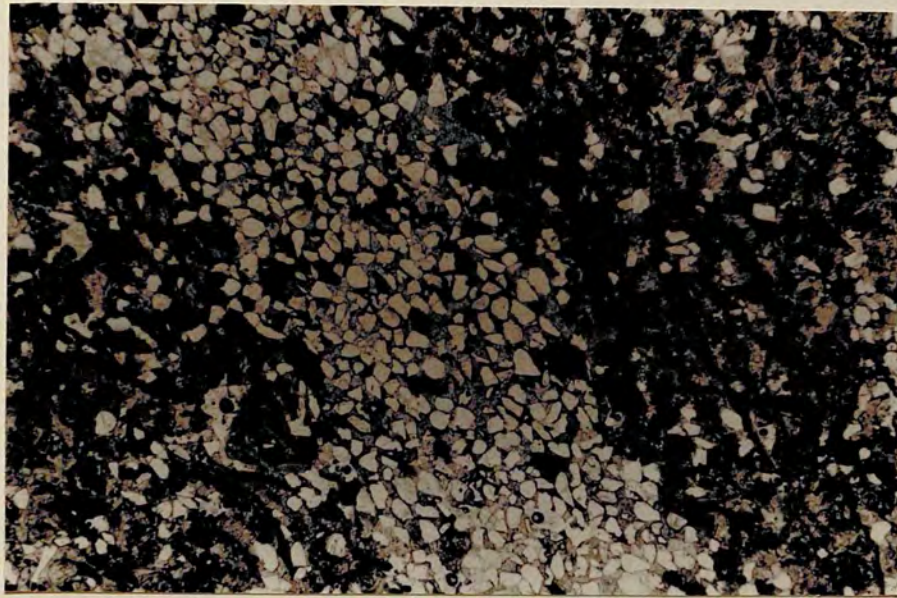
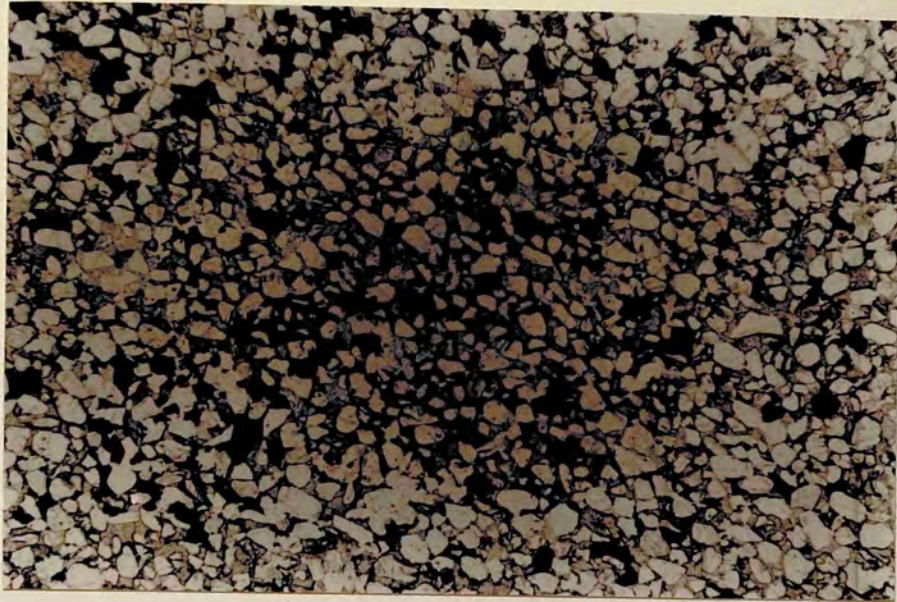


Plate 3.26 Serra Lunga. Sandy limestone with poorly sorted medium to coarse sand size subangular to well rounded quartz grains along with glauconite pellets (opaque), Globigeriniids, algal debris and a single small Rotaliid (left). Pore space is cement filled. Scale 105 x

Plate 3.27 Serra Lunga. Sandy limestone with poorly sorted subangular to well rounded quartz grains along with opaque glauconite pellets, Globigeriniids and fragments of algae and benthonic foraminifera. Compaction is represented by areal pressure solution contacts between some grains. Pore space is cement filled. Scale 105 x

Plate 3.28 Cardellia. Grainstone with common glauconite pellets along with small Rotaliids, Textulariids (one arrowed) and fragments of benthonic foraminifera, echinoids and algae. Compaction is represented by areal pressure solution contacts between some grains. Pore space is cement filled. Scale 105 x

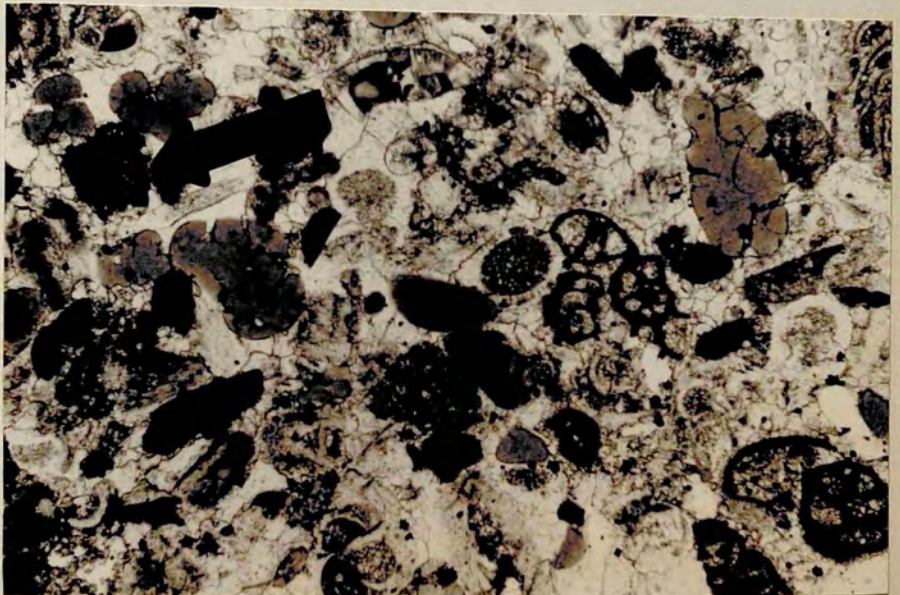
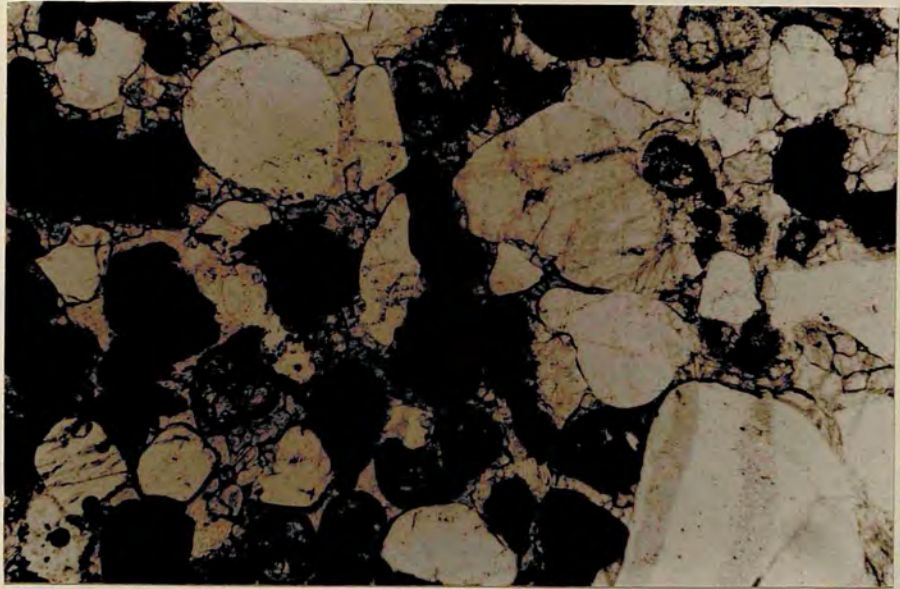
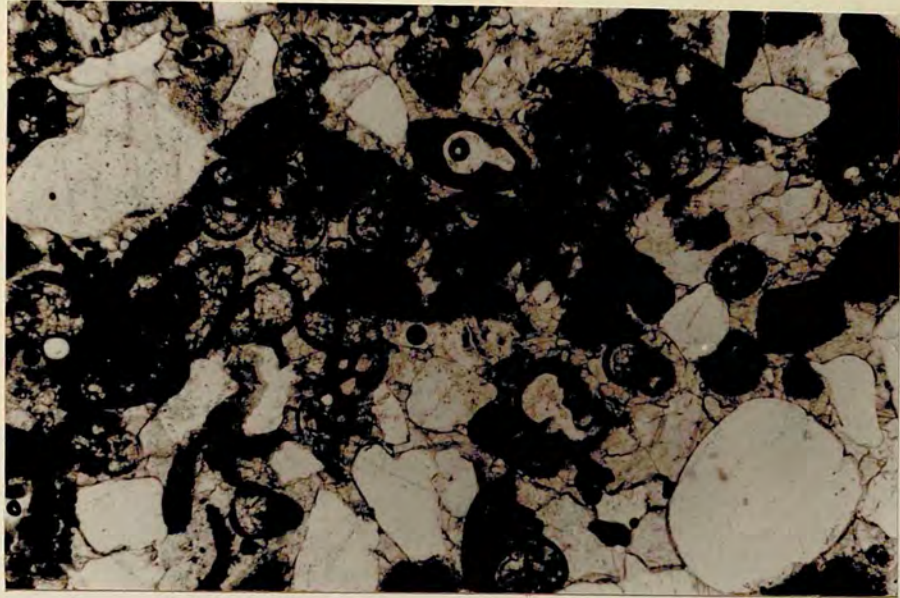
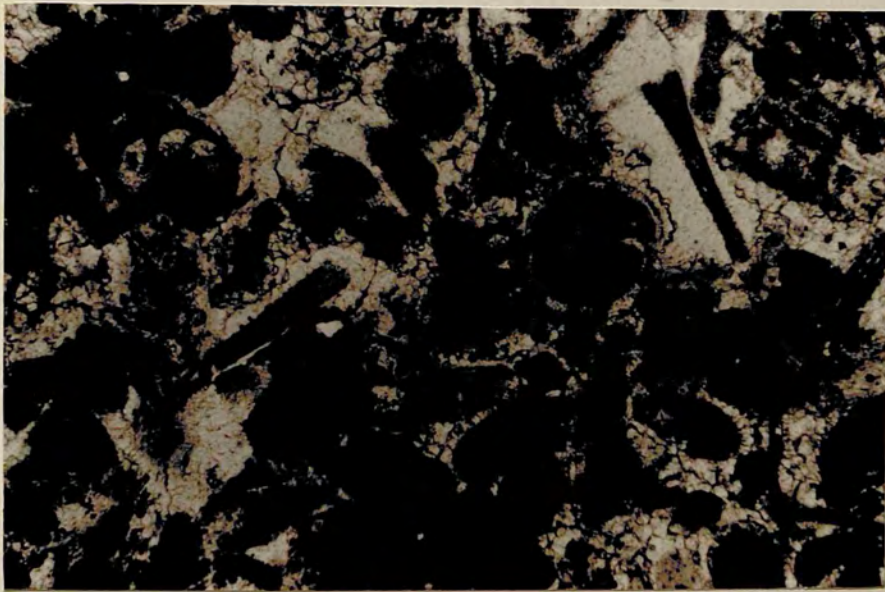
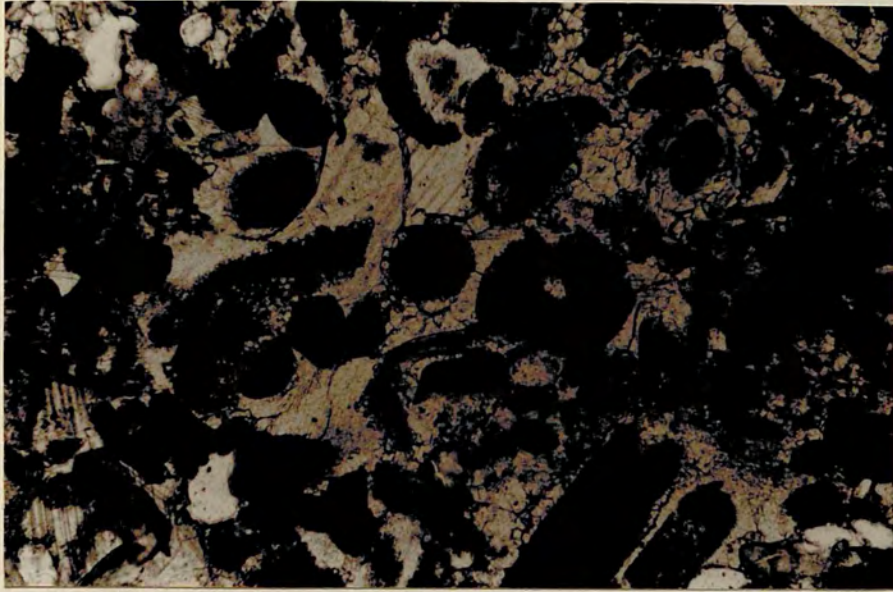


Plate 3.29 Cardellia. Grainstone composed of fragments of algae, echinoids, benthonic foraminifera and bivalves. A few glauconite pellets (opaque - subopaque) and quartz grains are present. Pore space is cement filled. Scale 105 x

Plate 3.30 Cardellia. Grainstone composed of Globigeriniids, small Rotalliids and fragments of echinoids, algae and benthonic foraminifera along with some glauconite pellets (opaque). Pore space is cement filled. Scale 105 x



PALAEONTOLOGY: CORALLINE RED ALGAE
(all photomicrographs are from Nadorello east samples)

Plate 4.1 *Archaeolithothamnium saipanense*. Typical branching growth form: short narrow branches connected by thin layers of thallus. Sporangia are numerous and concentrated into layers. Scale 41 x

Plate 4.2 *A. saipanense*. Four to five thalli are superimposed, each is fertile and contains sporangia in layers in the area of the low relief protuberance. Scale 41 x

Plate 4.3 *A. saipanense* forms the outer encrustation of a rhodolith previously encrusted by *Lithoporella melobesioides*. The thin simple multilayered hypothallus and the threaded nature of the perithallus can be seen. Scale 105 x

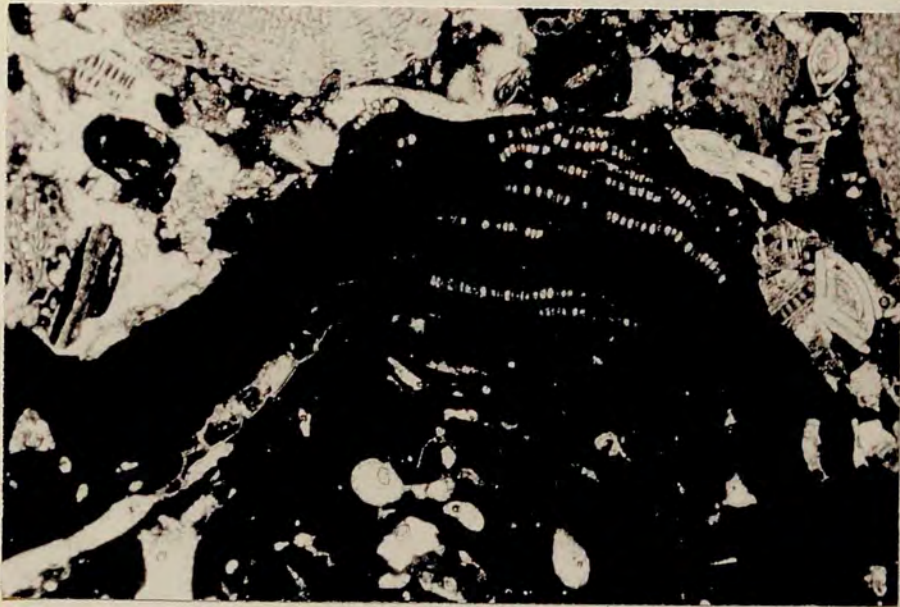


Plate 4.4 *A. saipanense*. Infertile tissue, showing well developed simple hypothallus and threaded to boxwork perithallus. Scale 105 x

Plate 4.5 *A. saipanense*. Close view of the tissue in Plate 4.4 showing the irregular order of the cells in the hypothallus and the selected calcification of the vertical walls in the perithallus giving a threaded appearance. Scale 410 x

Plate 4.6 *A. saipanense*. Fertile tissue showing thin simple hypothallus, threaded perithallus and sporangia in layers. Scale 410 x



Plate 4.7 *Lithothamnium aggregatum* (top and right) forms the outer encrustation of a rhodolith previously encrusted by *L. cf. marianae* (bottom). *L. aggregatum* is represented by a typical thin thallus composed of a prominent hypothallus and threaded perithallus. Conceptacles are rectangular in shape and form a relief at the surface of the thallus. Scale 105 x

Plate 4.8 *L. aggregatum* forms two separate encrustations on a rhodolith composed of *L. cf. marianae* in its core (bottom). The prominent hypothallus, threaded perithallus and rectangular shaped conceptacles can be seen (centre). Scale 105 x

Plate 4.9 *L. aggregatum*. Close view of the thallus right of centre in Plate 4.8 shows the simple multi-layered hypothallus, threaded perithallus and a single conceptacle. Scale 410 x



Plate 4.10 Thin thalli of *L. aggregatum* form several encrustations (right) around a rhodolith originally composed of *L. cf. marianae* (left).
Scale 41 x

Plate 4.11 *Lithothamnium cf. marianae*. Typical thick, short branch growth form showing common rectangular shaped conceptacles concentrated into the branches. Scale 41 x

Plate 4.12 *L. cf. marianae*. A single detached thick short branch (which would have been attached to the thallus at its narrow end, on the left) containing numerous rectangular shaped conceptacles.
Scale 41 x



Plate 4.13 Bored thallus of *L. cf. marianae* showing a thick simple multi-layered hypothallus and a threaded perithallus with lensoid growth zones. Scale 105 x

Plate 4.14 *L. cf. marianae*. Close view of the thallus showing a typically thin simple multi-layered hypothallus and threaded perithallus. Scale 410 x

Plate 4.15 *Lithophyllum ovatum* forms the outer thin encrustation on a rhodolith. The thallus is typically thin, with a coaxial hypothallus (best seen, right centre) and a perithallus containing a single unipored conceptacle (left centre). Scale 105 x

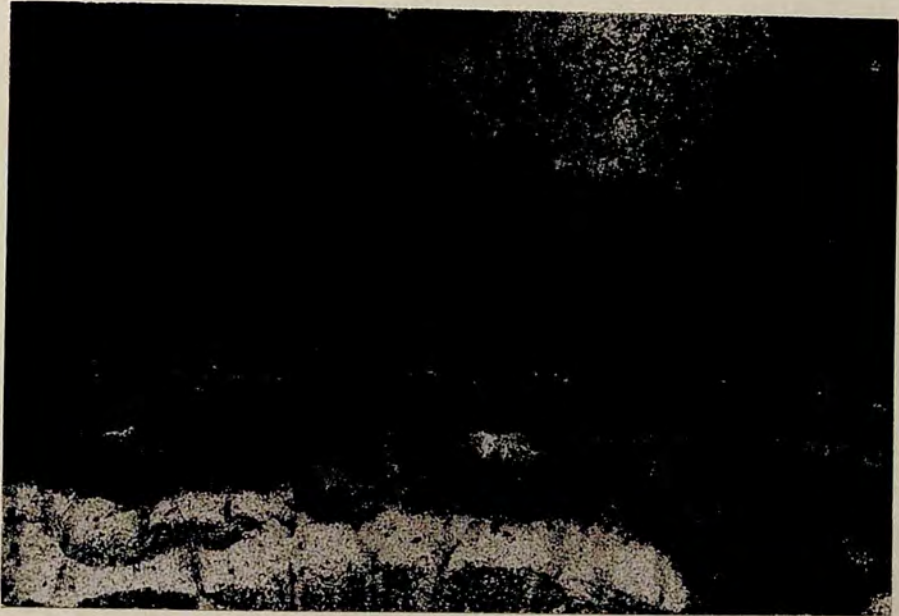


Plate 4.16 *L. ovatum*. Close view of the thallus in Plate 4.15 showing the coaxial hypothallus and layered perithallus. Scale 410 x

Plate 4.17 *Lithophyllum personatum*. Two thick, short, closely spaced, fertile branches (bottom left and right) containing large unipored conceptacles which have a flat base and convex roof. Scale 41 x

Plate 4.18 *L. personatum*. Close view of the branch on the bottom right of Plate 4.17 showing the layered and lensoid nature of the perithallus tissue, and the absence of this layering on the upper surface of the conceptacles. Scale 105 x

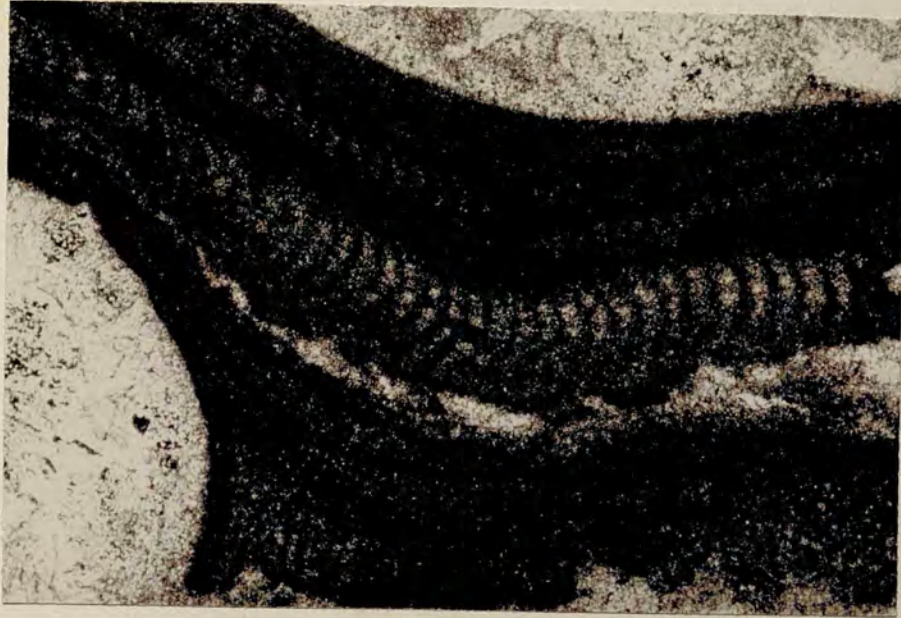


Plate 4.19 *L. personatum*. Close view of a conceptacle in Plate 4.18 showing the absence of layering and larger size of cells in the thallus on the upper surface of the conceptacle. Scale 410 x

Plate 4.20 *L. personatum*. Close view showing the poorly developed simple multi-layered hypothallus and layered perithallus of the rhodolith illustrated in Plate 4.17. Scale 410 x

Plate 4.21 A single detached branch of *L. personatum* showing a well developed layered and lensoid perithallus with numerous flat based convex roofed unipored conceptacles. Scale 105 x



Plate 4.22 *Mesophyllum* cf. *vaughanii*. Typical short thick, branch growth form with abundant conceptacles still containing sporangia. Scale 41 x

Plate 4.23 Bored thallus of *M.* cf. *vaughanii* containing abundant sporangia filled conceptacles in a protuberance of low relief. Scale 41 x

Plate 4.24 *M.* cf. *vaughanii*. Close view of the thallus on the right of Plate 4.23 showing a well defined thick, coaxial hypothallus; lensoid growth zones in the layered perithallus; and numerous conceptacles containing sporangia. Scale 105 x



Plate 4.25 A branch of *M. cf. vaughanii* showing pronounced lensoid growth zones in the area of the branch. Growth zones are non lensoid, parallel, in the thallus outside the area of the branch (bottom left). A single sporangia filled conceptacle is present (bottom right). Scale 105 x

Plate 4.26 *M. cf. vaughanii*. Close view showing the detail of a poorly developed plumose hypothallus and a layered perithallus. Scale 410 x

Plate 4.27 *Lithoporella cf. melobesioides*. Several monostromatic thalli with vertically elongate cells which vary in size within and between thalli. Scale 105 x

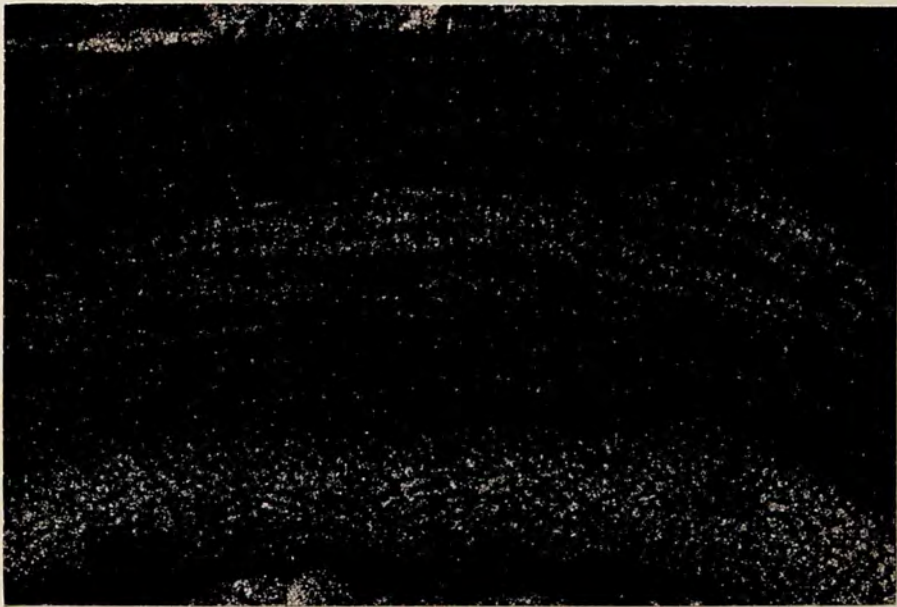
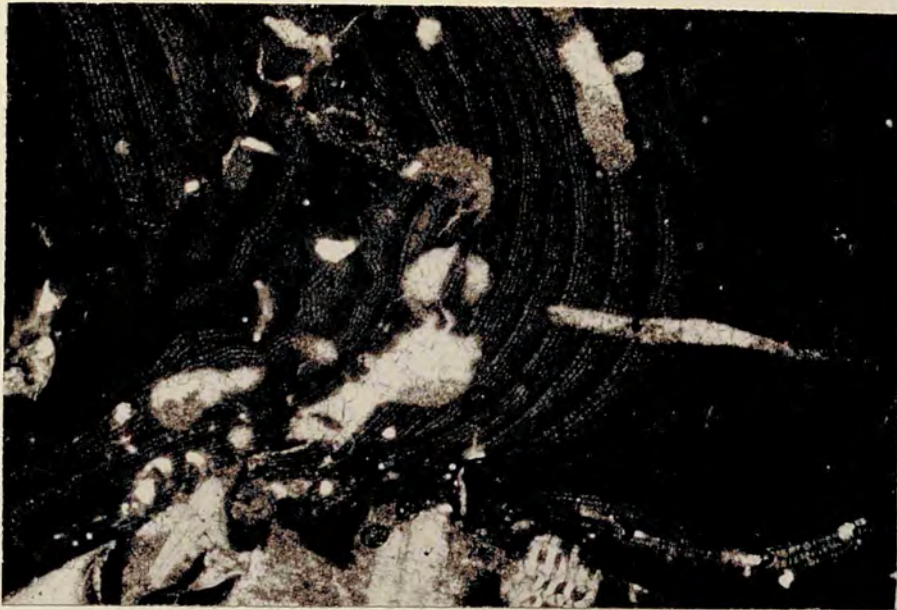


Plate 4.28 Thalli of *L. cf. melobesioides* (vertically elongate cells) are interleaved with thalli of *Melobesia cf. cuboides* (square and horizontally elongate cells) Scale 410 x

Plate 4.29 Thalli of *L. cf. melobesioides* and *M. cf. cuboides* in a rhodolith of *L. cf. marianae*. Scale 105 x

Plate 4.30 Thalli of *M. cf. cuboides* form the first encrustation on a *Lepidocyclina* (*Eulepidina*) foraminifera. Scale 105 x

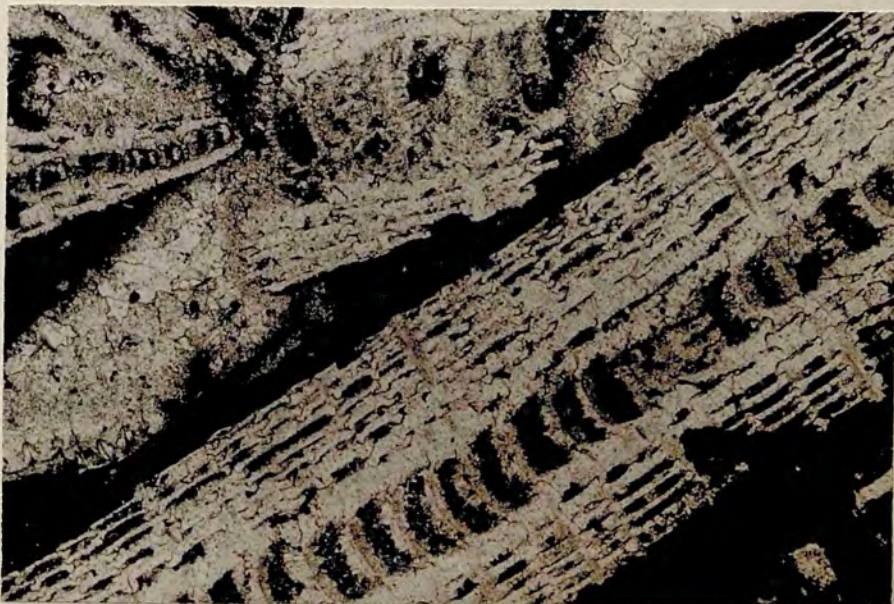
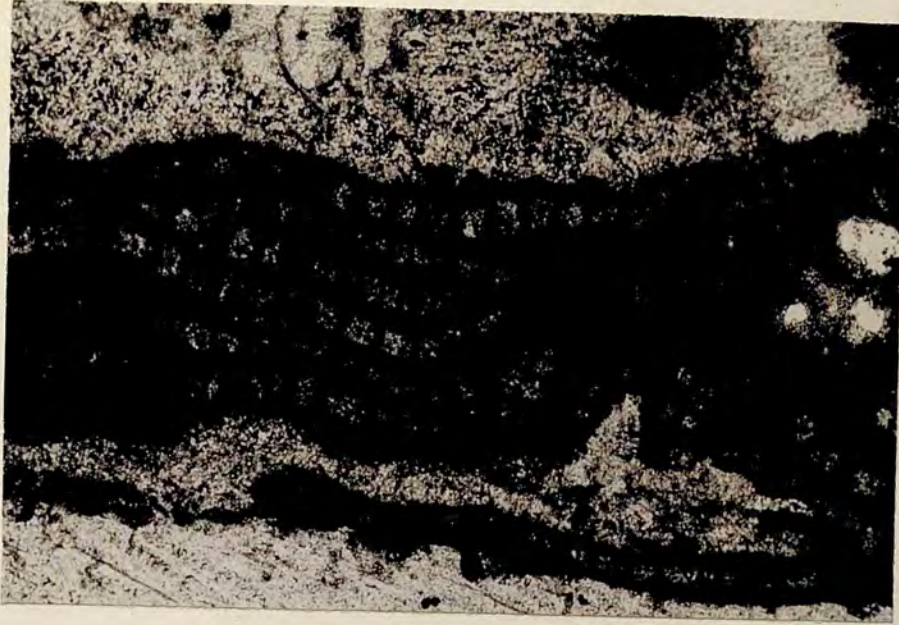


Plate 4.31 *M. cf. cuboides*. Close view of the thalli in the top right of Plate 4.30 showing the typical horizontally elongate cells. Scale 410 x

Plate 4.32 Thalli of *M. cf. cuboides* form the first encrustation (left) on an abraded rhodolith composed of *Archaeolithothamnium* (threaded thallus) and *Melobesia*. Scale 105 x

Plate 4.33 Rhodolith compact branching growth form seen at Nadorello east. The rhodoliths are composed of dense algal thallus, have short closely spaced branches and show good sphericity. The lens cap is 55 mm dia.

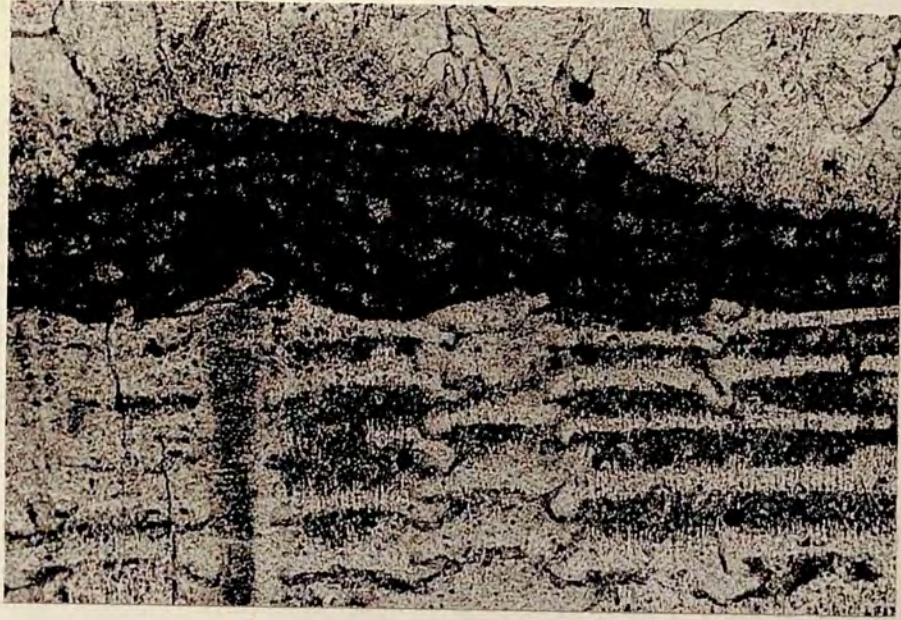
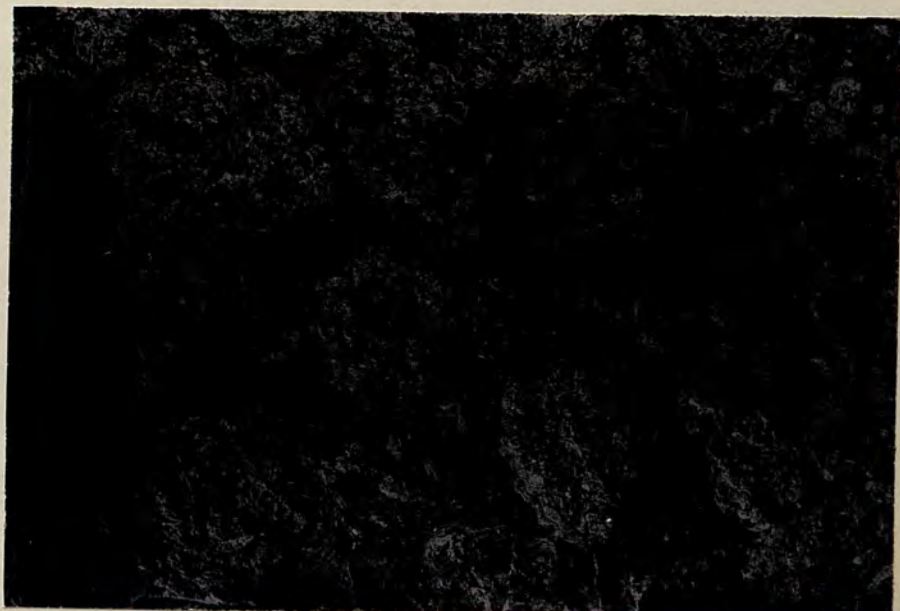


Plate 4.34 Rhodolith compact branching growth form seen at Nadorello east. Rhodoliths with good sphericity are formed of dense algal thallus with common short protuberances. The lens cap is 55 mm dia.

Plate 4.35 Rhodolith compact-laminar growth form seen at Nadorello east. The rhodolith (centre) has a core of dense compact branching algae, this is later encrusted by numerous thin thalli of another alga commonly displaying conceptacles (top left of the rhodolith). Millimeter gradations are seen on the rule.

Plate 4.36 Rhodolith laminar growth form seen at Nadorello east. The rhodoliths are composed entirely of an alga with a thin thallus growth form. There is no dense core and common alternating layers of sediment (grey) and alga (white) can be seen. The rule is 150 mm long.



- Plate 4.37 Rhodolith open branching growth form seen at Nadorello east. Branches which are relatively long and thin are widely spaced around the otherwise thin thallus of the rhodolith. Layers of sporangia, represented by faint grey lines, can be seen in the branches, thus identifying this alga as *Archaeolithothamnium*. Millimeter gradations are seen on the rule.
- Plate 4.38 Rhodolith open branching growth form seen at Nadorello east. Well spaced, long, thin branches are seen on an alga with a thin thallus which encrusts a benthonic foraminifera. Millimeter gradations are seen on the rule.
- Plate 4.39 Rhodolith compact non branching growth form seen at Contrada Giovanni. Non-branching rhodoliths of poor sphericity are formed of dense algal thallus mostly encrusting *Lepidocyclina* (*Eulepidina*) foraminifera. The lens cap is 55 mm dia.

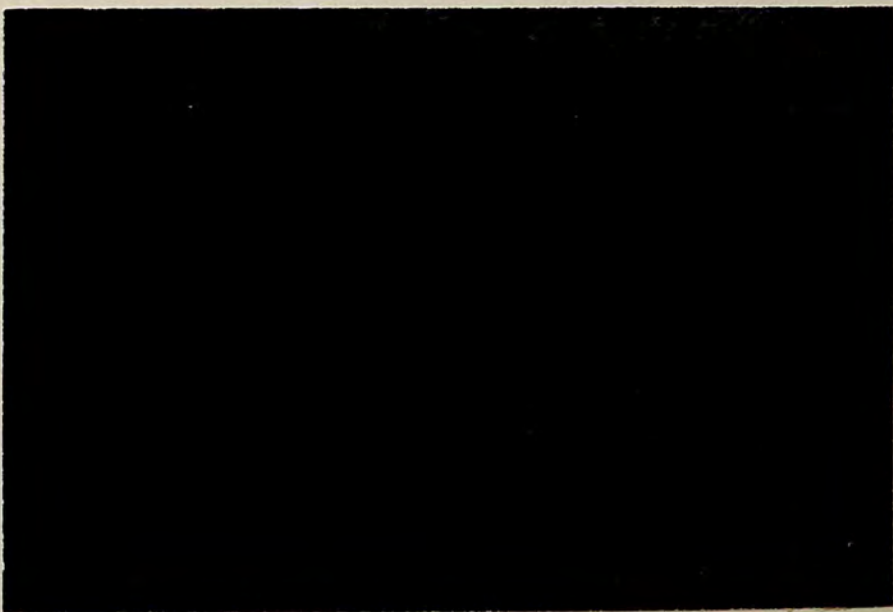
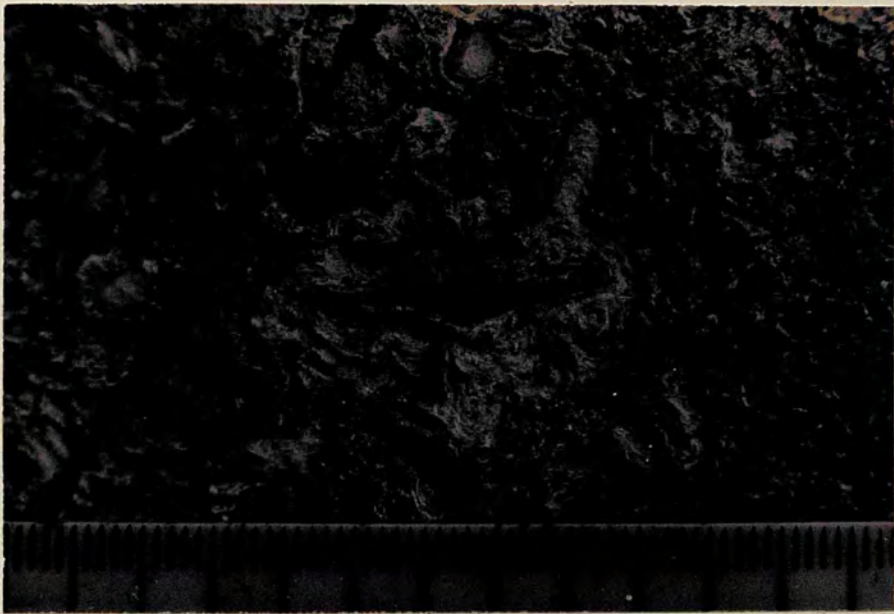
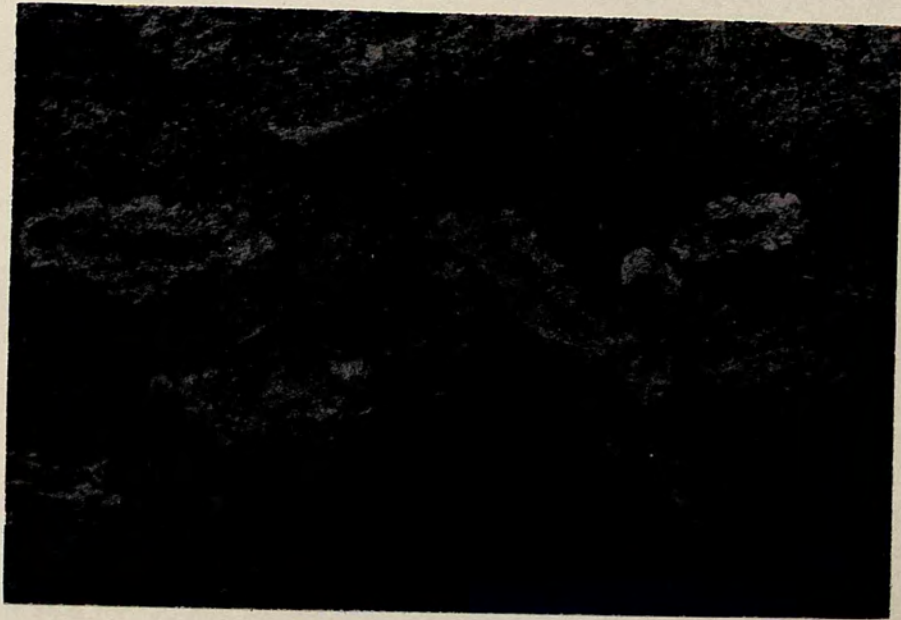


Plate 4.40 Rhodolith compact non-branching growth form seen at Contrada Giovanni. Close view of some rhodoliths towards the bottom centre of Plate 4.39, emphasising the poor sphericity of the rhodoliths and the compact nature of the thallus (no interleaving of sediment and thallus can be seen). The lens cap is 55 mm dia.



PALAEONTOLOGY: TRACE FOSSILS

- Plate 4.41 *Thalassinoides paradoxica* at Nadorello east on the Upper Cretaceous-Upper Oligocene unconformity. The view shows burrowed Upper Cretaceous chalk plastered to the underside of the massive Upper Oligocene algal limestone bed shown in Plate 2.4. The burrows, filled with Upper Oligocene limestone, are horizontal-subhorizontal in aspect, branch at angles of 45-90° at irregular intervals, and show swelling at the branch points. Scattered black phosphatic chalk clasts are present in the basal Upper Oligocene. The rule is 150 mm long.
- Plate 4.42 *T. paradoxica* at Donnalucata beach, SE Sicily. The view shows the upper surface of a Lower Miocene hardground which is perforated by numerous vertical tubes of *T. paradoxica*. The smaller openings (3-5 mm dia.) represent borings of *Trypanites* sp. The hardground limestone is dark in colour because it is phosphatised whereas the light coloured infill to the burrow tubes is composed mostly of non-phosphatised limestone with some phosphatic clasts. The lens cap is 55 mm dia.
- Plate 4.43 An example of very large burrows of *T. paradoxica* seen 200 mm below the phosphatised Lower Miocene hardground illustrated in Plates 4.42 and 7.1. The lens cap is 55 mm dia.

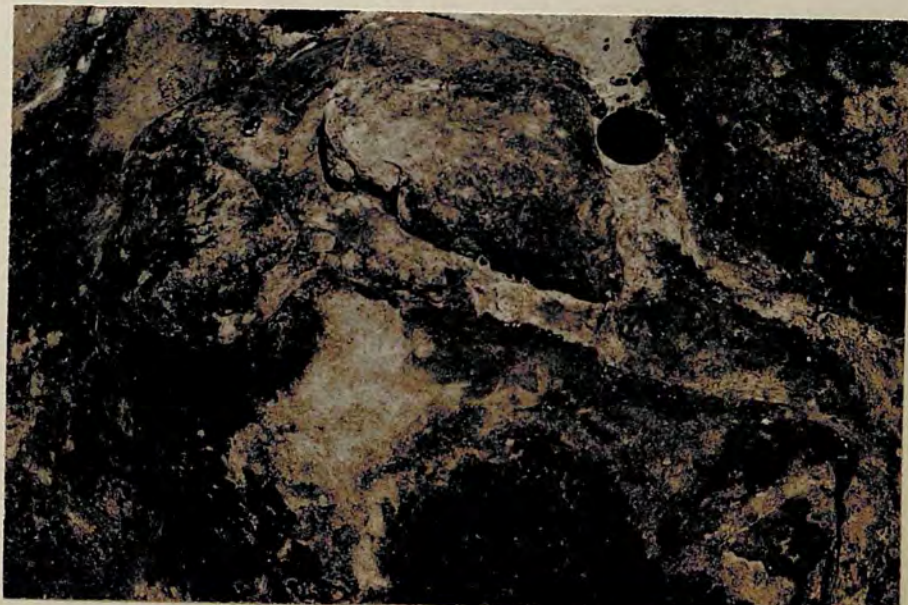


Plate 4.44 Burrows of *T. suevicus* seen in a beach exposure of Lower Miocene limestones at Donnalucata, SE Sicily. A c. 90° burrow branch (right centre) shows minor swelling at the branch point. The lens cap is 55 mm dia.

Plate 4.45 Burrows of *T. suevicus* in a beach exposure of Lower Miocene limestones at Donnalucata, SE Sicily. The burrows bifurcate and show negligible swelling at the branch point. Burrow walls are smooth. The lens cap is 55 mm dia.

Plate 4.46 A Lower Miocene limestone bed located immediately below the hardground at Donnalucata, SE Sicily, is thoroughly bioturbated by *T. suevicus*. The lens cap is 55 mm dia.

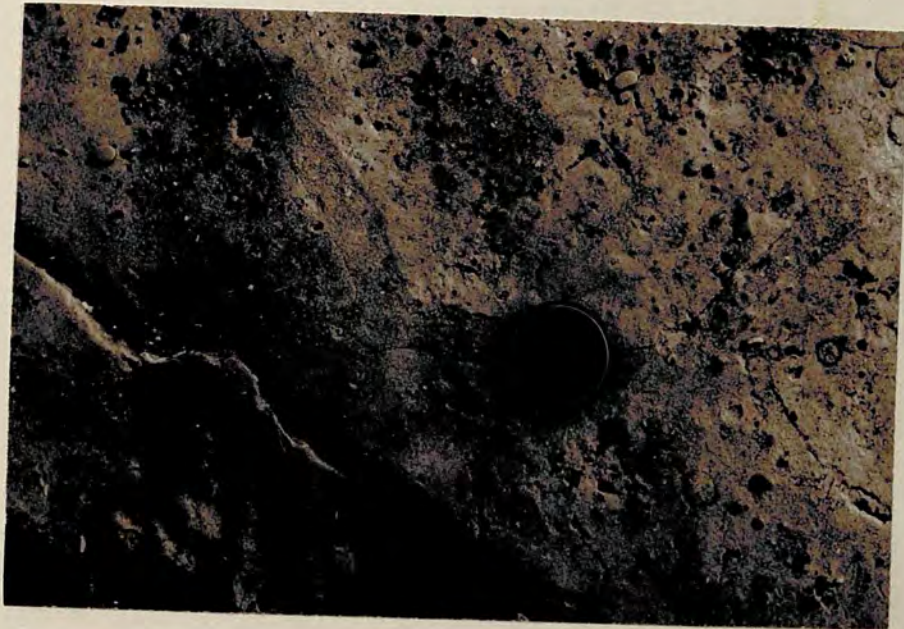
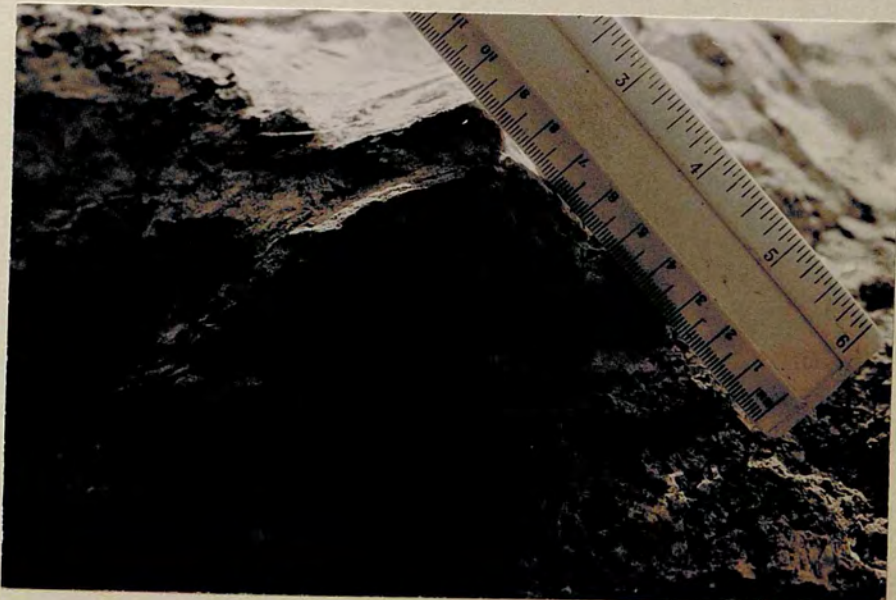
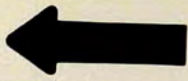


Plate 4.47 Small bifurcating burrows of *T. suevicus* located immediately below a Lower Miocene phosphorite bed at Pizzo Capra d'Oro, southeast of Ragusa, SE Sicily. The lens cap is 55 mm dia.

Plate 4.48 Borings of *Trypanites weisei* are seen (as black spots) on clasts of phosphatised limestone in the Lower Miocene phosphorite conglomerate at Contrada le Serre, north of Ragusa, SE Sicily. The lens cap is 55 mm dia.

Plate 4.49 Borings of *Trypanites* sp. seen on the surface of a fissure in Upper Oligocene and Upper Cretaceous limestones at Nadorello east in southwest Sicily. The borings are infilled with Lower Miocene glauconitic sandy limestone.



DIAGENESIS: UPPER OLIGOCENE LIMESTONES

Plate 5.1 Carboj Dam. Two periods of cement are present (Periods 1 and 2). The first is represented by a thin, dusty, syntaxial overgrowth on the echinoid grain (right centre). The second is represented by a wide clear overgrowth on the echinoid grain and by a thin coating of scalenohedra and equant spar on the foraminifera. The algal fragment (right) has no cement coating. Compaction post dates the second period cement evidenced by the echinoid overgrowth forming a pressure solution contact with neighbouring grains. Scale 105 x

Plate 5.2 Carboj Dam. Two periods of cement are present (Periods 1 and 2). The first is represented by a thin dusty syntaxial overgrowth (just visible) on the two echinoid grains (left and bottom right). The second cement forms wide overgrowths on the echinoid grains and thin coatings of scalenohedra (visible centre) on the foraminifera but is absent from the algal clasts. Compaction post dates the second cement since one echinoid overgrowth forms a pressure solution contact with the *Amphistegina* (right centre). Scale 105 x

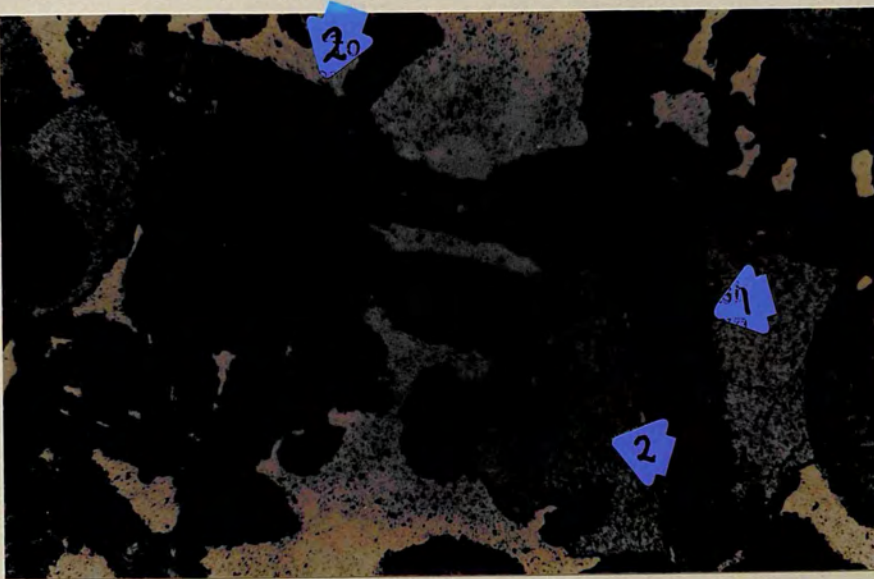
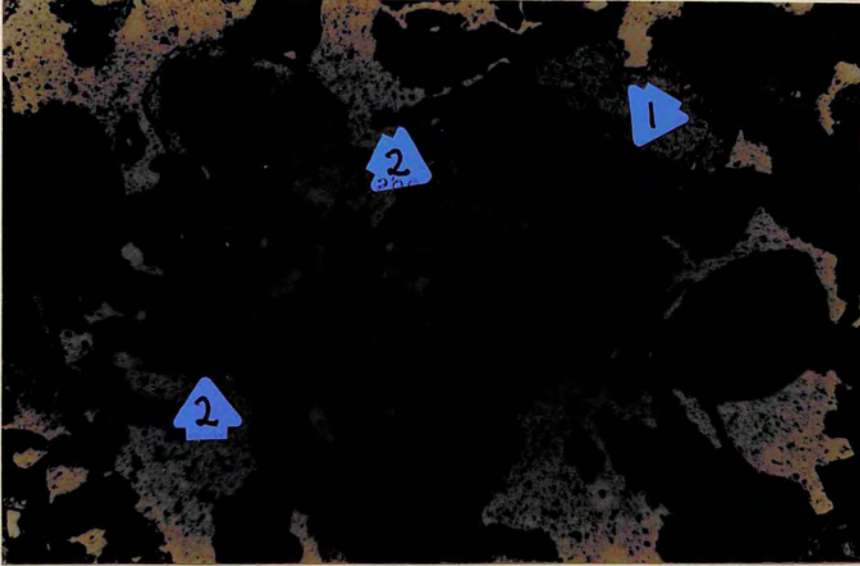
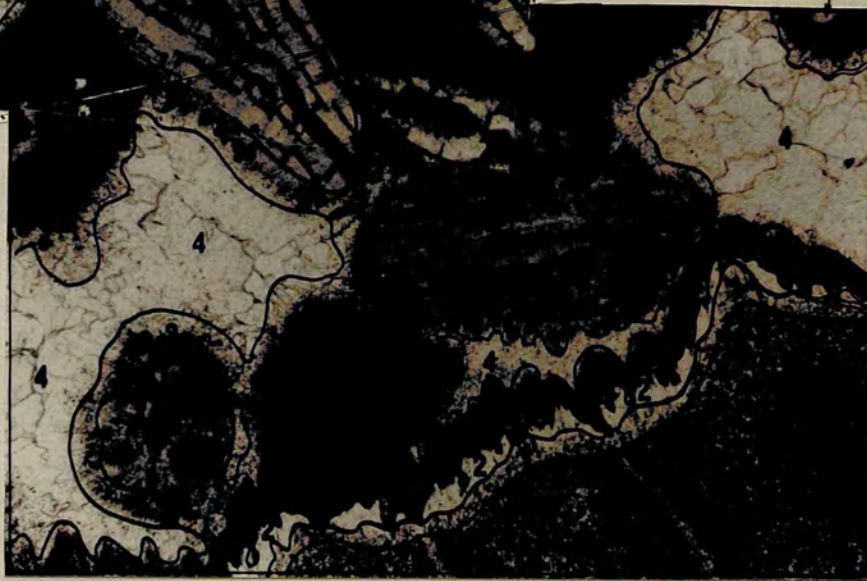
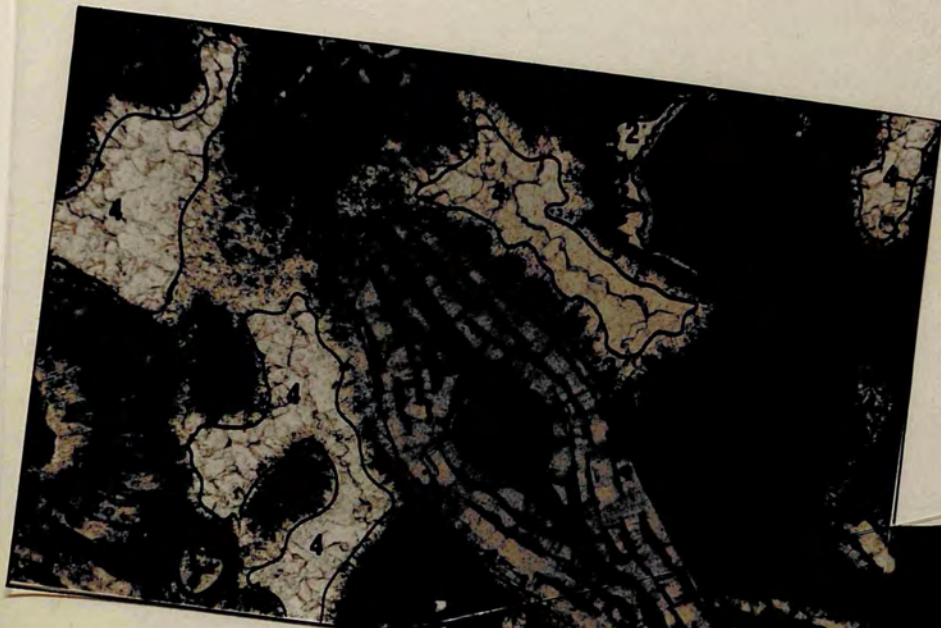


Plate 5.3 Nadorello east. Four periods of cement (Periods 1 to 4, alternating dusty and clear) are present on the echinoid grains where they show preferential growth in the c-direction of the grain (top). Two periods of cement (Periods 3 and 4) are present elsewhere. Scale 105 x



- | | |
|-----|-----------------------|
| 1-4 | CEMENTS |
| A | Algae |
| B | Bioclast |
| E | Echinoid |
| F | Foraminiferid |
| W | Wackestone intraclast |

Plate 5.4 Nadorello east. Four periods of cement (Periods 1 to 4, alternating dusty and clear) are present on the echinoid grain (left centre) where they show preferential growth in the c-direction of the grain. Two periods of cement (Periods 3 and 4) are present elsewhere. Scale 41 x

Plate 5.5 Carboj Dam. Close view showing the scalenohedral to bladed habit of the second period cement on a *Heterostegina/Operculina* foraminiferid. Scale 410 x

Plate 5.6 Western Nadorello. Stained peel photomicrograph of an echinoid grain and its syntaxial cement overgrowth. Seven zones of alternating non-ferroan and ferroan (stained blue with potassium ferricyanide) calcite are present. They are serrated in appearance with the apices extended in the c-direction of the crystal forming the echinoid grain. Scale 410 x

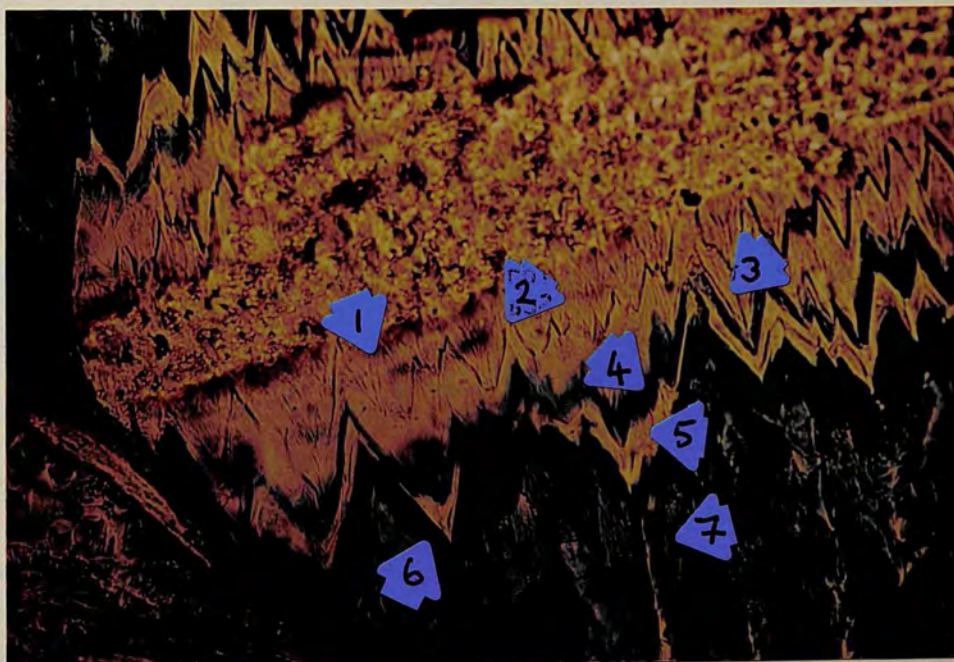
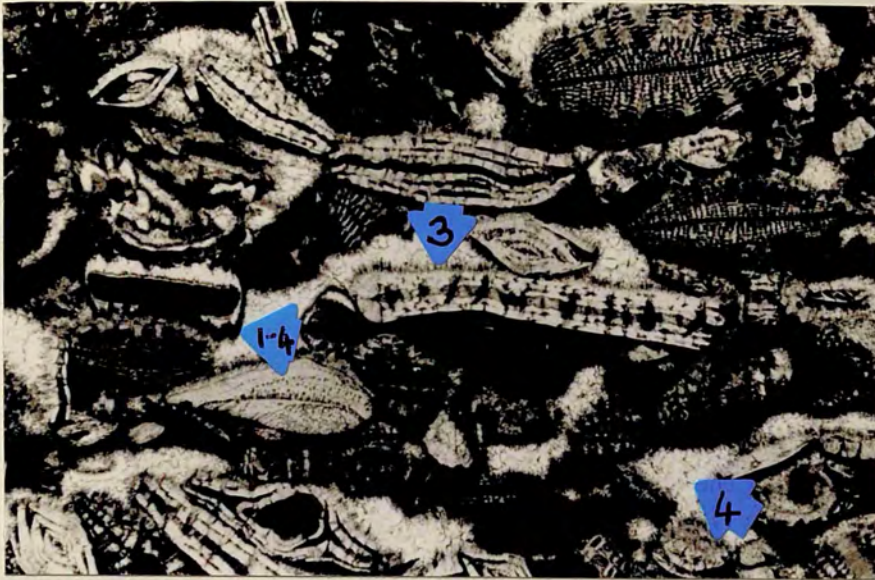


Plate 5.7 Nadorello east. Three periods of cement (Periods 2, 3 and 4) are seen on the echinoid grain (top left) but only two periods (Periods 3 and 4) are seen elsewhere. The dusty (Period 3) cement lines the pore space and forms a thicker coating on the foraminifera than on the algal (black) material. The blocky period 4 cement fills the remaining porosity which was protected from loss in compaction by the rigidity provided by the pore lining period 3 cement. Scale 41 x

Plate 5.8 Nadorello east. Two periods of cement (Periods 3 and 4) are present. Period 3 cement forms a dusty coating on the grains whilst period 4 cement forms a clear blocky fill. Scale 105 x

Plate 5.9 Nadorello east. Close view of a pore wall showing the dusty (Period 3) cement, with many inclusions, coating the grains and the clear blocky period 4 cement filling the pore space. The dusty cement is thicker on the foraminiferid substrate than on the algal substrate (right) and it shows faint crystal terminations (arrowed) to suggest an acicular or bladed habit. Scale 410 x

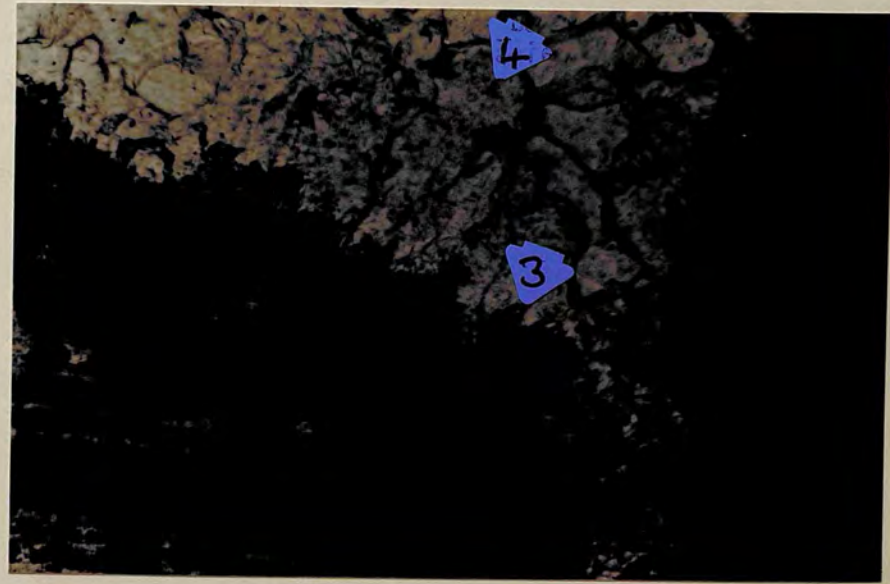
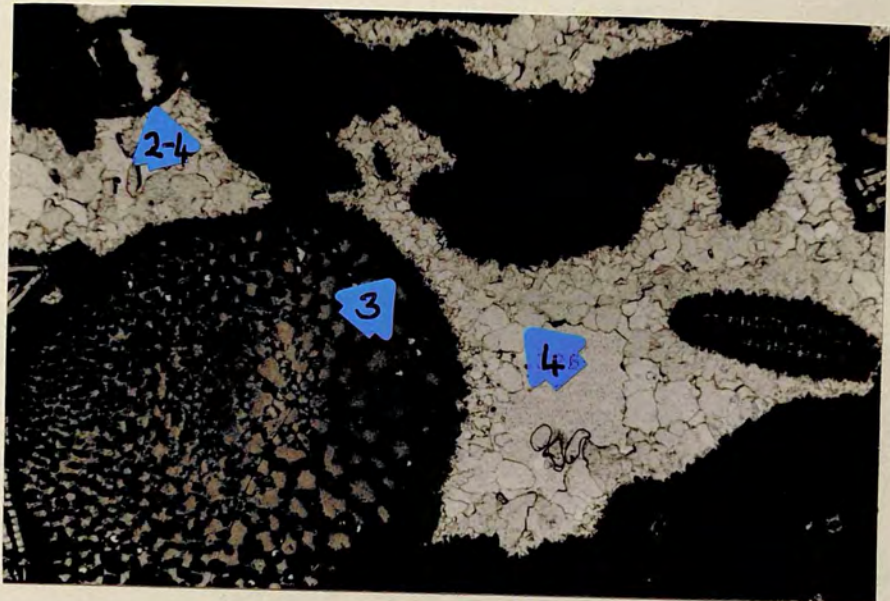


Plate 5.10 San Biagio. Two periods of cement (Periods 3 and 4) are present. The dusty period 3 cement coats the grains and fills some of the smaller pore spaces. The clear blocky period 4 cement (just visible and in the white areas) fills the remaining pore space. Scale 41 x

Plate 5.11 Contrada Giovanni. Echinoid grain overgrowths of period 2 cement (right centre) preserve point contacts and the original distribution of grains in their immediate vicinity. Whereas, elsewhere in the rock porosity is reduced and areal pressure solution contacts between grains prevail. Scale 41 x

Plate 5.12 La Conca. The echinoid overgrowth (Period 2 cement, bottom centre) preserves the original relative positions of the grains around it. Elsewhere in the rock compaction has occurred, there is an interlocking texture between *Nephrolepidina*, and areal pressure solution contacts prevail. Scale 41 x

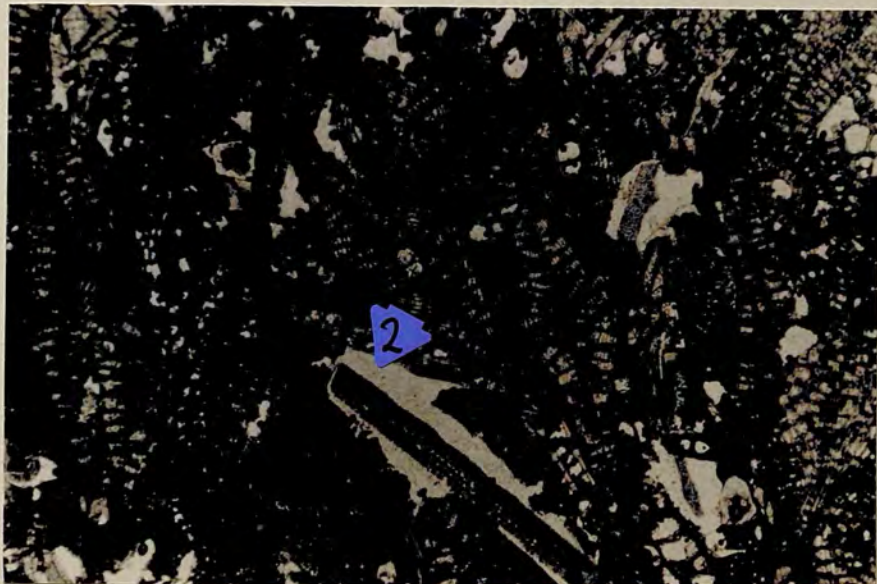
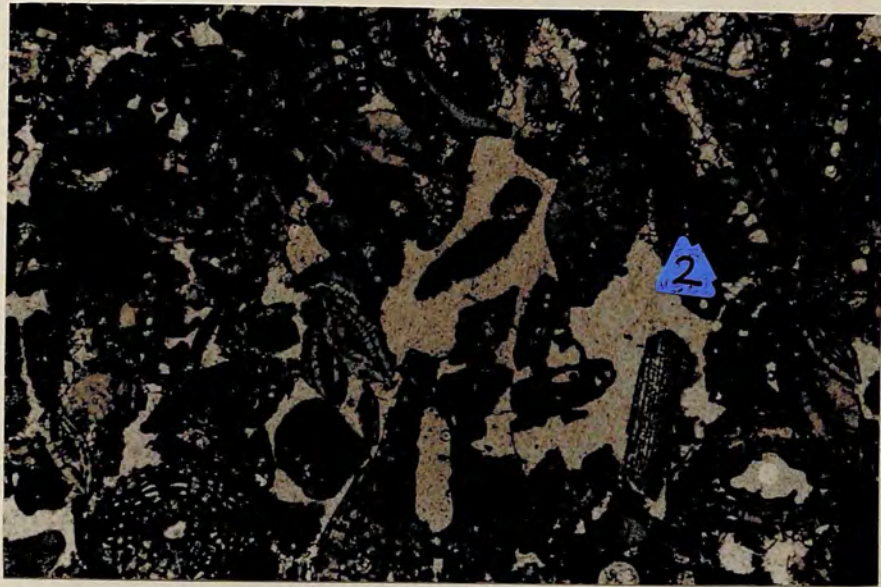


Plate 5.13 Nadorello east. Thoroughly compacted foraminiferal packstone showing very little intergranular porosity and numerous areal pressure solution contacts between grains. Scale 41 x

Plate 5.14 Carboj Dam. Compaction produces microstylites between the two foraminifera (top) whilst other foraminifera (centre and bottom) react by fracturing. Scale 105 x

Plate 5.15 Carboj Dam. Compaction in this coarse grained foraminiferal grainstone is much more pronounced than that seen in the finer grained rock (Plate 2.31) collected from the same locality. The grains have been rotated into parallel alignment, large areal pressure solution contacts prevail and algal clasts (black material) now occupy "interstitial" positions due to excessive pressure solution. Scale 105 x

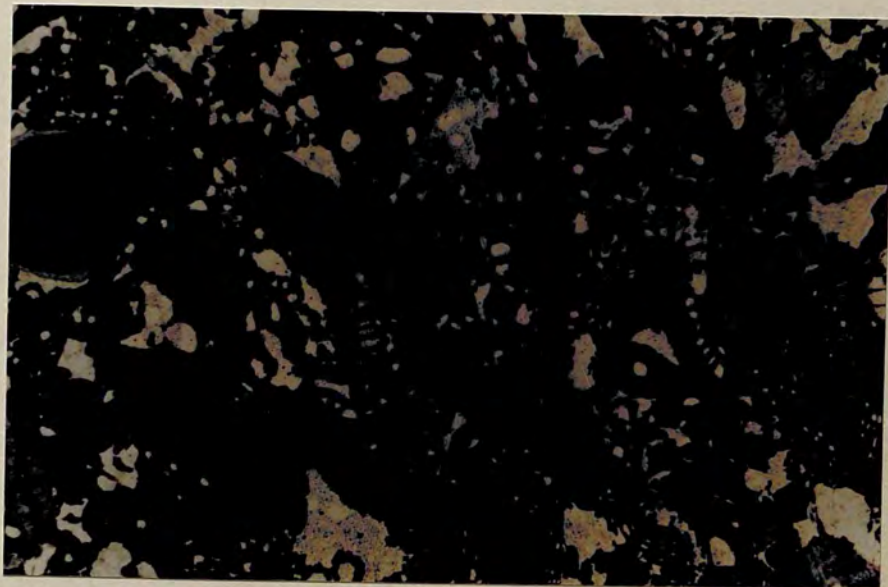
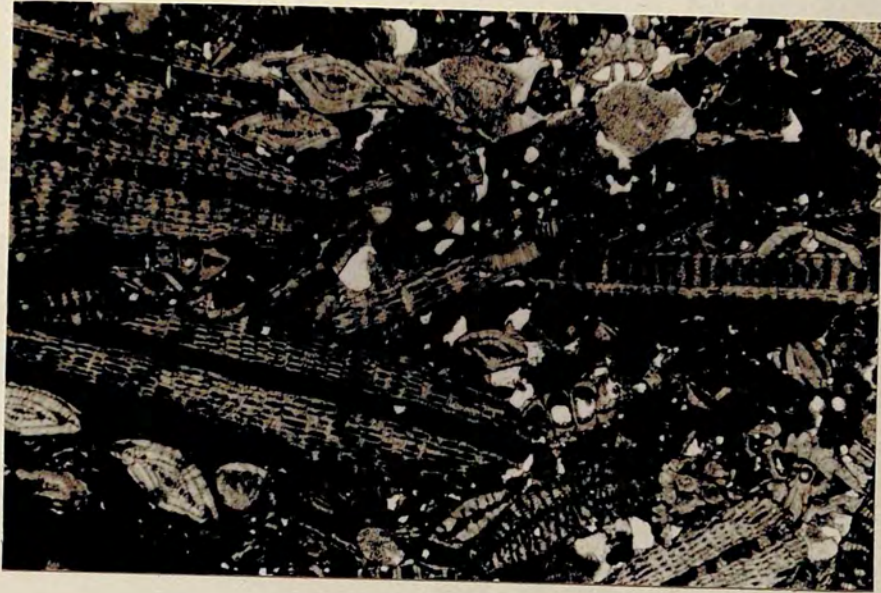


Plate 5.16 Tombe Sicani. The two *Heterostegina/Operculina* (top and centre) have reacted to compaction by fracturing. Scale 105 x

Plate 5.17 Carboj Dam. The two *Heterostegina/Operculina* (top left and left) have reacted to compaction by fracturing and by pressure solution of their internal septal walls (arrowed). Scale 105 x

Plate 5.18 San Biagio east. Compaction has resulted in the parallel alignment of foraminifera, fracture of some, and the apparent ductile deformation of others (arrowed). Scale 41 x

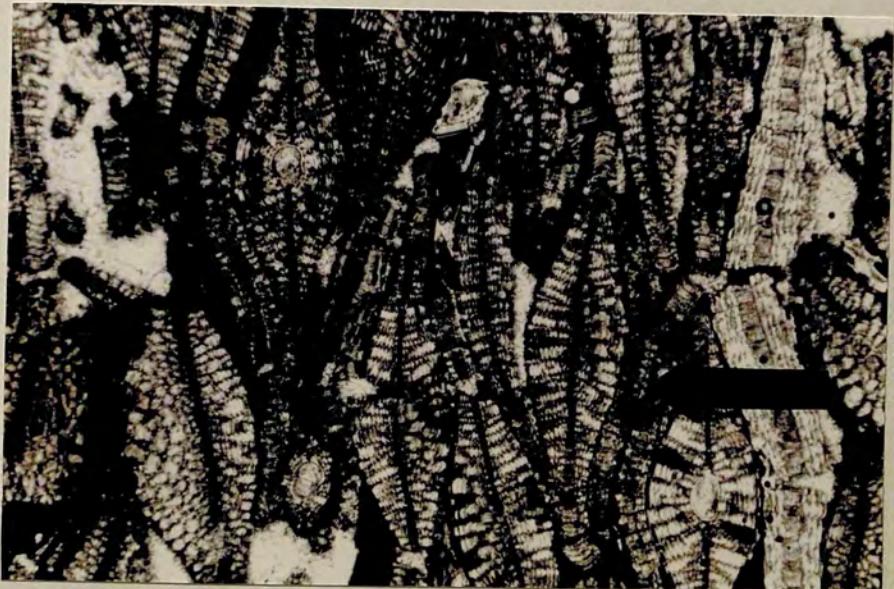
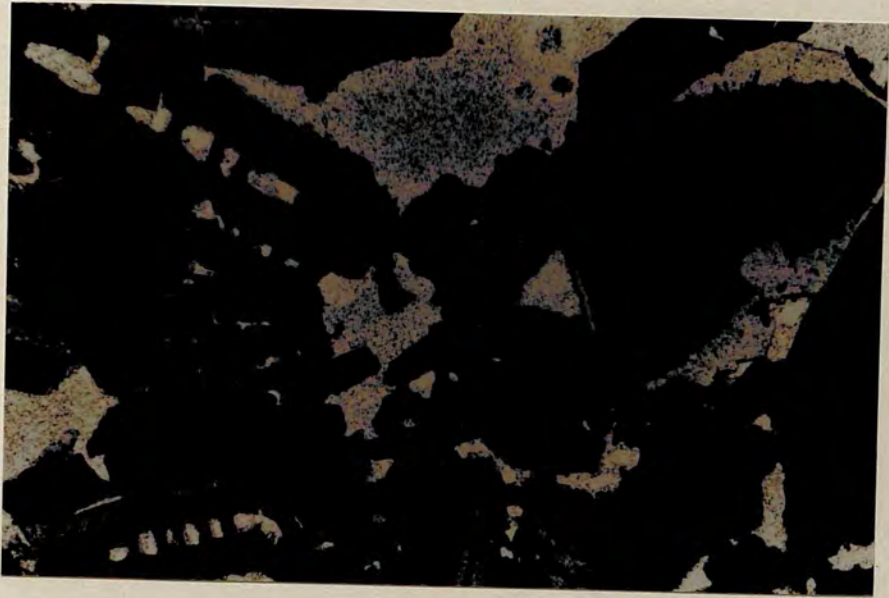
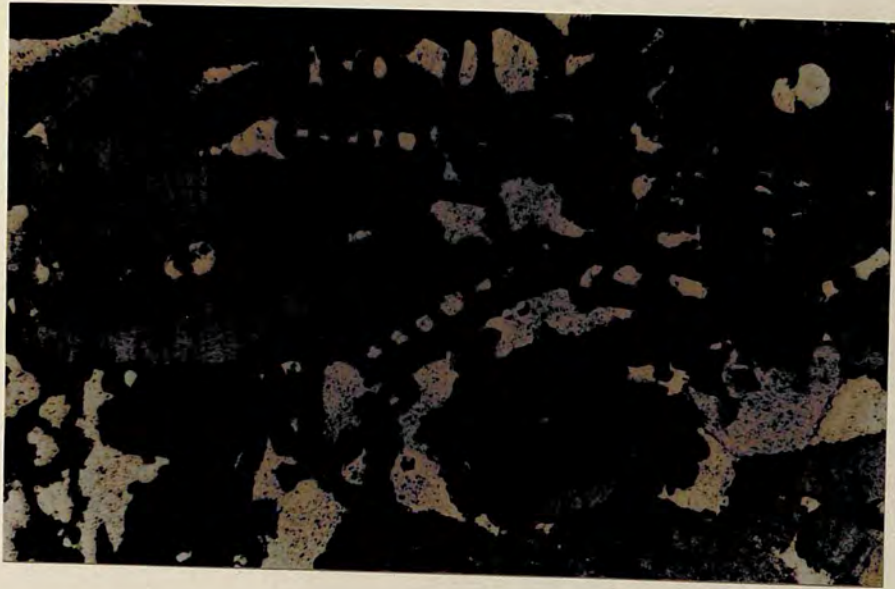


Plate 5.19 Contrada Giovanni. A large rock fragment (right centre) is resistant to pressure solution. Neighbouring grains have preferentially gone into solution against it. Scale 41 x

Plate 5.20 Nadorello east. Mud (A) microspar (B) and pseudospar (C) fill most of the pore space. The echinoid overgrowths (top and right) must, in part, be neomorphic, for the reasons set out in the text. Scale 41 x

Plate 5.21 Nadorello east. Cemented packstone (way up to the right) filling a *Thalassinoides* burrow. The lower part of the burrow fill (left) contains areas of mud (A) and microspar (B). The echinoid overgrowth (top left) must, in part, be neomorphic for the reasons set out in the text. The top of the burrow fill (right) has pore space filled by the fourth period cement. Scale 41 x

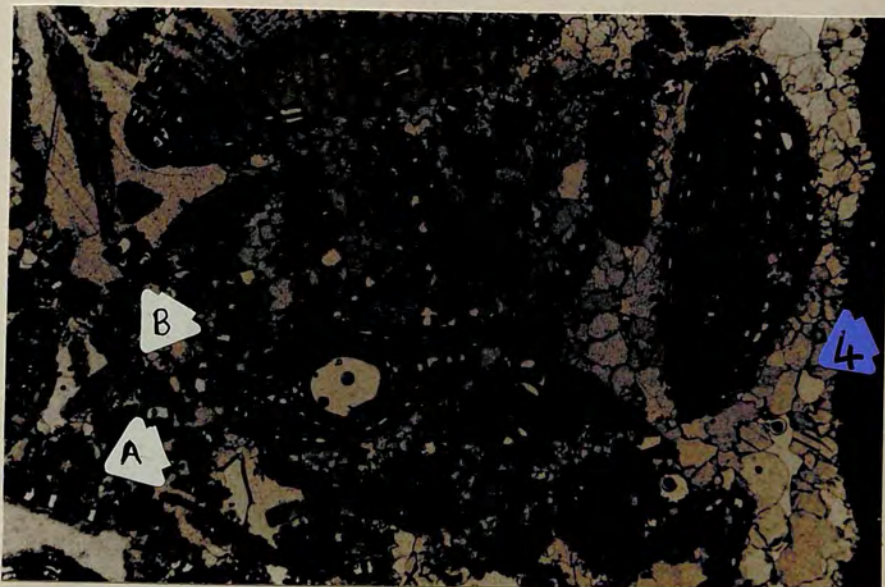


Plate 5.22 Tombe Sicani. All pore space filled by depositional matrix, syntaxial neomorphic overgrowths are seen on echinoid grains and foraminifera (arrowed). Scale 41 x

Plate 5.23 Tombe Sicani. Wackestone with true wackestone (grain floating) textures (top left and top right) and elsewhere intergranular pore space filled by depositional matrix. Neomorphic syntaxial overgrowths are found on the numerous echinoid grains in the rock. Scale 41 x

Plate 5.24 Nadorello east. Pelletal silts (arrowed) occupy primary pore space and have a different petrographic appearance to the depositional matrix upon which they rest. The upper surfaces of the silts are not flat and rest at an angle to the bedding in the depositional matrix. Scale 41 x

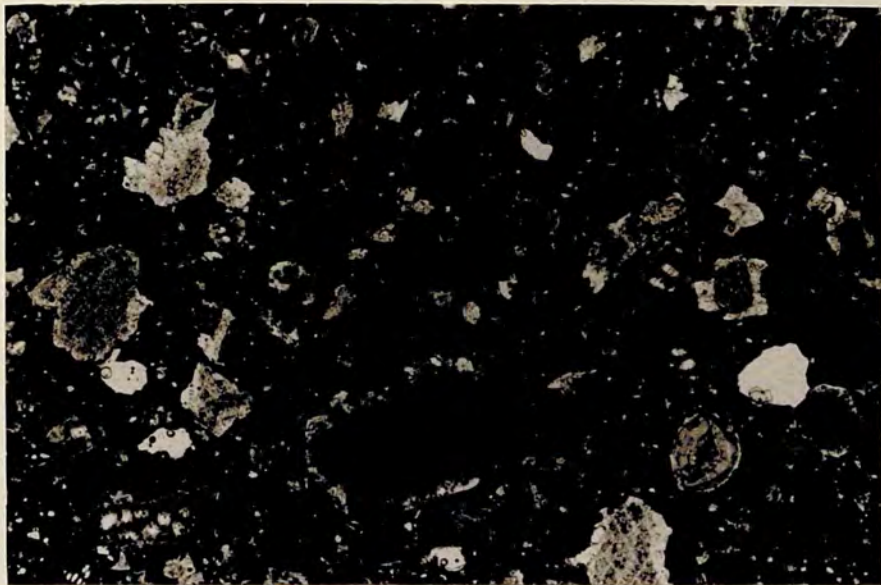


Plate 5.25 Nadorello east. Pelletal silts occupy the lower parts of primary pore space where they rest on depositional matrix. Scale 41 x

Plate 5.26 Nadorello east. A pelletal silt with faintly detectable pellet boundaries fills the lower part of a primary pore space. The silt post dates the pore lining (Period 3) cement (since it is not coated by it) and predates the blocky pore fill (Period 4) cement. Scale 105 x

Plate 5.27 San Biagio west. A mixture of mud opaque pellets and some small crystals fills most of the pore space which is lined by period 2 cement (arrowed). Way up is to the right, evidenced by umbrella structures produced by some of the foraminifera. Scale 41 x

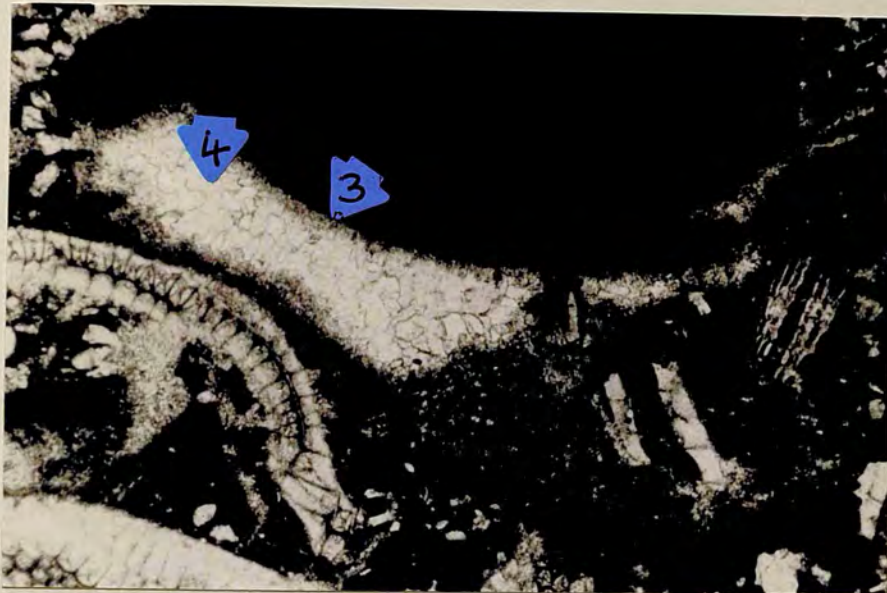


Plate 5.28 San Biagio west. A close view of the bottom centre of Plate 5.27 shows the period 2 cement coating the grains, the opaque pellets and small crystals in the pore filling mud, and the blocky period 4 cement filling the remaining pore space (bottom left). Scale 105 x

Plate 5.29 San Biagio east. Dolomite rhombs replace matrix and algae in a bioclastic packstone. Scale 105 x

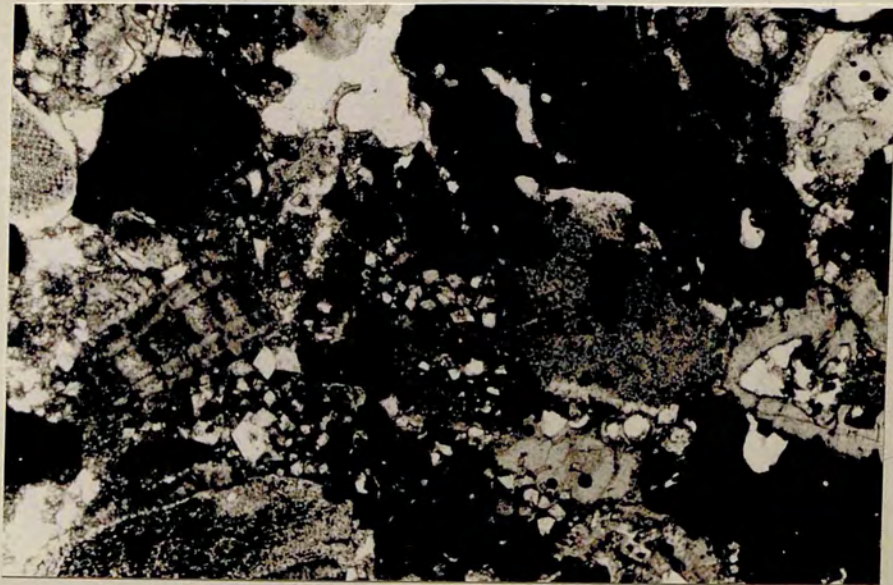
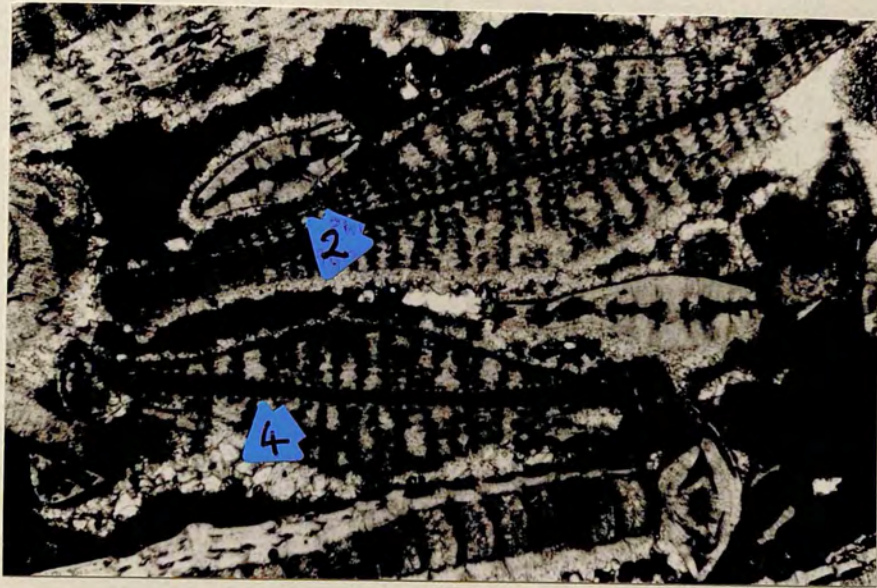
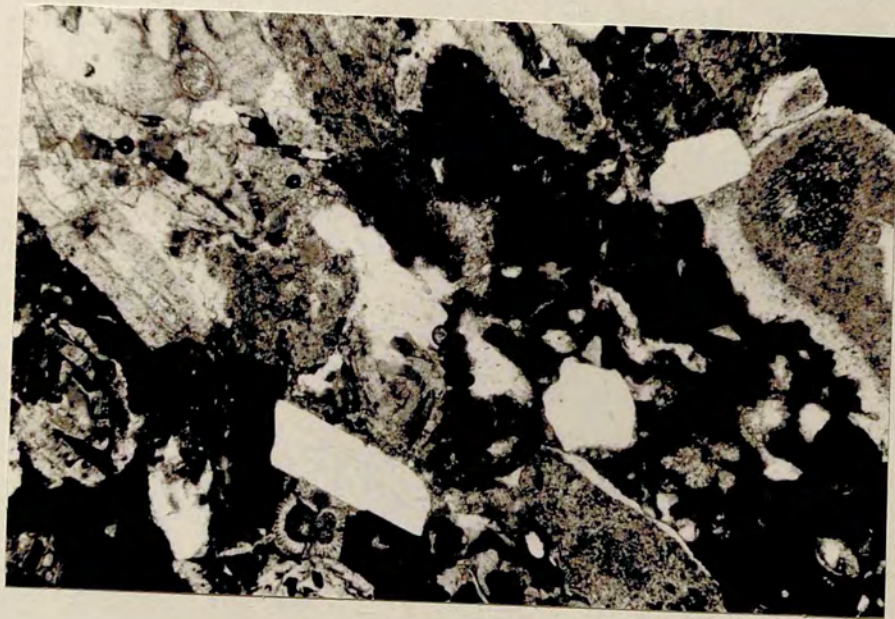


Plate 5.30 Western Nadorello. Subhedral unweathered crystals of feldspar with no inclusions form pressure solution boundaries with all neighbouring grains. Scale 105 x

Plate 5.31 Western Nadorello. A single subhedral crystal of feldspar forms pressure solution boundaries with neighbouring grains. Scale 105 x



DIAGENESIS: LOWER MIOCENE LIMESTONES

- Plate 5.32 Costa del Conte, glauconitic limestone facies. Cement overgrowths on the two echinoid grains (left centre and right centre) hold the neighbouring grains in their original relative positions. Elsewhere in the rock, compaction has occurred resulting in a reduction in porosity and areal pressure solution contacts between grains. The echinoid cements therefore pre-date compaction and represent a first period cement. Scale 41 x
- Plate 5.33 Costa del Conte, glauconitic limestone facies. First period cement is represented by syntaxial overgrowths on echinoid grains (which hold the neighbouring grains in point contact, bottom right and left) by small equidimensional crystals on the Textulariid (centre) and the algal clasts (top right), and by syntaxial overgrowths on the *Heterostegina/Operculina* fragments (right centre). Second period cement forms the blocky pore fill. Scale 105 x
- Plate 5.34 Battellaro, sandy limestone facies. First period cement is represented by slightly elongate to bladed crystals on one bivalve fragment (left arrowed) by a syntaxial overgrowth on another bivalve fragment (top right, arrowed), and by small equidimensional crystals lining the small Rotaliid (left). Second period cement is represented by large crystals forming subpoikilopic textures around quartz grains and by granular mosaics filling pore space around Globigeriniids (bottom right). Scale 105 x

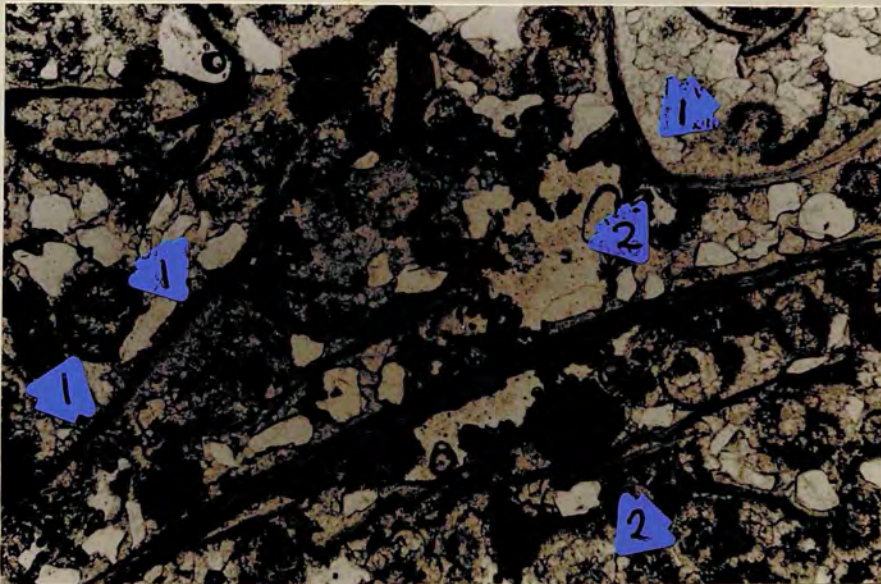
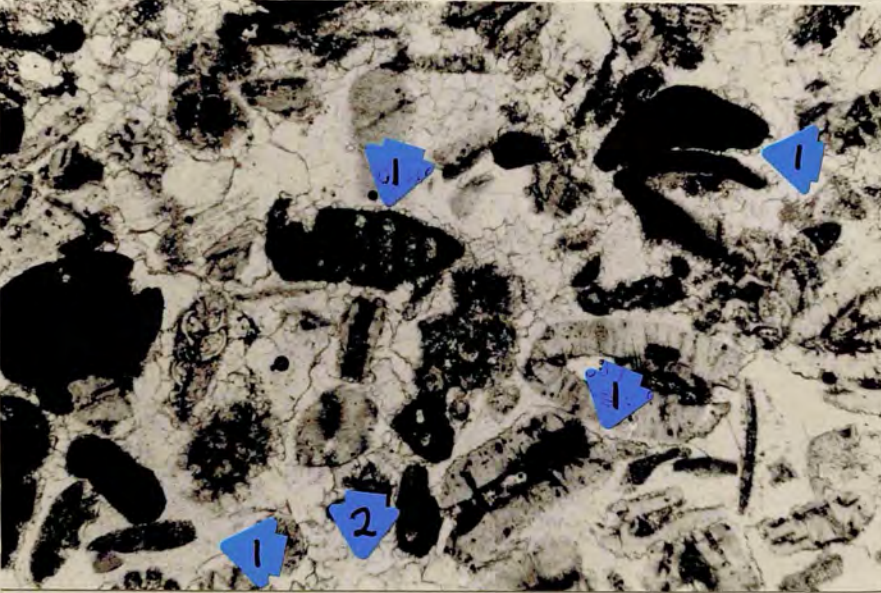


Plate 5.35 Mt Cardellia, glauconitic limestone facies. First period cement is represented by a syntaxial overgrowth on the echinoid grain (right centre) and on the *Heterostegina/Operculina* or *Spiroclypeus* fragment (left, arrowed) and by small equidimensional crystals on the algal fragment (top centre). Second period cement is represented by a blocky pore fill (best seen centre and left). Scale 105 x

Plate 5.36 Mt Cardellia, glauconitic limestone facies. First period cement is represented by wide syntaxial overgrowths on echinoid grains (right) and by small equidimensional crystals on the algal fragments (arrowed, top centre and left). Second period cement is represented by pore filling granular and blocky mozaics (best seen right centre). Scale 105 x

Plate 5.37 Battellaro, glauconitic limestone facies. First period cement is represented by syntaxial overgrowths on echinoid grains (top left and bottom right) and by small equidimensional crystals lining the Rotaliid fragment (arrowed, left centre) and the rock fragment (arrowed, right). Second period cement is represented by the crystals forming the sub-poikilotopic textures around the quartz grains (right centre). Scale 105 x

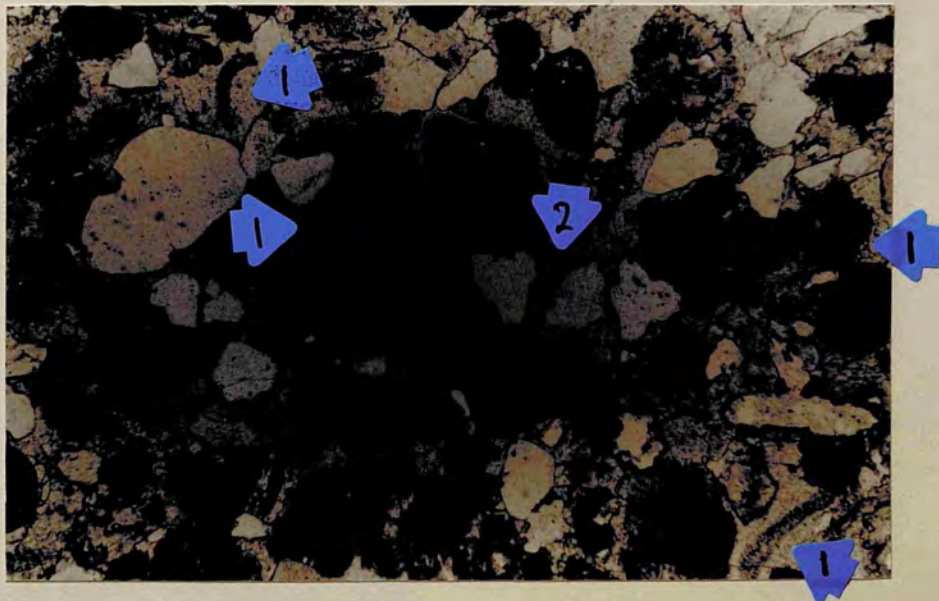
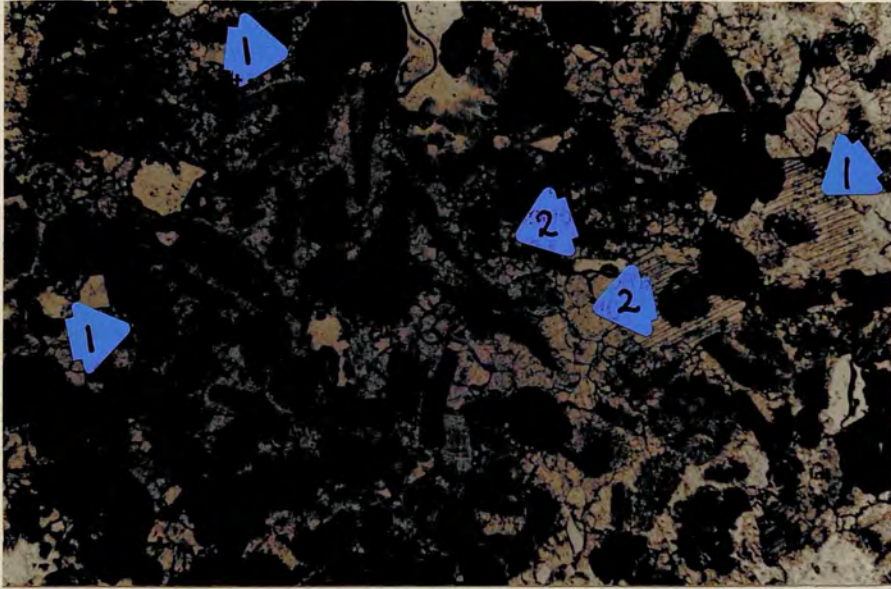
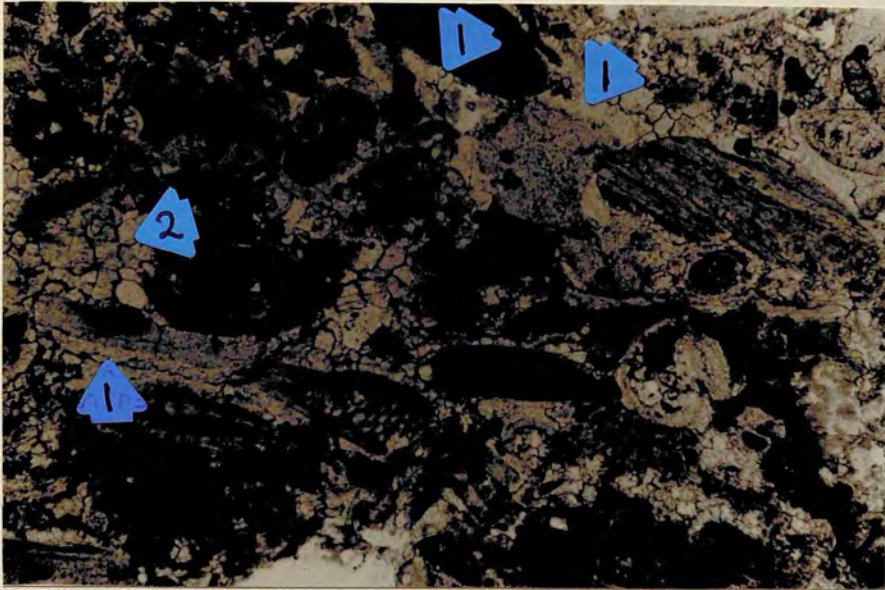


Plate 5.38 Costa del Conte, glauconitic limestone facies. First period cement is represented by equidimensional to slightly elongate crystals around the foraminifera. Second period cement is represented by a blocky pore fill. Scale 105 x

Plate 5.39 Costa del Conte, glauconitic limestone facies. First period cement is represented by equidimensional to slightly elongate crystals around the *Nephrolepidina* and *Miogypsina* foraminifera. Second period cement is represented by a blocky pore fill. Scale 105 x

Plate 5.40 Battellaro, sandy limestone facies. Sub-poikilotopic cement textures are seen throughout the sediment; no centripetally enlarged spars are present. The cement which fills pore space, belongs to the second period generation since small amounts of compaction, represented by pressure solution contacts between grains (arrowed) can be recognised. Scale 105 x

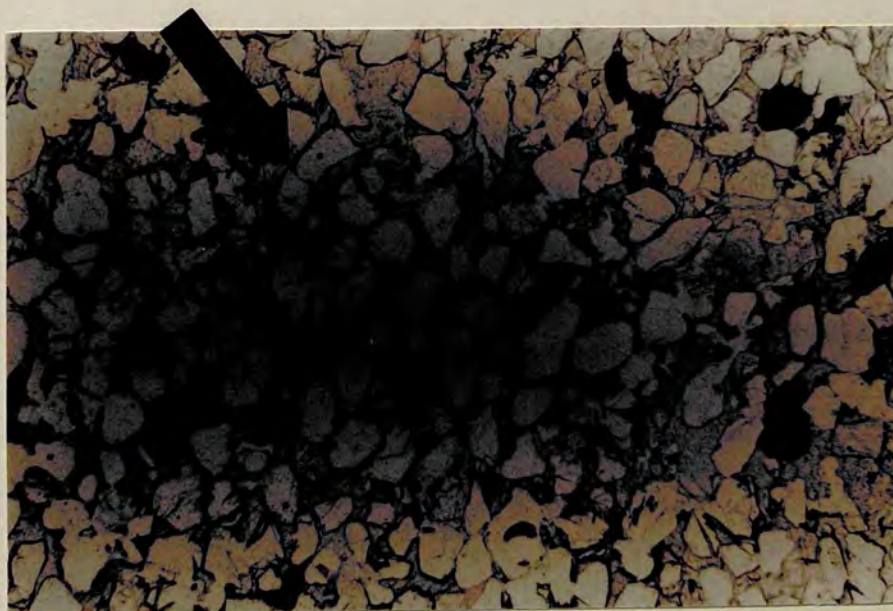
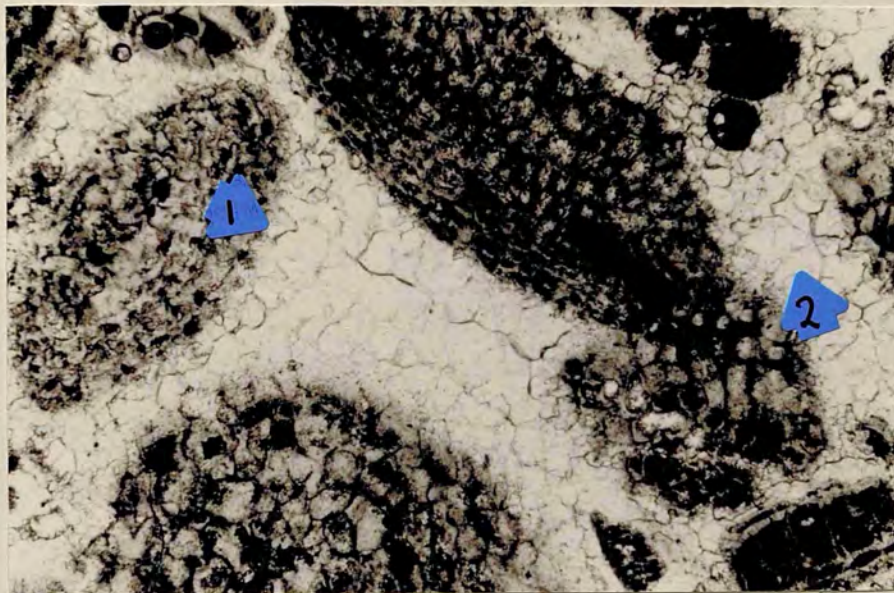
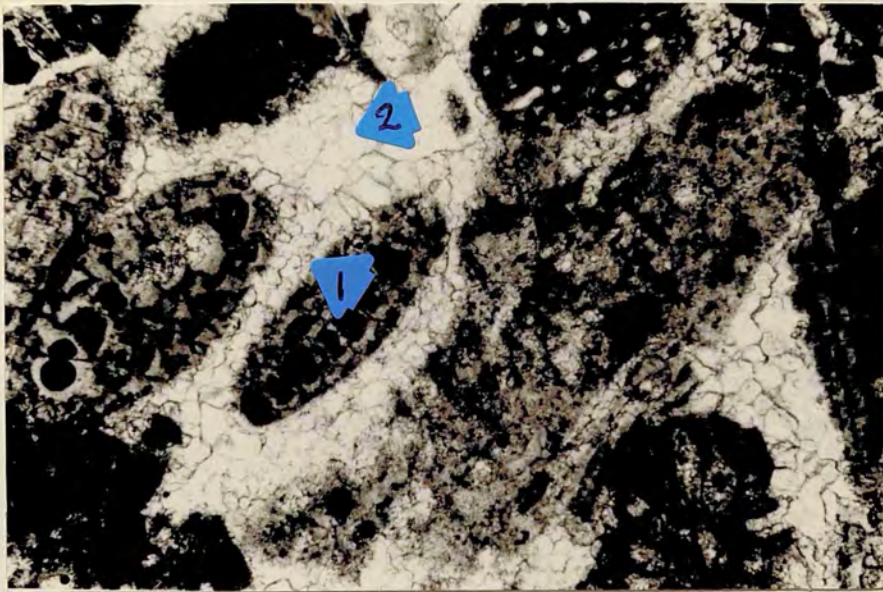


Plate 5.41 Battellaro, sandy limestone facies. Poikilotopic (arrowed) and sub-poikilotopic cement textures are present throughout the rock, filling pore space. The cement belongs to the second period generation since small amounts of compaction can be recognised. Scale 105 x

Plate 5.42 Costa del Conte, glauconitic limestone facies. Stained peel photomicrograph showing zones of ferroan (stained blue with potassium ferricyanide) and non-ferroan calcite (unstained) in the first period cement which coats some grains (arrowed). The second period cement, which fills the remaining pore space, is not zoned and is formed of ferroan calcite throughout. Scale 105 x

Plate 5.43 Battellaro, glauconitic limestone facies. The angular quartz grain (centre) is resistant to pressure solution. The neighbouring *Amphistegina* (arrowed) and glauconite grain (arrowed) preferentially go into solution to accommodate it. Scale 105 x

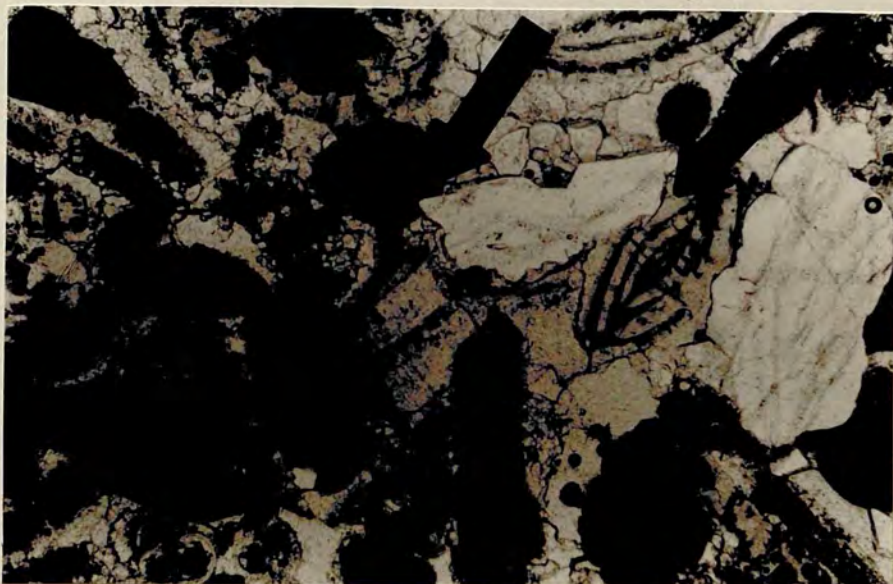
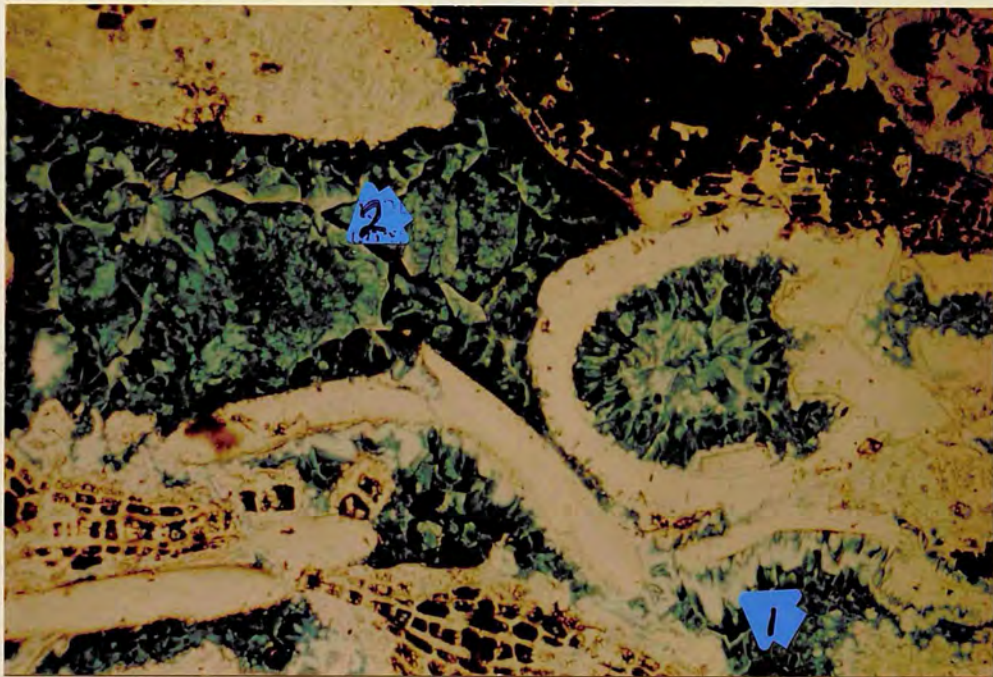
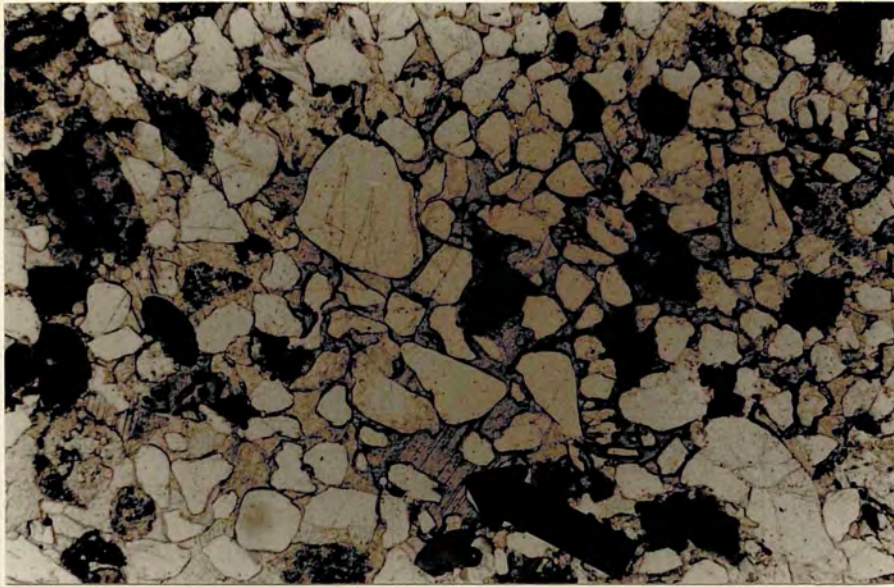


Plate 5.44 Battellaro, glauconitic limestone facies. Compaction has resulted in the foraminiferid (arrowed) preferentially going into solution to accommodate the large quartz grain (centre). This quartz grain also shows a pressure solution contact with the quartz grain on its right which has fractured and shows signs (strained extinction) of lattice distortion at the pressure solution contact. (Cross polarised light). Scale 105 x

Plate 5.45 Battellaro, glauconitic limestone facies. The *Spiroclypeus* fragment (arrowed) and the echinoid fragment (arrowed) preferentially go into solution to accommodate the neighbouring glauconite pellet. Scale 105 x

Plate 5.46 Serra Lunga, sandy limestone facies. Compaction has resulted in the fracturing of the two neighbouring quartz grains (centre). A single crystal of second period cement fills the fracture in the lower grain. Scale 105 x

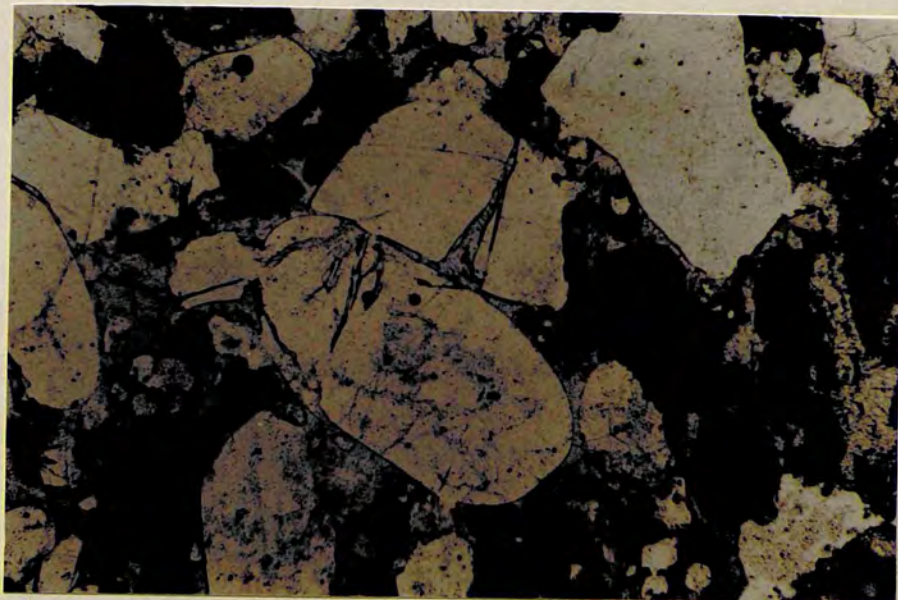
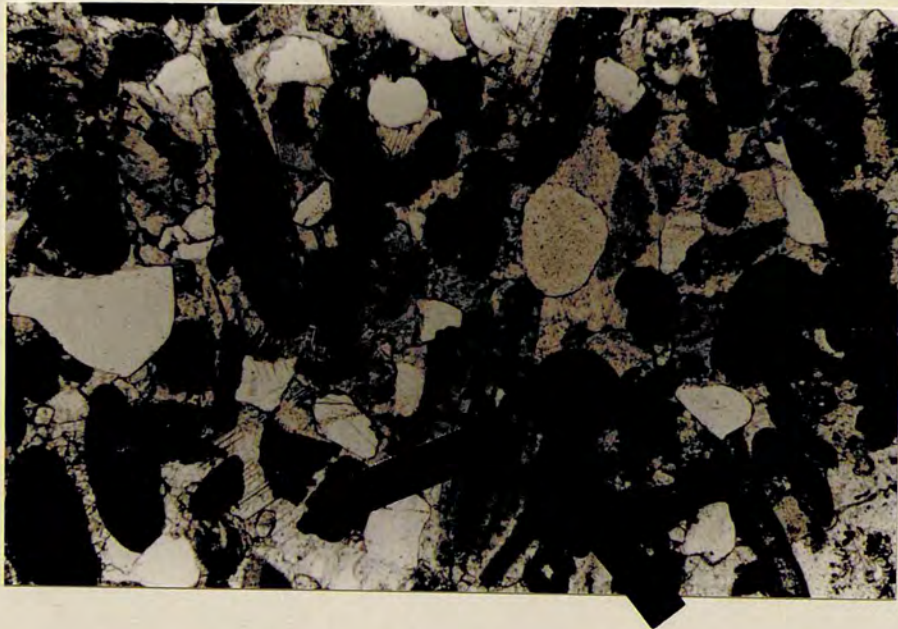
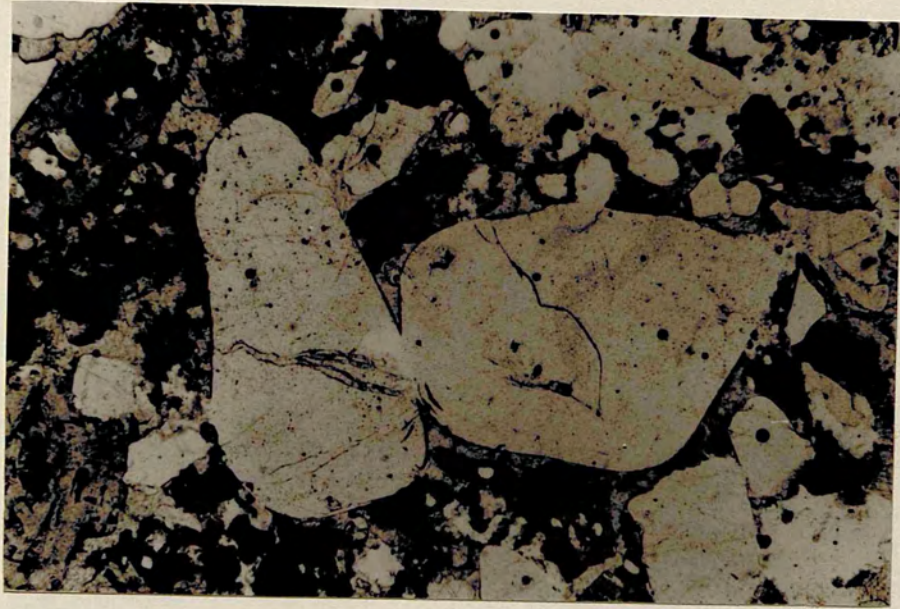


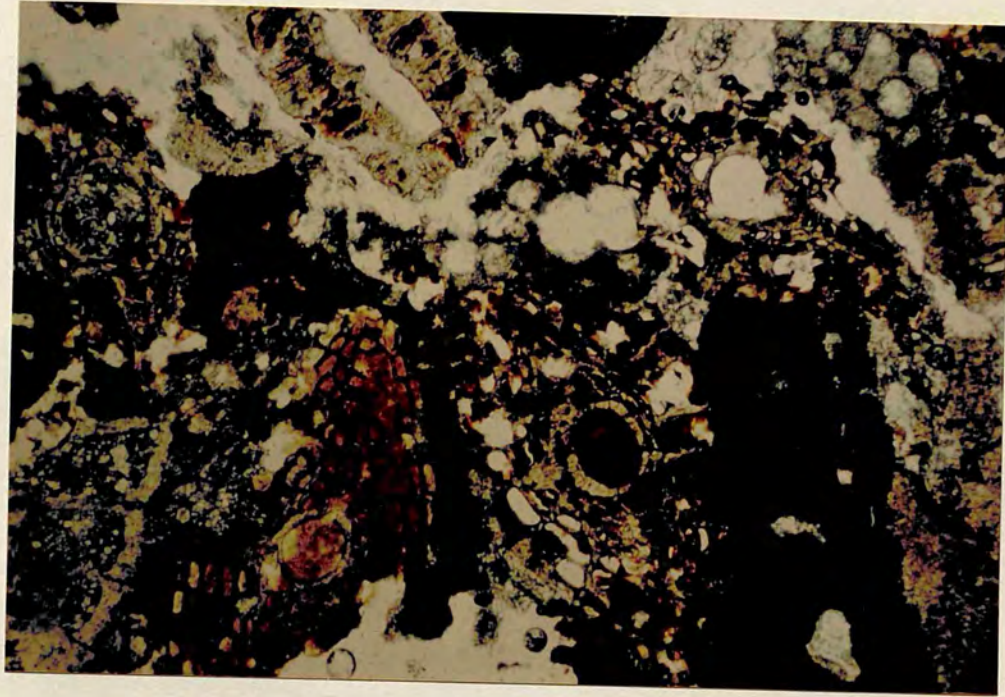
Plate 5.47 Serra Lunga, sandy limestone facies. Compaction has resulted in the fracturing of the quartz grain (left centre). The fractures are later filled by second period cement which is therefore post compaction in timing. Scale 105 x



GLAUCONITE

Plate 6.1 Western Nadorello Upper Oligocene. Glauconite is present as yellow, orange-brown and opaque infills to the chambers of four abraded *Nephrolepidina* foraminifera and as orange-brown and opaque infillings to borings and pores in a single *Heterostegina/Operculina* foraminiferid (top). Scale 105 x

Plate 6.2 Western Nadorello Upper Oligocene. Glauconite is present as orange-brown and opaque infills to foraminiferid chambers; pores in the walls of *Amphistegina* (top right); and pores in the echinoid grain (top left) which it also partially replaces. Scale 105 x



PHOSPHORITES: FIELD VIEWS

Plate 7.1 Donnalucata, SE Sicily. The dark limestone (centre) is phosphatised and forms a flat topped hardground. The mottled appearance to the top of the bed is caused by the infill of a *Thalassinoides paradoxica* burrow system with the overlying light grey limestone which contains small phosphatic limestone clasts (seen as black specks in the limestone, top right). The hammer is 260 mm long.

Plate 7.2 A general view (looking east) of the local succession at Contrada le Serre, north of Ragusa, SE Sicily. The prominent massive unit is the "livello a banchi calcarenitici" of the literature. The two phosphorite beds of Plate 7.3 are located at the top of the massive unit.

Plate 7.3 Close view of the two phosphorite horizons (top and bottom) at Contrada le Serre (Plate 7.2). The phosphorite conglomerates are formed of clasts of Globigeriniid wackstone held in a matrix of benthonic foraminiferid limestone. The lens cap is 55 mm dia.

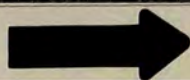
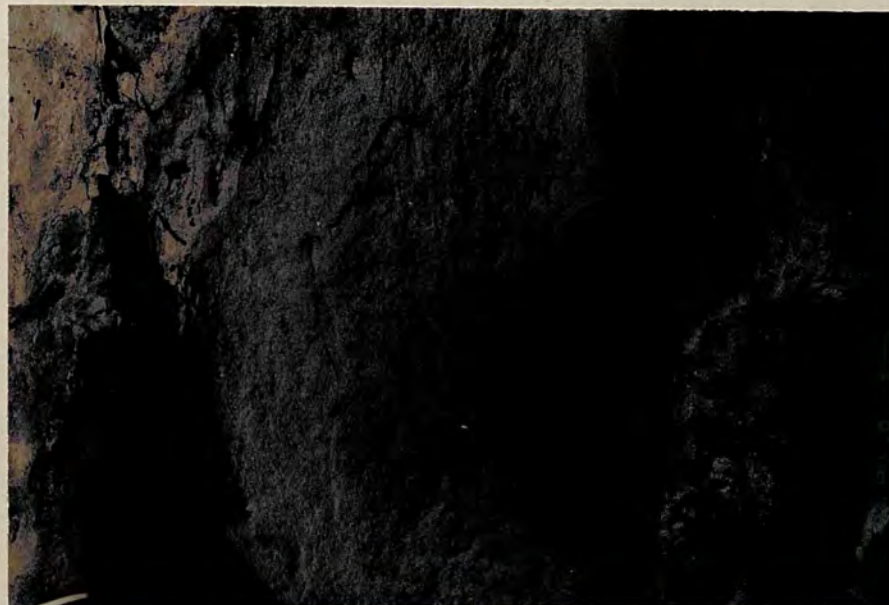


Plate 7.4 The lower main phosphorite bed of the Maltese islands exposed on the north coast of Gozo west of Xwieni Bay. The Lower Globigerina Limestone (bottom) terminates in a phosphatised hardground with rough, hackly relief (centre). The hollows of this hardground are then infilled by a dark coloured phosphorite conglomerate which extends down into the Lower Globigerina Limestone Formation by means of infill to a *Thalassinoides* burrow system. The hammer is 290 mm long.

Plate 7.5 A closer view of the hardground and phosphorite conglomerate in Plate 7.6 shows the depth and extent of the hollows in the hardground, the thickness of the conglomerate, and a clearer view of the conglomerate infilling the *Thalassinoides* burrow system. The hammer is 290 mm long.

Plate 7.6 A hollow in the Lower Globigerina Limestone below the hardground is infilled with phosphorite conglomerate which contains phosphatised limestone pebbles and phosphatised solitary coral moulds. The lens cap is 55 mm dia.



Plate 7.7 The upper main phosphorite bed (centre) of the Maltese islands exposed on the north coast of Gozo, west of Xwieni Bay. The bed, 1-1.5 m thick and dark in colour, forms a resistant lithology at the base of the Upper Globigerina Limestone Formation.



Plate 7.8 Close view of the base of the conglomerate bed in Plate 7.7. The conglomerate is composed of phosphatised limestone clasts held in a matrix of foraminiferal wackestone. The top of the white Middle Globigerina Limestone is heavily bioturbated and its burrows are infilled by the conglomerate. The lens cap is 55 mm dia.

Plate 7.9 Close view of the base of the conglomerate bed in Plate 7.7 showing it infilling the bioturbated top of the Middle Globigerina Limestone. The lens cap is 55 mm dia.



PHOSPHORITES: MICROFACIES

Plate 7.10 Dark and opaque francolite occurring as diffuse spots sometimes infilling and replacing *Globigerina* foraminifera (bottom right) in a chalk clast from the Upper Oligocene basal conglomerate at Nadorello east, SW Sicily. Light coloured francolite is also present, progressively replacing the limestone around a boring (bottom left). Scale 41 x

Plate 7.11 Alternating laminae of dark and opaque francolite with light coloured francolite observed parallel to a surface boring in a chalk clast from the Upper Oligocene basal conglomerate at Nadorello east, SW Sicily. The dark and opaque laminae are discontinuous and contain rounded spots (arrowed). (The interior of the clast is towards the top of the view). Scale 410 x

Plate 7.12 Dark clasts of phosphatised limestone (bottom left and top) are held in a matrix of light phosphatised limestone which infills the burrows of the hardground at Donnalucata, SE Sicily (Plate 7.1). Francolite is present as dark and opaque irregular shaped areas in the clasts and as the light coloured matrix (which is petrographically the same as that illustrated in Plate 7.14) in the sediment between the clasts. Scale 41 x

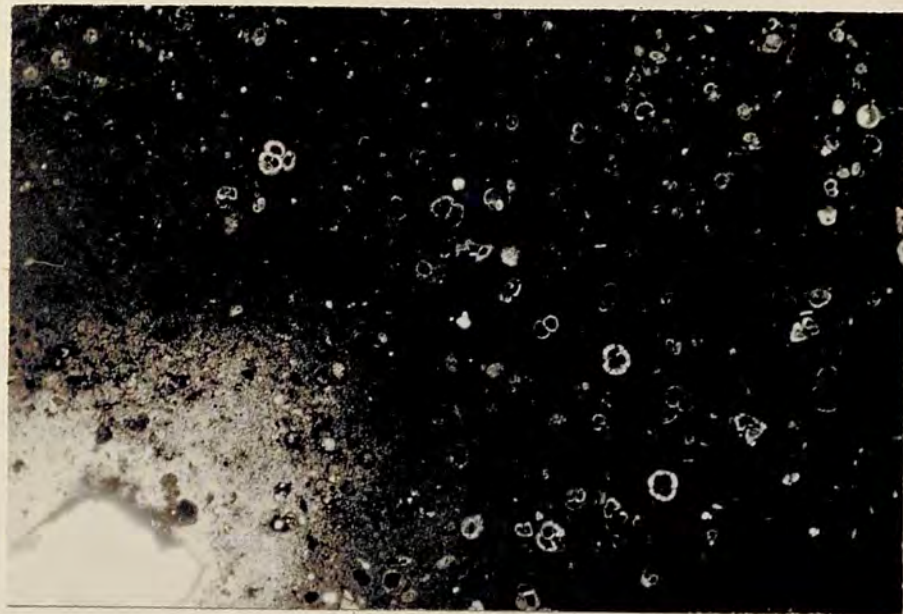


Plate 7.13 Francolite is present as dark and opaque pellets (top left, right centre) and as opaque infills to Globigeriniids in the sediment immediately overlying the hardground at Donnalucata, SE Sicily. Scale 105 x

Plate 7.14 Yellow orange to orange brown francolite has replaced the carbonate mud matrix of this limestone which forms the hardground at Donnalucata, SE Sicily. Scale 105 x

Plate 7.15 Francolite, a similar colour to that seen in Plate 7.14, forms the matrix of this hardground limestone from Donnalucata, SE Sicily. The francolite forms a carious texture with calcite crystals (arrowed) suggesting it is replacing them or being replaced by them. Scale 105 x



Plate 7.16 Donnalucata, SE Sicily. Francolite in the Globigeriniid chambers (centre) forms a carious texture with the calcite cement. Scale 410 x

Plate 7.17 Francolite forms thin light coloured coatings on clasts from the lower phosphorite conglomerate of the Lower Miocene at Qammieh, Maltese islands. The sharp boundaries to the coatings suggest that they are a primary precipitate, rather than a replacement of the limestone. Scale 41 x

Plate 7.18 The photomicrograph shows a boring in the surface of the hardground at the top of the Lower Globigerina Limestone at Qammieh, Maltese islands. This boring has been coated with francolite (A) partially filled with sediment (B) further coated by francolite (C) filled with sediment (D) and finally coated with the opaque francolite (E) which also extends over the surface of the hardground. Scale 41 x

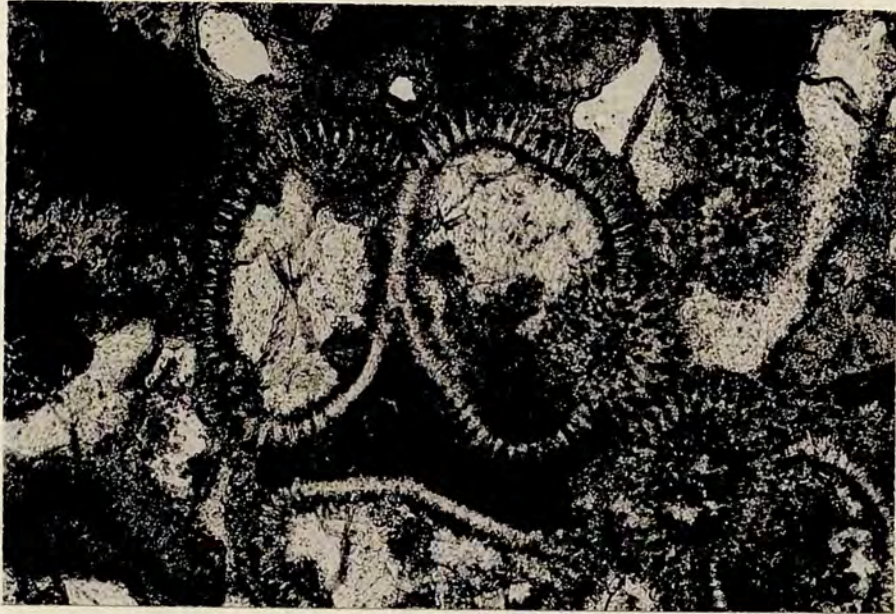


Figure 1.5 Outcrop and locality map
 Upper Oligocene and Lower Miocene Limestones
 (adapted from Mascle 1979)

